

AD 740724
AGARD-CP-98

AGARD-CP-98

1

AGARD

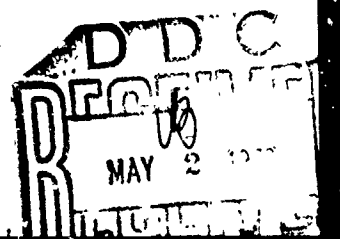
ADVISORY GROUP FOR AEROSPACE RESEARCH & DEVELOPMENT

7 RUE ANCELLE 92 NEUILLY SUR SEINE FRANCE

AGARD CONFERENCE PROCEEDINGS NO. 98

Specialists Meeting on Stress Corrosion Testing Methods

Details of illustrations in
this document may be better
studied on microfiche



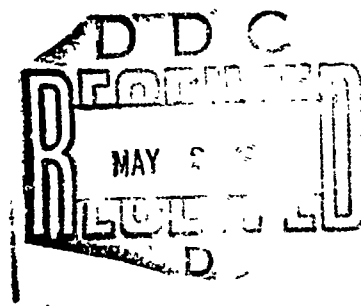
NORTH ATLANTIC TREATY ORGANIZATION



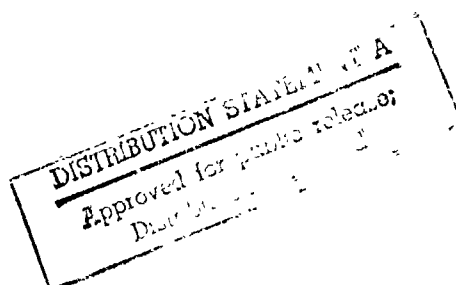
DISTRIBUTION AND AVAILABILITY
ON BACK COVER

Reproduced by
NATIONAL TECHNICAL
INFORMATION SERVICE

NORTH ATLANTIC TREATY ORGANIZATION
ADVISORY GROUP FOR AEROSPACE RESEARCH AND DEVELOPMENT
(ORGANISATION DU TRAITE DE L'ATLANTIQUE NORD)



SPECIALISTS MEETING ON STRESS
CORROSION TESTING METHODS



THE MISSION OF AGARD

The mission of AGARD is to bring together the leading personalities of the NATO nations in the fields of science and technology relating to aerospace for the following purposes.

- Exchanging of scientific and technical information;
- Continuously stimulating advances in the aerospace sciences relevant to strengthening the common defence posture.
- Improving the co-operation among member nations in aerospace research and development,
- Providing scientific and technical advice and assistance to the North Atlantic Military Committee in the field of aerospace research and development;
- Rendering scientific and technical assistance, as requested, to other NATO bodies and to member nations in connection with research and development problems in the aerospace field.
- Providing assistance to member nations for the purpose of increasing their scientific and technical potential,
- Recommending effective ways for the member nations to use their research and development capabilities for the common benefit of the NATO community.

The highest authority within AGARD is the National Delegates Board consisting of officially appointed senior representatives from each Member Nation. The mission of AGARD is carried out through the Panels which are composed of experts appointed by the National Delegates, the Consultant and Exchange Program and the Aerospace Applications Studies Program. The results of AGARD work are reported to the Member Nations and the NATO Authorities through the AGARD series of publications of which this is one.

Participation in AGARD activities is by invitation only and is normally limited to citizens of the NATO nations.

The material in this publication has been produced
directly from copy supplied by each author.

Published January 1972

06 053
620 194 2



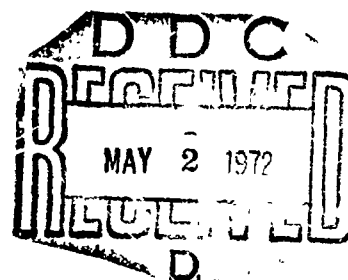
*Printed by Technical Editing and Reproduction Unit
Harford House, 9 Charlotte St. London W1P 1HD*

SYMPOSIUM CHAIRMAN

Dr. A. M. Lovelace
Director, Air Force Materials Laboratory
Wright-Patterson AFB
Ohio, 45433, USA

SYMPOSIUM VICE-CHAIRMAN

Prof. Dr. Ing. F. Bollenrath
Institut für Werkstoffkunde
Rhein-Westf. Technische Hochschule
Templergraben, 55
51-Aachen, West Germany



STRUCTURES AND MATERIALS PANEL CHAIRMAN

Dr. A. J. Barrett
Director, Engineering Sciences Data Unit
Royal Aeronautical Society
251-259 Regent Street
London, W1R7AD, England

COORDINATOR

Dr. D. E. Piper
Staff Scientist
Metallurgy & Composites Laboratory
Lockheed Palo Alto Research Laboratory
Lockheed Missiles & Space Company, Inc.
3251 Hanover Street
Palo Alto, California, 94304, USA

PANEL EXECUTIVE

Mr. Peter K. Bamberg
AGARD

FOREWORD

The problem of stress-corrosion cracking was identified by the Structures and Materials Panel of AGARD as a major area of concern to the aerospace industry. A Working Group on Stress Corrosion Cracking was formed in 1965 with a basic objective to evaluate and disseminate current knowledge about the phenomenon. A Specialists meeting held in 1966 (recorded in AGARD publication R-540/1966 entitled "Corrosion of Aircraft") and a Symposium held in Spring 1967 (AGARD publication CP-18/1967 entitled "Stress-Corrosion Cracking in Aircraft Structural Materials") attracted leading personalities of the NATO nations in the stress-corrosion field and resulted in the identification of two areas for further study:

1. The need to survey and publish current knowledge about the engineering practices to avoid stress-corrosion cracking, and
2. The need to survey and publish current recommendations concerning a standard method of test for stress-corrosion with particular emphasis on the generation of data significant to the designers of aerospace components.

A survey of NATO countries carried out in 1968 (AGARD publication R-570/1969) and a Symposium held in Fall 1969 (AGARD publication CP-63/1969) have highlighted those engineering practices used to avoid stress-corrosion cracking. A similar survey conducted during 1969 (AGARD publication AR-25/1970) and a Specialists meeting on Stress-Corrosion Testing Methods convened during the 33rd Structures and Materials Panel Meeting in October 1971 (with proceedings published in this AGARD report) constitute the efforts of the Working Group toward the second assignment mentioned above.

The program of this Specialists meeting on Stress-Corrosion Testing Methods was prepared to encourage discussion of (a) the utility and significance of stress-corrosion cracking data to current engineering and design practices, (b) the progress being made by NATO countries toward standardization of test techniques for stress-corrosion cracking, and (c) those test methods which might be recommended as standard techniques in the immediate future. Another important purpose of the meeting was to bring together those key personnel from North America and Europe who are striving on a voluntary basis to formulate standard methods and recommended practices for stress-corrosion testing. It is expected that the meeting will stimulate the interchange of information concerning such techniques and eventually lead to joint participation in any cooperative testing programs planned as a result of the meeting.

The opening lecture introduces the types and quality of data which are useful in design analysis and the following five papers describe the activities and attitudes of the various corrosion and fracture committees in the United States and Europe toward standardization of testing methods. The next contribution summarizes the proceedings of the recent NATO Science Committee Conference (April, 1971) on Theory of Stress Corrosion Cracking of Alloys with special reference to testing methods. The remaining invited papers were solicited on the basis that they provided new information about stress-corrosion cracking in general and/or stress-corrosion testing methods in particular.

CONTENTS

	Reference
ENGINEERING UTILITY AND SIGNIFICANCE OF STRESS CORROSION CRACKING DATA by W. E. Anderson	1
PROGRESS TOWARD STANDARDIZATION OF SCC TEST TECHNIQUES BY THE AMERICAN SOCIETY FOR TESTING AND MATERIALS by H. Lee Craig, Jr.	2
PROGRESS TOWARD STANDARDIZATION OF SCC TEST TECHNIQUES BY THE NATIONAL ASSOCIATION OF CORROSION ENGINEERS AND THE ALUMINUM ASSOCIATION by D. O. Sprowls	3
STRESS CORROSION TEST METHODS - THE EUROPEAN FEDERATION OF CORROSION CONTRIBUTION by R. N. Parkins	4
SOME IMPORTANT CONSIDERATIONS IN THE DEVELOPMENT OF STRESS CORROSION CRACKING TEST METHODS by R. P. Wei, S. R. Novak, and D. P. Williams	5
CURRENT PROGRESS IN THE COLLABORATIVE TESTING PROGRAMME OF THE STRESS CORROSION CRACKING (FRACTURE MECHANICS) WORKING GROUP by A. H. Priest and P. McIntyre	6
THE SCIENCE COMMITTEE CONFERENCE ON THE THEORY OF STRESS CORROSION CRACKING OF ALLOYS by J. C. Scully	7
MEASURING THE DEGREE OF CONJOINT ACTION BETWEEN STRESS AND CORROSION IN STRESS CORROSION by F. H. Cocks	8
pH AND POTENTIAL MEASUREMENTS DURING STRESS CORROSION OF ALUMINUM ALLOYS by J. A. Davis	9
STRESS CORROSION TESTING OF WELDED JOINTS by T. G. Gooch	10
SCREENING TESTS OF SUSCEPTIBILITY TO STRESS CORROSION CRACKING by G. J. Biefer and J. G. Garrison	11
STRESS CORROSION TESTING OF TITANIUM ALLOYS by S. J. Ketcham, C. E. Neu, and S. Goldberg	12
FACTORS INFLUENCING STRESS INTENSITY VALUES AND CRACK PROPAGATION RATES DURING STRESS CORROSION CRACKING TESTS OF HIGH STRENGTH STEELS by A. H. Priest and P. McIntyre	13
AN APPARATUS FOR STRESS-CORROSION TESTING WITH LARGE PRECRACKED WOL SPECIMENS by L. J. Ceschini and W. G. Clark, Jr.	14
TENSILE-LIGAMENT INSTABILITY AND THE GROWTH OF STRESS CORROSION CRACKS IN A HOMOGENEOUS Zn-Mg-Cu ALUMINUM ALLOY by J. H. Mulherin	15
AN ULTRAHIGH VACUUM SYSTEM FOR DETERMINING THE EFFECTS OF GASEOUS ENVIRONMENTS ON FATIGUE AND FRACTURE PROPERTIES OF METALS by H. L. Marcus and P. J. Stocker	16
ACOUSTIC EMISSIONS AND SLOW CRACK GROWTH IN HIGH STRENGTH STEEL by R. W. Staehle and G. E. Kerns	17
A CONTRIBUTION TO STRESS CORROSION TESTING OF ALUMINUM ALLOYS by G. Bollani	18

	Reference
INFLUENCE OF TEST METHOD ON STRESS-CORROSION BEHAVIOR OF ALUMINUM ALLOYS IN SEA WATER	
by G. J. Danek	19
DISCUSSION OF PAPER ENTITLED INFLUENCE OF TEST METHOD ON STRESS CORROSION BEHAVIOR OF ALUMINUM ALLOYS IN SEA WATER (PAPER 19)	
by D. O. Sprowls and J. G. Kaufman	19A
PARTICIPATION A L'ETUDE DE LA CORROSION SOUS TENSION DE CERTAINS ALLIAGES D'ALUMINIUM A HAUTE RESISTANCE	
par R. Doste	20
RESULTS OF COMPARATIVE STRESS-CORROSION TESTS ON Al-Zn-Mg-Cu ALLOYS USING DIFFERENT TYPES OF SPECIMENS	
by W. Lehmann	21
STRESS CORROSION CRACKING OF MARTENSITIC PRECIPITATION HARDENING STAINLESS STEELS	
by M. Henthorne	22
INVESTIGATION OF AN ACCELERATED STRESS CORROSION CRACKING METHOD	
by M. Hugo, J. Bellot, and E. Herzog	23
MICROSCOPIC IDENTIFICATION OF STRESS-CORROSION CRACKING IN STEELS WITH HIGH YIELD STRENGTH	
by E. H. Phelps	24
HOT SALT STRESS CORROSION CRACKING OF TITANIUM ALLOYS-OVERVIEW AND IMPACT ON SPACE SHUTTLE APPLICATION	
by W. B. Lisagor and J. E. Gardner	25
THE USE OF SLOW STRAIN-RATE EXPERIMENTS IN EVALUATING RESISTANCE TO ENVIRONMENTAL CRACKING	
by J. E. Reinoehl and W. K. Boyd	26
EXPERIMENTAL TECHNIQUES USED TO STUDY STRESS CORROSION MECHANISMS IN AIRCRAFT STRUCTURAL ALLOYS	
by G. M. Hoch, W. E. Krupp, and K. E. Weber	27
FRACTURE INITIATION AND STRESS CORROSION CRACKING OF WELDED JOINTS OF ALPHA- TYPE TITANIUM ALLOYS	
by C. Chassain and P. R. Krahe	28
PRELIMINARY REPORT ON RESEARCH ON THE INFLUENCE OF THERMOMECHANICAL TREATMENTS ON STRESS CORROSION CRACKING BEHAVIOR OF AISI 4340 STEEL	
by R. DeSantis, L. Matteoli, and T. Songa	29
PRELIMINARY RESULTS OF MECHANICAL AND STRESS-CORROSION TESTS ON PLATES OF 7075 ALLOY PRODUCED BY A NEW PROCESSING TECHNIQUE	
by E. DiRusso, M. Conserva, and M. Buratti	30
	Page
WRITTEN DISCUSSIONS OF PAPERS PRESENTED AT MEETING	1

ENGINEERING UTILITY AND SIGNIFICANCE
OF STRESS CORROSION CRACKING DATA

W. E. Anderson

BATTELLE
PACIFIC NORTHWEST LABORATORIES
Richland, Washington 99352
USA

SUMMARY

An engineering design analyst traces through some historical experiences with cracking and fracture problems to indicate the significance of corrosion acting concomitantly with stress. These experiences suggest a description that cracks develop either in "open" or "closed" areas; i.e., either at regions accessible to the ambient environment and direct view, or, at regions which are structurally hidden. These latter regions can be thought of as "nooks and crannies" having the same geometric nature as cracks or crevices.

Stress corrosion cracking is, first, a geometric disruption of the affected material; e.g., by fretting, mechanical damage like nicks and scratches, corrosion pits and internal fissures or cavities. Then follows an expansion of the disrupted region into the form of a crack, and, subsequent enlargement of the crack border.

Useful tests and evaluation methods now exist for the structurally "open" problems; this permits reasonable estimation of crack enlargement rates and hence service performance for short-lived components under simple loading and environmental experiences. Similarly credible tests and methods for longer-lived items or the structurally "closed" problems seem not yet in hand, even for the most elementary loading and environmental sequencing. Such problems presently defy practical prediction.

Lots of low-cost, moderately accurate data from many sources appears to have more utility for the analyst than limited amounts of very specific data. Specimen configurations and methods suitable for low-cost testing are examined and "new" possibilities suggested.

ENGINEERING UTILITY AND SIGNIFICANCE OF STRESS CORROSION CRACKING DATA

W. E. Anderson

INTRODUCTION

My "landmark" experience with ambient-environment airframe stress-corrosion cracking (SCC) came about in the late '50's as a result of a broken landing gear beam on a transport-type aircraft. Figure 1 shows the broken beam; Figure 2, the fracture face region. The break occurred at night, while the airplane was quiescent, having been refueled a little earlier, prior to an intended early morning flight to the customer. Rain had been falling for about two hours; the first in more than two weeks. Review of the craft's operations showed that it had been in lightweight flying status, but that a flat tire had been experienced two weeks previously and it was changed on the field runway. There seemed to be no question as to the initiating structural defect.

The locally dented tube broke from the inside first, developing an effective crack length of about two wall-thicknesses prior to the "wetting" experience. The fracture toughness of this material was estimated at $G_c = 105 \text{ lb/in.}$, whence, for the final crack length indicated by the change in rusting, the local bending stress figured at about 50,000 psi. A check with the geometry and load conditions at the time provided verification of this estimate.

The timing of this event was important; we had been accumulating confidence in the crack-strength-analysis methods of Irwin and Kies (1), who had visited the company on occasion. Our work was initially centered on the damaged-fuselage problem (2), but the principles seemed generally useful for much of the high-strength aircraft structure. Relevance to fatigue crack propagation occurred to Paris in 1957 (3) and soon enough data was accumulated from new tests reported in the literature (4-7) to permit evaluation of the scheme; it turned out that crack extension rate per cycle was correlated very nicely on the basis of the elastic stress field parameter, K , but it was to be some time before we could get the idea into published form (8 and 9). We recognized the potential effects of environmental influences on cracking (10), and by the April 1959 meeting on stress corrosion in Pittsburgh, we were thoroughly ready to "see" the significance of wedging-type corrosion products on SCC behavior described by Nielsen (11).

Meanwhile, we had been struggling with the "thickness effect" on toughness of cracked aluminum structures (12 and 13) and possible metallurgical influences on cracking resistance generally (14 and 15). There was a lot to do.

Sometime earlier we had been having troubles with high strength steels and "static fatigue." The conditions behind the 1954 summary of B-36 (Figure 3) experiences by Sachs (16) probably influenced thinking generally toward some method for steel protection which didn't cause more trouble than it cured. Among other means (like painting) there was developed a "porous cadmium plating" as a consequence of undesigned nocturnal urea addition to a plating solution.

The porous plating would indeed permit the baking-out of hydrogen at low temperatures. After a number of uneasy service difficulties, however, it became brutally clear that oxide of hydrogen could reenter the "pores" and serve as a very efficient electrolyte for the cadmium-steel "battery" at each interface-deep pore. The behavior was so regular that we could place a wet cotton wad on a strip so plated and, under a particular bending strain, could predict its early failure time much too accurately (we had them breaking at $30 \text{ min.} \pm 5 \text{ min.}$). The "fix" was to fill the pores with a polymer.

Zoeller and Cohen (17) showed some of these structural aluminum and steel stress corrosion cracking problems; several of their figures are reproduced here (see Figures 4, 5 and 6).

THE HISTORICAL PERSPECTIVEEARLY EXPERIENCES

These modern difficulties took on a different perspective when, in 1963, I was privileged to explore the older engineering journals at Lehigh University. Along with some remarkable descriptions of early American steamboating boiler explosions (one of which, by Ewbank (18) in 1843, seems likely to have involved stress corrosion cracking of copper), there was reported in 1844 by one John M. Batchelder the "Explosion of Hardened Steel" (19). His experience is portrayed in Figure 7, which he explains this way, "...The cause of the fracture is, probably, the same as observed in the glass toy called Prince Rupert's drops, made by pouring melted glass into cold water; the outside is suddenly contracted, while the particles in the interior, cooling more gradually, assume a different crystalline form, and burst asunder as soon as the cohesion of the external coating is destroyed." View his remarks as showing marvelous insight.

Water storage tanks of iron and steel seemed susceptible to unexpected failures under quiescent conditions; let me mention a few. The tank containing water from "...the silvery Tweed..." which burst in 1867 (20) was possibly due to stress-corrosion aggravated cracking. So also might have been the 10:30 A.M., June 29, 1881 water tank failure at Cincinnati (21). One episode in the rather droll account of this event is rendered in Figure 8. Perhaps the 1904 early morning failure of the water tank at Sanford, Maine, stemmed from such crack aggravating causes, too (22). I shall not deny that triggering mechanisms for such accidents may have included temperature-differential stressing between the relatively warm interior and coldish outside winds, but the influencing factor of combined stress and corrosion effects is difficult to discard entirely.

It is even more difficult to find any other reason but stress corrosion for the unfortunate cause of failure in the second attempt to span the St. Lawrence River with a "Quebec Bridge." The dramatic sequence of events is pictured in Figure 9. The truss was lost because a cast steel support rocker broke unexpectedly under perfectly quiescent conditions; a view of the rocker region is shown in Figure 10. (Reference 23)

There were problems with unexpected fractures of manganese bronze and tobin bronze bolts in the same time period; one was at the Panama Canal (24). An imaginary rendering of this difficulty is given in Figure 11; what else but stress-corrosion? The residual stresses in ordnance and helmets of WWI vintage caused rather unusual spontaneous fractures; these were mentioned by Howe and Groesbeck in 1920 (25). An attempt at picturing the problem is shown in Figure 12. During lunch break in a 1934 German construction shop, a freshly cut beam split open; Campus showed a picture of this event (26), and it is reproduced here as Figure 13. Can these cracking mechanisms be anything but concomitant action of stress and environment?

How shall all these incidents and accidents be described? What rationale might explain their precise atomic-level mechanisms? These problems are clearly important to the structural designer and he must include them in his considerations. But how?

To this observer there are two classes of cracking problems depicted in these historical events. One is cracking of "open" regions and the other is a class of structurally "closed" regions. Whether the distinction is fundamental or trivial seems not yet clear. But from this point of view it is easy for me to appreciate the 1930 remarks on corrosion in aircraft by Rawdon (27) (referencing U.R. Evans' 1927 papers on the subject), who pointed out that the rate of corrosion in a crevice "...on the basis of an oxygen concentration-cell is often very much greater than elsewhere on the same structure..."

RECENT AEROSPACE EXPERIENCES

Aircraft and their engines in 1930 may have been somewhat less structurally complex than those of today, but the SCC problem certainly didn't lessen with the increased complexity! Duttweiler (28) has provided an example of elevated temperature stress corrosion in titanium alloy. Originally blamed on fretting alone (Figure 14), the test disc (Figure 15) caused the spin-pit mess shown in Figure 16. It was later found that there was deposition of silver along with the fretting shown at the hole, and the assigned cause was stress corrosion.

Typical structural problems in transport aviation were kindly outlined by Weesner (29) in connection with another work. Figures 17-26 are taken from his offerings. All are traced to stress corrosion as the initiating or crack-extending phase of these service problems with modern turbine-powered airframes. Other survey work within the industry (30) indicated that the corrosion problem in civil aircraft generally was not astonishingly more severe in overwater operations than overland operations; these figures, then may be considered "typical" examples.

A summary to this point must recognize clear evidence of concern by aircraft structural designers, manufacturers and operators for the very real problem of stress corrosion cracking. Review of the figures presented suggests classification of the experiences into "open" problems, where the influencing environment can readily reach the affected area, and into "closed" problems where the cracking is initially "hidden" by fasteners and faying surfaces of other structural components.

Two of the documented cases reproduced here were obviously associated with fretting as the causative factor in geometric disruption of the affected material surface. The writer interjects personal views he believes are correct that other forms of disruption are similarly effective, e.g. corrosion pits, intermetallics, atomic structure voids and plain old mechanical damage. Furthermore, the view is held that if either the stress or the causative environment were absent from the affected region, the cracking process would be significantly retarded or altogether voided.

ACTUAL CONDITIONS AND THE TESTS WE USE TO MODEL THEM

AN UPPER WING SKIN

An example of the structural loads experience of an airplane component may help point out what I regard as real-life complexity of the SCC problem. Consider a certain portion of the upper wing skin on a conventional civil transport aircraft. Figure 27 depicts an "average" day's experience; it is important to note that about two-thirds of the load-time history is tensile.

Local residual stresses, somewhere in this region, may very well be nearly at yield. As the nominal stress level fluctuates from positive to negative, it can be assumed that this local region will experience the same range of fluctuations, but with an elevated mean.

A simplified representation, in real time, of the diurnal loads experience is shown in Figure 28. Both the nominal stresses at some region and the likely stresses at some other (residually stressed) region, are depicted as the approximated service cycles occur. This representation is probably the most elementary form of stress corrosion load-time cycling which would be credible to design analysts like me. It appears I shall have to resort to ad hoc approximations of the "worst likely" services experiences until something along the lines of "Miner's Law" is established for SCC. I am heartened at the progress along these lines (31 and 32).

The loading problem of Figure 28 emphasizes to me the need for considering the conjoint action of SCC and fatigue. I know that fatigue cracks as small as 0.1 mm seem to behave as the larger ones when they are defined by the stress field parameter concept (33), and providing the plastic zone surrounding the crack border is small compared to the minor crack dimension. If the residual stress maximum of 440 MN/m² is considered in this light, the case of a crack 0.1 mm deep is associated with a plastic zone only a few times smaller than the crack depth. However, for the nominal condition of a stress maximum at 125 MN/m², the plastic zone is about 1/40 the minor crack dimension of 10⁻⁴m. But whether these cracks might or might not behave in a manner described by the stress-field-parameters concept, they are real problems because defects like intermetallics as well as mechanical damage or corrosion pits 0.1 mm deep may occasionally be found. It is clear that concern for their effects on structure needs careful attention.

Figure 29 is presented at a scale of interest. The stress corrosion cracking data are from Hyatt (34), and the fatigue cracking rates are estimated from the literature for the short-transverse grain direction.

Both conditions are assumed to be "worst-likely" circumstances which might arise in civil transport service. At the nominal condition, maximum $K_I = 2.5 \text{ MN}\cdot\text{m}^{-3/2}$, and the 7079-T651 short-transverse plate exhibits stress corrosion cracking rates of 10^{-5} mm/sec ; about 1 mm per day! If the condition of $8.8 \text{ MN}\cdot\text{m}^{-3/2}$ arose, the cracking rate could exceed one millimeter per hour!

On the basis of five cycles per day, the cracking (due to cycling loads only) might range from about 10^{-3} mm/day to some very much lower value. Using this comparison then, it can be seen that mechanical cycling alone is several orders of magnitude less serious than the worst stress corrosion cracking. What is not clear is how the two might interact if the two conditions were to be imposed simultaneously, as they could very well be in practice.

Consideration of the upper wing skin example should demonstrate that not only is it important to have a measure of static-load stress-corrosion cracking resistance, but also it is necessary to have an evaluation of the combined effects of load-cycling and environment. In the present case, the other realities of temperature and pressure have not been implicated. At some time these must be considered as part of the total environmental and load sequencing variations. From the sheer immensity of this problem it is easy to appreciate why civil aircraft designers make very real attempts to provide structures that can safely contain large amounts of cracking damage.

Before continuing to specific specimen testing remarks, consider Figure 29 again. Two other abscissa scales besides cracking rates in millimeters are shown. The aluminum unit cell is considered to be about 4 Å across, and requires the separation of three atomic bonds per unit cell for complete fracture (if the process can be averaged for one unit cell thickness). At the lower stress-corrosion cracking rates of a few unit cells per second or slower, each atom has the opportunity to vibrate 10^{10} or more times before a bond is broken. As the cracking speeds reach that of brittle fracture, the atoms have the chance for only about one vibration before breaking apart. This kind of information is not only interesting to me, but I feel I gain some "perspective" from it.

TESTS

Conventional SCC test methods have not correlated well with actual cracking behavior of structures. For example, conventional testing (Figure 30)(35) failed to identify the unusual cracking rates of 7079 aluminum alloy. Is it possible that the SCC crack tip is sometimes blunted? That's suggested by Figure 31, from Creager and Paris (36), who referenced Mulherin's work. However, regardless of the details, the dominant message of experience is that SCC testing must take on broader dimensions than the important but incomplete story told by 600 seconds of immersion in 3.5% NaCl solution followed by 3000 seconds out of it.

Harking back to the upper wing skin and the stress history of Figure 27, one of the most apparent needs is for tests which include various cycles of hold-time. The results of some of our own experimentation in this area are shown in Figures 32a and 32b (37). Altogether the combined fatigue and environment effects may be described as shown in Figure 33. It appears that some materials behave as "A", and others as "B". Perhaps this generalization is broadly true and perhaps some of you can say why and under what conditions the observed behavior will occur. But to get quantitative behavior numerous experiments are needed to find which are the "A's" and which are the "B's". We are trying to make these "timed-hold" tests in the simplest, least costly but credible apparatus we can conjure up. At the present time our cycling hydraulics (38) are off-the-shelf items arranged as shown in Figure 34.

TEST SPECIMENS

Part of the course in "new" SCC developments may be guided by the specimen configuration. Different specimens can provide different kinds of useful data. Smith and Piper (39) summarized many of these, Figure 35; for some of these, the crack-tip stress field intensity varies with crack length as shown in Figures 36 and 37.

There are at least two additional specimen types which may prove of value in SCC testing, Figure 38; they cause variation with crack length as shown. All the selected examples are compared in Figure 39.

Both the ring specimen and (certain configurations of) the wedge-loaded center-hole specimen have the interesting property of an increasing, then decreasing, crack-tip stress field as the crack extends. Such behavior may be particularly useful for obtaining several items of crack-resisting data from one test. This possibility is illustrated in Figure 40.

NEW TEST SPECIMENS

Between the foregoing several specimen types there may be sufficient diversity to meet most practical problems of SCC material testing. However, further refinements for structural testing can be suggested.

An adaptation of the center-hole rectangular-perimeter design is illustrated in Figure 41. Pressing the boundaries of this specimen will cause the hole wall to yield in compression. Following load removal, the yielded region will be in residual tension. The specimen is now self-stressed, and may be subjected to appropriate environments. Building on this approach, representative faying materials and fasteners may be affixed to provide representative crevices. This scheme might prove well-suited to temperature and pressure cycling patterns of real aircraft structures. The specimens are inexpensive and can be destructively sectioned as needed.

With just a little more imagination we can doubtless "invent" other tests that are both inexpensive and credible to the likes of me. There is still a lot to do.

CONCLUDING REMARKS

The problem of SCC in aircraft structures has been reviewed, as I see it, using an historical approach that I have found helpful. The important point is that SCC problems are still very much with us, and the

total "ecology of the crack" is a very complex inter-relationship between loads, load-cycles, chemical interactions of the structure with the environment, and normally occurring abuse in service.

I have intended to point up the need for further attention to realistic modeling of the complex parameters affecting real structures in the tests we choose to apply to materials. In this respect, we have come full cycle to a return to the original sense of the word "test", which means to abuse a material or structure sufficiently well that its satisfactory behavior means we can use it for its intended purpose with confidence that it will perform its function safely and economically.

The essential contributions of physicists, metallurgists, and chemists and the crucial contributions of traditional testing must continue. These contributions have been and will surely remain invaluable. However, I believe there is a trend toward more complete modeling of actual service conditions in SCC testing, and I look forward with great hope and anticipation to substantial progress in coping with these failure mechanisms over the next decade. It distresses me to think that I might someday become a victim of SCC and have to petition a city, somewhere, to get back my fee for a car wash, like Mr. Reid of Seattle (Figure 42)(43).

REFERENCES

1. J.A. Kies and G.R. Irwin, "Fracturing and Fracture Mechanics," Welding Research Supplement, Feb. 1952.
2. A. Sorensen, "Some Design Considerations for Tear-Resistant Airplane Structures," JAS Meeting, Jan. 23, 1956.
3. P.C. Paris, "A Note on Variables Effecting the Rate of Crack Growth Due to Cyclic Loading," Addendum N, 9-12-57, D-17867, The Boeing Company.
4. W. Weibull, "The Propagation of Fatigue Cracks in Light-Alloy Plates," SAAB TN 25, 1954.
5. W. Weibull, "Effect of Crack Length and Stress Amplitudes on Growth of Fatigue Cracks," Mem. 65, Aero Res. Inst. of Sweden, 1956.
6. D.E. Martin and G.M. Sinclair, "Crack Propagation Under Repeated Loading," Proc. Third US Cong. Appl. Mech., June 1958.
7. A.J. McEvily, Jr. and W. Illg, "The Rate of Fatigue-Crack Propagation in Two Aluminum Alloys," NACA TN 4394, Sept. 1958.
8. P.C. Paris, M.P. Gomez, and W.E. Anderson, "A Rational Analytic Theory of Fatigue," The Trend in Engineering, Vol. 13, No. 1, Jan. 1961.
9. J.R. Donaldson and W.E. Anderson, "Crack Propagation Behavior of Some Airframe Materials," Crack Propagation Symposium, Cranfield, England, 1961.
10. Ref. 4, p. 11.
11. W.E. Anderson in discussion of N.A. Nielsen, "The Role of Corrosion Products in Crack Propagation in Austenitic Stainless Steel. Electron Microscopic Studies," Physical Metallurgy of Stress Corrosion Fracture, Metallurgical Society Conferences, Vol. 4, 1959, pp. 147 and 148.
12. P.C. Paris and W.E. Anderson, "On the Brittle Fracture of Structures," The Trend in Engineering, University of Washington, Vol. 12, No. 2, April 1960.
13. W.E. Anderson and P.C. Paris, "Evaluation of Aircraft Material by Fracture," Metals Engineering Quarterly, Vol. 1, No. 2, May 1961, pp. 33-44.
14. W.E. Anderson, Patent No. 3,284,194, Aluminum Alloy (with W.E. Quist) assigns to the Boeing Co., 1964.
15. D.E. Piper, W.E. Quist, and W.E. Anderson, "The Effect of Composition on the Fracture Properties of 7178-T6 Aluminum Alloy Sheet," Met. Soc. Conf., Vol. 31, AIME, 1966.
16. G. Sachs, Survey of Low-Alloy Aircraft Steels Heat-Treated to High Strength Levels, WADC TR-53-254, Dept. of Comm. PB 121667, 1954.
17. H.W. Zoeller and B. Cohen, "Shot Peening for Resistance to Stress-Corrosion Cracking," Metals Engineering Quarterly, Feb. 1966.
18. T. Ewbank, J. Franklin Inst., 3rd Series, Vol. V, 1843, p. 400.
19. J. M. Batchelder, J. Franklin Inst., 3rd Series, Vol. VIII, 1844, p. 133.
20. "Bursting of a Reservoir at Kelso," Engineering, (London), Vol. 4, Dec. 20, 1867, p. 568.
21. "An Accident at Cincinnati," Engineering News, Vol. 8, July 9, 1881, p. 278.
22. C.W. Sherman, "A Standpipe Failure at Sanford, Me.," Engineering News, Vol. 52, Dec. 1, 1904, p. 507.
23. H. Barker, "Quebec Bridge Suspended Span Falls Into River in Hoisting," Engineering News, Vol. 76, Sept. 14, 1916, pp. 524-528.

24. "More Evidence of Unreliability of the Stronger Bronzes," Engineering News, Vol. 76, Nov. 23, 1916, p. 998.
25. H.M. Howe and E.C. Groesbeck, Trans. Am. Inst. of Min. and Metall. Engrs., Vol. 62, 1920, p. 522.
26. F. Campus, in Residual Stresses in Metals and Metal Construction, Ed. W.R. Osgood, Reinhold, N.Y., 1954.
27. H.S. Rawdon, "Corrosion Prevention Methods as Applied in Aircraft Construction", Proc. ASTM, Vol. 30, Part II, 1930, pp. 61-67.
28. Letter to R.E. Duttweiler, Evendale Works, from Schenectady Laboratory, General Electric Co., August 29, 1963.
29. Letter from J. Weesner, Pan American World Airways to W.E. Anderson, Feb. 24, 1971.
30. P.C. Johnson, American Airlines, Enclosure #3 to Ref. 29.
31. R.P. Wei and J.D. Landes, "Correlation Between Sustained-Load and Fatigue Crack Growth in High Strength Steels," Materials Research and Standards, Vol. 9, 1969, pp. 25-27, 44 and 46.
32. J.M. Barsom, "Corrosion-Fatigue Crack Propagation Below K_{ISCC} ," Engineering Fracture Mechanics, Vol. 3, No. 1, 1971, pp. 15-25.
33. J. Schijve, "Significance of Fatigue Cracks in Micro-Range and Macro-Range," Fatigue Crack Propagation - ASTM STP-415, 1967, pp. 415-459.
34. M.V. Hyatt, "Use of Precracked Specimens in Stress Corrosion Testing of High Strength Aluminum Alloys," Corrosion, Vol. 26, No. 11, Nov. 1970, pp. 487-503.
35. D.O. Spowls, "Reporting and Evaluating Stress Corrosion Data," Stress Corrosion Testing, ASTM STP-425, 1966, pp. 292-316.
36. M. Creager and P.C. Paris, "Elastic Field Equations for Blunt Cracks with Reference to Stress Corrosion Cracking," International Journal of Fracture Mechanics, Vol. 3, No. 4, Dec. 1967, pp. 247-252.
37. F.R. Vollert, F.J. Lewis and W.E. Anderson, "Exploratory Cracking-Rate Studies with Aluminum Alloy 7075-T6 in Wet and Dry Air Under Triangular and Trapezoidal Cyclic-Load Wave Forms," Battelle-Northwest BNWL-SA-3270, March 1970.
38. F.J. Lewis, F.R. Vollert and W.E. Anderson, "An Inexpensive Electro-Hydraulic Cyclic-Load Test System," Battelle-Northwest BNWL-SA-3182, March 1970.
39. H.R. Smith and D.E. Piper, "Stress-Corrosion Testing with Precracked Specimens," The Boeing Co. D6-24872, ARPA #878, June 1970.
40. W.F. Brown, Jr., and J.E. Srawley, "Plane Strain Crack Toughness Testing of High Strength Metallic Materials," ASTM STP-410, 1966.
41. J.C. Newman, Jr., "An Improved Method of Collocation for the Stress Analysis of Cracked Plates with Various Shaped Boundaries," NASA TN D-6376, August 1971.
42. J.P. Gallagher, "Experimentally Determined Stress Intensity Factors for Several Contoured Double Cantilever Beam Specimens," Engineering Fracture Mechanics, Vol. 3, No. 1, July 1971, pp. 27-43.
43. "WHAT HAS 4 WHEELS, 2 EYES AND CAN'T SEE?

One of the smallest dollar-amount ordinances to clear through City Council for many years was a recent claim payment for \$2.25 to reimburse Floyd H. Reid, 8561 30th Ave. N.W., for a car wash.

Reid was driving past a city sewer-pumping truck in Elliott Avenue West when "something broke" and his car was deluged with mud.

"It was just like someone tossing a blanket over the car," Reid said.

The Seattle Times, Washington, Nov. 8, 1966.

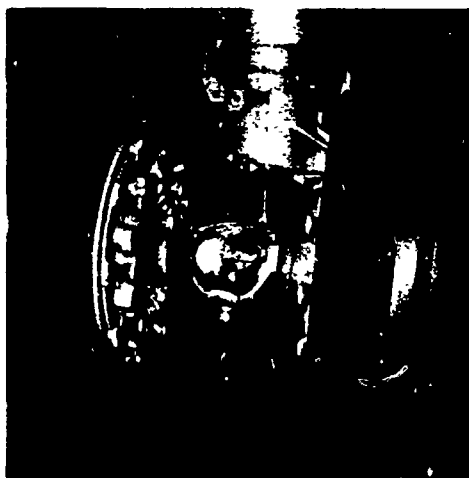


FIGURE 1. FRACTURED LANDING GEAR

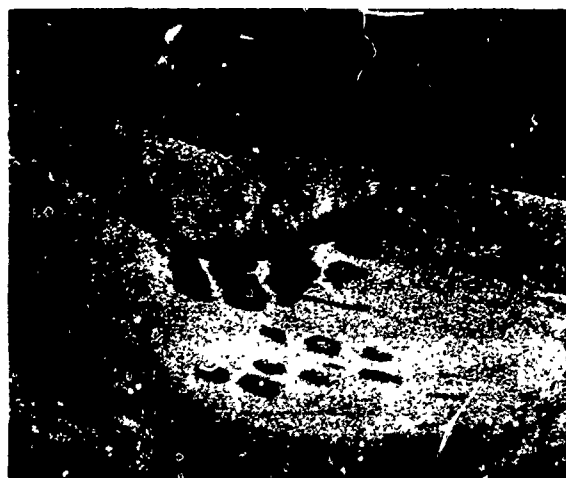
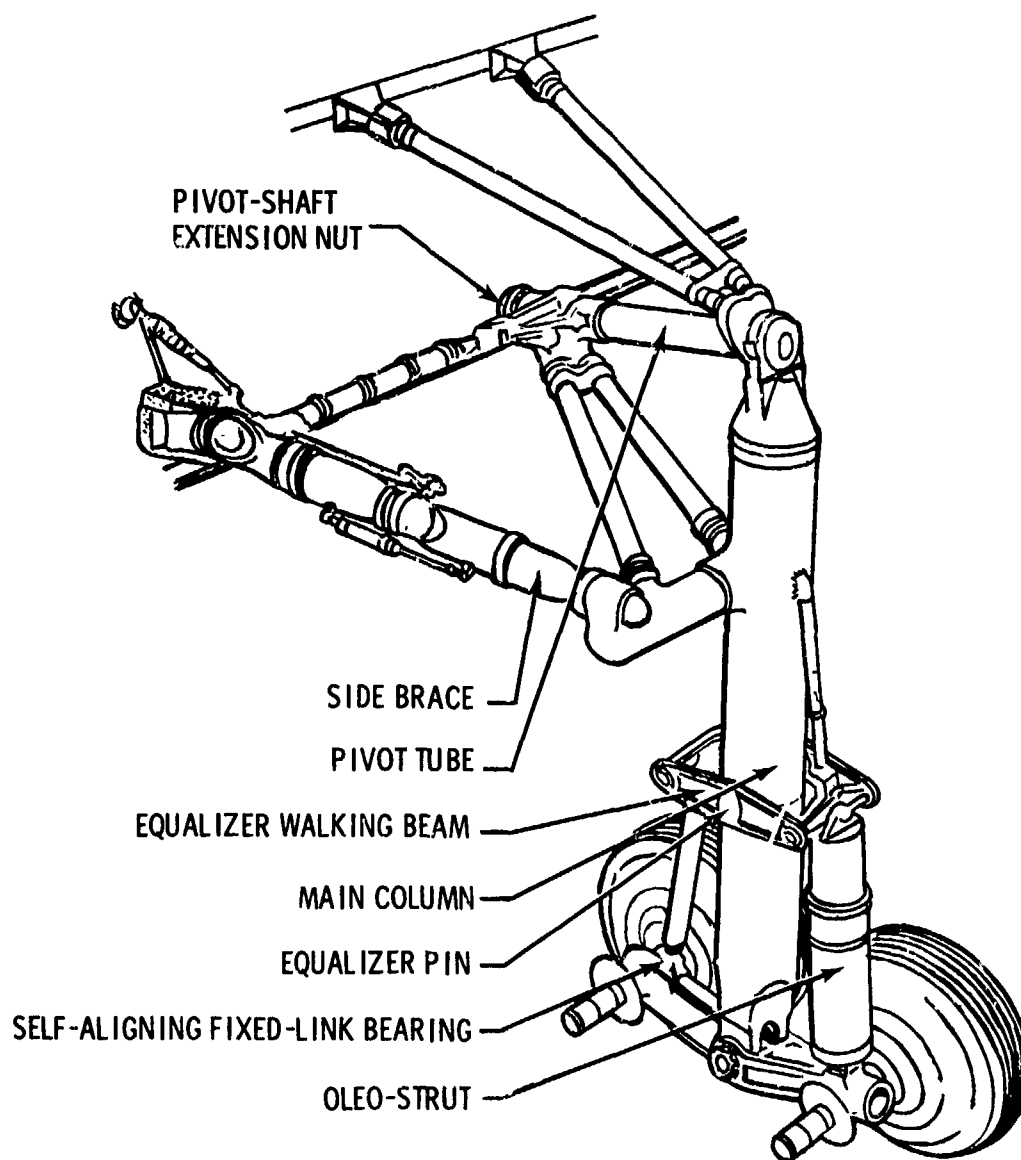


FIGURE 2. FRACTURE AREA OF FAILED LANDING GEAR

FIGURE 3. PROBLEMS WITH HIGH-STRENGTH STEEL, 1954⁽¹⁶⁾



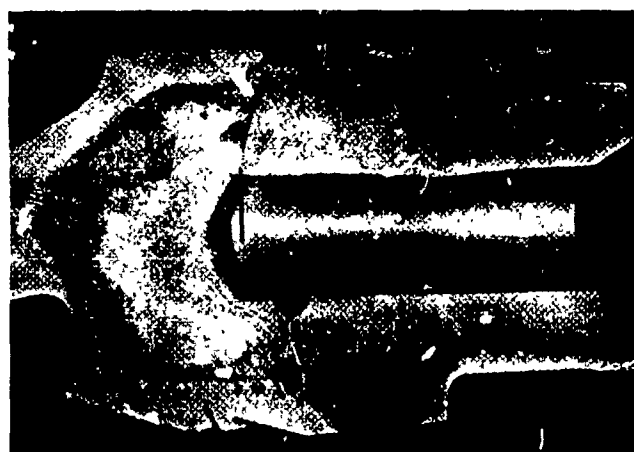
Landing gear made of forged 7079-T6 alloy. Arrows show problem areas.



Fracture showing stress-corrosion cracking in lug area

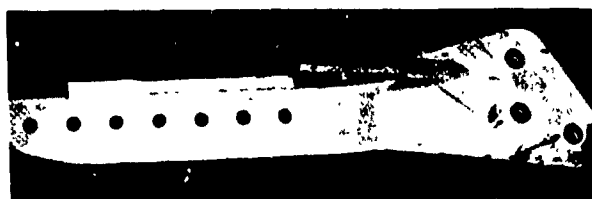


Fracture showing stress-corrosion cracking in parting plane of cylind.

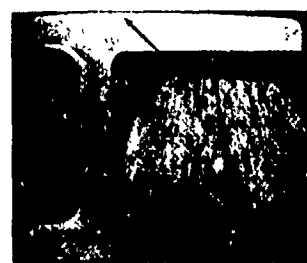


Fracture showing stress-corrosion cracking in parting plane of arm

FIGURE 4. CRACKING IN LANDING GEAR (7079-T6 Al)⁽¹⁷⁾



Dagger fitting showing stress-corrosion crack.



Cross-section of fitting showing grain run-out at parting plane. Insert shows close-up of grains.

FIGURE 5. CRACKING IN DAGGER FITTINGS (7079-T6 Al)⁽¹⁷⁾



Crack in trunnion fitting of 4330M steel (220 to 240 ksi).



Microsection of trunnion fitting showing typical intergranular cracks. $\times 100$

FIGURE 6. CRACKING IN A 4330M STEEL TRUNNION FITTING⁽¹⁷⁾

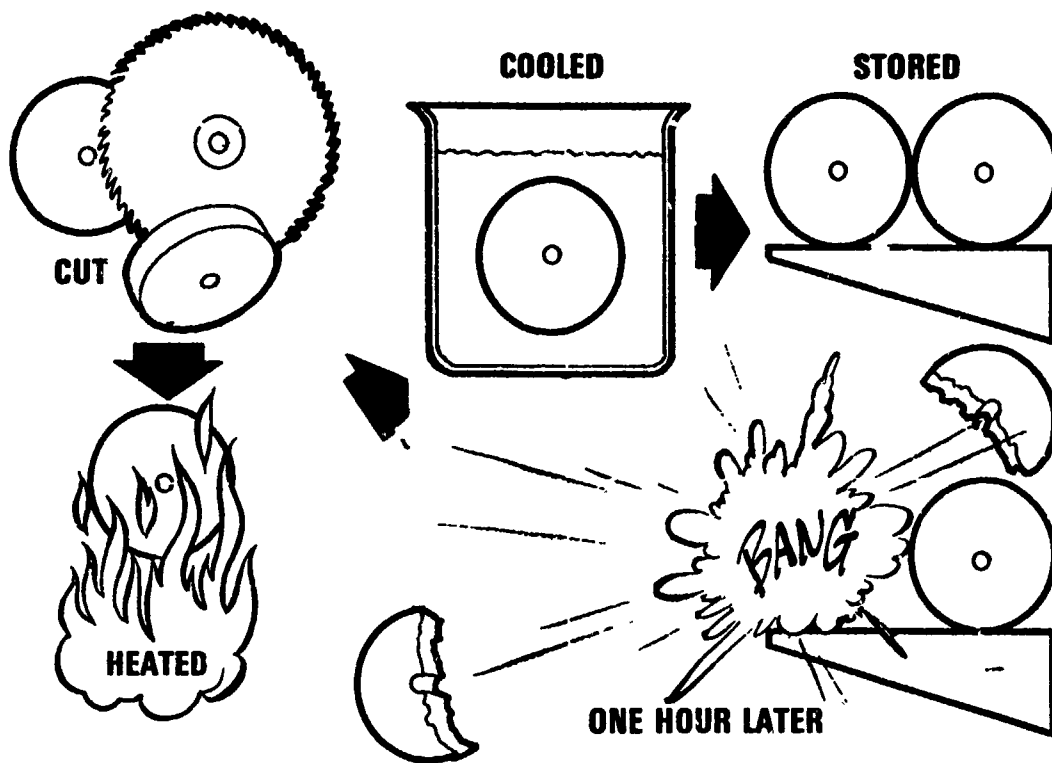


FIGURE 7. A MARTENSITIC PRINCE RUPERT'S DROP⁽¹⁹⁾



FIGURE 8. THE CINCINNATI FLUSH (1881)⁽²¹⁾

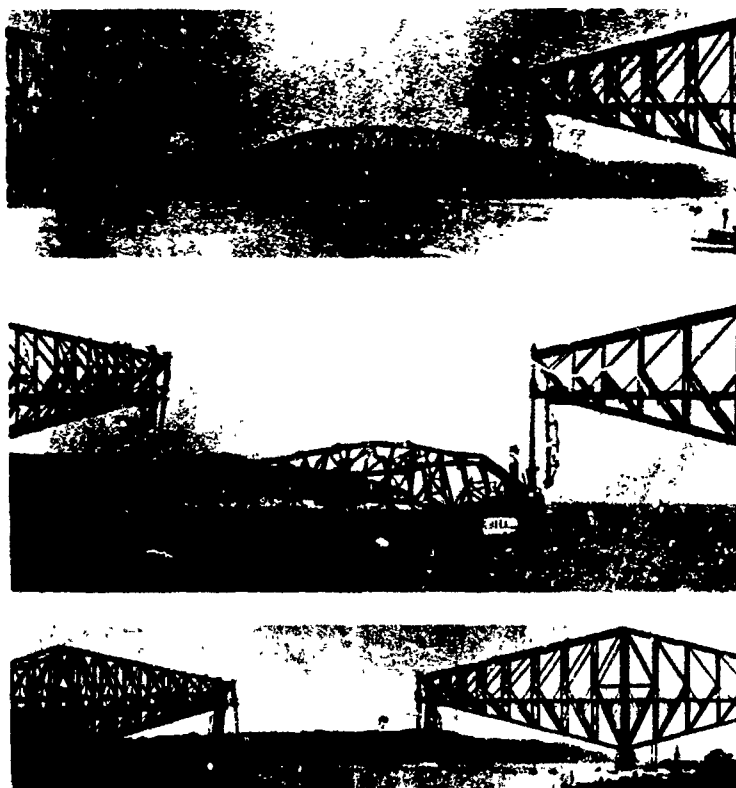


FIGURE 9. FAILURE OF THE QUEBEC BRIDGE⁽²³⁾

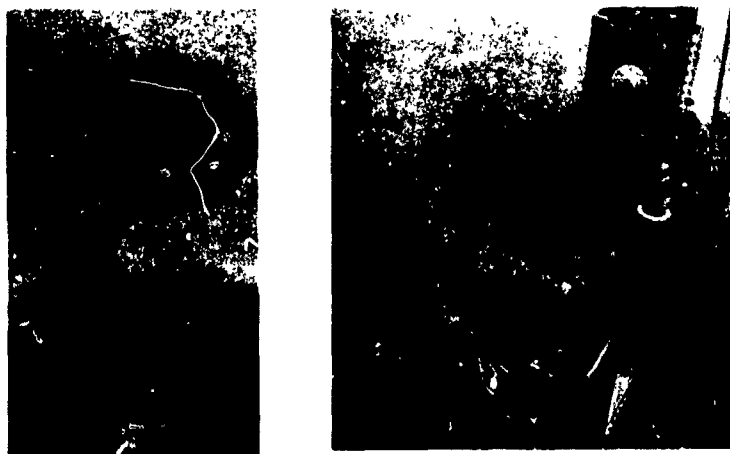


FIGURE 10. SUPPORT ROCKER FROM QUEBEC BRIDGE; BEFORE AND AFTER⁽²³⁾

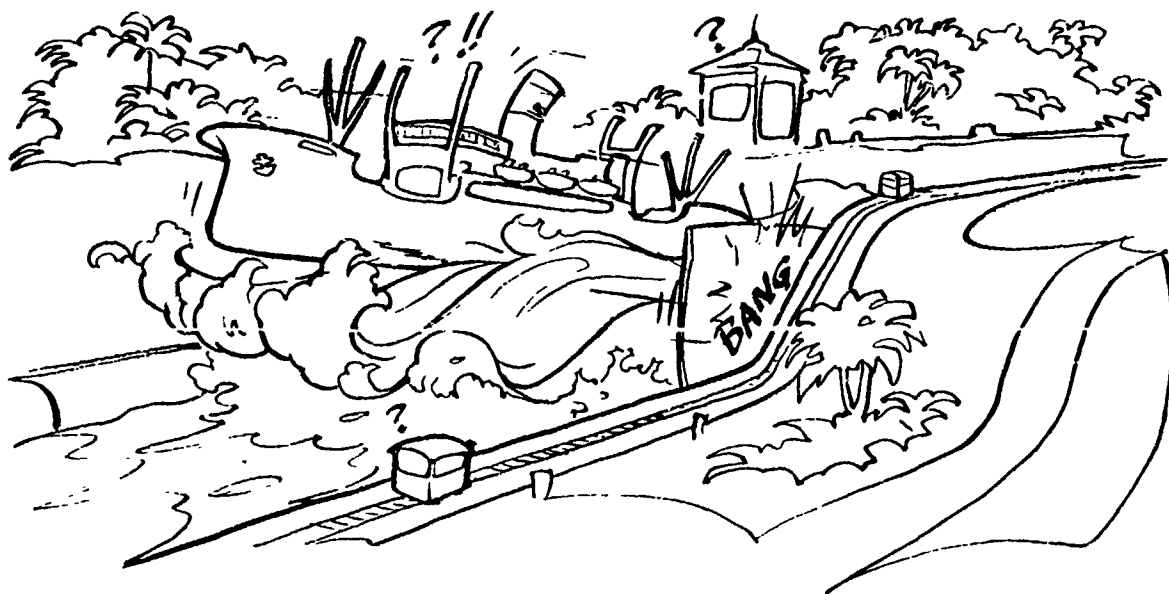


FIGURE 11. BRONZE COUNTERWEIGHT ASSEMBLY BOLT FAILURE, PANAMA⁽²⁴⁾



FIGURE 12. THE HELMET WAR (1920); VOLUTE CRACKING⁽²⁵⁾

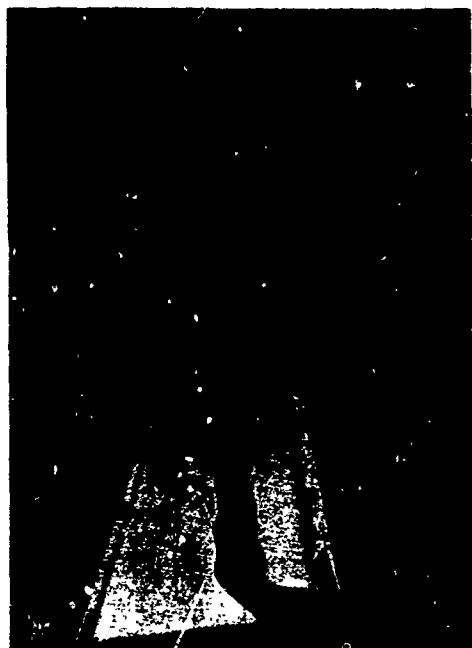


FIGURE 13. FAILURE OF A STEEL I-BEAM⁽²⁶⁾



FIGURE 14. FRETTING AT A BOLT HOLE (Ti ALLOY)⁽²⁸⁾



FIGURE 15. RECONSTRUCTION OF A FAILED Ti DISC⁽²⁸⁾

Reproduced from
best available copy.



FIGURE 16. SPIN-PIT FOLLOWING FAILURE Ti DISC⁽²⁸⁾

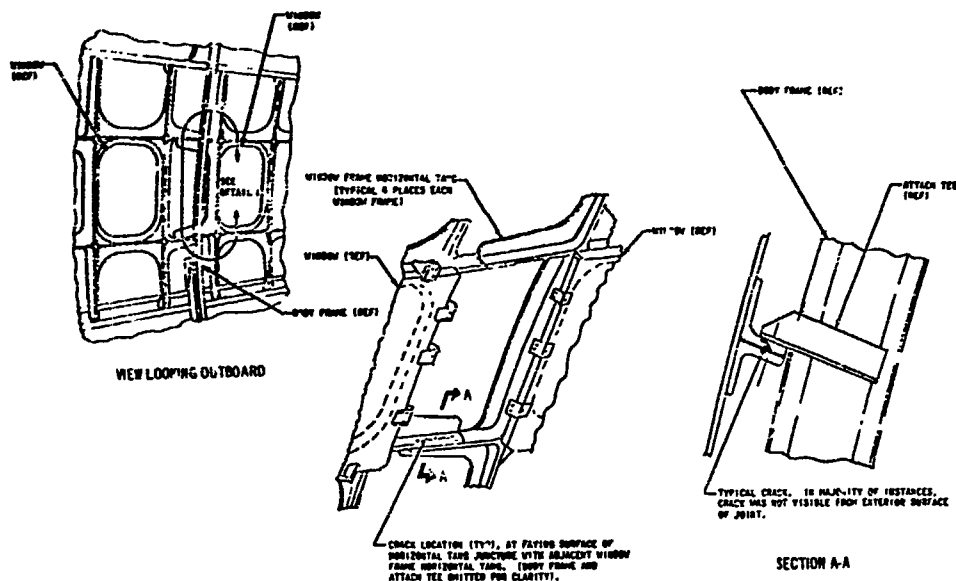


FIGURE 17. WINDOW FRAME FORGING FAYING SURFACE ADV #37
SERVICE HOURS: 22,000 TO 23,000⁽²⁹⁾

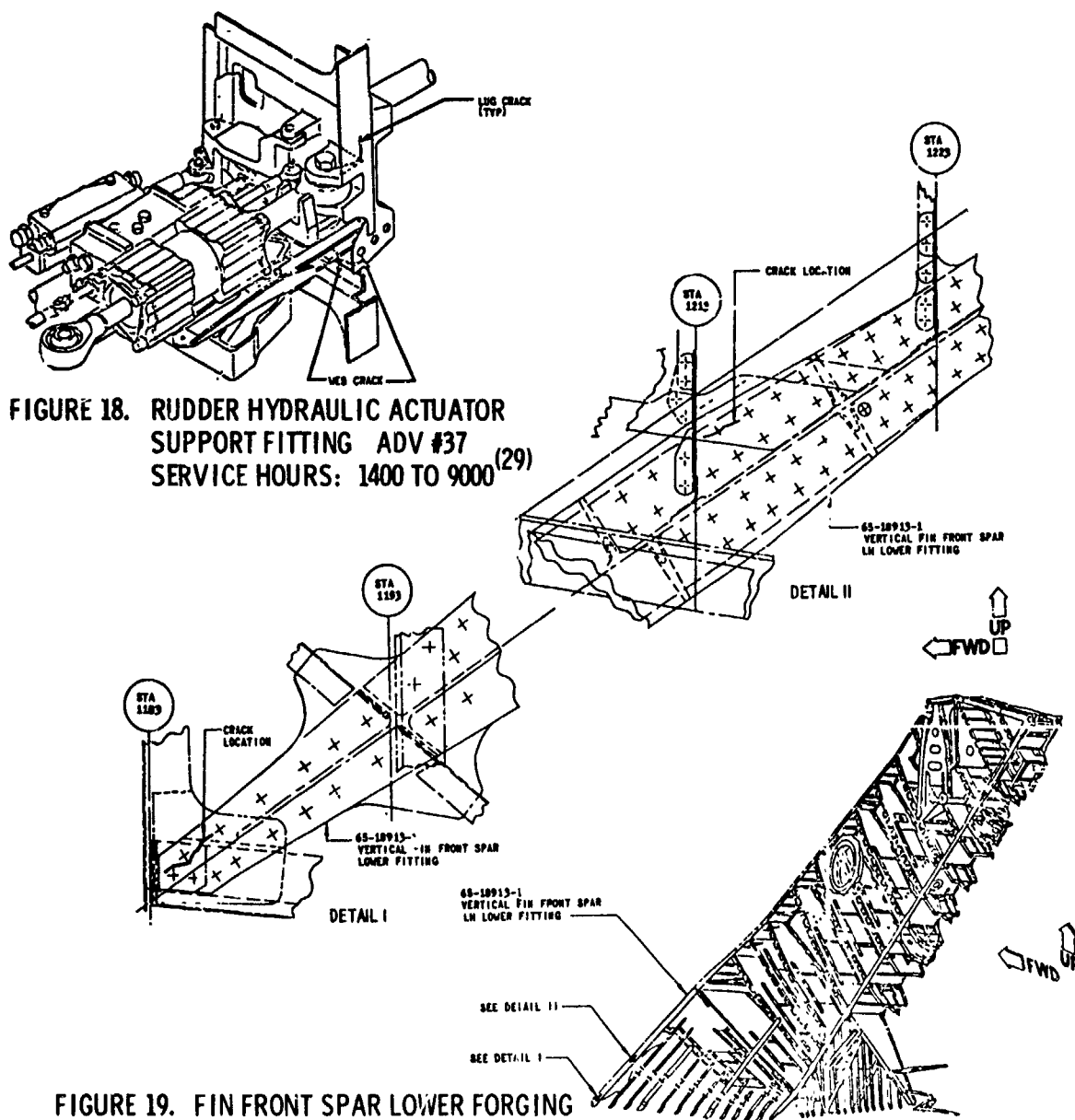


FIGURE 18. RUDDER HYDRAULIC ACTUATOR
SUPPORT FITTING ADV #37
SERVICE HOURS: 1400 TO 9000⁽²⁹⁾

FIGURE 19. FIN FRONT SPAR LOWER FORGING
ADV #18
SERVICE HOURS: 5600 TO 6800⁽²⁹⁾

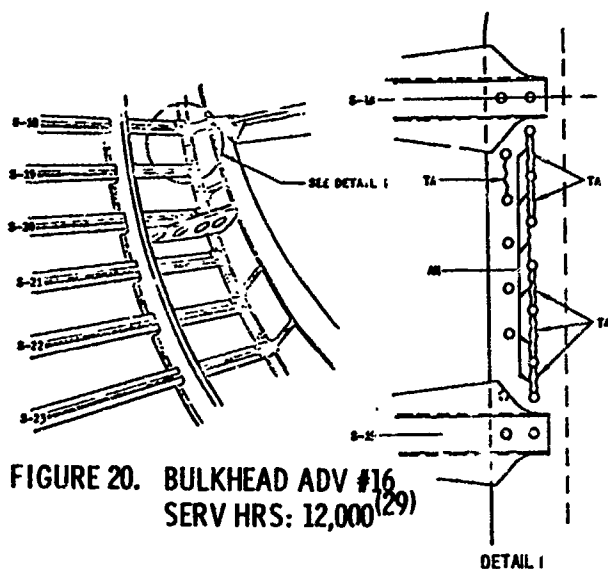


FIGURE 20. BULKHEAD ADV #16
SERV HRS: 12,000⁽²⁹⁾

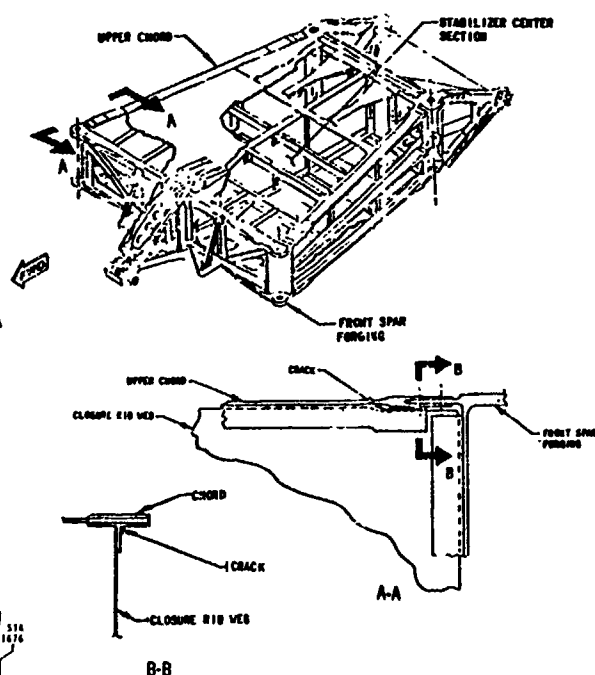


FIGURE 21. STABILIZER CENTER SECTION
ADV #46 SERV HRS: 11,000⁽²⁹⁾

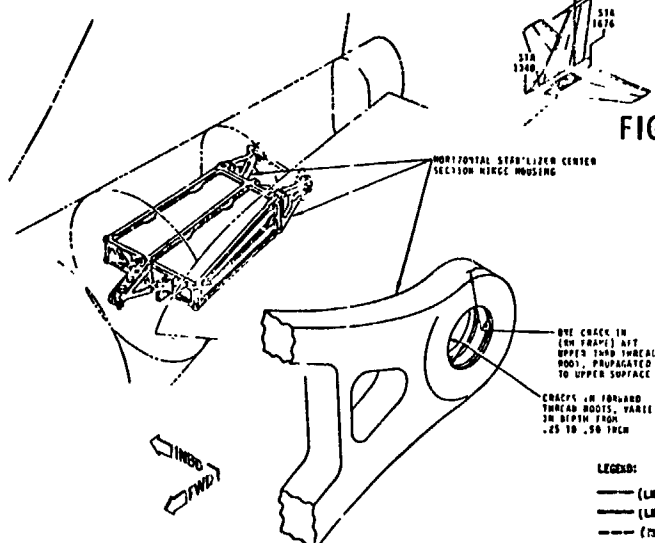


FIGURE 22. HORIZONTAL STABILIZER CENTER
SECTION HINGE HOUSING ADV #63
SERV HRS: 9500 TO 10,000⁽²⁹⁾

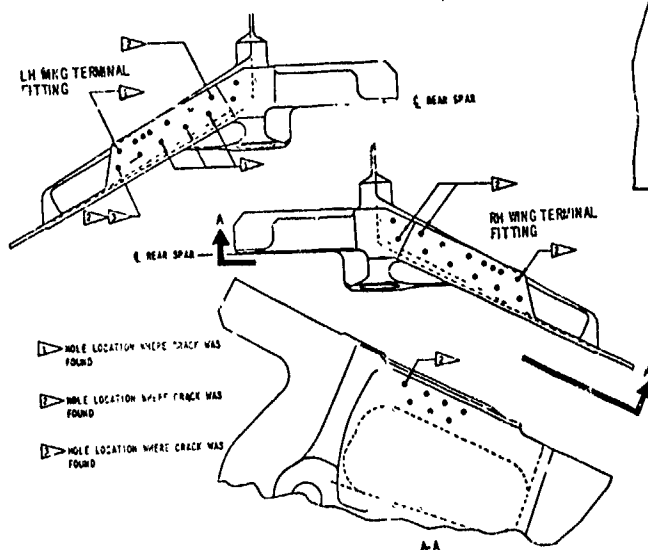


FIGURE 23. REAR SPAR TERMINAL FITTING ADV #43
SERVICE HOURS: 28,000 TO 36,000⁽²⁹⁾

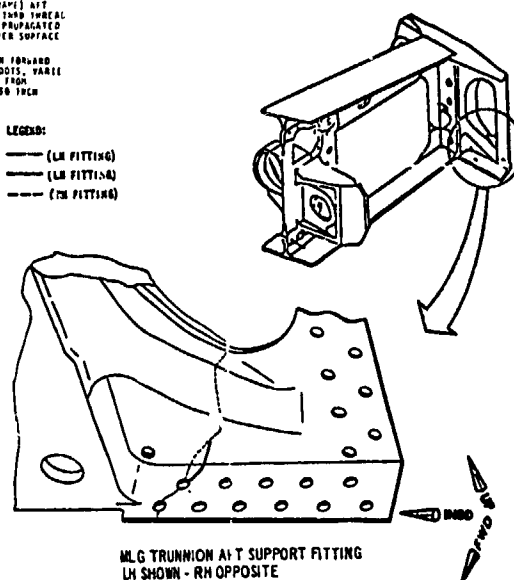


FIGURE 24. LANDING GEAR
SUPPORT STRUCTURE
ADV #42
SERVICE HOURS:
26,000 TO 32,000⁽²⁹⁾

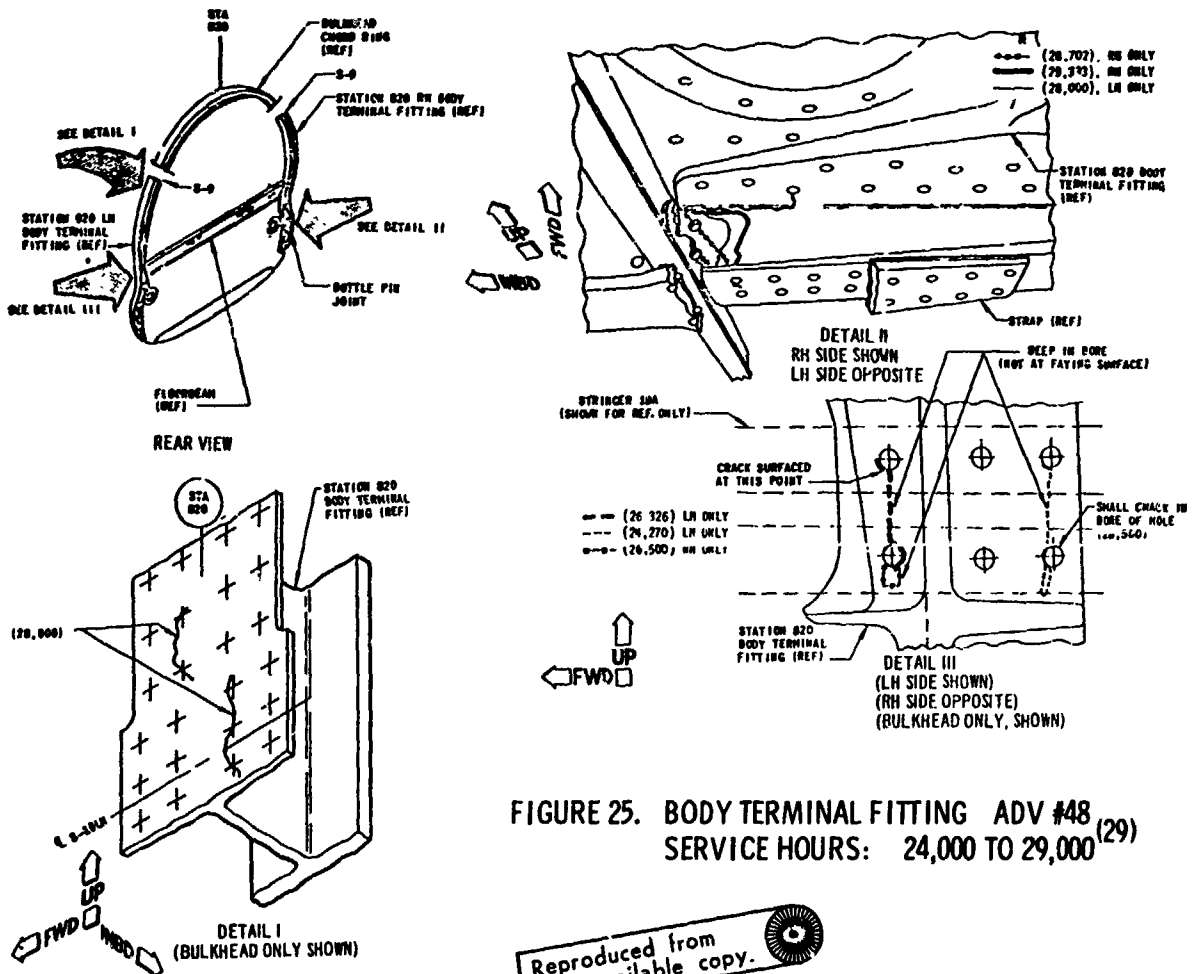


FIGURE 25. BODY TERMINAL FITTING ADV #48
SERVICE HOURS: 24,000 TO 29,000⁽²⁹⁾

Reproduced from
best available copy.

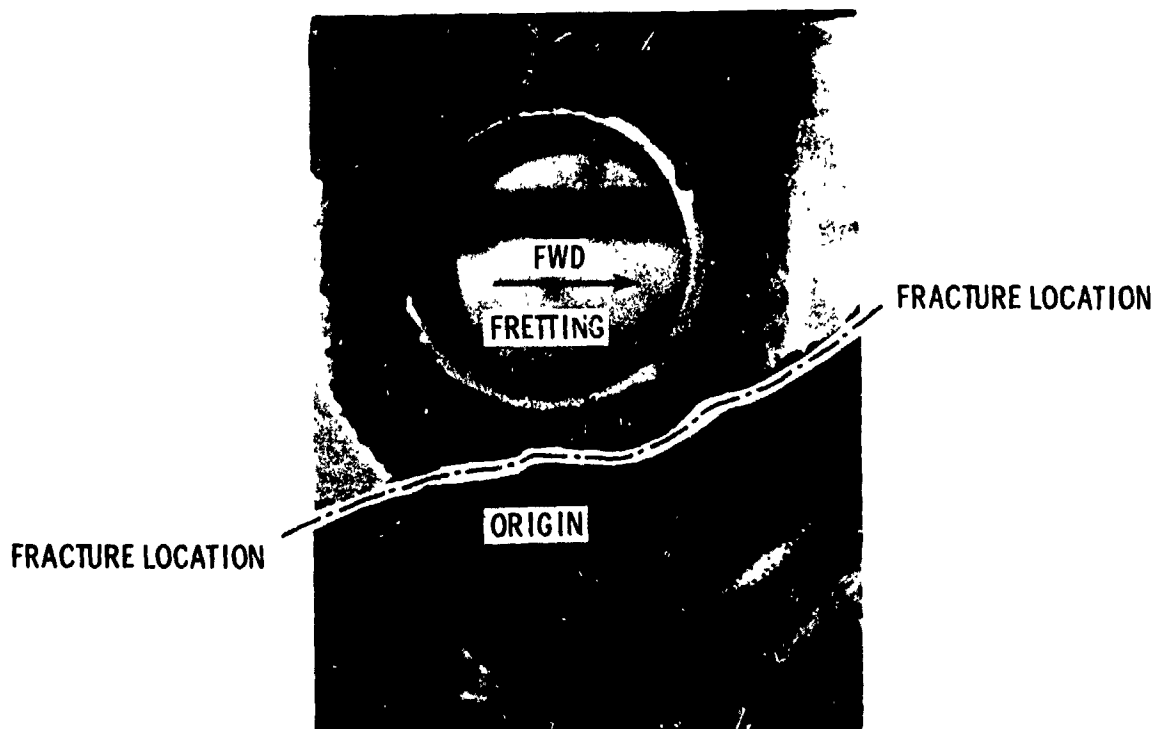
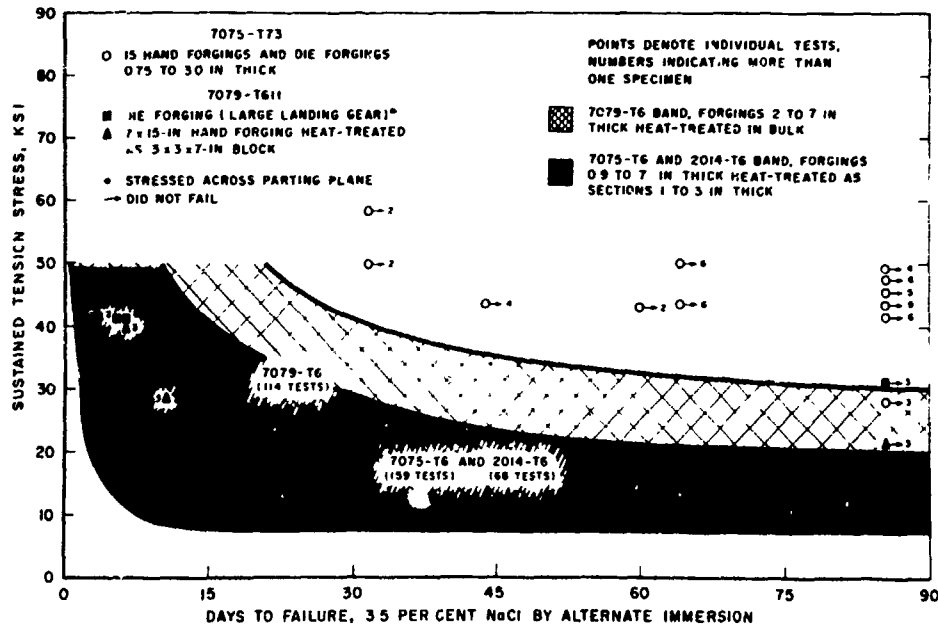


FIGURE 26. FAILURE OF STEEL TRUNNION FITTING⁽²⁹⁾



Tests taken in the short transverse direction compare the resistance to stress corrosion cracking of several high strength aluminum alloy forgings. The T73 Temper of 7075 alloy was developed specifically to provide high resistance to stress corrosion cracking.

FIGURE 30. SCC DATA FROM THE LITERATURE⁽³⁵⁾



FIGURE 31. CRACK TIP IN 2024-T35 ALUMINUM⁽³⁶⁾

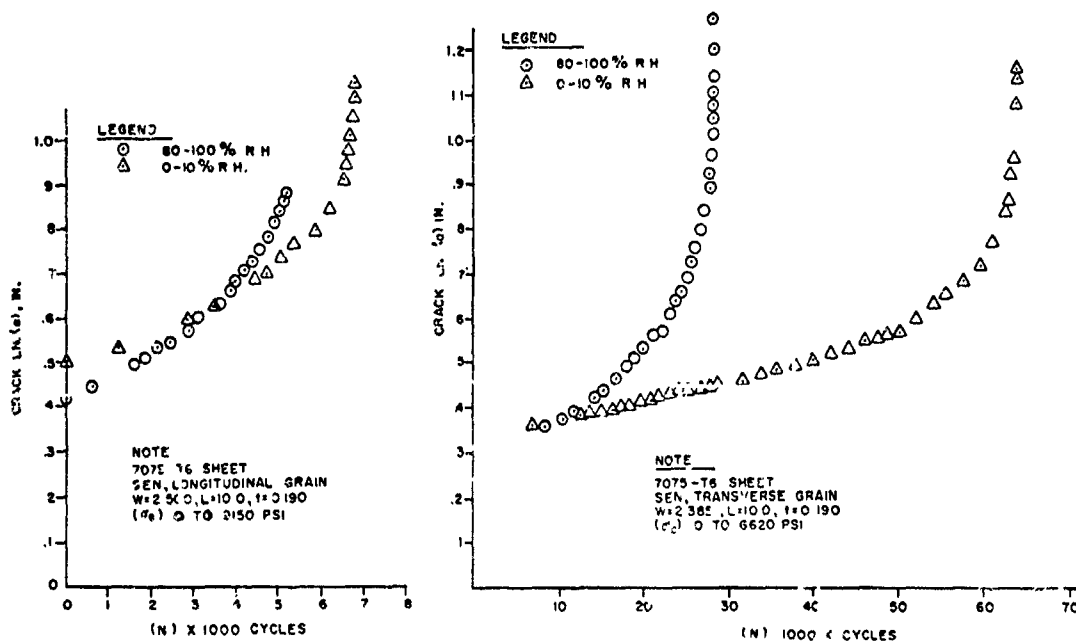


FIGURE 32 a. (a) Vs (N),
50 SEC HOLD⁽³⁷⁾

FIGURE 32 b. (a) Vs (N), 50 CPM⁽³⁷⁾

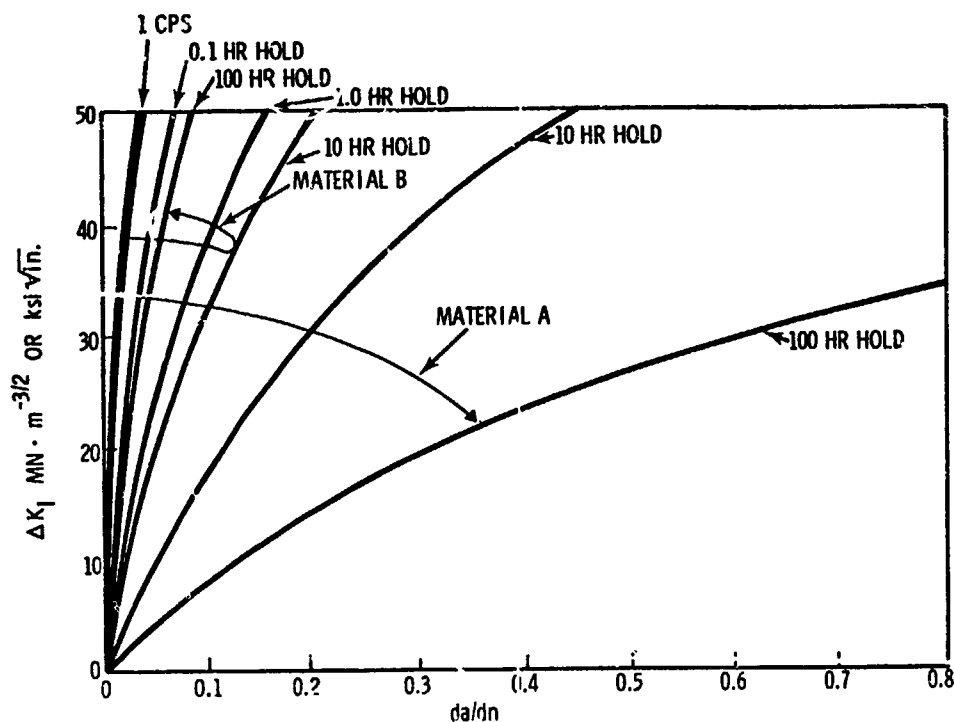


FIGURE 33. TWO APPARENTLY FUNDAMENTAL KINDS OF CRACKING BEHAVIOR

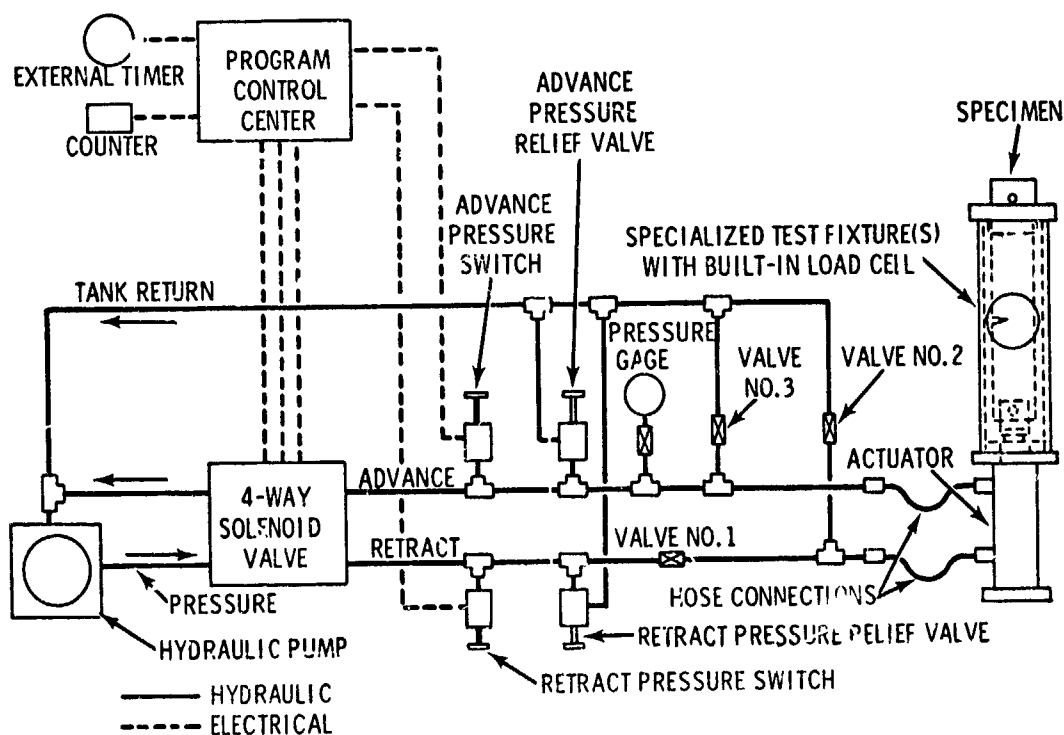


FIGURE 34. ELECTRO HYDRAULIC TEST SYSTEM⁽³⁸⁾

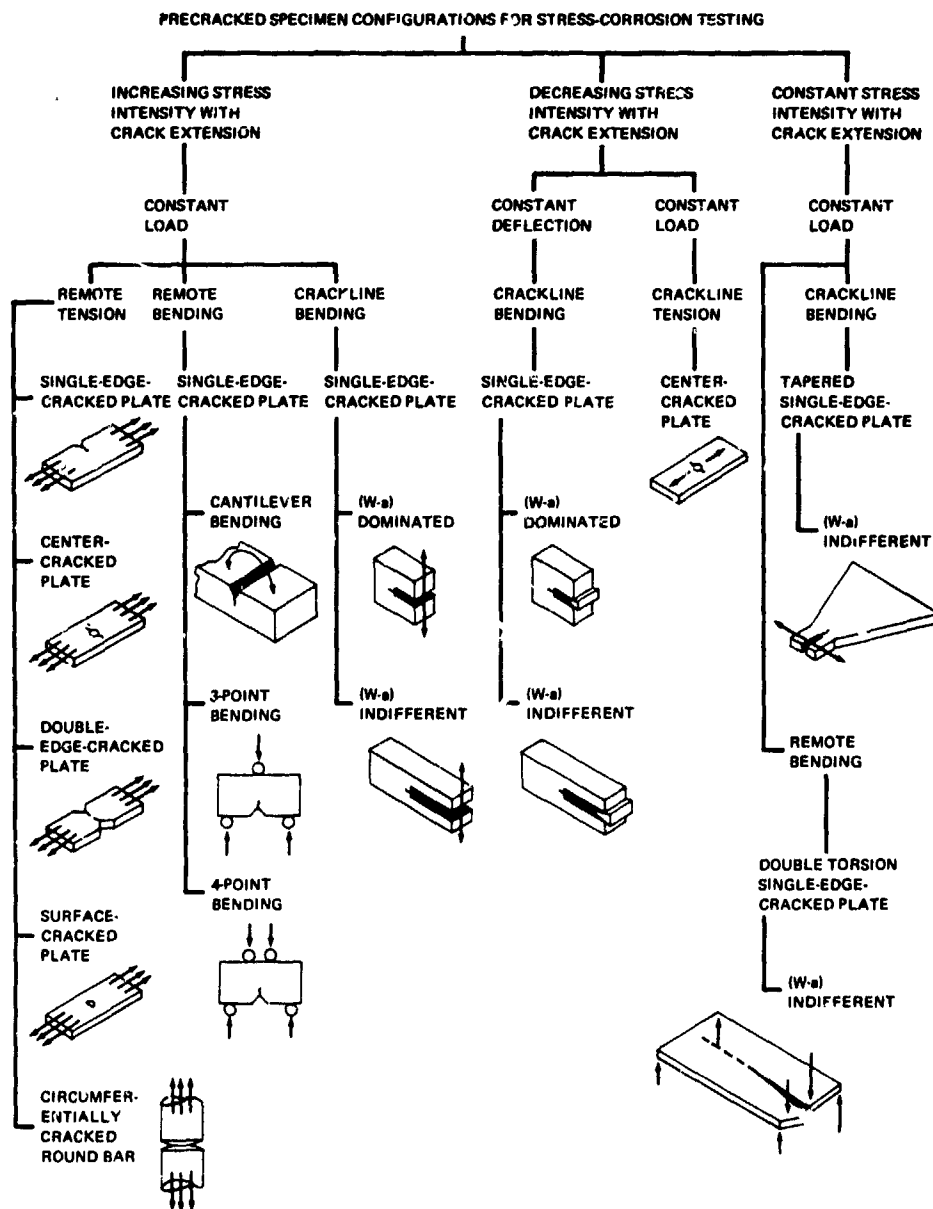


FIGURE 35. CLASSIFICATION OF PRE-CRACKED SPECIMENS FOR SCC TESTING

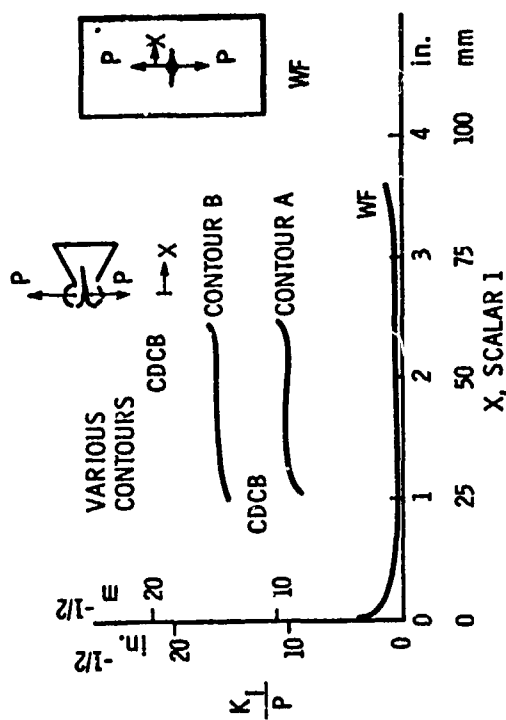


FIGURE 37. EXAMPLE SPECIMENS OF DECREASING⁽⁴¹⁾ AND OF NEARLY CONSTANT⁽⁴²⁾ STRESS FIELD PARAMETERS

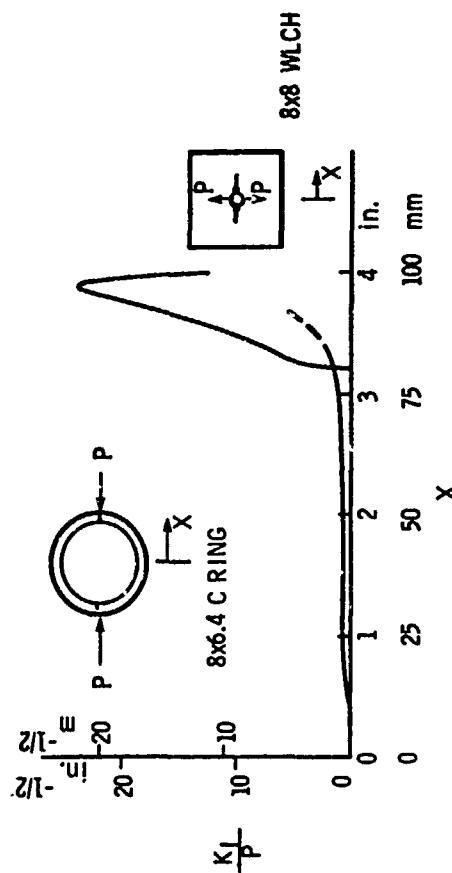


FIGURE 38. SUGGESTED ADDITIONAL SPECIMEN TYPES

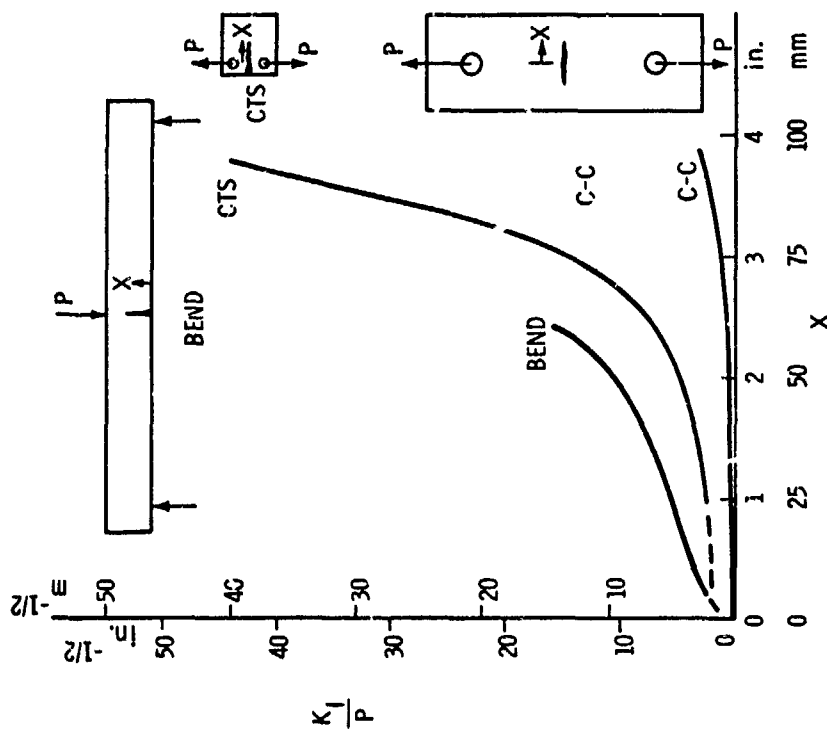


FIGURE 36. EXAMPLE SPECIMENS OF INCREASING STRESS FIELD PARAMETER⁽⁴⁰⁾

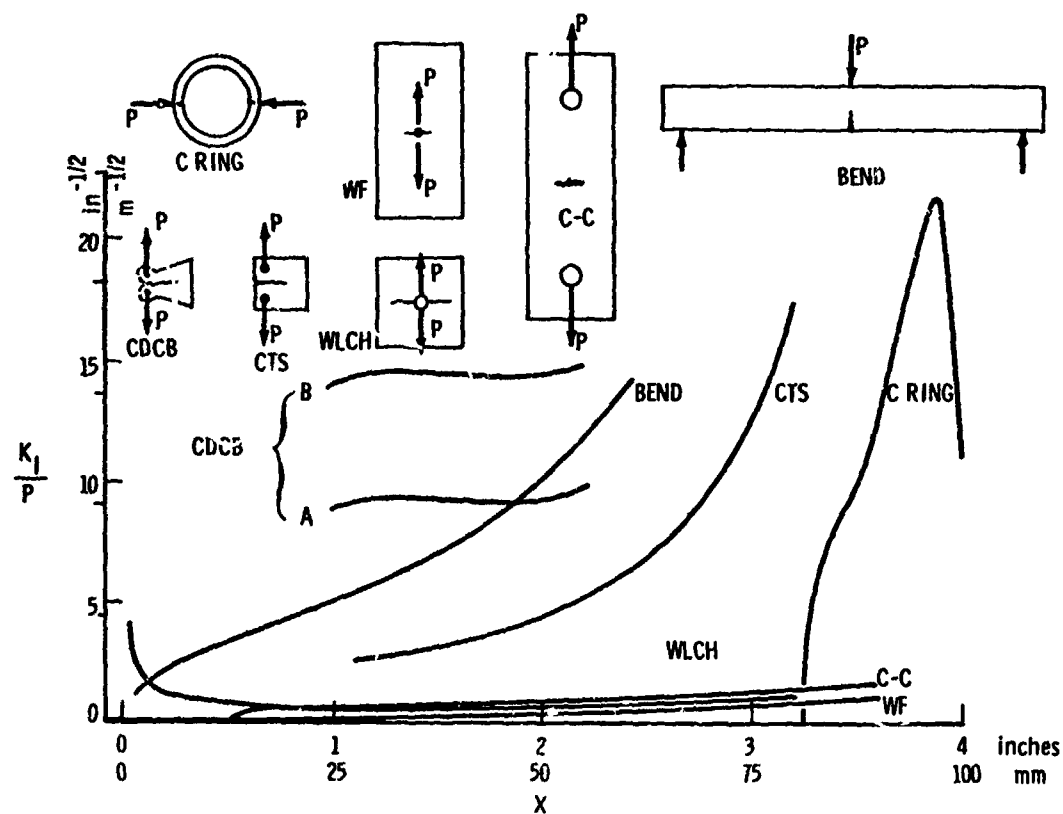


FIGURE 39. COMPARISON OF SELECTED EXAMPLE SPECIMENS

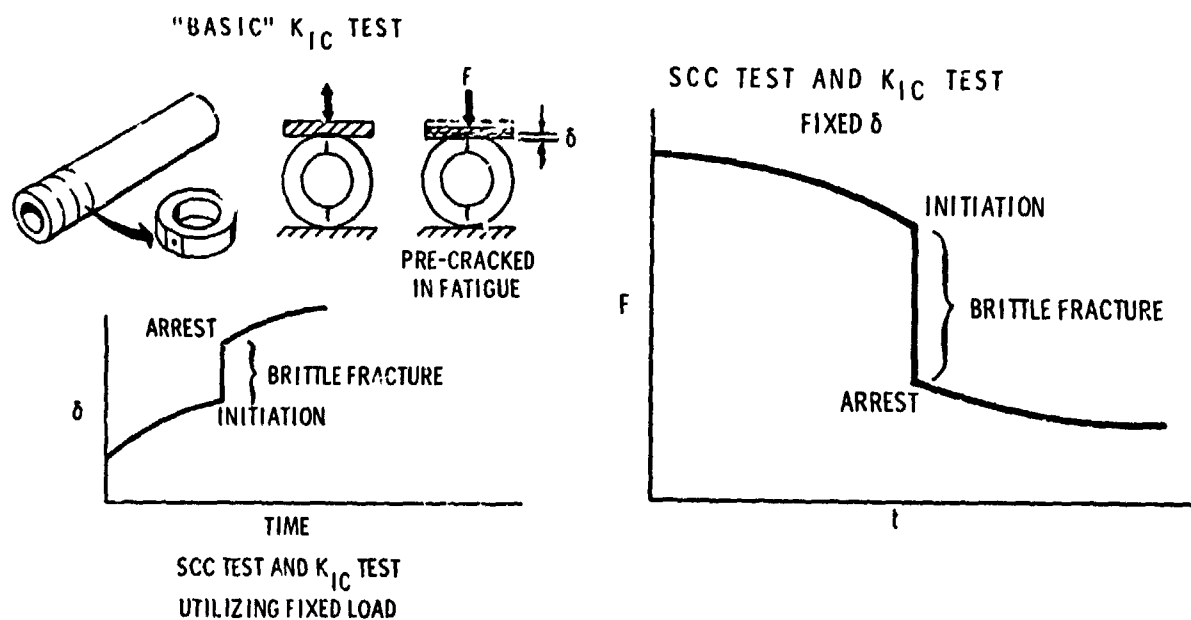


FIGURE 40. COMBINED FRACTURE ARREST AND SCC TESTS WITH THE RING SPECIMENS

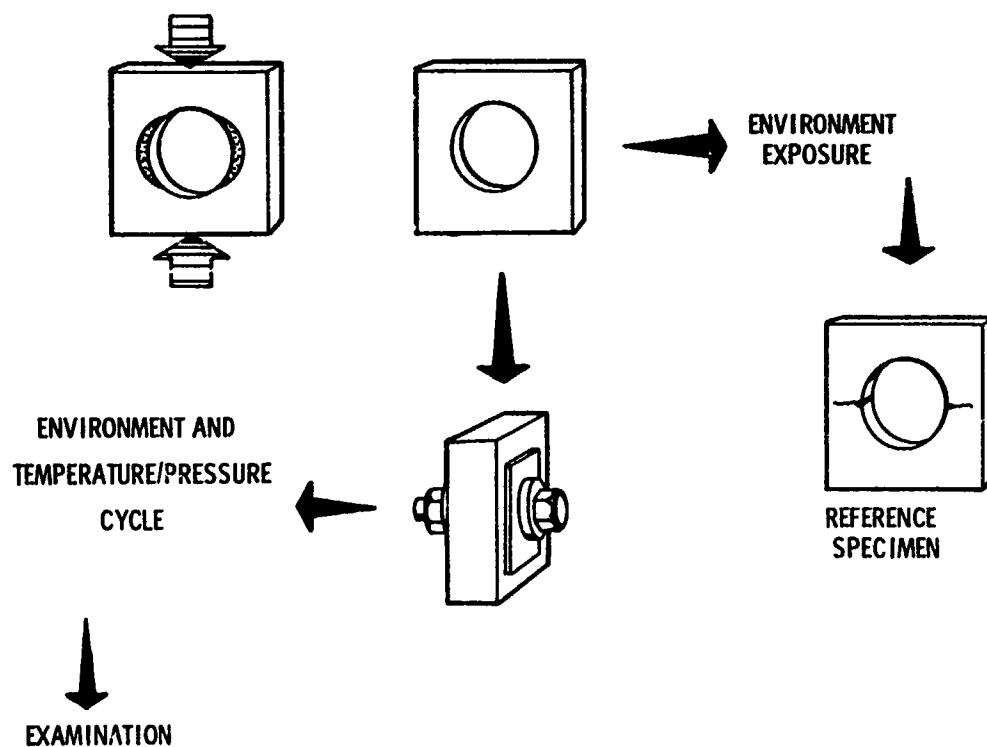


FIGURE 41. STRUCTURAL SIMULATION WITH SELF-STRESSED SCC SPECIMENS

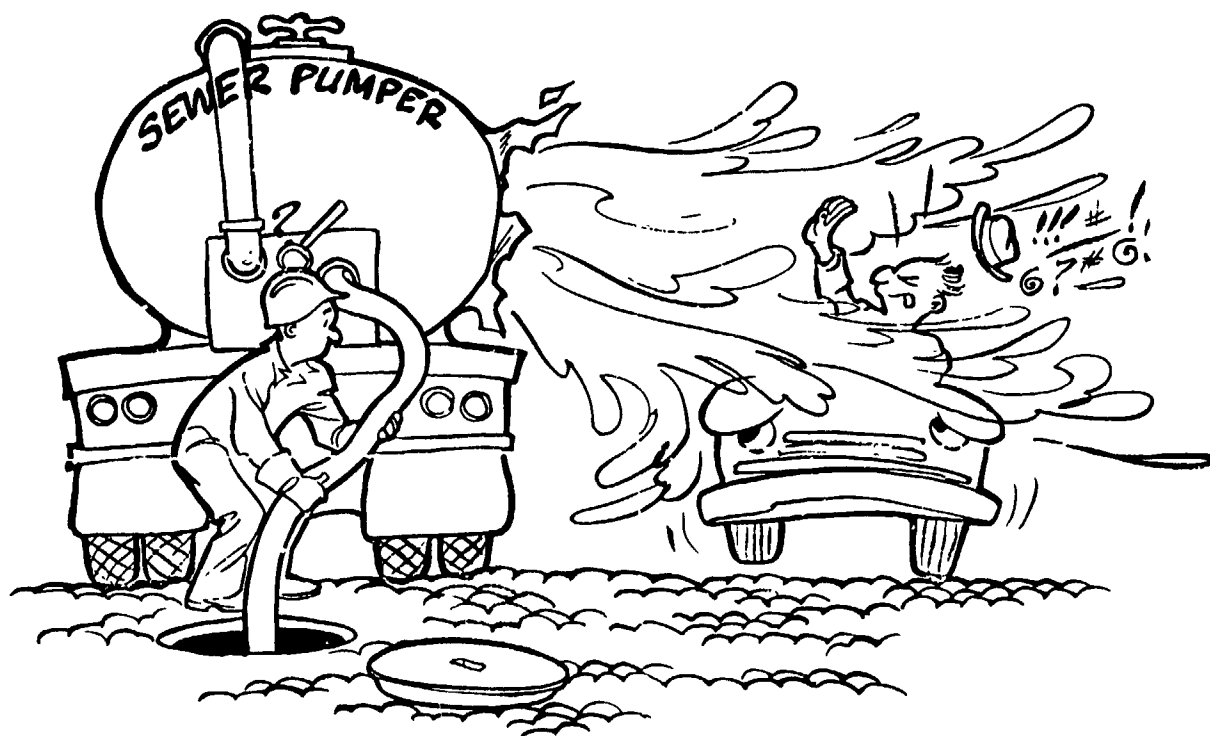


FIGURE 42. FLOYD REID'S LAMENT⁽⁴³⁾

PROGRESS TOWARD STANDARDIZATION OF
SCC TEST TECHNIQUES BY THE
AMERICAN SOCIETY FOR TESTING AND MATERIALS

By

H. Lee Craig, Jr.
Reynolds Metals Company
Metallurgical Research Division
Fourth and Canal Streets
Richmond, Virginia 23219
U.S.A.

SUMMARY

Subcommittee 6 of ASTM Committee G-1 on the Corrosion of Metals is responsible for developing standard test methods for stress corrosion testing. The ASTM is a voluntary, democratic organization of consumers, producers and persons with a general interest in test standardization. The Subcommittee is divided into four sections: 1) Smooth specimens and test jigs; 2) Test environments and specific material tests; 3) Corrosion fatigue; and, 4) Precracked specimens. Under the sections, task groups carry out the work of writing recommended practices and standard test methods. These are then voted upon at the Subcommittee, Committee and Society level. Some practices that are currently being balloted are: C-ring specimen, Bent beam specimen, U-bend specimen, direct tension specimen, boiling magnesium chloride test, polythionic acid test, and the 3.5% sodium chloride alternate immersion test. Among the precracked specimen types that are being developed are: the wedge opening load specimen, the double cantilever beam specimen, and the single cantilever beam specimen.

PROGRESS TOWARD STANDARDIZATION OF
SCC TEST TECHNIQUES BY THE
AMERICAN SOCIETY FOR TESTING AND MATERIALS

H. Lee Craig, Jr.

Stress corrosion is a plague of modern industrial society. It is a problem for the basic materials producer, the designer, the manufacturer, and eventually, the user who must maintain and service the complex structures that are aircraft, missiles, rockets in the latter half of the twentieth century. Even the scientist who studies the phenomenon is perennially confounded by the marriage of mechanics, electrochemistry and metallurgy that form the basis for understanding stress corrosion as a scientific discipline. No less troubled is the engineer who must deal with stress corrosion as one of the many facets which come with modern, high strength materials. When the standard engineering answer is, "Test it", the problem then becomes one of "which test" and "what do these results mean".

This, then is the conundrum that the Subcommittee G.01.06 has set out to solve within the framework of the voluntary, cooperative group of industrial, government and academic interests known as the American Society for Testing and Materials. In a world marketplace where there exists side by side all shades of economic systems, in addressing this group, I feel it is necessary to stress the two adjectives I have used above: voluntary and cooperative. The ASTM is not associated with the United States government, other than having received a charter from its Congress. Neither is it a professional organization, dedicated to the advancement of some engineering branch. Rather, it is a body of persons representing various groups of our industrial society who have voluntarily come together to use the methods of science and engineering to achieve a common goal. When there exists a community of interests on a given subject, a Committee is formed to concern itself with that subject. Experts and others with a strong interest in the subject are invited to join, and make up the membership of the Committee. It is then that the cooperation among these persons provides the activity which ultimately results in published Standards, Symposia, Data and other salable items from which the Society derives its income, in part, to support the cadre of headquarters personnel.

When the ASTM publishes a Standard, it is strictly a voluntary compliance that is sought. Because of the rigor and thoroughness with which these Standards are compiled, they are seldom questioned and have been accepted in courts of law as representing the last word, similar to the expert testimony of professional men such as doctors and engineers. ASTM standards may be incorporated into government specifications or those used by industry as a basis for purchase agreements.

In this paper I plan to give the background of the formation of our Subcommittee, some of its accomplishments and the way these were brought about, and some of the problems we plan to face in the near future. I will also discuss our relations with other societies, both on the national and international level.

Subcommittee G.01.06 was formed when the parent Committee G-1 was established in 1964. Prior to that time, corrosion problems were handled within the different materials committees, such as A-1, A-5 and A-10 on ferrous metals or B-1 on corrosion of non-ferrous metals. The shifting of all corrosion activities into a single committee recognized the value of having all experts in the field of corrosion coming together at one time to discuss their mutual problems. This Committee is one of the largest within ASTM, having over 300 members, with an active program of symposia, special technical publications, meetings and the promulgation of standards. The various subcommittees deal with the types of corrosion commonly met, such as atmospheric, marine, soil, the phenomena, for example, stress corrosion or galvanic corrosion, or means of studying corrosion, including laboratory tests, electrochemical methods or in plant tests. The present organization of the committee is shown in Figure 1.

Subcommittee 6 has over 100 members. Such a large number made it desirable to divide the effort into more narrow areas of interest. Therefore, four sections were formed: Section 1, Smooth specimens and test jigs; Section 2, Test environments and specific material tests; Section 3, Corrosion fatigue; and Section 4, Precracked specimens. This arrangement provides the permanent framework by which the committee functions. On the other hand, the working of the committee is carried on by Task Groups. A task group is established to solve a single problem or investigate a single point, as opposed to a Section and Subcommittee, which has an area of interest. Consequently, when the work of a task group is completed, it is discharged. The Section, Subcommittee, and Committee continue to function as long as they hold meetings and conduct such business

as they find appropriate. Normally, as talk groups are discharged, new ones are formed, with ever changing membership, depending on the nature of the problem to be handled. Thus the work of the Subcommittee continues. When a Standard is adopted by the Society, the Committee that sponsored it remains responsible for it, and must review each Standard at least once every five years.

The adoption of a Standard follows the structure described above, but in inverse order. Problems are brought to the attention of the Subcommittee or Section. The members vote to establish a task group. This task group meets and redefines the problem, and starts a program which will lead to a solution. The program, in its fullest extent, may involve a literature survey, holding a symposium, circulating a questionnaire, discussion of these results, selection of one or more promising methods of test. Drafts are prepared and circulated to task group members and others invited to comment because of their special knowledge. Usually, drafts undergo several revisions. Sometimes alternative methods are found. Then, round robin tests are performed to determine the relative merit of each procedure. Finally, a proposed standard method is drawn up. This is submitted for balloting by the entire subcommittee. In order to become official, a standard must receive the approval of at least 90% of those voting affirmatively or negatively. A ballot may be returned, marked, "Not Voting". This is an important point, for in order for a vote to count, at least 60% of the ballots must be returned. Negative ballots must be accompanied by a statement giving reasons for this action. These objections are reviewed by the Subcommittee, and evidence that each negative has been carefully considered and the objections met must be presented to the main Committee in the report of the balloting. The standard is then balloted by the entire Committee following the same rules as above. Thereafter, the standard is forwarded for approval by the Society, either by an affirmative vote of two-thirds of the members voting at the Annual Meeting, or by the return of at least 25 letter ballots with a 90% affirmative vote.

I have been asked to explain the reasons behind the way we have approached the subject of stress corrosion test standardization. As was mentioned above, G-1 was formed largely from Committee B-3. That committee had a subcommittee, number ten, devoted to stress corrosion. Fred Reinhart was its first chairman, and I became its second chairman when Fred resigned. It seemed logical to us to first divide the subcommittee into three task groups, with the objective of determining the state-of-the-art of each subject area. From these state-of-the-art reports would come information as to whether standards or recommended practices could be written from knowledge in hand, or perhaps, some further cooperative research needed to be done.

These task groups were as follows:

- | | |
|---|------------------------------|
| TG 1 - Stress Corrosion Testing Methods | - S. J. Ketcham,
Chairman |
| TG 2 - Stress Corrosion Environments and
Test Durations | - H. B. Romans,
Chairman |
| TG 3 - Evaluating and Reporting Stress
Corrosion Results | - D. O. Sprowls,
Chairman |

At this time, the nonferrous industry supplied many of the officers and chairman, simply because B-3 was a nonferrous metals committee. When the change was made to a G classification committee, we added an excellent and dedicated group of specialists from the ferrous industry, many of whom occupy positions of leadership at the present time.

Two important Task Groups were soon added, one on Nomenclature and the other, as sponsor for a Symposium on Stress Corrosion Testing. One of the most important functions of ASTM is to publish lists of definitions in the technical fields it covers. Our Nomenclature Task Group, under the splendid leadership of Floyd Brown, wrestled for many sessions with the concepts and assumptions that go into defining the phenomenon of stress corrosion, hydrogen embrittlement and many other basic terms. These were forwarded to the Subcommittee on Nomenclature, which has the responsibility for gaining Society approval for the definitions of terms commonly or uniquely used in corrosion. Presently, there is no Nomenclature task group with Sub 6, but rather, any task group working in a problem area and needing a definition, must develop one and submit it to Sub 2 and G-1 for approval.

Another ASTM function is to hold Symposia on topics of current interest, bringing together all those in the Society who have contributions to make and inviting persons outside the Society to present their work. In the mid Sixties, stress corrosion was being actively researched by many groups. Thus a task group to sponsor a symposium was established, and at the June 1966 annual meeting, a two-day, (four session) symposium was

held, with thirty papers, plus a working session during the subcommittee meeting at which three papers were presented which were received too late for inclusion in the formal symposium. The ASTM then published the book, Special Technical Publication 425, Stress Corrosion Testing, with most of the papers from the symposium. Included in this volume were reports of the first three task groups, listed above. With the publication of these reports, the task groups were discharged. This represented not the end of the work, but merely the beginning, for the task groups were each charged with determining the state-of-the-art in their subject and recommending appropriate action for our Subcommittee to take. The large number of test specimens found in the literature, their lack of standardization, the many test environments used by different laboratories, and the several methods of test reporting led to the conclusion that a very large task lay in front of us, indeed, to bring any semblance of standardization to this subject.

At this point it was decided to establish sections within the subcommittee. They were:

- Section 1 - Test Specimens and Loading Equipment
D. O. Sprowls, Chairman
- Section 2 - Test Environments
D. S. Neill, Chairman
- Section 3 - Corrosion Fatigue
No Chairman at Present
- Section 4 - Precracked Test Specimens
D. E. Piper, Chairman

Sections 1 and 2 were the natural extensions of the original two task groups. Section 1 is limited to what are termed "Smooth" specimens, as opposed to the precracked variety which were introduced in the mid-sixties for stress corrosion testing. Thus Section 4 was established to promulgate recommended practices for making and using the precracked specimens. The parent committee assigned us the area of corrosion fatigue, but to date, very little interest in this subject has been found among our members.

Section 1 has had the following task groups:

- Task Group 3 - C-Rings - D. O. Sprowls, Chairman
- Task Group 4 - U-Bends - M. Henthorne, Chairman
- Task Group 5 - Bent Beams - A. W. Loginow, Chairman
- Task Group 6 - Tensile Specimens - E. G. Haney, Chairman
- Task Group - Weldments

Each of these groups has decided that it would be impractical to specify a single configuration, size or material for each class of specimen, so they have written, "Recommended Practices". The difference between a Recommended Practice and a Standard in this instance is that some choice is left to the user in the selection of values for parameters such as thickness, length, or diameter. However, guidelines are set down where it is felt appropriate, for ratios of gauge to length, for instance.

As an example of the ASTM method at work, let us look at the steps which formed the basis for the C-Ring Recommended Practice. Task Group 1 prepared a state-of-the-art report on test specimens. Using the combined knowledge of the task group members, plus literature searching, a report was assembled which listed the following specimen types which appeared to be in use in more than one laboratory. (The "more-than-one-laboratory" criterion is often a convenient way to begin to eliminate many methods when looking for a standard test procedure. This automatically provides you with several persons who qualify by reason of familiarity as experts on a given method or specimen, in this case.)

- Bent Beam Specimen (Constant Deflection)
- Tension Specimens (Constant Deflection or Constant Load)
- C-Ring Specimen (including tuning fork specimen)
- Sheet-Type Preform Specimen
- Welded Beam Assemblies
- Interference Ring Specimen
- Tubing Specimen
- U-Bend Specimen

At the same time, a task group was being formed to study aluminum alloy 7039. This task group selected the C-Ring specimen as the most desirable one to test thick armor plate in the short transverse direction. There were five laboratories actively engaged in using large quantities of C-Rings for quality control testing of armor plate production.

As a result of these circumstances, Section 1 found that the largest body of active interest available dealt with C-Rings, and therefore established Task Group 3. (The numbers 1 and 2 were not used to avoid confusion with the original still active Subcommittee task groups as their reports had not yet been published, and they were not yet discharged).

The chairman wrote a draft of a recommended practice for making and using C-Ring specimens. This was based on earlier documents that had been circulated among the five laboratories using C-Rings which participated in a round robin test of 7039 alloy. This draft was circulated to the task group members and to other persons who were considered to have an interest in this type of specimen.

A deadline was set for the receipt of written comments, and after these had been received the chairman rewrote his first draft, making a second draft which incorporated the comments of the task group members. The time interval usually encompassed one or more meetings of the ASTM, which holds an annual meeting and a committee week, six months later. At these times the task group members meet face to face and discuss the written drafts at length, deciding if there is need for any experimental work to solve points at issue which are not agreed upon by the group. For instance, in the C-ring method it is left to the user to decide the surface preparation appropriate to his material, so no attempt is made to be specific in this area. On the other hand, the ratio of wall thickness to diameter of the ring is specified, within limits, since this parameter has an effect on the precision of the stress determination, for all materials.

The user is referred to other ASTM recommended practices for corrosive environments, such as the 3 1/2% sodium chloride solution-alternate immersion method. In this manner, the user can select any one of a number of ASTM specimen methods. Usually choosing one which is most appropriate to his material and form (sheet, plate, tubing and so on) and combine it with one of the ASTM environment methods, that suits his needs, (For instance, the boiling 42% magnesium chloride solution used with stainless steels).

When the task group is satisfied with a draft of the document, it is agreed to submit it to the Section for a vote. If the Section approves the work, then the document is reported to the Subcommittee as being ready for letter ballot. The Subcommittee then mails out a copy of the document to each member with a ballot. In order for a vote to be validated, 60% of the ballots mailed must be returned, marked either affirmative, negative, or not voting. As stated above, at least 90% of the total affirmative and negative votes must be affirmative to proceed.

If this be the case, as it was in the instance of the C-ring method, then the task group chairman proceeds to resolve the negative votes. Many times the points raised are changes accepted by the task group, as they had overlooked some facet which all concerned recognized to be valid. Occasionally, an objection may be raised which a majority of the task group feels is not sustained. In this case, a formal vote is taken and recorded. The person who voted negatively is informed of the action. When the results of the vote are presented back to the Subcommittee, all negatives are reported and the way that they were resolved is given in enough detail so that the Subcommittee can decide for itself if the vote to override an objection was valid or not.

This was the case in the C-ring voting, so the Subcommittee voted to forward the method to the entire G-1 committee for ballot. The above procedure is repeated once again, with the larger group. The C-ring method is currently at this stage today. Assuming no valid objections will be received, the Committee will forward the document for approval by the entire Society. Once this approval is obtained, the recommended practice will be published in the Book of Standards. It will remain active unless action is taken against it. Every five years the Subcommittee will be asked to ballot the desirability of continuing the method. In this way, methods which fall into disuse are removed from the Book of Standards, when they no longer meet with the approval of the Subcommittee which promulgated them.

As I mentioned earlier, this particular practice was believed to be so well established by usage among the several laboratories whose representatives comprised the task group, that no round robin or other laboratory testing stage was needed. If the publication of the method as a standard promotes wider use of the C-ring, then, users may come up with alterations or improvements. These can be incorporated into the document with the periodic revisions noted above.

To complete my report on the status of Section 1, the U-bend method is also being balloted by G-1. The bent-beam method was slightly delayed by one member of the Subcommittee, who shall remain anonymous, who thought he spotted a mathematical error in the derivation of the bent beam formula used to calculate the stress. He voted negatively, pointing out this error to the task group chairman. It took a heated exchange of letters and resort to an expert stress analyst to convince our subcommittee member that it was his math that was in error, and not that of the method. I mention this, really, to pay tribute to those members who do take the time to study carefully and derive for themselves the formulas and other details that go into making up a complex procedure such as this. Their fortitude in voting negatively should also not be overlooked, since it takes courage to put forward your own convictions. However, the procedures of the ASTM are designed so that each person's valid objections are heeded. This contributes immeasurably to the rigor of the final published document.

A comparison of the original Task Group 1 document which used three paragraphs and a brief procedure for calculating the stress level in a C-ring with the recommended practice for making and using C-rings will demonstrate the increase in thought and detail that has been put into the latter, thereby greatly increasing its usefulness, particularly to the novice.

Except for the U-bends, bent beams and tensile test specimens, there had not been any interest among Subcommittee members in writing recommended practices for other specimen types. For example, the tuning fork specimen, a favorite of many laboratories, has often been brought up, but without any members found willing to undertake the effort needed to write a document. Part of the reason for this, I am sure, is the recent upsurge of interest in precracked specimens, which has occupied the attention of those who might otherwise be actively developing tuning forks and other smooth specimens.

At our recent meeting, however, a new member came forward to express an interest in specimens for weldments. This was another area which had been discussed by older members through the years, but without much action. Now, I use this as an example of how a new problem gets introduced and handled in the framework of an established subcommittee. Presently, this member is drafting a recommended practice that will be circulated to the task group and other persons interested in the subject.

Section 2 similarly grew out of task group 2 on test environments and test duration. It has converted into a section whose area of interest deals with specific materials and environments used to test these materials. Stress corrosion is a problem shared by all materials, but each family seems to have as its nemesis, one or more specific corrodents, as ammonia compounds in the case of copper base alloys. These corrodents are generally widely distributed throughout our natural and man-made environments, so no real effort can be made to control the problem from this standpoint. However, when testing a given material for susceptibility to stress corrosion, it has been a common and useful practice to limit the test environment to some formulation that includes the specific corrodent for the material of interest. With this assumption underlying its work, Section 2 has had the following task groups:

- Task Group 7 - Hot salt test for titanium alloys
W. B. Lisagor, Chairman
- Task Group 8 - Stress Corrosion test for 7039 alloy
T. J. Summerson, Chairman
- Task Group 9 - Boiling magnesium chloride test
D. S. Neill, Chairman
- Task Group 10 - Polythionic acid test
D. S. Neill, Chairman
- Task Group 11 - Intergranular and exfoliation corrosion of aluminum alloys
S. J. Ketcham, Chairman
- Task Group 12 - 3 1/2% Sodium chloride-alternate immersion test
D. O. Sprowls, Chairman
- Task Group 13 - Stress corrosion test for magnesium base alloys
A. Gallaccio, Chairman
- Task Group 14 - Stress corrosion test for copper base alloys
R. Popplewell, Chairman
- Task Group 15 - Stress corrosion test in organic media
E. G. Haney, Chairman
- Task Group 16 - Stress corrosion tests in atmospheric environments
No Chairman

**Task Group 1 - Stress corrosion test of insulating materials used
with stainless steels
D. S. Neill, Chairman**

Each task group has had its own special history which has influenced the position in which we find them today. Task group 13 was discharged upon receipt of a report which included a literature survey of the field, and a conclusion that there was insufficient interest among members to prepare a recommended practice for the stress corrosion testing of magnesium based alloys.

Task Groups 9 and 10 have recommended practices currently being balloted by G-1. In the boiling magnesium chloride test, a major contribution was made by a non-member, I. B. Casale, through the efforts of M. A. Streicher a G-1 member who was not originally a member of the subcommittee. Dr. Streicher became a member and contributed greatly to this document. It is appropriate to mention at this time that the originator of this particular test, M. A. Scheil, was a member of Committee G-1 and also has participated in the committee. The other task groups are at various stages of voting on drafts within the task group, or, in some cases, preparing first drafts. Task Group 11 was formed within Subcommittee 6 because many of its members were active in this subcommittee, and the problems were felt to be somewhat related. However, this task group was later transferred to the jurisdiction of Subcommittee 5, on laboratory tests, and is nearing completion of its work.

Section 4, on precracked specimens started to write methods for specific materials, high strength steels, titanium alloys and high strength aluminum alloys. This effort did not reach fruition. A reorganization was made and now, this section will follow Section 1's modus operandi, and write a recommended practice for each of several particular types of specimens:

Task Group 1 - Wedge Opening Load Specimen
S. R. Novak, Chairman

Task Group 2 - Double Cantilever Beam
D. E. Piper, Chairman

Task Group 3 - Single Cantilever Beam
B. F. Brown, Chairman

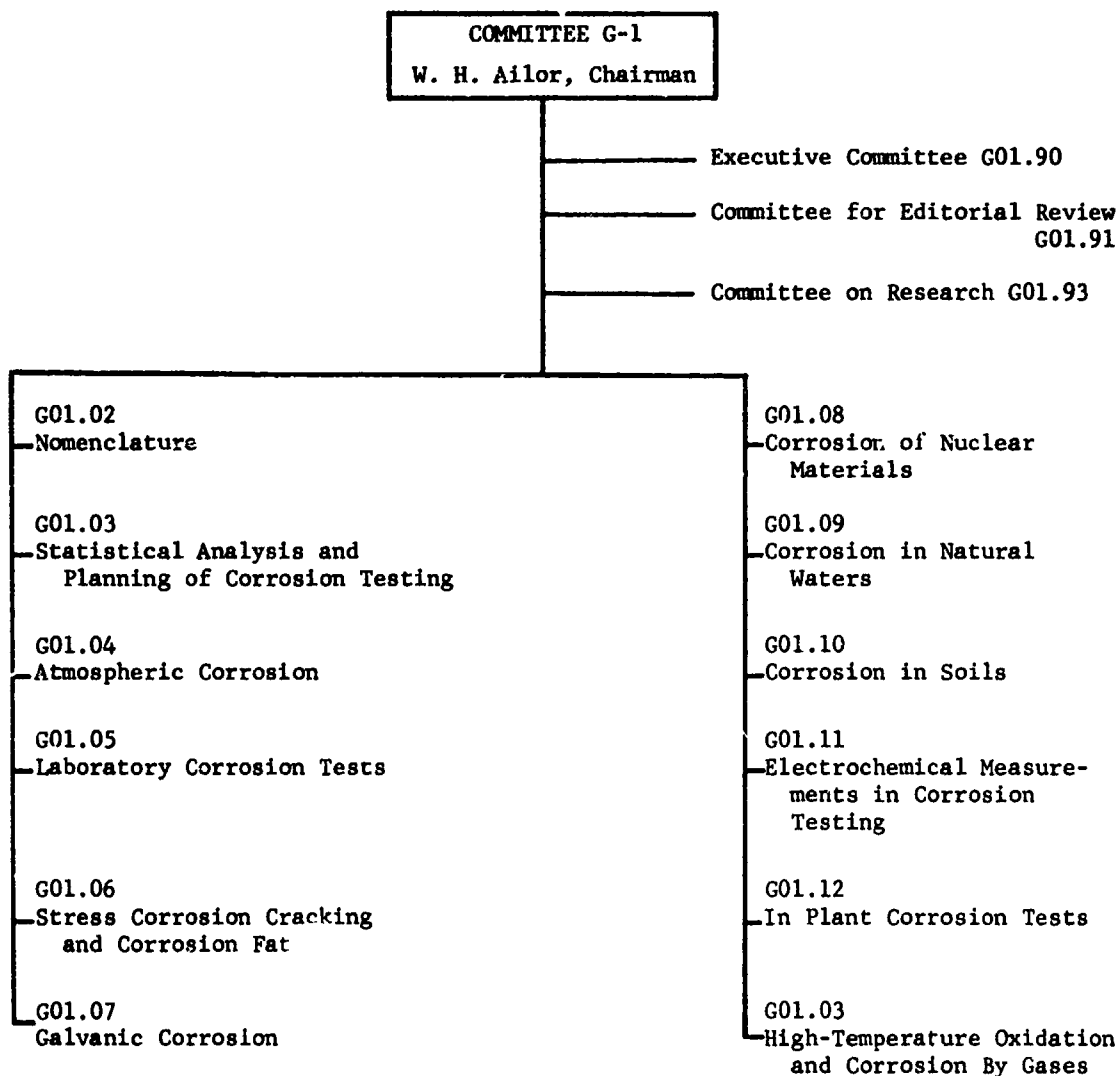
The most significant part of this effort is the cooperation being afforded to G-1 by Committee E-24. This committee is involved in the area of fracture mechanics, a branch of mechanical testing. One of their subcommittees, number 4, has the more narrow interest of environmentally controlled sub-critical crack growth. This is, of course, stress corrosion, viewed from the more narrow discipline of mechanics, which generally neglects the effects of environment - but then - who can do this today? This subcommittee established a task group, at first assigned the task of reviewing the draft for a recommended practice being written by Section 4, and now, to cooperate fully in the work of this Section.

It is contemplated that three methods will be proposed and that a round robin test of two or more of them will be carried out. These methods are currently being drafted by task group chairmen.

In addition to the work of the task groups and sections, the Subcommittee carries on several other functions. One of these has been mentioned, that of sponsoring a symposium, from which grew much of the work of the task groups and a volume of papers which serve as a permanent record of the state-of-the-art in stress corrosion testing as of 1966. Since then, the Subcommittee has co-sponsored or otherwise participated in several symposia and other meetings. One of the latest efforts was to contribute a chapter on Stress Corrosion Testing to the Handbook on Corrosion Testing being edited by W. H. Ailor. This will be published under the sponsorship of the Electrochemical Society as one of a series of volumes to replace H. H. Uhlig's classic but long out of date Corrosion Handbook.

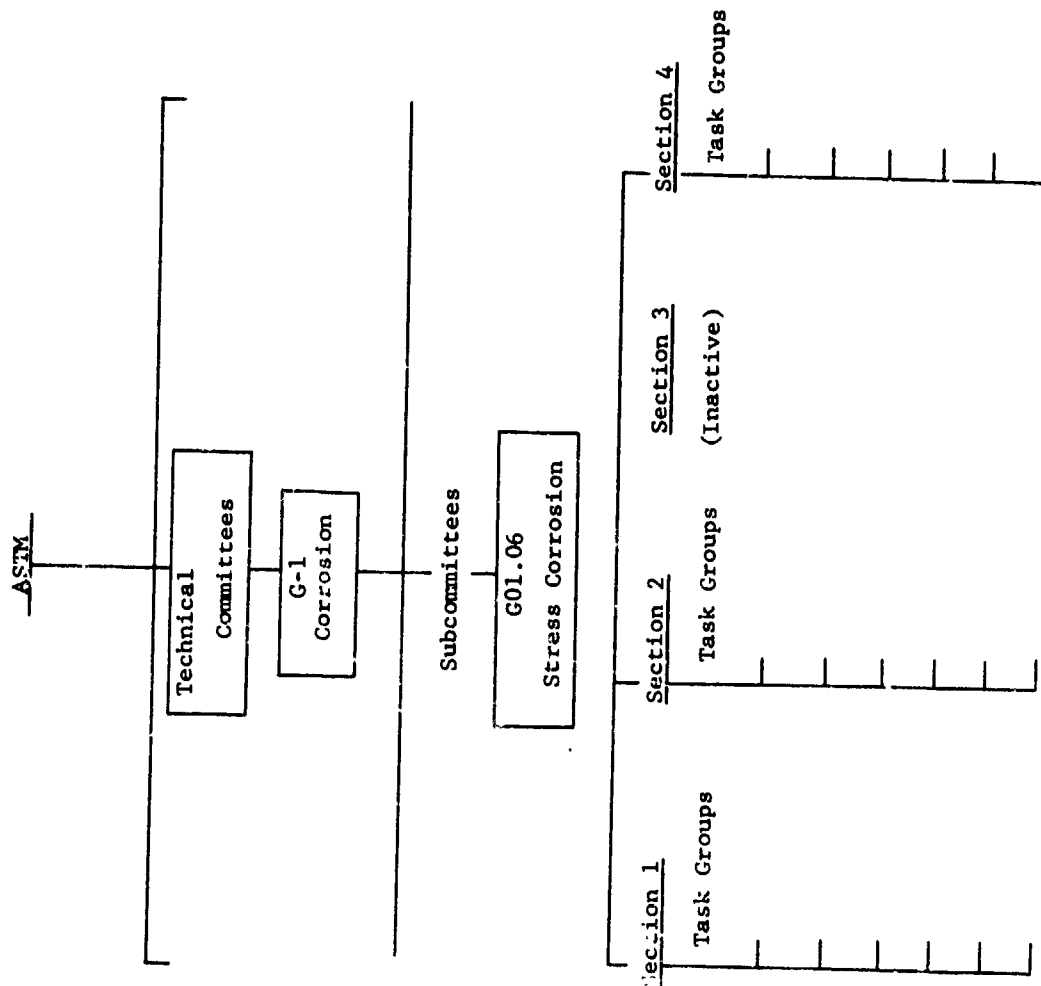
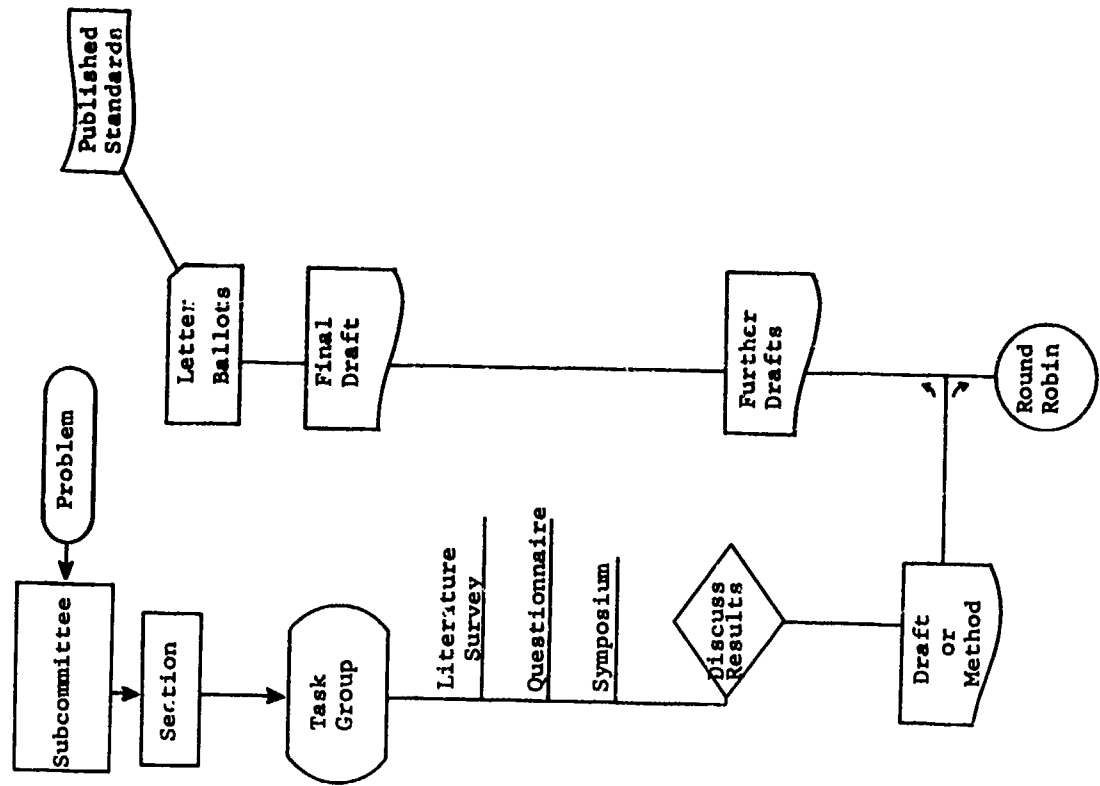
I would like to close my remarks by stressing the philosophy whereby we have guided this committee. The hallmark of our efforts has been "to provide a forum where those interested in stress corrosion could exchange views and cooperate in mutual endeavors to advance the art and knowledge of stress corrosion testing." We have not tried to be exclusive in this work, but rather have actively pursued liaison with other ASTM committees and other national organizations, such as the National Association of Corrosion Engineers, the Metals Property Council, the American Society for Metals, the Aluminum Association, the Welding Council, and other groups.

There have been some overtures for cooperation on the international level. ASTM held its first meeting outside the United States in Toronto, Canada just a little over a year ago, in June, 1970. John Stanners, of the British Iron and Steel Research Association met with us, and told us of the program of round robin testing being carried on in his country with precracked specimens. We have had correspondence with Redvers Parkins, of the European Federation of Corrosion. Now, I expect this meeting to accelerate the exchange of ideas and methods that we use, looking forward to an eventual cooperation under the aegis of the International Standards Organization. The ASTM is entering the seventies with a new, expansionary program to meet the demands of our truly modern, completely worldwide industrial society. I fully expect this meeting to be but the first of many with the objective of promoting the standardization of stress corrosion tests on a worldwide basis.



GRAPH 1

ORGANIZATION OF ASTM COMMITTEE G-1



PROGRESS TOWARD STANDARDIZATION OF SCC TEST TECHNIQUES
BY THE NATIONAL ASSOCIATION OF CORROSION ENGINEERS
AND THE ALUMINUM ASSOCIATION

Donald O. Sprowls
Section Head
Chemical Metallurgy Division
Alcoa Research Laboratories
P.O. Box 2970
Pittsburgh, Pennsylvania 15230

SUMMARY

There is just one NACE Standard for stress corrosion test techniques: it is entitled, "Evaluation of Metals for Resistance to Sulfide Stress Cracking at Ambient Temperatures". This document is in process and it is expected that it will be given final approval and issued in 1972.

The Aluminum Association is sponsoring jointly with the ASTM a task group for the stress corrosion testing of 7XXX series high strength aluminum alloys. Members of the task group include five producers of aluminum alloys, five U. S. Government agencies and one aircraft manufacturer. An inter-laboratory test program is in progress on three tempers of 7075 alloy for the purposes of: (1) comparing three types of smooth test specimens, (2) ascertaining the uniformity of test results that can be expected with a closely controlled procedure for the 3.5% NaCl alternate immersion test (Federal Method 823), (3) evaluating other corrodents that do not cause severe pitting of these alloys, and (4) relating the SCC performance in these laboratory tests with that in outdoor atmospheres.

PROGRESS TOWARD STANDARDIZATION OF SCC TEST TECHNIQUES
BY THE NATIONAL ASSOCIATION OF CORROSION ENGINEERS
AND THE ALUMINUM ASSOCIATION

Donald O. Sprowls

PART I - NATIONAL ASSOCIATION OF CORROSION ENGINEERS

The National Association of Corrosion Engineers is a technical society composed of approximately 7000 members who are interested in the various aspects of corrosion prevention and control. The Association was founded in 1943 and has grown from its initial beginnings with the pipeline industry to a membership that encompasses all aspects of industry. Its membership is not restricted to the United States but includes several hundreds of members from Canada, Japan, Mexico, and the European countries.

TECHNICAL COMMITTEES function as the technology arm of NACE. Meetings of these committees serve as forums for discussion of specific corrosion problems. From these discussions, informational reports and NACE Standards are evolved. All Standards issued by the Association are written, reviewed, and approved by procedures set forth in the "NACE Standards Manual", to be described in a later paragraph.

The following is a list of the Technical Group Committees organized under the general Technical Practices Committee as shown in Figure 1.

- T-1 Corrosion Control in Petroleum Production
- T-3 General Corrosion
- T-5 Corrosion Problems in the Process Industries
- T-6 Protective Coatings and Linings
- T-7 Corrosion by Waters
- T-8 Refining Industry Corrosion
- T-9 Corrosion of Military Equipment
- T-10 Underground Corrosion Control

Each Technical Group Committee consists of several Unit Committees, and these in turn are generally organized into Task Groups with specific assignments. For example, one of the Unit Committees of Committee T-1 is "Metallurgy of Oil Field Equipment", and this Unit Committee has several Task Groups, one of which (T-1F-9) is devoted to testing techniques for sulfide corrosion cracking. This Task Group has the assignment to prepare a standard for evaluating materials for sour crude service.

The NACE Standards Manual provides a guide which must be followed for the development and preparation of new or revised standards. An NACE standard shall be initiated by a Technical Unit Committee with at least ten members. The interests of the individual members shall be recorded under the categories of "Consumer", "Producer", and "General Interest". Every effort will be made to have equal representation between the "Consumer" and the "Producer", but in no event will the membership consist of less than 51% in the "Consumer" plus "General Interest" categories. The proposed standard is drafted by the appointed Task Group which may use the services of uniquely qualified persons external to NACE as "Advisors". A flow diagram showing the procedure for review and approval of a proposed standard is shown in Figure 2. The Central Office of NACE shall submit a standard to the originating Unit Committee after the first two (2) years for reapproval, change, or recommendation that the standard be submitted to the American National Standards Institute for Adoption by that body.

The proposed NACE Standard (Test Method) entitled "Evaluation of Metals for Resistance to Sulfide Stress Cracking at Ambient Temperatures" is currently out for letter ballot of Group Committee T-1. This document probably will be completed and given final approval early in 1972. It would be premature to distribute copies of the draft at this time, but a copy of another NACE Standard is appended to illustrate the format.

Group Committee T-5 has a Unit Committee on the "Stress Corrosion Cracking of Metallic Materials", which sponsors symposia and conducts forums for discussion of stress corrosion problems, new stress corrosion resistant alloys, protective measures, etc. There are several task groups representing different metal alloy systems, and the assignments involve informational reports on service failures and case histories (Figure 1). This committee maintains effective liaison with the ASTM Subcommittee on Stress Corrosion Testing, and inasmuch as the latter is actively working on SCC testing methods, Unit Committee T-5E has not moved in this direction.

There are no other Unit Committees or Task Groups in NACE that are concerned with stress corrosion testing methods.

PART II - ALUMINUM ASSOCIATION - ASTM JOINT TASK GROUP

The Aluminum Association, with its membership consisting of representatives of producers and fabricators of aluminum and aluminum alloys in United States and Canada, has among its technical committees one on Finishes and Corrosion. In May, 1971, the Aluminum Association Technical Policy Committee requested the formation of an Ad-Hoc Committee to consider the problems associated with the stress corrosion testing of high

strength heat treatable aluminum alloy products. This committee sponsored a technical presentation of the problem at the U.S. Air Force Materials Laboratory on June 3, 1971, for representatives of the Air Force, the Naval Air Systems Command and the U.S. Army. An abridged version of that presentation is given in the sections to follow. In response to the interest and support pledged by the armed services, a task group was organized in June, 1971, entitled, Aluminum Association and ASTM (G01.06.91) Joint Task Group for Stress Corrosion Testing 7XXX Aluminum Alloys Containing Copper. Members include five producers of aluminum alloys, five U. S. Government agencies and one aircraft manufacturer.

What is the Problem?

1. Stress-corrosion cracking (SCC) problems have occurred with parts made of high strength aluminum alloys such as 2014-T6, 2024-T3, 7075-T6 and 7079-T6. Generally the SCC is associated with sustained tension stress at the surface of the metal and acting in the short transverse direction relative to the grain flow pattern in the metal. Machining parts from forgings, plate, etc. often has left end-grain structure at the surface of the finished part. The stresses that have been responsible for the SCC usually are not caused by the design loads that are watched closely by fatigue conscious engineers. Rather, SCC is generally caused at unexpected locations by relatively high tension stresses that are locked into components as a result of heat treatment or assembly practices.

2. Although alloy 7075-T73 has provided a good solution to SCC of high strength aluminum alloys, the attendant decrease of 10 to 15% in T.S. and Y.S. compared to 7075-T6 is undesirable for many applications. Nevertheless, it often has been possible to substitute 7075-T73 directly for 2014-T6. Satisfactory performance has been given by 7075-T73 products in structures for up to 8 years operation. Also, accelerated laboratory tests and exposures of up to 10 years in industrial and seacoast atmospheres have demonstrated the virtual immunity to SCC of a wide variety of products and shapes. To define the resistance to SCC of 7075-T73 products for specification purposes, a SCC test requirement was incorporated into the military specification for the heat treatment of aluminum alloys, MIL-H-6088E. Subsequent experience has shown that the conditions of this test, summarized in Table I, are too general when used for the evaluation of products of newer alloys and tempers. An illustration of the wide variety of test conditions used is shown in Table II with information from sixteen different laboratories. Because this is the most widely used accelerated test for these alloys, it is expedient to regulate conditions to make the test as reliable as possible.

3. The aerospace industry has indicated that for many applications an alloy with a resistance to SCC less than that of 7075-T73, but substantially better than that of 7075-T6 or 7079-T6, would be very desirable, provided it has mechanical properties similar to 7075-T6 or 7079-T6. This has become a prime target for alloy development for the aerospace industry, and new alloys and/or tempers, such as 7075-T76, 7075-T736, 7175-T736, 7049-T73, X7050-T73*, X7050-T736* and RX720 have appeared on the scene.

It is not practical to use SCC tests only in natural environments for alloy development because of the long exposure periods required, and so accelerated tests are used. The T73 temper, and later the T76 temper, were developed principally by exposures to the 3.5% NaCl alternate immersion test; the salt solution was made to purity standards meeting ASTM B117 (salt spray test solution) and the exposures made under ambient conditions of laboratory atmosphere. The reliability of this test for predicting the atmospheric SCC performance of 7075 alloy in the T6, T73 and T76 tempers is illustrated by the test data shown in Figure 3.

4. Problems have arisen in defining "intermediate" resistance to SCC of aluminum alloy products. Not only do variables in the SCC test procedure have a marked influence on the SCC test results, but of even greater importance is the selection of representative products and the sampling procedure. These critical factors influence both R & D efforts to develop new alloys and the establishment of meaningful specification acceptance tests. Figure 4 is a schematic representation of data from a number of investigations showing the wide variation in performance that may be encountered in SCC tests of 7XXX-T7X alloy products compared to those of 7075-T6 or 7075-T73, when proper account is not taken of the test conditions.

In the upper graph it is shown that at the relatively high stress level of 75% Y.S. (usually about 40-50 ksi for 7XXX-T7X products) 7075-T73 is highly resistant to SCC regardless of test conditions and product tested. At this high stress level specimens of T6 temper products fail rapidly in all cases. The performance of specimens from intermediate resistance T7X temper products can vary widely depending upon the grain directionality of the product, type and location of the specimen tested, and the make-up of the test solution: on the basis of a "30-day A.I. test" a specific 7XXX-T7 alloy may appear to be the equal of 7075-T73, or it may not appear appreciably better than 7075-T6 or 7079-T6.

At the 25 ksi stress level (lower graph) 7075-T73 will not stress-corrosion crack and the 7075-T6 may, on the basis of extended specimen life, appear to be fairly resistant. The performance of T7X temper specimens, on the basis of a 30-day test, may

* Preliminary temper designations still in development stage.

appear distinctly superior to the T6 temper and equal to T73, but on the basis of longer exposures, the performance may overlap both that of T73 and T6 tempers.

The effects of some of the variations in test conditions will be discussed in the following paragraphs.

The 3.5% NaCl Alternate Immersion Test

Method No. 823 of U.S. Federal Standard 151B was issued on November 24, 1967 to regulate the procedure for this test in SCC specifications for aluminum alloy products. The regulations set forth are shown in Table III. To evaluate this test method an interlaboratory testing program sponsored by ASTM Subcommittee G01.06.02 was conducted in five different laboratories on C-ring specimens of 7039 alloy plate. Appreciable variation was observed in the alternate immersion test results obtained in different laboratories, although the repeatability of the test results in any one laboratory was fairly good. Comparison of the detailed procedure used in the five laboratories revealed that all had not adhered strictly to the specified procedure.

Another small interlaboratory test was performed by Alcoa under the sponsorship of a government contract, and a portion of the data is shown in Figure 5. The graphs illustrate a marked variation in corrosion and SCC of transverse 0.125-in. diameter tensile specimens of 7079-T651 exposed to 3.5% NaCl A.I. tests in four different laboratories. All four tests would conform to the general requirements of MIL-H-6088E. Procedure A is an Alcoa test using solution made with commercial salt and tapwater which meets the water purity limits of ASTM B117-64 (<200 ppm total solids). Procedures B and C satisfied Federal Method 823 (Procedure B conducted by Alcoa, C by another laboratory). With Procedure D (a third laboratory) the salt solution met the purity standards of Method 823 but the atmospheric conditions varied over a wider range. While Procedures C and D were more corrosive to 7079-T651 alloy, Procedure B caused more rapid SCC. Procedure A was the milder test on both counts.

A problem of interpretation that arises with the 3.5% NaCl alternate immersion test is illustrated by data plotted in Figure 6 for a single lot of 7075-T7351 plate. When operated without close control of atmospheric conditions, solution chemistry, etc. the test yields variable results, as one might expect. When an attempt is made to regulate the test, as in Federal Method 823, test results may be more uniform in a given laboratory, but there still can be appreciable variation in test results between laboratories. In this instance the more aggressive Method 823 versions of the test do not relate with 4-year outdoor exposure tests as well as the less aggressive test (dashed line). The reason, as revealed by metallographic examinations of failed specimens, is that the specimens exposed to the two Method 823 tests failed as a result of transgranular cracks caused by tensile overload that occurs as the corrosion pits develop and not by characteristic intergranular SCC. Such transgranular cracks have never been observed in specimens exposed to the atmosphere.

Subcommittee G01.06 of the ASTM is presently balloting a Recommended Practice for Performing the 3.5% NaCl Alternate Immersion Test that follows closely the conditions called out in Federal Method 823. A new interlaboratory test program evaluating this test procedure is presently being started by the Aluminum Association - ASTM Joint Task Group.

The Stress Corrosion Test Specimen

The type and size and method of loading of the stress corrosion test specimen can have marked effects upon the probability of its failing and the time to failure. Also, small test specimens are particularly liable to tensile overload failures when exposed to environments that cause severe pitting of the specimen.

Because the per cent loss in strength of the test specimen is a function of the specimen diameter and the exposure time, it may be concluded from Figure 7 that the 0.225-in. diameter specimen is less likely to incur pitting-failures in a 30-day exposure than the 0.125-in. diameter specimen. Although there has been widespread use of the 0.125-in. diameter tensile test specimen, the occurrence of such failures in the 3.5% NaCl alternate immersion test has resulted in many laboratories adopting larger diameter tensile specimens.

A disadvantage or risk involved with the use of larger diameter tensile specimens is a sacrifice in the sensitivity of the test to true stress-corrosion cracking. The results summarized in Table IV for high resistance tempers show that these "pitting-type" failures almost can be eliminated by use of the 1/4-in. diameter specimen. However, tests of intermediate resistance items at high stresses and of low resistance items at low stresses showed that use of 1/4-in. specimens reduced the percentage of legitimate SCC failures. Thus, the use of larger specimens to avoid "nuisance" pit-type failures may also reduce the ability to detect susceptibility to SCC. This is particularly true for a 30-day exposure of items with intermediate resistance to SCC. Atmospheric exposure data for specimens of both sizes are needed to determine which size of test specimen gives the most realistic data.

Method of Sampling Products to be Evaluated

In a simple product such as sheet, the choice of specimen type and orientation is limited. However, for thick sections, and especially for complex shapes, the sampling

procedure becomes more complicated and of fundamental importance. It is necessary to take into account the grain structure of the material resulting from the metal flow pattern induced during fabrication of the product.

Because of the sequence of working operations in making forgings, and the variation that is possible, the metal flow pattern may not always be simply related to the cross section of the finished product. Consequently, true longitudinal and long-transverse specimens may be difficult to locate without first making a careful examination of the grain structure. It is recognized that in hand forgings the grain structure is usually elongated in the longitudinal and the long-transverse directions with relation to the external shape of the part. In a square cross section, the grain structure pattern may not be as well defined in relation to the external shape as in a rectangular section; however, as the width-to-thickness ratio increases, the long-transverse characteristics usually become more apparent.

Even a square section, however, may exhibit different degrees of directional structural characteristics. An extreme example of the complicated metal flow pattern that may be developed in a square hand forging is shown in Figure 8. From this 8-inch square section "transverse" specimens were removed with three different orientations relative to the grain structure as shown on the etched section. The specimen blanks, 5/16-inch square x 2 inches long, were reheat-treated to the -T6 temper. A sustained stress of 35 ksi was applied to the machined 0.125-inch diameter tension bars during exposure to the 3-1/2 per cent sodium chloride alternate immersion test. Specimen P (parallel to metal flow) was intact after 180 days' exposure, whereas specimen D (45° to metal flow) stress-corrosion cracked after 70 days' exposure, and specimen N (normal to metal flow) after only 14 days. A duplicate P specimen, exposed while under a stress of 60 ksi, also was intact after 180 days' exposure.

Thus, from a square section, "transverse" specimens which might be expected to exhibit a relatively low resistance to stress-corrosion cracking exhibited a wide variation in resistance, including both short-transverse and longitudinal specimen behavior. In some instances test specimens removed longitudinally from hand forgings have exhibited a tendency for transverse specimen behavior.

An example of how specimen location in an extrusion affected SCC test results is shown in Figure 9. For the intermediate resistance T76 temper the "transverse" grain structure at the base of the outstanding leg had higher resistance than the short-transverse grain structure in the web. The effect of grain structure was not evident on the very high resistance T73 temper, nor on the relatively low resistance T6 temper. The difference in performance for the T76 temper is attributed to difference in grain structure, rather than to specimen type.

Effect of Size and Shape of Products to be Evaluated

An example of the marked effects that the configuration of a forging and the directionality of the grain structure can have on the stress corrosion performance is shown in Figure 10. The performance of the web-flange type die forging was relatively poor because the short-transverse-parting plane flow was more severe than that in the cylindrical forging; however, the grain structure of the latter was more critical than that of the thick hand forgings. All of the forgings of the experimental alloy were of similar composition and had been given the same nominal heat treatment. It is possible by the choice of appropriate thermal treatments to develop similar SCC performance in the various products.

Conclusions

1. The introduction of new 7XXX-type alloys and tempers with intermediate resistance to SCC has posed new problems in performing SCC tests and evaluating the results.
2. There is a need for refined test procedures and the adoption of uniform practices for all investigators. Work in this direction already in progress under the sponsorship of ASTM and the Aluminum Association should be accelerated. In this area there is a need for:
 - (a) Close control of the widely used 3.5% NaCl alternate immersion test;
 - (b) Evaluation of other corrodents that do not cause severe pitting of these alloys; and
 - (c) Determination of the possible effects of the use of specimens of different types and sizes and of methods of loading.
3. To obtain valid comparisons of the resistance to SCC of alloys and tempers it is essential that like products and configurations be tested by uniform procedures. Standard products and methods of sampling should be adopted through the Aluminum Association, ASTM and through U.S. Government agencies.
4. An improved rating system for classifying the relative resistance to SCC of an alloy and temper is needed. This should be based upon standard products tested by uniform procedures.

TABLE I

STRESS CORROSION TEST FOR 7075-T73 PRODUCTS
MIL-H-6088E (SECTION 4.4.5)

1. STRESS IN SHORT TRANSVERSE GRAIN DIRECTION
2. THIRTY (30) DAY EXPOSURE
3. ALTERNATE IMMERSION (10 MIN. IMMERSION +50 MIN. OUT OF SOLUTION)
4. SOLUTION OF 3.5% NaCl WITH PURITY AND pH PER METHOD 8II OF FEDERAL STD. 151 (METHOD 8II CANCELLED, BUT SIMILAR TO ASTM B117-64 (99.7 MIN. % NaCl, 0.1 MAX. % NaI + WATER CONTAINING <200 ppm TOTAL SOLIDS)

TABLE II
VARIATIONS IN 3.5 % NaCl A.I. -- 16 LABORATORIES

1. <u>ATMOSPHERE CONTROL</u>			
A.	HUMIDITY CONTROLLED		3 LABS
	NOT CONTROLLED		13 LABS
B.	AIR TEMPERATURED CONTROLLED		11 LABS
	NOT CONTROLLED		4 LABS
2. <u>SALT SOLUTION MAKE-UP</u>			
A.	DISTILLED WATER		6 LABS
	DEIONIZED WATER		7 LABS
	TAP WATER (METHOD 811 < 200 ppm SOLIDS)		3 LABS
B.	ANAL. REAGENT NaCl		3 LABS
	CHEM. PURE NaCl		7 LABS
	COMM. PURE NaCl		5 LABS
	SYN. SEAWATER		1 LAB
3. <u>METHOD OF IMMERSION</u>			
	FERRIS WHEEL] IMMERSION	13 LABS
	SAMPLES INTO SOLUTION		
	PUMP SOLUTION		
	PUMP SOLUTION INTO CELL		3 LABS
4. <u>TEST SPECIMEN</u>			
	TENSILE ROUND		
	1/8 INCH DIA.		8 LABS
	>1/8 INCH DIA.		6 LABS
	C-RINGS		6 LABS
	OTHERS		1 LAB

(KAISER ALUMINUM AND CHEMICAL CORPORATION, T. J. SUMMERSON)

TABLE III
REGULATIONS FOR 3.5% NaCl ALTERNATE IMMERSION TEST

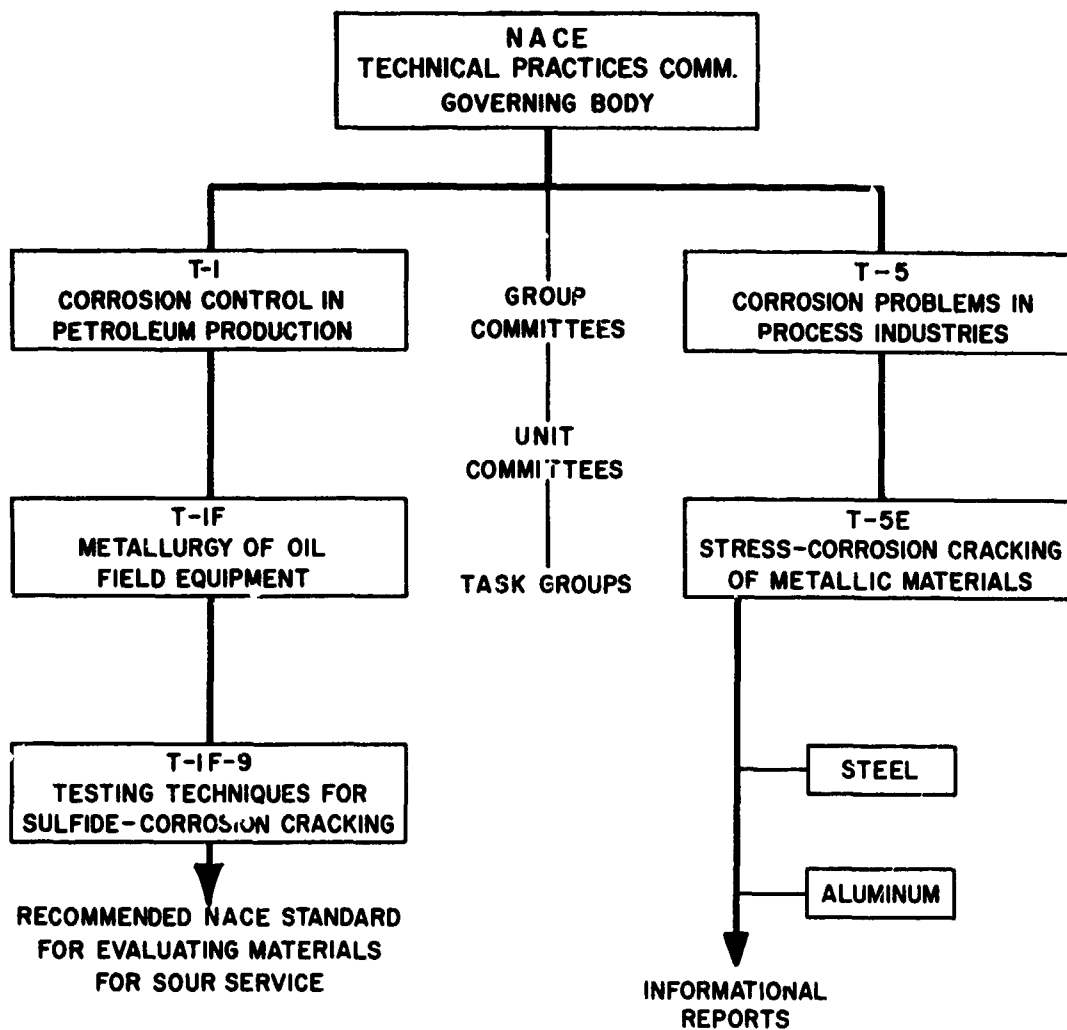
NaCl	<u>MIL-H-6088E</u>		<u>FEDERAL METHOD 823</u>
	99.7 MIN. % NaCl, 0.1 MAX. % NaI		C.P.
WATER	<200 ppm TOTAL SOLIDS		DISTILLED
SOLUTION pH	6.4 - 7.2		6.4 - 7.2
SOLUTION TEMP.	AMBIENT		75 ± 2°F
AIR TEMP.	AMBIENT		80 ± 2°F
AIR REL. HUMIDITY	AMBIENT		45 ± 6°F

TABLE IV

SUMMARY OF 3.5% NaCl A.I. TESTS (FEDERAL METHOD 823) COMPARING RESULTS
OF 1/8 VS 1/4 IN. TENSILE ROUNDS SHORT-TRANSVERSE SPECIMENS FROM
PLATE AND DIE FORGINGS

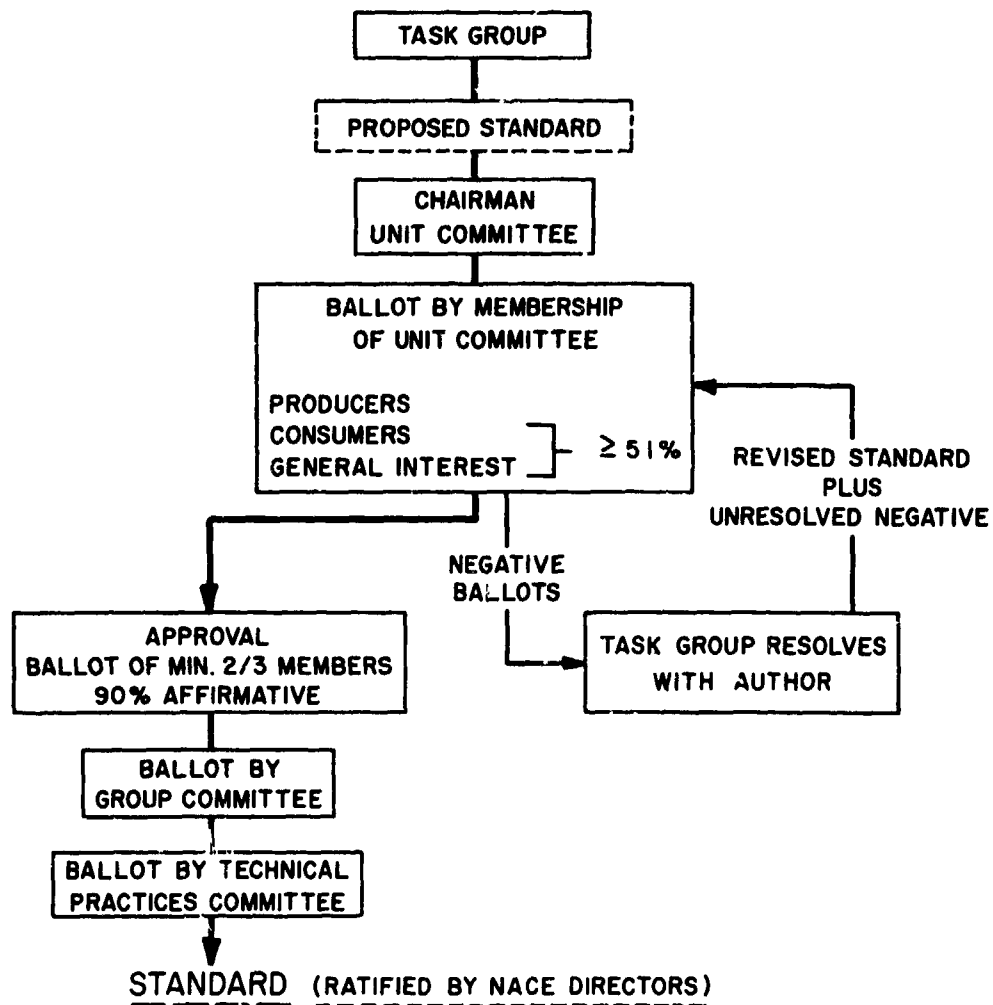
TYPE OF MATERIAL	PERIOD OF EXPOSURE		1/8 IN. DIA.		1/4 IN. DIA.	
	DAYS		F/N	% FAIL.	F/N	% FAIL.
TRANSGRANULAR PIT-TYPE FAILURES						
HIGH RESISTANCE HIGH STRESS	30		11/45	24	2/65	3
	84		36/45	80	9/65	14
INTERGRANULAR SCC FAILURES						
INTERMEDIATE RESISTANCE HIGH STRESS	30		27/38	71	10/37	27
	84		38/38	100	27/37	72
LOW RESISTANCE LOW STRESS	30		17/20	85	10/20	50
	84		20/20	100	15/20	75

(ALCOA RESEARCH LABORATORIES, B. W. LIFKA)



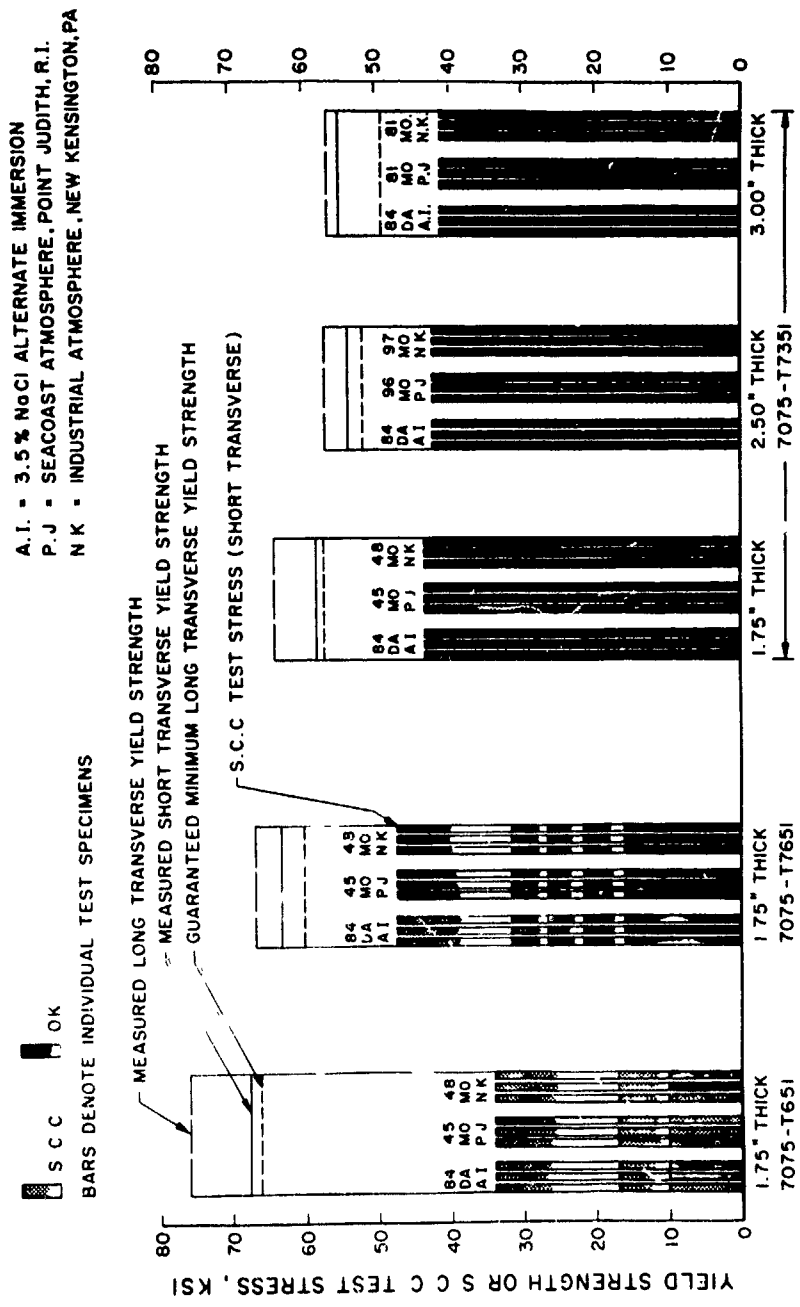
ORGANIZATION OF NACE TECHNICAL COMMITTEES
(PARTIAL)

FIGURE 1



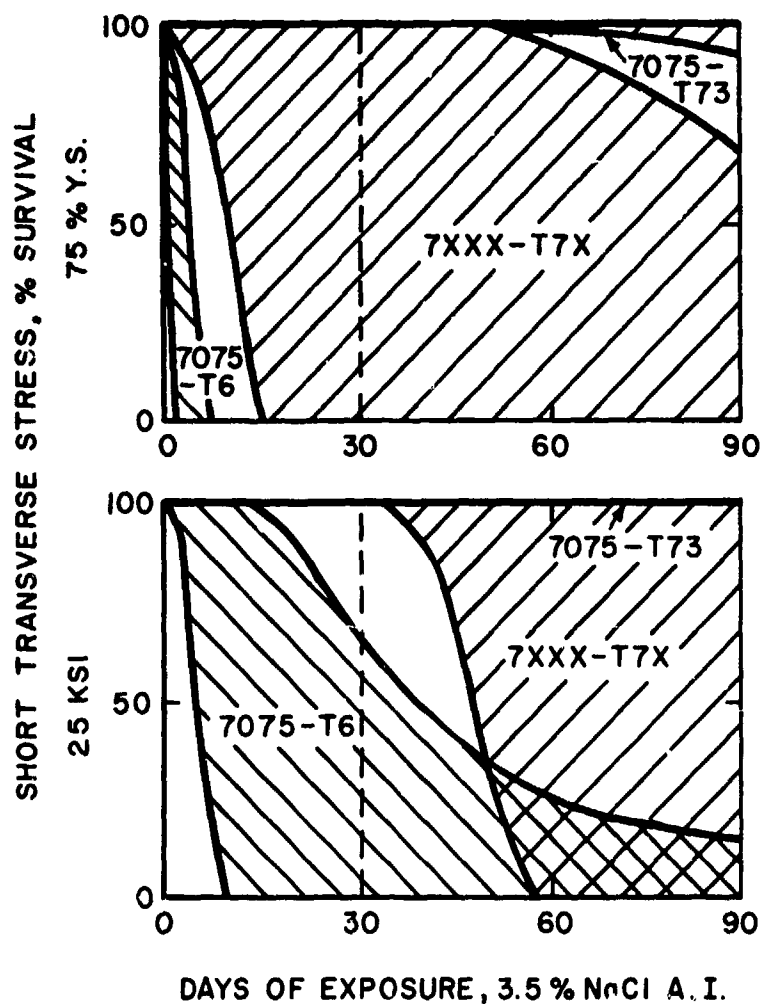
PROCEDURE FOR APPROVAL OF PROPOSED NACE STANDARDS

FIGURE 2



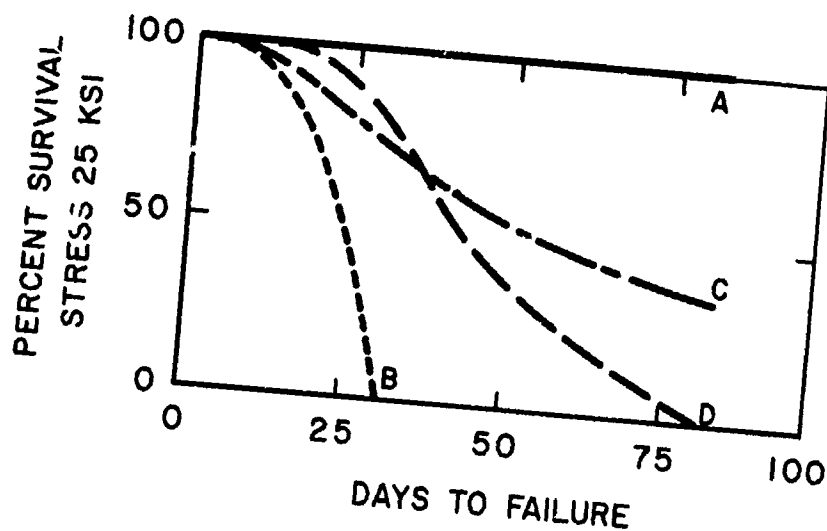
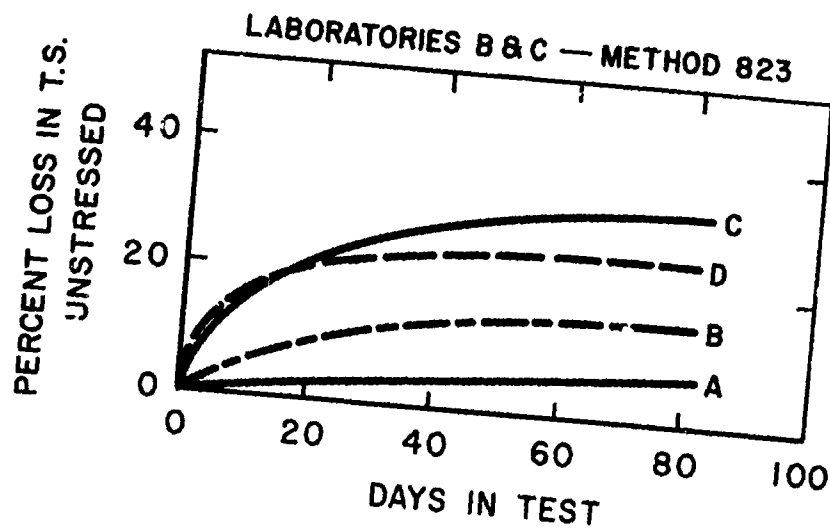
COMPARISON OF PROLONGED ATMOSPHERIC EXPOSURE WITH 3.5% NaCl ALTERNATE IMMERSION STRESS-CORROSION TESTS OF 7075-T7351 AND 7075-T651 PLATE.
(ALCOA RESEARCH LABORATORIES, R.H. BROWN, D.O. SPROWLS & B.W. LIFKA)

FIGURE 3



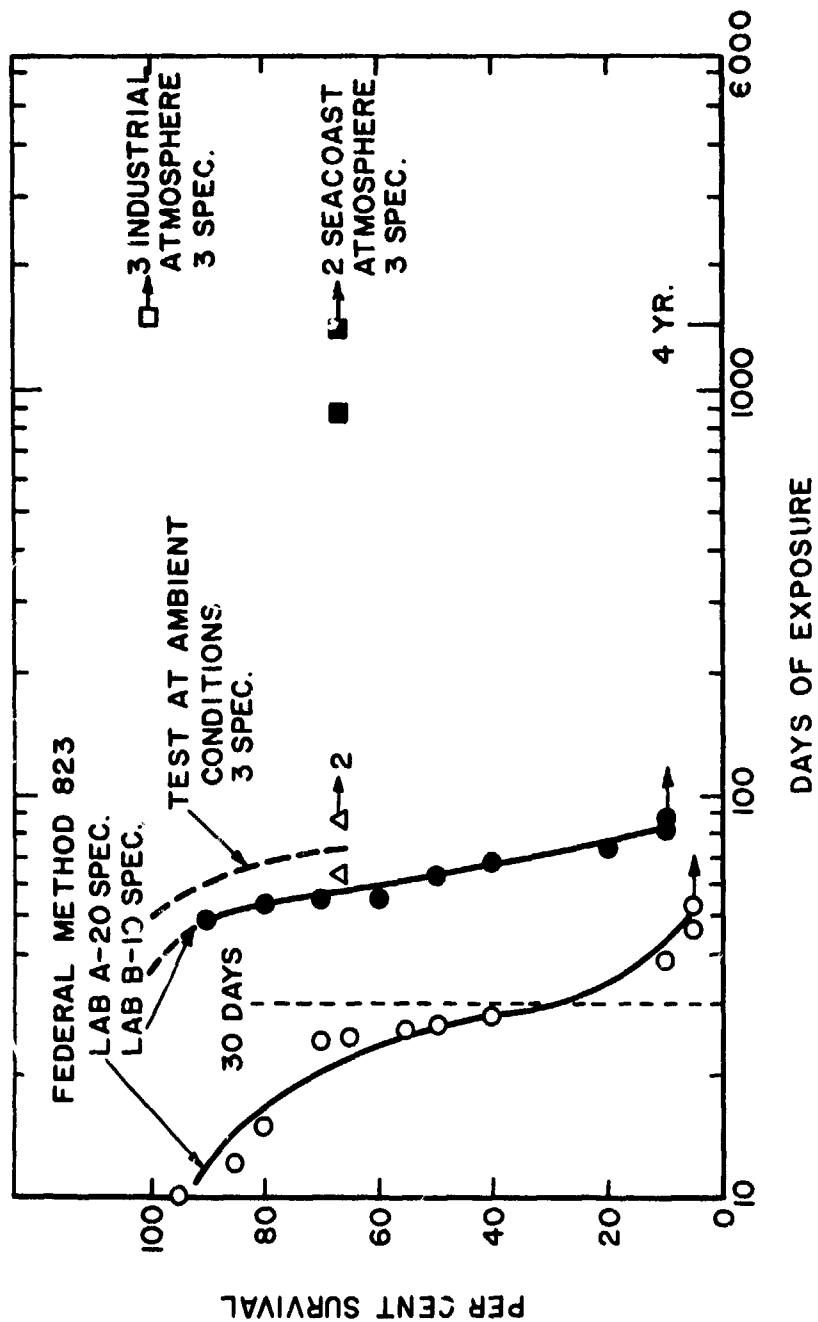
EFFECT OF TESTING VARIABLES ON S.C.C. PERFORMANCE
OF PRODUCTS WITH INTERMEDIATE RESISTANCE TO S.C.C.
(T.J. SUMMERSON, KAISER RESEARCH & D.O. SPROWLS ALCOA
RESEARCH)

FIGURE 4



VARIATIONS IN CORROSION & SCC UNDER DIFFERENT
 CONDITIONS OF ALTERNATE IMMERSION IN 3.5% NaCl
 TRANS. 0.125 IN. DIA. TENSILE SPECS. FROM 7079-T651 ROLLED ROD
 (ALCOA RESEARCH LABORATORIES, D.O. SPROWLS & D.G. VANDENBURGH)

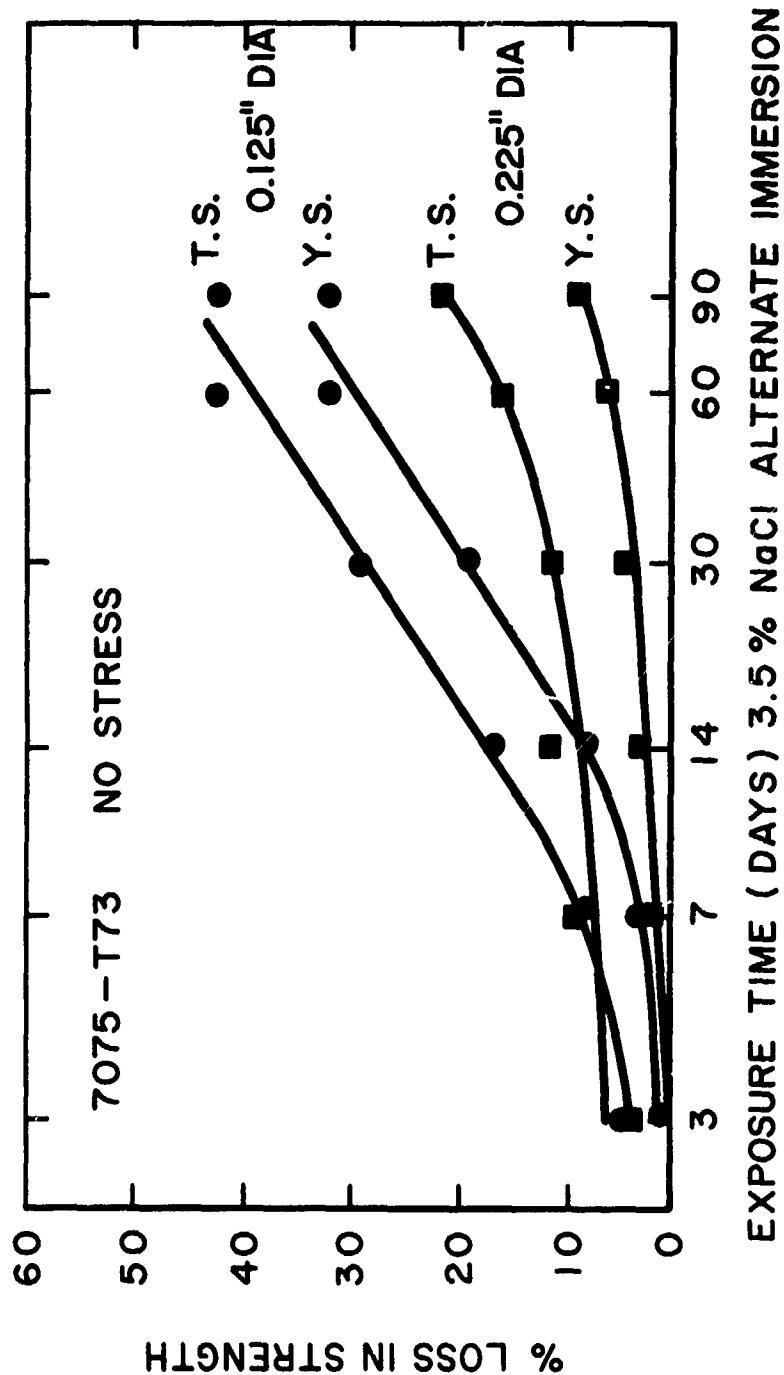
FIGURE 5



SHORT TRANSVERSE SCC TESTS OF A SINGLE LOT OF 1.75 IN. THICK 7075-T7351 PLATE (0.125 IN. T.B.) EFFECT OF VARIATIONS IN THE 3.5% NaCl ALTERNATE IMMERSION TEST

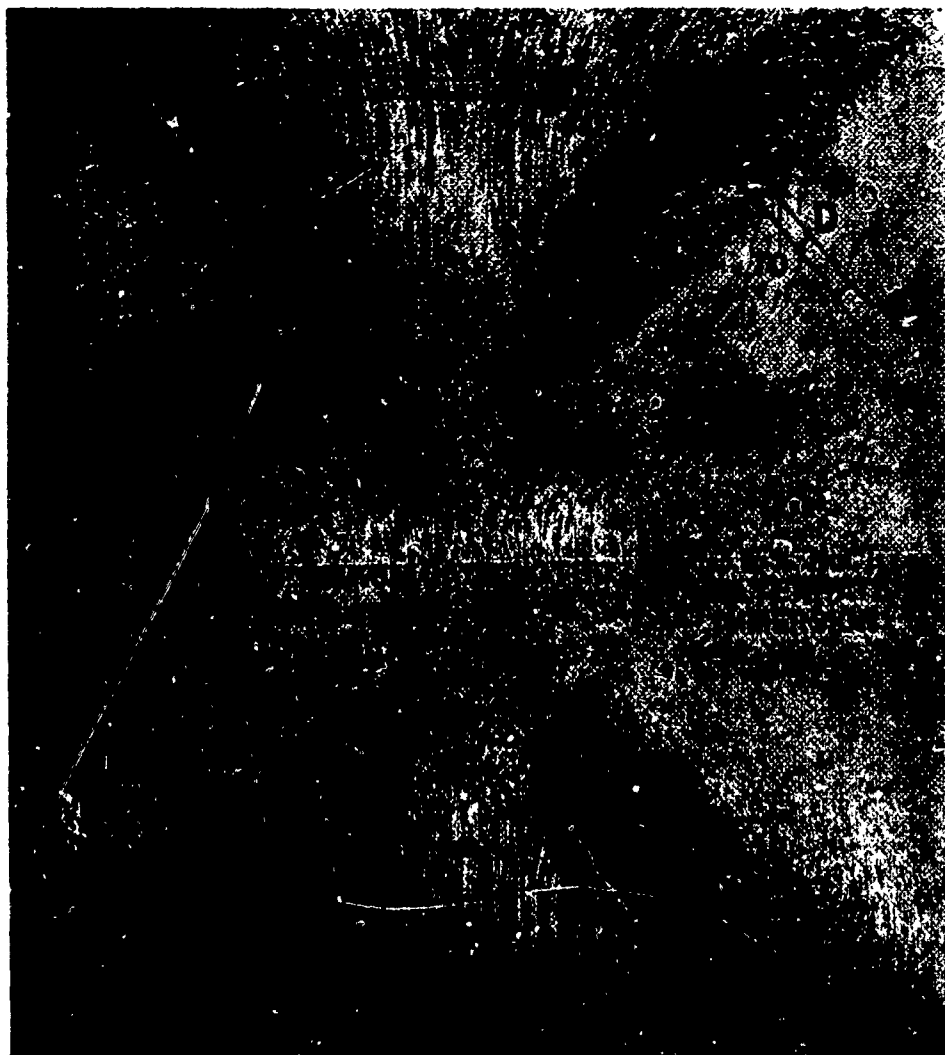
(H.L. CRAIG, JR., REYNOLDS RESEARCH & D.O. SPROWLS, ALCOA RESEARCH LABORATORIES)

FIGURE 6



**% LOSS IN PROPERTIES AS A FUNCTION OF TIME AND
DIAMETER OF TENSILE SPECIMEN**
(REYNOLDS METALLURGICAL RESEARCH LABORATORIES, H.L.CRAIG, JR.)

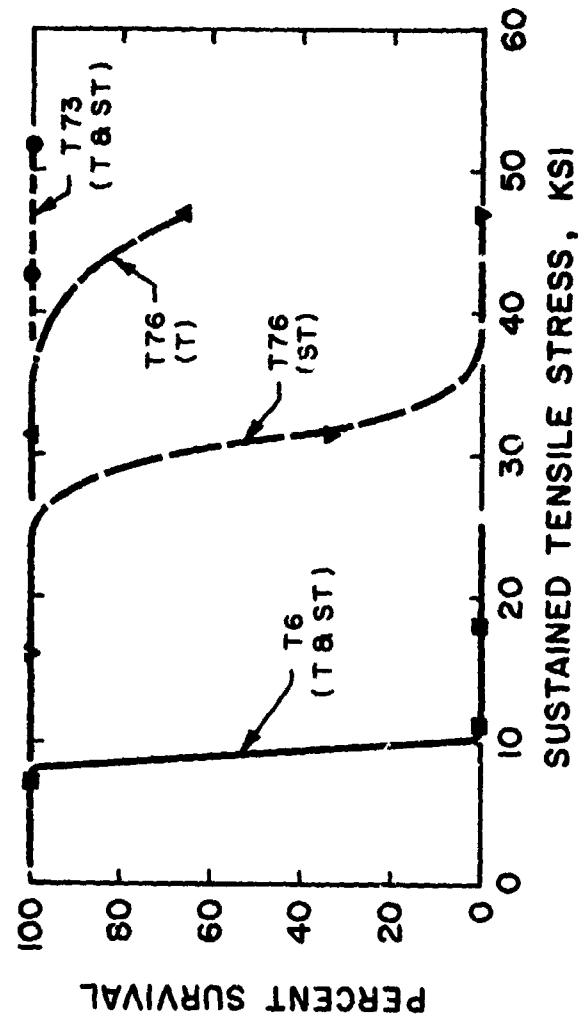
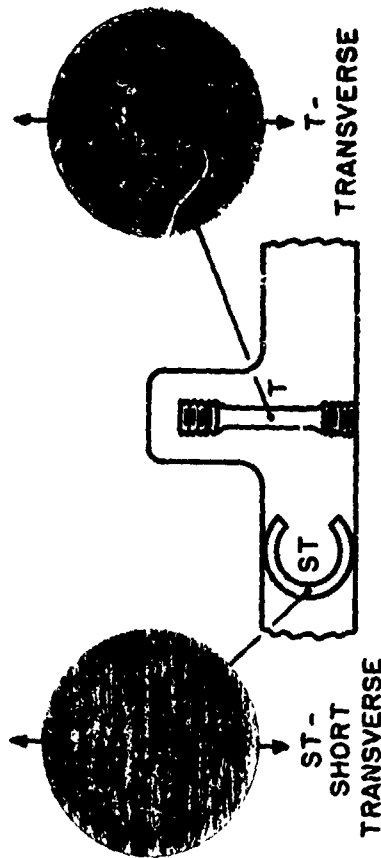
FIGURE 7



Superimposed on a photograph (IX) of a macroetched transverse section of a special 8in. x 8in. x 24in. hand forging of 7075-T6, fabricated so as to produce a complex grain flow, are the outlines of three stress-corrosion specimens along with their days to failure in the 3 % NaCl alternate immersion. These specimens showed widely different stress-corrosion resistance, as would be expected in view of their orientation to the grain structure. Noteworthy is the high order of resistance of specimen (P).

(D.O. SPROWLS & R.H. BROWN, METAL PROGRESS VOL.81, NO.4 (1962), P.P.79-85)

FIGURE 8



EFFECT OF LOCATION OF TEST SPECIMEN ON STRESS-CORROSION PERFORMANCE OF 7075 ALLOY EXTRUDED WING FLANK.
(ALCOA RESEARCH LABORATORIES, B.W. LIFKA & D.O. SPROWLS)
FIGURE 9

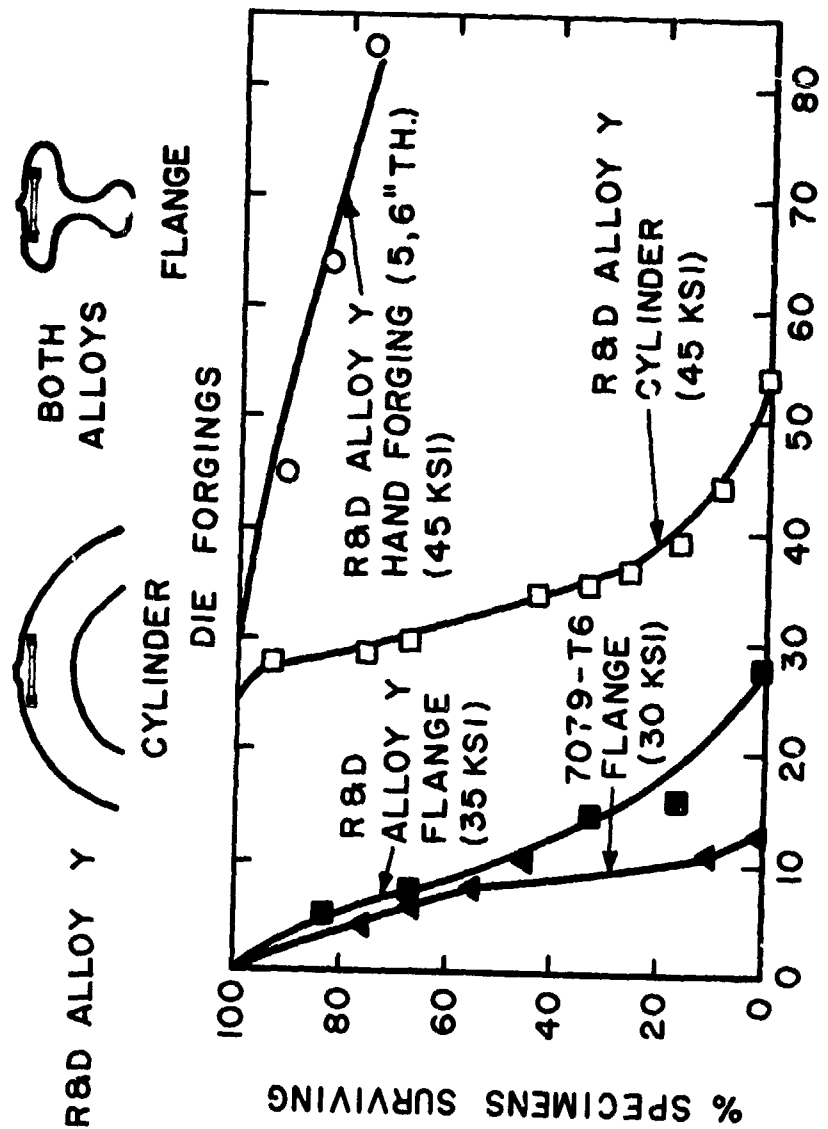


FIGURE 10
 DAYS OF EXPOSURE, 3.5% NaCl - A.I.
 (ALCOA RESEARCH LABORATORIES, B.W. LIFKA & D.O. SPROWLS)

1

STRESS CORROSION TEST METHODS -
THE EUROPEAN FEDERATION OF CORROSION CONTRIBUTION

R.N. Parkins
Department of Metallurgy
The University
Newcastle upon Tyne, NE1 7RU, England.

SUMMARY

The European Federation of Corrosion Working Party on Stress Corrosion Test Methods has prepared a review of this subject and the present paper is a precis of the major points in this review. It points to some of the problems associated with the various methods of testing, such as the extensive use of time to failure as a parameter that measures susceptibility and the apparently poor reproducibility of K_{ISCC} values as reported in the literature. On the environmental side of testing, the dangers in the use of 'standard' solutions are indicated and the necessity, in simulating service failures, of precisely reproducing the composition of the environment and the relevant electrode potential are shown.

The European Federation of Corrosion, which is an amalgam of the various corrosion societies of Europe, set up, in 1969, a Working Party on Stress Corrosion Test Methods. This Working Party was set two immediate tasks, one involving a cooperative testing programme to compare the results from different test methods and the reproducibility of results from different laboratories, and the second to prepare a critical essay on test methods in which the emphasis would be placed upon consideration of the factors that can influence test results, rather than upon collecting together the details of test methods. The first task is not yet completed, but the critical essay has almost reached its final form prior to its simultaneous publication in English, French, German and Spanish. The present paper constitutes a précis of the major points made in the more detailed article that is to be published in the summer of 1972.

It may be reasonably assumed, from the fact that there are so many different stress corrosion test methods currently in use, that there is no single method that is markedly superior to all others. Nevertheless, some rationalization of the present situation appears desirable and it is as well to remember in this context that, ideally, a test method should not be so severe that it leads to the condemnation of a material that would prove adequate for a particular service condition, or so trifling as to permit the usage of a material in circumstances where rapid failure would ensue. Recognition of such requirements has frequently led to the use of tests that closely simulate a practical situation, especially in regard to the structure and composition of the material and usually in relation to environmental aspects, but less frequently in respect of the manner in which the stress has been generated in the test specimen. For the convenience of discussion, the present article is divided into two main sections, the first concerned with stressing systems and the second with environmental aspects of testing.

STRESSING SYSTEMS

Irrespective of whether the specimen is plain or contains a pre-crack at the start of the test, the method of stressing the test piece involves either

- (a) a constant total strain
- (b) a constant load
- or (c) a constant strain rate.

Insofar as the majority of stress corrosion failures are probably the result of the incorporation of fabrication stresses into structures, tests employing a constant total strain are probably most frequently the more realistic. Constant load tests may simulate more closely failure from applied or working stresses, whilst tests involving the application of a constant strain rate, although used relatively little in the past and apparently not very relevant to service failures, may well find considerable application in the future.

Constant Total Strain Tests

These are by far the most popular type of test as a group, since bend tests, in a variety of forms and usually employing simple, cheap, restraining jigs come into this category. The stiffness of the restraining frame can be an important parameter in influencing the results obtained, not least because the initial elastic strain in the specimen is converted in part to plastic strain as the crack propagates. This is because the net section stress increases as a crack propagates until the yield stress is reached when the crack yawns, frequently accompanied by the propagation of a Lüders band and a resultant reduction in the elastic strain and hence, in effect, the load. Once load relaxation has been initiated the extent to which it proceeds will depend upon the material being tested, the characteristics of the restraining frame and even upon the number of cracks that the specimen has developed. Thus in a specimen that develops a number of cracks, each of which causes a Lüders band to be propagated, marked load relaxation will be observed as compared with a similar specimen in which only one or a few cracks are present. In the latter case the stress corrosion crack will not need to grow to large dimensions before sudden, fast fracture occurs because the applied load remains high, whereas with the marked load relaxation associated with the presence of many stress corrosion cracks the latter must propagate much further before one of them becomes large enough to create the stress conditions at a relatively small load for sudden fracture. Consequently a specimen that is more susceptible, in the sense that it develops more cracks, may take a longer time to fail than one that contains fewer cracks and is less susceptible. This indicates the dangers in comparing stress corrosion susceptibilities in terms of time to failure, especially when the results are from different laboratories using restraining frames of varying stiffness.

The point may be illustrated with some results of stress corrosion tests on a mild steel immersed in a boiling nitrate solution, in which the time to failure was determined for a range of initial stresses (Figure 1) using the same equipment for each test. If the effects of cold work upon the cracking susceptibility are compared at 18 tons/sq.in. initial stress, then it would be concluded that cold working increased the resistance of the steel to failure, whilst a comparison at 10 tons/sq.in. would lead to a very different conclusion, in terms of time to failure. It could be argued that neither of these results is correct because the drawing would result in different yield strengths being developed in the three different conditions and that the results should be rationalized by making the comparison as a function of the respective yield strengths. Here again, however, the order of susceptibility varies according

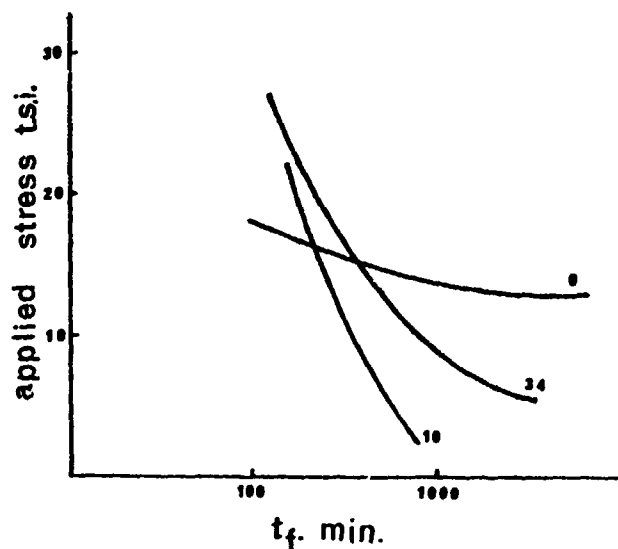


Figure 1. The effects of different amounts of prior cold work on the stress corrosion of a 0.07% C steel in boiling 4N NH_4NO_3 .

to the rationalized stress at which the comparison is made, as the results shown below indicate.

Initial Stress	Susceptibility of different cold worked conditions.		
	Most	Intermediate	Least
18 tsi.	0%	10%	34%
10 tsi.	10%	34%	
100% TS.	34%	10%	0%
30% YS.	10%	34%	0%

Constant Load Tests

Since the effective cross section of a test piece reduces by crack propagation constant load tests involve an increasing stress situation. Consequently such tests are more likely to lead to early failure or total failure than constant strain tests. The latter, because of the associated relaxation, can produce cracks that eventually stop propagating and so total failure may not be observed. In fact, cracks that cease to propagate may also occur in constant load tests, probably as the result of creep exhaustion where the latter is an important parameter in cracking. If constant load tests are employed in relation to test pieces of relatively large cross section they will involve the use of massive loads or lever systems. This is sometimes avoided by reducing the size of the specimen, possibly to very fine wires. The latter is dangerous unless failure by stress corrosion cracking is confirmed by, say, metallography, since failure may result from simple pitting and an attendant increase in the effective stress to the U.T.S. in some stress corrosion environments.

Constant Strain Rate Tests

Such tests have not as yet had extensive application, possibly because it may be thought that the pulling of specimens to failure at a slow strain rate shows little relation to the reality of service failures. In point of fact in constant total strain and constant load tests, crack propagation also occurs under conditions of slow dynamic strain to a greater or less extent depending upon the initial value of stress in relation to the effective yield stress of the test piece. There are some additional features associated with constant strain rate tests that in the future may lead to their more extensive use in routine laboratory testing. Thus, they are a relatively severe type of test in the sense that they frequently promote stress corrosion failure in the laboratory where other tests on plain specimens do not promote cracking, and in this sense they are in a similar category to tests on pre-cracked specimens. Moreover, constant strain rate tests are positive in that they invariably produce fracture, either by stress corrosion or some other mechanism and this in a relatively short period of time. Since the results from most stress corrosion tests are simply used for comparative purposes, the data they provide having little absolute significance, there is clearly sometimes merit in having a form of test that is severe, positive and rapid, especially for purposes of initial sorting.

The most important feature of constant strain rate tests is concerned with the particular value of the strain rate employed. Clearly if this is too high ductile fracture will ensue before the necessary reactions can take place, consequently relatively low strain rates, usually in the region of 10^{-6}sec^{-1} ,

need to be employed. It is possible in some cases however for the strain rate to be too low. Thus, if the environment is one that produces filming of the metal surface, and probably almost every stress corrosion environment comes into this category, then at very slow strain rates film repair may be fast enough to keep pace with the rate at which bare metal is formed so that the cracking reaction is not sustained. Figure 2 illustrates this point schematically and suggests that the most appropriate strain rate for

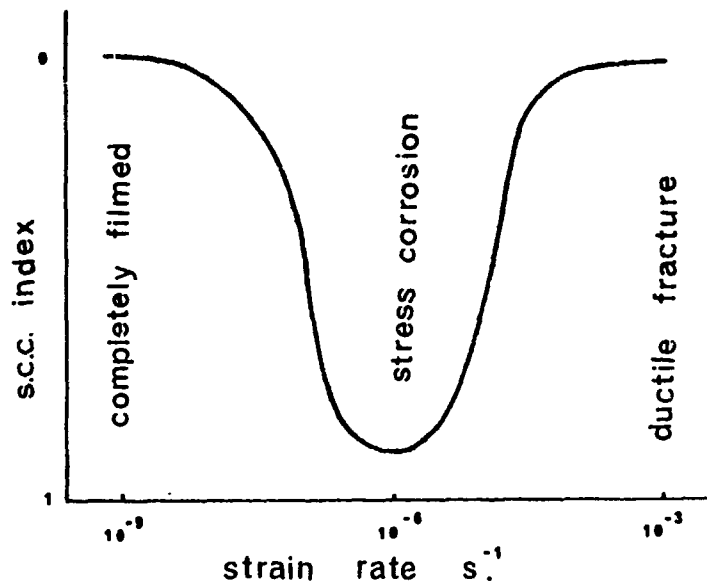


Figure 2. Schematic illustration of the effect of strain rate upon stress corrosion susceptibility in a filming environment.

producing stress corrosion cracking will vary from system to system and should be determined for each case.

The usual means of indicating whether or not stress corrosion cracking has occurred in a static test is the time to failure, whereas such a parameter would not appear, at least at first sight, to be appropriate in the case of constant strain rate tests. Metallographic examination can confirm whether or not stress corrosion cracking has occurred during a constant strain rate test, although this does not usually lead to a quantifiable result for purposes of comparison. The more obvious quantitative measures of stress corrosion susceptibility in a constant strain rate test are ductility parameters, such as percent reduction in area or elongation, the maximum load achieved or the area under the stress-strain curve, all of which will be reduced from the values observed with ductile failure when stress corrosion cracks are present. In fact the time to failure in a constant strain rate test also may be used in comparing cracking tendencies, since the lesser the intensity of stress corrosion cracking the greater will be the ductility to fracture and, therefore, the greater the time to fracture at a constant strain rate.

Pre-Cracked Test Pieces

The developments in fracture mechanics in the last decade have resulted in the evolution of a whole new field of stress corrosion testing involving the use of specimens containing a sharp pre-crack, usually produced from a notch by subjecting the specimen to fatigue. It frequently has been claimed of pre-cracked specimens that they circumvent the initiation stage of cracking in plain specimens, erroneously assumed invariably to be related to the creation of a corrosion pit that eventually leads to cracking and failure. Whilst the initiation of stress corrosion cracking may be different in plain and pre-cracked specimens, because of their differing geometries promoting different stress distributions, it is extremely doubtful if initiation is circumvented with pre-cracked specimens because the initiation of stress corrosion cracks in many cases involves the establishment of a localized electrochemical condition within the confines of a geometrical discontinuity. What may be more disturbing in this context is the possibility that in some instances the mechanism of cracking may be changed when a stress corrosion crack is initiated from the tip of a fatigue crack rather than at a plain surface. Thus, instances are known of materials failing by intergranular cracking, and possibly therefore resulting from an active path mechanism, when tested as plain specimens but failing in a transgranular mode, and therefore possibly by a different mechanism, when the crack is propagated from a sharp discontinuity. To argue as to which type of test is correct in the light of such results is invidious, but such differences have inevitably led to queries as to whether the same phenomena are occurring in the different tests. However, in most cases it appears reasonable to assume that the difference between the two types of test will be minimal, not least because once a crack initiated in a plain specimen has reached an appropriate size the test has obvious similarities to one involving the use of a pre-cracked specimen, i.e. the concepts of fracture mechanics are applicable to an initially plain specimen.

There are presently two major problems associated with the use of pre-cracked specimens in stress corrosion testing, one concerned with specimen dimensions and the other with the reproducibility of results. In order to achieve the plane strain conditions that must obtain if elastic stress analysis

is to be applicable, the specimen size for highly ductile materials is impracticably large. Since it is probable that most service stress corrosion failures occur in highly ductile materials in relatively thin sections it is clear that fracture mechanics, as currently developed, is not applicable in many instances.

Where the data from pre-cracked specimen tests is used for design purposes, e.g. in defining the maximum permissible crack size for non-propagation, it is necessary to recognise that fracture toughness properties are not so reproducible as those parameters, yield stress and ultimate tensile stress, that engineers are more familiar with in design calculations. Thus, the variability between different heats of nominally the same composition and heat treatment determined in the same laboratory, or between results available in the literature from different laboratories, can be alarmingly large. For 18% Ni maraging steel heat treated to a nominal yield stress of 250 ksi and tested in 3-3.5% NaCl solution K_{ISCC} values reported in the literature vary from 10 to 50 ksi $\sqrt{\text{in}}$, whereas the yield or ultimate tensile stress would not be likely to vary by more than a few per cent. Whether such variations in K_{ISCC} are due to inherent differences between heats of nominally the same material or are the result of small differences in technique between different laboratories is not known.

ENVIRONMENTAL ASPECTS OF TESTING

Whilst it is inevitable that the environment will always remain as one of the variables that may need to be assessed by stress corrosion tests, nevertheless certain solutions, by their widespread use over many years, have tended to become 'standard test solutions' for certain types of alloy, e.g. MgCl₂ for austenitic steels, 3.5% NaCl for aluminium alloys and nitrates for ferritic steels. Whilst the preparation of nominally identical solutions in different laboratories would not be expected to lead to differences in the solutions that would markedly influence stress corrosion test results, this is not invariably so. Thus, variations in the boiling points of MgCl₂ solutions may result from the preparation of solutions from salts that have picked-up different amounts of moisture, 3.5% NaCl may contain different amounts of oxygen and boiling nitrate solutions may acquire widely differing pH values, all of which may influence the results from stress corrosion tests. Even where the use of 'standard' solutions does not raise such problems, there are other situations where their use is questionable. Thus, they are sometimes used to indicate the relative susceptibilities of a range of alloys or heat treatments and the assumption made that this order will remain the same in other environments. Such practice may sometimes be permissible, but in other cases the results may be very different from those expected. For example, the addition of about 0.5% Al to a carbon steel will considerably increase its resistance to cracking in nitrate solution but in higher pH environments, such as strong NaOH solutions, the Al addition has virtually no effect.

Electrochemical Aspects of Testing

The electrochemical nature of the reactions involved in stress corrosion cracking permit the cracking to be influenced by the application of current or potential from an external source. The usual reason for impressing current upon stress corrosion test specimens, where data collecting is the objective, is to reduce the time to failure and there is no reason why such a method should not be used providing adequate care is taken to ensure that the mechanism of failure is not changed from that which operates at the free corrosion potential and that the data correlates well with service experience. It should not be assumed that if a galvanostatic technique is used the effect will simply be to influence the kinetics of cracking, since the applied current is also likely to alter the potential and this could promote a different response.

The effect of potential upon cracking response will vary from one system to another, but some aspects of this part of stress corrosion testing may be conveniently discussed in relation to the cracking of carbon steels. These materials fail in different ranges of potential according to the environment in which they are immersed, Figure 3 showing the cracking ranges for a mild steel in hydroxide, carbonate and nitrate solutions respectively. The tests used in determining the results shown in Figure 3 involved potentiostatic control whilst the specimen was subjected to a constant slow strain rate and the times to failure in such tests have been normalized by dividing by the time to failure in oil at the same strain rate and at the appropriate temperatures for each solution. The free corrosion potentials for this steel in these three different environments are also indicated on Figure 3 and show that whilst failure could occur in the nitrate at the free corrosion potential, this would not be so in the hydroxide or carbonate solutions. This does not mean that carbon steels will never fail by stress corrosion cracking in these latter two environments at the free corrosion potential, but simply that this particular steel in the particular solutions used in these experiments did not fail at the free corrosion potential. The latter is, of course, dependent upon the composition of the steel and, more markedly so, upon the composition of the environment. It is possible therefore that as the result of, say, small additions to the environment, added intentionally or present as impurities, or of changes in the composition of the steel, the corrosion potential can be caused to lie within the cracking range so resulting in stress corrosion without applied potential. It is apparent from Figure 3 that relatively small changes in potential, not exceeding about 100 mV, may produce a marked change in cracking response. This points to the necessity, especially in laboratory tests attempting to simulate a service failure, of reproducing the environmental conditions with precision and especially so the relevant potential.

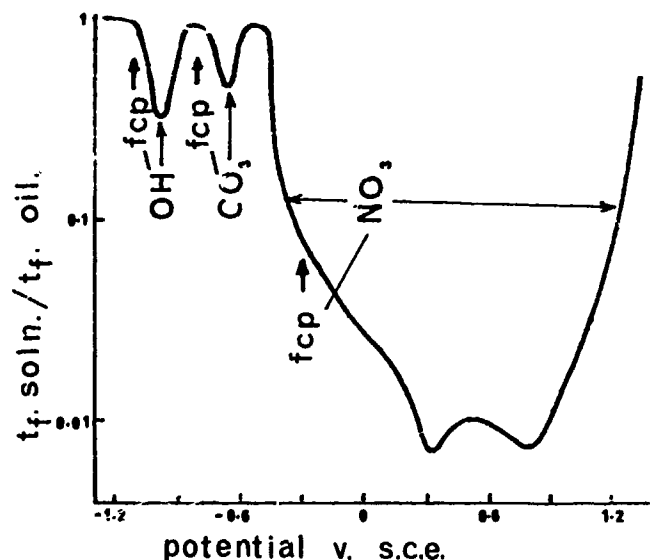


Figure 3. Stress corrosion susceptibility of low carbon steel in constant strain rate tests in various environments at different potentials.

CONCLUSION

Various other aspects of stress corrosion testing, such as the effects of surface finish and exposed area, the design of test cells and experimental details concerned with the initiation of tests, are dealt with in some detail in the fuller paper of the European Federation Working Party and which space restrictions have prevented mention of herein. Whilst these points, together with those mentioned in the present paper, serve to indicate the complexities and potential pitfalls in stress corrosion testing, they also point to the need for some rationalization in the field of stress corrosion test methods. And yet there is a case for some diversity in relation to simulation of service conditions, since stress corrosion failures in service do initiate at plain surfaces, and frequently without pitting, as indeed they do at geometrical discontinuities, whether the latter be cracks or other defects or intentional features of design. It is necessary constantly to remember that in the final analysis laboratory tests must relate to service experience, pointing to the continuing necessity for simulative tests.

**SOME IMPORTANT CONSIDERATIONS IN THE DEVELOPMENT
OF STRESS CORROSION CRACKING TEST METHODS**

**R. P. Wei
Lehigh University
Bethlehem, Penna., U. S. A.**

**S. R. Novak
U. S. Steel Corporation
Monroeville, Penna., U. S. A.**

**D. P. Williams
NASA Ames Research Center
Mountainview, Calif., U. S. A.**

SUMMARY

In this paper, the need for recognizing certain potentially serious problems in the development of standard test methods for stress corrosion cracking studies is discussed. The importance of recognizing and satisfying the basic assumptions of the linear-elastic fracture mechanics analysis in experimentation is re-emphasized. The effects of nonsteady-state crack growth, including incubation, must be taken into account in determining the crack growth kinetics. These effects and the influences of steady-state crack growth kinetics, as well as, a host of geometrical, material and environmental variables, must be considered in arriving at suitable criteria for K_{Isc} determinations.

LIST OF SYMBOLS

a	crack length
da/dt	rate of crack growth
K	crack-tip stress-intensity factor
K_I	crack-tip stress-intensity factor for the opening mode
K_{Ic}	plane-strain fracture toughness
K_{II}	initial value of K_I
K_{Isc}	apparent threshold K_I for stress corrosion cracking
t	time
t_F	time-to-failure or life
t_{INC}	incubation time
t_{SC}	time for crack growth
T	temperature
W	specimen width
$Y(a/W)$	a geometrical parameter
σ	nominal applied stress or gross-section stress

APPENDIX

ASTM COMMITTEE E-24 ON FRACTURE TESTING OF METALS

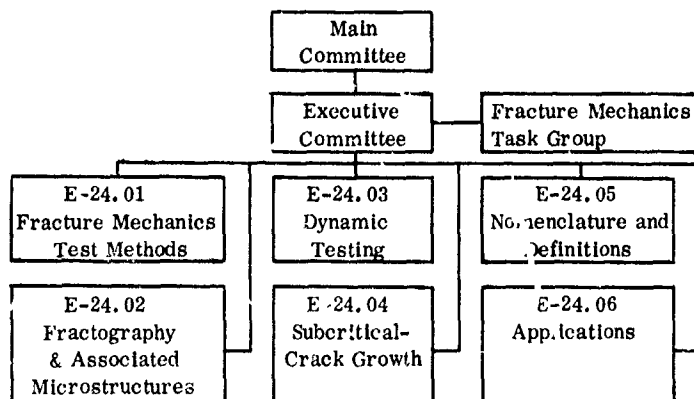
ASTM Committee E-24 on Fracture Testing of Metals is one of the standing committees of the American Society for Testing and Materials. The scope of the Committee is as follows:

To promote knowledge and advancement in the field of fracture testing by:

- (a) Promoting research and development on methods for appraisal of the fracture resistance of metals.
- (b) Developing recommended practices, methods of test, definitions, and nomenclature for fracture testing of metals, exclusive of fatigue testing.
- (c) Sponsoring technical meetings and symposia independently or in cooperation with other organizations.
- (d) Coordinating the committee activities with those of other relevant ASTM committees and other organizations.

It is organized into six Subcommittees and one Task Group as shown in the accompanying organizational chart. Three of the Subcommittees (E-24.01, E-24.03 and E-24.04) are primarily responsible for test methods development. E-24.02 and E-24.06 serve in an advisory capacity relating to metallurgical and design aspects of fracture and subcritical-crack growth. E-24.05 is concerned with nomenclature and definition of terms used in fracture testing. The Fracture Mechanics Task Group provides support in the theoretical aspects of fracture mechanics.

ORGANIZATIONAL CHART



R. P. Wei, S. R. Novak, and D. P. Williams

INTRODUCTION

The application of linear elastic fracture mechanics analyses to the study of stress corrosion cracking and other subcritical-crack growth problems has undergone considerable development during the past ten years and has met with considerable success. Members of both ASTM Committee E-24 on Fracture Testing of Metals and ASTM Committee G-1 on Corrosion of Metals have participated actively in the development and use of fracture mechanics in stress corrosion cracking studies (more generally, subcritical-crack growth studies) in the United States, through their respective subcommittees and task groups. Justification for the use of K_I (the crack-tip stress-intensity factor for opening mode) to characterize the mechanical crack driving force in stress corrosion cracking has been reviewed by Johnson and Paris [1] and by Wei [2]. Further experimental verification has been provided by the recent results of Smith et al [3] and Novak and Rolfe [4]. With the increasing acceptance of the fracture mechanics approach, and the attendant proliferation of new test methodology and terminology, it has become necessary and desirable to establish test standards, as early as possible, for the orderly development of this important field. ASTM Committees G-1.06 and E-24.04 have jointly undertaken this task for developing fracture mechanics based test methods. Like all other ASTM committees, Committee E-24 functions through the interest and voluntary efforts of its individual and corporate members. The organizational structure and scope of ASTM Committee E-24 and of its various subcommittees are summarized in the Appendix. In developing these recommended test methods, it is worthwhile to re-examine the basic assumptions of the analyses and the various other problems associated with stress corrosion testing to ensure proper development and utilization of test methods and correct interpretation of test results.

Experimental measurements of stress corrosion cracking susceptibility using precracked specimens follow essentially two related approaches. The choice of a particular approach is determined in part by tradition and motivation and in part by practical considerations of experimentation and cost. The simpler and more commonly used approach involves the measurement of the time-to-failure, t_f , (or, life) for precracked specimens under different applied loads, and the determination of a so-called threshold K_I (designated as K_{Isc}) below which, presumably, no failure can occur as a result of stress corrosion cracking [4,5]. The level of K_{Isc} in relation to K_{Ic} , the plane-strain fracture toughness of a material, gives a measure of its stress corrosion cracking susceptibility, and is often used in material selection and design [1]. This approach is akin to that utilized in conventional stress corrosion testing with smooth or mildly notched specimens, and is widely used in engineering and scientific research at the present time. The other approach is somewhat more complex and involves the determination of the crack growth kinetics, that is, measurements of the rate of crack growth, da/dt , as a function of the mechanical crack-driving-force, characterized by K_I , under controlled test conditions. This approach requires greater effort and more sophisticated instrumentation. It promises, however, to provide more useful information for quantitative design and life estimation, and for understanding the basic mechanisms for stress corrosion cracking. The kinetic approach has begun to receive greater attention in recent years, and has been of primary interest to the members of Committee E-24.04.

Experiences acquired during recent studies of the crack growth kinetics suggest that there are several problems which can affect both the determination of crack growth kinetics and that of K_{Isc} . These problems must be taken into consideration in developing standard methods of test for stress corrosion cracking. A brief review of these problems is made. The implication of these problems in terms of suggested criteria for K_{Isc} determination and in terms of the K_{Isc} concept itself are discussed. Possible methods for circumventing these problems are considered. Since the test methods are based on linear elastic fracture mechanics, it is appropriate to review briefly the essential assumptions of this approach. The basic test methods are also indicated.

ANALYTICAL FRACTURE MECHANICS CONSIDERATIONS

Since crack growth and stress corrosion attack would be expected to occur in the highly stressed region at the crack-tip, the stress (or, strain) distribution in this region is of primary importance. It has been shown that the crack-tip stress and displacement fields for an isotropic elastic body can be characterized in terms of a single parameter K , the crack-tip stress-intensity factor, which governs the intensity or magnitude of the local stresses at the crack-tip [6-8]. The crack-tip stress-intensity factor K depends on the type of loading and on the configuration of the body, including the size and shape of the crack. K factors for many different loading conditions and body configurations, and numerical solutions for K factors of practical test specimens have been well documented in the literature [7,9,10]. For engineering materials, some plastic deformation will occur in a region near the crack-tip. If the zone of plastic deformation is small in comparison with the crack size and with other planar dimensions of the body, the stress distribution in the large will not be seriously disturbed. The elasticity solutions will then represent a reasonable approximation of the stress and displacement fields near the crack-tip. Since the small zone of plastically deformed material at the crack-tip is contained within the surrounding elastic material, it is reasonable to expect that the behavior in this region would be governed by the surrounding elastic material and, thus, be characterized by the crack-tip stress-intensity factor K . Hence, it seems most appropriate to use the crack-tip stress-intensity factor K to characterize the mechanical crack-driving-force. For stress corrosion cracking studies, the stress-intensity factor for the opening-mode (mode I) of crack growth, K_I , is generally used, since the opening-mode predominates in stress corrosion cracking [2,6,7].

The use of the crack-tip stress-intensity factor K_I , defined by linear elasticity, to characterize the mechanical crack driving force is predicated, therefore, on the assumption of limited plasticity. The applicability of this approach to stress corrosion cracking and other fracture studies will depend on the experimental fulfillment of this fundamental assumption. Specimen size requirements based on this assumption have been discussed by Brown and Srawley [9] and by Wei [2]. Specific requirements pertaining to valid determinations of K_{Isc} and the influence of specimen size on the apparent K_{Isc} are discussed in detail by Novak in a separate paper [11]. These requirements and specimen size effects must be clearly understood before meaningful standard test procedures can be developed.

BASIC TEST METHODS

Various types of specimens and methods of loading can be used to determine the stress corrosion cracking properties of materials. The fracture mechanics based specimens may be broadly separated into three groups:

1. Constant load, increasing K_I specimens
2. Constant displacement, decreasing K_I specimens
3. Constant K_I specimens.

The first group of specimens is exemplified by the cantilever-bend specimens; the second, by the bolt-loaded WOL specimens; and the third, by tapered DCB specimens subjected to constant applied load. Of course, by judicious placement of loads and choice of loading conditions, increasing or decreasing K_I conditions may be obtained on any of these specimen groups. Specimens of the first and second groups have been commonly used for kinetic studies and/or K_{Isc} determinations. Problems associated with the use of these types of specimens will be discussed below.

KINETICS OF CRACK GROWTH AND LIFE (TIME-TO-FAILURE)

In studying crack growth under stress corrosion conditions, it has been generally assumed that there is a one-to-one correspondence between the rate of crack growth and the mechanical crack driving force characterized by K_I . This correspondence certainly exists for the case of steady-state crack growth, and must be true if K_I is to be a proper representation of the crack driving force. This correspondence, however, does not preclude the occurrence of a number of non-steady-state phenomena. Close examination of the crack growth process shows that crack growth occurs in six stages:

1. Crack growth on rising load
2. Initial transient crack growth
3. Incubation period*
4. Crack acceleration
5. Steady-state crack growth
6. Onset to failure or crack growth instability.

The occurrence of crack extension on loading, followed by transient growth, has been observed by Li et al. [12], Barsom [13], and Landes and Wei [14]. This behavior is illustrated schematically in Figure 1. Following the initial transient growth, the crack appears to stop growing, or enter an incubation period, before accelerating again to some steady-state rate of growth appropriate to the prevailing K_I . Landes and Wei showed that this nonsteady-state growth period is a function of K_I and of the test temperature, Figures 2 and 3 [14]. The incubation period and the period of accelerating crack growth, leading to steady-state growth are illustrated more clearly by the recent results of Hudak and Wei [15], Figure 4. ** The existence of an incubation period for precracked specimens has been demonstrated by Benjamin and Steigerwald [16] on AISI 4340 steel tested in water. These authors showed that the incubation period is affected by prior history [16]. The strong dependence of the incubation period on K_I is shown by the recent results of Novak [17] for a highly alloyed 180 ksi yield-strength steel tested in synthetic sea water (ASTM Designation D-1141-52) at room temperature, Table I. These results show that the incubation period can be quite long in certain alloy-environment systems.

TABLE I
Influence of K_I on Incubation Time
CONSTANT-DISPLACEMENT WOL SPECIMENS
(Decreasing K_I)

K_{II} (ksi $\sqrt{\text{in}}$)	Extent of Crack Growth (inch) after					
	300 hrs	700 hrs	1400 hrs	2200 hrs	3500 hrs	5000 hrs
180	ND	0.35	0.76	1.00	1.12	---
150	ND	ND	ND	0.28	0.52	0.61
120	ND	ND	ND	ND	0.03	0.045
90	ND	ND	ND	ND	ND	0.045

ND - No Detectable Growth

* Incubation period is defined as that period during which the rate of crack growth is much less than 10^{-6} inch per minute.

** Crack growth was monitored by a displacement gage. The oscillatory nature of the steady-state growth rate shown in Fig. 4 is principally an artifact introduced by changes in displacement that result from oscillations in the dead-weight loading device.

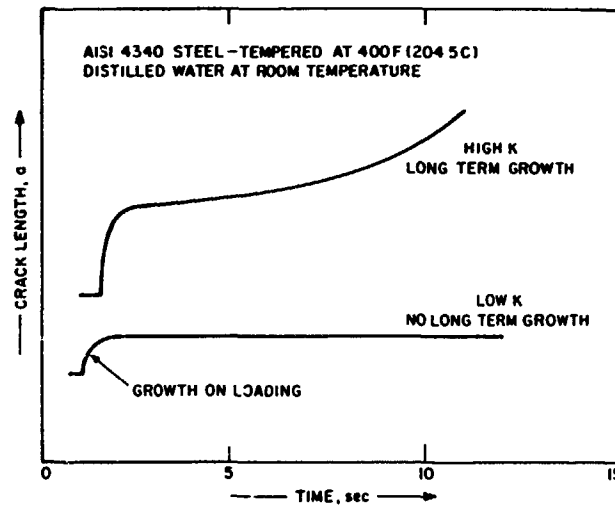


Figure 1: Schematic Illustration of Sustained-Load Crack Growth Behavior [14]

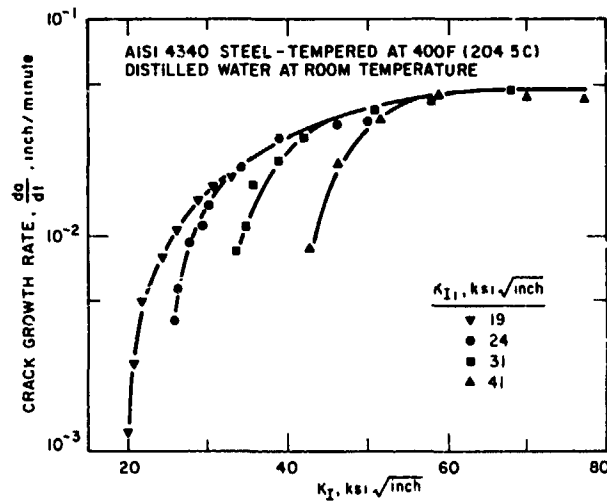


Figure 2: Kinetics of Sustained-Load Crack Growth Showing the Effect of Initial K_I [14]

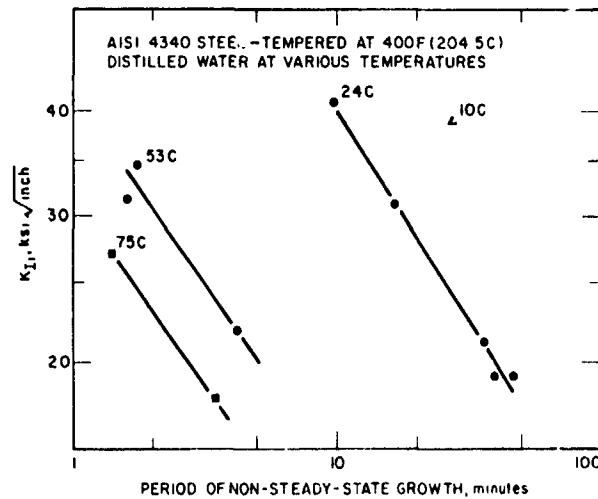


Figure 3: The Influence of K_{II} and Test Temperature on the Period of Non-Steady-State Crack Growth [14]

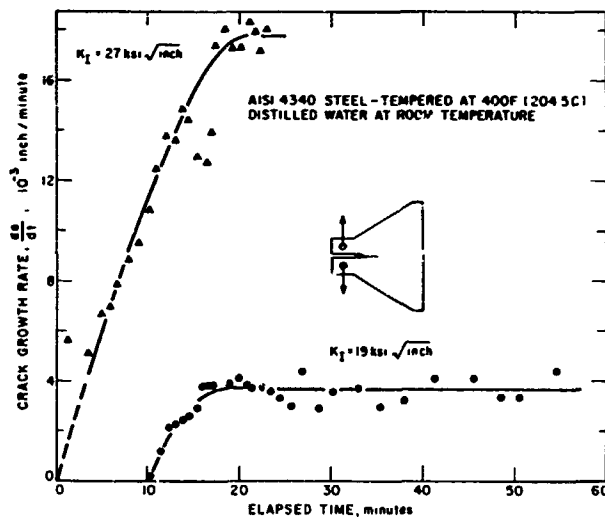


Figure 4: Sustained-Load Crack Growth under Constant K_I Showing Incubation, Crack Acceleration and Steady-State Stages of Crack Growth [15].

Typical steady-state crack growth response as a function of K_I is illustrated by the results of Williams [18], Figure 5, and is also shown schematically in Figure 6a. Steady-state crack growth kinetics may be divided into three regions. Region I is highly dependent on K_I , and may reflect crack acceleration for certain types of tests.

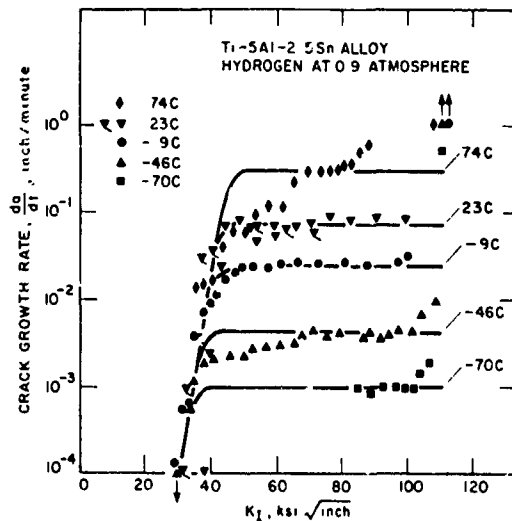


Figure 5: Typical Steady-State Crack Growth Kinetics [18]

Region II is nearly independent of K_I and represents a range where crack growth is limited by the embrittling chemical process. In region III, crack growth approaches the condition for unstable growth. For high strength materials, under conditions approximating plane-strain, the condition for the onset of unstable growth is defined by $K_I = K_{IC}$, where K_{IC} is the plane-strain fracture toughness of the material.

The life of a specimen is a function of both the incubation and crack growth processes. A typical time-to-failure (life) versus K_{II} curve for a constant-load, increasing K specimen is illustrated schematically in Figure 6b, where K_{II} denotes the initial applied stress-intensity factor. The time-to-failure (t_F) is composed of an incubation period (t_{INC}) and a period of slow crack growth (t_{SC}).

$$t_F = t_{INC} + t_{SC} \quad (1)$$

The incubation time is a function of K_I and of prior history [15-17]. The period for slow crack growth depends on the specimen configuration, type of loading and the details of the crack growth kinetics [2, 18]. The time-to-failure is related inversely to the rate of crack growth, Figure 6, and may be estimated from the kinetic data. The general form of the crack growth kinetics may be expressed as follows:

$$\frac{da}{dt} = G(K_I, K_{II}, T, \text{ and other material, environment and test variables}) \quad (2)$$

where T is the test temperature. The inclusion of K_{II} , the initial stress-intensity factor, reflects the recognition that a steady-state rate of crack growth may not be established immediately on loading. Thus, da/dt can be dependent on time for a given K_{II} . For steady-state crack growth, da/dt becomes simply a function of K_I and of variables other than K_{II} , and is, therefore, independent of time.

$$\frac{da}{dt} = F(K_I, T, \dots) \quad (3)$$

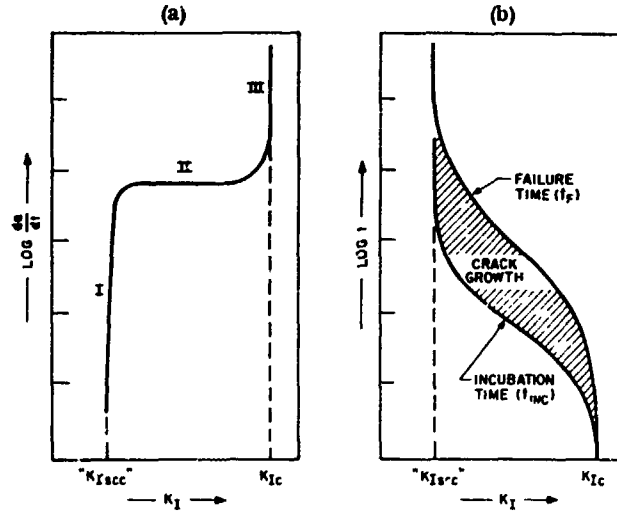


Figure 6: Schematic Representations of the Crack Growth Kinetics and Time-to-Failure under Sustained Loads

Under the assumption of steady-state crack growth, the time-to-failure for a typical test specimen may be obtained by direct integration, when the applied load and all of the other variables are maintained constant. For constant load tests:

$$\frac{dK_I}{dt} = \frac{dK_I}{da} \frac{da}{dt} = \frac{dK_I}{da} F \quad (4)$$

Since, for the steady-state case, the rate of crack growth is time independent Equation 4 may be integrated directly. Separation of variables and integration gives the time-to-failure as:

$$t_F = t_{INC} + \int_{t_{INC}}^{t_F} dt = t_{INC} + \int_{K_{II}}^{K_{Ic}} \left[\frac{dK_I}{da} \cdot F \right]^{-1} dK_I \quad (5)$$

The incubation time t_{INC} is a function of K_{II} , the initial stress-intensity factor. K_{Ic} is the plane-strain fracture toughness of the material. The stress-intensity factor K_I can be expressed in the form [9]:

$$K_I = \sigma a^{\frac{1}{2}} Y \left(\frac{a}{W} \right) \quad (6)$$

where σ = the nominal applied stress, a = the crack length, $Y \left(\frac{a}{W} \right)$ = a parameter representing the crack and specimen geometries, and W = the specimen width. Inspection of Equations (5) and (6) indicates that the time-to-failure will depend on the specimen geometry and size. For example, the time-to-failure for geometrically similar specimens loaded to identical K_{II} levels are expected to be different. Similarly, specimens with different initial crack sizes, loaded to the same initial K_{II} , will produce different lives. Typical time-to-failure curves computed on the basis of crack growth kinetics and assumed crack geometries are shown in Figures 7 and 8 [18]. Even though the incubation time and non-steady-state crack growth were neglected in these calculations, the essential features of the t_F versus K_{II} curves are reproduced. It is clearly seen that the time-to-failure is related to the crack growth kinetics, and that it is dependent on geometry and environmental conditions.

IMPLICATIONS FOR STRESS CORROSION CRACKING STUDIES

In the foregoing discussion, it has been shown that the steady-state rate of stress corrosion crack growth is uniquely related to the crack driving force, with other conditions being constant. The mechanical component of the crack driving force may be characterized, under the assumption of limited plasticity, by the crack-tip stress-intensity

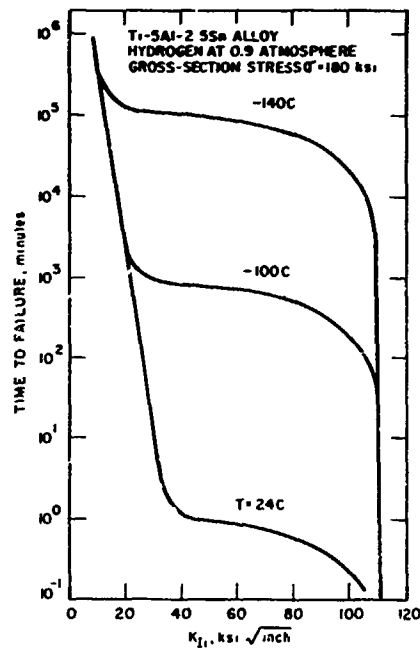


Figure 7: Computed Time-to-Failure Curves (Excluding Incubation Time) Showing the Influence of Test Temperature [18].

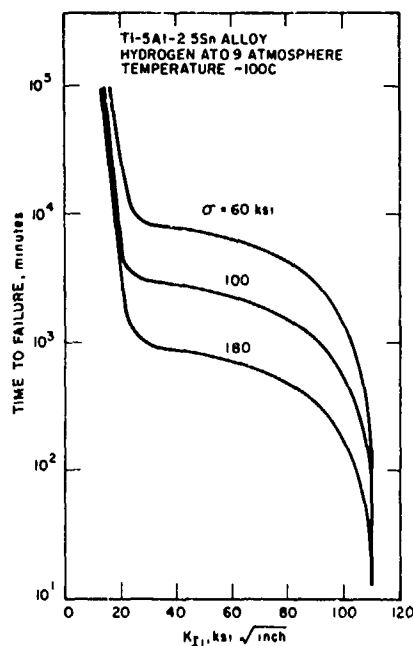


Figure 8: Computed Time-to-Failure Curves (Excluding Incubation Time) Showing the Effect of Gross-Section Stress or Initial Crack Size [18].

factor, K_I , defined by linear elastic fracture mechanics. The kinetic information can be quite useful in making quantitative estimates of the service lives of structural components, provided that the incubation time and the period of non-steady-state crack growth can be handled in some satisfactory way. The existence of an incubation period and non-steady-state crack growth presents serious practical problems in the determination and utilization of crack growth kinetics. Figures 2 and 4 show that the incubation phenomenon and non-steady-state crack growth can lead to an under-estimation of the steady-state rate of crack growth, with a consequent over-estimation of the safe operating life.

The incubation phenomenon and the crack growth kinetics (for both the steady-state and non-steady-state cases) can affect the evaluation and use of the so-called threshold stress-intensity factor for stress corrosion cracking,

K_{Isc} , as well. Kinetic data are sometimes used for estimating K_{Isc} . If the apparent rapid decrease in the rate of crack growth shown in Figure 2 is interpreted as an approach to the threshold K_I level, erroneously high estimates of K_{Isc} would result. The estimated value of K_{Isc} would appear to depend on the starting K_I level (K_{I1}) used in testing. For the usual stress corrosion cracking (life) tests, some type of criteria is normally used to terminate the test and to define an estimated value of K_{Isc} . Usually, K_{Isc} is defined as that K_I level at which "no failure" or "no observable crack growth" has occurred after some prescribed period of time. Since it has been shown through consideration of the crack growth kinetics that the time-to-failure is quite dependent on the loading condition, specimen size and geometry, and environmental conditions, such criteria can lead to serious errors in the estimation of K_{Isc} . The problem is compounded by the existence of incubation. The combined effects of incubation and crack growth kinetics on the apparent K_{Isc} obtained from constant load, cantilever bend tests of another 180 ksi yield strength, high alloy steel in synthetic sea water at room temperature, are shown in Table 2. It is seen that by increasing the cut-off time from 100 hours to 10,000 hours (or, from approximately 4 days to over one year), the apparent K_{Isc} is decreased from 170 ksi $\sqrt{\text{in.}}$ to 25 ksi $\sqrt{\text{in.}}$ [17]. Thus, substantial error can be introduced by using short-time test data in design. Because the apparent K_{Isc} are so dependent on test procedures and conditions, its practical utility must be carefully re-evaluated.

TABLE II
Influence of Cut-Off Time on Apparent K_{Isc}
CONSTANT-LOAD CANTILEVER BEND SPECIMENS
(Increasing K_I)

ELAPSED TIME (hours)	APPARENT K_{Isc} (ksi $\sqrt{\text{in.}}$)
100	170
1,000	115
10,000	25

In developing test specifications, one must be certain that the incubation period and the non-steady-state crack growth processes are reduced or eliminated in experimentation, and/or taken into proper consideration in data reduction and interpretation. The influence of the kinetics of steady-state crack growth should also be considered. For kinetic studies, constant K specimens may be used. The testing time at each K_I level, however, must be sufficiently long to ensure the establishment of steady-state conditions. The incubation time at low K_I levels may be too long to justify the use of this test method. Since the incubation time is expected to be much shorter at high K_I levels, Table I, the use of a constant displacement, decreasing K specimen may be more attractive. Experience with this type of specimen for kinetic studies is limited at this time. Further development will be required. For K_{Isc} determinations, this type of specimen has been used and offers definite advantages. By starting at high K_I levels, it is expected that the long incubation times can be avoided. Schematic representation of typical test results from such tests is illustrated in Figure 9. Consideration of the proper cut-off time must still be established. Design of specimen must be such that the decrease in K_I with crack prolongation is not too rapid. A rapid decrease may produce delays in crack growth or exhibit the pre-stressing effect reported by Carter [12], with consequent over-estimation in K_{Isc} .

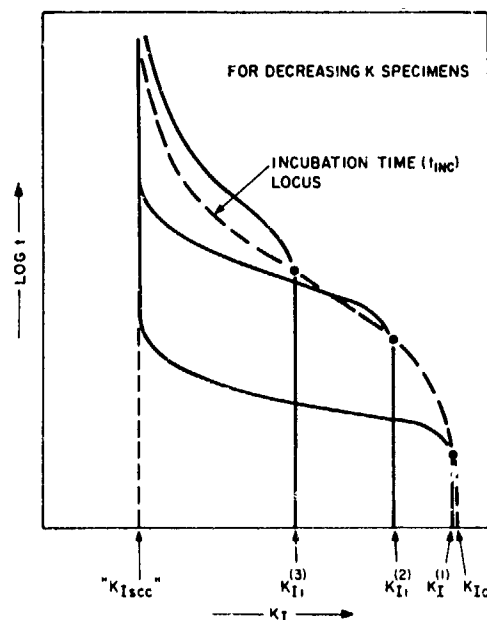


Figure 9: Schematic Representation of Typical Stress Corrosion Cracking Behavior in a Decreasing K Test

SUMMARY

In this paper, the need for recognizing certain potentially serious problems in the development of standard test methods for stress corrosion cracking studies is discussed. To obtain valid data from fracture mechanics based test methods, the basic assumptions of the linear-elastic fracture mechanics analyses must be clearly recognized and satisfied in experimentation. The effects of incubation and non-steady-state crack growth must be taken into account in determining the crack growth kinetics. These effects and the influence of steady-state crack growth kinetics, as well as, a host of geometrical, material and environmental variables, must be considered in arriving at suitable criteria for K_{Isc} determinations.

REFERENCES

1. H. H. Johnson and P. C. Paris, *Journal of Engineering Fracture Mechanics*, **1**, 3-45 (1968).
2. R. P. Wei, in *Proceedings of Conference - Fundamental Aspects of Stress Corrosion Cracking*, Ohio State University, 104 (1969).
3. H. R. Smith, D. E. Piper and F. K. Downey, "A Study of Stress-Corrosion Cracking by Wedge-Force Loading," *Engineering Fracture Mechanics*, Vol. 1, No. 1 (June 1968), pp. 123-128.
4. S. R. Novak and S. T. Rolfe, "Comparison of Fracture Mechanics and Nominal Stress Analyses in Stress Corrosion Cracking," *Corrosion*, Vol. 26, No. 4 (April, 1970), pp. 121-130.
5. B. F. Brown and C. D. Beachem, *Corrosion Science*, **5**, 745-50 (1965).
6. G. R. Irwin, in *Structural Mechanics*, Pergamon Press, New York, N. Y., 557 (1960).
7. P. C. Paris and G. C. Sih, *Fracture Toughness Testing and Its Applications*, ASTM STP 331, 30-83 (1965).
8. G. C. Sih and H. Liebowitz, in *Fracture - An Advanced Treatise*, Vol. II, H. Liebowitz, editor, Academic Press (1970).
9. W. F. Brown, Jr. and J. E. Srawley, *Plane Strain Crack Toughness Testing of High Strength Metallic Materials*, ASTM STP 410 (1966).
10. H. R. Smith and D. E. Piper, "Stress Corrosion Testing with Precracked Specimens," Boeing Document D6-24872, (June 1970).
11. S. R. Novak, "Critical Aspects in the Evaluation of K_{Isc} ," to be published (1971).
12. Che-Yu Li, P. M. Talda and R. P. Wei, unpublished results (1965).
13. J. M. Barsom, unpublished results (1969).
14. J. D. Landes and R. P. Wei, "The Kinetics of Subcritical Crack Growth under Sustained Loading," to be published.
15. S. J. Hudak and R. P. Wei, unpublished results (1971).
16. W. D. Benjamin and E. A. Steigerwald, *Transactions of the ASM*, **60**, 547-8 (1967).
17. S. R. Novak, unpublished results (1971).
18. D. P. Williams, "A New Criterion for Failure of Materials by Environment-Induced Cracking," to be published (1971).
19. C. S. Carter, "Effect of Prestressing on the Stress-Corrosion Resistance of Two High-Strength Steels," Boeing Document D6-25275, (May, 1970).

ACKNOWLEDGMENT

One of the authors (R. P. Wei) wishes to acknowledge the support of this work by the Office of Naval Research through Contract N00014-68-A-0514.

CURRENT PROGRESS IN THE COLLABORATIVE TESTING PROGRAMME OF THE
STRESS CORROSION CRACKING (FRACTURE MECHANICS) WORKING GROUP

A. H. Priest
Section Leader
The Corporate Laboratories of the
British Steel Corporation
Hoyle Street
Sheffield S3 7EY, England

P. McIntyre
S.S.O.
The Corporate Laboratories of the
British Steel Corporation
Hoyle Street
Sheffield S3 7EY, England

S Y N O P S I S

A preliminary analysis is presented of the initial results of the Collaborative Testing Programme of the Stress Corrosion Cracking (Fracture Mechanics) Working Group of the BSC Corporate Laboratories. In this analysis the results are interpreted in terms of the influences of specimen geometry, maximum fatigue pre-cracking stress intensity, test temperature and laboratory error. It is concluded that the only significant errors can be attributed to differences in the calibration and accuracy of testing equipment between the participating laboratories and to failure to adhere to the recommended testing procedure which is found to be satisfactory for the material and environment which were used.

CURRENT PROGRESS IN THE COLLABORATIVE TESTING PROGRAMME OF THE
STRESS CORROSION CRACKING (FRACTURE MECHANICS) WORKING GROUP

A. E. Priest and P. McIntyre

INTRODUCTION

The Stress Corrosion Cracking (Fracture Mechanics) Working Group of the British Steel Corporation, Corporate Laboratories was originally formed in October, 1969 by members of the Fracture Mechanics (High Strength Steels) Working Group who were interested in the application of fracture mechanics to the study of stress corrosion cracking.

The present structure of the Working Groups in the field of fracture mechanics is illustrated in Figure 1.

Thirty members representing twenty-seven organisations are named in the constitution list of the Stress Corrosion Cracking (Fracture Mechanics) Working Group whose chairman is Mr. J. E. Truman of the Brown-Firth Research Laboratories.

At the first meeting of the Working Group the following terms of reference were agreed:

"To collaborate in the collection and presentation of data on the stress corrosion cracking of metallic materials. To provide a forum for exchange of views on testing techniques, and interpretation and application of data. To carry out supporting studies with the emphasis on crack growth, and to recommend preferred testing techniques".

The first activity of the Working Group was to conduct a survey of the involvement of members in the field of stress corrosion testing and of their present testing techniques. This survey was reviewed at the second meeting of the Working Group and it revealed that, although several laboratories were committed to the conventional testing of uncracked specimens, the majority were either already equipped or were prepared to equip for the stress corrosion testing of pre-cracked test pieces.

It was decided that the interests of the Working Group would be best served by a collaborative test programme with regard to the eventual standardisation of fracture mechanics stress corrosion testing procedures. The purpose of the present paper is to review the progress that has been made with the preliminary stage of this collaborative programme - the determination of K_{ISCC} for 300M steel.

MATERIAL AND EXPERIMENTAL TECHNIQUES

The material and experimental techniques to be used in the collaborative programme were discussed at the next meeting of the Working Group.

It was decided that a material possessing a reasonably high K_{ISCC} value and freedom from crack branching should be used. For these reasons 300M steel was selected for the programme. Supply of this material and its heat treatment were kindly undertaken by Brown-Firth Laboratories. Details of the analysis and heat treatment are given in Tables 1 and 2. It was decided that for the initial investigation the experimental techniques to be used should not be specified too rigidly - if necessary more rigorous control could be introduced into subsequent test programmes. The choice of specimen geometry was, therefore, left open to each participant so that existing test facilities could be used wherever possible. A solution of 3.5% by weight of analar quality sodium chloride in de-ionised water was recommended for the environment, to be either drip fed on to the specimen or contained in a stirred bath surrounding the specimen. In laboratories where de-ionised water was unavailable, distilled water was to be used. Since it had been observed for some steels that the subsequent stress corrosion behaviour depended on whether or not pre-cracking was conducted in air or in salt solution it was specified that sodium chloride solution should be introduced during the fatigue operation and testing commenced immediately afterwards. In those laboratories without fatigue facilities where specimens were to be pre-cracked in batches elsewhere it was suggested that the specimens should be both fatigued and then stored in the presence of acetone which, like salt solution, eliminates the long incubation periods often observed with specimens which have been pre-cracked in air.

Other specified experimental details were that the environment should be introduced before load application which should be made in as smooth a manner as possible. It was requested that records should be kept of times to failure, test temperature, maximum fatigue load (which was to be kept as low as possible, and preferably below 20 ksi/in.), crack branching - where this occurred, and, where possible, incubation periods and crack growth rates.

In order to determine K_{ISCC} accurately and with the minimum amount of material this was to be provided in the form of 1.375 in. by 0.625 in. bar - sufficient for $\frac{1}{2}$ in. thick specimens, and use was to be made of a binary search technique for K_{ISCC} measurement. The binary search procedure which is schematically illustrated in Figure 2, enables K_{ISCC} to be determined, at least in theory, to within $1/64$ of K_{IC} from only seven specimens. The first specimen is used to determine K_{IC} using the same test rig as for subsequent stress corrosion tests, the initial stress intensities for which are expressed as fractions of K_{IC} beginning with $\frac{1}{2} K_{IC}$ and subsequently depending on whether or not failure occurs within the prescribed time limit. The time limit chosen for these tests was 100 hours as originally proposed for low alloy steels by A.S.T.M.⁽¹⁾

Of the 27 organisations belonging to the Working Group, 19 agreed to participate in the collaborative programme. Each laboratory was responsible for the machining of its own test pieces, but heat treatment was carried out in a single batch. The heat-treated specimens were returned for final machining and testing at the end of last year, since when two participating laboratories have dropped out of the programme, eleven laboratories have submitted their results and six laboratories are still conducting tests. It was

originally anticipated that completion of this preliminary test programme would be within ten months, but, as is shown in Figure 3, testing is incomplete after two years. Major obstacles to progress have been delays due to machining and testing difficulties.

An early set-back to the programme was that the size specification for the rolled material was not met. This precluded the possibility of using tension specimens possessing the same orientation as bend specimens. It was therefore necessary for bend specimens to be notched transversely to the rolling direction whereas tension specimens were notched longitudinally to the rolling direction. However, two laboratories, using both bend and tension specimens have shown the K_{ISCC} values for the two orientations to be the same to within 1 ksi $\sqrt{\text{in}}$.

RESULTS AND DISCUSSION

Tables listing all of the test data from the participating laboratories are given in Appendices 1 and 2.

Figure 4 shows the values of time to failure as a function of initial stress intensity during stress corrosion and also the values of fracture toughness which were measured on the stress corrosion testing rigs. In this figure no attempt has been made to correct for the variations in specimen width which occurred as a result of the different specimen geometries used and there is a clear tendency for the times to failure at a given stress intensity level to increase with increasing specimen width.

A considerable reduction of scatter is obtained by normalisation of the results in terms of time to failure per inch of specimen width by dividing the times to failure by the ligament depth below the fatigue crack ($W - a$). This treatment eliminates the systematic variation of time to failure with specimen size so that the results for any given specimen geometry occur randomly within the scatter band.

A further slight reduction in scatter is obtained when the initial stress intensities are also normalised. This is achieved by dividing the initial stress intensities used in each laboratory by the value of K_{IC} determined on the stress corrosion test rig in order to eliminate the influence of test rig calibration. Figure 5 shows the reduced scatter due to these normalisation procedures when applied to specimens in which failure was observed.

It is evident from the experimental data that there are two distinct regimes in the relationship between time to failure and initial stress intensity. In the first group of results, at fairly high initial stress intensities, the time to failure is relatively independent of initial stress intensity while in the second group of results, at lower initial stress intensities there is a strong dependence of time to failure on initial stress intensity so that a small change in initial stress intensity can change the time to failure by several orders of magnitude. This behaviour precludes the possibility of determining absolute values of K_{ISCC} from the experimental data and therefore the highest stress intensity values of tests which did not produce failure within 100 hours have been taken as the K_{ISCC} values in the analysis of the collaborative test programme results.

The observation of two regions of behaviour on the plot of time to failure against initial stress intensity can be explained by differences in the exact mechanism of failure within each region. In the first group, where the time to failure is relatively independent of initial stress intensity, the fracture surfaces in the stress corrosion region were entirely intergranular right from the tip of the fatigue crack where initiation occurred. However, the fracture surfaces of those specimens in the second group, which display a marked dependence of time to failure on initial stress intensity, revealed, on close examination, the presence of a narrow, almost featureless, zone between the tip of the fatigue crack and the onset of the intergranular stress corrosion region. The width of this band increased as the time to failure increased and Figure 6 illustrates such a zone of width 0.006 in. which was observed on a specimen which failed after 1,210 hours.

These fracture observations suggest that general corrosion at the tip of the fatigue crack can play an important role in the failure of specimens belonging to the second group where low initial stress intensities are associated with prolonged failure times. In the first group of specimens the initial stress intensities applied were sufficiently high to promote the immediate onset of stress corrosion cracking, while in the second group of specimens the initial stress intensities were insufficient to promote stress corrosion cracking until general corrosion had effectively increased the stress intensity to the required threshold value. Additional evidence for this conclusion was supplied by those laboratories which monitored crack growth rates and reported no incubation periods or extremely slow crack extension until just prior to failure for those specimens belonging to the second group.

The contribution of general corrosion is not solely limited to an extension of the fatigue crack and Figure 7 shows the effects of general corrosion on the surface of a $\frac{1}{2}$ in. CKS (compact tension) specimen which failed after 1,072 hours. In this case a reduction in thickness of 0.013 in. occurred due to general corrosion, as well as a reduction of 'W' and an increase in 'a' by 0.006 in. This effectively increased the initial stress intensity from 13.6 ksi $\sqrt{\text{in}}$. at the onset of the test to 14.3 ksi $\sqrt{\text{in}}$. at the onset of stress corrosion cracking.

This work emphasises the need for extreme care in selecting a failure criterion for K_{ISCC} determinations. For this material the transition between groups 1 and 2, the stress corrosion motivated and general corrosion motivated regions, respectively, occurred at about 10 hours test duration but even after 100 hours duration the contribution by general corrosion was negligible and so it would appear that the selected failure criterion of 100 hours is appropriate for this material.

THE INFLUENCE OF SPECIMEN GEOMETRY

The following specimen geometries were used by participants in the test programme:

10 x 10 mm (Charpy) Bend
 6 x 1 x $\frac{1}{2}$ in. Bend
 14 x 30 x 150 mm Bend
 8 x 0.8 x 0.2 in. Tension
 $\frac{1}{2}$ in. C.K.S. (Compact Tension)
 $\frac{1}{2}$ in. T - WOL (Tension)

The analysis of specimen geometry influence is complicated because while most of the specimens were notched transversely to the rolling direction, the $\frac{1}{2}$ in. C.K.S. and $\frac{1}{2}$ in. T-type WOL specimens were notched longitudinally. It is evident from the experimental results shown in Figure 8, however, that with the exception of the constant displacement specimens, all of the test results fall within the same scatter band, indicating that for this material neither specimen orientation nor geometry have a marked effect on the K_{ISCC} values. The large amount of scatter in the results obtained with constant displacement specimens can be explained in the light of the recent work at the BSC Corporate Laboratories on crack blunting during stress corrosion cracking⁽²⁾. This has shown that intergranular stress corrosion cracks become progressively more blunt as they propagate. The value of the arrest stress intensity is therefore a function of the initial stress intensity. Stress corrosion cracks in those specimens loaded to an initial stress intensity well in excess of K_{ISCC} will therefore propagate for a considerable distance prior to arrest which, because of the blunting effect, will occur at a much higher stress intensity than that required for initiation of a stress corrosion crack from a fatigue crack. On the other hand, the application of an initial stress intensity only just above K_{ISCC} would result in arrest after a small amount of growth before noticeable blunting could occur. In this way, laboratory J, using a constant displacement specimen, obtained a very high arrest value of 24.2 ksi $\sqrt{\text{in.}}$ for K_{ISCC} using an initial stress intensity of 24.5 ksi $\sqrt{\text{in.}}$ whereas laboratory B obtained an arrest K_{ISCC} value of 16.0 ksi $\sqrt{\text{in.}}$ using an initial stress intensity of 16.3 ksi $\sqrt{\text{in.}}$. The K_{ISCC} values determined by all the other laboratories lay in the range 15.7 to 18.9 ksi $\sqrt{\text{in.}}$ using the 100 hour criterion, and a one-way analysis of variance of the results showed the deviations between specimens of different geometry were not significant within a 5% confidence limit. The results of this analysis are shown in Table 3.

THE INFLUENCE OF MAXIMUM FATIGUE PRE-CRACKING STRESS INTENSITY

Previous work had indicated that the maximum stress intensity used during the fatigue pre-cracking of specimens can influence the value of K_{ISCC} subsequently determined so that high maximum fatigue loads result in high K_{ISCC} values. It was therefore recommended that the maximum stress intensity in fatigue ($K_f \text{ max}$) should be limited to 20 ksi $\sqrt{\text{in.}}$ but in practice most of the laboratories used higher values than this. Figure 9 shows K_{ISCC} values plotted as a function of $K_f \text{ max}$ and shows that for this material the fatigue stress intensity has no influence. The distribution of data points appears to be completely random despite the fact that $K_f \text{ max}$ values in excess of twice the recommended level were used.

THE INFLUENCE OF TEST TEMPERATURES

Test temperatures in the range 15-27°C were reported by the participating laboratories; the maximum individual range being 12°C.

The K_{ISCC} results are plotted as a function of test temperature in Figure 10 which, apart from two results appears to indicate a trend towards lower K_{ISCC} values as the temperature increases. To test this trend a test was conducted 40°C but this indicated no reduction in K_{ISCC} below that measured at ambient temperature. It must therefore be concluded that variations of test temperature within the normal range have no significant influence on the value of K_{ISCC} .

ANALYSIS OF LABORATORY ERROR

Two approaches have been adopted in the analysis of results for errors attributable to individual laboratory procedures:

Firstly, the results of all tests conducted by laboratories using an initiation rather than an arrest technique have been interpreted in terms of the binary search procedure which was the recommended testing method and which is illustrated in Figure 2. This procedure required each laboratory to determine K_{IC} on the stress corrosion rig and then to conduct six stress corrosion tests in order to pinpoint K_{ISCC} to within $1/64 K_{IC}$. Unfortunately, not all of the laboratories adhered rigidly to this practice, as is apparent from Table 4 which shows for each laboratory the result of the K_{IC} determination and the number and outcome of tests conducted on the basis of the binary search procedure. Also shown are the K_{ISCC} values determined which are expressed in terms of K_{IC}

64

Difficulties in the prediction of the exact initial fatigue crack length from the unbroken specimen prior to testing precludes the possibility of applying an initial stress intensity accurate to better than $1/64 K_{IC}$.

Therefore, only those deviations from the mean value of K_{ISCC} which exceed $1/64 K_{IC}$ can be considered to be significant. Table 4 shows most of the K_{ISCC} values determined to be within the range $(\frac{20}{64} \pm \frac{1}{64}) K_{IC}$ and of these results, deviations from the absolute mean values, which are reflected by deviations of the K_{IC} value from the mean value of 57.5 ksi $\sqrt{\text{in.}}$, can be attributed to errors in the calibration of the testing equipment. Errors of this type would, for instance, be due to an inaccuracy in the assessment of the mechanical advantage of the loading system and such errors have evidently occurred since one laboratory conducted stress corrosion tests of more than 20 minutes duration at a nominal initial stress intensity which was in excess of the K_{IC} values obtained by six other laboratories.

One form of error which is not apparent in this analysis of the results is that due to failure to take into account the weight of the balance pan on the end of the loading beam. Such an error would have caused an otherwise inexplicable deviation of the ratio K_{ISCC}/K_{IC} from the mean. In fact only two

of the results fall outside the range $(\frac{20}{64} \pm \frac{1}{64}) K_{IC}$.

Laboratory E obtained a value of K_{ISCC} equal to only $16/64 K_{IC}$. However, their value of K_{IC} , at $62.2 \text{ ksi}\sqrt{\text{in.}}$ was the highest obtained by any laboratory and also the specimen thickness used, at 0.20 in. was the smallest used and only just within the size criterion for a valid K_{IC} determination with this material. It is likely that the larger proportion of predominantly plastic behaviour at the edges of these specimens contributed to a higher K_{IC} value than was obtained from the thicker specimens used elsewhere. Such plasticity effects would be insignificant at the lower stress intensities used during stress corrosion testing and so although the K_{ISCC} value obtained was a relatively small fraction of K_{IC} , its absolute value was comparable with those from other laboratories.

Laboratory G2 also obtained a low value of K_{ISCC} equal to $\frac{17}{64} K_{IC}$. In this case the laboratory error can be attributed to failure to observe the prescribed testing technique since Table 4 shows that an incomplete binary search was conducted. Because of this the initial stress intensities used were not sufficiently closely spaced to allow an accurate determination of K_{ISCC} . Several other laboratories also failed to complete the binary search procedure but fortuitously succeeded in determining K_{ISCC} with reasonable accuracy.

It can be concluded that analysis of the results in terms of the binomial search procedure enables sources of laboratory error to be readily ascertained and also enables errors due to failure to observe the correct testing procedure to be determined.

The alternative method of interpreting the results is to assume that all errors are associated with differences in the test machines used by the laboratories.

Two main sources of error are considered likely to influence the test results. The first type is arithmetical error, E_A , and is associated with the incorrect assessment of the weight of the loading arm of the test machine. The assumption must be made that the means of the K_{ISCC} and K_{IC} results are the correct values for the material. If this is so, then:

$$\frac{K_{IC} + E_A}{K_{ISCC} + E_A} = \frac{\bar{K}_{IC}}{\bar{K}_{ISCC}} = \bar{R};$$

where \bar{K}_{IC} and \bar{K}_{ISCC} are the mean values and \bar{R} is their ratio.

Hence:

$$E_A = \frac{K_{ISCC} \cdot \bar{R} - K_{IC}}{1 - \bar{R}} \text{ ksi}\sqrt{\text{in.}}$$

The second type of error is geometrical error, E_g , which may arise through either inaccuracies in the measurement of the length of the loading arm of the test machine or incorrectly calibrated weights. This causes erroneous bending moments in the case of bend tests or erroneous tensile loads in the case of tension tests. This form of error is apparent if both K_{ISCC} and K_{IC} values are significantly higher or lower than the mean values. Geometrical error can be calculated from the relationship:

$$E_g = \frac{K_{IC} - \bar{K}_{IC} - E_A}{\bar{K}_{IC}} = \frac{K_{ISCC} - \bar{K}_{ISCC}}{\bar{K}_{ISCC}} E_A$$

The relationships between K_{IC} and K_{ISCC} values of the individual laboratories are illustrated in Figure 11 in which the straight line indicates the locus of \bar{R} .

Data points lying on the locus line but at positions either higher or lower than the mean possess the geometrical error E_g .

Data points lying above or below the locus line possess the arithmetical error E_A .

A summary of the K_{ISCC} and K_{IC} values obtained by the laboratories is given in Table 5 together with the relevant E_A or E_g values. In determining the mean value of K_{IC} and K_{ISCC} , those values which were erroneous for some obvious reason were omitted from the calculation. Thus K_{IC} and K_{ISCC} values from the constant displacement tests were not considered for the reasons given earlier.

The arithmetical errors shown in the table vary between -3.82 and $+2.37 \text{ ksi}\sqrt{\text{in.}}$ while the geometrical errors vary between $+15$ and -13 per cent. It has already been shown that the binary search technique only enables K_{ISCC} values to be determined with an accuracy of not greater than $\pm 1/64 K_{IC}$, that is approximately $\pm 1 \text{ ksi}\sqrt{\text{in.}}$. Further errors also arise in estimating the length of the fatigue crack prior to the stress corrosion test and these probably give rise to errors in the order of $\pm 0.5 \text{ ksi}\sqrt{\text{in.}}$. The arithmetical errors in Table 4 which are less than $1.5 \text{ ksi}\sqrt{\text{in.}}$ are therefore insignificant and result from limitations imposed by the number of specimens available for the binary search. This leaves laboratories C, E and K with significant arithmetical errors (apart from Laboratories B and J which were not included in this analysis since they used an arrest technique).

Laboratory G had only completed four tests at the time of writing and from Table 3 it is evident that K_{ISCC} could only be determined to within $5/64 K_{IC}$, about $5 \text{ ksi}\sqrt{\text{in.}}$. In comparison E_A for this laboratory is insignificant.

The K_{IC} value for laboratory E of $62.2 \text{ ksi}\sqrt{\text{in.}}$ is significantly higher than those of the other laboratories but the K_{ISCC} value is toward the lower end of the latter band. It is possible that, as mentioned previously, the specimen thickness of 0.20 in. was approaching the limiting thickness for plane

strain at K_{IC} of 0.154 in. determined from the expression:

$$B = 2.5 \left(\frac{K_{IC}}{\text{yield stress}} \right)^2$$

The large arithmetical error could therefore result from an erroneous K_{IC} value rather than from miscalibration of the test rig.

The result from laboratory K is, therefore, the only one showing a significant arithmetical error which can only be attributed to an incorrect assessment of the weight of the loading arm on the test machine.

The standard deviation for K_{IC} values shown in Table 3 is 3.11 ksi $\sqrt{\text{in.}}$ which is 5.4% of the mean; this compares with a value of 4.3% of the mean for valid K_{IC} tests of high strength steels which was determined from the collaborative programme of the MG/EB Fracture Toughness Working Group. In view of the relative simplicity in the method of the K_{IC} determinations in the present tests this indicates that the test machines used in the stress corrosion tests are of comparable accuracy with those used in the fracture toughness tests.

Most of the variation in the K_{IC} and K_{ISCC} values listed in Table 5 appears to be related to geometrical error, E_g . The scatter of K_{IC} values found in the MG/EB Fracture Toughness Working Group collaborative programme within individual laboratories amounted to about + 4% which can be attributed to material variations. Geometrical errors greater than this in Table 5 should therefore be considered significant, which means that only laboratories A1, G2, C, D and I showed insignificant levels of E_g .

CONCLUSIONS

A preliminary survey of the collaborative test programme results of the Stress Corrosion Cracking (Fracture Mechanics) Working Group which have been compiled to date has yielded K_{ISCC} values in the range 15.3 to 18.9 ksi $\sqrt{\text{in.}}$ with a mean value of 17.0 ksi $\sqrt{\text{in.}}$ from specimens tested with an initiation technique using pre-cracked specimens and a 100 hour failure criterion.

A study of the results has shown that large differences can occur between K_{ISCC} values determined by initiation from a fatigue crack, and arrest from a stress corrosion crack in this material due to the blunting effect of the intergranular corrosion crack.

Neither specimen geometry nor maximum fatigue load during the pre-cracking procedure has been found to influence significantly the value of K_{ISCC} determined by initiation from a fatigue crack, nor the temperature variations in the range 15 - 27°C.

The main sources of error appear to be associated with differences in the calibrations and accuracies of test rigs between the participating laboratories although failure to observe the prescribed testing techniques has also contributed to some scatter in the results.

REFERENCES

1. A.S.T.M. Committee G 0106 Section 04 "Draft Proposals of Test for Stress Corrosion Cracking"; Bisra Confidential Report No. MG/ES/168/71.
2. A. H. Priest and P. McIntyre, "Factors Influencing Threshold Stress Intensity Values and Crack Propagation Rates During Stress Corrosion Cracking Tests of High Strength Steels"; Bisra Open Report No. MG/59/71.
3. "A Preliminary Analysis of the Materials Tested so far in the Fracture Toughness (High Strength Steels) Committee, Fracture Toughness K_{IC} Testing Collaborative Programme"; Bisra Confidential Report No. MG/EB/237/70.

ACKNOWLEDGEMENTS

The authors wish to express their gratitude to the Chairman and members of the Working Group listed in Appendix 3 for their valuable discussions and practical contributions to the programme. It should be noted that the authors are responsible for all interpretations based on the results of the programme.

TABLE 1

Chemical Composition Cast No. VA7086

Steel	C	Si	Mn	Ni	Cr	Mo	V	S	P
300M	0.42	1.74	0.82	1.82	0.85	0.38	0.09	0.005	0.007

TABLE 2
Heat Treatment and Tensile Properties

Steel	Heat Treatment	Tensile Strength ksi	Proof Stress ksi	K_{IC} ksi \sqrt{in}
300M	Normalise 950 °C - Normalise 875 °C, Temper 320 °C	280 - 290	250 - 258	60 - 65

TABLE 3
ANALYSIS OF INFLUENCE OF SPECIMEN GEOMETRY

TYPE OF TEST	SOURCE OF ESTIMATE	SUM OF SQUARES	DEGREES OF FREEDOM	MEAN SQUARE	F	TABLED $F_{0.05}$ at 95% conf.
K_{Isc} 600 m/h	Between specimen types	6 5076	3	2 1692	2.1404	4.35
	Within types	7 0942	7	1 01346		No sig diff
	TOTAL	13 6018	10			
K_{Isc} 600 m/h	Between specimen types	4 0988	3	1 3663	1.5501	4.35
	Within types	7 5267	7	1 07524		No sig diff
	TOTAL	12 5255	10			
K_{IC}	Between specimen types	310545	3	10 3515	0.95498	4.35
	Within types	75 8675	7	10 8395		No sig diff
	TOTAL	106 922	10			

TABLE 4
APPLICATION OF THE BINARY SEARCH TECHNIQUE TO THE ANALYSIS OF INITIATION K_{Isc} VALUES

	Lab. No.	K_{IC} Value	Stress Corrosion Test Number						K_{Isc} (to nearest $V_{64} K_{IC}$)
			1	2	3	4	5	6	
1) TRANSVERSELY NOTCHED	A 1	54.5	F	NF	F	F	NF	NF	$19/64 K_{IC}$
	G 1	59.0	F	-	F	-	-	NF	$19/64 K_{IC}$
	G 2	59.0	F	-	F	F	-	NF	$11/64 K_{IC}$
2) $W \times 1 \times 1/2$ IN BEND	C	59.8	F	NF	F	F	-	NF	$9/64 K_{IC}$
	D	58.9	F	-	F	NF	F	F	$29/64 K_{IC}$
	F 1	54.7	-	-	F	F	NF	NF	$19/64 K_{IC}$
3) $W \times 0.8 \times 0.2$ IN TENSION	E	62.2	F	NF	F	F	F	F	$19/64 K_{IC}$
2) LONGITUDINALLY NOTCHED	I	61.2	F	NF	F	NF	F	-	$29/64 K_{IC}$
	K	55.3	F	NF	F	NF	F	NF	$21/64 K_{IC}$
	A 2	51.4	F	NF	F	NF	F	NF	$21/64 K_{IC}$
	F 2	55.9	-	-	-	NF	F	F	$29/64 K_{IC}$

F denotes failure within 100 hrs

NF denotes no failure within 100 hrs

TABLE 5.
ANALYSIS OF ERRORS

Lab	Specimen Type	R_{1500} ksi/in ²		R_{10} ksi/in ²	$\frac{R_{1500} - R_{10}}{R_{10}}$ %	$\frac{R_{1500} - R_{10}}{R_{10}}$ %
		6000 min	6000 max/min			
A1	10mm x 10mm Bend	15.3	15.3	54.5	-1.03	-5
G1		15.6	18.1	59.0	-2.48	+7
G2		17.4	17.4	59.0	-0.07	+2
C	1 x 1/2 in Bend	17.6	17.6	59.8	-0.02	+4
D		18.0	19.9	58.9	+0.96	0
F1		16.7	17.9	54.7	+0.87	-6
E	0.8 x 0.2 in Tension	15.6	15.6	62.2	-3.82	+15
B	Constant Deflection	16.0		73.3		
J		24.2		51.1		
I	1/2 in - Compact Tension	18.9	18.9	61.2	+1.27	+4
K		18.0	18.0	55.5	+2.37	-8
A2		16.3	16.4	51.5	+1.63	-13
F2		17.3	17.9	55.9	+1.22	-5

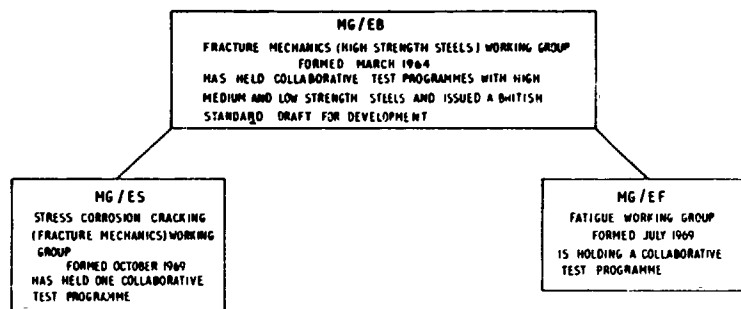


FIG 1 THE PRESENT STRUCTURE OF WORKING GROUPS IN THE FIELD OF FRACTURE MECHANICS.

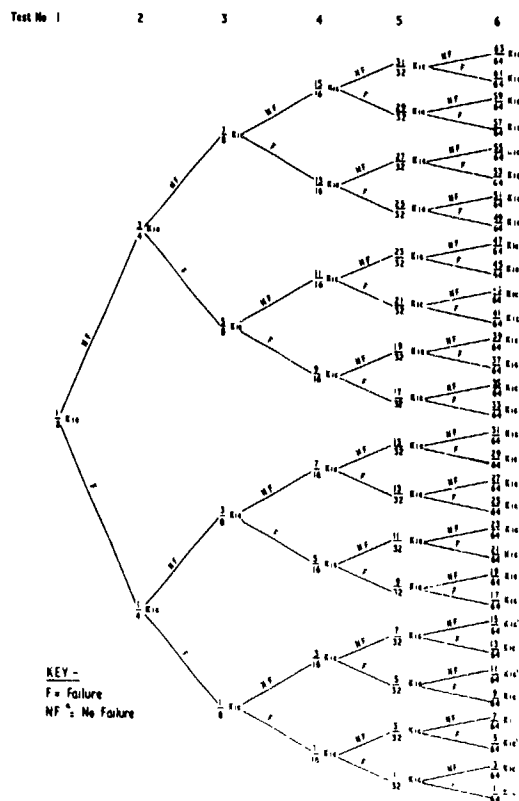


FIG 2 RATIONALISED TESTING PROGRAM FOR THE DETERMINATION OF K_{1sc}

FIG 3 COMPARISON BETWEEN PREDICTED AND ACTUAL PROGRESS WITH THE COLLABORATIVE TEST PROGRAMME

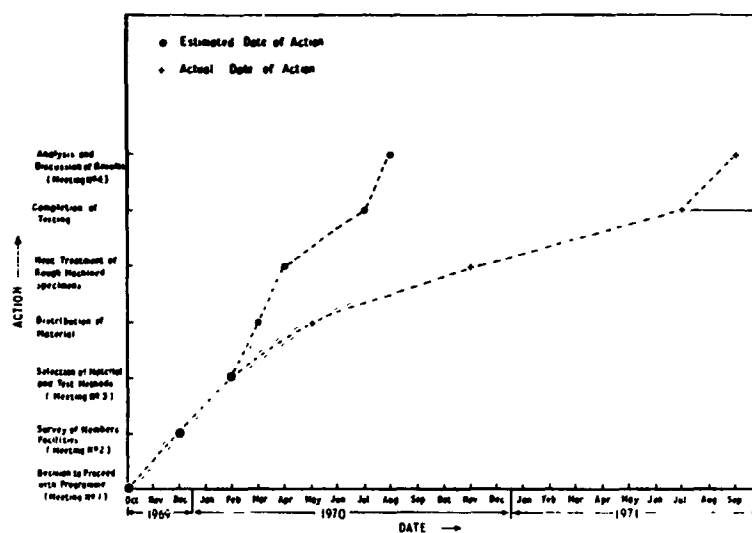
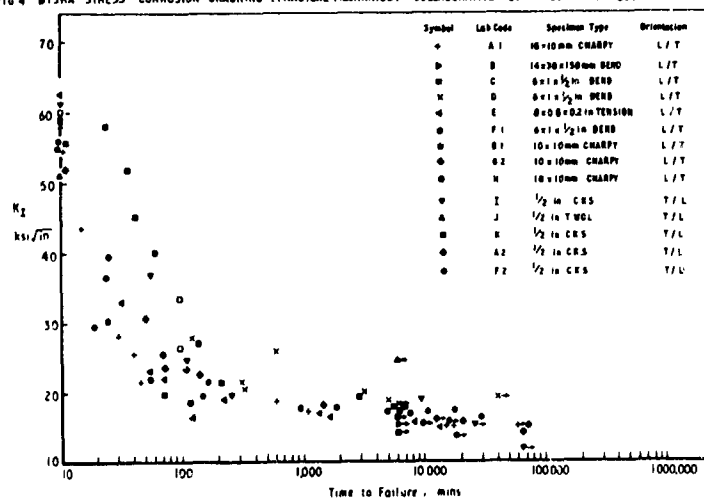
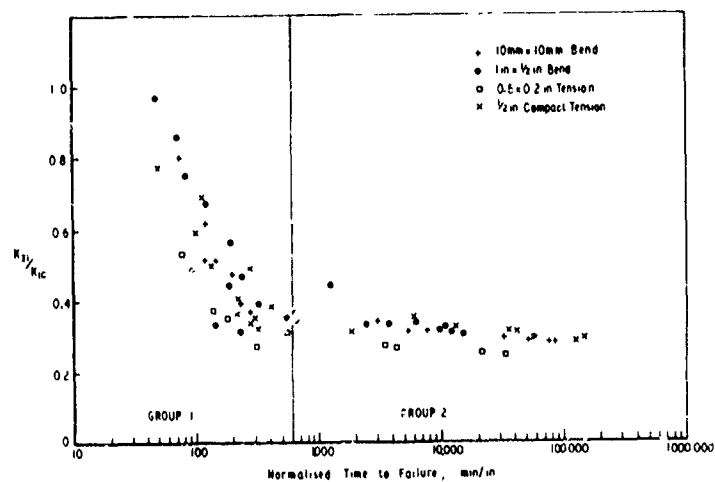
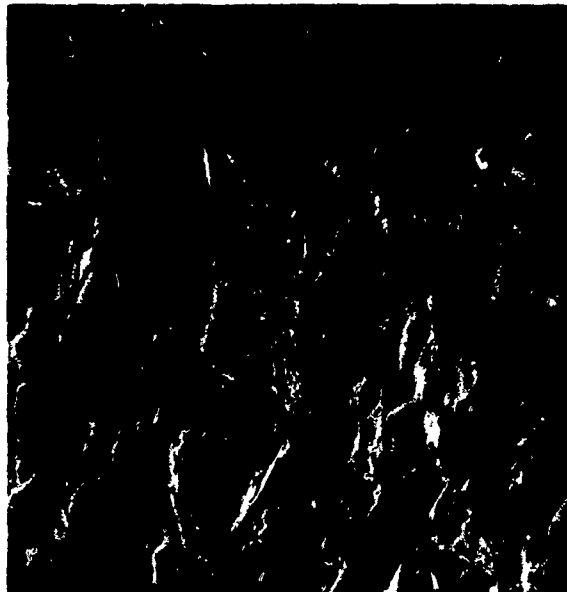


FIG 4 BISRA STRESS CORROSION CRACKING (FRACTURE MECHANICS) COLLABORATIVE TEST PROGRAMME RESULTS

FIG 5 TIME AND K_{IC} -NORMALISED RESULTS OF THE COLLABORATIVE PROGRAMME

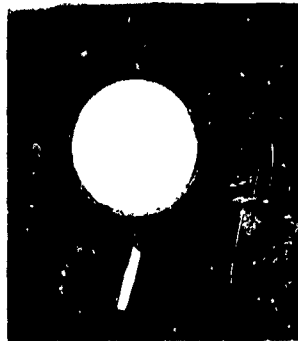


— 0.01 in —

FIG 6.

GENERAL CORROSION ZONE BETWEEN THE FATIGUE
CRACK AND STRESS CORROSION CRACK IN 300M STEEL.

Reproduced from
best available copy.



— 0.5 in —

FIG 7.

GENERAL CORROSION ON THE SURFACE OF A
SPECIMEN OF 300M STEEL.

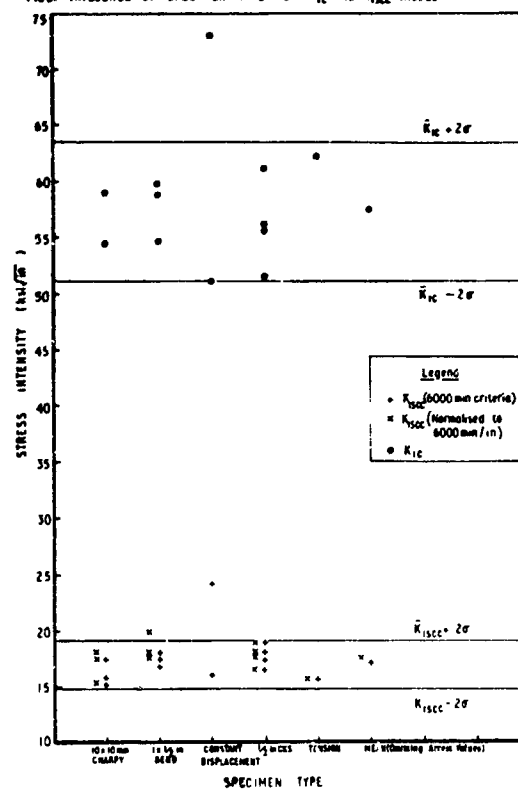
FIG. 8. INFLUENCE OF SPECIMEN TYPE ON K_{IC} AND K_{ISCC} VALUES

FIG. 9. INFLUENCE OF FATIGUE

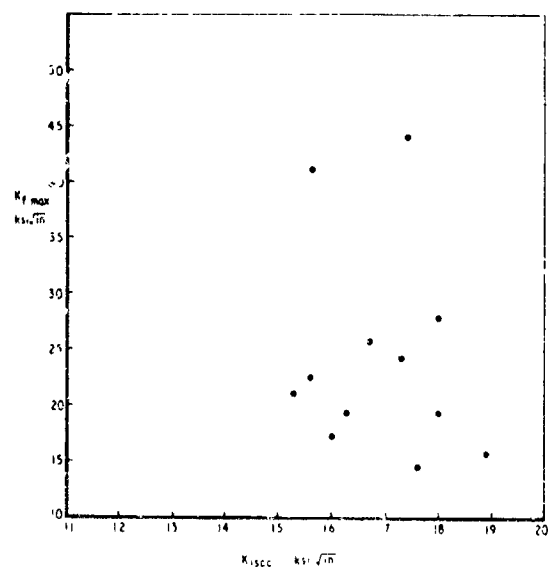


FIG 10. INFLUENCE OF TEST TEMPERATURE

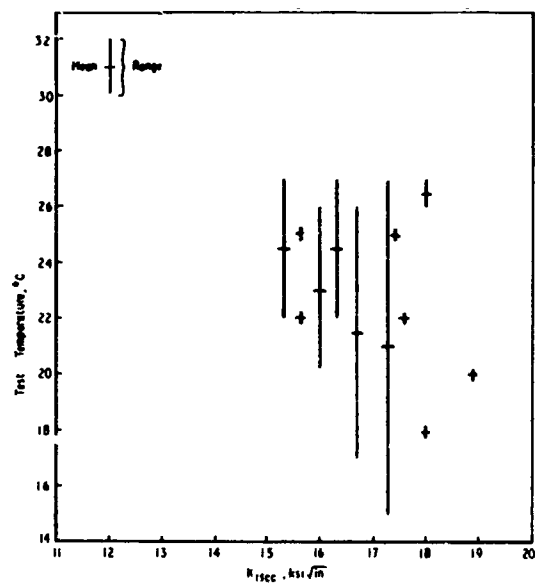
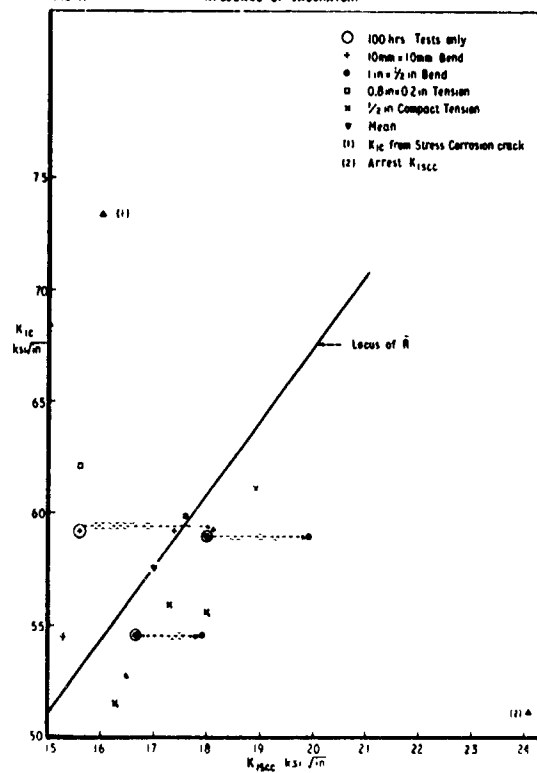


FIG 11. INFLUENCE OF LABORATORY



APPENDIX 1.

Laboratory	Code	K_{II} ksi $\sqrt{in.}$	Time to Failure Minutes
Bisra	A	43.5 28.0 25.5 21.4 18.5 17.1 15.3 15.1 15.0 14.5	15 29 40 45 600 1880 16880 K_{ISCC} 15600 60000 + 7200 +
Bisra	A2	39.6 30.5 25.8 18.5 17.5 16.4 15.8 14.8 14.4 14.5	25 50 69 108 138 6600 K_{ISCC} 20400 72000 64400 2900 + (40°C)
British Rail	B	26.9 16.3 11.5	No Arrest Crack Arrested 16.0 ksi $\sqrt{in.}$ 60000 +
BSC - River Don	C	58.0 51.7 45.0 40.0 33.3 26.3 19.8 18.5 17.6 16.4	24 36 42 60 96 95 72 115 6000 + K_{ISCC} 6000 +
Bristol Aerojet	D	27.8 25.7 21.2 20.6 20.5 19.9 19.0 18.9 18.0	122 610 309 303 280 3120 40000 + 5025 6000 + K_{ISCC}
English Electric	E	33.0 23.0 22.0 19.0 17.0 16.5 16.4 15.6 15.0	31 54 72 225 1360 120 1670 8300 K_{ISCC} 13600
M.V.E.E.	F	21.4 17.9 17.1 16.7 16.0 15.3	160 1229 - 1896 4875 7851 K_{ISCC} 28800 9600 +
M.V.F.E.	F2	19.4 17.7 17.3 15.4 13.6	149 < 927 17911 K_{ISCC} 16000 + 18700 +
Brown-Firth	G1	30.2 29.4 22.0 17.4 17.3	24 18 54 6918 K_{ISCC} 10572

APPENDIX 1 (CONTINUE)

Laboratory	Code	K_{II} ksi \sqrt{in}	Time to Failure Minutes
Brown-Firth	G	36.3 23.7 18.1 15.6	24 72 1572 12816 + K_{ISCC}
BSC - Swinden Laboratories	I	36.8 24.6 19.7 18.9 15.6 11.9	55 110 255 9300 27600 + K_{ISCC} 66000 +
R.A.E.	T	37.1 27.5 24.5	Crack Arrested 25.5 ksi \sqrt{in} . Crack Arrested 25.3 ksi \sqrt{in} . Crack Arrested 24.3 ksi \sqrt{in} .
UKAEA	K	27.0 21.2 19.3 18.0 17.5 14.0	132 210 2946 6000 + K_{ISCC} 6000 + 6000 +

APPENDIX 2

Laboratory	Code	Specimen Type	K_f max ksi \sqrt{in} .	Temp. °C.
Bisra	A1	10 x 10 mm Bend	21.0	22 - 27
Bisra	A2	1 x $\frac{1}{2}$ in. Compact Tension	19.3	22 - 27
British Rail	B	14 x 30 x 150 mm Bend Constant Deflection	17.3	20 - 26
BSC - River Don	C	1 x $\frac{1}{2}$ in. Bend	14.5	22
Bristol Aerojet	D	1 x $\frac{1}{2}$ in. Bend	19.4	18
English Electric	E	0.8 x 0.2 in. Tension	22.5	22
M.V.E.E.	F1	1 x $\frac{1}{2}$ in. Bend	25.9	17 - 26
M.V.E.E.	F2	$\frac{1}{2}$ in. Compact Tension	23.9	15 - 27
Brown Firth	G1	10 x 10 mm Bends	44.0	25
Brown Firth	G2	10 x 10 mm Bend	41.0	25
BSC - Swinden Laboratories	I	$\frac{1}{2}$ in. Compact Tension	15.6	20
R.A.E.	J	$\frac{1}{2}$ in. W.O.L. Constant Deflection	16.2	15 - 22
U.K.A.E.A.	K	$\frac{1}{2}$ in. Compact Tension	28.0	26 - 27

APPENDIX 3THE CORPORATE LABORATORIES OF THE BRITISH STEEL CORPORATIONSTRESS CORROSION CRACKING (FRACTURE MECHANICS) WORKING GROUPCONSTITUTION LIST

Mr. J. E. Truman (Chairman)	Brown-Firth Research Laboratories
Mr. R. J. Allen	British Railways Board
Mr. M. R. Armitage	British Aircraft Corporation Limited
Dr. J. E. Bowers	British Non-Ferrous Metals Research Association
Mr. A. R. G. Brown	Ministry of Technology, Royal Aircraft Establishment
Mr. K. A. Chandler	The Corporate Laboratories, BSC, Battersea
Dr. C. T. Cowan	The A.P.V. Company Limited
Dr. D. W. O. Dawson	A.P.V. Paramount Limited
Mr. J. W. Eggar	Henry Wiggin & Company Limited
Mr. T. E. Evans	International Nickel Limited
Mr. R. A. Faulkner	Rawker Siddoley Aviation Limited
Mr. R. K. Greenwood	Vickers Limited (Barrow)
Mr. T. G. Gooch	The Welding Institute
Mr. J. T. Heron	Royal Armaments Research Development Establishment
Dr. R. A. E. Hooper	BSC Midland Group
Mr. R. Jeal	Rolls-Royce (1971) Limited
Dr. J. F. Knott	Cambridge University
Mr. P. F. Langstone	Bristol Aerojet Limited
Mr. T. Harrison	Brown-Firth Research Laboratories
Dr. P. McIntyre	BSC, The Corporate Laboratories, Sheffield
Mr. J. I. Norwood	BSC River Don and Associated Works
Dr. R. N. Parkins	University of Newcastle
Mr. A. H. Priest	BSC, The Corporate Laboratories, Sheffield
Dr. J. C. Radon	Imperial College of Science and Technology
Dr. G. Sanderson	Fulmer Research Institute Limited
Mr. I. R. Scholes	Imperial Metals Industries
Dr. J. Scully	University of Leeds
Mr. T. V. Thornton	General Electric Company, Power Engineering
Mr. C. Tyzack	United Kingdom Atomic Energy Authority
Mr. D. Webber	Military Vehicle Experimental Establishment
Mr. T. Wilkinson (Technical Secretary)	BSC, The Corporate Laboratories, Sheffield

THE SCIENCE COMMITTEE CONFERENCE
ON THE THEORY OF STRESS CORROSION
CRACKING OF ALLOYS.

Dr. J.C.SCULLY
Reader in Corrosion Science
Department of Metallurgy
University of Leeds
Leeds LS2 9JT
England.

SUMMARY

The Conference covered general aspects of stress corrosion cracking as well as individual alloy systems. Of particular interest to testing methods were (i) repassivation, and (ii) measurements of crack velocity. These are discussed and their relevance to testing methods is emphasized. Comparison between different alloys or of different heat treatments of an alloy can only be made if the relationship between mechanical, metallurgical and electrochemical variables on crack propagation kinetics is fully determined. Separation of mechanism work and the development of testing procedures is not profitable and there is a strong need for more exchange of information between the two groups who work in these fields of stress corrosion cracking.

THE SCIENCE COMMITTEE CONFERENCE ON THE THEORY
OF STRESS CORROSION CRACKING OF ALLOYS

Dr. J.C. Scully.

1. INTRODUCTION

The NATO Science Committee Research Evaluation Conference on the Theory of Stress Corrosion Cracking in Alloys was held at Ericeira, Portugal during the period March 29 - April 2 1971. Approximately 75 people attended either as invited participants or as observers and 16 papers were presented on both general aspects of stress corrosion cracking and individual alloys systems. Two additional papers were on testing methods. Those not presenting papers were invited to present working material. A flexible timetable was devised which ensured that there was a very detailed discussion of the current understanding of the phenomenon. The Proceedings, which include summarized discussions, will shortly be available¹.

The principal objective of the Conference was to focus attention upon those areas in mechanistic studies of stress corrosion cracking that urgently require investigation. Both from the papers that were presented and from the lengthy discussions that ensued there was a large measure of agreement about these areas. It is scarcely possible to summarize with any completion the outcome of a major conference but there are two subjects of comparatively wide general interest that dominated the discussion and that also are of direct relevance to the subject of Testing Methods covered by this AGARD Specialists Meeting on Stress Corrosion Testing Methods. It is therefore the intention of this paper to draw attention to these two subjects by discussing each fairly briefly while at the same time emphasizing their continuing importance. The two subjects are: (i) Repassivation, and (ii) Measurements of Crack Velocity. The discussion of each illustrates that mechanistic investigations require a close understanding of the characteristics of the testing procedure that is adopted. The argument can also be made in reverse that the development of testing procedures is aided by an appreciation of mechanistic factors. It is the opinion of the author that the separation of workers into groups who work on testing procedures and groups who work on mechanisms is not profitable and cannot be justified. Stress corrosion cracking is a complex phenomenon and a unified effort by all parties would appear to offer the greatest hope of a successful resolution of the problem.

2. REPASSIVATION.

The breakdown of protective films consisting either of metal reaction product or of a noble constituent by either chemical or mechanical means has long been recognized as an essential event in the initiation and propagation of stress corrosion cracks. The result of such breakdown causes highly localized attack and the development of acidity with consequent hydrogen evolution in many alloy systems. It is only in recent years that attention has been focussed upon not the breakdown but upon the subsequent rate of repair of such films. The essence of the concept, published² in 1967, is that crack propagation occurs when there is a critical delay in the repair of such films at the tips of cracks. Too small a delay will not give sufficient current for the necessary corrosion event, while too great a delay will permit too large a current flow, giving pitting and generally not sufficiently localized attack. Cracking occurs in electrochemical borderline situations between the formation of a soluble and an insoluble product. Such events will depend upon both electrochemical³ and mechanical⁴ parameters. Cracking is likely to be associated with ranges of potential where protective films exhibit possible instability, i.e. in regions of active/passive transition. The local composition of the environment will be of critical importance since some anions, e.g. Cl^- , probably contribute significantly to delaying repassivation as a result of competitive adsorption on the freshly exposed metal at the crack tip⁵.

At the Conference much discussion centred about the role of repassivation. Work was presented by Professor Stachle on austenitic stainless steels which indicated that cracking in boiling concentrated MgCl_2 solutions might be explained as arising from critical repassivation events. In general, cracking in alloys might be described as arising when the amount of fresh metal created at the crack tip was greater than the volume of solution in the region of the crack tip could passivate. Such a simple description covers a number of complex interacting factors. The deformation processes at the crack, resulting in slip steps, gliding, stretching and dimple formation, will be important since they determine the amount of fresh area created. The repassivation processes will be dependent kinetically upon the value of the potential at the crack tip, the solution composition, hydrolysis reactions and hydrodynamic considerations. With so many variables it is not surprising that cracking occurs only in a relatively small number of alloy/environment systems.

A practical example was shown⁶ that demonstrates the importance of repassivation in a dynamic straining test, a testing procedure that is rapid, severe and unequivocal. The results are shown in Fig.1. Plain specimens of Ti-5Al-2.5Sn alloy were strained to fracture at different strain-rates in two different environments. Firstly, in neutral aqueous NaCl solutions, cracking was observed to occur over a comparatively narrow range of crosshead speeds. At high speeds there is insufficient time for crack initiation and dimple fracture occurs. As this speed is lowered there is time for initiation and propagation which is reflected in the decrease in elongation. At lower speeds the same surface deformation processes occur but at a lower speed so there is time for repassivation to take place and the surface regains its stable condition of being covered with a protective film. No crack initiation occurs. Secondly, in a particular mixture of methyl alcohol and HCl which is aggressive and causes intergranular corrosion, no cracking occurs at the high crosshead speed for the same reason as for the experiments in the aqueous environments. At lower speeds there is time for crack initiation and propagation. As this speed is further lowered, however, there is no possibility of repassivation and since there is an increasing length of time for propagation there is a decreasing elongation to fracture.

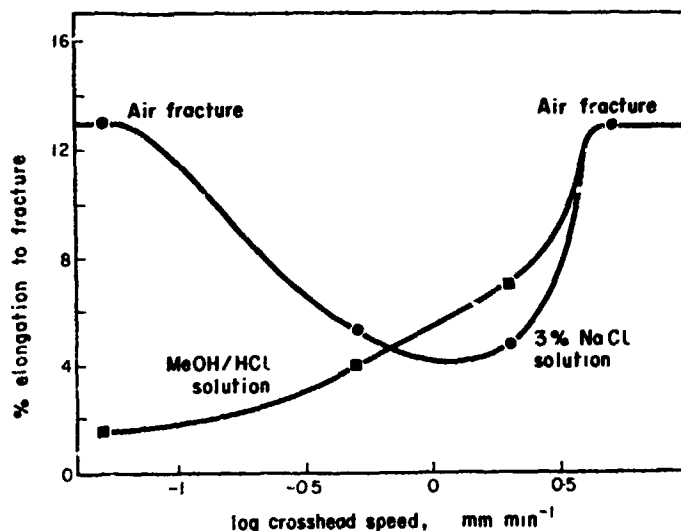


Fig.1. Elongation to fracture for specimens of Ti-5Al-2.5Sn alloy strained at various crosshead speeds in two different environments.

Such results are simply explained but there are considerable subtleties that should be included. Initiation can be associated with emergent slip steps the height of which will depend upon the grain size. The speed of emergence is not strain-rate dependent and initiation might be expected to be independent too. What is important is the nature of the event that occurs during the delay in repassivation. Since initiation is considered to arise from a hydrogen-induced cleavage, this process will depend upon reaching a critical stress level within a certain time. Such events require investigation and such tests should also be done under potentiostatic control, a method that has been employed by some authors.

These results were obtained during a mechanistic investigation but they are relevant to a particular testing method which has some unique advantages. There were opinion expressed that such a testing method should be developed and there was an increasing number of laboratories that were incorporating such tests into their programmes. In general, repassivation is relevant to all testing procedures and was discussed at the 1967 AGARD Meeting in Turin. At the simplest level, consideration must be given to whether a specimen loaded before or after adding the testing medium since different results can be obtained depending upon the method chosen.

3. MEASUREMENTS OF CRACK VELOCITY.

How stress corrosion cracks propagate is fundamental to an understanding of mechanisms. Much work has reported average velocities derived from a wide range of tests but it is only recently that instantaneous velocities have been measured as a function of mechanical, metallurgical and electrochemical variables. The Conference included several papers covering such investigations. It appears that for high strength materials there is a general pattern observed between the crack velocity and the stress intensity factor, K . This is illustrated in Fig.2 which is taken from a paper from Dr. Speidel on aluminium alloys.

The diagram illustrates 3 different stages in the relationship. Stage I covers a region in which the velocity is strongly dependent upon the value of K . The propagation process has an activation energy of 28 kcal./gm.mole. Stage II is a region which the velocity is independent of K . The process has an activation energy of 3-5 kcal./gm.mole. Stage III is observed only in highly susceptible alloys which are avoided where possible. Crack branching occurs in the Stage II 'plateau' region and both branches propagate. This occurs at a certain fixed value of K . At lower values of K branching may also occur. Dr. Speidel distinguishes between these phenomena as 'macro' and 'micro' branching and a diagram from his second paper is shown in Fig.3.

Fundamental data of this kind were reported to be not confined to aluminium alloys. Titanium and magnesium alloys exhibit similar behaviour with similar values of activation energy. Glass in moist atmospheres exhibits Stage I behaviour. Not surprisingly, there was considerable attention paid to these results. An understanding of Stage I behaviour was felt to be crucial to mechanism determination. Repassivation was important here perhaps since in completely non-aggressive environments only Stage II was observed, e.g. Ti alloys in neutral aqueous chloride solutions. With increasing K some critical process occurred so frequently that it was no longer rate-controlling. At this point Stage II was reached in which cracking was controlled by the diffusion of some species in the environment.

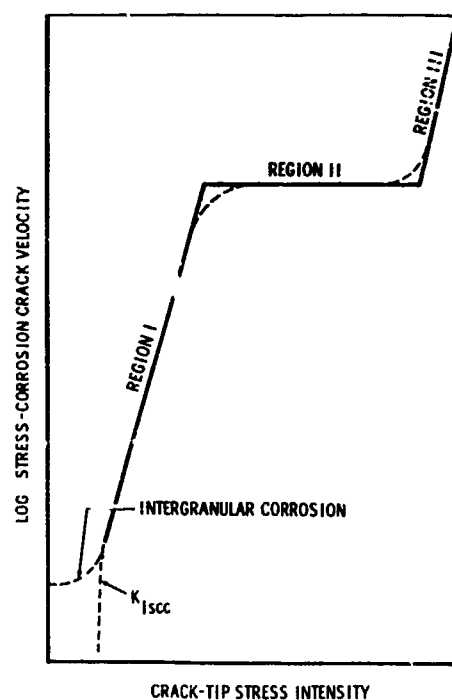


Fig. 2. Schematic diagram illustrating the relationship between stress corrosion crack velocity and stress intensity factor for aluminium alloys¹. (Speidel).

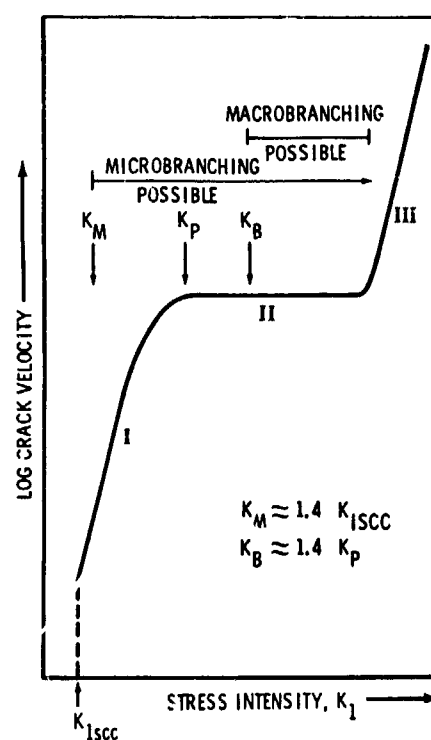


Fig. 3. Schematic diagram similar to Fig. 2 indicating regions in which macro and micro branching occur.¹ (Speidel).

A number of extremely important points of direct relevance to testing procedures arise from such data.

(a) Testing should be done under fixed conditions of mechanical, metallurgical and electrochemical conditions since values that determine the relationship shown in Fig.2 vary as these variables are altered. An example is shown in Fig.4.

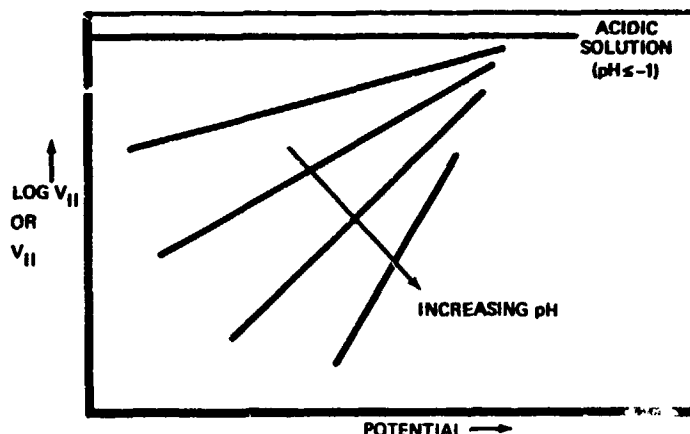


Fig.4. Schematic diagram illustrating the relationship between Stage II stress corrosion crack velocity and potential as a function of pH in titanium alloys.¹ (Feeney and Blackburn)

(b) Unless the complete relationship was established, testing procedures could only give incomplete and possibly misleading indications of behaviour. Where several alloys were being compared it was vitally important to ensure that a comparison was meaningful and this would appear to demand knowledge of the complete curve. The relationship shown in Fig.2 has an immediate use in alloy development and materials selection for a given environment.

(c) In many alloys a genuine value of K_{Isc} below which crack propagation does not occur is not observed and reported values may merely reflect upon the patience of the observer. In aluminium alloys velocities as low as 10^{-11} m/sec have been observed. It was suggested that instead of K_{Isc} a value of K might be designated corresponding to a low negligible velocity which would have to be agreed upon.

(d) The value of the potential was very important and this is usually not controlled during testing procedures. This makes comparison between alloys difficult. It also means that if the open-circuit potential is outside the potential range within which cracking occurs susceptibility can be missed and an alloy appear immune. In service use, however, the open-circuit potential might drift into the range, possibly as a result of temperature changes or aeration effects on high velocity surfaces, consequently resulting in cracking. By omitting the control of a major variable it was not surprising that there were common inconsistencies between laboratory tests and service experience.

At the moment the procedures covered by these points are not generally followed in testing laboratories. Perusal of many of the papers in this volume will confirm this. This is a great pity since it constitutes a considerable hindrance to progress in determining testing methods immediately relevant to service conditions. Stress corrosion cracking occurs as a result of the complex interaction of fracture mechanics, physical metallurgy and electrochemistry. To initiate tests in which only two of the variables are controlled and perhaps even measured is incorrect and cannot be expected to give satisfactory answers except by chance.

4. CONCLUSION

The points above, (a) - (d), are capable of considerable amplification. Taken together with considerations of repassivation they do emphasize that the development of testing procedures and mechanistic studies have much in common and groups working in each area have much to contribute to each other's endeavours. This was a widely expressed feeling at the meeting. The Conference Proceedings show that much has been discovered about stress corrosion cracking over the last few years. This very brief summary of only two general points was not intended to cover the wide range of ideas that were presented at the Conference. Currently the problem is to ensure that this knowledge is widely disseminated and thoroughly discussed. This in turn should ensure that the principal objective of the Conference is achieved and also that testing procedures are devised which give results more related to service conditions.

REFERENCES

1. The Theory of Stress Corrosion Cracking in Alloys. (Ed. J.C. Scully), obtainable from NATO Scientific Affairs Division, 1110 Brussels, Belgium for \$4.00 including postage.
2. J.C. Scully, Corros. Sci., 7, 197 (1967)
3. J.C. Scully, Corros. Sci., 8, 513 (1968)
4. J.C. Scully, Corros. Sci., 8, 771 (1968)
5. J.C. Scully, Brit. Corros. J., 1, 355 (1966)
6. J.C. Scully and D.T. Powell, Corros. Sci., 10, 719 (1970).

MEASURING THE DEGREE OF CONJOINT ACTION BETWEEN
STRESS AND CORROSION IN STRESS CORROSION

by

Franklin H. Cocks
Assistant Head
Materials Science Department

Tyco Laboratories, Inc.
Bear Hill
Waltham, Massachusetts
U. S. A. 02154

SUMMARY

A stress corrosion testing method which allows a quantitative separation between the effects of stress and those of corrosion in causing stress corrosion damage is described. This test involves the measurement of the reduction in subsequent stress corrosion life which is brought about by initially exposing the sample to the corrosive environment without any stress being applied (pre-corrosion). If a given alloy is susceptible only to the combination of stress and corrosion (true stress corrosion), then such a preexposure would not be expected to greatly reduce its subsequent stress corrosion lifetime. If, however, a corrosion process that is not accelerated by stress is required to initiate the failure process, then such preexposure without applied stress may be found to be almost as damaging as an equal amount of exposure carried out under stress. A stress corrosion index (SCI) is defined which quantitatively measures these effects. Data obtained by this method are presented for a high strength aluminum alloy (7075) tested in buffered NaCl solution. For specimens of this alloy having a machined surface finish, 80% of the time required to produce failure in normal stress corrosion tests is found to be due to a process which is not accelerated by applied stress. An explanation for this behavior is offered in terms of the existence of a highly deformed surface layer within which any well defined grain boundaries have been destroyed. This surface layer must be penetrated by pitting before a true stress corrosion process can begin.

MEASURING THE DEGREE OF CONJOINT ACTION BETWEEN STRESS AND CORROSION IN STRESS CORROSION

Franklin H. Cocks

Stress corrosion implies by definition that stress and corrosion acting together produce a greater deterioration than each acting separately. The 1948 American Society for Metals Subcommittee on Stress Corrosion¹ proposed that the relative subsequent breaking loads of specimens which were: (a) stressed but not corroded, (b) corroded but not stressed, and (c) corroded while stressed, be taken as a measure of the acceleration of corrosive damage by stress. This method has not been widely used because breaking loads measured on dry specimens provide relatively little information on the rate of progress of damage under corrosive conditions. To provide an improved index of the acceleration of corrosion damage caused by the application of stress, a novel test procedure has now been developed.² According to this method what is measured, rather than breaking loads, is the reduction in subsequent stress corrosion lifetime brought about by preexposure to the corrosive environment (precorrosion) without the application of stress. By quantitatively determining the reduction in resistance to subsequent stress corrosion as a function of increasing precorrosion exposures, one can assign a numerical value to the degree of conjoint action between corrosion and the applied stress. As will be shown, this testing procedure has proven particularly valuable in explaining the protective effects afforded by many mechanical surface treatments as well as in providing a quantitative tool for the investigation of basic stress corrosion processes.

If an alloy is susceptible only to true stress corrosion, then preexposure to the corrosive environment without any stress applied would not be expected to lead to a large reduction in the time required to produce failure in a subsequent normal stress corrosion test. If, however, a corrosion process that was not accelerated by stress were important initially in the total failure process, then exposure to the corrosive environment without stress (precorrosion) would lead to a substantial decrease in the subsequent time required to produce stress corrosion failure, as measured from the time at which the stress was applied. These two cases are illustrated schematically in Fig. 1. As shown, the vertical axis is the stress corrosion time-to-failure, measured after application of the stress, while the horizontal axis is the precorrosion time; that is, the time during which the sample was exposed to the corrosive environment without an applied stress. The horizontal line (A) shows the behavior to be expected if only a true stress corrosion process operates, since, in this case, corrosion without stress does not change the subsequent failure time. The line (B), however, shows the result which will be found if stress corrosion does not occur and failure results only from normal corrosion. Thus, in this case, one unit of precorrosion exposure time is seen to be just as damaging as one unit of exposure time with both stress and corrosion applied. Arbitrary time units are shown on this figure and, of course, the time required to produce failure by normal corrosion will usually be considerably longer than that required by a stress corrosion mechanism. What is of primary importance, however, is the way in which the time-to-failure, when both stress and corrosion are applied together, varies as the alloy is subjected to increasing precorrosion treatment. This variation gives, of course, the slope of the precorrosion curve. By adding unity to the value of this slope, one can define a stress corrosion index (SCI) as

$$SCI = 1 + \frac{dy}{dx}$$

where y is the measured time-to-failure after precorrosion and x is the time for which the specimen was exposed to the corrosive environment without stress. By defining the index in this way, it will be zero in the case where a stress corrosion process does not occur at all (line B) and unity in the case where only a true stress corrosion process causes damage (line A).

An example of the application of this technique may be found in the case of aluminum alloy 7075 (in wt %, 5.6 Zn - 2.5 Mg - 1.6 Cu - 0.3 Cr - balance Al) in the high strength T651 temper (yield stress, 73,000 psi).³ Stress corrosion and precorrosion tests were carried out in deaerated one normal NaCl solution buffered to pH 4.7 with CH_3COONa and CH_3COOH in a recirculating system at 30°C. The applied load was 90% of the yield stress. Corrosion was galvanostatic with an anodic current density of 0.3 mA/cm². The specimens were cut in the short transverse direction from 1.5 in thick plate and machined to a 25 microinch (rms) surface finish. One set of these samples was tested without further surface preparation except cleaning. Another set was reheat-treated to the T6(51) temper, while a third set was similarly reheat-treated and then electropolished in 25 vol % HNO_3 and 75 vol % methanol at -50°C. The results of precorrosion tests on these samples are shown in Fig. 2. Those points along the ordinate at zero precorrosion time give, of course, the results of normal stress corrosion tests (stress and corrosion applied simultaneously).

Several features are evident from this figure. The time-to-failure of the electropolished specimens is relatively independent of precorrosion exposure ($SCI \approx 1$) over the whole range of precorrosion treatments examined (from 5 to 40 times the normal stress corrosion time-to-failure). For the as-machined specimens, however, the stress corrosion susceptibility index is zero for precorrosion treatments of up to somewhat less than one times the normal time-to-failure; thereafter, $SCI \approx 1$ as in the case of electropolished specimens. Significantly also, in the region where their SCI values are unity, all specimens show the same subsequent time-to-failure. That is, no matter what the starting surface condition, the behavior of all specimens becomes almost identical for precorrosion treatments of more than 0.5 hours, and all points fall on a line almost parallel to the abscissa. The ordinate value of this line thus gives the true stress corrosion resistance of these specimens, independent of starting surface conditions.

For both the reheat-treated as well as the as-machined samples, it is seen that a large fraction (80% in the case of the as-machined samples) of the time-to-failure as measured in a normal stress corrosion test is taken up by a corrosion process that is not accelerated by applied tensile stress.

A high residual surface tensile stress could, of course, cause the specimens to stress corrode in the absence of an external applied stress, but similar specimens deformed 2% either by cold compression or by stretching to eliminate residual stress⁴ showed similar large initial precorrosion effects. Thus, it is necessary to explain why, especially in the case of the as-machined samples, a stress corrosion process does not initially occur. The observation that no precorrosion effect is observed on the electropolished specimens leads to the conclusion that a surface layer is involved. To investigate the surface condition of these samples, transverse metallographic sections were prepared. Although these sections gave evidence for grain boundary distortion within approximately 1μ of the surface, the characteristics of this distortion were not clear. To investigate more closely the condition of the grain boundaries near the surface, therefore, the method of direct surface etching was used.

Fig. 3 shows the appearance of each type of specimen surface after etching for 25 sec in Keller's etch (1% HF, 1.5% HCl, 2.5% HNO₃, balance H₂O). In this sequence of photomicrographs it can be seen that the grain boundary structure of the reheat-treated and electropolished sample is quite clearly developed, while the as-machined specimen shows almost no evidence for a surface grain boundary structure. The samples which were only reheat-treated and which showed an intermediate precorrosion effect also show only a partially developed surface grain structure.

The interpretation of this difference in grain boundary structure and precorrosion behavior is particularly informative in the light of the paper by Borchers and Tenckhoff,⁵ who show that the well-known beneficial effect of shot peening in increasing resistance to stress corrosion does not primarily result from residual stress effects, but rather arises because of the destruction of grain boundaries at the surface. Because stress cracking almost always occurs intergranularly in high strength aluminum alloys, the stress corrosion process evidently cannot begin until the cold-worked surface layer, within which any well-defined grain boundary structure has been destroyed, has been penetrated by corrosion and well-defined grain boundaries exposed. What the results of Fig. 2 demonstrate is that this penetration occurs via a pure corrosion and not a stress corrosion process. Thus, corrosion without applied stress is initially just as damaging as corrosion with applied stress because no stress corrosion process can occur until the underlying region of well-defined grain boundaries has been reached. This sequence of events is illustrated in Fig. 4. As seen in Fig. 4(a), any well-defined grain boundary structure has been fragmented at the surface by mechanical deformation. When the sample is exposed to the corrosive environment, either with or without an applied tensile stress, this surface layer must be penetrated by a non-stress corrosion process, e.g., pitting (Fig. 4(b)), before a true stress corrosion process can begin (Fig. 4(c)). The extreme practical importance of this effect can be seen from Fig. 2, which shows that even the less than 1μ thick surface layer introduced by machining can increase the time-to-failure as measured in a normal stress corrosion test by more than a factor of four. It is probably also that similar surface structure considerations can be used to explain other precorrosion effects which have been reported for high strength aluminum alloys.^{6,7}

It is evident that the effects described here may occur quite generally for alloys and environments where cracking occurs intergranularly. In the case of Ti-6 Al-4 V in brominated methanol, less than half of the time required to produce failure in a normal stress corrosion test is actually related to the resistance of the alloy to stress corrosion.⁸ Similar results have also been obtained for low alloy steel samples in hot nitrate solutions.⁹ In addition, the testing procedure itself may have applications in corrosion fatigue and liquid metal embrittlement studies, as well as in investigations of stress corrosion processes.

The uses of this test method may be broadly described as two-fold: First, technologically, precorrosion testing provides a direct and quantitative means for evaluating the effectiveness of surface treatments such as glass bead or shot peening in inhibiting stress corrosion. Not only is the increase in the overall time-to-failure determined, but the dependence of this increase on (a) residual stress effects, and (b) surface deformation effects, can be separately evaluated because the degree of inhibition of the conjoint action of stress and corrosion can be accurately determined. For example, in the case of the aluminum alloy 2219 (in wt %, 6.3 Cu - 0.5 Mn - 0.18 Zr - 0.1 V - 0.06 Ti - balance Al) in the T31 temper (yield strength 34,000 psi), the protective effect of shot-peening is due almost completely to residual compressive stress effects, since a true stress corrosion process operates even in the absence of well-defined grain boundaries.¹⁰ In the case of glass bead peened steel specimens tested in hot mixed nitrate solutions, however, the measured increase in resistance to cracking under stress corrosion conditions is partly due to residual compressive stress and partly due to surface grain boundary disruption.⁹ Second, in basic investigations of stress corrosion, it is crucial that the effects of such variables as heat-treatment, environment, and temperature be related to their influence on the stress corrosion process itself and not to the combination of pure corrosion as well as stress corrosion processes. It would seem that only by carrying out the test procedure outlined here can this separation of effects be assured.

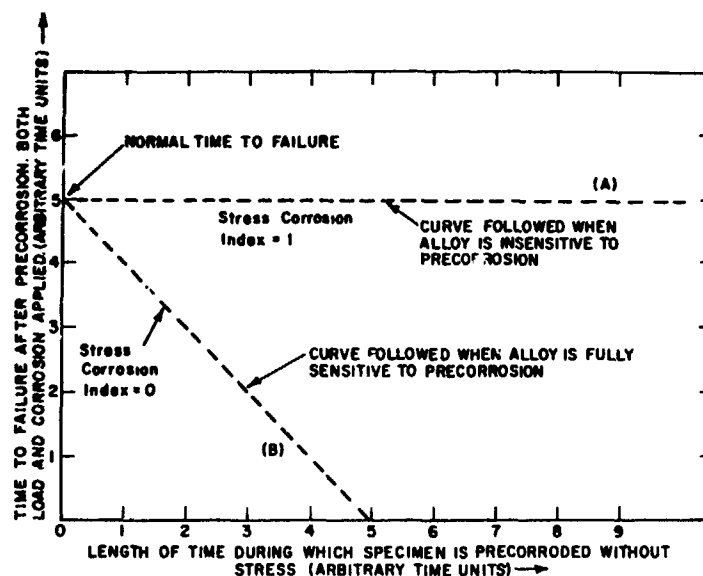


Fig. 1

Schematic drawing showing two extreme cases for the effect of precorrosion (corrosion exposure without applied stress) on subsequent stress corrosion time-to-failure (measured after the application of the load).

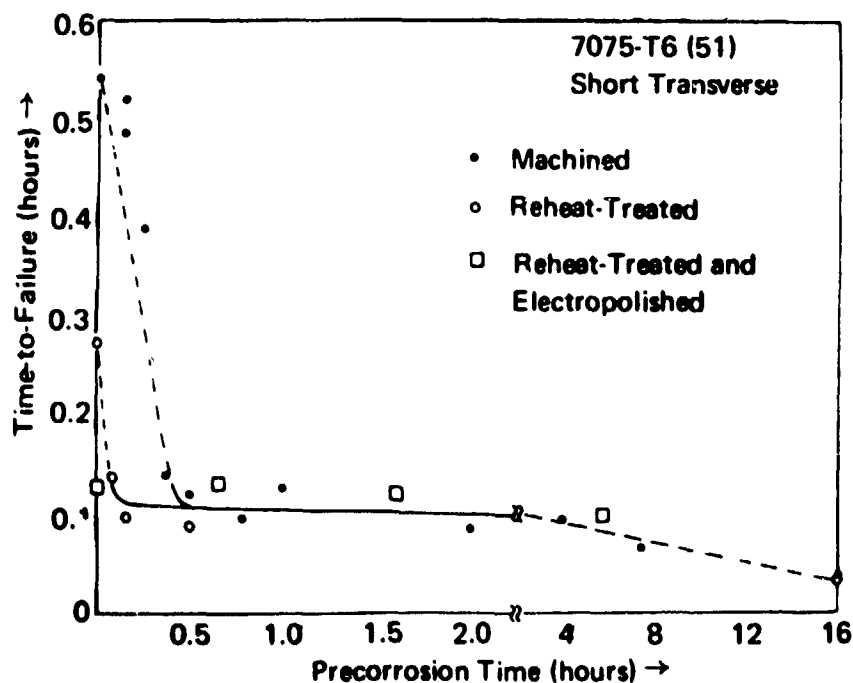


Fig. 2

Subsequent stress corrosion time-to-failure versus precorrosion time (corrosion exposure without applied stress) for as-machined, reheat-treated, and reheat-treated and electropolished samples of 7075-T651.

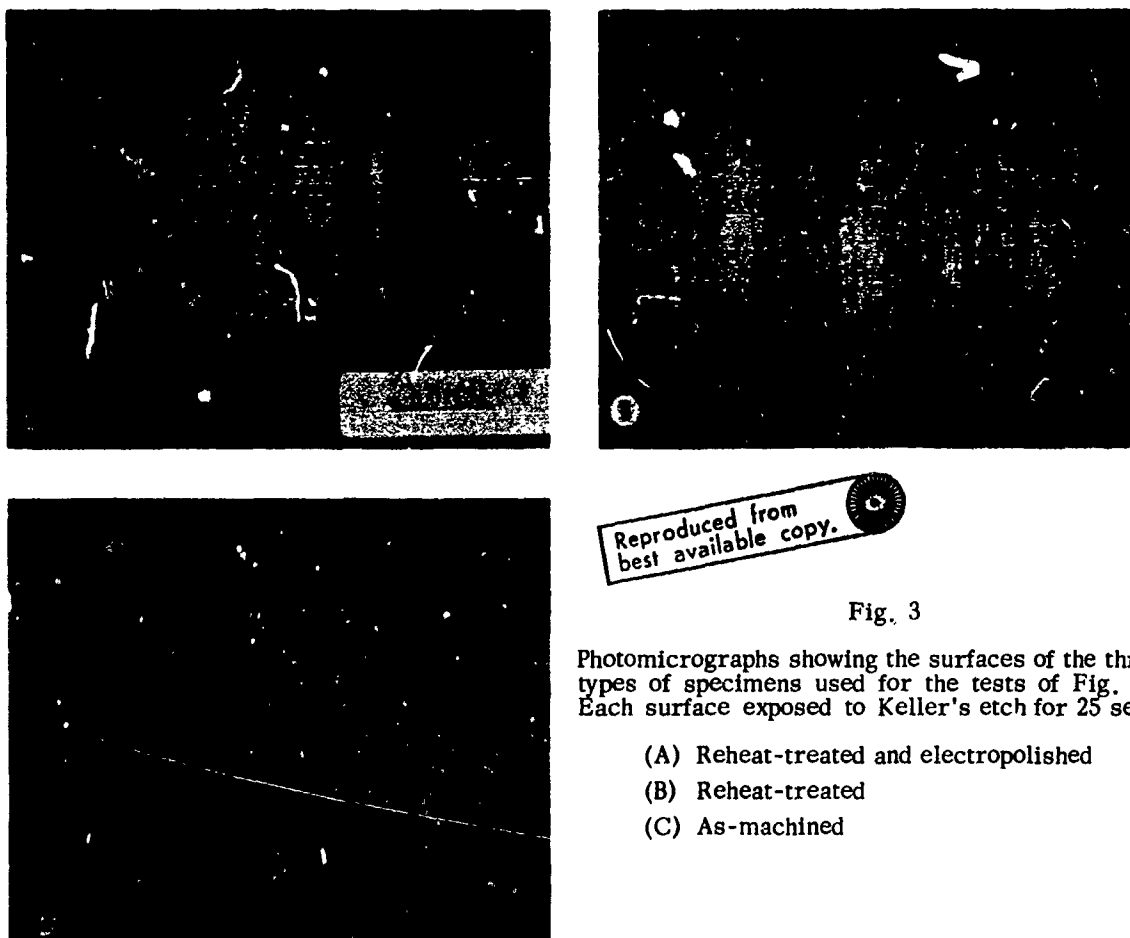


Fig. 3

Photomicrographs showing the surfaces of the three types of specimens used for the tests of Fig. 2. Each surface exposed to Keller's etch for 25 sec.

- (A) Reheat-treated and electropolished
- (B) Reheat-treated
- (C) As-machined

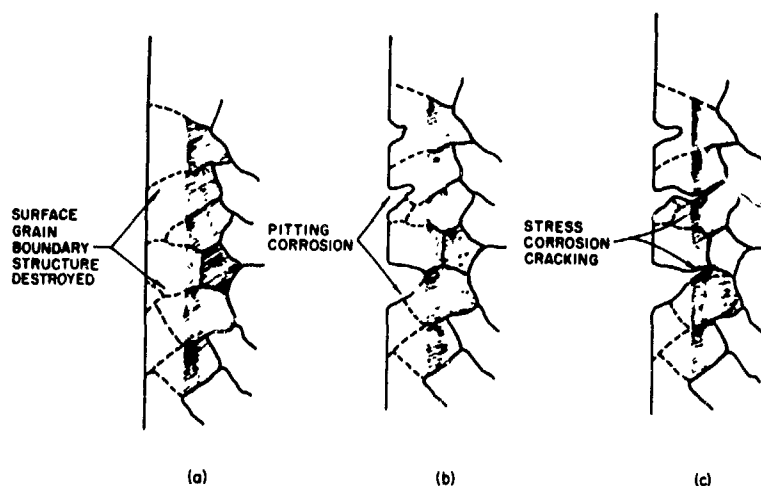


Fig. 4

Schematic drawing showing, (a) deformed surface layer devoid of any well-defined grain boundary structure, (b) penetration of this deformed layer by pitting corrosion, and (c) initiation of stress corrosion once the underlying region of well-defined grain boundaries has been reached.

REFERENCES

1. M. A. Hunter, R. H. Brown, E. H. Dix, Jr., A. L. Jamieson, and H. H. Uhlig, "The Stress Corrosion of Metals" in Metals Handbook, 1948 ed., American Society for Metals, Metals Park, Ohio, 227.
2. F. H. Cocks, "The Separation of Corrosion and Stress Effects in Stress Corrosion Testing," Mat. Res. Stds. 9 (1969) 29.
3. F. H. Cocks, J. F. Russo, and S. B. Brummer, "The Separation of Corrosion and Stress Effects in Stress Corrosion: The Critical Role of Surface Preparation," Corrosion 25 (1969) 345.
4. R. S. Barker and J. G. Sutton, "Stress Relieving and Stress Control," in Aluminum 3, K. R. van Horn, ed., American Society for Metals, Metals Park, Ohio, 1967, 355.
5. H. Borchers and E. Tenckhoff, "The Influence of Surface Condition on the Stress Corrosion of AlMgZn Casting Alloys," Zeitschrift für Metallkunde 59 (1968) 58.
6. H. K. Farmery and U. R. Evans, "The Stress Corrosion of Certain Aluminum Alloys," J. Inst. Metals 84 (1955-56) 413.
7. W. Gruhl, "Investigations on the Problem of the Stress Corrosion of AlZnMg₃," Zeitschrift für Metallkunde 54 (1963) 86.
8. F. H. Cocks, J. F. Russo, and S. B. Brummer, "The Separation of Corrosion and Stress Effects in Stress Corrosion: Ti-6Al-4V in Bromine-Methanol Solutions," Corrosion 24 (1968) 206.
9. F. H. Cocks and A. J. Bradspies, "The Separation of Corrosion and Stress Effects in Stress Corrosion: Low Alloy Steel in Hot Mixed Nitrate Solutions," to be published.
10. F. H. Cocks and S. B. Brummer, "Stress Corrosion of High Strength Aluminum Alloys," Fourth International Congress on Metallic Corrosion, Amsterdam, The Netherlands, 7-14 September 1969.

**pH AND POTENTIAL MEASUREMENTS DURING
STRESS CORROSION OF ALUMINUM ALLOYS**

by

**J. A. Davis
Bell Aerospace Company
Division of Textron, Inc.
Buffalo, New York**

SUMMARY

A technique has been described for using small tip diameter microelectrodes to study the stress corrosion behavior of various aluminum alloys exposed to chloride environments. Several general observations concerning the stress corrosion behavior of aluminum alloys were made: (1) propagation of a stress corrosion crack is always accompanied by a decrease in pH near the crack tip; (2) increasing the stress intensity to above K_{ISCC} results in a rapid active shift in corrosion potential; and (3) as cracks progress, the corrosion potential slowly drifts in the active direction. A general mechanism for stress corrosion based on these observations is that crack propagation occurs by active-path dissolution with a minimum applied stress required to rupture the passive film and initiate crack propagation.

pH AND POTENTIAL MEASUREMENTS DURING STRESS CORROSION OF ALUMINUM ALLOYS

by

**J. A. Davis
Bell Aerospace Company
Division of Textron, Inc.
Buffalo, New York**

ABSTRACT

The pH and potential profiles down stress corrosion cracks have been determined on 1100-0, 2024-T3, 5456-H343, 5456-H117, and 7075-T651 aluminum alloys and 1020 steel exposed to potassium chloride solutions. The pH was observed to decrease near the crack tip when the crack was propagating by stress corrosion. Active jumps in the corrosion potential followed by rapid repassivation were associated with mechanical crack propagation. A film-rupture-anodic dissolution mechanism was used to explain the results.

INTRODUCTION

The local solution chemistry in the crack tip vicinity during stress corrosion cracking has recently received considerable attention since Brown et al.⁽¹⁾ directly measured the crack tip pH. Brown et al.⁽¹⁾ froze the crack tip solution of a growing stress corrosion crack in situ, broke the specimen open, gently warmed the solution, and measured the pH using pH-sensitive paper. On aluminum alloys stress corroded in neutral chloride solutions, they measured a crack tip pH of about 3.5. Rosenfeld and Marshakov⁽²⁾ have measured similar pH values during crevice corrosion of aluminum alloys.

Edeleanu and Evans⁽³⁾ predicted that a constant pH should result during a localized anodic reaction by the hydrolysis of metallic ions or atoms and subsequent precipitation of the hydroxide formed by the reaction. The final pH is dependent on the aluminum ion concentration, the solubility product constant of the hydroxide, and the dissociation constant of water, ranging from about 3.5 to 4.5. Sedricks et al.⁽⁴⁾ have recently extended the work of Edeleanu and Evans⁽³⁾ and have shown that by using the solubility product constant of freshly precipitated aluminum hydroxide, they can accurately predict the pH at the crack tip during stress corrosion of aluminum in chloride environments.

While the work of Edeleanu and Evans⁽³⁾ and Sedricks⁽⁴⁾ allow prediction of the crack tip pH and the work of Brown et al.⁽¹⁾ the measurement of the pH at the crack tip, no method previously described permits the direct measurement of pH near the crack tip or pH gradients from the crack tip to the bulk solution during the actual progress of stress corrosion cracks. In the present investigation, micro-electrodes having tip diameters of one to five microns were developed and used to measure pH gradients during stress corrosion of various aluminum alloys and 1020 steel exposed to neutral potassium chloride.

MATERIALS AND EXPERIMENTAL WORK

The materials used in this investigation were commercial 1100-0, 2024-T3, 5456-H343, 5456-H117 and 7075-T651 aluminum alloys. All materials were in the form of 1/4 or 1/8 inch thick sheet.

Stress corrosion specimens were machined from the sheet material in the form of single edge notched, sheet tensile specimens (Figure 1) such that stress corrosion cracks would grow in the long transverse direction. The specimens were descaled followed by degreasing with methylene chloride for a minimum of 8 hours in a soxhlet extractor. The specimens were then thoroughly rinsed in distilled water and stored in a vacuum dessicator. A 25- to 40-micron hole was drilled at the base of the notch on some specimens while others were fatigue precracked prior to the degreasing treatment.

The test solution was contained in the notch of the specimen by Teflon tape securely held in place by electrical tape, as shown in Figure 1. Restriction of the solution to the notch area proved to be advantageous for two reasons. Contamination of the microelectrodes was reduced to a minimum and observation and manipulation of the microelectrodes was greatly simplified.

The stress corrosion test environment for microelectrode studies was 4.46 percent potassium chloride dissolved in double distilled water of pH 5.9 to 6.5. Potassium chloride rather than sodium chloride was used because sodium ions significantly shorten the lifetime of the pH microelectrode and affects its response at high pH values. Short term comparison experiments using neutral sodium chloride for the test environment yielded identical results to tests using potassium chloride.

Two types of microelectrodes have been developed for this investigation; a pH and a reference microelectrode. A schematic representation of the pH microelectrode is shown in Figure 2. A one micron sealed tip approximately 150 microns long was drawn in a pipette puller from a one millimeter O.D. glass pipette (Corning type 0150 pH glass). The tip was then examined at a magnification of 600X to insure the tip was sealed. The microelectrode was filled with double distilled water and a five mil platinum wire, cleaned with a hot solution of sulfuric acid - sodium dichromate, was inserted into the water. The platinum wire was externally connected to a copper lead wire.

The silver/silver chloride (Ag/AgCl) reference microelectrode, shown in Figure 3, was drawn from a one millimeter O.D. pyrex pipette to a 5-micron tip diameter approximately 150 microns long with the tip left open to the solution. The microelectrode was then filled with a buffered 0.1N potassium chloride-saturated silver chloride solution. The reference probe was a 5-mil platinum wire coated with silver that was chloridized to about half the thickness. Finally, the platinum wire was externally connected to a copper lead wire. Both the pH and Ag/AgCl microelectrodes were conditioned for at least one hour in 4.46 percent KCl and calibrated before each series of measurements.

A schematic representation of the experimental apparatus is shown in Figure 4. For pH measurements, the pH microelectrode was inserted into the crack or into the 25- to 40-micron hole drilled at the base of the notch and the reference electrode was placed about 25 microns from the root of the notch. The depth of microelectrode immersion in microns into the crack was measured by micro-manipulators with motion controlled by a micrometer dial. The pH was determined by measuring the potential of the pH microelectrode with respect to the Ag/AgCl microelectrode with a high input impedance (10^{15} ohm) battery powered electrometer. The corrosion potential was determined by measuring the potential of the specimen with respect to the Ag/AgCl microelectrodes and all potentials are reported on the Ag/AgCl scale in volts. The specimen, microelectrodes and electrometer are enclosed in a Faraday cage to reduce the pickup of external electrical noise.

The pH microelectrodes were calibrated after conditioning in 4.46 percent KCl by measuring the potential with respect to a Ag/AgCl microelectrode in 4.46 percent KCl solutions buffered to pH values in the range of interest. The most common pH solutions used as standards for calibration were pH 2, 4, 6 and 8. A typical calibration curve with a slope of 58 millivolts per pH unit is shown in Figure 5. Microelectrodes were discarded that produced less than 50 millivolts per pH unit, a nonlinear response, or considerable drift between calibrations. The Ag/AgCl microelectrodes were calibrated by measuring the potential with reference to a saturated calomel electrode. If the potential difference was between 35 and 45 millivolts and exhibited less than 5 millivolts drift in 24 hours, the Ag/AgCl reference electrode was considered usable.

The load on the specimen was determined with a load cell and transducer and the load as well as potential were recorded on a dual channel strip chart recorder. The stress intensity was calculated (5) from the load by the expression:

$$K_I = \frac{Pa^{1/2}}{B \cdot W} Y(a/W)$$

where P is the load, a is the crack length, B is the thickness, W is the height, and Y(a/W) is the compliance correction given by (5) :

$$Y\left(\frac{a}{W}\right) = 1.88 - 9.41 \left(\frac{a}{W}\right) + 18.78 \left(\frac{a}{W}\right)^2 + 18.78 \left(\frac{a}{W}\right)^3 - 38.48 \left(\frac{a}{W}\right)^4 + 53.85 \left(\frac{a}{W}\right)^5$$

Selected fracture surfaces were examined by transmission electron microscopy using two-stage, plastic-carbon replicas. The plastic replicas were shadowed at 45° with platinum - 20 percent palladium to enhance surface relief and carbon was applied normal to the plastic replica. Corrosion products were removed from the fracture surface by making several plastic replicas that were discarded and a final plastic replica that was shadowed and examined.

RESULTS

For comparative purposes, the stress corrosion resistance of 2024-T3 and 7075-T651 aluminum alloys was determined using center precracked, sheet tension specimens exposed to 3.5 percent sodium chloride. The stress intensity below which failure did not occur in 100 hours, K_{ISCC} , was determined by loading specimens to a given stress intensity and recording the time-to-failure. The values of K_{ISCC} determined were 17 ksi/ $\sqrt{\text{in.}}$ for 2024-T3 and 11 ksi/ $\sqrt{\text{in.}}$ for 7075-T651. The values of K_{ISCC} were probably slightly higher than the values obtained under valid plane strain conditions because of the use of subsized specimens. However, the values agree reasonably well with results of other investigators.

The results of potential and pH measurements on aluminum alloys exposed at various stress intensities are summarized as follows:

Al 1100-0

Al 1100-0 is commercially pure aluminum and is generally considered immune to stress corrosion cracking. Figure 6 shows the results of microelectrode studies with pH and corrosion potential behavior at various stress intensities shown as a function of time. The pH is given in terms of depth above (+) or below (-) the base of the notch in microns. At low stress intensities, the corrosion potential reached a steady state value of -0.750V (Ag/AgCl) and the pH was relatively constant when going 1000 microns into the bulk solution to 250 microns into the hole drilled at the base of the notch. When the stress intensity was increased to 11 ksi/ $\sqrt{\text{in.}}$, a pH gradient developed with a one pH unit difference between the bulk solution and the crack tip and the corrosion potential shifted to -800V (Ag/AgCl). This gradient in pH quickly disappeared (within 10 minutes) indicating the anodic reaction at the base of the notch could not be sustained. Additional increases in stress intensity resulted in small (10 to 20 mV) jumps in corrosion potential in the active direction and a return of the pH gradient. Again, the gradient disappeared within 10 minutes and the corrosion potential rapidly returned to the value before the increment of stress intensity was added. If sufficient time between increments in stress intensity were allowed, the corrosion potential returned to -0.750V (Ag/AgCl) or the value before stressing.

Al 2024-T3

K_{ISCC} for Al 2024-T3 was determined as 17 ksi/ $\sqrt{\text{in.}}$ and is, therefore, susceptible to stress corrosion at higher stress intensities. Figure 7 shows the pH and corrosion potential at various stress intensities below and above K_{ISCC} as a function of time. Below K_{ISCC} , no pH gradients developed, the corrosion potential reached a steady-state value of -0.700V (Ag/AgCl) and increases in stress intensity had no effect on the corrosion potential. Above K_{ISCC} , pH gradients developed and persisted as long as the stress intensity was maintained above K_{ISCC} . Increases of the stress intensity above K_{ISCC} resulted in active jumps in the corrosion potential with the peak potential exceeding -1.0V (Ag/AgCl). The corrosion potential quickly returned (2 to 5 minutes) to the original value before the increment in stress intensity. Just prior to final failure, the stress intensity was increased with a resultant jump in corrosion potential. The potential rapidly decayed to within 20 mV of the value before stressing then shifted in the active direction to about -0.800V (Ag/AgCl). This shift in corrosion potential was accompanied by a drop in stress intensity. Finally, the corrosion potential began to shift in the noble direction with the corrosion potential at -0.750 (Ag/AgCl) at the time of failure.

Al 5456-H343

Al 5456-H343 is generally considered susceptible to stress corrosion in chlorides. The results of microelectrode measurements are shown in Figure 8. Large pH gradients were noted at stress intensities as low as 8 ksi/ $\sqrt{\text{in.}}$ and a difference in behavior from earlier alloys was noted. The bulk solution pH rose to pH 9 while the pH of the solution in the hole decreased to a value of 5.7 from the initial bulk solution value of 6.5. After about 30 minutes, the pH gradient disappeared and the bulk solution increased to a value of about 7.8. The solution was replaced with fresh solution of pH 6.0 and the test continued. At higher stress intensities, the pH gradients again developed with the bulk solution pH increasing with time and the crack tip pH decreasing with time. Finally, after a large crack had formed, copious hydrogen evolution was noted, and this hydrogen evolution caused a mixing and a reduction in the magnitude of the pH gradient.

Al 5456-H117

Alloy 5456-H117 has been developed for its immunity to stress corrosion by reducing the number of intergranular precipitates. The results of microelectrode measurements are shown in Figure 9. Even at 4 ksi/ $\sqrt{\text{in.}}$, large pH gradients were developed shortly after application of a load. The crack tip pH was about 4.7 while the bulk solution pH increased to 8.5 to 9.0. After 10 to 15 minutes, the pH gradient disappeared and did not return until the stress intensity was increased whereupon it once again

disappeared after about 10 to 15 minutes. The solution was replaced with fresh solution of pH 6 after leveling off as the bulk solution pH had increased to about 8. At higher stress intensities with fresh solution, the crack tip pH reached a value of 4.3 with the bulk solution pH of 6. However, after 10 to 15 minutes, the gradient disappeared and the solution pH slowly shifted to higher values. At very high stress intensities, i.e., 26 ksi/ $\sqrt{\text{in.}}$, the crack propagated mechanically to an extent that the applied stress intensity dropped by 150 ksi/ $\sqrt{\text{in.}}$ before the crack arrested. Even at the higher stress intensities, crack propagation could not be sustained.

Al 7075-T651

K_{ISCC} for Al 7075-T651 was determined to be 11 ksi/ $\sqrt{\text{in.}}$. Results of microelectrode measurements are shown in Figure 10. At low stress intensities, below K_{ISCC} , no pH gradients developed. At a stress intensity above K_{ISCC} a pH of 3.8 at the crack tip was reached. The bulk solution pH at this stress intensity also decreased to about pH 5. At 7 ksi/ $\sqrt{\text{in.}}$ with fresh solution, the crack tip pH was 5 while the bulk solution pH reached 8.2. Finally, at 36.7 ksi/ $\sqrt{\text{in.}}$, copious hydrogen evolution produced mixing of the solution in the crack and leveled the pH gradient at about pH 4. Also noted were the active shift in corrosion potential with increases in stress intensity. Failure followed shortly after this leveling.

A specimen of 1020 steel was also examined using the microelectrode technique as shown in Figure 11. The 1020 steel showed pH gradients both at low stress intensities and at high stress intensities. The pH at the crack tip reached a minimum value of about 4.7 while the bulk solution pH was never higher than 6. Also, increases in stress intensity caused a much smaller active shift in corrosion potential. The corrosion potential did show a slow, active shift as the crack lengthened.

Fractography

Transmission electron micrographs of two-stage, plastic-carbon replicas of selected fracture surfaces were taken to substantiate that stress corrosion crack growth and the development of pH gradients could be correlated. A specimen of 2024-T3 was stressed to 28 ksi/ $\sqrt{\text{in.}}$ in 4.46% KCl and microelectrodes inserted. As soon as a pH gradient developed, the solution was removed and the specimen mechanically broken open. A replica of the fracture surface just below the notch root was taken as shown in Figure 12. The fracture was intergranular with evidence of secondary grain boundary cracks, typical for stress corrosion of aluminum alloys in chloride environments.

Some question existed concerning the development of pH gradients for Al 1100-0 and Al 5456-H117, since both alloys are considered to be immune to stress corrosion. Figure 13 shows a micrograph of a fracture surface after microelectrode measurements on 5456-H117. Indications of intergranular stress corrosion are clearly evident on the fracture surface (Figure 13a) in contrast to the dimple rupture (Figure 13b) on the area of the fracture surface produced by mechanical crack propagation. Figure 13c shows the grain boundary structure with only random grain boundary precipitates present.

Finally, replicas were taken to correlate the jumps in corrosion behavior with fracture mode. Figure 14 shows the fracture surface from a specimen of 7075-T651 showing a region of predominately dimple rupture between two regions of quasi-cleavage. The dimple rupture area was formed by mechanical crack propagation and exposed unfilmed metal to the solution. The potential immediately jumped to about -1.8V (Ag/AgCl). Once the area repassivated, stress corrosion proceeded.

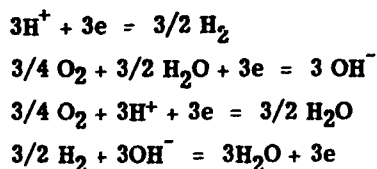
DISCUSSION

The results of this program show several observations that are specific to stress corrosion of aluminum alloys: (1) crack propagation is always associated with acidification at the crack tip; (2) increases in stress intensity cause rapid jumps in the corrosion potential only when the stress intensity is above K_{ISCC} ; and (3) the corrosion potential drifts in the active direction if extensive crack propagation occurs. Furthermore, the microelectrode technique has been shown to be very sensitive for determining the susceptibility of aluminum alloys to stress corrosion cracking. Each of these aspects of stress corrosion will be discussed as follows.

The acidification associated with stress corrosion crack propagation was originally predicted by Edeleanu and Evans⁽³⁾ and extended by Sedricks et al.⁽⁴⁾. The anodic reaction is originally:



while several possibilities exist for the cathodic reaction:



all of which remove hydrogen ions from solution. When the solubility product constant for aluminum hydroxide is exceeded, the anodic reaction becomes $\text{Al} + 3\text{OH}^- = \text{Al}(\text{OH})_3 + 3\text{e}$ and a constant pH results. This pH has been calculated by Edeleanu and Evans (3) and Sedricks et al. (4) from the expression:

$$\text{pH} = \frac{1}{3} \log \left(\frac{K_w^3 [\text{Al}^{+3}]}{K} \right)$$

where K_w and K are the solubility product constants for the dissociation of water and the formation of insoluble hydroxide, respectively, and $[\text{Al}^{+3}]$ is the concentration of aluminum ions in solution. Hence, the pH depends only on the aluminum ion concentration in solution, all remaining terms being constants.

The present results indicate acidification occurs close to the crack tip while an increase in pH occurs at some distance from the crack tip. The reason for a difference in pH for different distances from the crack tip is that anodic and cathodic reactions are separated by a finite distance. Once precipitation of aluminum hydroxide begins, the pH stabilizes both at the crack tip and in cathodic areas. Hydroxide produced at cathodic areas is consumed by hydroxide formation in anodic areas and a steady state is achieved. Measurement of the pH can be used to calculate the concentration of aluminum ion in solution.

The rapid shifts in corrosion potential accompanying increases in applied stress intensity were only observed when the final stress intensity was above K_{ISCC} on aluminum alloys. The increase in stress intensity apparently ruptures the passive film, exposing unfilmed aluminum to the solution. Film formation is rapid and the corrosion potential returns quickly to the value that existed before the stress intensity was increased. Electron micrographs of the fracture surface indicate zones of quasi-cleavage typical of stress corrosion, separated by zones showing dimple rupture typical of mechanical crack propagation as shown in Figure 14 to substantiate that unfilmed metal was exposed to the solution. Since this behavior occurs only above K_{ISCC} , apparently K_{ISCC} is the stress intensity required to rupture the passive film.

The flow active drift in the corrosion potential accompanying crack propagation was originally observed during stress corrosion of stainless steel in hot chloride environments. The explanation generally given for this type of behavior is that an increasing area of active crack tip is exposed to the solution, giving a more active corrosion potential.

The final aspect of the present program to be considered is the ability of this technique to evaluate materials concerning susceptibility to stress corrosion cracking. Of the alloys examined using micro-electrodes, 5456-H117 is considered immune to stress corrosion while 7075-T651 is considered very susceptible. Comparison of Figure 9 after 2.5 hours with Figure 10 at 70 hours shows the pH profile down a stress corrosion crack shortly after the application of stress for both alloys. As can be seen, the profile is very nearly the same for the two materials, indicating both are susceptible to stress corrosion. About 10 to 15 minutes after the application of the stress, the behavior of the two materials was quite different. The pH gradient on 7075-T651 had not changed while no pH gradient was observed on 5456-H117. This behavior indicates that cracks will initiate and propagate on 7075-T651 while cracks will not propagate on 5456-H117. This behavior is similar to the behavior observed by Sprowls for actual exposure tests.

The results of this investigation indicate that a film rupture-anodic dissolution mechanism is operating during stress corrosion cracking of aluminum alloys. Two observations have led to this conclusion: (1) the behavior of the corrosion potential with increases in stress intensity; and (2) the decrease in pH associated with crack propagation. Increasing the stress intensity does not affect the corrosion potential unless the final stress intensity is above K_{ISCC} . The effect is to cause a rapid active shift in the corrosion potential. This behavior has been interpreted such that K_{ISCC} is the minimum stress intensity required to rupture the film. The decrease in pH near the crack tip can only be associated with anodic dissolution at the crack tip. The only way that a decrease in pH can occur is for aluminum ions to be produced and hydrolyzed. Hence, with the above observations, a film rupture-anodic dissolution mechanism appears most plausible.

REFERENCES

1. B.F. Brown, C.T. Fujii, and E.P. Dahlberg, Jnl. Electrochem. Soc., 116, (1969) p. 218.
2. J.L. Rosenfeld and I.K. Marshakov, Corrosion, 20, (1964) p. 115t.
3. C. Edeleanu and U.R. Evans, Trans Faraday Soc., 47, (1951) p. 1121.
4. A.J. Sedricks, J.A.S. Green, and D.L. Novak, RIAS Technical Report No. 4 to ONR, (Dec. 1970).
5. P. Paris and G. Sih, ASTM STP 381, (April 1965).
6. D. Sprowls, Private Communications.

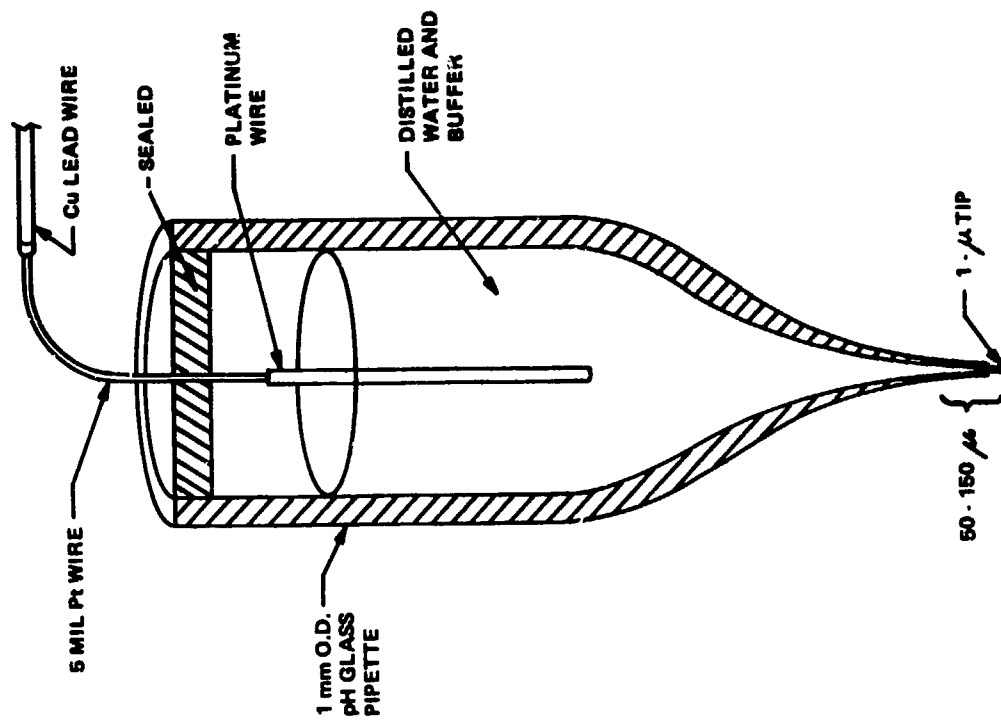


Figure 2 Schematic representation of pH microelectrode.

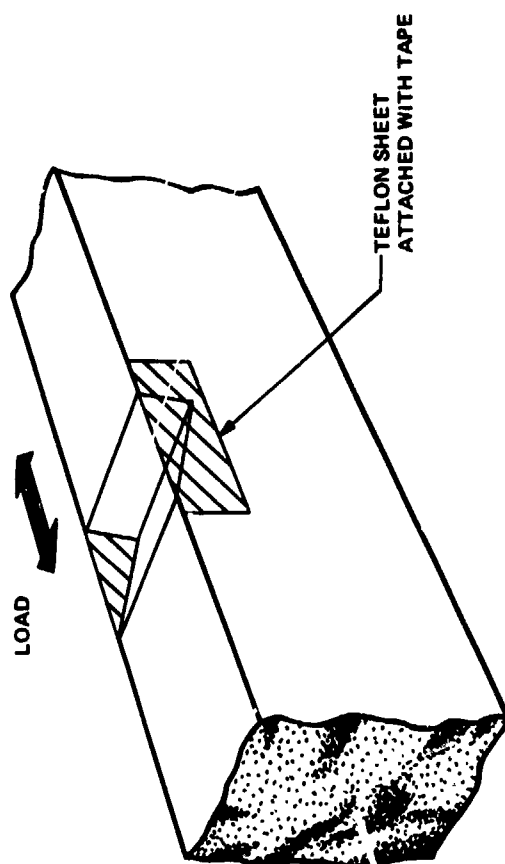


Figure 1 Schematic representation of specimen.

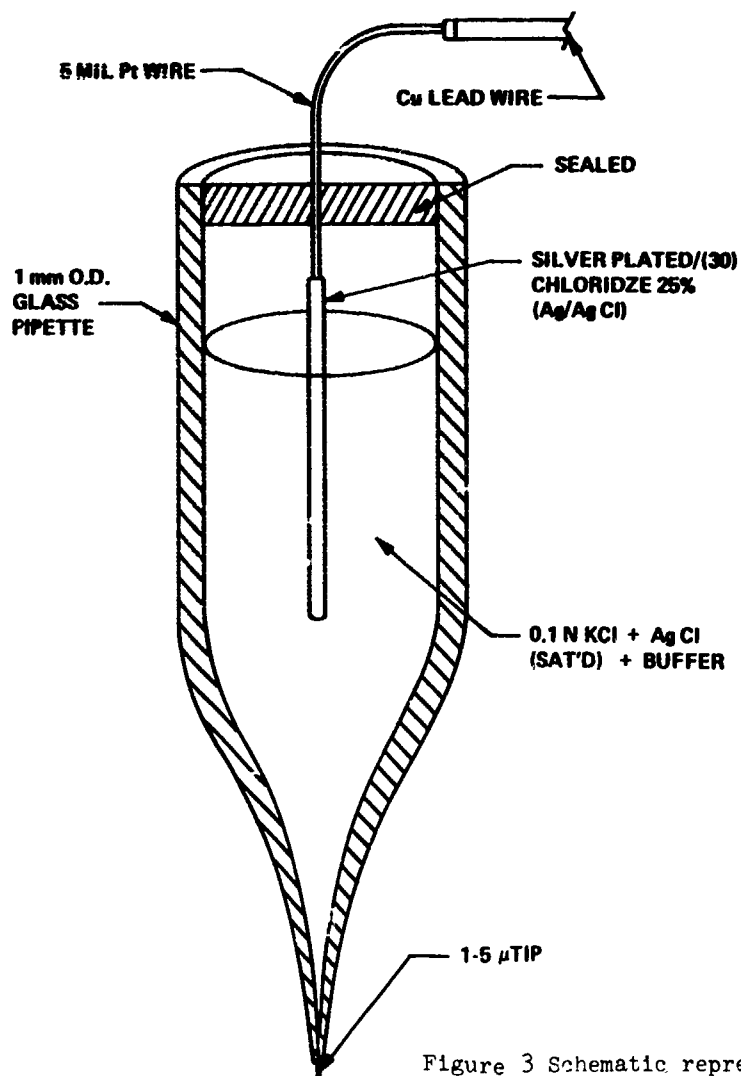


Figure 3 Schematic representation of reference electrode.

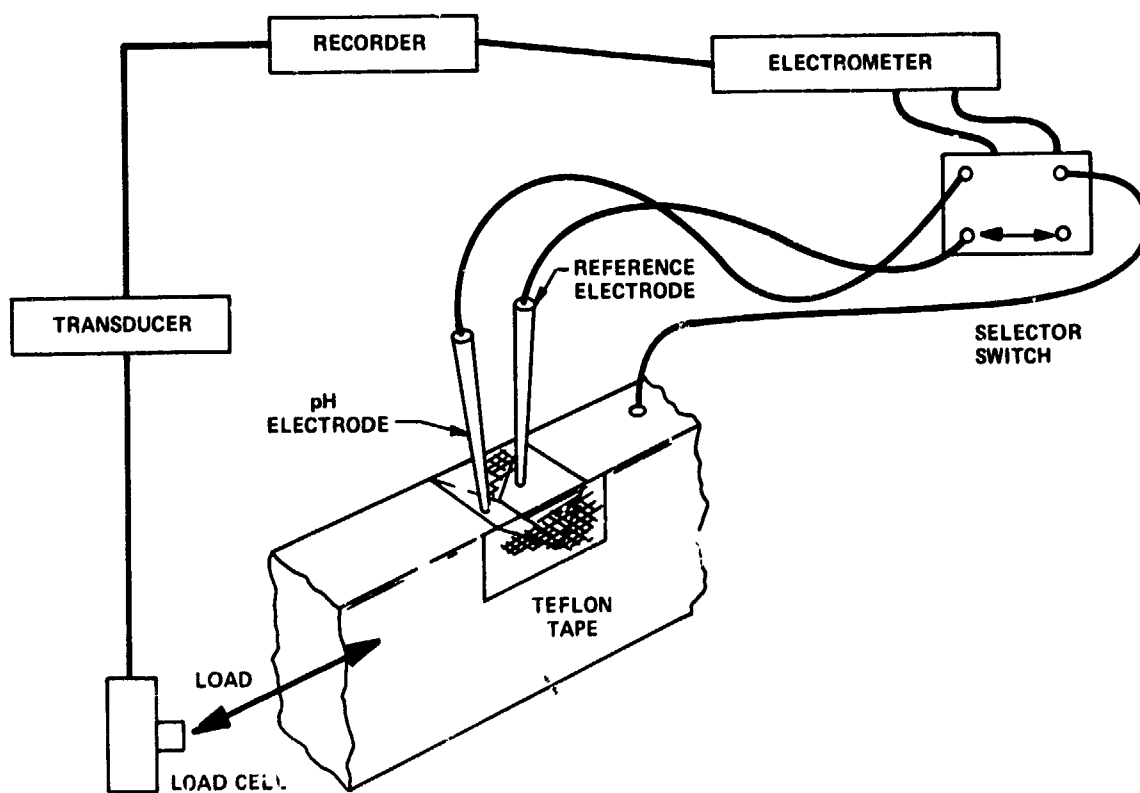


Figure 4 Schematic representation of experimental apparatus.

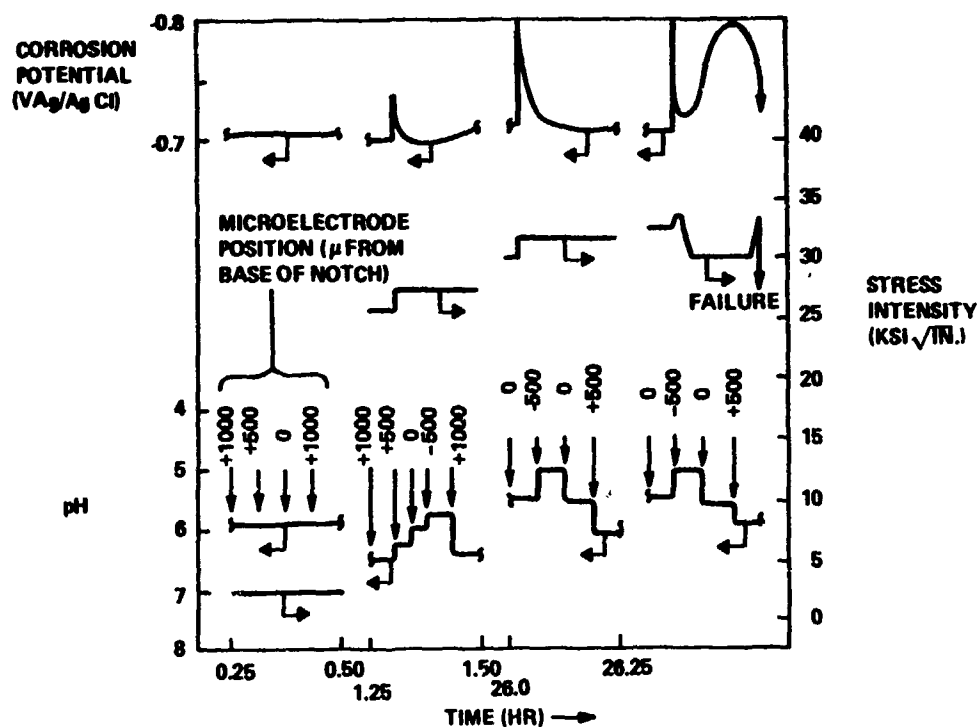


Figure 7 Crack tip pH and potential as a function of applied stress intensity for 2024-T3 aluminum alloy exposed to 4.46% KCl.

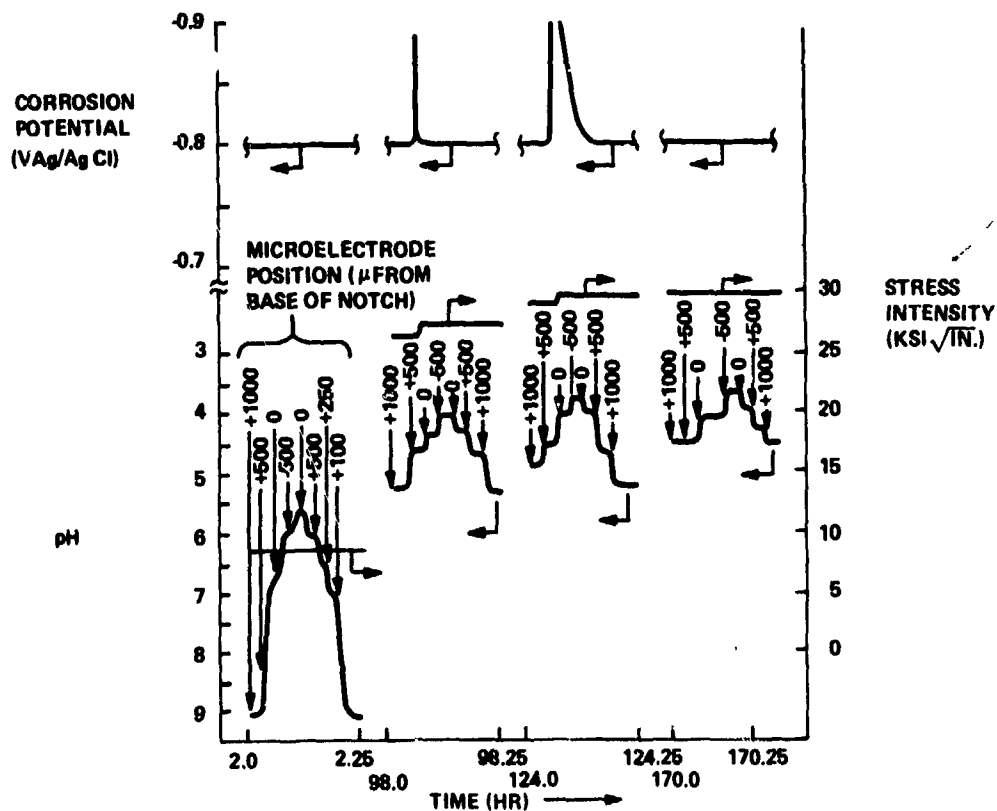


Figure 8 Crack tip pH and potential as a function of applied stress intensity for 5456-H343 aluminum alloy exposed to 4.46% KCl.

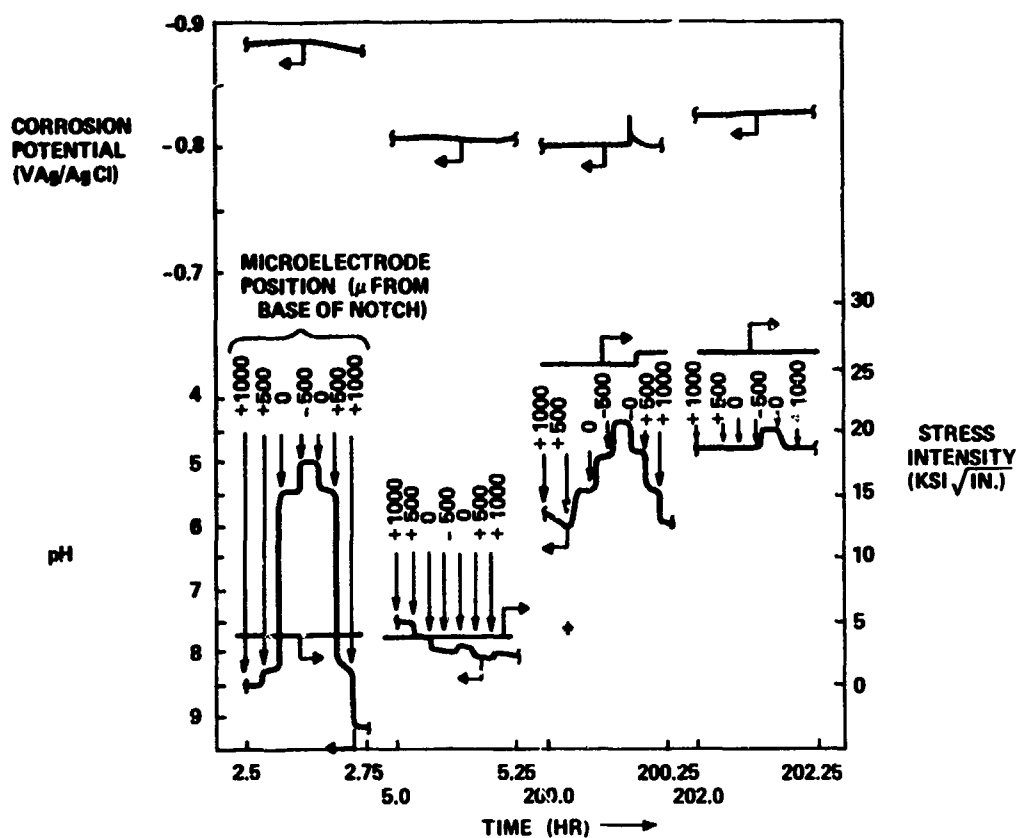


Figure 9 Crack tip pH and potential as a function of applied stress intensity for 5456-H117 aluminum alloy exposed to 4.46% KCl.

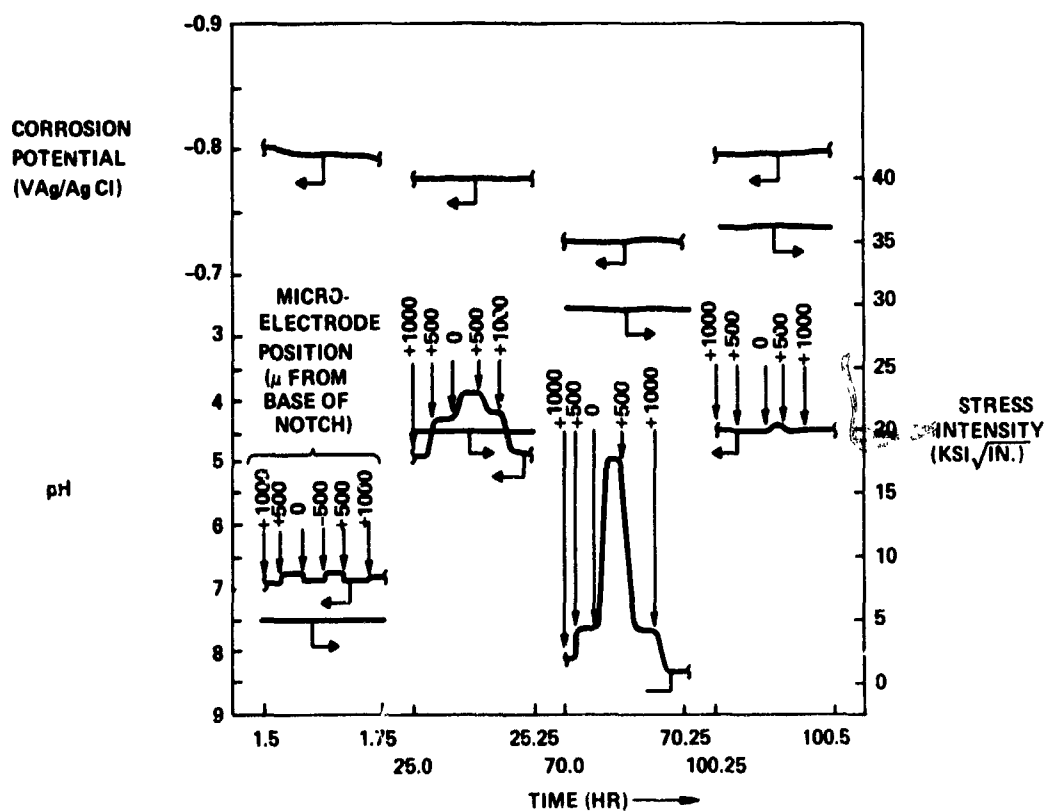


Figure 10 Crack tip pH and potential as a function of applied stress intensity for 7075-T651 exposed to 4.46% KCl.

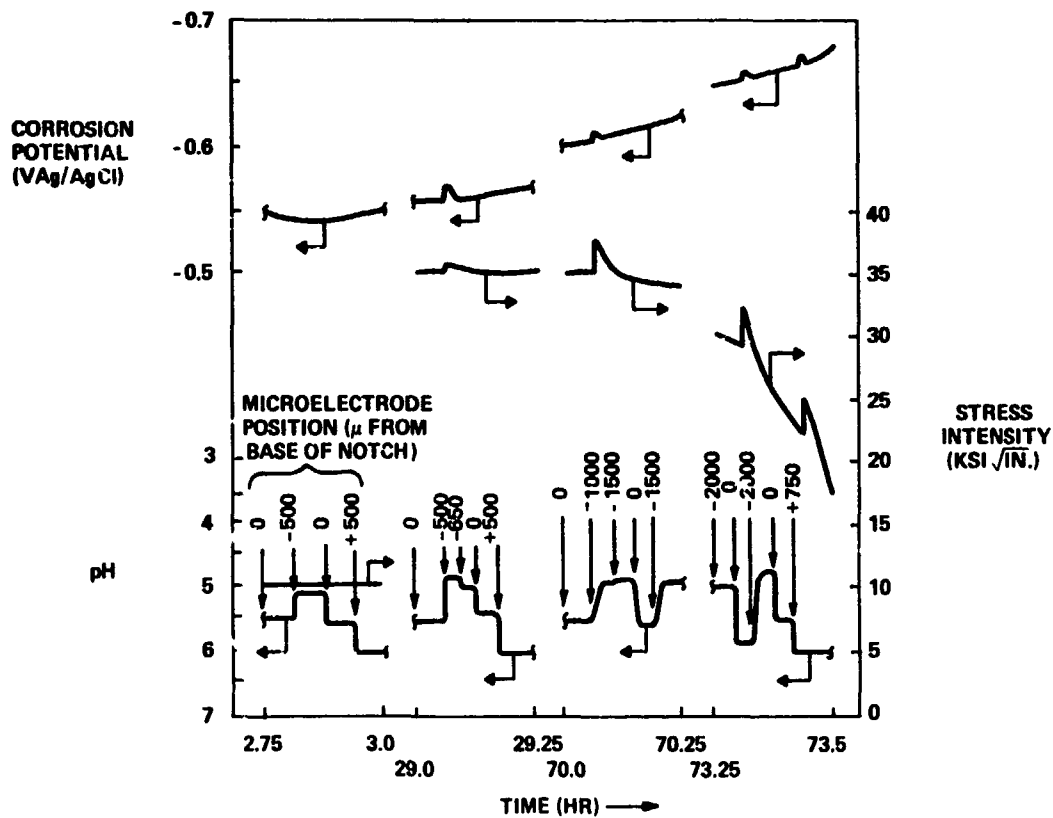


Figure 11 Crack tip pH and potential as a function of applied stress intensity for 1020 steel exposed to 4.46% KCl.



7000X

Figure 12 Fractograph showing stress corrosion fracture surface on 2024-T3.



20,000X



25,000X



6000X

Figure 13 Fractographs showing (a) stress corrosion fracture surface, (b) dimple rupture fracture surface and (c) grain structure on 5456-H117.

Reproduced from
best available copy.



2000X

Figure 14 Fractograph showing stress corrosion fracture surfaces separated by dimple rupture on 7075-T651.

**STRESS CORROSION TESTING OF
WELDED JOINTS**

by

**T.G.Gooch
The Welding Institute,
Abingdon, Cambridge, UK**

STRESS CORROSION TESTING OF WELDED JOINTS

By C. G. Gooch

SYNOPSIS

Service stress corrosion failures are frequently associated with welded joints. The present paper outlines the technique used at The Welding Institute for assessing the stress corrosion behaviour of weldments, and gives some illustrative results. Reference is made to aspects of weld testing requiring particular attention.

1. INTRODUCTION

Stress corrosion cracking (SCC) is likely to be particularly associated with welded joints in consequence of a number of factors. Unless the structure is effectively stress relieved, tensile residual stresses will remain in the weld area, while the irregular weld reinforcement will provide a stress concentration, and favour hideout of aggressive chemical species in the environment. Further, the welding thermal cycle may induce metallurgical changes causing local susceptibility to SCC greater than that of the parent material. Since welding is the most common method of fabrication of metallic structures, it is imperative that attention be paid to the SCC behaviour of welded joints during a material development or evaluation programme.

The application of fracture mechanics principles using pre-cracked specimens offers a number of advantages in SCC testing of welded joints. The conditions necessary for propagation of a weld defect by SCC can be determined, and related to the type and orientation of defects that may be encountered in practice. Further it is possible to site the pre-existing defect in any region of a test weld, and assess the SCC behaviour of that region independently of defects elsewhere.

An investigation is in progress at The Welding Institute to study the SCC behaviour of welded joints⁽¹⁾. Attention has been paid to quantitative assessment of the susceptibility of weldments in a range of transformable steels, and also to the cause of failure and the effects of material composition and micro-structure. The present paper outlines the SCC testing approach adopted, and gives some illustrative results.

2. EXPERIMENTAL TECHNIQUE

2.1. General Approach.

SCC testing is carried out using single edge notched (SEN) specimens, stressed in 3-point bend. The corrodents generally employed are 3% NaCl or simulated seawater as representative of media causing SCC of hardenable steels.

K_{ISCC}* determinations are made conventionally using a number of specimens, each stressed at constant load, although an incremental loading technique has been employed and found to give similar results.

2.2. Specimen Preparation

When testing welded joints, two distinct methods of specimen preparation are adopted, namely deposition of an actual weld, or weld simulation. The former is essential if weld metal studies are to be carried out, but it may be difficult to directly test the heat affected zone (HAZ) of a single pass weld, since weld and specimen dimensions may prove restrictively small. In such cases weld simulation is particularly useful, as single run microstructures can be reproduced in a conveniently sized specimen.

2.2.1. Weld Testing

The welding technique normally employed is illustrated in Fig. 1. A K-preparation is used, with a buttering technique, to give a planar through-thickness HAZ, as shown in Fig. 2. The completed butt weld is machined into SEN specimens, and the pre-existing notch sited in the region of interest. The fatigue crack tip can generally be positioned to within a 1 mm radius without the necessity for side grooving. However, the precise area of the weld sampled by the fatigue crack tip is positively identified after SCC testing by hardness measurement and metallographic examination. The results obtained can thus be correlated with each region of the weld.

2.2.2. Simulated Weld Testing

The thermal cycle associated with welding may be simulated in one of three ways, viz:-

- 1) Furnace simulation, followed by quenching in a suitable medium.

This is useful for the production of large specimens, but it may be difficult to achieve the high heating and cooling rates encountered in an actual weld. It may further require considerable experimentation on heat treatment conditions to accurately

*It is not always possible to define the yield stress of a given region of a weld; thus, although plane strain conditions are aimed at for parent material, it is not certain that these are obtained in weld testing.

reproduce the required HAZ microstructure.

ii) Use of a Weld Thermal Simulator.

By electrical resistance or induction heating a specimen held in high heat sink grips, high heating and cooling rates can be obtained, programmed to reproduce a given weld thermal cycle⁽²⁾. Typically, specimens of 10 x 10 mm cross-section can be prepared, although some limitation on cooling rate must be accepted, together with the necessity for experimentation to reproduce the desired microstructure.

iii) Electron beam (EB) welding.

EB welding may be used in its own right as a fabrication process, and specimen SCC welds produced having planar HAZs with no necessity for weld preparation. The process also enables high cooling rates to be obtained by virtue of a large heat sink adjacent to the weld bead. Thus, EB welds may be prepared to give HAZs of maximum hardness in relatively large specimens. The method is particularly applicable to alloys of low hardenability, to reproduce the severe practical case of the hard microstructures found adjacent to small weld beads deposited under conditions giving rapid cooling.

3. RESULTS

3.1. Typical SCC data

Tables 1 to 3 show material compositions, heat treatment and welding conditions representative of those studied at The Welding Institute. Associated SCC data obtained using the above techniques are given in Table 4, and illustrate the discrimination possible between various regions of welds made by a variety of processes.

3.2. Overall findings

Results so far obtained on welded joints in a wide range of ferritic steels have enabled the following general conclusion to be reached:-

- i) Differentiation must be made between low alloy steels, and low carbon precipitation hardening materials.
- ii) With alloys giving marked HAZ hardening, post-weld heat treatment is essential to restore SCC resistance. If such treatment is not applied, increased SCC susceptibility will be found in the transformed HAZ, although softening associated with the sub-critical HAZ may decrease the susceptibility of this region.
- iii) With low carbon precipitation hardening alloys, the susceptibility of the softened, as-welded, transformed HAZ will probably be a little higher than that of parent material. However, post-weld heat treatment to restore HAZ mechanical properties generally results in a HAZ SCC resistance comparable with that of parent material.
- iv) If post-weld heat treatment is not applicable, the use of a temper bead welding technique is recommended.
- v) The necessity for post-weld heat treatment is dependent on the HAZ microstructure⁽³⁾ if twinned martensite is formed during the welding cycle, SCC susceptibility increases markedly, and a tempering treatment becomes essential. Other martensites have comparable and higher SCC resistance. This is illustrated by reference to Fig. 3.

4. GENERAL COMMENTS

It is well recognised that loss of fracture toughness associated with SCC may result in a very high sensitivity to defects. This is particularly apparent if welded joints are considered, and K_{ISCC} values obtained experimentally are expressed in terms of a defect tolerance parameter by, for example, the general relationship

$$K = \sigma \sqrt{\pi a}$$

where 'K', ' σ ', and 'a' have the usual meanings.

However, it is difficult to define a value of stress applicable to weld joints in service. It can be appreciated that allowance should be made for design loading, residual contractual and transformation stresses, and geometric stress concentrations, but as yet it is only an approximate resultant stress that can be obtained. Prudence dictates that any approximation should be conservative, and thus direct quantitative application of K_{ISCC} data to obtain a defect tolerance may result in a defect size for a weldment that is prohibitively, and perhaps unrealistically, small. While K_{ISCC} data readily enable comparison to be made between areas of a weld, or between different materials, it must be recommended at the present time that conventional SCC testing of welds representative of practice be undertaken conjointly with pre-cracked specimen studies. It is remarked that such testing is further desirable to enable assessment to be made of the contribution of service corrosion and pitting etc. to SCC initiation.

When SCC testing welded joints, reference must be made to welding process and conditions. This is particularly true in the constructional field, where post-weld heat treatment is seldom applicable, and welding technique largely determines HAZ and weld metal microstructure, and associated SCC susceptibility. Even if post-weld heat treatment is applied, process and conditions must be considered particularly since weld metal composition, inclusion distribution etc. will vary from process to process.

Recognition should also be made of the effects of service environment on SCC behaviour. The cause of SCC of high strength steels is in dispute, but work at The Welding Institute has indicated failure in the general case to be due to hydrogen embrittlement⁽⁴⁾. The amount of hydrogen entering a steel structure in service will depend on the environment, and allowance for this should be made during testing. As an illustration, Snape⁽⁵⁾ found 6-7 ml/100g of hydrogen in steel exposed to an acid H₂S test solution for 7 hrs. At The Welding Institute, only 2 ml/100g was found after exposure to 3% NaCl after 1000 hrs, indicating this common test solution to be by no means an environment causing most embrittlement. At the same time, comparative data obtained in 3% NaCl should be generally applicable unless service corrosion of a given alloy differs markedly, in, for example, tendency towards pitting etc.

REFERENCES

1. Welding Institute Research Investigations 7022 and 3239.
2. WIDGERY, D. J. Met. Constr. and B.W.J., 1, 7, p. 328 (July 1969).
3. GOOCH, T. G. Welding Institute Confidential Report C239/7/70.
4. GOOCH, T. G. Welding Institute Confidential Reports M/41/69, C239/2/69 and subsequent unpublished work.
5. SNAPE, E. Corrosion, 23, 6, p. 154 (June 1967).
6. CANE, M. W. F. Unpublished work.

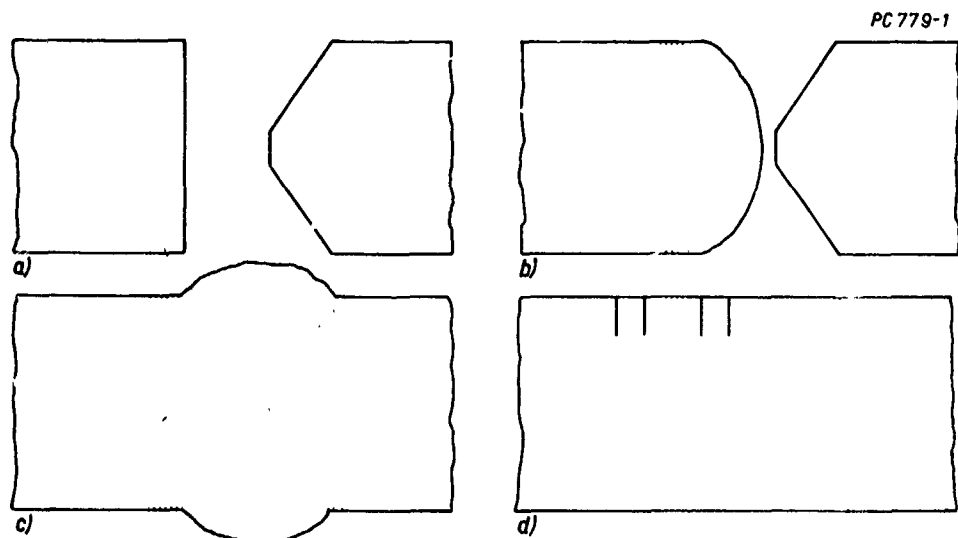


Fig. 1. K-preparation welding procedure (a) joint preparation, (b) one side buttered with weld metal, (c) joint completed, and, (d) joint machined and notched as required.

Table 1. Material analyses.

Material	Element Wt, %									
	C	Si	Mn	Ni	Cr	Mo	Cu	V	Ti	Co
RS 140	0.39	0.30	0.51	0.30	3.0	1.06	-	0.20	-	-
FV 520S	0.07	0.45	1.26	5.57	15.3	1.73	1.7	-	0.15	-
18% Ni	0.009	0.005	0.09	18.0	-	3.19	-	-	0.31	9.25
NCMV	0.45	0.80	0.47	1.74	1.32	0.94	-	0.25	-	-

Table 2. Heat treatment conditions.

Steel	Heat treatment		Parent material mechanical properties		
	Before welding	After welding	Hardness HV 20*	Yield stress N/mm ²	(tonf/in ²)
RS 140	900°C, 1 hr OQ: T 600°C 1 hr AC	T 600°C, 1 hr AC	442	1150	(75)
FV520S ^x	1050°C, 5 min AC: 750°C, 2 hr AC: 20°C 2 hr.	750°C, 2 hr AC: O°C, 2 hr: PH 450°C, 2 hr AC	410	1140	(74)
18%Ni	820°C, 1 hr OQ: PH 480°C, 3 hr AC	PH 480°C, 3 hr AC	408	1230	(80)
NCMV	920°C, 1 hr OQ: T 350°C, 1 hr AC	T350°C, 1 hr AC	460	1630	(106)

Notes: * Mean of 10 determinations
+ Mean of 3 tests
^x With electron beam welding, post-weld heat treatment was -70°C, 1 hr:PH450°C, 2hr AC.
OQ = Oil quenched to ambient temperature.
AC = Air cooled to ambient temperature.
T = Tempered.
PH = Precipitation hardened.



a) OC 2286



b) OC 2285

Fig. 2. Longitudinal sample weld. (a) as buttered, x 2, (b) completed x 3.5

Table 3. Welding Conditions.

Steel	Process	Material thickness mm (ins.)	Buttering layer				Final weld			
			Voltage V	Current A	Speed mm/min (in./min)	No. of runs	Voltage V	Current A	Speed mm/min (in./min)	No. of runs
RS 140	MMA	Matching composition	20	110	-	4	20	110	-	20
FV520S	TIG	FV520B	11	110	150 (6)	10	12	180	100 (4)	14
	EB	Autogenous	NA	NA	NA	NA	140x10 ³	35x10 ⁻³	250 (10)	1
18Ni	MIG	Telmar-90/110	24	160	500 (20)	7	24	160	250 (10)	14
	EB	Autogenous	NA	NA	NA	NA	140x10 ³	35x10 ⁻³	250 (10)	1
NCMV	MIG	A532	27	230	275 (11)	3	27	230	275 (11)	11

Notes: MMA = Manual metal arc; TIG = Tungsten inert gas; EB = Electron beam; MIG = Metal inert gas; NA = Not applicable; square edge close butt weld made.

Table 4. Typical SCC data.

Steel	Weld	Region tested	K_Q		K_{ISCC}	
			$N_{mm}^{-3/2}$	$(ksi/\sqrt{in.})$	$N_{mm}^{-3/2}$	$(ksi/\sqrt{in.})$
RS 140	MMA	Parent material	4630	(133)	1740	(50)+
		Transformed HAZ	NA		1810	(52)
		Subcritical HAZ	NA		2610	(75)
FV520S	Simulated*	As-welded single pass transformed HAZ	1220	(35)+	240	(7)+
		Parent material	3410	(98)	2090	(60)+
		Transformed HAZ	3480	(100)	2720	(78)
18Ni	EB	Subcritical HAZ	3130	(50)	2610	(75)
		Transformed HAZ	4520	(130)	2780	(80)
		Weld metal	4500	(129)	2610	(75)
18Ni	MIG	Parent material	3510	(101)	2260	(65)+
		Transformed HAZ	3650	(105)	2780	(80)
		Subcritical HAZ	3480	(100)	2610	(75)
NCMV	EB	Transformed HAZ	3480	(100)	2960	(85)
		Weld metal	2090	(60)	1390	(40)
		Parent material	2020+	(58)	310	(9)+
NCMV	MIG	Transformed HAZ	2960	(85)	696	(20)
		Weld metal	2710	(78)	2440	(70)

* Furnace simulation; 950°C, 30 min, followed by glycerine quench.
+ Plane strain values.

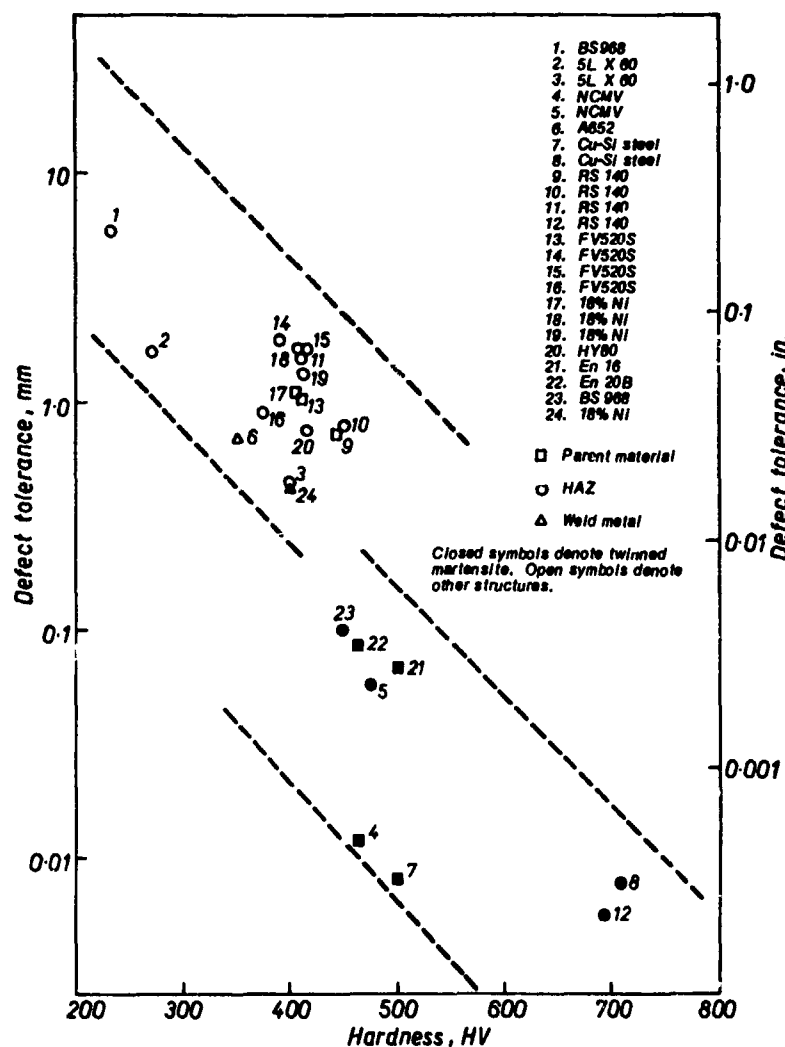


Fig. 3. Relationship between hardness and defect tolerance, calculated from $K = \sigma/\sqrt{ra}$, where σ is the sample yield stress, or an approximation after M. W. F. Cane (6).

SCREENING TESTS OF SUSCEPTIBILITY
TO STRESS CORROSION CRACKING

by

G. J. Biefer* and J. G. Garrison**
Research Scientist* and Senior Technologist**
Corrosion Section, Physical Metallurgy Division
Mines Branch, Department of Energy, Mines and Resources
568 Booth Street
Ottawa, Ontario, K1A 0G1, Canada

SUMMARY

For five high-strength alloys, susceptibilities to the propagation of stress-corrosion cracking (SCC) have been assessed. Using 3.5% NaCl solution as the medium, both parent and weld metals were investigated. Specimens were studied under freely corroding conditions, and also cathodically protected at the potentials given by cadmium and by zinc sacrificial anodes. The well-known cantilever test was used; the test specimens, cut from 1/2- and 3/4-in. plates, were bars notched on both the sides and the top. Prior to tests, a pre-crack was always produced at the base of the top notch by fatiguing in air. The equipment was designed so that specimens, loaded as cantilevers, were broken by means of a steadily rising load. This was applied by dripping water at a constant rate into a container suspended from the end of the cantilever beam.

Results were reported in terms of the nominal stress intensities K^* at fracture. While, strictly speaking, only of qualitative significance, reproducibility of the K^* values was good and the effects of metallurgical and environmental factors could be readily estimated. For example, it appeared clear that for each of 18% Ni (200) maraging, HP9-4-25 and HY 140 steels, resistance to SCC propagation is noticeably impaired by cathodic protection at the potential provided by zinc, i.e., about -1.05 volts saturated calomel electrode (SCE). Resistance to cracking is considerably greater than this at the potential provided by cadmium, i.e., about -0.75 volt SCE. For the maraging and HP9-4-25 steels, weld metal is notch-sensitive under dry conditions and is considerably less resistant to SCC than parent metal. Titanium 6211 and Inconel 718 are both highly resistant to SCC propagation under all test conditions investigated.

SCREENING TESTS OF SUSCEPTIBILITY TO STRESS CORROSION CRACKING

G. J. Biefer and J. G. Garrison

INTRODUCTION

The Physical Metallurgy Division (PMD) of the Canadian Department of Energy, Mines and Resources became involved with the stress-corrosion cracking (SCC) of high-strength materials because of its close working relationship with the Canadian Department of National Defence. In particular, we have been connected with the Canadian FHE 400 prototype Hydrofoil Craft. The material chosen for the foils system of the Hydrofoil was 18% Ni (250) maraging steel, which has a yield strength of 250,000 psi. However, there have been operational difficulties because of stress-corrosion cracking of the foils in sea water, much of the cracking being of the hydrogen-embrittlement type. It therefore appeared that a more crack-resistant alloy would have to be used if more hydrofoil craft were to be constructed.

Consequently, the Canadian Navy asked PMD to investigate a number of alternative high-strength materials which might be used instead of the 250 grade maraging steel in future Hydrofoils, or in other demanding marine applications. An important part of this investigation was an assessment of SCC susceptibility. We decided to use the SCC test developed by B. F. Brown (1), in which notched, pre-cracked metal specimens are stressed in cantilever bending. To economize on technician operating time and also on total lapsed time in the tests, we decided to fracture the specimens by application of a steadily rising load.

EXPERIMENTAL

The alloys selected for study were those described in Tables 1 and 2. Both parent and weld metal were investigated. The welding was carried out at PMD and was TIG, except for the titanium alloy, which was pulsed-arc MIG. Both parent and weld metal of 200 grade maraging steel had been aged at 900°F prior to testing. Inconel 718 plate had been received in the solution-treated condition; specimens cut from this plate had then been given a two-stage ageing treatment at 1325°F then at 1150°F, before testing. The Inconel 718 welds had been solution treated at 2000°F; the specimens had then been machined and the ageing treatment performed as for the parent specimens. No heat treatments had been given to the other three alloys tested.

Our test specimens, similar to those used by B. F. Brown and co-workers, have been bars 6 to 8 in. in length cut from 1/2- and 3/4-in. plate, the lengths of the bars being in the rolling direction and their depths in the direction of the plate thickness. Weld metal specimens were cut with their lengths transverse to a butt weld. As shown in Figure 1, the bars were notched on their sides and also on their upper surfaces; weld metal specimens were notched on the weld centre plane. Prior to tests, specimens were always pre-cracked in the upper notch to a depth of 0.010 to 0.030 in. by fatiguing in air. The pre-crack plane, therefore, was normal to the L direction of the plate; when the specimen was stressed, the crack would be expected to propagate in the T direction (LT crack).

Specimens were mounted in the test rig by clamping one end to a solid vertical post, and the other end to a cantilever arm. The specimen was then stressed to failure by adding water, at a constant rate, to a container hanging from the end of the cantilever arm (Figure 2). The water had been transmitted from the main reservoir through a siphon tube, the upper end of which passes through a float within the reservoir. The water then exits through a delivery nozzle which is always the same vertical distance below the surface of the reservoir. Therefore, the driving hydraulic pressure remains constant as the reservoir empties, keeping the rate of flow of water into the container constant. By inserting nozzles with different internal diameters, steady loading rates in the range 0.125-360 lb/hr are obtainable. It was found necessary to add a germicide to the water, to prevent a build-up of organic growths from clogging the nozzles and reducing flow rates.

For all materials, specimens were first of all broken dry, the loading being carried out at a rapid rate which will be specified later. Fracture of the specimen and consequent descent of the container operated a micro-switch which then activated a cut-off valve in the siphon line and also deactivated a timer. Pre-crack depth was then measured on the fracture face and, along with the total breaking load, was used to calculate the nominal stress intensity at fracture K^* according to the equations shown in Figure 3. K^* is obtained using the equations given by Brown (1) for evaluating K_{I1} but includes the correction for the side notching $\left(\frac{B}{B_N}\right)^{3/2}$ as proposed by Freed and Krafft (2).

In most cases, specimen dimensions did not provide plane-strain conditions according to the criteria proposed by the ASTM (3) and hence the K^* values we obtained on dry specimens cannot be considered to have the significance of true stress intensities. However, K^* is directly proportional to

the load at fracture, multiplied by an essentially geometrical term, so it appeared acceptable to use it in a purely comparative way, to reveal large differences in behaviour caused by environmental changes.

After testing under dry conditions, K^* was then measured for specimens broken in contact with 3.5% NaCl solution. This was done in the usual way by enclosing the specimen, in the notched area, with a plastic bottle containing the solution, which was replenished at a rate of about 5 liters/day. Specimens were tested under free-corrosion conditions, and also cathodically polarized, by means of a bar of cadmium or of zinc immersed in the specimen vessel and connected externally to the specimen. Despite the replenishment of the 3.5% NaCl solution, the use of the sacrificial anodes sometimes caused rises in pH, in an erratic fashion. From occasional sampling, in tests which had lasted overnight or longer, pH was 5.3 to 7.6 for solution in contact with freely corroding specimens. When specimens were coupled to zinc, pH values were usually in the range 6.3 to 7.5, but a few readings in the range 8.0 to 8.7 were obtained. For specimens coupled to cadmium, pH values were often higher than 9.0, and lay in the range 6.1 to 9.6**.

In our initial rising-load tests in 3.5% NaCl solution, for the most part on 250 grade maraging steel, we had found that the K^* values obtained were highly dependent upon specimen loading rate⁽⁴⁾. K^* also tended to be higher than the threshold value K_{ISCC} , because it was affected by such factors as induction periods, slow crack propagation during loading, and crack branching or delamination along the plate rolling plane. At rapid loading rates, the latter factors could even yield artificially elevated K^* values which were considerably higher than K^* determined under dry conditions. However, it was found that wet K^* values became lower and more consistent as the specimens were loaded more slowly. In contrast, the results obtained with dry specimens were more or less unaffected by loading rate.

On the basis of this earlier experience, standard test conditions were selected. The initial load, deriving from the cantilever beam, the empty container and its supporting straps, etc., was generally in the vicinity of 20 kpsi/in. For the most crack-susceptible alloys, a lightweight container giving an initial load of about 10 kpsi/in. was used. The loading rate employed for dry specimens was such that the stress intensity increased by 2-4 kpsi/in./min. For tests in 3.5% NaCl solution, a much lower rate of increase in stress intensity was used - 0.005 to 0.010 kpsi/in./min. Therefore, for example, a dry test might be over in 20 min, while a test in 3.5% solution might last as long as 200 hr.

RESULTS AND DISCUSSION

Table 3 presents the results obtained, in terms of K^* values, for the alloys studied. Results are given for both parent and weld metals broken dry, freely corroding, and coupled to cadmium or to zinc. Some of the trends indicated by these data are the following:

1. As freely corroding parent metal, the 200 grade maraging steel has very little tendency to propagate stress-corrosion cracks, but can be hydrogen-embrittled at the potential supplied by zinc. As recommended by International Nickel Co., we had used the 250 grade wire for welding this alloy; weld properties, as shown by our work, were definitely inferior to those of the parent metal.
2. The HP9-4-25 steel tested appeared to be generally less resistant to crack propagation than the 200 grade maraging steel. In particular, it was highly susceptible to hydrogen-embrittlement cracking. The weld metal showed inferior properties and was exceptional in that it showed crack propagation at an angle to the plane of the pre-crack.
3. When freely corroding, both parent and weld metal of HY-140 were quite resistant to crack propagation, and resistance was even greater at the potential supplied by cadmium. However, there was evidence of hydrogen embrittlement at the potential supplied by zinc.
4. Inconel 718 parent metal was resistant to crack propagation under all test conditions. The solution-treated and aged weld metal was also resistant.
5. Titanium 6211 was resistant to crack propagation under all test conditions, as both parent and weld metal. There was a tendency for the free-corrosion K^* values obtained for the parent metal to be slightly higher than the dry K^* values. From examination under low-power stereomicroscope, this appeared to result from delamination in the rolling plane near the pre-crack tip, which had a slight "crack-blunting" effect.
6. With respect to the three high-strength steels, it appears that their worst deficiency is a susceptibility to hydrogen-embrittlement cracking at the rather negative potentials usually used in cathodic protection systems in sea water. These may be in the vicinity of the potential given by zinc, or even more negative. For the 200 grade maraging and the HP9-4-25 steels, there seems to be a rather severe lowering of properties in welds.

** For saturated $Zn(OH)_2$ solution the equilibrium pH value should be 8.3, whereas for saturated $Cd(OH)_2$ it should be 9.3.

Other comments could be made, and other examples of its application cited, but the foregoing data are considered sufficient to show that the rising-load cantilever test is a reasonably good screening method for testing susceptibility to stress-corrosion crack propagation, in that useful preliminary information can be gained regarding the probable effects of metallurgical and environmental variables. More extensive and quantitative testing can then be carried out in the areas of greatest interest.

REFERENCES

1. B. F. Brown, "A New Stress-Corrosion Cracking Test for High-Strength Alloys", *Materials Research and Standards* 6, (March 1966), 129.
2. C. N. Freed and J. M. Krafft, "Effect of Side Grooving on Measurements of Plane-Strain Fracture Toughness", *Journal of Materials*, 1, (December 1966), 770.
3. "Tentative Method of Test for Plane-Strain Fracture Toughness of Metallic Materials", *ASTM E399-70T Standards*, Part 31 (1971).
4. B. C. Syrett and G. J. Bieffer, "The Rising-Load Cantilever Test: A Rapid Test for Determining the Resistance of High-Strength Materials to Environmental Cracking", *Mines Branch Research Report R227*, Department of Energy, Mines and Resources, Ottawa, Canada (July 1970).

ACKNOWLEDGEMENTS

Specimens were welded by personnel of the Welding Section of the P.M.D. Test rig and specimen fabrication were carried out at the Mines Branch Machine Shop.

TABLE 1

General Description of Alloys

Alloy	Source and Shipping Slip Identification	Additional Heat Treatments Given	Nominal YS, kpsi	Parent Metal Hardness, Rc
18% Ni (200) maraging steel	Cameron Iron Works, Camvac 200, 1/2-in. vacuum-melt plate, solution annealed at 1500°F for 1 hr.	3 hr at 900°F	200	44
HP9-4-25 steel	Republic Steel Co., 3/4-in. vacuum-melt plate, quenched and tempered at 1000°F.	None	190	44.5
HY-140 steel	U.S. Steel Co., 3/4-in. plate from heat 4P1435, heat-treated to 150,000 psi yield strength.	None	140	34.5
Inconel 718	Huntington Alloy Products Division of International Nickel Co., 1/2-in. annealed plate from heat HT-43A8EV.	8 hr at 1325°F, then cool to 1150°F and hold at this temperature 8 hr.	166	40.5
Titanium 6211	Reactive Metals Inc., 1/2-in. plate from heat 303065.	None	110	33.1

TABLE 2
Analyses of the Alloys, %

Alloy	C	Mn	Si	S	P	Cu	Co	Cr	Mo	Ni	Other Elements
18% Ni (200) maraging steel (a)	0.01	0.05	0.01	0.007	-	-	8.57	-	3.24	18.81	Al 0.07 B 0.004 Ti 0.19 Zr 0.004
HP9-4-25 steel (a)	0.27	0.21	0.02	0.014	0.005	-	3.86	0.39	0.51	9.48	V 0.08
HY-140 steel (b)	0.11	0.83	0.24	0.008	0.007	0.07	-	0.52	0.50	4.78	Ti 0.001 V 0.08
Inconel 718 (b)	0.05	0.07	0.18	0.007	-	0.07	0.08	19.03	3.02	51.10	Al 0.57 Fe 19.50 Nb 5.20 Ta 0.04 Ti 1.6
Titanium 6211 (b)	0.02	-	-	-	-	0.005	-	-	1.1	-	Al 6.0 Fe 0.18 N 0.009 Nb 2.2 Ta 0.95

(a) Analyzed at the Canadian Department of Energy, Mines and Resources.

(b) Analyzed by the Supplier.

TABLE 3
Nominal Stress Intensity K* at Fracture

Alloy	Nominal YS, kpsi	K*, kpsi√in.			
		Dry	Freely Corroding	Coupled to Cd	Coupled to Zn
18% Ni (200) maraging steel, parent weld	200	121.5, 114.62 114, 56.5	118, 118.5 45.1, 47.3	106, 99.4 57.4, 55.5	52.5, 50.0 33.4, 30.9
HP9-4-25 steel parent weld	1	106, 108.9 71.4, 81.3	67.6, 57.2 36.9, 41.0	94, 115 37.9, 42.3	28.5, 22.4 18.3, 24.3
HY-140 steel parent weld	140	122.3, 122.4 119.2, 122.5	107, 106.5 100.5, 89	124.8, 116.6 110.2, 110.2	65.5, 69.1 44.1, 54.2
Inconel 718 parent weld	166	104.2, 109.8 108, 108.8	93.6, 103 113, 108	- -	95.4, 91.9 88.6, 85.8
Titanium 6211 parent weld	110	72.5, 69 81, 74	79.6, 93.3 79.7, 79, 74.6	- -	84.4, 88.4 73, 73.6

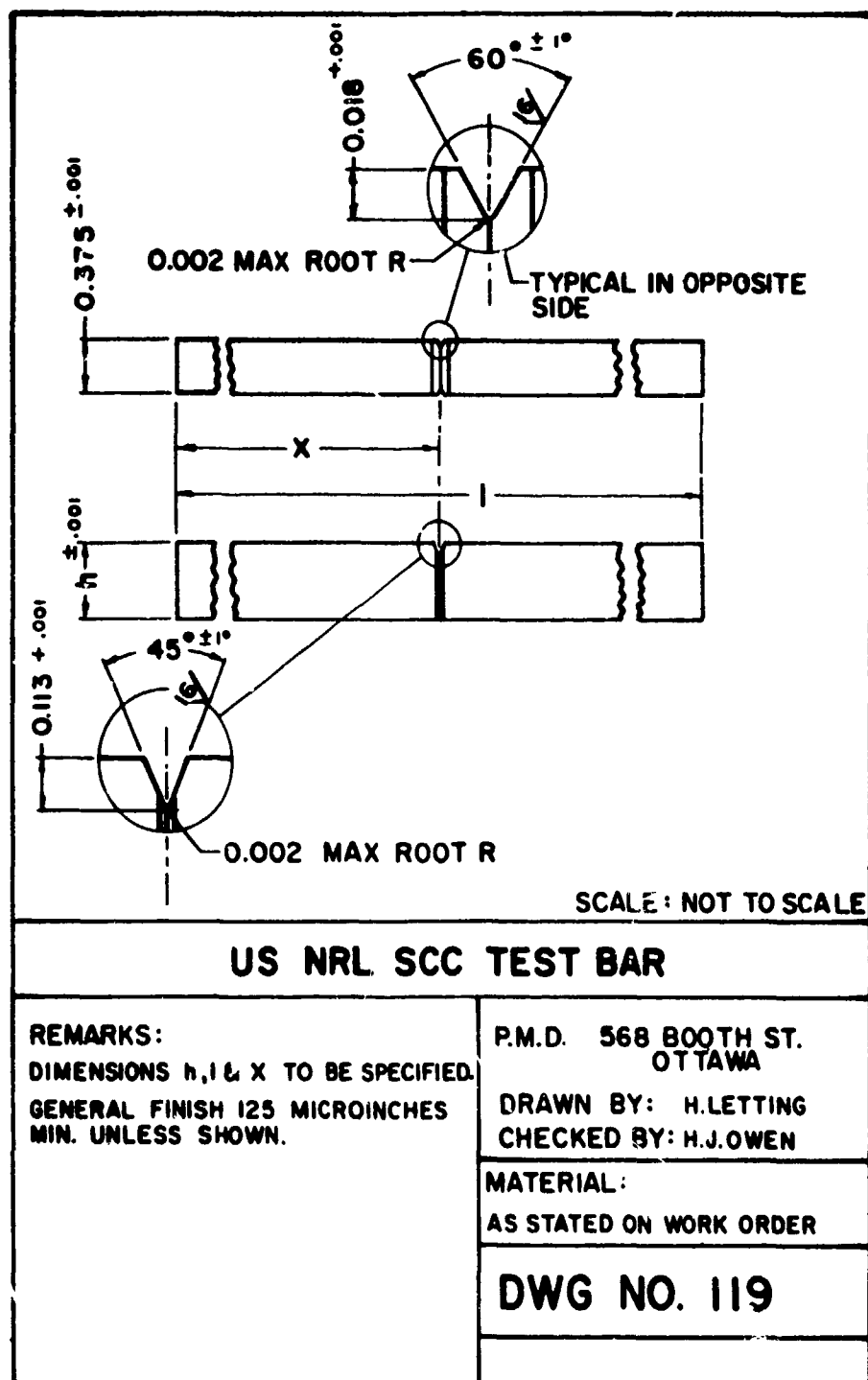


Figure 1. Shop drawing of cantilever test specimen.

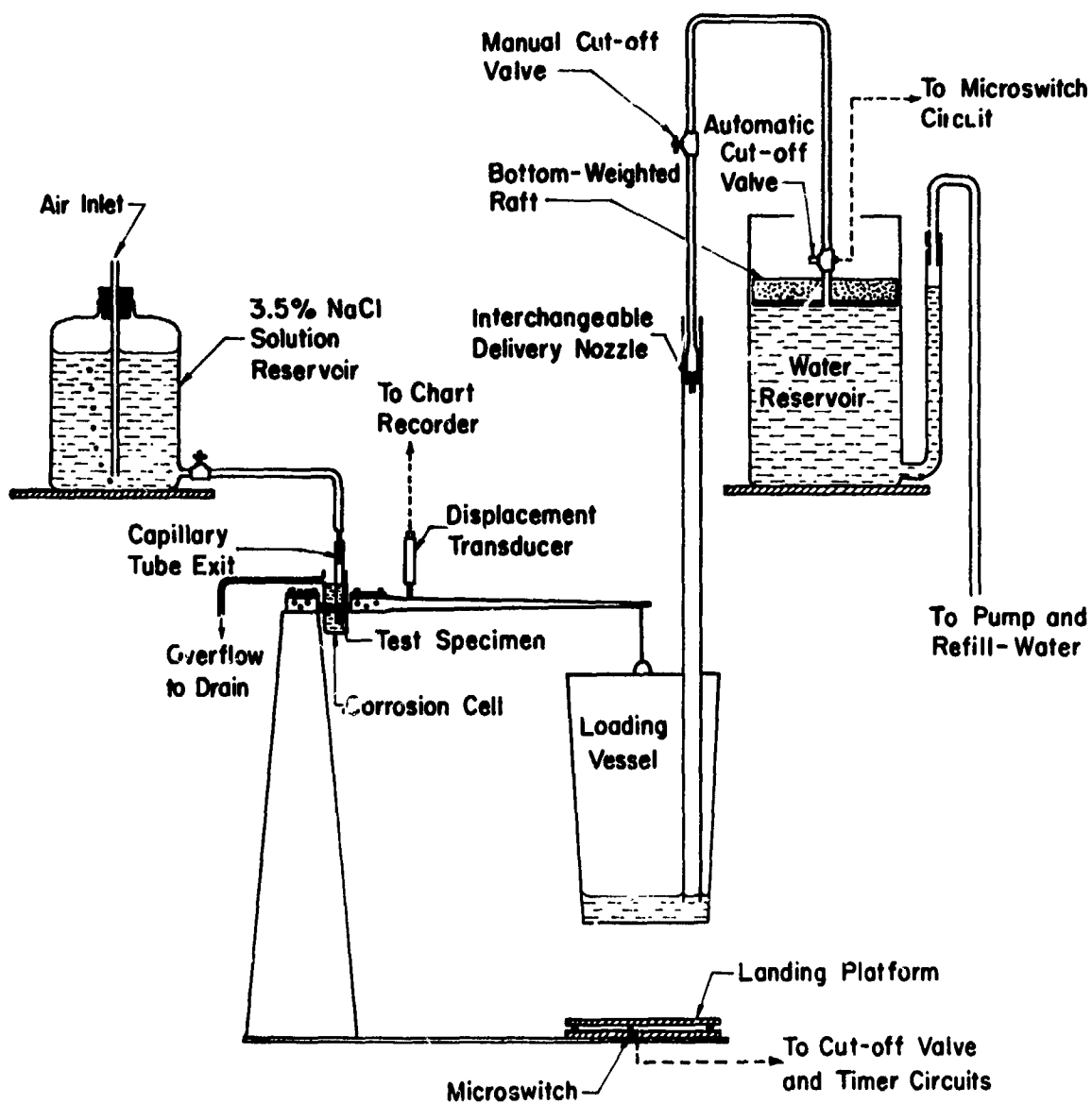
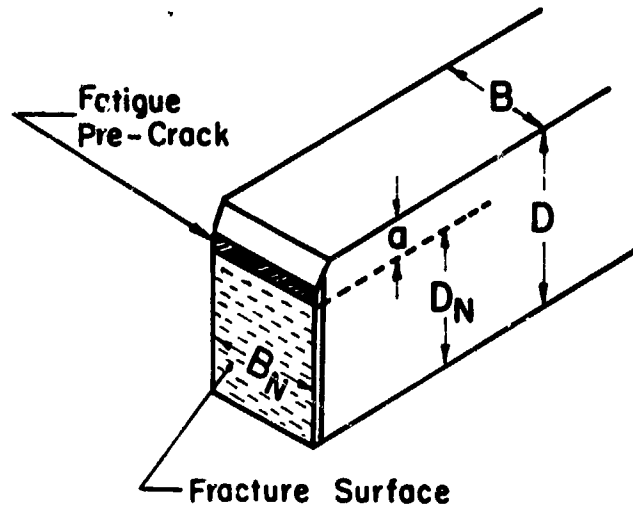


Figure 2. Diagram of the cantilever test rig.

$$K^* = \left(\frac{B}{B_N} \right)^{\frac{1}{2}} \frac{\beta L w}{B D^{3/2}}$$

$$s = \frac{6 L w}{B_N D_N^2}$$



$$\beta = 4.12 \sqrt{\frac{1}{(1 - a/D)^3} - (1 - a/D)^3}$$

K^*	= Stress Intensity at Fracture,	kpsi $\sqrt{\text{in}}$
B	= Specimen Thickness,	in
B_N	= Specimen Thickness at Notches,	in
D	= Specimen Depth,	in
D_N	= Specimen Depth at Notches,	in
L	= Total Length of Cantilever Arm,	in
w	= Total Weight Causing Fracture,	p
s	= Stress at Notches,	kpsi
a	= Upper Notch Depth, Including Pre-Crack	in

Figure 3. Equations used in this work.

**STRESS CORROSION TESTING
OF TITANIUM ALLOYS**

by

S.J. Ketcham*

C.E. Nau*

S. Goldberg**

*** Naval Air Development Center
Warminster, Pennsylvania 18974**

**** Naval Air Systems Command
Washington, D.C. 20360**

SUMMARY

Results are presented of two studies, 1) effect of grain flow orientation on stress corrosion susceptibility of two titanium alloys and 2) stress corrosion tests of titanium electron beam weldments. Emphasis is on test specimens used and on some properties of titanium alloys which have to be considered when conducting stress corrosion tests.

STRESS CORROSION TESTING OF TITANIUM ALLOYS

S.J. Ketrham
C.E. Neu
S. Goldberg

INTRODUCTION

This paper will cover testing experience gained in two studies. The first was concerned with determining whether titanium alloys in thick sections exhibit the anisotropic stress corrosion behavior characteristic of high strength alloys. The second was to determine the stress corrosion behavior of electron beam welded titanium alloys. Alloys studied were Ti-6Al-6V-2Sn, and Ti-6Al-4V.

EXPERIMENTAL PROCEDURE

For the grain flow orientation study, titanium plates 1.75 inch thick (44mm) of Ti-6Al-6V-2Sn, and 2.5 inch thick (63mm) of Ti-6Al-4V were tested in both the annealed, and solution treated and aged (STA) conditions. Mechanical properties and heat treatments are given in Table I.

Notched C-rings were used for the specimen type, (Figure 1). (1) The directionality terminology with respect to the rolling direction is shown in Figure 2. Two sizes of C-rings were used for the Ti-6Al-4V, 1.98 inch (51mm) and 1.65 inch (42mm). For the Ti-6Al-6V-2Sn, a 1.65 inch (42mm) diameter ring was used. The nuts and bolts were Ti-100A alloy.

The procedure for testing the C-rings was as follows:

- (1) Strain gages were attached to the center of smooth C-rings of the same wall thickness as that below the notch in the notched specimens. These rings were tested in compression to determine load versus nominal outer fiber tensile stress by a simple Hook's Law relationship.
- (2) Notched specimens were also tested in compression to determine breaking load in air. Load-deflection curves were obtained.
- (3) Notched rings were then loaded to desired percentages of breaking load (50-85%) by bolt tightening to the corresponding deflection established by the load deflection curves obtained in step (2) above. Specimens were loaded in the testing environment of 3 1/2% NaCl solution to preclude repair of the oxide film in the notch.

In the investigation into the stress corrosion susceptibility of electron beam welded annealed Ti-6Al-4V alloy, three types of specimens were used. Double edge notched tensile specimens and pre-cracked cantilever bend specimens were fabricated from a 2 inch (51mm) thick weldment. The weld crown and drop through on this plate were machined flush. Figure 3 shows the manner in which the specimens were removed from the plate. The plate had been stress relieved at 650C.

Four point bend specimens, 0.25 inch (6.3mm) thick were removed from the face and root side of a 1 inch (25.4mm) thick weldment as shown in Figure 4. The weld crown and drop through were left intact on this plate so as to provide stress raisers. This plate was not stress relieved.

The three types of specimens are shown in Figure 5. For the annealed 6Al-6V-2Sn alloy, only precracked specimens were tested from a 0.5 inch (12.7mm) plate which had been stress relieved at 732C.

All the welds had been inspected by radiographic, ultrasonic and penetrant methods and no flaws were reported.

The double edge notched tensile specimens were subjected to a sustained load of various percentages of the notched breaking strength (75-90%) in stress rupture machines while exposed to 3 1/2% NaCl solution.

The pre-cracked cantilever beam specimens were fatigue cracked in air. Difficulty was encountered in precracking because the face side of the weld tends to crack more rapidly than the opposite side. The precracked specimens were immersed in 3 1/2% NaCl and then deadweight loaded in cantilever bending using the technique described by Brown (2).

On the four point loaded bend specimens, stresses on the outer fibers up to 130 ksi were applied. The deflection required for stressing the welded beam assembly is obtained by use of the following formula:

$$d_s = \frac{2fs}{3Et} (3L - 4a) \quad \text{where}$$

- d_s = change in the distance between the plates along the longitudinal axis of the bolts, in.
 f = the required stress, psi
 E = modulus of elasticity, psi
 t = thickness in.
 L = length (center to center of bolts) in.
 a = distance from center of bolts to nearest flange of "H" section.

RESULTS OF GRAIN FLOW ORIENTATION STUDY

Run-out times were arbitrarily chosen as 200 hours, however any failure that occurred took place

within thirty minutes. Results are shown in Figures 6 and 7. The long transverse direction in annealed material of both alloys was more susceptible than the longitudinal or short transverse directions. Fager and Spurr observed similar behavior with Ti-8Al-1Mo-1V using precracked specimens. (3) The STA condition of both alloys exhibited no clear-cut directional differences.

It was found that specimens that did not fail at low loads should not be subsequently stressed to higher loads. Incremental increases in loading resulted in failures at values near the failure stresses in air. In other words, incremental loading appeared to pre-condition the specimens to endure higher loads.

Metallographic examination of the annealed condition of both Ti-6Al-6V-2Sn and Ti-6Al-4V revealed that the structure of the longitudinal and short transverse directions were similar; the long transverse differed from the other two directions. Microstructural differences however did not appear to account for the increased susceptibility of the long transverse direction.

RESULTS OF ELECTRON BEAM WELDMENTS STUDY

No failures occurred with the notched tensile specimens in 200 hours. Likewise none of the four point loaded bend specimens failed in 200 or more hours.

Results with the precracked specimens are presented in Figure 8. The Ti-6Al-4V weldment had a K_{Isc} value of 29.4 ksi $\sqrt{\text{in.}}$ as opposed to a K_I value in air of 38.0 ksi $\sqrt{\text{in.}}$. The Ti-6Al-6V-2Sn weldment had a K_{Isc} value of 22 ksi $\sqrt{\text{in.}}$ as compared with a K_I value in air of 36.9 ksi $\sqrt{\text{in.}}$.

As with the notched C-rings, incremental loading of the precracked specimens after a run-out of 200 hours, resulted in failures at stress intensities close to that in air.

DISCUSSION OF THE TESTING METHODS

Stress corrosion tests are conducted for a variety of reasons, the reason frequently determining the type of test. The type of specimen to be used is also frequently determined by the form and size in which the metal is available.

For the grain flow orientation study it was necessary to obtain information for titanium that could be related to that already obtained for steels and aluminum alloys.

There is a general specification for design and construction of aircraft weapon systems. This document specifies that for high strength alloys used in naval aircraft, maximum allowable sustained tensile stresses are 50% of the yield strength in the longitudinal direction, 35% in the long transverse direction and 25% in the short transverse direction. Such limitations for titanium alloys were questioned. The specification limitations were based on stress corrosion tests on smooth specimens of high strength steel and aluminum alloys but titanium would not crack without a flaw of some kind. This dictated the use of either pre-cracked or notched specimens. Notched C-rings were chosen for the study because the limitations of plate thickness necessitated a compact specimen for short transverse tests and because it is possible to obtain the nominal stresses at the root of the notch by using smooth C-rings with the same thickness as that below the notch. It developed that at the breaking loads in air, the nominal bending stresses at the base of the notch were considerably above the ultimate tensile strength of the material. The maximum percentages of the breaking loads in 3 1/2% NaCl, which ranged from 55-80%, all represented values above the yield strength of the material. It was therefore decided that a maximum allowable of 60% of the yield strength would be a conservative figure for all directions in Ti-6Al-4V and Ti-6Al-6V-2Sn plate.

The study of the electron beam weldments was instigated by the need to determine the quality of the electron beam weldments being furnished by a contractor. A precracked specimen was the primary specimen selected for this study so that results could be compared with existing data on weldments.

The double edge notched tensile specimen had a notch radius of only 0.01 inch (0.3mm). This specimen had proved to be satisfactory for assessing hydrogen embrittlement effects on steels and titanium alloys. Lane, studying the effect of notches on stress corrosion cracking of titanium, found that a .002 inch (0.05mm) notch radius gave the same results as a fatigue crack. The notched C-ring used for the grain orientation study had a much sharper notch, .003 inch (0.8mm) than the notched tensile, and the C-ring proved to be a satisfactory specimen for the purpose. With a sharper notch the flat tensile specimen might be more useful.

The four point loaded tests of the electron beam welded specimens provided useful information. The specimen simulated an actual component design where the weld drop through would be left intact and where the maximum design stress was below the highest stress level used in the test. The results of these tests indicated that no stress corrosion problems should be encountered under those conditions in that particular application.

The fact that incremental loading preconditioned titanium to endure higher stresses has been recognized by others. One investigator instead of step loading used a constant loading rate of about 6 ksi/min after an initial stress of 50% of the estimated fracture stress was obtained. This was said to provide more consistent data (4). The beneficial effect of preloading on K_{Isc} was also reported in a Boeing study on 4340 steel (5).

References

1. F.S. Williams, W. Beck and E.J. Jankowsky, ASTM Proceedings, Vol. 60, 1192 (1960)
2. B.F. Brown, ASTM Materials Research and Standards, 66, 129 (1966)
3. D.W. Fager and W.F. Spurr, ASM Transactions, Vol. 61, 285 (1968)
4. Reactive Metals Research Report No. R471 of October 1965; Study of Stress Corrosion Cracking of Titanium Alloys in Sea Water with Emphasis on Ti-6Al-4V and Ti-8Al-1Mo-1V Alloys
5. G. Sandoz, Naval Research Laboratory Memorandum Report 2101 of March 1970.

Table I

Data for Titanium Plates Used in Directionality Study

Mechanical Properties

<u>Alloy</u>	<u>Condition</u>	<u>Direction</u>	<u>ksi</u>		<u>Elongation</u>
			<u>.2% Offset Yield</u>	<u>Ultimate Tensile</u>	
Ti-6Al-4V	Annealed	L	130	139	13
		LT	130	139	16
		ST	129	143	12
	STA	L	136	149	12
		LT	137	150	13
		ST	136	153	10
Ti-6Al-6V-2Sn	Annealed	L	144	154	17
		LT	144	154	17
		ST	141	153	7
	STA	L	172	181	11
		LT	170	179	11
		ST	165	177	6

Heat Treatments

Ti-6Al-4V Annealed : 704C (2 hours), air cooled

STA : 843C (1 hour), water quench +
566C (4 hours), air cooled

Ti-6Al-6V-2Sn Annealed : 732C (2 hours), air cooled

STA : 954C (1 hour), water quench +
538C (4 hours), air cooled

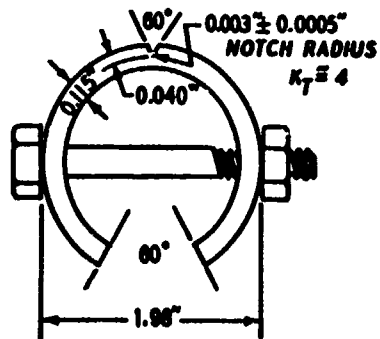


Figure 1 Drawing of notched C-ring

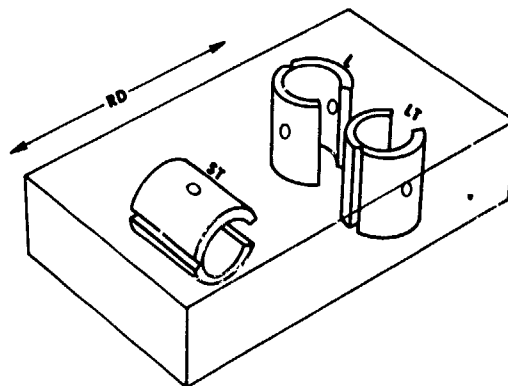


Figure 2 C-ring specimen orientation for titanium plate with respect to rolling direction (RD)

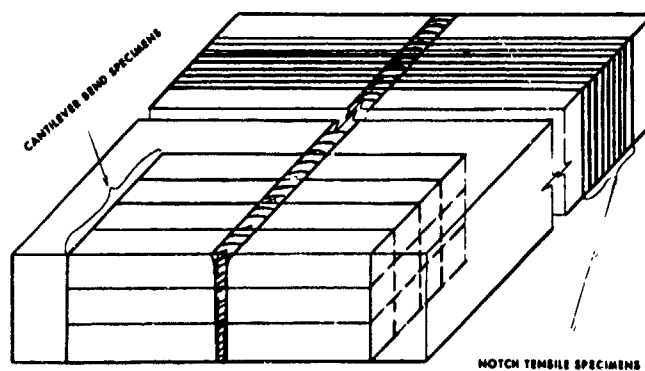


Figure 3 Specimen layout from two inch electron beam weldment

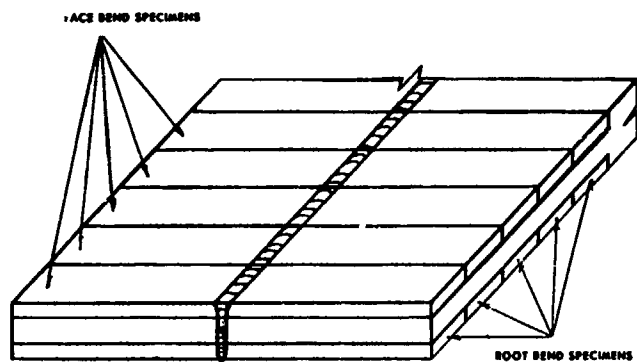


Figure 4 Specimen layout from one inch electron beam weldment



Figure 5 Three types of specimens used for electron beam weld

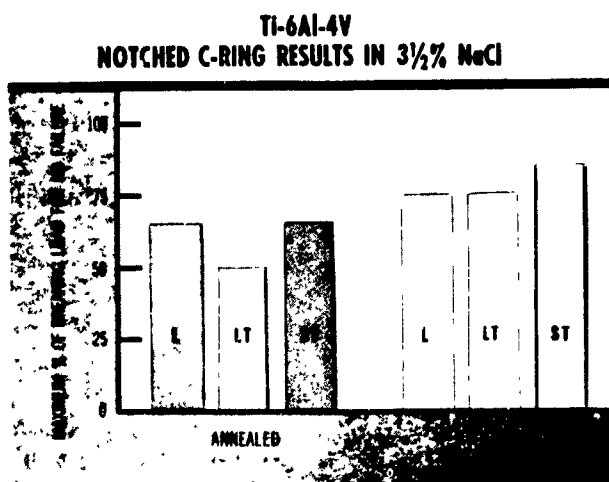


Figure 6 Results of directionality study in Ti-6Al-4V

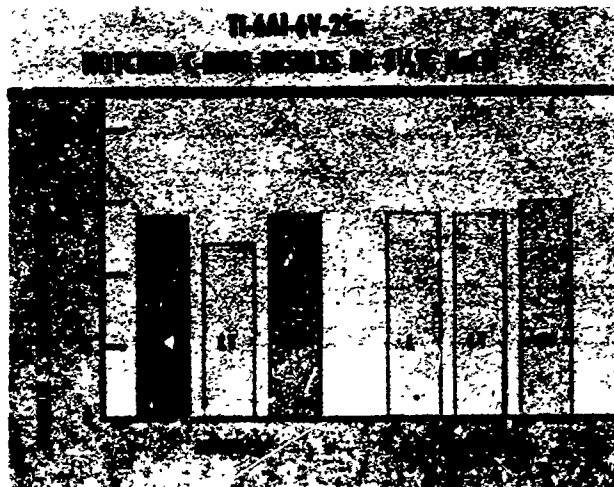


Figure 7 Results of directionality study in Ti-6Al-4V-2Sn

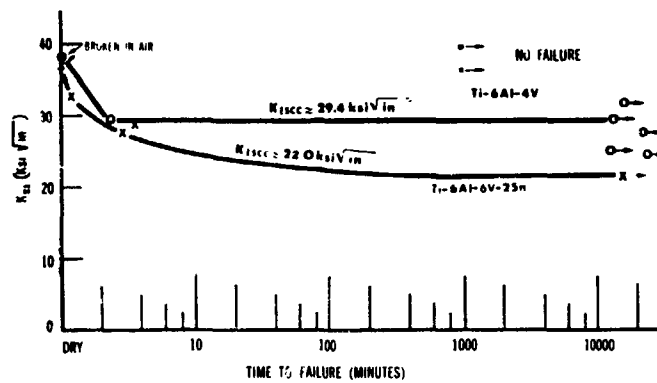


Figure 8 Results for precracked specimens from electron beam weldments

FACTORS INFLUENCING THRESHOLD STRESS INTENSITY VALUES AND CRACK PROPAGATION
RATES DURING STRESS CORROSION CRACKING TESTS OF HIGH STRENGTH STEELS

A. H. Priest
Section Leader
The Corporate Laboratories of the
British Steel Corporation
Hoyle Street
Sheffield S3 7EY, England

P. McIntyre
S.S.O.
The Corporate Laboratories of the
British Steel Corporation
Hoyle Street
Sheffield S3 7EY, England

SYNOPSIS

A number of factors have been identified which influence both observed threshold stress intensity values and crack propagation rates for the stress corrosion of high strength steels in aqueous environments. More specifically: K_{ISCC} values for a number of steels have been shown to be related to the formation of a continuous stretch zone at the fatigue crack tip; both K_{ISCC} and K_{IC} values are influenced by the yield strength and inclusion density of the steel; the relative values of K_{ISCC} determined by arrest and initiation methods and stress corrosion crack growth rates are influenced by the effectiveness of stress corrosion cracks as stress concentrators since intergranular cracks become progressively blunter as they propagate while the reverse can be true of transgranular cracks; observed stress corrosion crack propagation rates are also influenced by the failure to attain equilibrium in specimens of conventional length and by the presence of crack curvature and crack branching where these occur.

**FACTORS INFLUENCING THRESHOLD STRESS INTENSITY VALUES AND CRACK PROPAGATION
RATES DURING STRESS CORROSION CRACKING TESTS OF HIGH STRENGTH STEELS**

A. H. Priest and P. McIntyre

INTRODUCTION

Research on the application of fracture mechanics to stress corrosion cracking has been directed towards a study of the factors governing both the threshold stress intensity for stress corrosion cracking, K_{ISCC} , and stress corrosion crack growth rates. Whilst final conclusions concerning these factors have not been reached, the present report is devoted to a brief summary of some of the more significant current findings.

1. FACTORS INFLUENCING K_{ISCC}

(a) Stretch Zone Formation

A recent study of factors governing the validity of C.O.D. measurements on pre-cracked specimens of mild steel (1) revealed the formation of a small stable ductile stretch zone situated at the tip of the fatigue crack and at 45° to the plane of the fatigue crack under stress corresponding approximately to the onset of general yield in the specimen.

An extension of this work to steels of higher strength levels which are susceptible to stress corrosion cracking has revealed that similar stretch zones are formed at the fatigue crack tip at stress intensity values closely approximating to K_{ISCC} .

Figure 1 shows the fracture surface of a 10 mm. square bend specimen of a Ni-Cr-Mo-V steel tempered at 200°C, for which the K_{ISCC} value is 22 ksi√in. This specimen was pre-cracked and then pre-loaded to a stress intensity of 17 ksi√in. prior to being broken in impact after cooling to 70°K. The transition from fatigue crack (on the left) to rapid fracture (on the right) is not clearly delineated and no stretch zone is evident.

Figure 2 shows a similar specimen which was pre-loaded to a stress intensity of 27 ksi√in. (i.e. just above K_{ISCC}). In this case a continuous stretch zone, consisting of a row of ductile voids, and not exceeding 2 μm in width, is just perceptible at the fatigue crack tip.

In a similar manner, continuous stretch zones were observed to form on pre-loading to stress intensities closely approximating to K_{ISCC} in specimens tempered at 500°C and 600°C. These stretch zones are shown in Figures 3 and 4 respectively. Once again no continuous stretch zones were observed in specimens pre-loaded to below K_{ISCC} .

From these observations it appears that the formation of a stretch zone is a necessary initial step in the stress corrosion process and that the stress intensity required to form this zone governs K_{ISCC} . Such a zone formed at the oxidised tip of a fatigue crack would provide a clean surface to act as a catalyst for the dissociation of the aqueous stress corrosion solution into hydrogen and oxygen, in much the same way as slip steps in the case of smooth tensile specimens. Some of the hydrogen thus evolved could be atomically adsorbed on to the metal surface and diffuse into the plastic zone where it may be instrumental in promoting sub-critical flaw growth by hindering plastic deformation and facilitating micro-void nucleation in the region of maximum triaxial stress.

The stretch zones form at approximately 45° to the fatigue crack, which corresponds to the elastic plastic interface surrounding the plastic zone at the crack tip.

The stress intensity at which the zone forms is observed to be inversely proportional to the yield strength of the material, since an increase in tempering temperature causes a reduction in yield stress but increase in the stress intensity required to form the zone. In the limiting case of mild steel such zones have not been observed at stress intensities below that required to promote general yield. It is evident that as the ability to absorb interfacial stresses in the elastic-plastic region diminishes with increase in yield strength due to the hindrance of dislocation movement, the propensity towards micro-void nucleation rather than ductile deformation is increased. This behaviour reflects the influence of yield strength on stress corrosion cracking susceptibility; those materials with higher yield stresses being most susceptible.

(b) Influence of Inclusions

Recent work at Birsra has shown the fracture toughness of high strength steels (K_{IC}) to be a function of the empirical expression:

$$\sigma^* - \sigma_y$$

$$\sqrt{N}$$

as illustrated in Figure 5, where: σ^* is some critical fracture stress;

σ_y is the yield stress;

N is the number of inclusions per unit area in the plane normal to the fracture plane.

Because there are, in general, close parallels, between K_{IC} values and K_{ISCC} values a similar relationship exists between K_{ISCC} , yield strength and inclusion density and this further illuminates the mechanism of stretch zone formation.

(c) Measurement Technique

The values of K_{ISCC} can be determined either by initiation from a fatigue crack under constant load or by arrest from a stress corrosion crack under constant displacement. The relative values obtained by these techniques have been found to be sensitive to the stress corrosion crack path, i.e. whether the path is intergranular or transgranular.

Figure 6 illustrates for an EN30B steel (4% Ni-Cr-Mo), notched transversely to the rolling direction, the relationship between the crack blunting coefficient,

$$\frac{K_{IC}^1}{K_{IC}}$$

and the stress intensity during stress corrosion, where K_{IC} is the fracture toughness of the material measured conventionally from a fatigue crack and K_{IC}^1 is the fracture toughness measured from a stress corrosion crack.

The values of K_{IC}^1 were obtained by unloading specimens after various amounts of crack growth in stress corrosion under constant load, drying out the crack tip and then conducting a conventional fracture toughness determination.

The stress corrosion crack path in this material is intergranular and the results show that as the stress corrosion crack propagates it becomes progressively less sharp due to the formation of an "interlocking zone" of incompletely separated grains resulting from multiple small scale branching around individual grains. The corrosion crack becomes progressively more blunt until the stress intensity reaches 50 ksi $\sqrt{\text{in.}}$ above which no further effect is observed. It therefore follows that the stress corrosion crack in this material is a less effective stress concentrator than a fatigue crack and therefore the K_{ISCC} value measured in such a material by an arrest technique would be expected to be greater than that measured by initiation from a fatigue crack. This has been borne out by the results of the Collaborative Test Programme of the Birsra Stress Corrosion Cracking (Fracture Mechanics) Working Group.

Figure 7 illustrates the opposite behaviour observed with another high strength steel (REX539, 2% Ni-Cr-Mo), notched longitudinally, in which the stress corrosion crack path is transgranular. In this case it is unnecessary for the plane of cracking to change at the onset of rapid fracture and so the stress corrosion crack is a more effective stress concentrator than the fatigue crack. Because of this it may be expected that the K_{ISCC} value measured from the arrest of a stress corrosion crack need be no greater than that measured by initiation from a fatigue crack. This point is under investigation at present.

(d) Accuracy of Stress Intensity Measurement

Another important factor which can influence the accuracy of K_{ISCC} measurement is the dependability of the compliance calibration used in the calculation of stress intensities. This was emphasised recently in a project to evaluate a $\frac{1}{2}$ in. thick contoured double cantilever beam specimen possessing a W-value of less than 2 in. A compliance calibration following the method devised by Gallagher (2) indicated a region of apparently constant stress intensity between a/W values of 0.25 and 0.62. However, fracture toughness determinations from specimens pre-cracked to various a/W - values within this range yielded the data shown in Figure 8. Although the compliance calibration indicated a large region of constant stress intensity, it is clear that the actual stress intensity in this region was increasing as the crack propagated under constant load. An analysis of the results in terms of the stress per unit area on the remaining ligament at failure revealed that failure always occurred when a particular stress level was attained, that is to say that the close proximity of the crack tip to the back face of the specimen was responsible for the observed deviation.

Experiments with modified specimens to which parallel-sided extensions have been added to the back face are being conducted at present and initial results show that the problem has been overcome by increasing the stress-bearing ability of the remaining ligament. This phenomenon has not been apparent in the larger contoured specimens previously utilised because of the greater distance of the crack tip within the constant stress intensity region from the back face of the specimen.

2. STRESS CORROSIONFactors Influencing Growth Rates(a) Failure to Attain Equilibrium

A comparison of subcritical flaw growth in high strength steels when tested under constant load in both aqueous and gaseous environments has yielded remarkable similarities between stress corrosion and hydrogen cracking. The K_{ISCC} values and fracture surface appearance are indistinguishable for steels tested in either purified hydrogen gas or 3.5% sodium chloride in deionised water but the growth rates differ markedly, as shown in Figure 9. Crack growth rates were monitored by an electrical resistance technique (3). In the case of cracks grown in gaseous hydrogen an equilibrium growth rate, which is independent of stress intensity and therefore chemically controlled, is rapidly attained, whereas the cracks grown under stress corrosion conditions propagate at a much slower rate which increases progressively during a test but never attains equilibrium. Although hydrogen cracking and stress corrosion cracking are basically similar, the rate controlling process in stress corrosion is obviously much slower so that test piece failure occurs prior to the attainment of an equilibrium growth rate. It is proposed to adopt the use of much longer test pieces in an attempt to obtain quantitative rather than qualitative stress corrosion data.

(b) Crack Branching

Crack branching during stress corrosion is responsible for much slower crack growth rates than would otherwise be the case. This is evident from Figure 10 which shows Brown-type curves for EN30B steel austenitised at both 830°C and 1000°C prior to oil quenching and tempering at 200°C. The material

austenitised at 1000°C exhibited marked crack branching at all stress intensities above 16 ksi $\sqrt{\text{in.}}$ and this was responsible for much slower crack growth rates than those observed in material austenitised at 830°C which showed no such tendency. At initial stress intensities above 40 ksi $\sqrt{\text{in.}}$ the branching tendency became so great that arm break-off occurred with the $\frac{1}{2}$ in. CXS specimens which were used. Cotterell (4) has shown that crack path stability during fracture toughness testing of such specimens is a function of the amount of deviation of the crack tip from the ideal plane. As the deviation increases, the ratio of bending stress to ligament stress increases and so the tendency to branch increases.

In EN30B steel the crack path follows the prior austenite grain boundaries. As the prior austenite grain size increases, larger deviations of the crack tip from the ideal plane can occur before the next grain boundary offering a path back towards the ideal plane is encountered. Thus, in material austenitised at 1000°C it is possible for sufficiently large deviations of the crack path to occur along grain boundaries so that the bending moment is large enough to cause crack path instability in the form of branching. It is to be expected that the use of test pieces in which the bending moment due to deviations of the crack from the ideal plane is less would attenuate branching even in material possessing a large prior austenite grain size. Tests are therefore being conducted on centre-cracked plate specimens to confirm this point.

(c) Crack Curvature

Simultaneous monitoring of stress corrosion crack growth by an ultrasonic probe situated at specimen mid-thickness and the electrical resistance technique, which monitors mean crack length, has illuminated the phenomenon of crack curvature during stress corrosion. Figure 11 shows the difference between mean crack length and crack length at mid-thickness during the stress corrosion of EN30B steel. It is clear that crack growth commences in the predominantly plane strain region at mid-thickness, giving rise to marked crack curvature. As the crack extends to the edges of the specimens the influence of the plane stress component retards continued rapid crack growth in the centre and both centre and edges continue to grow together at a somewhat diminished rate of acceleration. Towards the onset of rapid fracture the crack length at the edges of the specimen to some extent catches up with that at the centre, giving rise to the diminished crack curvature observed on the fracture surface. It is quite clear that crack growth rates monitored during stress corrosion are dependent to a large extent upon the monitoring technique adopted.

(d) Crack Blunting

The effectiveness of a stress corrosion crack as a stress concentrator (which was discussed earlier in connection with arrest versus initiation K_{ISCC} values) also influences crack growth rates under non-equilibrium conditions. Reference back to Figure 6 shows that for EN30B steel the intergranular crack path produces blunting which becomes progressively more severe up to a stress intensity of 50 ksi $\sqrt{\text{in.}}$. Figure 12 shows the growth rate behaviour of this material as a function of stress intensity. An initially high rate of crack acceleration at stress intensities below 50 ksi $\sqrt{\text{in.}}$ rapidly diminishes as the crack blunting increases, counteracting the influence of increasing stress intensity. At stress intensities of 50 ksi $\sqrt{\text{in.}}$ and above the lack of any further increase in crack bluntness enables an increase in the rate of crack acceleration to occur.

In comparison with this behaviour, Figure 7 revealed that for REX539 steel the transgranular crack path is a much more effective stress concentrator. The relationship between crack growth rate and stress intensity during stress corrosion shown in Figure 13 reflects this fact, a steady increase in crack growth rate being maintained throughout the propagation process, together with higher absolute values of growth rate.

CONCLUSIONS

Many factors must be taken into consideration during the determination and interpretation of both threshold K_{ISCC} values and stress corrosion crack growth rates. The present work has indicated the important role played by stretch zone formation, inclusions, method and accuracy of measurement of stress intensity or K_{ISCC} values. It has also identified the influence of crack branching, curvature and blunting as well as the non-attainment of chemical equilibrium on the observed crack growth rates in stress corrosion of high strength steels.

REFERENCES

1. D. Elliott and H. Stuart, Proceedings of the 3rd Annual S.E.M. Symposium, Chicago 1970, 305-312.
2. J. P. Gallagher, "Experimentally Determined Stress Intensity Factors for several Contoured Double Cantilever Beam Specimens", Ph.D. Thesis, Theoretical and Applied Mechanics Department, University of Illinois, Feb. 1968.
3. P. McIntyre and A. H. Priest, "Measurement of Sub-Critical Flaw Growth in Stress Corrosion, Cyclic Loading and High Temperature Creep by the D.C. Electrical Resistance Technique". NASA Open Report MG/54/71, June, 1971.
4. B. Cotterell, International Journal of Fracture Mechanics, 6(1970) 189-192.

Fatigue Crack

Rapid Fracture



45° Tilt.

100 μm

FIG. 1. FRACTURE SURFACE OF NCMV STEEL TEMPERED AT 200°C AND PRE-LOADED TO $17 \text{ ksi}\sqrt{\text{in}}$ ($K_{Isc} = 22 \text{ ksi}\sqrt{\text{in}}$)

Fatigue Crack

S Z

Rapid Fracture



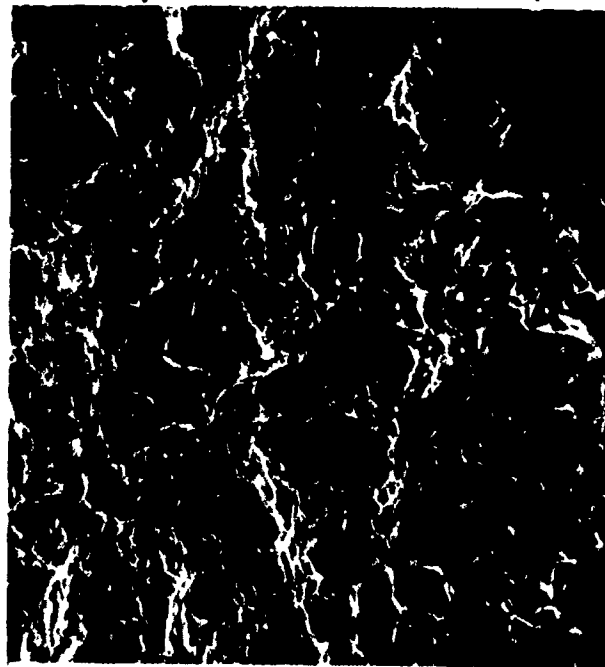
45° Tilt

100 μm

FIG. 2. FRACTURE SURFACE OF NCMV STEEL TEMPERED AT 200°C AND PRE-LOADED TO $27 \text{ ksi}\sqrt{\text{in}}$ ($K_{Isc} = 22 \text{ ksi}\sqrt{\text{in}}$)

Reproduced from
best available copy.

Fatigue Crack SZ Rapid Fracture

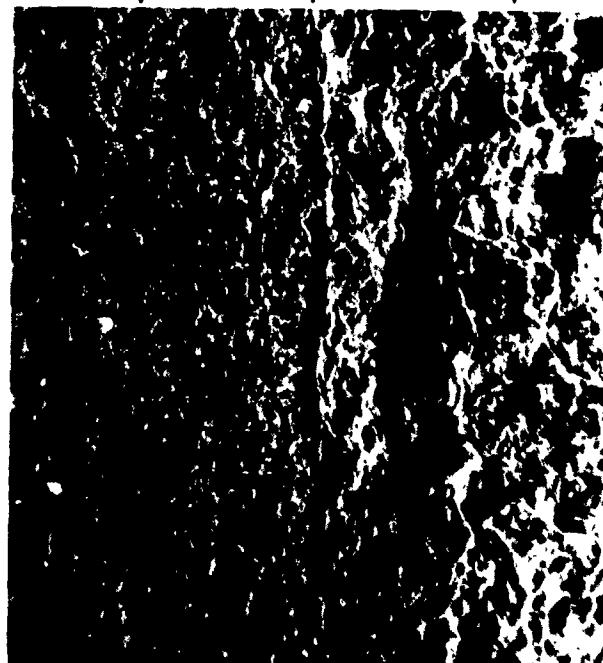


45° Tilt

50 μm

FIG 3 FRACTURE SURFACE OF NCMV STEEL TEMPERED AT 500 °C AND PRE-LOADED TO 35 ksi√in ($K_{ISCC} = 34 \text{ ksi}\sqrt{\text{in}}$)

Fatigue Crack SZ Rapid Fracture



45° Tilt

100 μm

FIG 4 FRACTURE SURFACE OF NCMV STEEL TEMPERED AT 600 °C AND PRE-LOADED TO 36 ksi√in ($K_{ISCC} = 35 \text{ ksi}\sqrt{\text{in}}$)

Reproduced from
best available copy.

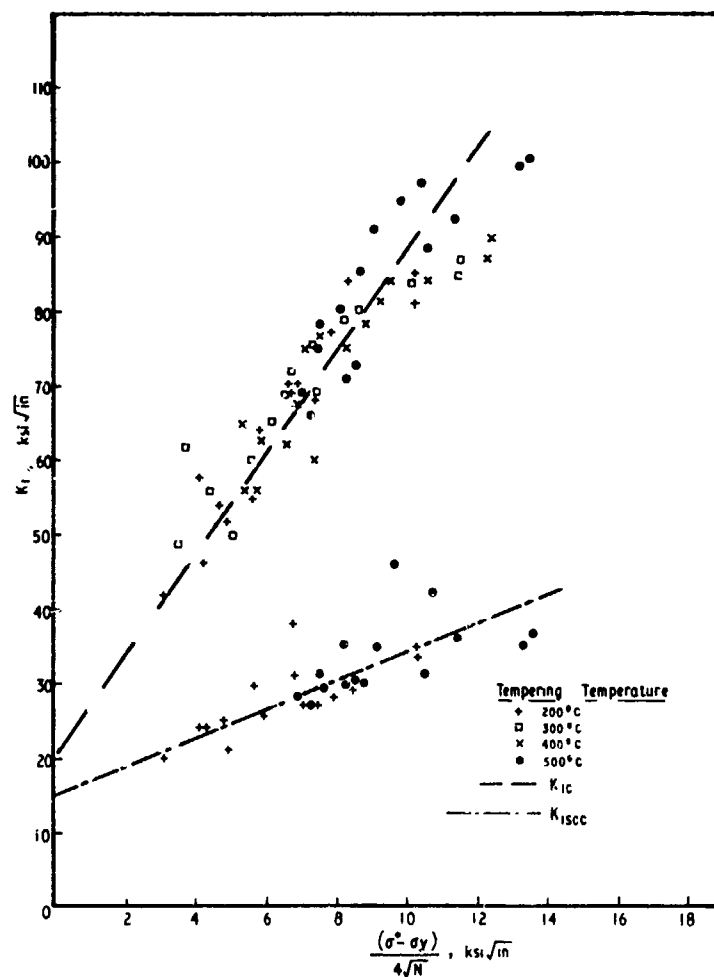


FIG 5. CORRELATION BETWEEN FRACTURE TOUGHNESS, STRESS CORROSION RESISTANCE, YIELD STRESS AND INCLUSION SPACING

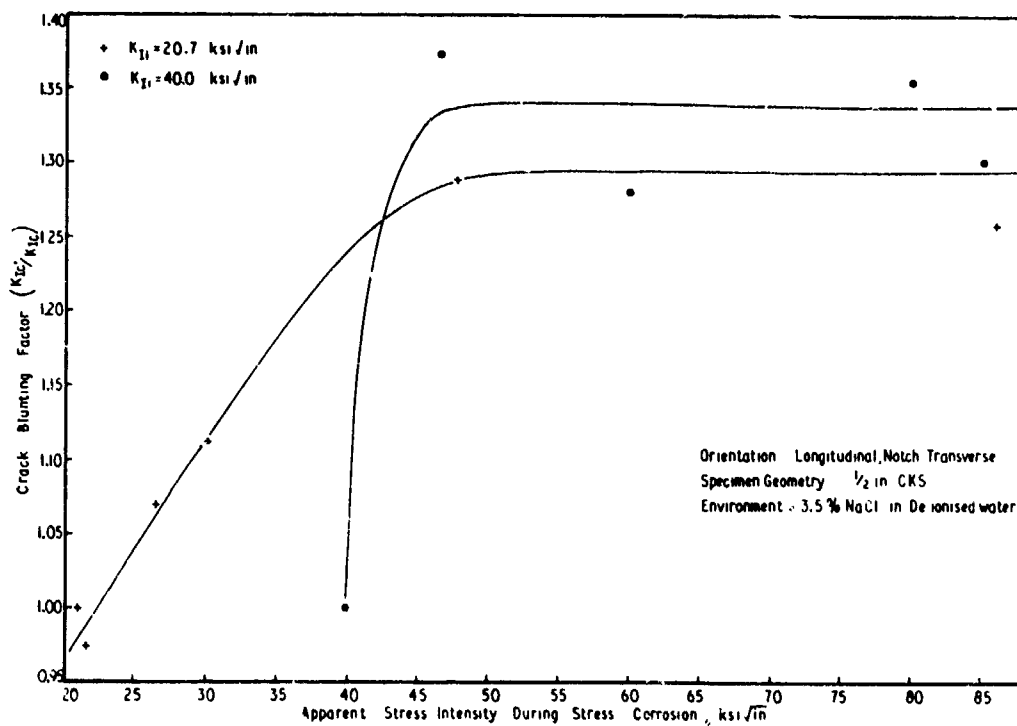


FIG 6 CRACK BLUNTING AS A FUNCTION OF STRESS INTENSITY DURING THE STRESS CORROSION OF EN30B STEEL

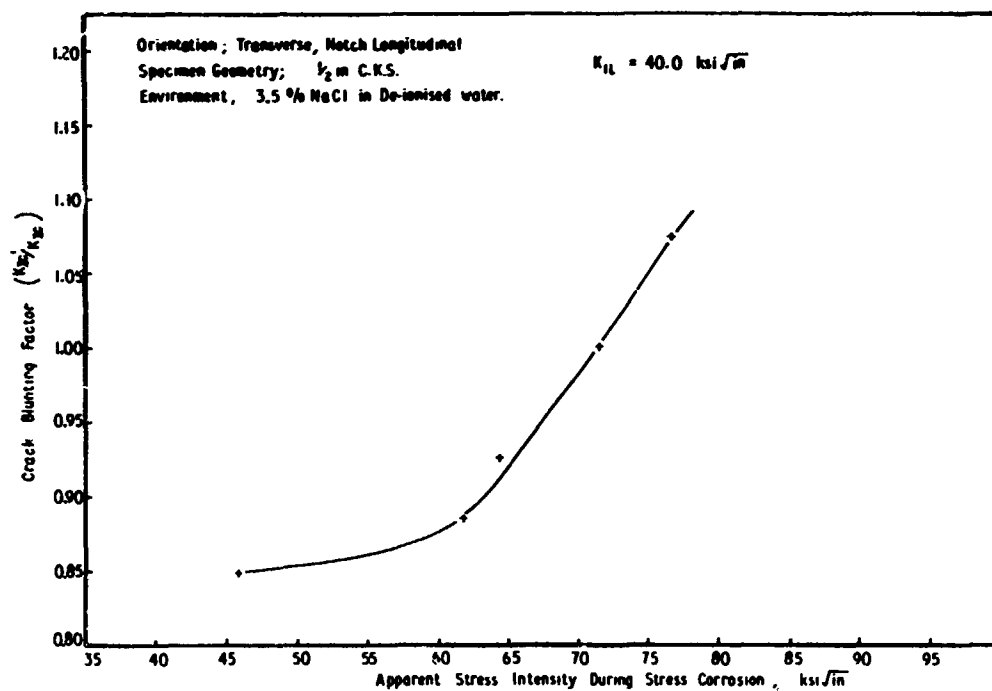


FIG 7 CRACK BLUNTING AS A FUNCTION OF STRESS INTENSITY DURING THE STRESS CORROSION OF REX 539 STEEL

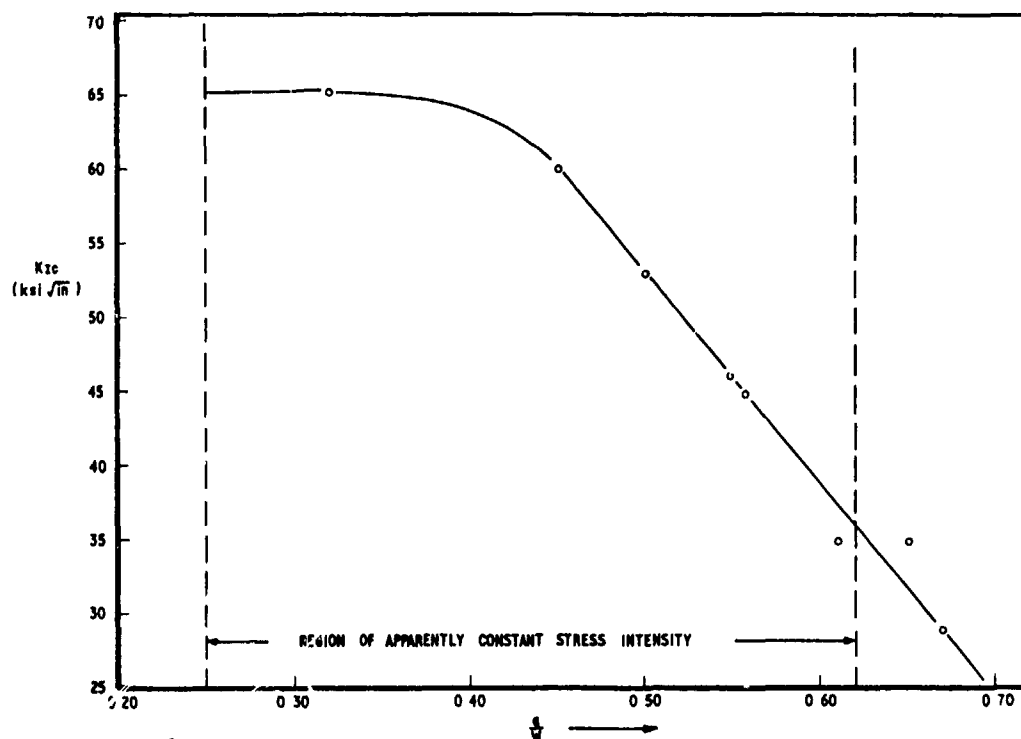


FIG 8 THE $\frac{a}{W}$ -DEPENDENCE OF K_{IIc} IN THE REGION OF APPARENTLY CONSTANT STRESS INTENSITY OF THE CONTOURED $\frac{1}{2}$ DCB SPECIMEN

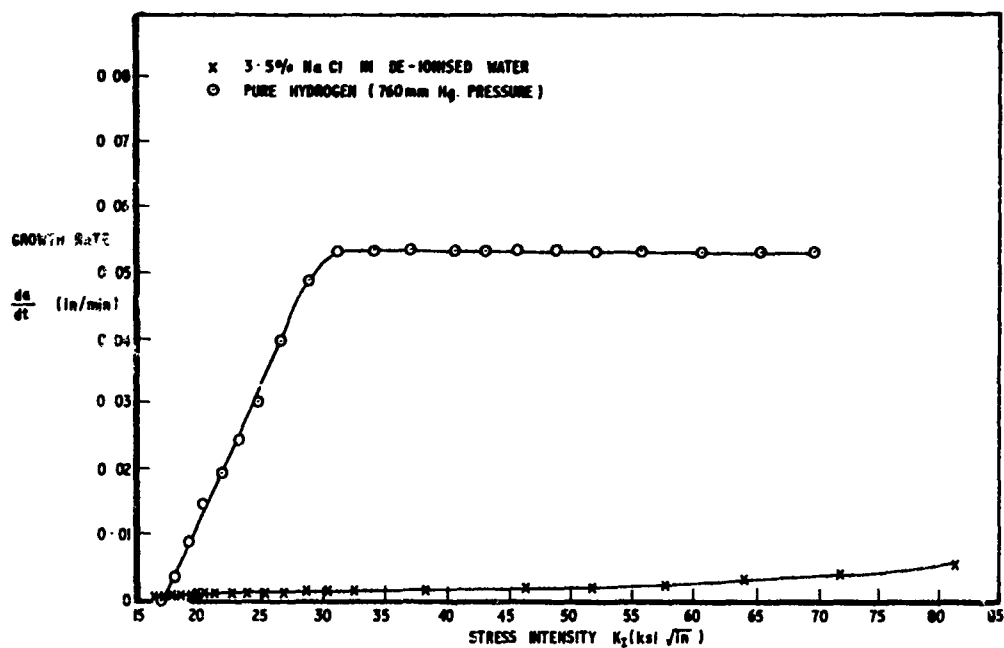


FIG 9 CRACK GROWTH RATE OF EN30B STEEL AS A FUNCTION OF STRESS INTENSITY AND ENVIRONMENT

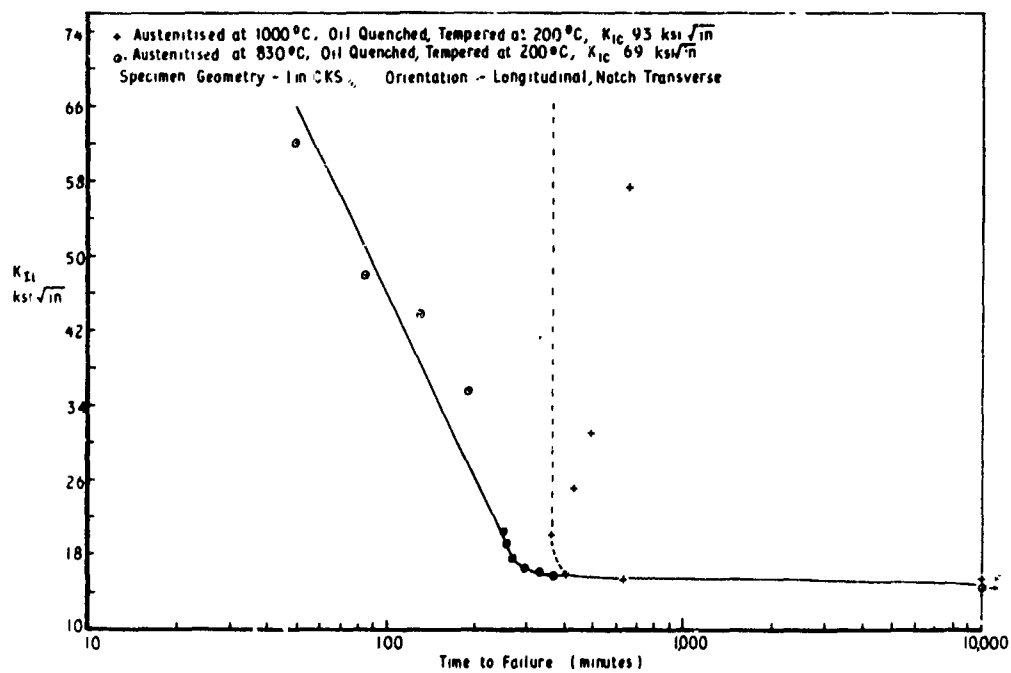


FIG 10 INITIAL STRESS INTENSITY VERSUS TIME TO FAILURE FOR EN30B STEEL (4 1/2% Ni-Cr-Mo)

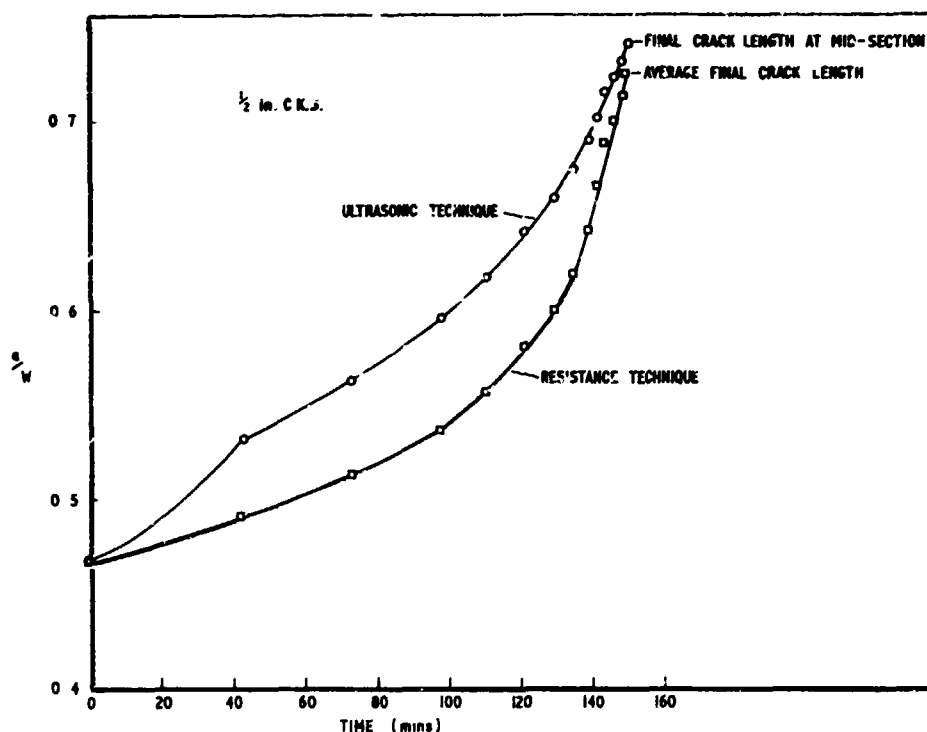


FIG 11 CRACK LENGTH IN STRESS CORROSION OF EN30B STEEL AS A FUNCTION OF TIME

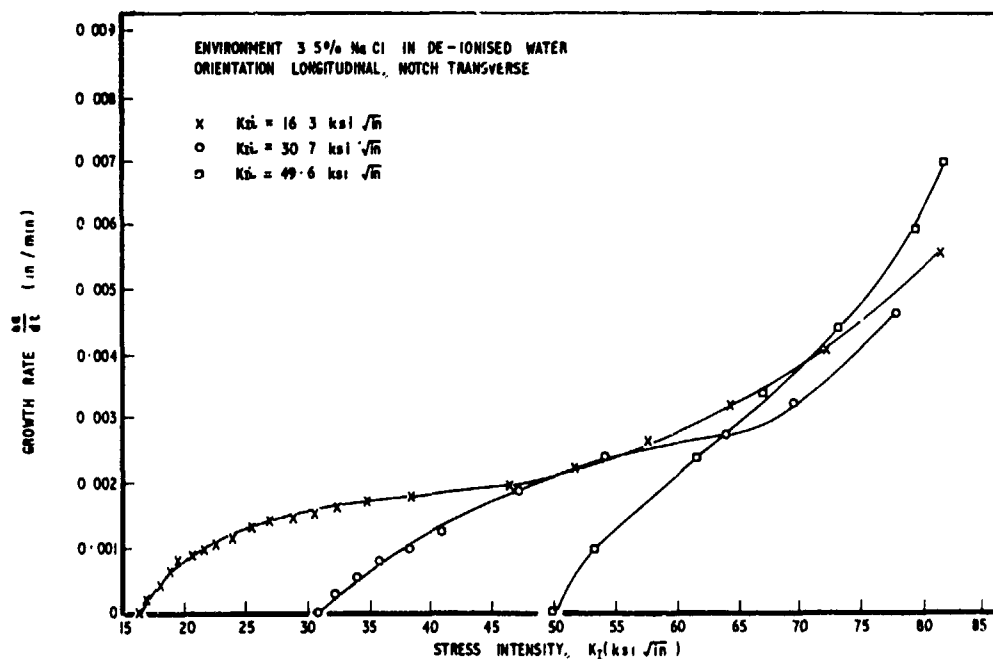


FIG 12 GROWTH RATE AS A FUNCTION OF STRESS INTENSITY DURING THE STRESS CORROSION OF EN30B STEEL

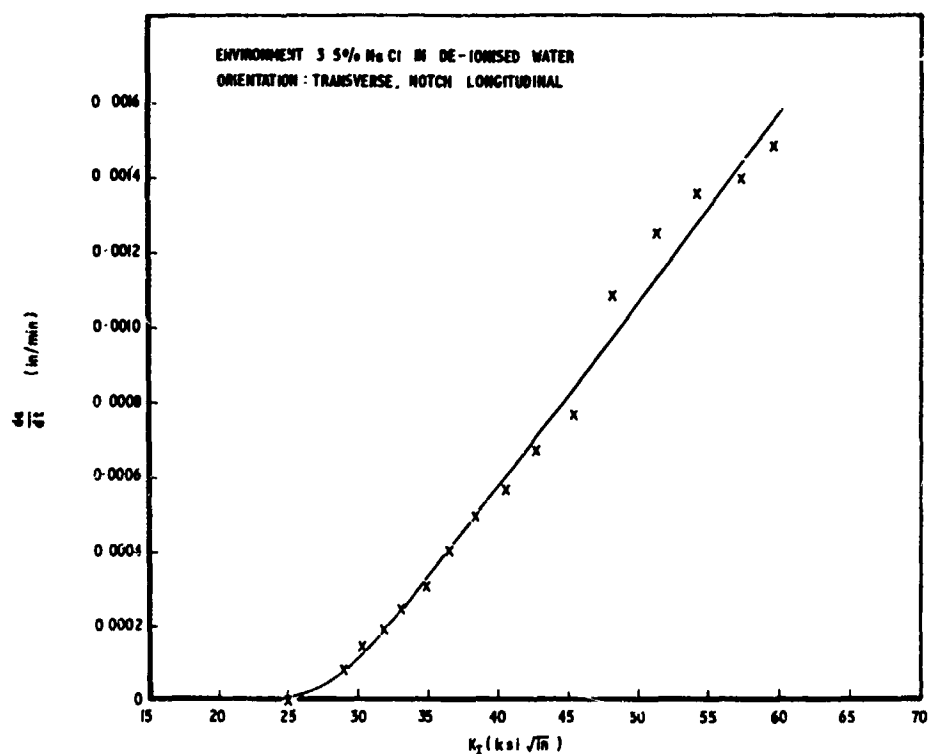


FIG 13 GROWTH RATE AS A FUNCTION OF STRESS INTENSITY FOR THE STRESS CORROSION OF REX 539 STEEL

AN APPARATUS FOR STRESS-CORROSION TESTING WITH LARGE PRECRACKED WOL SPECIMENS

L. J. Ceschini
Senior Engineer
Materials Testing and Evaluation
Westinghouse Research Laboratories
Beulah Road
Pittsburgh, Pennsylvania 15235

and

W. G. Clark, Jr.
Senior Engineer
Mechanics Department
Westinghouse Research Laboratories
Beulah Road
Pittsburgh, Pennsylvania 15235

Summary

A laboratory test unit designed for K_{Isc} and stress-corrosion crack growth rate testing with large (2-4 inch thick) precracked WOL specimens is described. The apparatus involves the use of a unique hydraulic loading arrangement which provides a convenient means of generating the relatively high loads required for stress-corrosion testing with large WOL specimens. Additional features of the test unit include the ability to continuously monitor crack growth during the test and also the ability to test in an enclosed environment at various temperatures and pressures.

Ce document présente un appareil de laboratoire qui mesure le coefficient K_{Isc} défini ci-dessous et le taux de croissance de fissurations. La disposition d'une charge hydraulique unique permet de produire, de façon commode, des forces relativement importantes nécessaires aux tests mesurant les forces de corrosion avec les spécimens WOL. L'appareil permet de contrôler, de façon continue, l'évolution des fissures durant l'essai. En outre, il permet de pratiquer l'essai dans un environnement clos, à différentes températures et différentes pressions.

L. J. Ceschini and W. G. Clark, Jr.

1. INTRODUCTION

Since the development of the fracture mechanics approach to stress-corrosion testing and the subsequent identification of a stress-corrosion threshold parameter, K_{Isc} (the value of plane-strain stress-intensity factor below which an existing crack will not grow due to stress-corrosion), several unique testing procedures have been proposed which can be used to evaluate the stress-corrosion susceptibility of structural alloys.⁽¹⁻⁶⁾ The first widely used stress-corrosion cracking test involving precracked specimens and fracture mechanics concepts was the cantilever beam test developed by Brown.⁽⁴⁾ In this test, a series of precracked cantilever beam specimens is stressed at constant load in the environment of interest and the time to failure recorded as a function of the initial applied stress intensity factor, K_{II} ; where K_{II} is a function of the applied stress and crack size. The initiation of cracking and subsequent crack growth are monitored by measuring the beam deflection as a function of time and subsequently relating the deflection to the crack length from the compliance of the specimen. A schematic illustration of the cantilever beam corrosion test is shown in Fig. 1. The primary disadvantages of this stress-corrosion testing technique are that a separate test facility is required for each test and several specimens are required to establish the K_{Isc} value (a series of tests at decreasing values of K_{II} is conducted until a K_{II} level is reached at which no cracking is observed.)

A more efficient technique for K_{Isc} testing involves the bolt-loaded WOL (wedge-opening-loading) specimen described by Novak and Rolfe⁽⁶⁾ and shown in Fig. 2. In this test procedure, a WOL specimen is self-stressed by means of a bolt and no additional loading equipment is required. Because the test is conducted under constant displacement rather than constant load, as in the cantilever beam test, the load on the specimen and, consequently, the nominal stress intensity factor decrease as the crack grows, leading to crack arrest as K_{II} approaches K_{Isc} . As a result, only a single test is required to establish the K_{Isc} value, although several duplicate tests are normally conducted in order to substantiate the results.

Although the bolt-loaded WOL K_{Isc} test has the distinct advantage of being a self-contained test which requires a minimum of test specimens, this procedure does have two major disadvantages: (1) a technique is not readily available for monitoring crack growth behavior during the test, as a result the test is primarily limited to K_{Isc} testing and; (2) the bolt-loading procedure is not easily adaptable to the testing of large specimens (WOL specimens larger than about 2 inches thick). More specifically, very high torque is required to produce the loads necessary for heavy section tests (several thousand foot pounds are required to bolt-load 3 and 4 inch thick steel WOL specimens to K_{II} levels on the order of 100 ksi $\sqrt{\text{in.}}$).

This report describes a modification to the bolt-loaded WOL stress-corrosion test procedure which readily permits the testing of large WOL specimens and also permits the continuous monitoring of crack growth behavior.

2. CRACK GROWTH MONITORING

An obvious approach to the instrumentation of the bolt-loaded WOL specimen to permit the monitoring of crack growth during a stress-corrosion test is to strain gage and calibrate the bolt to read load directly. From knowledge of the applied load and the displacement across the machined slot (measured with a clip gage and held constant during the test) it is then possible to determine the crack length from the compliance calibration of the specimen:⁽⁶⁾

$$EB \left(\frac{V}{P} \right) = C \left(\frac{a}{w} \right)$$

where:

- E = modulus of elasticity
- B = specimen thickness
- P = applied load
- V = displacement across the machined slot
- C = compliance constant dependent upon the relative crack length, a/w
- a = the crack length measured from the center line of loading
- w = specimen length, measured from the center line of loading

For the case of a given material and specimen size, loaded to a given displacement, it is then possible to use the above equation to construct a curve of applied load versus crack length, which in turn, can be used to generate crack growth rate data. However, because of the nature of loading, the compliance calibration of the loading bolt is strongly affected by the friction associated with the threads and also the friction developed at the area of contact between the bolt and the split pin, (Fig. 2). Kim has shown that it is possible to encounter as much as ± 20 percent difference in the compliance (slope of the load-displacement curve) of the bolt as measured in compression in a test machine and the same bolt threaded into an actual specimen.⁽⁷⁾ Because of the potential error likely to be encountered in an instrumented bolt-loaded WOL stress-corrosion test, consideration was given to modifying the loading arrangement such that accurate crack growth rate data could be obtained during the test. Figure 3 shows the modified loading arrangement developed to permit stress-corrosion crack growth rate testing with the WOL specimen.⁽⁸⁾ A schematic illustration of the loading arrangement is shown in Fig. 4. The loading bolt has been replaced with a clevis and loading stud. Because the loading stud or load cell does not rotate during the loading of the specimen and because the strain gages are located far enough away from the loading nut, no friction problems are encountered, and the load cell calibration is unaffected by the loading arrangement.

3. TEST SPECIMEN SIZE CONSIDERATIONS

It has long been recognized that the state of stress, brittle plane strain or ductile plane stress conditions, may have a significant effect upon the stress corrosion susceptibility of structural alloys. (3,5,9) More specifically, a limited amount of data is available which shows that the stress-corrosion threshold level is strongly affected by the state of stress (stress-corrosion cracks were found to grow under plane strain conditions, whereas they did not grow under non-plane strain conditions.) (5,9) In view of these observations and the absence of more definitive data, it is necessary to assume that stress-corrosion cracking is a more severe problem under plane strain conditions. Therefore, it is obvious that stress-corrosion data generated under plane strain conditions are required for use in the design of structures which operate or are assumed to operate under plane strain conditions. Consequently, depending upon the material and structure under consideration, adequate stress-corrosion testing may require relatively large test specimens. As pointed out earlier, bolt loaded, intermediate strength steel WOL specimens in excess of about 2 inches thick require torque levels which cannot be conveniently developed manually. Since many structures of concern to Westinghouse involve high-toughness materials used in very heavy sections, a procedure for stress-corrosion testing with large toughness specimens is required to evaluate the stress-corrosion susceptibility of these materials. As a result, consideration was given to the development of a stress-corrosion testing procedure which could be used to test relatively large (3 and 4 inch thick) WOL specimens. Additional requirements taken into consideration were the development of a loading arrangement which would permit the load to be changed easily during the test and a procedure which could be used for testing in gaseous environments at various temperatures and pressures.

Figure 5 presents a schematic illustration of the loading arrangement developed to satisfy the testing requirements described above.

This loading arrangement is essentially a modification of the clevis-loaded test fixture shown in Fig. 4. The significant features of the modified loading arrangement include: (1) the use of a "pancake" hydraulic cylinder to develop the high loads required for the stress-corrosion testing of large WOL specimens; (2) the use of a hydraulic cylinder also permits the load to be changed at any time during the test; (3) the use of a strain gaged loading stud which permits constant monitoring of the applied load and consequently crack length as discussed earlier; (4) the use of a L.V.D.T. (linear variable differential transformer) to permit the continuous monitoring of crack opening displacement during the test; and (5) the use of a gas tight chamber which permits stress-corrosion testing in gaseous environments at various temperatures and pressures. An additional feature which can be extremely valuable is the ability to subject the specimen to cyclic loading at any time during the test. This is done simply by replacing the hydraulic pump with a servo-hydraulic system. Figure 6 shows the stress-corrosion test unit and associated instrumentation used to monitor the test.

4. DISCUSSION AND SUMMARY

The bolt-loaded WOL specimen is the most efficient and least expensive test currently available for the K_{ISCC} testing of relatively small specimens. However, when it is necessary to generate stress-corrosion crack growth rate data, as well as K_{ISCC} threshold data, we recommend the use of the clevis loaded fixture shown in Fig. 4. The small increase in initial cost of the clevis loaded fixture is well worth the ability to generate accurate crack growth rate data.

With regard to the stress-corrosion testing of large WOL specimens, a bolt-loading arrangement is not satisfactory due to the excessive torque required to load the specimen and alternate means of loading the specimen are required. The apparatus described in this paper provides a convenient means of loading large WOL specimens as well as additional features which permit the continuous monitoring of crack growth during the test and the ability to test in an enclosed environment at various temperatures and pressures. Several of these stress-corrosion test units have been built and they are currently in operation in both liquid and gaseous environments at various temperatures and pressures. Experience to date with these units indicates that they work extremely well and no problems have been encountered.

REFERENCES

1. B. F. Brown and C. D. Beachem, "A Study of the Stress Factor in Corrosion Cracking By Use of the Precracked Cantilever Beam Specimen," Corrosion Science, Vol. 5, 1965, p. 745.
2. S. R. Novak and S. T. Rolfe, "Comparison of Fracture Mechanics and Nominal Stress Analyses in Stress Corrosion Cracking," Corrosion-NACE, Vol. 26, No. 4, April 1970, p. 121.
3. C. D. Beachem and B. F. Brown, "A Comparison of Three Precracked Specimens for Evaluating the Susceptibility of High-Strength Steel to Stress Corrosion Cracking," Stress Corrosion Testing, ASTM STP 425, Am. Soc. Testing Materials, 1967, p. 31.
4. B. F. Brown, "A New Stress-Corrosion Cracking Test for High-Strength Alloys," Materials Research and Standards, Vol. 6, No. 3, March 1966, p. 129.
5. H. R. Smith, D. E. Piper and F. K. Downey, "A Study of Stress-Corrosion Cracking by Wedge-Force Loading," Engineering Fracture Mechanics, Vol. 1, No. 1, June 1968, p. 123.
6. S. R. Novak and S. T. Rolfe, "Modified WOL Specimen for K_{ISCC} Environmental Testing," Journal of Materials, Vol. 4, No. 3, September 1969, p. 701.
7. D. S. Kim, Unpublished Westinghouse Research Laboratories Data.

8. W. G. Clark, Jr. and D. S. Kim, "Effect of Synthetic Seawater on the Crack Growth Properties of HY140 Steel Weldments," To be published.
9. D. E. Piper, S. H. Smith and R. V. Carter, "Corrosion Fatigue and Stress-Corrosion Cracking in Aqueous Environments," Boeing Co. Report D6-60067, March 1967.

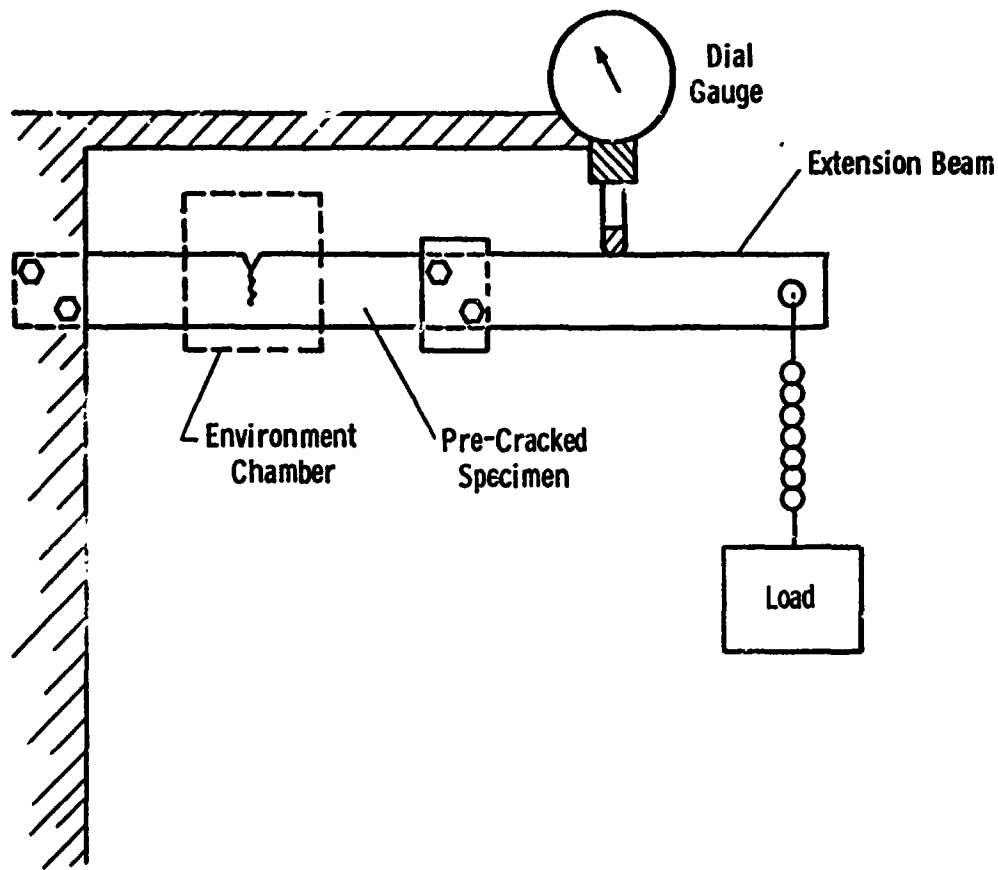


Fig. 1 -Schematic illustration of the cantilever beam corrosion test

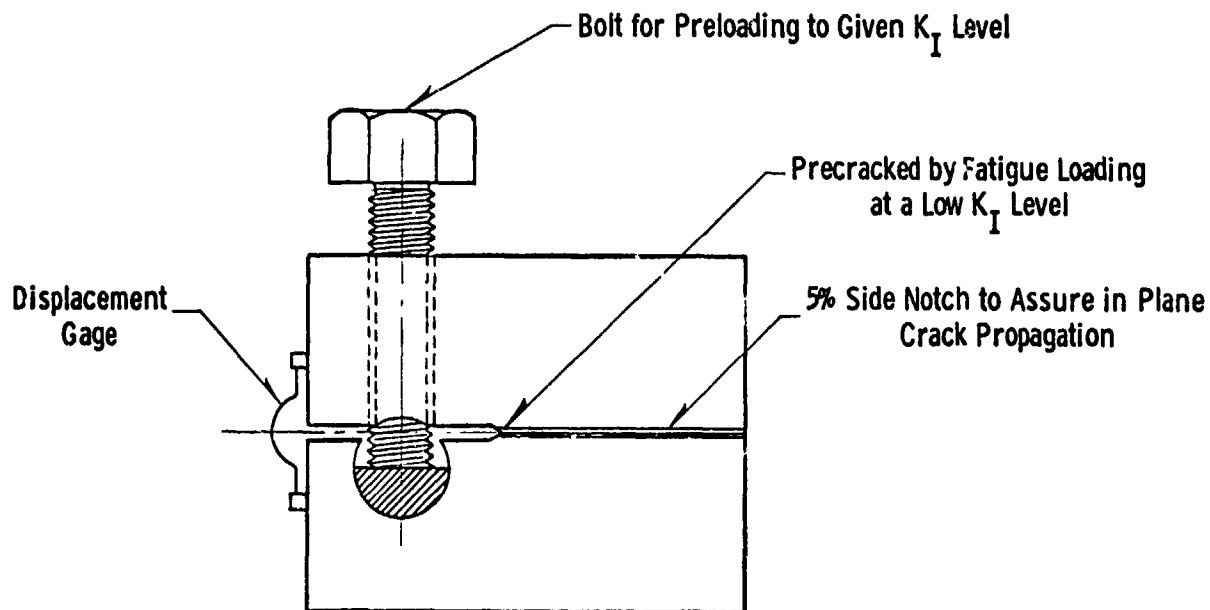


Fig. 2 -WOL specimen modified for use as a stress corrosion susceptibility test specimen

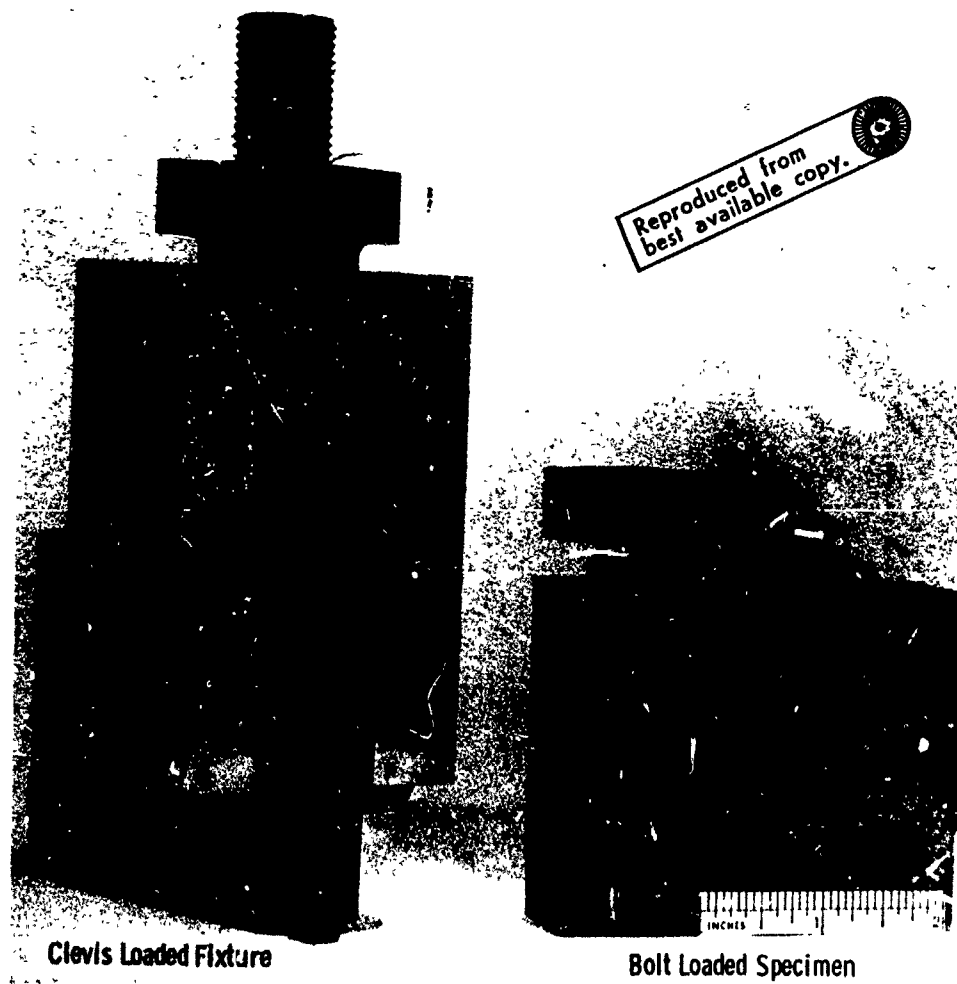


Fig. 3—Stress corrosion test fixtures

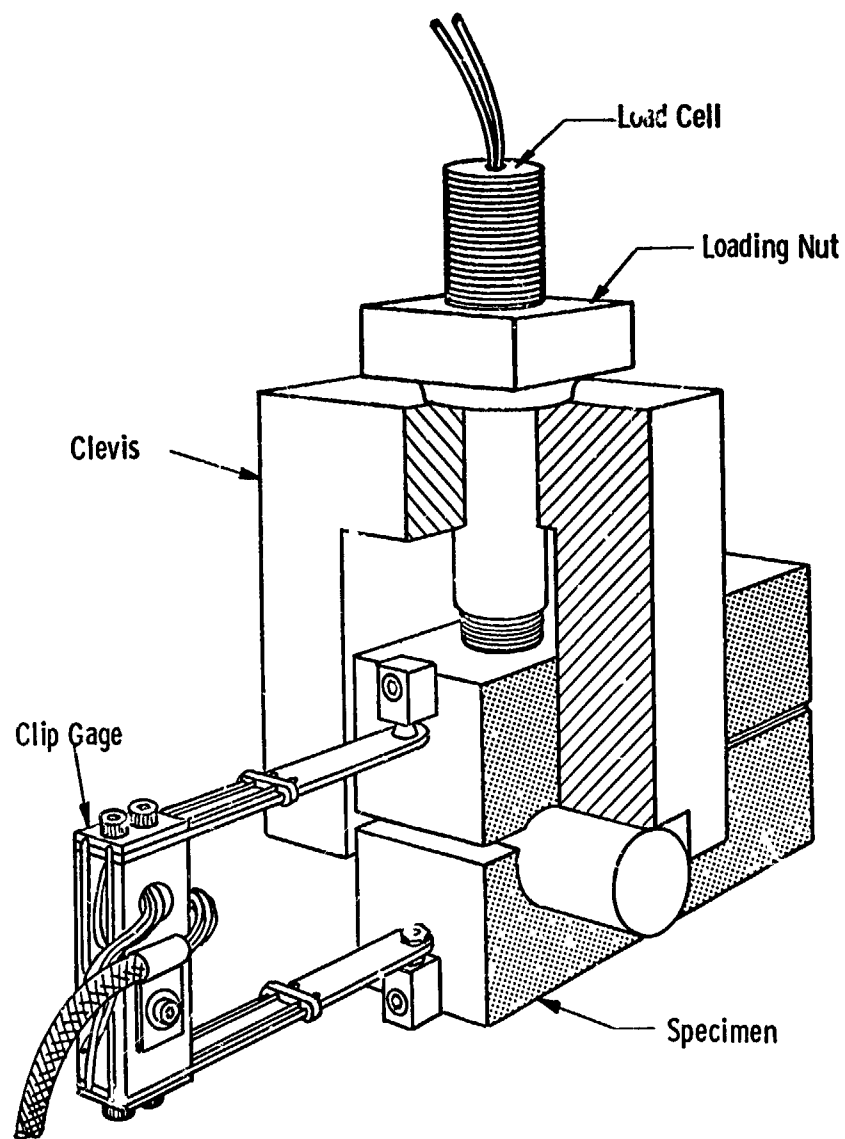


Fig. 4 -Loading arrangement and instrumentation used for stress corrosion testing

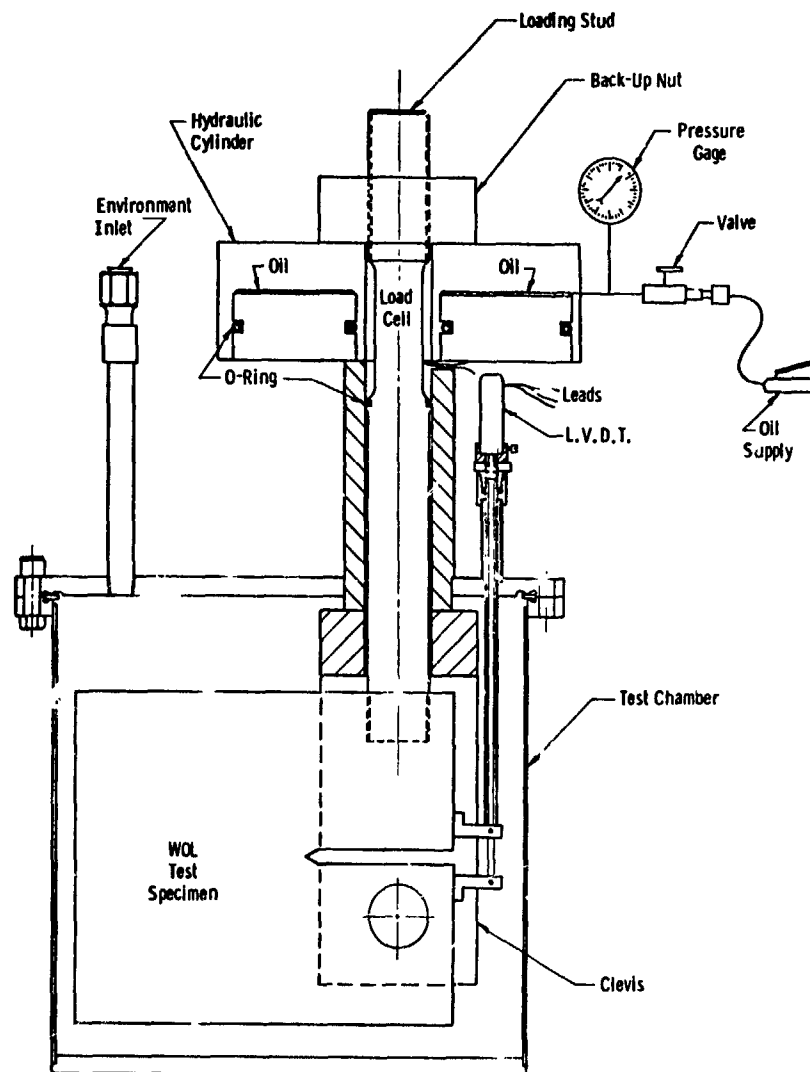


Fig. 5—Schematic illustration of the loading arrangement use to conduct K_{Isc} tests with large precracked WOL specimens

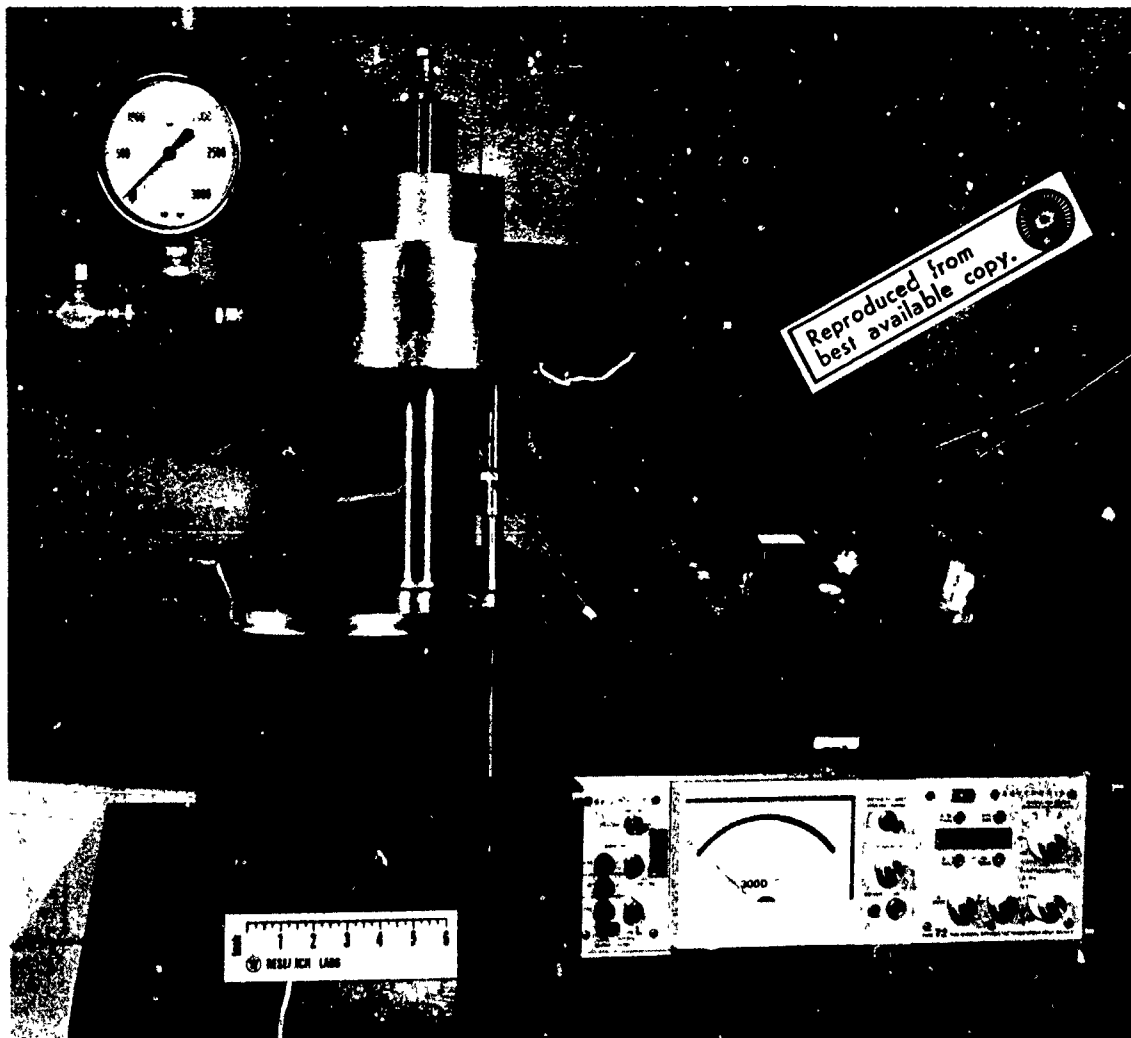


Fig. 6—The test unit and instrumentation used to conduct stress-corrosion testing with large WOL specimens

**TENSILE-LIGAMENT INSTABILITY AND THE GROWTH OF
STRESS-CORROSION CRACKS IN A
HOMOGENEOUS Zn-Mg-Cu ALUMINUM ALLOY**

by

Joseph H. Mulherin
Frankford Arsenal
Department of the Army
Philadelphia, Pa. 19137
U.S.A.

TENSILE-LIGAMENT INSTABILITY AND THE GROWTH OF STRESS-CORROSION CRACKS
IN A
HOMOGENEOUS Zn-Mg-Cu ALUMINUM ALLOY

JOSEPH H. MULHERIN

A contributory adjunct to stress-corrosion testing is the application of conceptual modeling. As an example of the technique, the Krafft tensile-ligament model was applied to results from a Zn-Mg-Cu aluminum alloy series. The variant in the series was the degree of homogeneity of the microstructure. According to the model, the largest variation in the susceptibility to stress corrosion crack propagation was attributable to an increase in the rate of surface-chemical attack around the circumference of the ligaments.

During a continuing research effort to produce an ultrahigh strength aluminum alloy, an intermediate phase consisted of the characterization of a homogeneous or essentially inclusion-free alloy. This presented an opportunity to study, in some detail, the influence of the undissolved alloy constituents, normally found in commercial material, on the stress-corrosion behavior.

As the basis for the study, the tensile-ligament model of Krafft was selected. The application of this model to the stress-corrosion phenomenon has been presented in a recent publication by Krafft and Mulherin.¹ This paper describes the stress-corrosion behavior, as a function of homogeneity, for a Zn-Mg-Cu aluminum alloy in terms of this model.

Experimental Material

The experimental material consisted of a 2 inch thick plate of the following analysis.

<u>Component</u>	<u>Weight Percent</u>
Zn	5.5
Mg	2.50
Cu	1.57
Cr	0.20
Ti	0.01
Fe	0.00
Si	0.01
Al	Balance

The plate was thermally treated to produce four different concentrations of the nonequilibrium particles (C_s) obtained through treatments A, B, C, and D. The determination of their volume fraction compared to a commercial control follows.

<u>Treatment</u>	<u>C_s (volume percent)</u>
Commercial	0.860
A	0.324
B	0.241
C	0.106
D	<0.050

Upon conclusion of the homogenizing treatment, the material was water quenched and aged at 120° C to produce a fine scale precipitation from the solid solution. The purpose of this precipitation treatment was to strengthen the alloy to the equivalent of the T6 condition. The resulting engineering mechanical properties in the short transverse direction as a function of the second phase were found to be the following.

<u>Treatment</u>	<u>Strength (ksi)</u>		<u>Elongation (%)</u>
	<u>Yield</u>	<u>Ultimate Tensile</u>	
Commercial	73.0	83.0	11.0
A	73.6	82.2	12.5
B	69.5	80.2	13.9
C	70.7	83.0	13.4
D	73.4	83.3	14.4

Metallographically, a general comparison of the grain morphology and concentration of second phase between commercial and experimental material is shown in Figure 1.

Rather complete discussion of the physical metallurgy aspects of this category of materials has been presented by Antes and Markus,² and on the mechanical behavior by Mulherin and Rosenthal.³

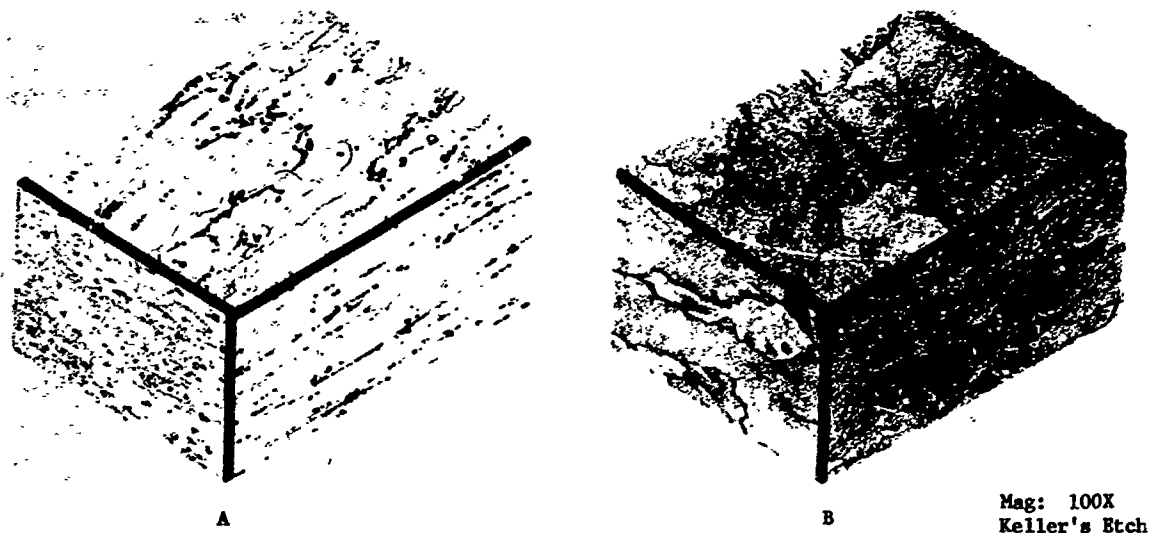


Figure 1. Composite Photomicrographs of the Three Principal Fabrication Planes to Demonstrate Grain Morphology and Distribution of Second Phases:
A - Commercial Material B - Experimental Material

Determination of Plastic Flow and Fracture Properties

To determine the plastic flow properties, stress-strain curves were obtained by measuring the diametral expansion strain on short compression specimens. The specimens were 1/4 inch in diameter and 7/16 inch long. The appearance of the compressive stress (σ_c) vs diametral areal strain (ϵ_A) record for both commercial and experimental material is illustrated in Figure 2.

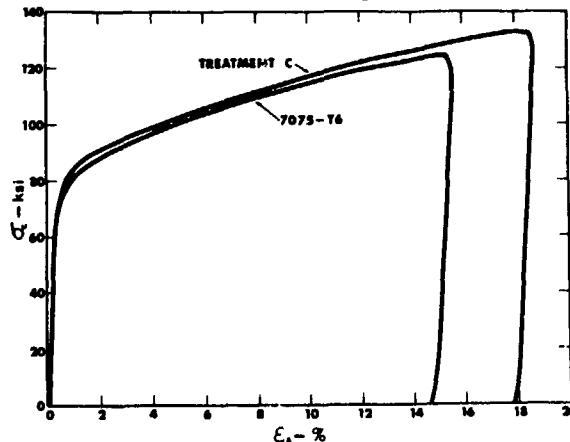


Figure 2. Compression Test Record of Stress (σ_c) vs Diametral Areal Strain (ϵ_A) for Commercial and Experimental Material

The elastic slope (θ_0) is related to the longitudinal elastic constant (E) by Poisson's ratio (ν) by

$$\nu = \frac{E}{2\theta_0}$$

The components of the compressive strain, in terms of elastic and plastic components, are

$$\epsilon_A = \epsilon_p + \frac{\sigma_c}{\theta_c}$$

where ϵ_p is the experimentally determined plastic strain. In turn, the compressive data is converted to the "true" ($\bar{\sigma}$) values by

$$\bar{\sigma} = \frac{\sigma_c}{(1 + \epsilon_A)}$$

and

$$\bar{\theta} = \theta_c - \bar{\sigma}$$

The conversion to longitudinal strain (ϵ_L) is simply

$$\epsilon_L = \epsilon_p + \frac{\bar{\sigma}}{E}$$

In this manner, the instability strain criterion, after Krafft, can be investigated; viz, where

$$\frac{\bar{\theta}}{\bar{\sigma}} - 1 = 0.$$

A convenient representation of the true stress-strain characteristic is obtained by plotting the

instability coefficient ($\bar{\theta}/\sigma_c$) against the reciprocal longitudinal strain (ϵ_L^{-1}). This representation is presented in Figure 3 for the C material, and is compared to the commercial control. Evaluation of each treatment resulted in the following determinations of the instability strain.

<u>Treatment</u>	<u>Instability Strain, ϵ_c</u> <u>(%)</u>
Commercial	11.6
A	12.9
B	13.3
C	12.7
D	12.8

These data indicate an insensitivity of the instability strain to a wide variation in the concentration of second phase.

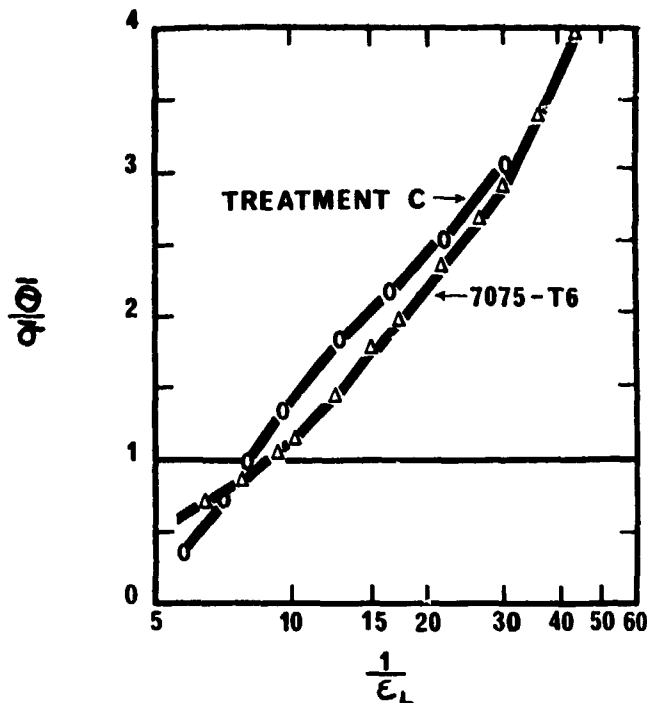


Figure 3. Graph of Stability Coefficient ($\bar{\theta}/\sigma$) against Reciprocal Longitudinal Strain (ϵ_L^{-1}) to Obtain Instability Condition ($\bar{\theta}/\sigma = 1$)

For the fracture investigation, the plane strain fracture toughness was obtained using a compact K_{Ic} specimen configuration (CKS) as described by Wessel.⁴ This is a pin-loaded single-edge-notched geometry. Specimen orientation fixed the plane of crack propagation parallel to the plate surface at mid-thickness. Prior to testing, a fatigue crack, 0.1 inch long, was introduced at the root of the machined notch. Non-linearity of the crack front was encountered in the experimental material due to the lack of a stretching operation, usually performed on mill products.

For the fracture toughness test, a double cantilever clip gage was used to obtain crack opening displacement. This was plotted, concurrently with the load, on an X-Y plotter. Loading was performed on a closed loop hydraulic machine. Analytically, a compliance power series was used to calculate the stress intensity. Instability was selected at the 4 percent offset intersection of the load-deformation plot. The results of the plane strain fracture toughness as a function of second phase are shown in Figure 4. From a commercial level of approximately 20,000 psi/in., an increase of 100 percent is experienced.

In the model it is postulated that tensile ligaments are formed at the crack front. It is these ligaments that not only are subject to the usual tensile behavior but, also, are sensitive to the environment-to-metal surface attack. As previously observed, the size of the ligaments (d_T) is

$$\sqrt{d_T} = \frac{1}{E \sqrt{2\pi}} \left(\frac{K_{Ic}}{\epsilon_c} \right)$$

which is, incidentally, the distance ahead of the crack front at which the validity of the elastic stress field singularity is attained.

With the previous determination of the instability strain and plane strain fracture toughness, the ligamental cell size is a simple computation. The results are shown in Figure 5. In view of the constancy of the instability strain, the results follow an anticipated power law relationship and are compared to a square root dependency.

Application of the Model to Stress-Corrosion Cracking

The tensile-ligament model identifies three factors as influential in the corrosion-assisted crack propagation phase of stress-corrosion cracking. These are: (1) the ligamental cell size, d_T ; (2) plastic

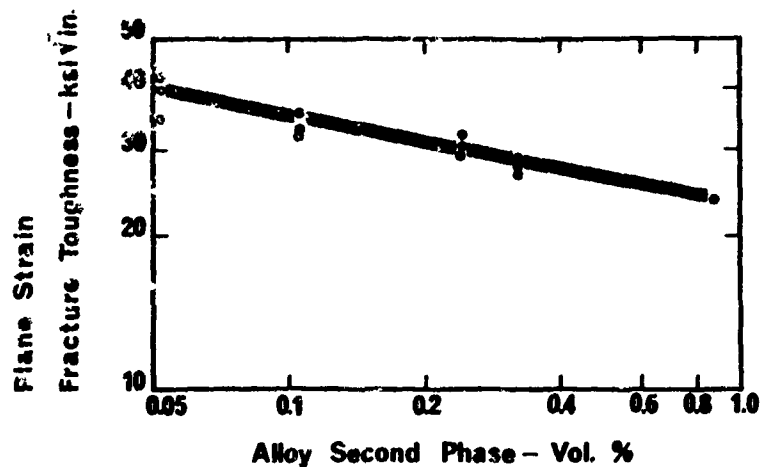
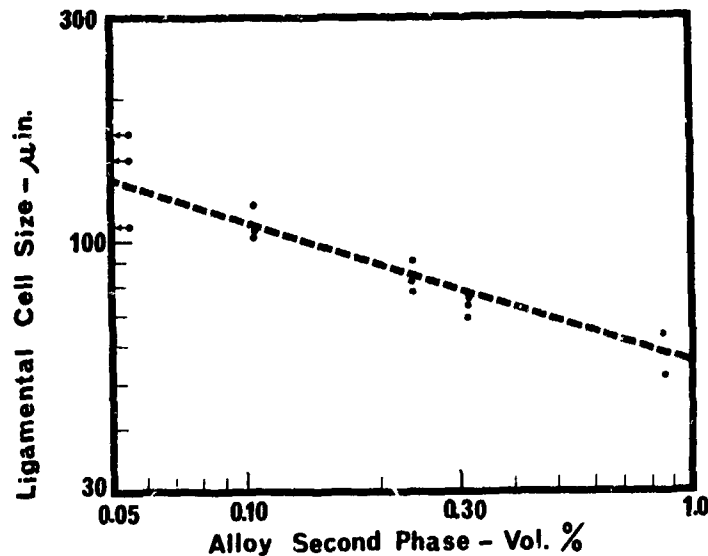


Figure 4. Relationship between the Plane Strain Fracture Toughness in the Short Transverse Direction and the Concentration of Second Phases of 7075-T6 Aluminum Alloy



NOTE: These data points are compared to a square root dependence.

Figure 5. Relationship between the Ligamental Cell Size and the Concentration of Second Phase

stability $\bar{\theta}/\bar{\sigma}$ (ϵ); (3) a surface chemical reaction rate, V_g , between the d_T cells and the spatial environment.

Recalling from the publication cited,¹ V_g can be stated in terms of flow properties such that

$$\frac{V_g}{V_c} = \frac{\epsilon_P}{8} \left(\frac{\bar{\theta}}{\bar{\sigma}} - 1 \right)$$

where V_c is the velocity of crack propagation. The reciprocal of the crack velocity relative to the surface chemical reaction rate is shown in Figure 6. If desired, the ϵ_L can be scaled to the stress intensity by scale matching at the instability strain. The constancy of the V_g/V_c ratio shown in these data has been experienced for commercial material as well.

For the particular case being studied, the observations of the crack propagation behavior are in the form of time-to-failure data. Therefore, a summation integral is used, namely:

$$V_{stf} = \int_{K_0}^{K_{Ic}} \frac{V_g}{V_c} (K_I) da$$

For scale matching, one assumes that the surface reaction rate is constant for the life of the ligament. This assumption appears reasonable in view of the nascent state and small diameter of the ligaments. With the evaluation of V_g , the actual data may be compared to the model prediction which is shown in Figure 7. Substantial agreement is indicated.

Also of significance is an evaluation of the V_g constants as a function of the homogenization treatments. These are

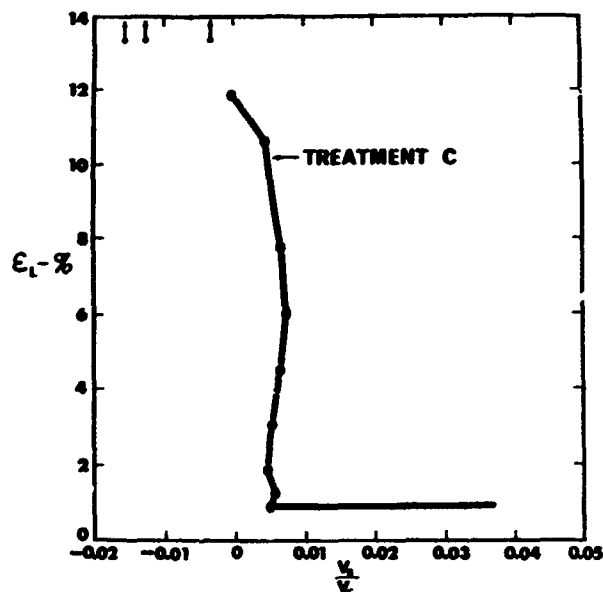


Figure 6. Reciprocal of the Crack Velocity (V_c) Relative to Surface Chemical Reaction Rate (V_s) Plotted against Longitudinal Strain

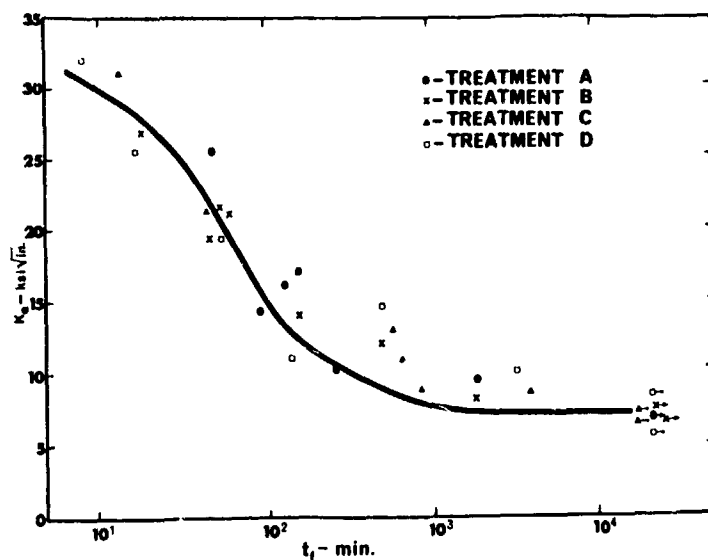


Figure 7. Comparison between the Model Prediction for Treatment C and Failure Time Data (t_f) for All Homogenizing Treatments

<u>Treatment</u>	<u>V_s</u> <u>(in./sec)</u>
Commercial	1.10×10^{-9}
A	4.35×10^{-6}
B	6.10×10^{-6}
C	1.40×10^{-5}
D	2.14×10^{-5}

These data indicate that the chemical reaction accelerated, causing an increase in the crack propagation velocity. Arithmetical manipulation shows crack velocities in the order of 1.6μ in./second for the commercial material and 2300μ in./second for the C treatment.

The model further identifies the threshold for stress-corrosion crack propagation with the tensile-yield strength (σ_{ys}), the ligamental cell size (d_T) and, for aluminum, the elastic Poisson ratio (ν) in the following manner

$$K_{Isc} = \frac{\sigma_{ys}}{(1 - 2\nu)} \sqrt{2\pi d_T}.$$

Actual determination of the K_{Isc} compared to the prediction is shown in Figure 8, using K_{IC} as the independent variable. These data are seen to be in close agreement with, but slightly above, the model values.

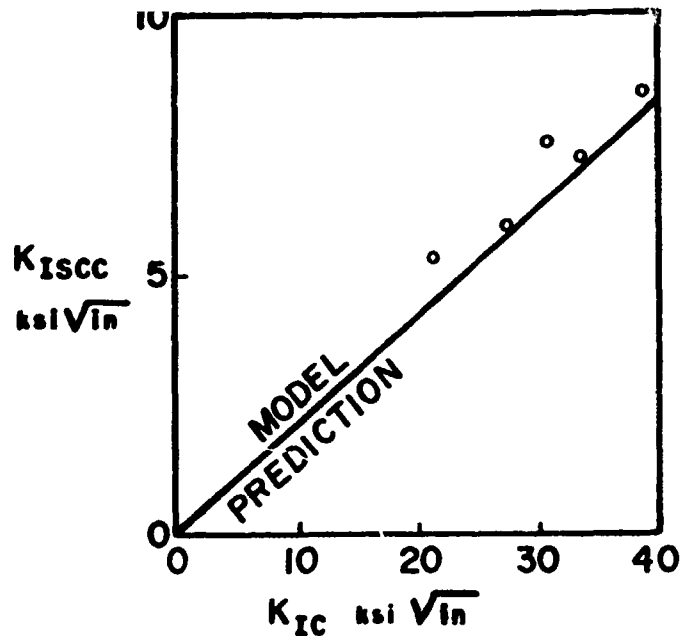


Figure 8. Comparison between the Predicted and Experimental Stress-Corrosion Threshold (K_{ISCC}) as a Function of the Plane Strain Fracture Toughness (K_{IC})

Conclusions

Specific observations which can be derived by using the tensile-ligament conceptual model for the evaluation of the material susceptibility to stress-corrosion crack propagation are:

1. In the stress intensity region between the commercial K_{IC} and the elevated K_{IC} , the experimental material will tolerate some crack propagation under a triaxial stress state, whereas the commercial material will not.
2. In the stress intensity region between K_{ISCC} and K_{IC} , the rate of crack propagation is much greater in the experimental materials.
3. A modest elevation of the K_{ISCC} was experienced in the experimental material due basically to an improvement in the plastic flow and fracture properties.
4. The kinetics of the surface chemical reaction increased by several orders of magnitude in the experimental material. The increased chemical reactivity is reflected in a higher crack propagation velocity.

Possibly two more general conclusions of greater significance can be made. The first is that an improvement in the toughness of a material, regardless of how dramatic, does not necessarily imply immunity to stress-corrosion cracking ($K_{ISCC} \approx K_{IC}$). The second conclusion concerns the chemical aspects, exclusive of chemical composition. Chemistry plays a vital role in material behavior; therefore, greater emphasis should be placed in such areas as polarization and potential studies.

References

1. J. M. Krafft and J. H. Mulherin, "Tensile-Ligament Instability and the Growth of Stress-Corrosion Cracks in High-strength Alloys," Trans ASM, Vol 62, p 64 (1969).
2. H. W. Antes and h. Markus, "Homogenization Improves Properties of 7000 Series Aluminum Alloys," Metals Engineering Quarterly, ASM (1970).
3. J. H. Mulherin and H. Rosenthal, "Influence of Nonequilibrium Second-phase Particles, Formed During Solidification, Upon the Mechanical Behavior of an Aluminum Alloy," Metallurgical Trans, ASM-AIME, Vol 2, p 247 (Feb 1971).
4. E. T. Wessel, "State of the Art of the WOL Specimen for K_{IC} Fracture Toughness Testing," Engineering Fracture Mechanics, Vol 1, p 77 (1968).

AN ULTRA HIGH VACUUM SYSTEM FOR DETERMINING THE EFFECTS OF GASEOUS
ENVIRONMENTS ON FATIGUE AND FRACTURE PROPERTIES OF METALS

H. L. Marcus and P. J. Stocker
North American Rockwell Science Center
Thousand Oaks, California 91360

SUMMARY

A high vacuum, 10^{-10} torr, all-metal system is described in which crack growth behavior of metals under static and dynamic loading can be studied. Provisions are made to introduce clean gases to the system, such as hydrogen and oxygen to study their effects on the crack growth phenomena. Crack growth results are presented for Ni-200 exposed to low pressures of hydrogen gas in the 10^{-8} to 150 torr pressure range.

AN ULTRA HIGH VACUUM SYSTEM FOR DETERMINING THE EFFECTS OF GASEOUS ENVIRONMENTS ON FATIGUE AND FRACTURE PROPERTIES OF METALS

H. L. Marcus and P. J. Stocker

Introduction

Many studies over the years have been made on the effects of hydrogen on the mechanical properties of metals, and, in particular, of the effects of hydrogen internal to metals, that is, of hydrogen put in by heat treatment, electro-plating, and other processes. The influence of gaseous hydrogen on the mechanical properties of metals has been investigated to a much lesser extent. Recently there has been a great deal of activity in this field in relation to the space program. In particular, the work of Chandler and Walters¹ has indicated pronounced effects of high pressure hydrogen gas on what were previously thought to be relatively insensitive materials. Others have also studied hydrogen at various pressures.²⁻⁸ Ni based alloys, in general, are those in which the hydrogen effects are significantly higher in gaseous hydrogen than when precharged with hydrogen.

Subcritical crack growth phenomena in steels has been studied by Nelson, Williams and Tetelmann.^{2,3} Their work on hydrogen effects on slow crack growth has shown that the effects of hydrogen gas below one atmosphere pressure can be rather significant. They have demonstrated that temperature dependence leads to a peak in crack velocity and that this peak apparently is associated with dissociation of the molecular hydrogen.

It is the purpose of this paper to describe equipment in which fatigue and static crack growth behavior could be established in an ultra high vacuum, of the order of 10^{-10} torr. In addition, crack growth rate as a function of partial pressure of gas, in particular of hydrogen gas, in a range of from 10^{-8} torr to 1 to 2 atmospheres can be made. The material used in the initial studies and to be described in this paper is commercially pure Ni-200.

System Description and Results

The system, shown in Fig. 1, is a stainless steel ultra high vacuum system which contains the specimen and transfers the specimen load through metal bellows to an MTS electro hydraulic universal mechanical testing machine. Three separate stages of oil-free pumping permit evacuation of the chamber with no possibility of contamination through oil backstreaming. The first, a sorption pump, reduces the pressure to about 5 torr, a range where an ion pump may be employed. The latter has the capability of reducing the pressure to the 10^{-10} torr range. For increased pumping speed, a titanium sublimation pump is available to be used in conjunction with the ion pump; however, the titanium surface is such an active getter that it cannot be used during hydrogen atmosphere work. The chamber pressure is measured with three different pressure gauges. An ion gauge operates in the range 10^{-10} torr to 10^{-3} torr, a thermocouple gauge functions from 10^{-3} torr to 1 torr and, finally, a Bourdon tube gauge is used from 1 torr to 1 atmosphere. The system is totally bakable and may be outgassed at temperatures up to 280°C. This feature not only makes possible the attainment of ultra high vacuum, but helps to reduce outgassing during studies at temperatures below 280°C. The sample temperature control arrangement depicted in Fig. 1 is a heat transfer device. The copper block is mounted to the specimen within the chamber and hot gas, cold gas, or liquid nitrogen is passed through it until a steady-state temperature is reached. The copper block minimizes the thermal gradients. The temperature gradient across the tapered cantilever beam specimen is less than 5°C. The temperature may then be varied while the crack is propagating.

Another feature of this system is a provision for the introduction of a gas, or gases, during the course of an experiment. Thus, one may obtain a crack velocity at ultra high vacuum, then introduce a known amount of a gas such as hydrogen and observe its effect on the crack growth behavior and subsequently insert a controlled amount of a second gas, such as oxygen, so as to attempt to determine interaction levels and the amount of the second gas necessary as a function of hydrogen pressure to influence the embrittling effect on the material. The ion pumps can be valved off from the main chamber containing the active gases. In practice the gases may be passed from bottles of commercially available research grades or from less pure sources through permeation transfer tubes or through a gas purification train. A Pd-Ag transfer tube is used for hydrogen, and pure Ag is used for oxygen. If the crack growth rate is extremely slow and the run becomes extended, outgassing may prove to be a problem. In this case the chamber may be re-evacuated, brought back to the proper gas pressure and then the run continued. A bakeable gas analyzer can also be incorporated into the system.

The specimen used in the experiments run in this system is a tapered double cantilever beam specimen developed initially by Mostovoy and Ripling¹¹ and analyzed by Srawley and Gross.¹² Marcus and Sih¹³ have given a discrete description of the particular specimen used in these studies. The specimen has the advantage of a constant stress intensity at the crack tip over a range of approximately two inches when a fixed load is applied. This allows continuous monitoring of the crack velocity while changing environmental or loading variables, such as the hydrogen gas pressure, while the crack is running.

The materials studied to date in this system have been Ti, Fe, Cu, Cb and Ni based alloys. In this paper, however, we will limit our discussions to the effects on commercially pure Ni 200. Fig. 2 shows crack velocity versus H_2 pressure for fixed stress intensity, K , at three different values of ΔK in Ni 200. ΔK is $K_{max} - K_{min}$ in sinusoidal cyclic loading. Thus, as you can see at 10^{-1} torr, you may start seeing an influence of hydrogen gas on the cyclic crack growth rate and by the time you get to 150 torr, which is the maximum pressure in these particular runs, you have an order of magnitude increase in the crack growth rate that is strongly dependent on hydrogen pressure, as is shown in Fig. 3.

Of particular interest is the temperature dependence of the Ni crack growth rate in the presence of hydrogen gas. This gives clues to the rate controlling processes. The hydrogen gas is introduced into the system and the Ni crack growth rate is monitored as the temperature of the sample is varied with the gas heat transfer system. A maximum at approximately 0°C is observed as shown in Fig. 4. These results are for three different runs up and down the temperature range on the same specimen. The maximum at the

lower temperature in both heating and cooling eliminates the possibility of outgassing being the cause. This maximum may be associated with a dissociation of the hydrogen molecule as was suggested by similar results for statically loaded steels.²

After the crack growth rate in clean 150 torr hydrogen was established oxygen was introduced into the system through a controlled leak valve. Addition of 50-100 torr partial pressure of oxygen reduced the cyclic crack growth rates back to those observed in hard vacuum. The work described here is not complete enough to determine if only the partial pressure of oxygen limits the growth or if it is controlled by a different partial pressure of oxygen for the varied hydrogen pressures. The system is set up so that it is possible to introduce several gases and mixtures of gases to determine their combined effects.

Discussion

The system described in this paper makes it possible to measure the crack velocity rate in ultra high vacuum. In addition it enables us to introduce external gases to establish some measure of the lower limit of gas pressure for which reactions will actually take place. One limitation in regard to this particular technique is the fact that the pressure is the external pressure and not necessarily the pressure at the crack tip. In particular, the problem with the tapered double cantilever beam specimens described is the fact that you have this tremendously high service area of very clean metal surface that tends to adsorb the gas. This may limit the amount of gas capable of getting at the crack tip. Therefore, the gas pressure observed is only the upper limit to the gas pressure at which interactions take place and this may be off by a couple of orders of magnitude from the absolute pressure at the crack tip where the interactions take place. What has been shown is that a very small amount of hydrogen gas does interact at the crack tip setting up stress-gas interaction configuration such that the crack velocity does increase with gas pressure. The system has the capability of keeping a very clean surface and has been used to introduce not only a gas to the vacuum, such as hydrogen, but a second gas such as oxygen to effectively passivate the surface in the presence of hydrogen. Although the pressure of 1 torr is a significantly low pressure, it is more than sufficient to keep the surface fully covered as the crack propagates. The results clearly demonstrate that hydrogen gas does implement the crack growth in Ni-200 and the crack growth rate is significantly changed as you go up in pressure of the hydrogen, in the low pressure ranges investigated. This result demonstrates that the gas hydrogen-nickel interaction is much more severe than that associated with internal hydrogen where it has been observed that there is very little hydrogen effect.

The fracture surface appearance of cyclicly loaded Ni-200 in gaseous environment is shown in Fig. 5. The Ni that is grown in 10^{-8} torr vacuum, 5B, has a ductile fracture mode. In 150 torr hydrogen, 5A, where a larger growth rate is observed, the fracture surface is flatter and microcracks in the direction perpendicular to the propagation direction are prevalent. These are characteristic of all the fracture surfaces of all materials where hydrogen effects crack growth. In one atmosphere of oxygen, 5C, the presence of striations is pronounced and microcracks that were characteristic of the hydrogen embrittlement are not present. Another interesting observation is that in the double cantilever beam specimen microcracks are formed in hydrogen on the fracture surface initially formed in hard vacuum. We know these are formed after the crack growth since microcracks are not significantly observed in regions fatigued in hard vacuum and not subsequently exposed to hydrogen. If you introduce the hydrogen, the flexing of the arms creates a high enough stress at the clean metal fracture surface to start hydrogen embrittlement and get the cracks forming perpendicular to the growth direction. Although the system described in this paper allows the use of the extremely high vacuum to initiate fatigue crack growth and permits subsequent exposure of the clean metal surface to gases such as hydrogen to see the interaction effects with the fatigue crack propagation rate it is necessary to be careful in evaluating the fracture surfaces due to this post fracture interaction. This was dramatically demonstrated in work on Ti-6Al-2Sn-4Zr-6Mo where the cold worked surface region formed during fatiguing vacuum completely formed a hydride after hydrogen was introduced.¹⁴

Conclusions

An all metal bakeable vacuum system coupled to an electrohydraulic system is described, which operates at pressures as low as 10^{-10} torr. It has facilities for introducing pure gases, separately or together, into the vacuum system at controlled pressures ranging from 10^{-8} torr to 1 atm. Both static and dynamic crack propagation tests can be run, initially in hard vacuum and then as a function of the gas or gases added. Temperature runs can be made from -100°C to $+200^{\circ}\text{C}$.

Studies of commercial Ni-200 are presented showing:

- 1) Hydrogen effects on fatigue crack growth rate are seen at hydrogen pressures under 1 torr, with as high an order of magnitude increase in growth rate at 150 torr.
- 2) A peak in growth rate is observed at 0°C for fixed loading conditions and hydrogen gas pressure.
- 3) Oxygen passivates the Ni-200 to the hydrogen interaction when added to the hydrogen gas.

References

1. R. J. Walter and W. T. Chandler, North American Rockwell Corporation, Rocketdyne, Canoga Park, Calif., Reports R-7780-1, R-7780-2, R-7780-3, NASA NAS8-19 (1968).
2. D. P. Williams and H. G. Nelson, Metallurgical Trans. 1, 63 (1970).
3. H. G. Nelson, D. P. Williams and A. S. Tetelman, Metallurgical Trans. 2, 953 (1971).
4. G. G. Hancock and H. H. Johnson, Trans. AIME 236, 513 (1966).
5. R. M. Vennett and G. S. Ansell, Trans. ASM 62, 1007 (1969).
6. J. E. Campbell, DMIC Report S-31 (1970).
7. J. P. Fidelle and M. Rapin, Proceedings of the Colloquium "Hydrogen in Metals", organized by the CEA at Valduc, September (1967).
8. P. M. Lorenz, NASA-CR-100208, N69-19152.
9. W. A. Spitzig, P. M. Talda and R. P. Wei, Engr. Fracture Mech. 1, 155 (1968).
10. G. F. Pittinato, Trans. ASM 62, 410 (1969).
11. S. Mostovoy, P. B. Crosley, and E. J. Ripling, J. of Matls. 2, 661 (1967).
12. J. Srawley and B. Gross, NASA Tech Report NASA TN D-3820 (1967).
13. H. L. Marcus and G. C. Sih, J. Engr. Fracture Mech. (in press).
14. H. L. Marcus, P. J. Stocker, N. E. Paton, and J. C. Williams (to be published).

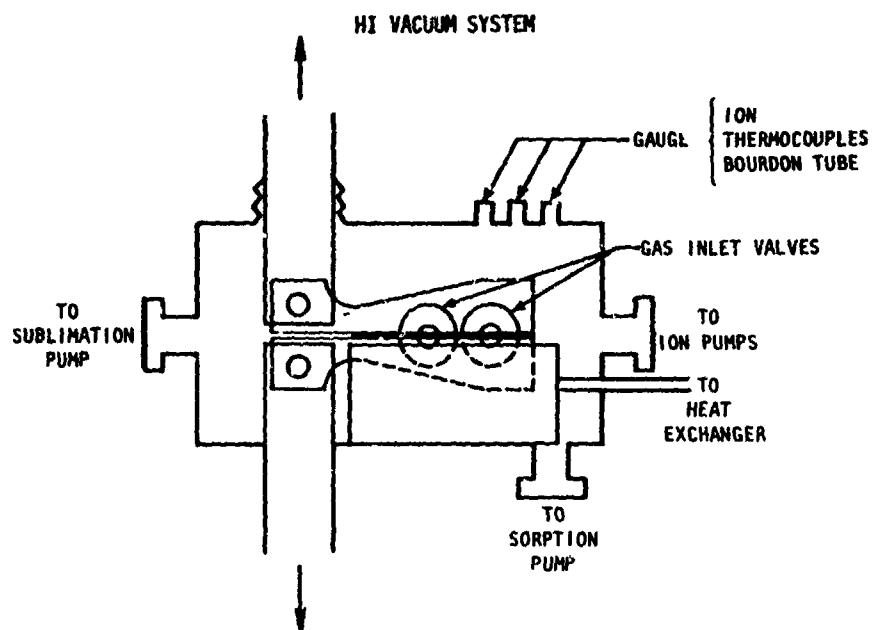


Figure 1 Schematic of all metal stainless steel ultra high vacuum system

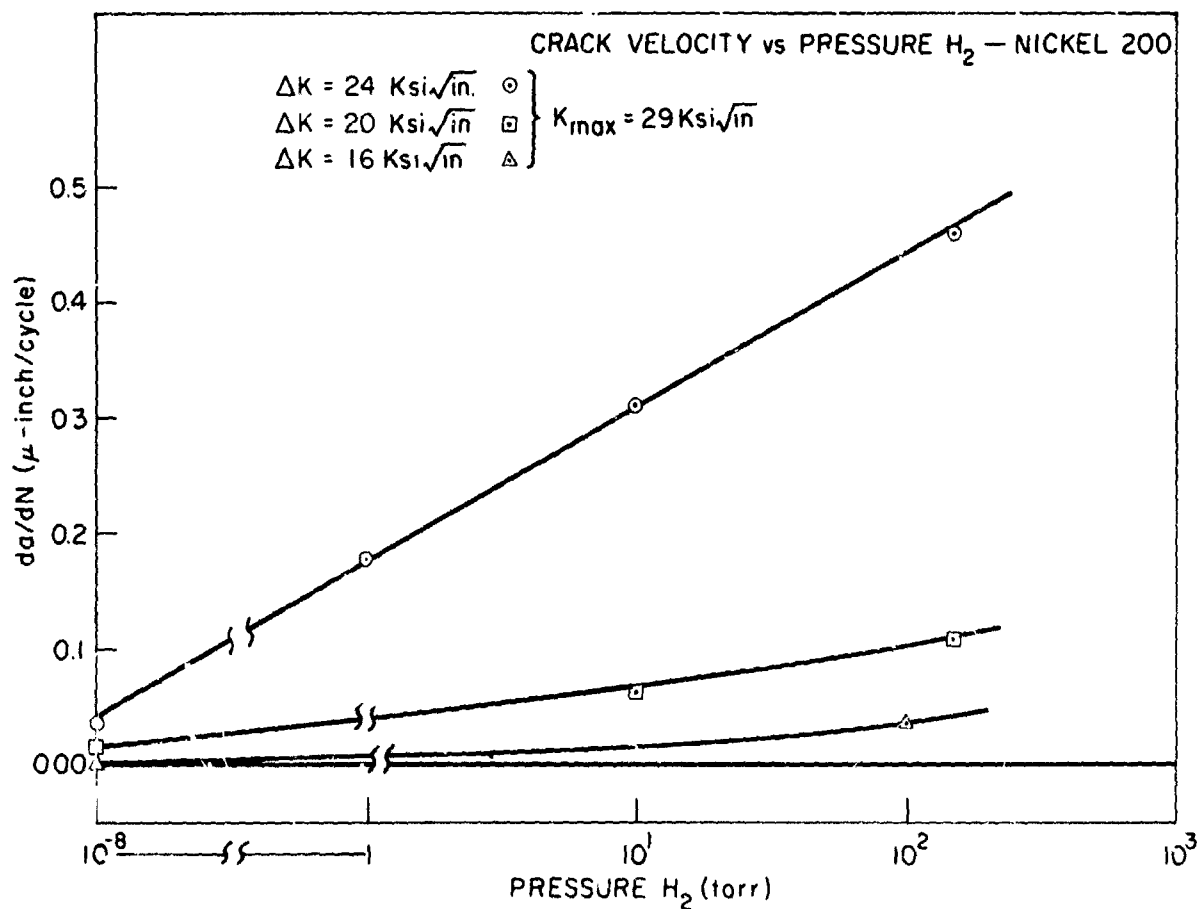


Figure 2 Fatigue crack growth rate of Ni-200 exposed to various hydrogen pressures at three ΔK levels.

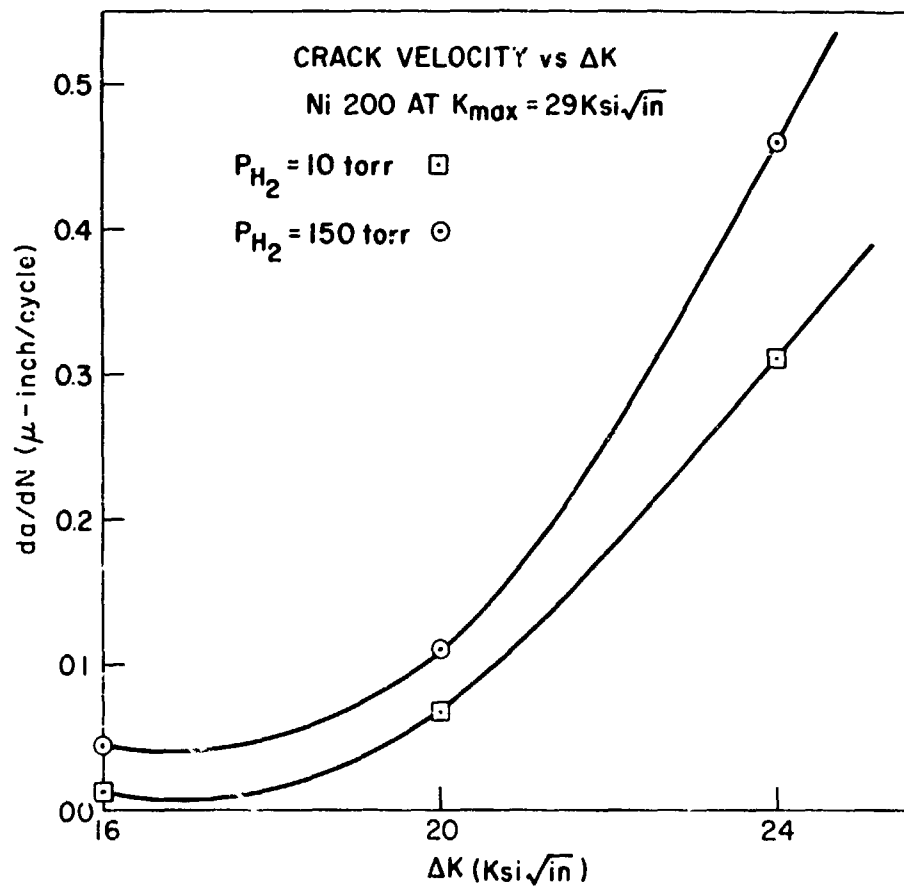


Figure 3 Fatigue crack growth rate of Ni-200 as a function of ΔK for two hydrogen pressures.

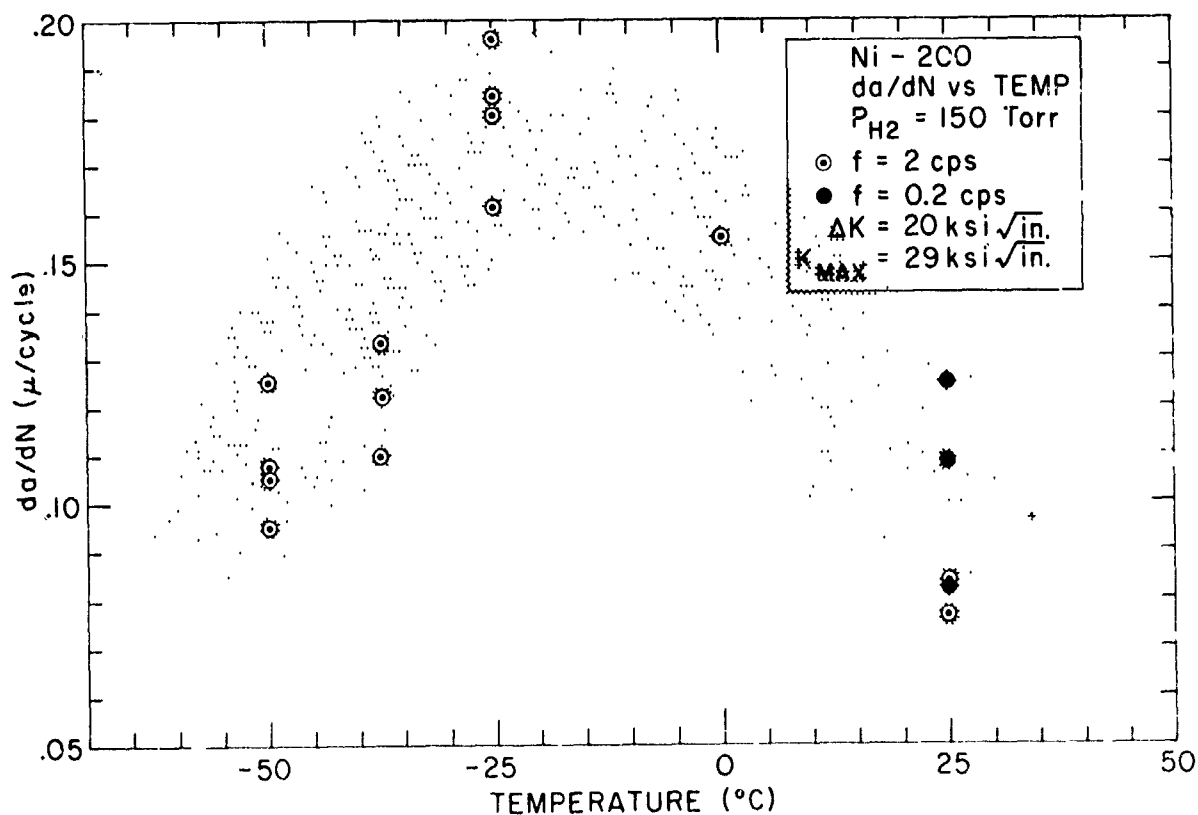


Figure 4 Fatigue crack growth rate of Ni-200 in 150 torr hydrogen gas over the temperature range -50 to +25°C

Ni-200

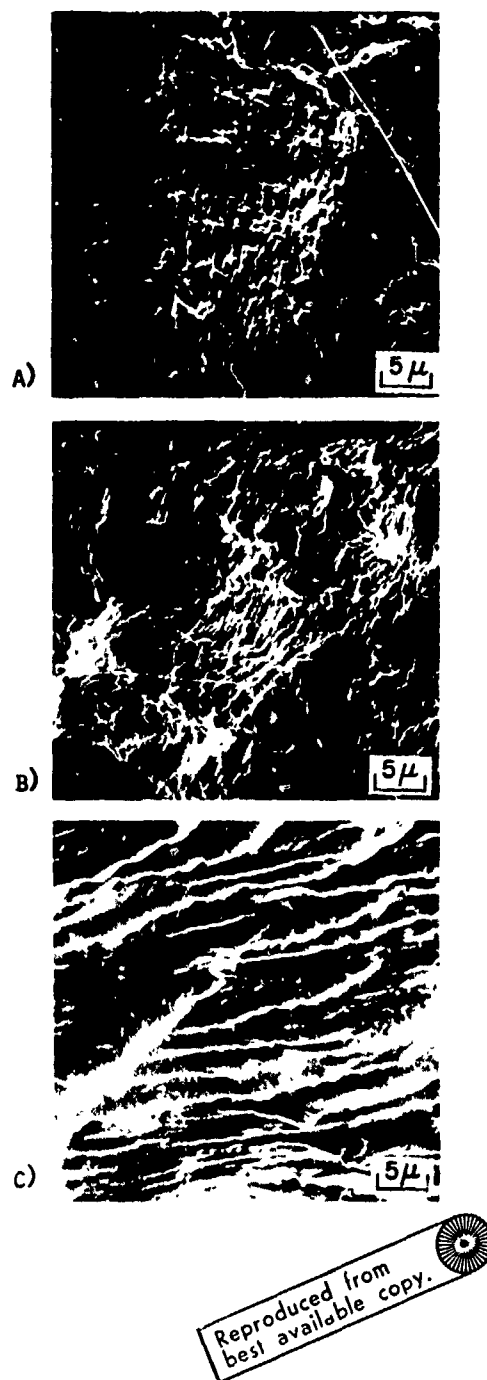


Figure 5 Scanning electron micrographs of Ni-200 fatigue fracture surfaces. A) Fatigued in 150 torr hydrogen; B) Fatigued in 10^{-8} torr vacuum; C) Fatigued in 1 atmosphere oxygen

Acoustic Emissions and Slow Crack Growth
in High Strength Steel

R. W. Staehle, International Nickel Professor
of Corrosion Science and Engineering
G. E. Kerns, Research Assistant
Department of Metallurgical Engineering
The Ohio State University
Columbus, Ohio 43210

Acoustic emission techniques have been used in the study of stress corrosion cracking in high strength material. Pre-fatigue cracked single cantilever specimens were loaded and exposed to gaseous and aqueous environments. Acoustic emission signal shape and total resonance counts were recorded for specimens of different strength levels tested in different environments. Also, the phenomenon of wave reflection was reduced in order to examine the frequency content and energy of the emission.

The results show that a higher strength level produces more acoustic activity, regardless of environment. Also, the generated stress wave is of a high frequency and low energy nature.

ACOUSTIC EMISSIONS AND SLOW CRACK GROWTH IN HIGH STRENGTH STEEL

R. W. Staehle*
G. E. Kerns

INTRODUCTION

The propagation of stress corrosion cracks in high strength steel is accompanied by the generation of high frequency stress waves. Such acoustic emissions are functions of both the material and the fracture process, in that stress wave generation is favored by high strength levels, cleavage mode failure, large grain size, plane strain conditions, and twinning⁽¹⁾. However, several questions regarding such stress waves remain unanswered:

1. How much elastic energy is associated with an acoustic emission?
2. Can fracture events be determined by the characteristics of the emissions?
3. Is the technique capable of giving information regarding the process controlling fracture?
4. With what specific microstructural detail is each stress wave associated?

The first question is, at present, unanswered, although estimates of 1 erg per emission⁽²⁾ have been made by generating known energy pulses to give similar detector responses. Also parameters related to stress wave energy (square of the amplitude) have been related to the energy input from linear elastic fracture mechanics⁽³⁾. The second question is unanswered since the frequency content of such waves limits the use of conventional detecting techniques on a quantitative basis. In spite of the lack of knowledge regarding stress wave characteristics, acoustic emission techniques have been used to determine the rate-controlling process during crack propagation⁽⁴⁾.

The aims of this study are to determine:

1. the extent to which emissions are functions of both material properties and environmental conditions.
2. the nature of the stress wave (i.e. amplitude, pulse shape, frequency content).

Experimental Procedure

The material used in this investigation was AISI 4335 steel, in the as-quenched or quenched and tempered condition. Test specimens were of the single cantilever beam type, as shown in Figure 1. In order to determine the effect of environment on acoustic behavior, specimen heat treatment was not varied (1500°F/1 hr., O.Q. + 400°F/1 hr., A.C.). The specimens were 0.495 - 0.525" thick, 1" wide, and 6" long, providing plane strain test conditions. The specimens were pre-fatigue cracked in air and tested in three environments: 1. 100% dry H₂ gas, 2. a H₂/Ar gas mixture containing 23.1% H₂, and 3. 3-1/2% sodium chloride solution. The solution pH was adjusted to 13.0 by addition of sodium hydroxide, and the specimen was tested potentiostatically, at +1500 mV w.r.t. a saturated calomel electrode. A Eranson 16 MHz transducer was used to detect the emissions, as shown in Figure 2. The specimens were tested until catastrophic failure occurred.

In the second series of tests, the specimen heat treatment was varied. Approximate tensile strength values were obtained by R_c hardness measurements. The test environments were 9.1% H₂ in H₂/Ar mixture and 3-1/2% sodium chloride solution (pH not adjusted). In the latter environment, specimen potential was maintained at -1.0 volts w.r.t. a saturated calomel electrode. An Endevco 2272 accelerometer was used to detect the emissions, and resonance peak counts were recorded as a function of beam deflection. The resonance frequency of the accelerometer is 37 kHz. In prior studies, beam deflection (as measured by an LVDT) was found to be proportional to crack length under constant load conditions. The electronic system is shown in Figure 3.

In the third study, an attempt was made to determine wave mode, amplitude, and energy. In order to avoid free surface reflection of the stress wave before it strikes the detecting transducer, sections of AISI 4335 steel (same heat treatment) were coupled to the sides of the specimen. Similarly, the two PZT-4 detecting discs (.049" thick, .350 diameter) were mounted on the bottom surface of the specimen and backed by 1/2" thick sections of PZT-4. This technique inhibited thickness mode resonance of the detecting disc by providing an acoustically matched medium into which the wave could pass, without undergoing reflection or refraction within the detecting element. This procedure provides a period of approximately 6 microseconds during which no reflected portions of the incident wave should excite the piezoelectric ceramic disc. Examination of the actual pulse, without the superimposed effects of specimen or transducer resonance, is therefore possible. The specimen-transducer arrangement is shown in Figure 4.

Results

Examination of the signals in Figures 5-7 shows that no significant differences in signal size or shape occur by changing the stress corrosion environment. In all environments, acoustic signal size increased just prior to catastrophic failure. Initial stress intensities were 39-49 ksi-in^{1/2} for the specimens tested, and no significant effect of starting stress intensity factor on acoustic activity was observed. Figures 8 and 9 show that, with the exception of the 240 ksi specimen, higher strength levels promote more acoustic activity (regardless of environment) for the same amount of crack growth. In both aqueous tests crack bifurcation occurred.

In Figure 10, the signals seen in the latter three photographs were latter attributed to electronic noise. However, in the first two photographs, spike pulses of microsecond duration are observed. Also, some thickness mode resonance of the detecting element is seen to occur (2.5 MHz). Considering the crack front to detector distance and stress wave velocities in steel, the presence of the closely spaced signals in the first two photographs could not be explained by the simultaneous generation of both dilatational and shear waves. Emission energy can be calculated using a published value⁽⁵⁾ of g_{33} for PZT-4 (24.9×10^{-3} volt-meters/newton) and approximating elastic energy as $1/2 (\sigma^2/E)$, where σ is the maximum stress on the piezoelectric element, and E is Young's modulus for the ceramic. The value of σ is determined using the maximum voltage generated by the ceramic, and the piezoelectric constant g_{33} . It is assumed that the amplitude of the wave, for such short pulses, determines the energy. Frequency content is not considered. A study in comparing the square of the mission amplitude with energy has been done by Gerberich⁽³⁾. In the present study the wave is assumed to be of spherical geometry and generated by a point source at the crack front in the mid-thickness of the specimen. The amount of spherical attenuation is estimated by multiplying the apparent energy by the ratio of detector area to the area of a sphere (whose origin is at the emission source) with radius equal to the source-to-detector distance. Since this energy is dissipated over a spherical surface, the ceramic disc is struck by only a fraction of the total energy. Energy losses at the metal-ceramic interface are estimated using the wave refraction equation (found in the text by Mason⁽⁶⁾) for the case of a normally incident dilatational wave. The acoustic impedance for the ceramic was obtained from the same source⁽⁶⁾. The impedance of steel was obtained from published data⁽⁷⁾. The calculated energy per emission was less than 10^{-2} ergs. These calculations are available.

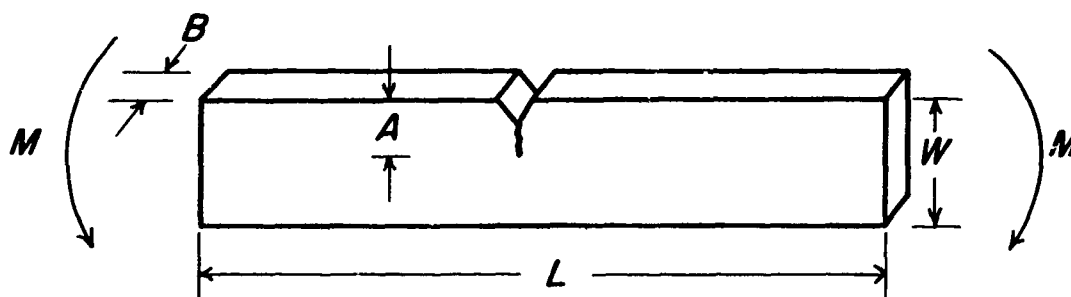
Conclusions

The acoustic emission studies have shown that:

1. Higher strength levels promote greater acoustic activity in both gaseous and aqueous environments.
2. Acoustic signals generated by cracks in high strength steel are of a low energy and high frequency nature.
3. The absence of reflection phenomena allows for the examination of acoustic signals on a more quantitative basis.

References

1. Dunagan, H. L., and Green, A. T., "Factors Affecting Acoustic Emission Response from Materials", Materials Research and Standards, March 1971, pp. 21-24.
2. Baker, G. S., "Acoustic Emission and Prefracture Processes in High Strength Steel", Tech. Rep. AFML-TR-67-266, Aerojet General Corporation, Sacramento, California, March 1968.
3. Hartbower, C. E., Gerberich, W. W., and Liebowitz, H., "Investigation of Crack-Growth Stress-Wave Relationships", Engineering Fracture Mechanics, Vol. 1, 1968, pp. 291-308.
4. Hartbower, C. E., and Gerberich, W. W., "Monitoring Crack Growth of Hydrogen Embrittlement and Stress Corrosion Cracking by Acoustic Emission", Proc. Conf. on Fundamental Aspects of Stress Corrosion Cracking (Ohio State Univ.), Sept. 1967, pp. 420-438.
5. Clevite Corp., "Modern Piezoelectric Ceramics", Publ. No. PD-9247.
6. Mason, Warren P., Physical Acoustics, Vol. 1, Part A, Academic Press, New York, 1964, pp. 204, 275.
7. Haulein, Stuart, L., et al., "Comparison of Mechanical and Acoustic Properties for Selected Non-ferrous, Ferrous, and Plastic Materials", Naval Ordnance Laboratory, White Oak, Maryland, July 1, 1970.



B = Specimen Thickness (in.)

W = Specimen Width (in.)

L = Specimen Length (in.)

A = Crack Length (in.)

M = Applied Moment (in. lbs.)

Plane - Strain Stress Intensity Factor

$$K = 4.12M \frac{\sqrt{(1/a^3) - a^3}}{BD^{3/2}}$$

(psi-in^{1/2})

$$\text{Where: } \alpha = 1 - A/D$$

Fig. 1 - Single Cantilever Beam Test Specimen.

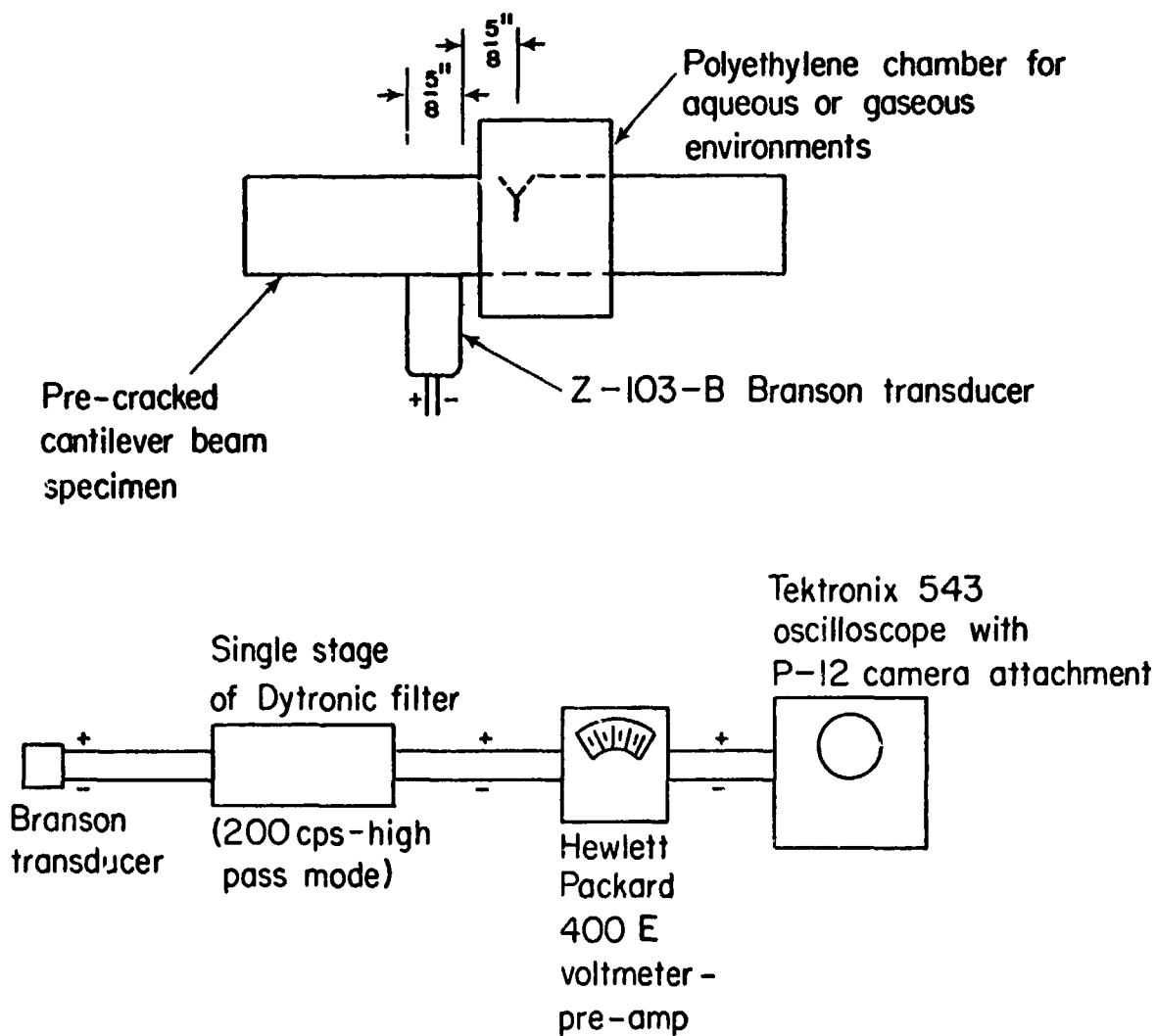


Fig. 2 - Test Apparatus for Experiments with Branson Transducer.

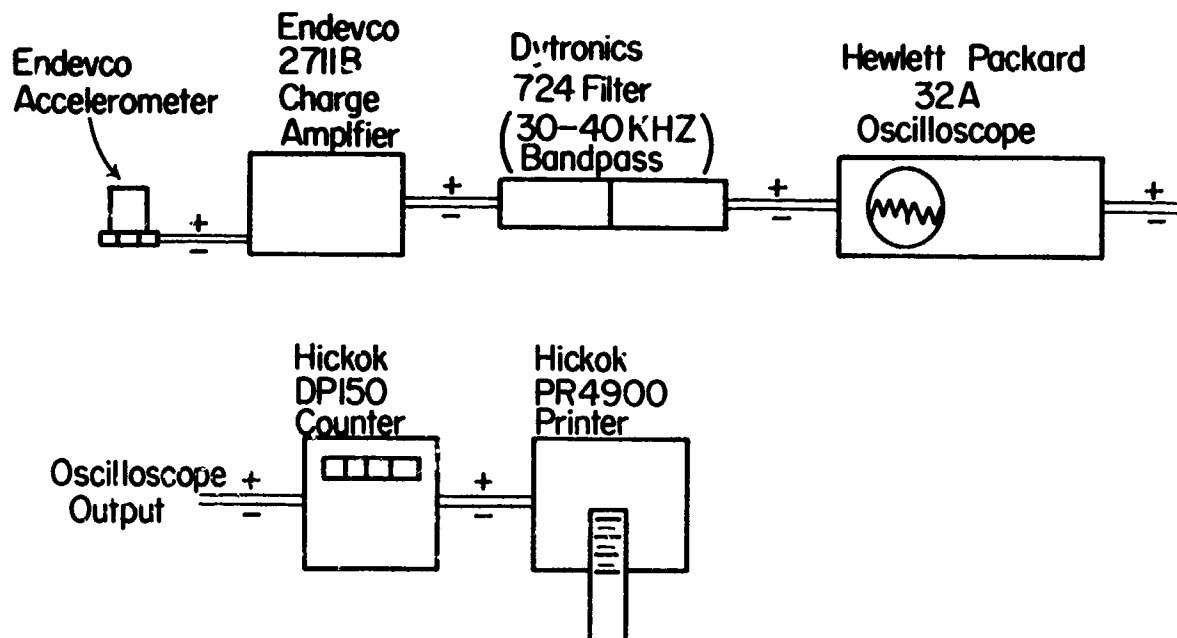


Fig. 3 - Electronic System for Testing with Endevco 2272 Accelerometer.

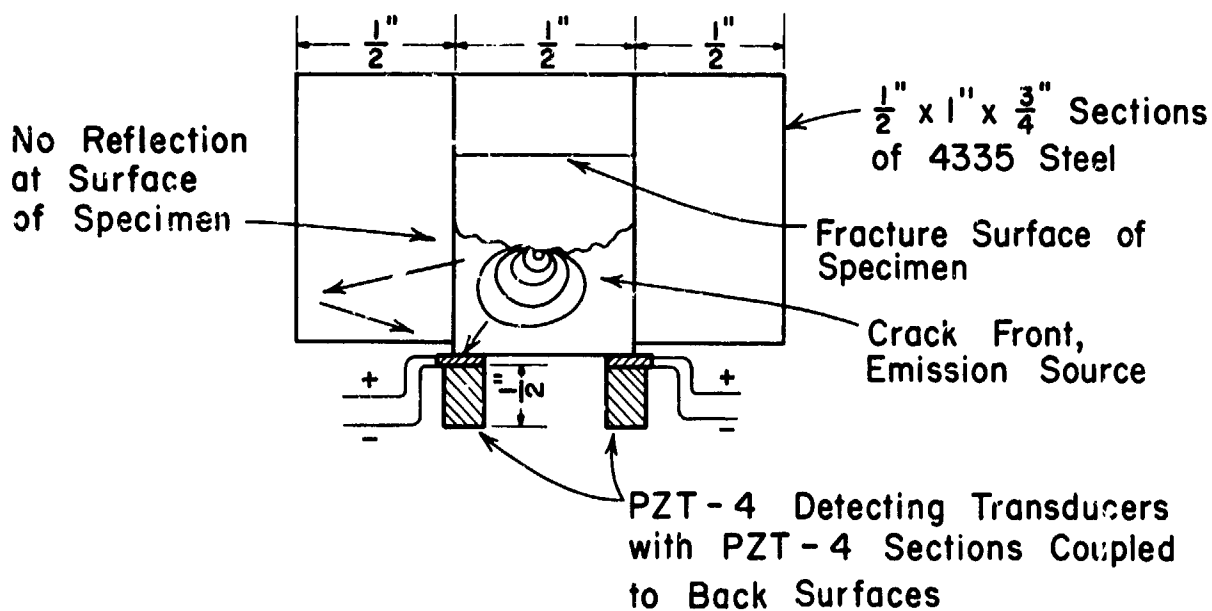
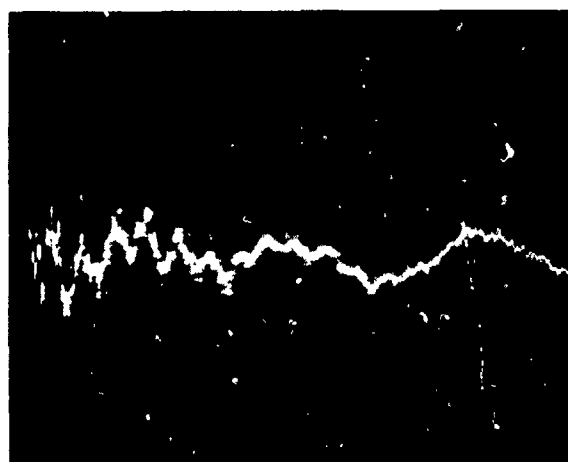
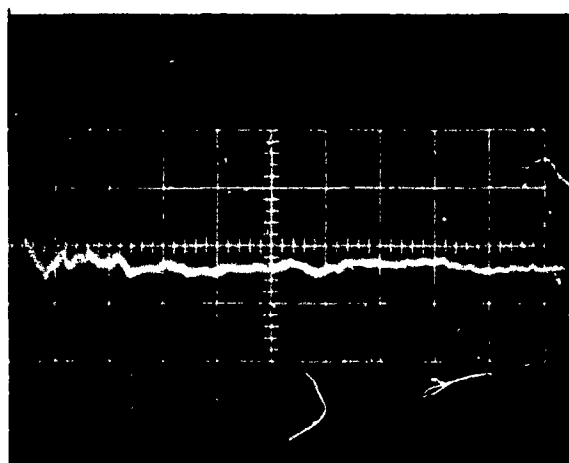
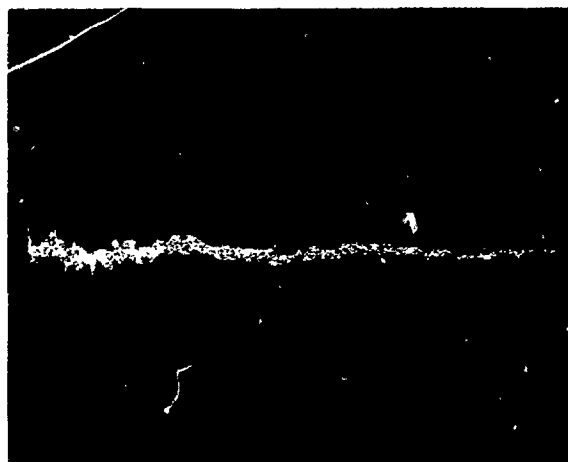
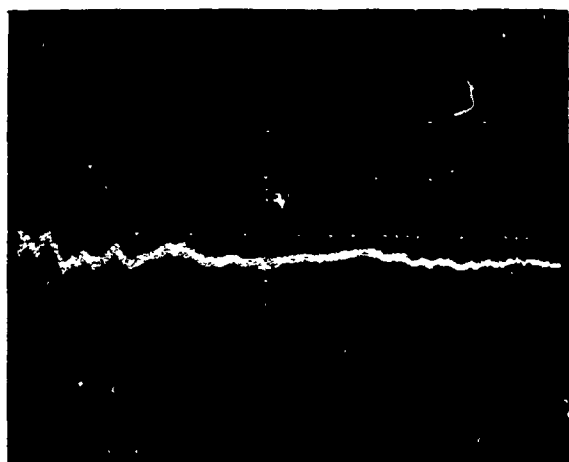
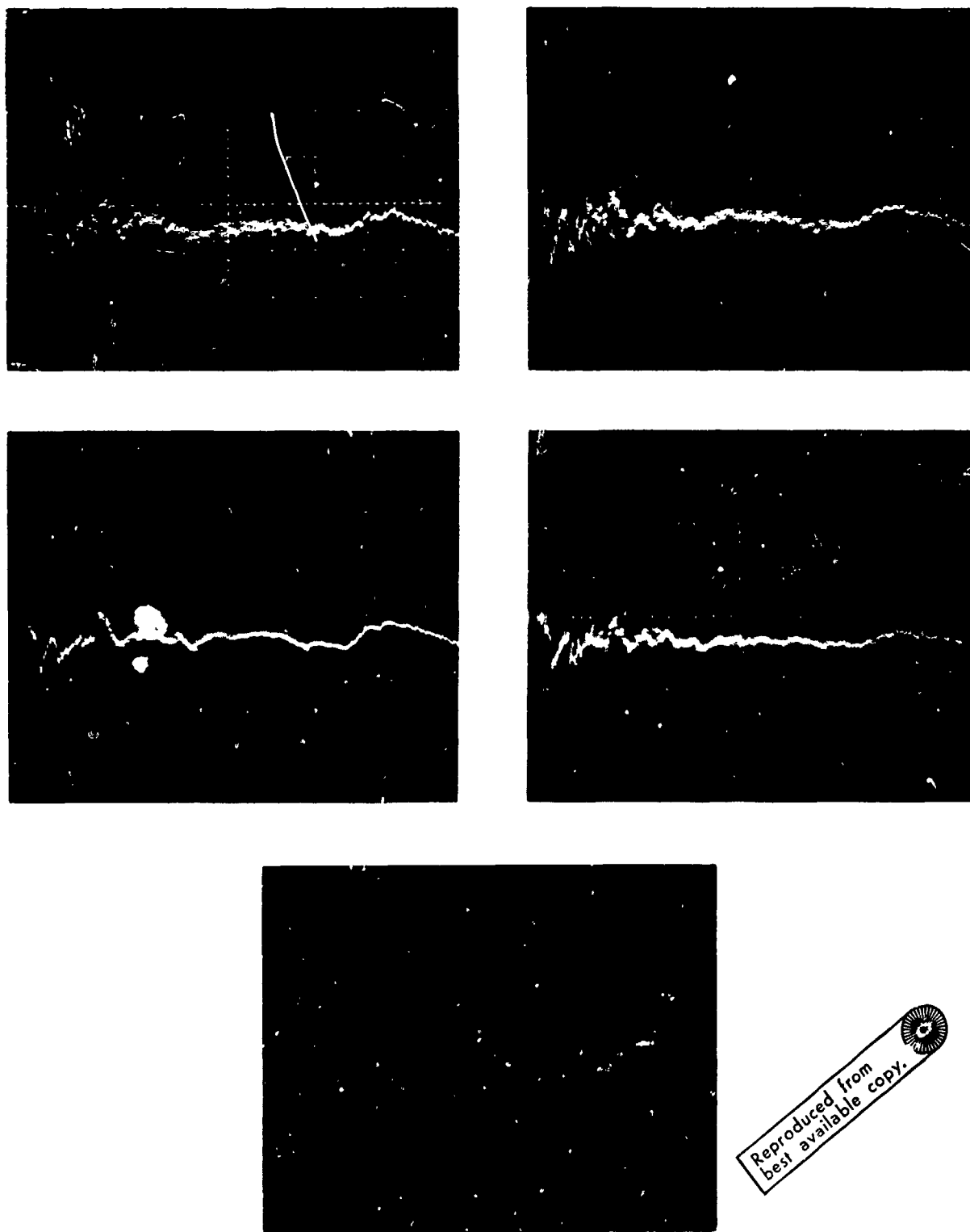


Fig. 4 - Cross Sectional view of Specimen and PZT-4 Transducers



Reproduced from
best available copy.

Fig. 5 - Photographs of Acoustic Emissions in 23.1% H_2 (Spec. CDG-80_3 horizontal scale - 50 sec/cm vertical scale - 10 mV/cm)



Reproduced from
best available copy.

Fig. 6 - Photographs of Acoustic Emissions in Pure H_2 (Spec. CDG-81), horizontal scale - 50 sec/cm
vertical scale - 10 mV/cm

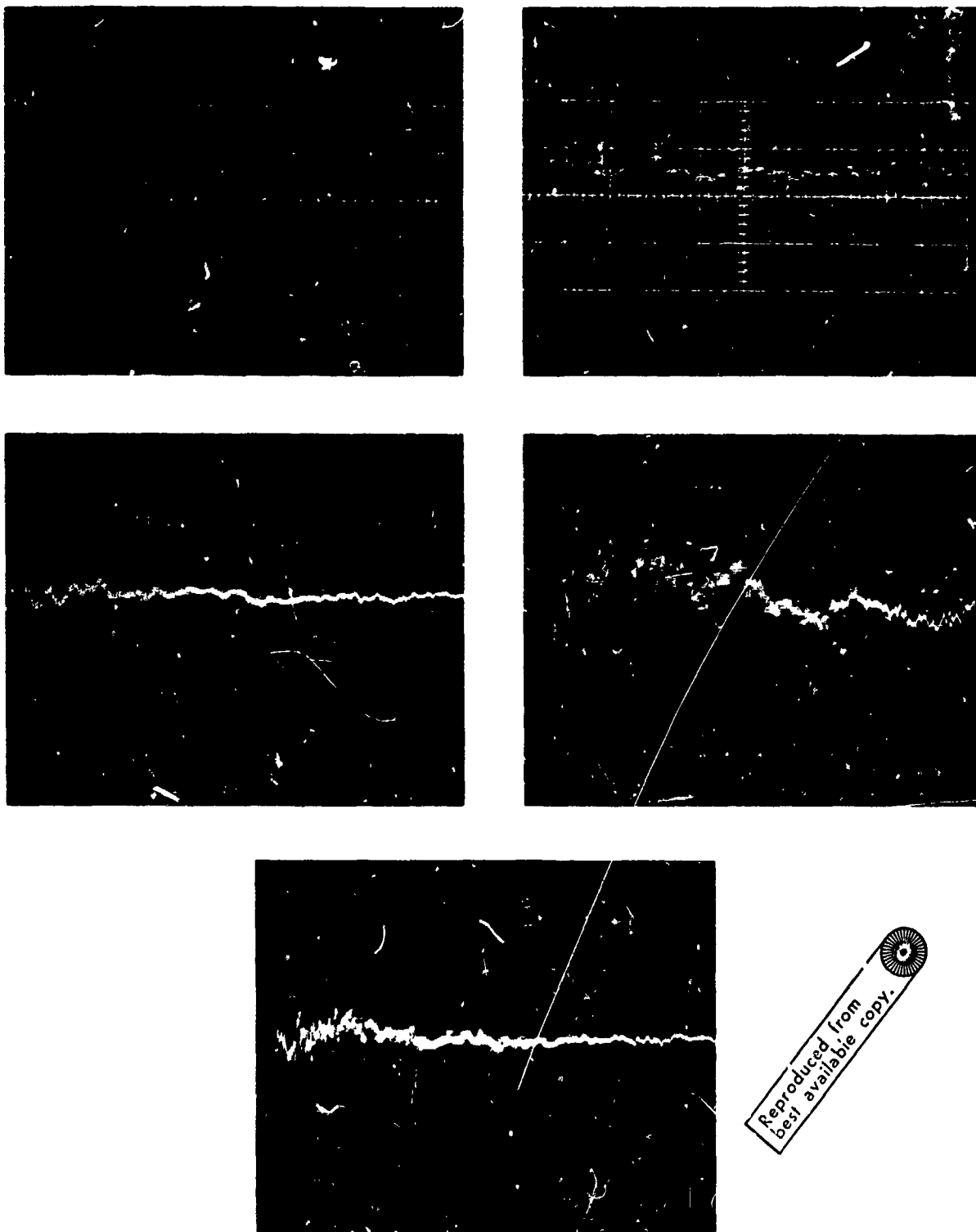


Fig. 7 - Photographs of Acoustic Emissions in $3\frac{1}{2}\%$ NaCl (adjusted to pH = 12.0 with NaOH) at +1500 nV WRT (SCE) (Spec. CDG-84).
horizontal scale - 50 sec/cm
vertical scale - 10 mV/cm

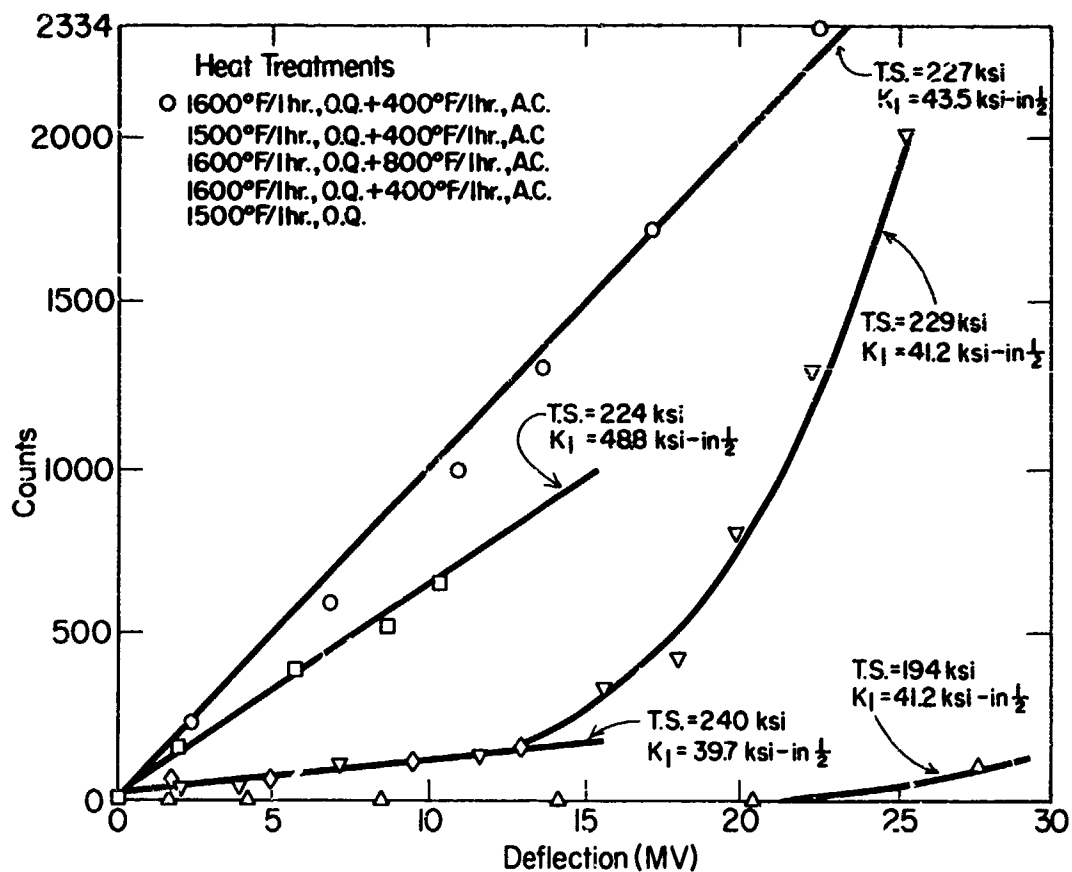


Fig. 8 - Counts vs. Deflection for Specimens of Various Strength Levels in H₂-AR Gas Environment. (9.1 Vol. % H₂).

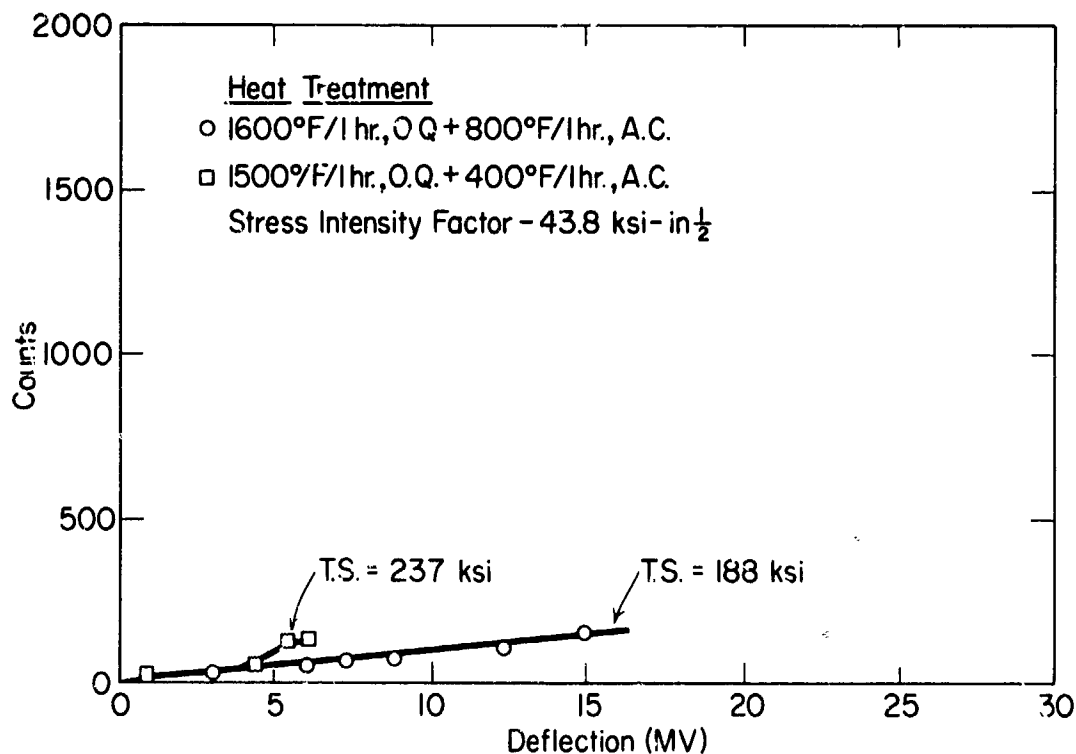
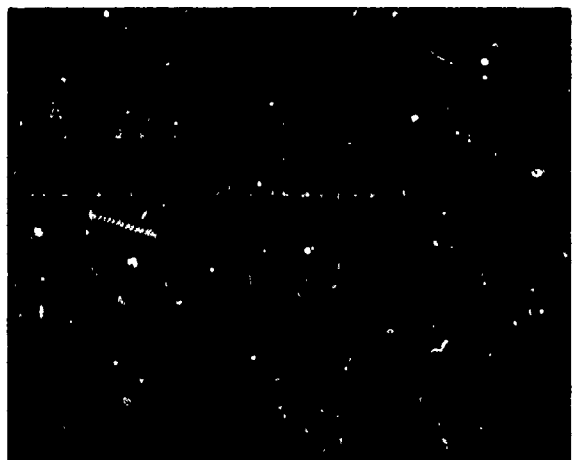
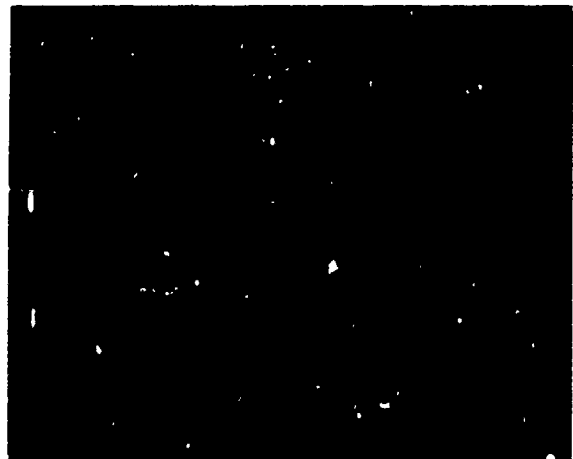


Fig. 9 - Counts vs. Deflection for Specimens in 3 1/2% NaCl Solution and at -1.0 Volt WRT Sat. Calomel Electrode.



Reproduced from
best available copy.

Fig. 10 - Photographs of Acoustic Emissions in Pure H₂ (Spec. CDG-88), horizontal scale - 1 s/cm

A CONTRIBUTION TO STRESS-CORROSION TESTING OF ALUMINUM ALLOYS

By

Giovanni Bollani

Direzione Laboratori Centrali - Laboratori Auto Avio
FIAT - Corso Giovanni Agnelli 200 - 0100 TORINO (Italy)

SUMMARY

The results of an extensive investigation for the improvement of the stress-corrosion testing methods on high-strength Al-alloys are briefly outlined.

For the evaluation of the crack initiation period under different stress conditions, two smooth specimens of original design are recommended.

For the measure of the crack propagation rate, the D.C.B. prefissured specimen has been found effective.

** **

RESUME

On présente les résultats les plus importants d'une recherche approfondie pour l'amélioration des méthodes d'essai à la corrosion sous tension dans les alliages légers.

Pour l'évaluation de la période d'incubation de la fissure sous de différentes conditions de contrainte on recommande ici deux éprouvettes lisses de dessin original. Pour la mesure de la vitesse de propagation l'éprouvette D.C.B. prefissurée s'est démontrée efficace.

A CONTRIBUTION TO STRESS-CORROSION TESTING OF ALUMINUM ALLOYS

by

G. Bollani

1 - INTRODUCTION

It is well known that a very important point in the evaluation of the resistance of materials to stress-corrosion cracking is the assessment and the standardization of laboratory testing procedures, suitable to give consistent and low-scatter results, that may be readily used in design (1), (2). To this aim it is firstly appropriate to define as clearly as possible the nature of the informations that should be achieved with a particular test: this criticism does usually imply specific requirements for the kind of specimen and experimental set-up. A special care must be given to the features of the crack initiation and propagation, that as far as possible must be discernible from each other in the evaluation of the results. Secondly it will be necessary to take into account a set of experimental conditions extensive enough to reproduce all the relevant practical situations: this will generally involve the performance of tests on different kinds of specimen, loading system and environment.

In the following report will be shown the most relevant points of an investigation carried out on this subject making use of:

- smooth, mechanically notched (edge V or hole) and pre-cracked (D.C.B.) specimens
- simple state of stresses (uniaxial, as arising from a classical test in bending or in tension), and more complex states (biaxial, as e.g. in torsion).

The testing materials have been selected among some high-strength Al-alloys, as reference environment was used in all tests the standard NaCl 3.5% aqueous solution.

2 - EXPERIMENTS AND RESULTS

2.1 SMOOTH SPECIMEN

This kind of specimen is obviously intended to evaluate the initiation phase of the stress-corrosion cracking. The principal requirements that have however to be accomplished to get a meaningful information are:

- the specimen must break as soon as a crack of very limited depth has been developed, in order to avoid any influence of the subsequent phase of propagation
- the nominal stress must be clearly defined and as far as possible constant on the entire rupture section.

Whenever possible, it is also useful to arrange for a preferential fracture zone on the specimen, that makes easier an early detection of the crack nucleation and contributes to reduce the scatter of results.

After said requirements, the specimen for 4 points-bending loads shown in fig.1 has been designed. The following remarks are appropriate:

- the size of the specimen (maximum length = 48 mm) is small enough to allow tests to be made in the short-transverse direction of nearly all plates in use for structural applications
- the load required to obtain a nominal tensile stress $\sigma_{max} = 0.75 \cdot \sigma_y$ (maximum value of practical interest) is lower than 80 kg for all high-strength Al-alloys, and can be easily controlled by a low-stiffness spring system
- the stress distribution is always tensile in all the critical area (lower part of the central cross-section), and nearly constant for a length ± 2 mm from the central line, where most of the fractures do occur; the stress concentration factor due to the fillet and the hole is very small ($\alpha_K \approx 1.2$) and has been accounted for by strain-gages calibration
- the maximum crack length before rupture is only 1 mm.

It is interesting to point out that for high strength Al-alloys with one-step aging, tested in the standard environmental solution NaCl 3.5%, the lowest stress able to produce a stress-corrosion crack in the short transverse direction may range from 3 to 7 kg/mm². This value of stress gives rise to a maximum stress-intensity factor (assume $K = \sigma\sqrt{a}$) of about 10 kg/mm^{-3/2}; this figure of K is notably less than the minimum value of K_{Isc} , as evaluated on these alloys with pre-cracked D.C.B. specimens (see point 3). That is to say no K-controlled propagation of the crack was included in the long life evaluation obtained from smooth specimens.

The life values for some of the most common Al-alloys and aging treatments are reported in fig.2 (all specimens have been obtained from plates of 50 mm thickness): it is well demonstrated a very limited scatter of the results, that makes possible a good selection among different materials, and a tendency to obtain a safety figure of the strength, near the lower limit of the ALCOA scatter band as reported in reference (3).

To investigate the stress-corrosion behavior of the material under biaxial stress conditions, the tubular specimen for torsion loads shown in fig.3 has been designed. The size of the hollow cross-section (wall thickness = 1 mm; mean radius = 3.5 mm) is such that a maximum shear stress of $\tau = 0.75 \cdot \sigma_y$ can be imposed with a torque of only about $1.7 \cdot 10^3$ mm.kg (20 kg with a lever arm of 100 mm). From the equilibrium of stresses, we have at the external surface of the specimen a biaxial situation:

$$\tau = \sigma_{I} = -\sigma_{II}$$

where τ is directed both along the circumference of the cross section and parallel to the axis of the cylinder; σ_I and σ_{II} are the principal stresses, respectively oriented at +45° and -45° to the axis. The specimens have been obtained out of a plate of 7075-T651, 50 mm thick, both in the longitudinal and in the short-transverse direction (axis of the cylinder parallel to these directions). The test results shown in fig.4 give rise to the following comments:

- for the material investigated, with grains strongly elongated in the cold working direction, the fracture takes place along elongated grain boundaries (fibres) and is practically insensitive to the orientation of the principal tensile stress, that was conversely the major controlling factor in the case of bending loads
- the threshold values (τ) of stress-corrosion cracking for specimens taken in the longitudinal and in the short-transverse direction are very close together, and approximately coincident with the threshold (σ) obtained from bending tests in the short transverse direction.

These findings have been confirmed by further tests on an extruded bar of the same material an temper, with nearly equiaxed grains: the fracture in this case was probably started by the tensile component of the stress (45° to the axis of the specimen), but the lives in the longitudinal and the transverse direction did again not differ appreciably (170 hours against 140 hours, with an imposed stress of 15 kg/mm²).

It seems therefore that the tubular specimen tested under torsional load could find a good use also to evaluate the short-transverse resistance to stress-corrosion of sheets whose thickness is only 10 mm, that is insufficient for obtaining a bending specimen. Furthermore from a design point of view it is advisable to look at the torsional loads as critical stress situations with regard to stress-corrosion failures, and to prescribe careful controls when this will be encountered in practice.

It should also be mentioned that the torsion specimen might really not be considered as a truly initiation one: the deformation following the crack extension in the case of the longitudinal specimen is often actually large enough to make possible a control of the crack propagation and a study of morphological details of the fracture.

2.2 NOTCHED SPECIMEN

The principal aim of the tests made on this kind of specimen was to investigate the importance of the surface finish of the smooth specimens in fig.1 and fig.3.

The bending-load notched specimen was manufactured with a geometry substantially similar to that of fig.1, but with a couple of edge V notches ($\alpha_k = 3.5$) and a constant width of 24 mm : see fig.5. The torsion-load notched specimen was manufactured identical to that of fig.3, but with a hole ($\alpha_k = 1.5$, if calculated as T_{max}/T_{nom}), drilled in the mid-section as shown in fig.6.

Although no systematic investigation was carried on these specimens, it was easily demonstrated that the influence of the two kinds of mechanical notch on the crack initiation and development is limited to the high stress situation (quasi-static-ruptures); in the case of stresses near the threshold value a notch proves almost ineffective, particularly for the short-transverse specimen. This statement has been found to apply also for extruded structures, with grain boundaries not strongly elongated.

It is therefore advisable that a smooth stress-corrosion specimen be given a good surface finish by fine machining (to a roughness of say $R_a = 0.8 + 1.5\mu$), but it is believed unnecessary to provide a more expensive finishing by grinding or polishing as is required for a fatigue specimen. From a design standpoint it is worth noting that the stress-corrosion situation for a notched structure of Al-alloy appears to be more favourable than fatigue : this fact should be kept into account also when considering the relatively minor incidence of stress-corrosion in practice.

2.3 PRE-CRACKED D.C.B. SPECIMEN

A set of tests has also been carried on Double Cantilever Beam mechanically pre-cracked specimens, to evaluate their suitability for crack propagation measurements. As it is well known, this kind of specimen looks very attractive for the possibility of making tests representative of the actual stress-corrosion cracking with a minimum requirement of experimental facilities.

The geometry of the specimen used in our investigation is shown in fig.7 : it differs from that reported in the ref. (4) only in the width of the notch (the spacing between the notch surfaces is 2 mm, instead of 1 mm, for more ease of machining), and in the screw diameter (8 mm instead of 6 mm, to avoid some screw fractures in high toughness directions). After some trials, the radius at the tip of the mechanical notch was set 0.2 mm, as this would repeatedly give well aligned initial cracks, with a limited amount of plastic deformation.

To measure the initial COD a very simple fixture supporting a 0.01 mm accuracy dial-gage proved to be effective. The mechanical extension of the static crack was set between 2 and 4 mm : the main reason for the choice of this length is to evade from the plastic zone at the tip of the notch (typically of the size of 1 to 2 mm) and from the associated residual stresses. In so doing it was also possible to appreciate if the propagation in the environment was expected to be correct, that is on the central line of the specimen (see fig.7 - left specimen), or in a slant direction (right specimen). The measure of the crack propagation was optically made on both sides of the specimen and controlled by an eddy-current method (Magnaflux ED-520) : results differing by more than 5% have been discarded.

Among the materials investigated have been included two experimental Al-alloys with Zr addition, recently developed at the Istituto Sperimentale Metallurgico - Novara (Italy) - (5), whose typical composition and mechanical characteristics are the following :

Type of alloy	Zergal 3	Zergal 4
chemical composition (average data) - % -	5.8 Zn 2.4 Mg 1.5 Cu 0.8 Cu 0.2 Zr 0.5 (Mn+Fe+Si)	
ultimate tensile stress - kg/mm ² -	60	55
yield point - kg/mm ² -	54	50
elongation - % -	7.5	8.5

The pre-cracked specimens have been tested in the standard environment, both with continuous immersion (as it was the case for the smooth and the notched ones), and with alternate immersion (10' in - 50' out). The results are summarized in figs.8 to 11 as follows :

- fig.8 : stress-intensity factor (K_I) versus time (t), to evaluate the approximate K_{Isc} value for 7075-T651 (plate) and 7079-T6 (extruded bar)
- fig.9 : K_I versus t, and K_{Isc} for 7075-T7351 (plate) and 7075-T73 (forging)
- fig.10 : K_I versus t, and K_{Isc} for Zergal 3 and Zergal 4 (forging)
- fig.11 : crack propagation rate (da/dt) versus stress-intensity factor (K_I) for all the experimented materials.

For the calculation of the K_I value the approximate formula :

$$K_I = \frac{E D h}{4} \frac{[3h (a + 0.6 h)^2 + h^3]^{1/2}}{(a + 0.6 h)^3 + h^2 a}$$

valid for a D.C.B.specimen of very similar geometry (4) was assumed. From an examination of the results the following remarks may be drawn :

- the pre-cracked specimen proves to be a simple and efficient laboratory tool for the evaluation of the stress-corrosion crack propagation in materials; the best use of the specimen is made testing on plates in the short-transverse direction (or in the transverse for forging and extruded bars); some difficulty is expected when testing in the longitudinal direction. As this case is however not the most dangerous one, the limitation does not appear to have great enough interest in practice
- the repeatability of the test data obtained for da/dt versus K_I is good enough to make possible the selection of a material among those investigated after only a few days (less than 150 hours); an accurate estimate of K_{Isc} does however require about 3 weeks, in the classic environment.

As to some material performances, it may be noted that a forging of the experimental alloy Zergal 4 (one step aging) has proven nearly equivalent to the alloy 7075-T73 from the standpoint of stress-corrosion crack propagation, with 10% more of static resistance.

3 - CONCLUSIONS

In stress-corrosion testing it seems advisable to make use of two different kinds of specimens : the one suited to evaluate the initiation period (controlled by a threshold value of the applied stress), and the other intended to measure the crack propagation rate (controlled by a threshold value of the imposed stress-intensity factor). The first specimen, obviously smooth, will be necessary to evaluate practical situations where no surface damage is admissible for a structural element ; the second specimen, already pre-cracked, will be required to keep into account the fact that some structures may contain a limited defect during their life.

For an initiation test in the most common bending-load conditions, it is very useful the specimen shown in fig.1, that, without being appreciably more difficult to be manufactured than the classical ones, has given in our tests accurate and reproducible results. To investigate the behavior of materials under the effect of a more complex state of stresses, as arising from a torsion-load situation, the specimen shown in fig.3 is suggested. This specimen can also be used for a preliminary evaluation of the stress-corrosion resistance of plates with thickness lower than 50 mm (to a minimum of 10 mm), stressed in the short-transverse direction. The surface finish of a smooth specimen is not so important as in fatigue tests, particularly at the very long lives.

For a crack propagation test, the D.C.B. pre-cracked specimen has proven to be very effective and nearly inexpensive, particularly when stressed in the short-transverse direction, which is obviously the most interesting situation. Some difficulties may be expected when loading the specimen along other more resistant directions. The selection of a high strength aluminum alloy for resistance to stress-

corrosion crack propagation by means of this or similar specimens can be made on a sound analytical basis (K_{Isc}), and in a test time acceptable for industrial purposes.

* ** *
*

REFERENCES

- (1) - "Stress corrosion testing" - ASTM - S.T.P. No.425, 1967
- (2) - PIPER D.E. "Standardization of test methods for stress-corrosion cracking" - AGARD Advisory Report No.25, 1970
- (3) - BROWN R.H., SPROWLS D.O., SHUMAKER M.B. "Influence of stress and environment on the stress-corrosion cracking of high strength aluminum alloys" - AGARD Conference Proceedings No.53, 1970
- (4) - HYATT M.V. "Use of precracked specimens in stress-corrosion testing of high strength aluminum alloys" - Boeing Reports D6 - 24466 to 24471, 1969
- (5) - DI RUSSO E. "Metallurgical features of the stress-corrosion cracking of aluminum alloys" - La Metallurgia Italiana No.6, 1970



Fig.1 - Smooth specimen and test fixture for 4-points bending load



Fig.2 - Test results on smooth specimens in bending (different materials)



fig. 3 - Stress Corrosion Cracking Specimens Geometry

A = Specimen ready for deformation

B = Specimen ready for S. C. C. test

Reproduced from
best available copy.



Fig.4 - Test results on smooth specimens in torsion (7075-T651)



Fig.5 - Fractures of notched specimens in bending (7075-T651)

Reproduced from
best available copy.

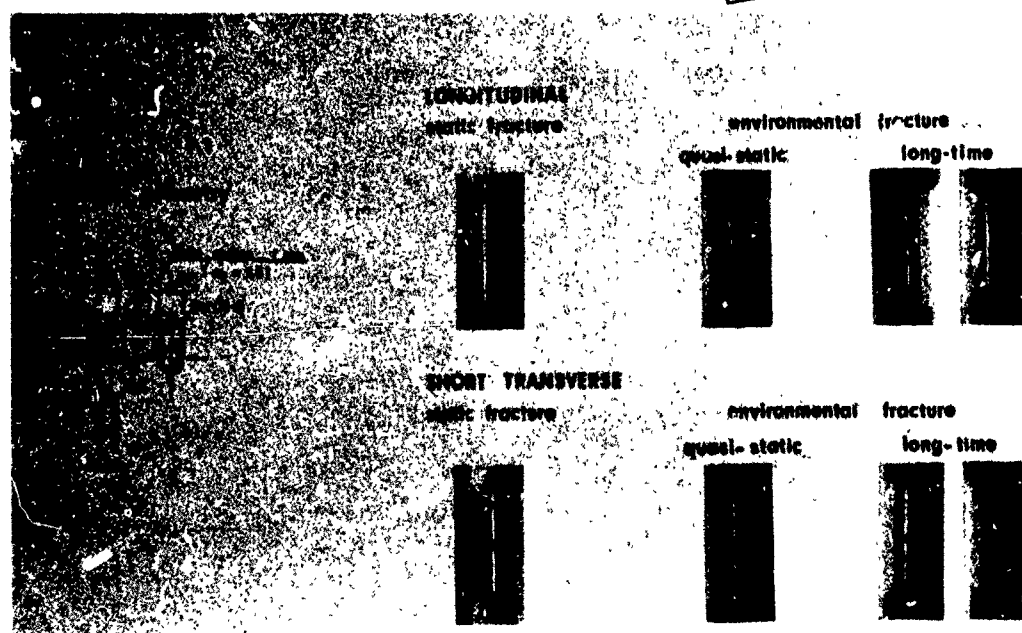
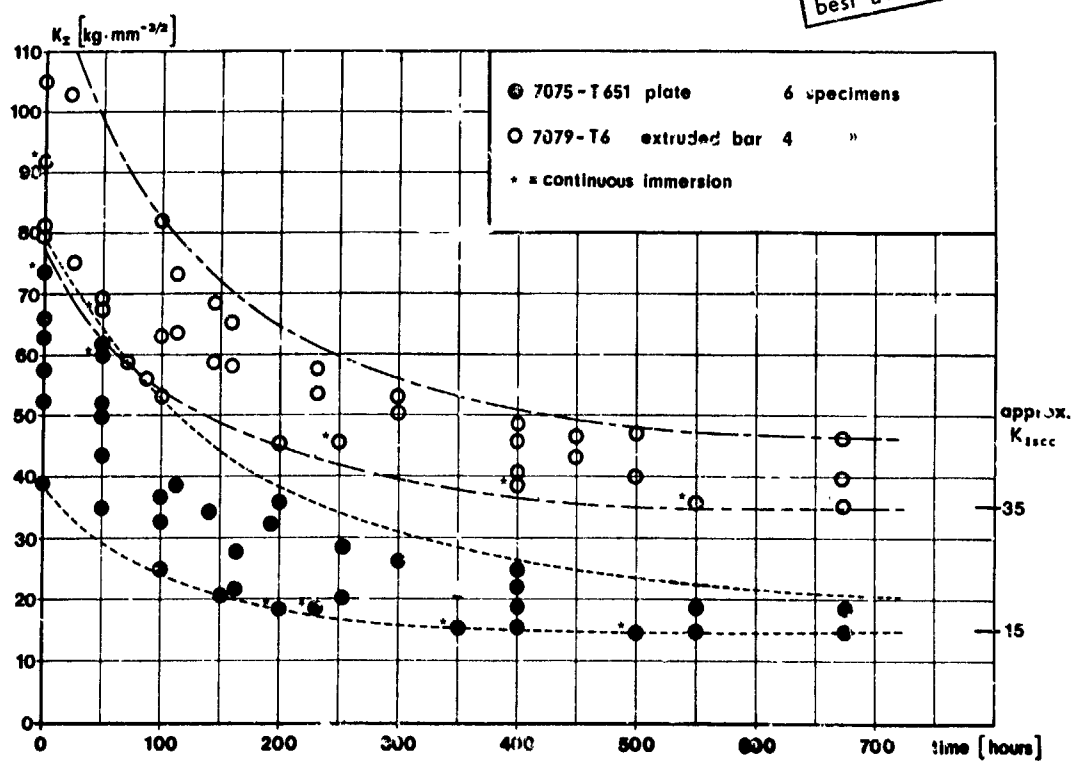


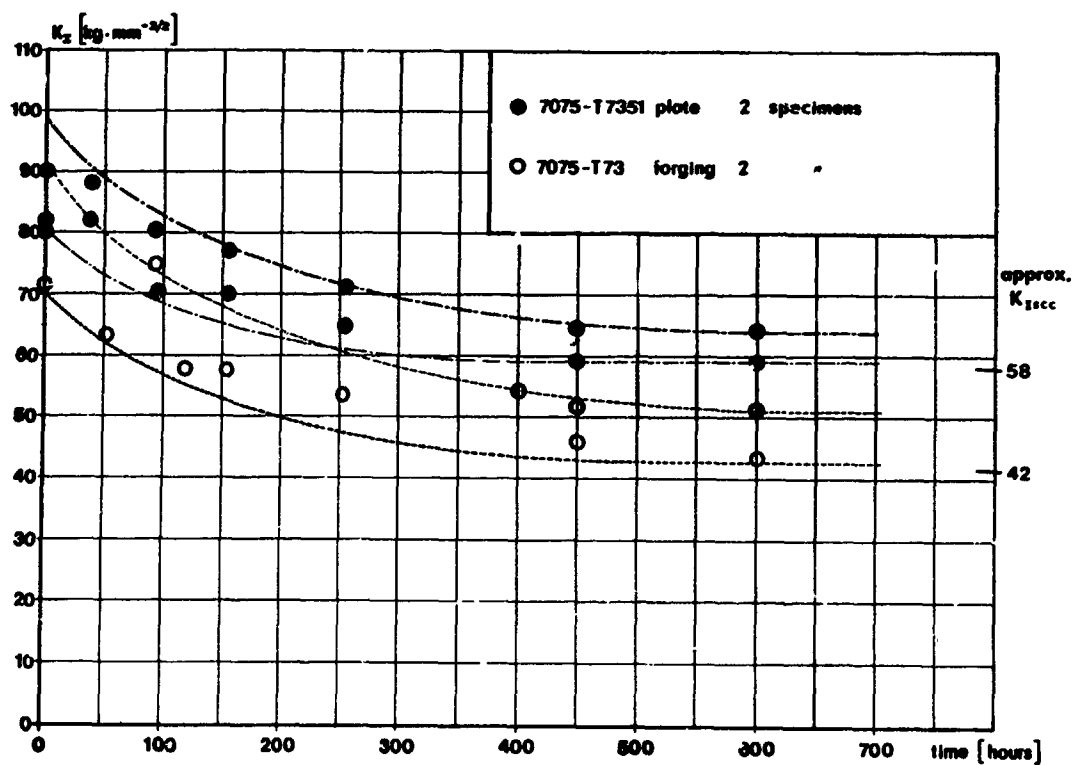
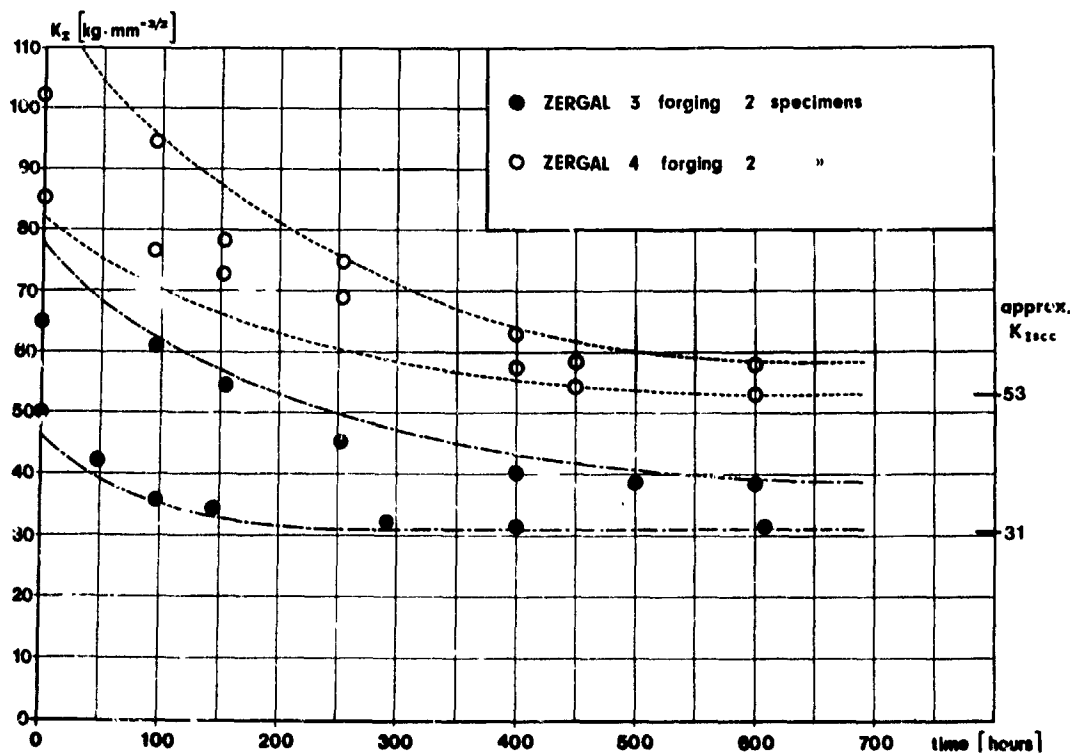
Fig.6 - Fractures of notched specimens in torsion (7075-T651)



Fig.7 - Pre-cracked D.C.B. specimen

Reproduced from
best available copy.

Fig.8 - K_I -time data for transverse D.C.B. specimens

Fig. 9 - K_I -time data for transverse D.C.B. specimensFig. 10 - K_I -time data for transverse D.C.B. specimens

INFLUENCE OF TEST METHOD ON STRESS-CORROSION BEHAVIOR
OF ALUMINUM ALLOYS IN SEA WATER

by

George J. Danek
Head, Corrosion Branch
Annapolis Laboratory
Naval Ship Research and Development Center
Annapolis, Maryland 21402

SUMMARY

Highlights are presented of recent investigations conducted at the Naval Ship Research and Development Center on sea-water stress-corrosion behavior of high-strength aluminum alloys. Rolled 7000-series plate was used to show a significant influence of specimen orientation on sea-water stress-corrosion response. The results suggested that tests in the short transverse direction are essential in ascertaining stress-corrosion behavior of high-strength aluminum alloys in either smooth or precracked specimens. Based on these results a number of high-strength hand forgings, representing the 2000-, 6000-, and 7000-series, were tested as bent-beam and precracked cantilever specimens taken in the short transverse direction. Inconsistencies are observed when the sea-water stress-corrosion results from precracked cantilever specimens are compared to those from smooth specimens. The results indicate that each of the two techniques provides important information, and both methods should be used in assessing the sea-water stress-corrosion behavior of high-strength aluminum alloys.

INFLUENCE OF TEST METHOD ON STRESS-CORROSION BEHAVIOR OF ALUMINUM ALLOYS IN SEA WATER

by
George J. Danek

INTRODUCTION

Stress-corrosion cracking behavior is a critical property in selecting high-strength materials for sea-water applications. Failure by this process can be insidious and catastrophic. Experience has shown that many high-strength-to-weight materials, developed for sophisticated marine applications, are particularly prone to failure by stress-corrosion cracking.

The classical methods used over the years for evaluating sea-water stress-corrosion cracking behavior involve sea-water immersion of a stressed specimen, usually in the form of a bent beam. Stress corrosion proceeds by two steps - initiation of a stress-corrosion crack and subsequent propagation. The initiation phase of the process entails the formation of a stress raiser (notch) from which the stress-corrosion crack can propagate. The stress raiser may be introduced as a mechanical notch or as a weld defect. However, initiation often occurs when a pit grows to form the stress raiser from which stress-corrosion cracks emanate, figure 1. For many high-strength alloys the pitting process consumes essentially the entire exposure time in a classical stress-corrosion test. The subsequent propagation in a susceptible material proceeds rapidly, and final failure occurs by mechanical rupture when the crack attains a critical size.



Figure 1 - Pits with Emanating Stress-Corrosion Cracks
12Ni-5Cr-3Mo Maraging Steel (Villela's Etch)

Reproduced from
best available copy.

A new stress-corrosion technique was introduced by Brown in 1966.⁽¹⁾ A specimen with a sharp notch is stressed in bending while exposed to a corrodent. For cases where initiation proceeds by environmental pitting in a classical stress-corrosion test, the sharp notch (usually a fatigue crack) can circumvent the time-consuming process of forming a defect. It is generally agreed that the technique is a significant advancement in technology and offers several important advantages over the classical method in addition to reducing the testing time:

- Permits evaluation of stress-corrosion behavior on materials which are immune to pitting.
- Permits quantitative expression of complex stress-corrosion behavior in terms of fracture toughness characteristics, defect size, and stress intensity
- Provides a tool for mechanism studies of electrochemical aspects of the stress-corrosion process as described by Brown, et al.⁽²⁾

The precracked cantilever-beam technique and some of its modifications have proven valuable in assessing the suitability of high-strength-to-weight ratio alloys for use in sea water. Classes of materials that have been studied at the Naval Ship Research and Development Center include ferrous, nickel, titanium, and aluminum alloys.

Our work on aluminum alloys which has been reported by Wacker and Chu^{(3), (4), (5)} will be highlighted in this paper. Particular emphasis is placed on inconsistencies that are observed when bent-beam results are compared with those from precracked cantilever specimens. Also the influence of anisotropy in aluminum alloys on stress-corrosion behavior is illustrated.

MATERIALS

Table 1 lists aluminum alloys (hand forgings and rolled plates) of the 2000-, 6000-, and 7000-series that are pertinent to this paper. Stress-corrosion data are given for many of the alloys listed, but some are used only to illustrate microstructural features and surface appearances.

Table 1 - Test Materials

Alloy	Fabrication Method	Size inches
6061-T652	Forging	9 x 24 x 24
6061-T652	Forging	6 x 12 x 24
2024-T352	Forging	6 x 12 x 24
2024-T852	Forging	6 x 12 x 24
7075-T7352	Forging	6 x 12 x 24
2014-T6	Forging	8 x 16 x 19
7039-T64	Plate	3 thick
7079-T6	Plate	3 thick
7002-T6	Plate	2 1/2 thick
X7106-T63	Plate	3 thick

METHOD OF TEST

Precracked specimens of the forged materials were taken in the short transverse orientation. Specimens from alloys received as plate were taken in the short transverse, long transverse, and longitudinal directions in order to illustrate orientation effects on stress-corrosion behavior. Specimens were loaded by deadweight as cantilever beams with the cracked region enclosed in natural sea water in a plastic container.

Conventional stress-corrosion tests were also conducted by using smooth specimens. They were loaded in natural sea water to different stress levels as bent beams by restricting their ends in fixtures. Here again, the forged alloys were considered as short transverse specimens only, and all orientations were studied in alloys received as plate.

Specimen lengths varied due to constraints imposed by as received material thicknesses. The data on smooth bent beams were analyzed in terms of load stress versus time to failure by conventional practice, whereas data on the precracked specimens were reduced to initial stress intensity versus time to failure according to Brown.⁽¹⁾

RESULTS AND DISCUSSION

Influence of Anisotropy

Specimen orientation has been observed to influence stress-corrosion behavior of wrought aluminum alloys. Data from plate material 7079-T6 will be used to illustrate stress-corrosion response as a function of orientation because the effect is more pronounced in rolled products.

Specimens can be taken in three directions; in the case of precracked specimens, they can be notched in two ways, as shown in figure 2. It can be seen in figure 3 that the three orientations yield different results when stressed as both specimens are exposed to sea water. Failure occurs much earlier in short transverse specimens than in either the longitudinal or long transverse samples. Analogous results are observed for specimens exposed as precracked cantilevers as illustrated in figure 4. Here again, the short transverse specimens are the least resistant to stress-corrosion failure.

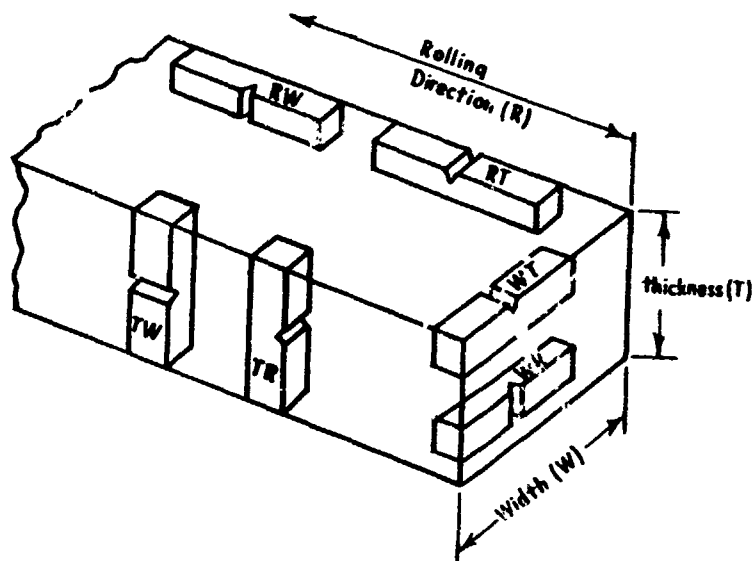
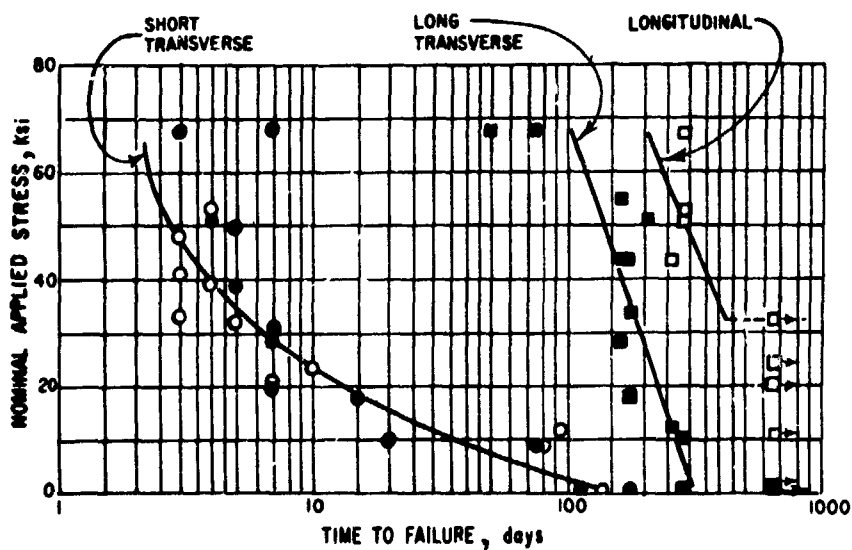


Figure 2
Direction of Specimens



Notes:

- - Short Transverse - Specimen thickness parallel to long-transverse plate direction (corresponding to TW direction).
- - Short Transverse - Specimen thickness parallel to longitudinal plate direction (TR direction).
- - Long Transverse (width direction).
- - Longitudinal (rolling direction)

Figure 3
Results of Directional SCC Cracking
Tests of 7079-T6 Smooth Strips in Bending

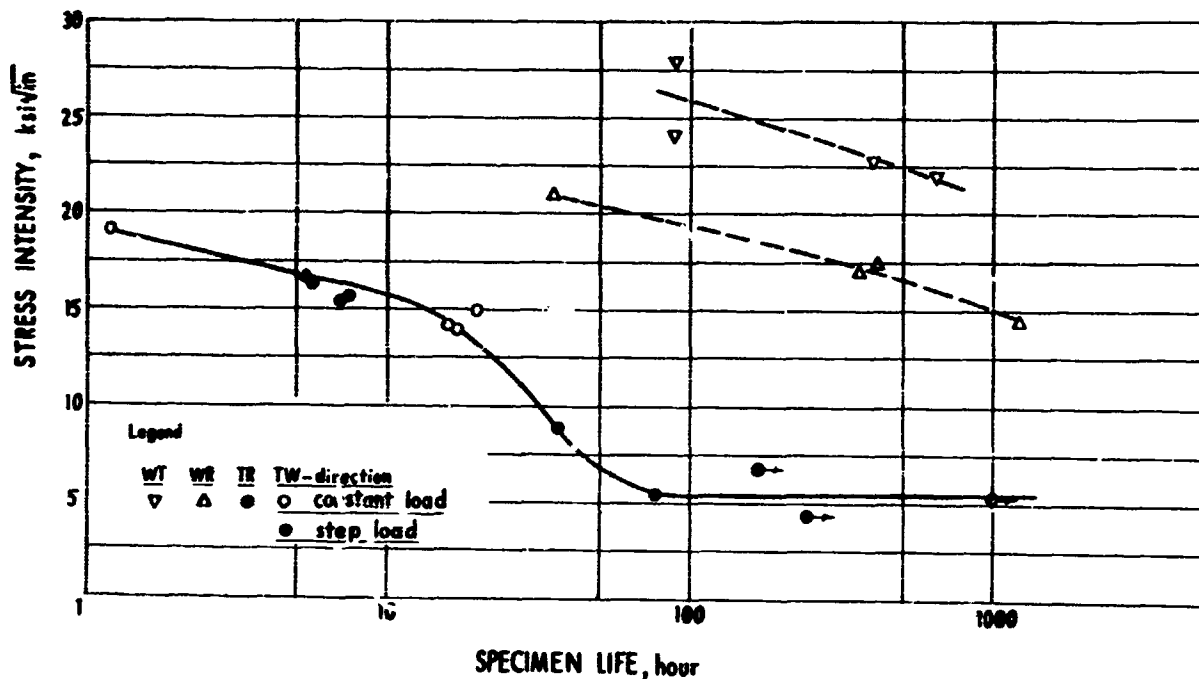


Figure 4
SCC Test Results of 7079-T6 Precracked Specimens

Typical microstructural directionality effects in high-strength aluminum alloys are illustrated by the composite photomicrograph shown in figure 5. Here it can be seen that the short transverse orientation is the most critical in terms of stress-corrosion susceptibility. Specimens taken in the short transverse direction (TR and TW) possess longer and more continuous corrosion-sensitive grain boundary paths than specimens taken in either the longitudinal or long transverse direction.

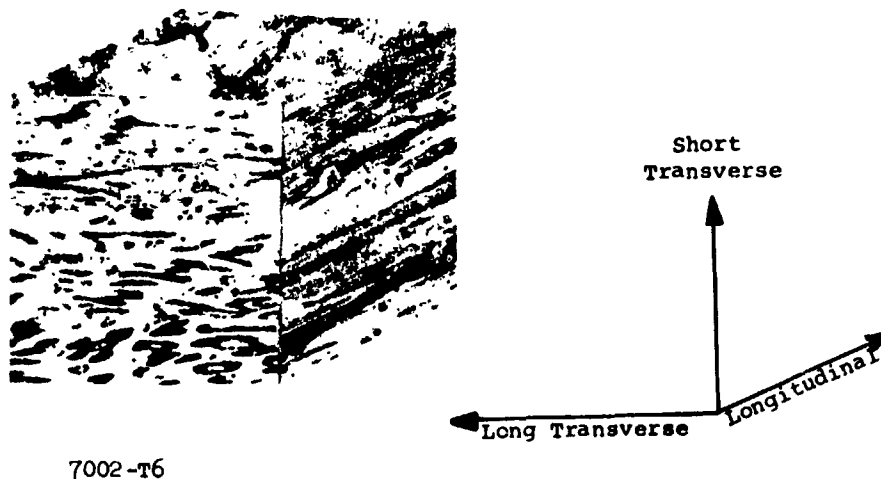


Figure 5
Microstructural Directionality Effects in
High-Strength Aluminum Alloys (Kellers Etch - 100X)

That stress-corrosion crack propagation is directionally sensitive can be seen in figures 6 and 7. Stress-corrosion attack in smooth specimens is shown in figure 6. Deterioration of a short transverse specimen is compared to that of one taken in the longitudinal direction. For the short transverse specimen, where the intergranular grain boundary corrosion path is perpendicular to the specimen tension surface, stress-corrosion attack is able to progress rapidly through the specimen thickness. In the longitudinal specimen, on the other hand, a susceptible, continuous grain-boundary path is oriented parallel to the specimen tension surface. Instead of progressing normal to the tension surface, corrosion attack will now proceed parallel to it along the intergranular corrosion sensitive path.

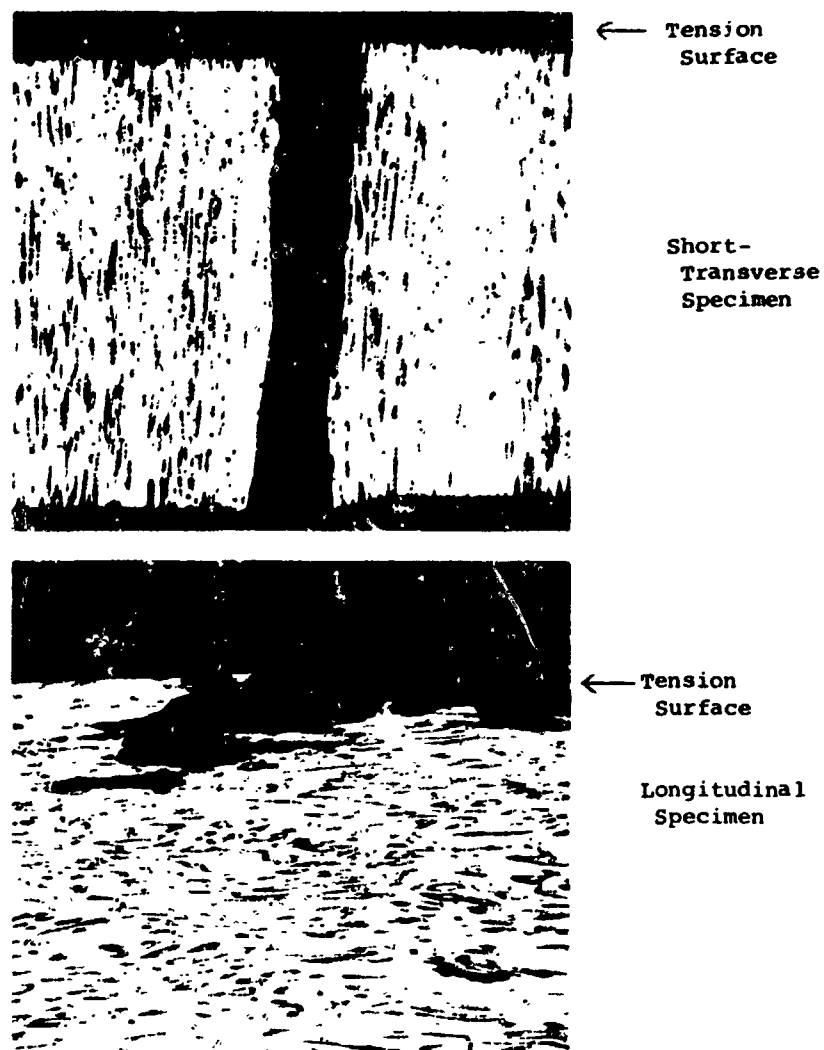


Figure 6
Corrosion Directionality Effects in Alloy 7002-T6
(Kellers Etch - 50X)

Reproduced from
best available copy.



Figure 7
Longitudinal (RT Type) Stress-Corrosion Cantilever Specimen
(Alloy 7039-T64) (6X)

Figure 7 shows stress-corrosion failure in a precracked cantilever specimen of the RT type. Although the specimen was fatigue precracked, corrosion penetration followed the corrosion-sensitive, laminated grain-boundary paths perpendicular to the fatigue crack. This behavior is even more dramatically illustrated in the microsection shown in figure 8. Here, fatigue crack blunting by corrosion along sensitive grain boundaries provides a pseudostrengthening process. The short transverse and longitudinal specimens represent the two extremes in stress-corrosion response. Intermediate are the long transverse specimens. These results suggest that tests in the short transverse direction are essential in ascertaining stress-corrosion behavior of high-strength aluminum in either the smooth or precracked specimen.

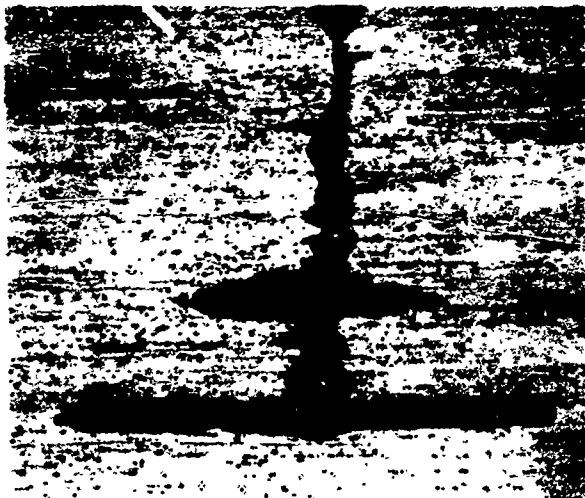


Figure 8
Corrosion Directionality Effects in
Cantilever Specimens of
Aluminum 2014-T651 Alloy
(Kellers Etch - 50X)

Reproduced from
best available copy.

Influence of Test Method

Based on results of directionality studies, short transverse specimens were used in subsequent stress-corrosion exposures of a number of high-strength alloys, listed in table 1, in the form of hand forgings. Bent-beam and cantilever stress-corrosion test results are presented in figures 9 and 10.

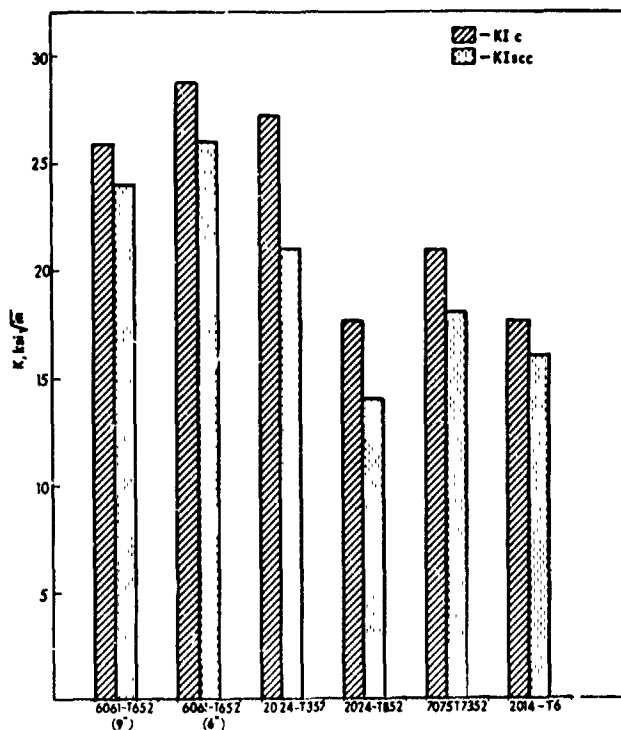


Figure 9 - Properties of Aluminum Alloy Forgings
in Short Transverse Orientation

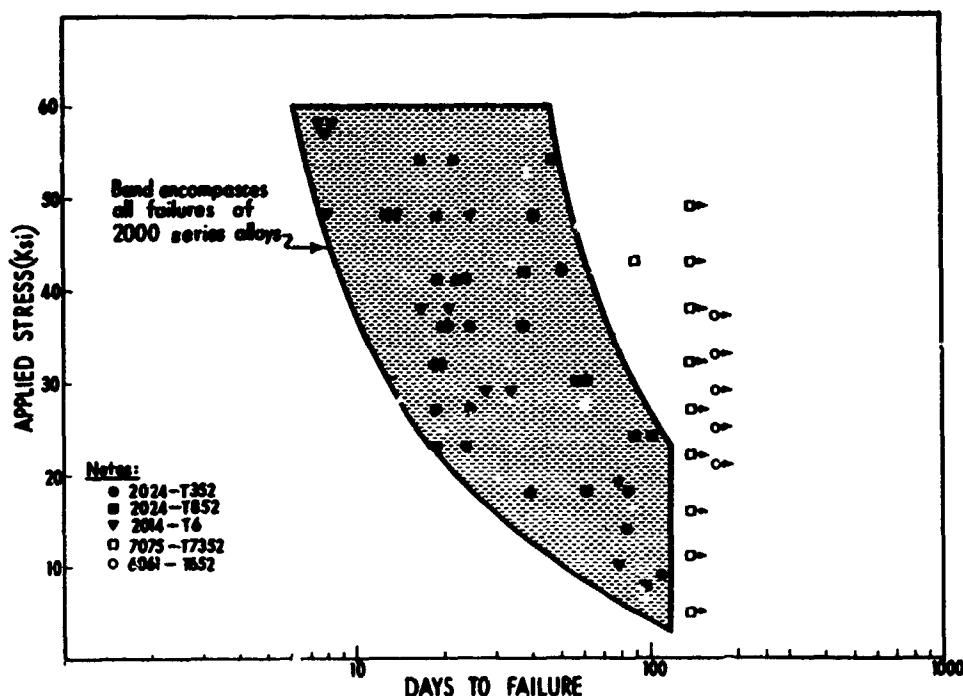


Figure 10
Results of Bent-Beam Stress-Corrosion Tests
Short Transverse Orientation (Forgings)

Comparison of the data in these figures indicates that the two methods yield inconsistent results. As shown in figure 9, all of the alloys tested as precracked cantilever specimens exhibited K_{Isc} values that are close to the K_{Ic} air values. This might be considered to indicate that the alloys are, at most, only mildly susceptible to stress-corrosion cracking. The smooth data illustrated in figure 10, on the other hand, show that all of the 2000-series specimens exposed as bent beams failed after about 100 days, regardless of applied stress. Only one specimen of all the 6000- and 7000-series failed in the same time frame. This 7075-T7352 specimen, loaded to 80% of the 0.2% yield strength, failed due to excessive pitting and not stress-corrosion cracking. The variation in behavior observed in the two test methods can be dramatically illustrated by specifically comparing the data for 6061-T652 and 2024-T352. In the precracked test, the two alloys rank numbers 1 and 2 among the group tested, and the K_{Isc} values are not too different: 26 ksi $\sqrt{\text{in.}}$ for 6061-T652 versus 21 ksi $\sqrt{\text{in.}}$ for 2024-T352. In contrast, when the smooth specimen data are examined critically, it can be seen that the 2024-T352 is highly susceptible to stress-corrosion cracking and 6061-T652 is very resistant. There is a wide variation in pitting characteristics among aluminum alloys as evidenced by figures 11 and 12.

6061-T652
(167-Day Exposure)



Reproduced from
best available copy.

7075-T7352
(142-Day Exposure)



Figure 11 - Pitting Attack on
General Corrosion Specimens (Approximately 3X)

2024-T352
(167-Day Exposure)

2024-T852
(142-Day Exposure)



(80-Day Exposure)

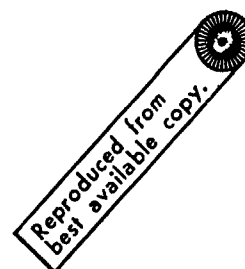
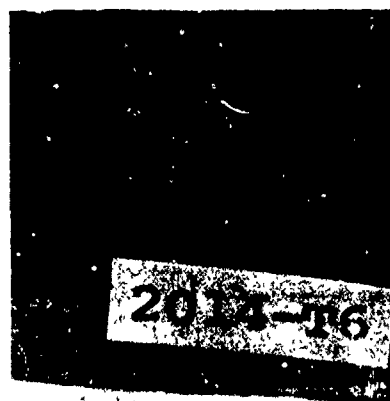


Figure 12
Pitting Attack on General Corrosion Specimens
(Approximately 3X)

In the 2024-T352 and other 2000-series alloys, pitting attack occurs rapidly with deep penetration. In these alloys the initiation phase of stress-corrosion cracking becomes a significant part of the overall process. The 6061-T652 alloy exhibits greater resistance to pitting. The absence of the pit producing stress raiser might contribute to the superior behavior of this alloy in bent-beam exposures.

Another inconsistency, apparent by looking at figures 9 and 10, relates to the behavior of 2024-T352 and 2024-T852. The 2024-T352 temper is superior in the precracked cantilever test but inferior when tested as long time exposures of bent beams. Lowering of the $K_{I_{SCC}}$ value appears to correspond to lower ductility and fracture toughness (K_{IC} value) of the 2024-T852 condition.

The implication of these results is that we should not rely entirely on the precracked cantilever test for evaluating the sea-water stress-corrosion characteristics of high-strength aluminum alloys. Both techniques provide useful information. The precracked cantilever test offers the opportunity to focus attention on the propagation stage of stress-corrosion cracking. Information of this type is obviously valuable for the analysis of cases where stress-corrosion cracking may propagate from a preexisting stress concentration such as a weld defect or a mechanical notch. When stress raisers are formed by environmental pitting, precracked cantilever tests are again useful because they provide the opportunity to separate the initiation and propagation phases for analysis purposes. Bent-beam exposures shed light on pitting characteristics as a part of stress-corrosion behavior. This is a particularly important consideration in the case of aluminum alloys because of their wide variation in pitting behavior.

The results presented suggest that both the precracked cantilever test and the classical, long-term, bent-beam exposure provide important data. These testing techniques should therefore be used together as complementary methods when selecting high-strength aluminum alloys for sea-water applications.

REFERENCES

- 1 - Brown, B. F., "A New Stress-Corrosion Cracking Test for High Strength Alloys," Materials Research and Standards, March 1966, p. 126.
- 2 - Brown, B. F., Fujii, C. T., and Dahlberg, E. P., "Methods for Studying the Solution Chemistry Within Stress Corrosion Cracks," Journal Electrochemical Society, February 1969, p. 218.
- 3 - Chu, H. P., and Wacker, G. A., "Stress Corrosion Testing of 7079-T6 Aluminum Alloys in Sea-water using Smooth and Precracked Specimens," Journal of Basic Engineering, December 1969, p. 565.
- 4 - Wacker, George A., and Chu, Huai-Pu, "Stress-Corrosion Characteristics of High Strength Aluminum Alloys in the Marine Environment," Paper No. 28, Corrosion/71 (to be published by NACE).
- 5 - Chu, H. P., and Wacker, G. A., "Fracture Toughness and Stress Corrosion Properties of Aluminum Alloy Hand Forgings," Presented at ASTM E-24 Meeting on Fracture Testing of Metals, Atlanta, Ga., March 1971 (to be published by ASTM).

DISCUSSION OF PAPER, "INFLUENCE OF TEST METHOD
ON STRESS-CORROSION BEHAVIOR OF
ALUMINUM ALLOYS IN SEAWATER" BY GEORGE J. DANEK

Donald O. Sprowls
Section Head
Chemical Metallurgy Division
Alcoa Research Laboratories
P. O. Box 2970
Pittsburgh, Pennsylvania 15230

J. G. Kaufman
Chief
Mechanical Testing Division
Alcoa Research Laboratories
P. O. Box 2970
Pittsburgh, Pennsylvania 15230

SUMMARY

Stress corrosion evaluations of thick sections of aluminum alloy products are markedly influenced by the sampling procedure, especially the orientation of the test specimen to the grain structure. The work reported by Mr. Danek shows that the method of testing with precracked specimens may be affected just as much, or more, than traditional smooth specimen methods. On the basis of estimated threshold stress intensities (K_{Isc}) obtained with precracked cantilever beam specimens, Mr. Danek reported rankings of alloys that are unrealistic compared to service experience and to estimated threshold stresses obtained from tests of smooth beam specimens. On the other hand, tests of the same alloys at Alcoa Research Laboratories with bolt-loaded precracked double cantilever beam specimens ranked the alloys in good agreement with rankings obtained with tests of smooth tensile specimens.

DISCUSSION OF PAPER, "INFLUENCE OF TEST METHOD
ON STRESS-CORROSION BEHAVIOR OF
ALUMINUM ALLOYS IN SEAWATER" BY GEORGE J. DANEK

Donald O. Sprowls
J. G. Kaufman

These investigations conducted at the Naval Ship Research & Development Laboratory provide a timely comparison of two quite different methods of performing stress-corrosion cracking (SCC) tests on a group of aluminum alloys that have established a wide range of stress corrosion resistance in service. Mr. Danek has presented information in an area of stress corrosion testing that is very complex because of the anisotropy of the materials studied. These remarks, based on our experience, will help place these findings in perspective.

Rankings of the alloys obtained with the two SCC test methods are in poor agreement, as shown by the recap of the author's data in Table D1. With the results of the smooth specimen tests, the alloys can be classed in three distinct groups that are consistent with service experience (1,2,3,4): (a) 6061-T652 and 7075-T7352 with no SCC failures, (b) 2024-T852 failing at high and medium stresses, and (c) 2024-T352 and 2014-T6 with failures at high, medium and low stresses. However, with the results of the precracked specimen tests there was no distinct ranking of the alloys. Moreover, the apparent " K_{Isc} " value for alloy 2024-T352 appeared similar to those for 6061-T652, yet the virtual immunity to SCC of 6061-T652 under service conditions is well established, as is also the relatively poor service record of various products of 2024-T3 when stressed in the short-transverse direction. It is equally unrealistic that 2024-T352 and 2014-T6 should rank the same as 7075-T7352. Actually all of the " K_{Isc} " values reported are in the range of 80 to 93% of K_{Ic} ; thus, these values appear to represent a measure of fracture toughness more than of resistance to SCC.

Unfortunately a valid comparison of the two test methods used in this investigation may have been obstructed by the anisotropy that is characteristic of forgings. For example, the surprisingly good ranking of alloys 2014-T6 and 2024-T352 in the tests of precracked specimens could be explained by a curve in the grain structure near the tip of the precrack, with the effect that the specimen was not truly short-transverse. Failure to orient test specimens so that the applied load is acting in a true short-transverse direction relative to the grain flow can markedly influence stress corrosion test results, as was shown previously for a 7075-T6 hand forging(2). The grain flow in hand forgings cannot be predicted from the geometric shape of the forging. It is necessary to survey the metal flow pattern by macroetching machined slices to determine whether each of the short-transverse specimens is similarly oriented to the grain structure. The variability of grain structure is less likely to have affected the performance of the smooth beam specimens because of their relatively large stressed area compared to the small area stressed at the tip of the crack in the precracked specimens.

In tests recently completed at the Alcoa Research Laboratories on these same alloys in the form of rolled plate with a uniform directional grain structure, a much better agreement was obtained between the two stress corrosion test methods(5). Environmental crack growth curves obtained with bolt-loaded TL double-cantilever beams by the test procedure by Hyatt(6) are shown in Figure 1. Estimates of a stress intensity factor, calculated from the length of the crack at "arrest", and maximum sustained SCC growth rates derived from these curves are compared in Table D2 with estimated threshold stresses determined with short-transverse smooth 0.125 in. diameter x 2 in. long tension specimens. On the basis of the residual stress intensity factors (which may be considered as an estimate of K_{Isc}), the performances of the very resistant 6061-T651 and 7075-T7352 alloys are clearly distinguished from performances of the low resistance 2014-T651 and 7079-T651 alloys; however, the performances of the 2024-T351 and T851 items could not be readily distinguished from each other or from that of the 7075-T7351 plate. Part of this problem stems from the difficulty in establishing the arrest, as may be noted especially in the curve for 2024-T351. Comparison of the maximum stress corrosion crack propagation rates helps to bring the precracked specimen data in line with the smooth specimen data for the 2024-T351 and T851 items.

In alloy development work, two criteria can be used with the precracked specimen test method; one is an increase in the threshold stress intensity for SCC (K_{Isc}); the other is a decrease in the stress corrosion crack propagation rate. It is evident from Figure 1 that the SCC growth rate of 2024-T351 has been greatly reduced by artificial aging plate to the T851 temper even though the improvement in the estimated threshold stress intensities was small. We believe that in stress corrosion testing aluminum alloys with precracked specimens, consideration must be given both to the threshold stress intensity and SCC propagation rate. When this is done, the ranking of alloys tested in this manner probably will be similar to the ranking of alloys tested with smooth specimens.

With both methods of testing it is of fundamental importance to: (1) determine possible variations in grain structure of the products being tested and position test specimens accordingly, and (2) make suitable allowance for artifact mechanical effects (such as creep) which are not, in fact, a part of the SCC process. For example, there was considerable variation in the K_{Ic} values for individual specimens of 6061-T652 tested by Chu and Wacker, more than enough to account for the 7 to 9% reduction identified

with their " K_{Isc} " values. Thus, there is reason to believe that the criterion of failure of the 6061-T652 and possibly the 7075-T7352 specimens may not have been related to environmental crack growth, but rather to the problem of interpreting residual stress intensity levels close to K_{Ic} .

REFERENCES

- (1) Hooker, R. N. and Waisman, J. L., "Control of Stress-Corrosion Cracking In Airframe Components", Corrosion, Vol. 10, No. 1C (1954), pp. 325-334.
- (2) Sprowls, D. O. and Brown, R. H., "What Every Engineer Should Know About Stress Corrosion of Aluminum", Metal Progress, Vol. 81, No. 4, pp. 79-85 (1962) and Vol. 81, No. 5, pp. 77-83 (1962).
- (3) Jackson, J. D. and Boyd, W. K., "Preventing Stress Corrosion Cracking of High Strength Aluminum Alloy Parts", Materials in Design Engineering, (May, 1966), p. 70.
- (4) Brownhill, D. J., Babilon, C. F., Nordmark, G. E., and Sprowls, D. O., Technical Report AFML-TR-70-10, issued by Alcoa Research Laboratories, February, 1970, Re: Mechanical Properties, Including Fracture Toughness and Fatigue, Corrosion Characteristics and Fatigue-Crack Propagation Rates of Stress-Relieved Aluminum Alloy Hand Forgings.
- (5) Sprowls, D. O., Shumaker, M. B., and Lifka, B. W., Contract NAS 8-21487, Evaluation of Stress-Corrosion Cracking Susceptibility Using Fracture Mechanics Techniques, Eleventh Quarterly Report (Jan. 1 - March 31, 1971) issued by Alcoa Research Laboratories.
- (6) Hyatt, M. V., "Use of Precracked Specimens in Stress Corrosion Testing of High Strength Aluminum Alloys", Corrosion, Vol. 26, No. 11 (Nov., 1970), pp. 487-503.

Table D1
RELATIVE PERFORMANCE OF SMOOTH BEAM SPECIMENS AND FATIGUE PRECRACKED
CANTILEVER BEAM SPECIMENS FROM THICK HAND FORGINGS - "SHORT" TRANSVERSE STRESS

Alloy	Smooth Specimens			Precracked Specimens		
	Yield Strength, ksi	Estimated Threshold Stress for SCC ksi	% Y.S.	K _{IC} ksi $\sqrt{\text{in.}}$	"K _{ISCC} " ksi $\sqrt{\text{in.}}$	% K _{IC}
6061-T652	38.1	OK38*	OK100*	26 (23-28)	24	93
6061-T652	35.3	OK35*	OK100*	29 (27-32)	26	91
7075-T7352	56.3	OK51*	OK90*	21 (20-22)	18	86
2024-T852	53.9	20	37	17.6 (17.5-17.7)	14	80
2024-T352	43.3	<9.5	<22	27 (26.5-27.4)	23	85
2014-T6	61.0	<9.5	<15	17.5 (16-19)	16	90

* No stress-corrosion cracking (SCC) at highest stress tested.

Table D2

RELATIVE PERFORMANCE OF SMOOTH TENSION SPECIMENS AND TENSION PRECRACKED
DCB SPECIMENS FROM 2.5 IN. THICK PLATE SHORT TRANSVERSE STRESS

Alloy	Smooth Specimens			Precracked Specimens			
	Yield Strength, ksi	Estimated Threshold Stress for SCC, ksi	$\frac{\text{ksi}}{\% \text{ Y.S.}}$	K_{Ic} ksi $\sqrt{\text{in.}}$	K_{Ic} ksi $\sqrt{\text{in.}}$	$\frac{K_{Ic}}{\% K_{Ic}}$	Max. Crack Growth Rate, in./Hr.
6061-T651	42	OK32*	OK75*	21	32(1)	150	3×10^{-5} (2)
7075-T7351	55	OK41*	OK75*	21	18(1)	86	3×10^{-5} (2)
2024-T851	62	46>Th.>27	75>Th.>50	17	14(1)	82	2×10^{-4}
2024-T351	42	<10	<24	21	16,14,12(1)	76,67, 57	1×10^{-3}
2014-T651	60	<10	<17	19	10	53	1×10^{-3}
7079-T651	67	<10	<15	19	6	32	2×10^{-2}

Notes: * No SCC at highest stress tested.

- (1) Values based on crack length measured on fracture surface of exposed specimens; other values based on crack lengths measured on the specimen surface. The surprisingly high value for 6061-T651 is indicative of excessive plastic deformation.
- (2) Metallographic examination did not reveal presence of traditional intergranular SCC.

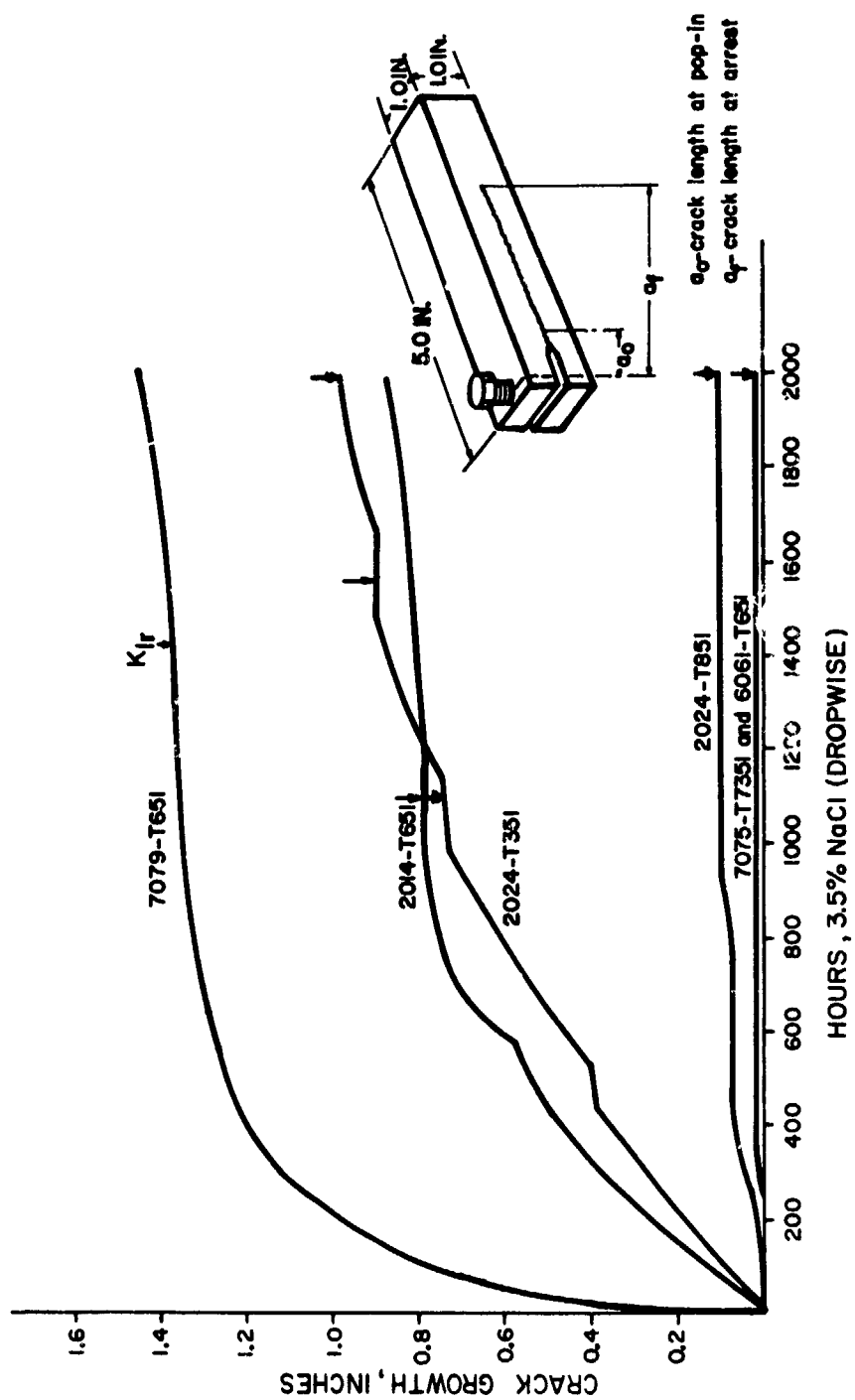


Figure 1

**PARTICIPATION A L'ETUDE DE LA CORROSION SOUS TENSION
DE CERTAINS ALLIAGES D'ALUMINIUM A HAUTE RESISTANCE**

par

Robert Doste
Ingénieur au Laboratoire Central
AEROSPATIALE
Boîte Postale 376
92-Suresnes
France

PARTICIPATION A L'ETUDE DE LA CORROSION SOUS TENSION DE CERTAINS ALLIAGES D' ALUMINIUM A HAUTE RESISTANCE

par

Robert DOSTE

RESUME

Les travaux mentionnés dans cette publication portent sur la corrosion sous tension de 2 des principaux alliages d'aluminium utilisés dans l'industrie aéronautique française : A-U2GN et A-U4SG. De nombreux essais systématiques ont été effectués par essais classiques, en flexion sous charge imposée constante.

Les processus intervenant dans la corrosion et la corrosion sous tension faisant le plus souvent appel à des réactions électrochimiques, nous décrivons quelques techniques d'étude par méthodes électrochimiques et tentons d'établir une corrélation entre les phénomènes observés et les microstructures particulières des alliages.

Dans le cas de l'A-U2GN, on peut avancer une explication concernant la sensibilité à la corrosion intercrystalline et le rôle de la contrainte dans le cas de cet alliage aux états sous-revenu, ainsi que la désensibilisation intervenant après un traitement thermique correct.

Dans le cas de l'A-U4SG, les traitements thermiques de revenu diminuent nettement la susceptibilité du matériau à la corrosion intercrystalline alors que la sensibilité à la corrosion sous tension demeure importante; l'influence de l'aération de la solution semble prépondérante.

1 - INTRODUCTION

La corrosion et la corrosion sous tension des métaux et alliages sont des phénomènes dont l'importance s'est considérablement accrue depuis une vingtaine d'années dans l'industrie aéronautique en raison de la longévité toujours plus grande qu'on exige des appareils et des performances qui ne cessent de croître. De tels progrès dans les performances supposent de la part du constructeur un souci constant d'allègement des structures, impliquant l'utilisation de matériaux à caractéristiques élevées auxquels on impose un taux de travail important.

La corrosion sous tension est ainsi devenue l'une des principales préoccupations des bureaux d'études et des métallurgistes et un nombre croissant d'études, tant dans les laboratoires industriels que de recherche, a accompagné le développement technologique d'alliages à hautes caractéristiques.

Nos travaux dans le domaine de la corrosion sous tension ont surtout porté sur les principaux alliages d'aluminium utilisés dans l'industrie aéronautique française, et plus particulièrement sur l'A-U2GN et l'A-U4SG.

Après avoir relaté les résultats d'études systématiques de ces deux alliages, portant sur les méthodes d'essais et sur les traitements thermiques, nous décrirons quelques travaux particuliers ayant pour but une meilleure compréhension des principaux phénomènes intervenant.

2 - CORROSION SOUS TENSION DE L'A-U2GN

L'A-U2GN est un alliage à durcissement structural de composition :

Cu	Mg	Ni	Fe	Si	Ti
2,0 - 2,6	1,2 - 1,8	0,9 - 1,4	0,9 - 1,4	0,1 - 0,25	0,05 - 0,15

De nombreuses pièces de structure de l'avion "CONCORDE" étant sollicitées par des contraintes permanentes de traction de 10 à 20 hb, il importait de connaître les risques encourus en corrosion sous tension et de déterminer les conditions de traitement optimales (variables selon le type de produit et la gamme de transformation.)

La comparaison de la tenue en C.S.T. des divers produits en A-U2GN a été essentiellement effectuée sur éprouvettes cylindriques prélevées en sens travers court des produits, et dont la gamme de préparation comprend un tournage fin, un dégraissage à l'acétone et un décapage (solution nitrique-fluorhydrique à ébullition) avant mise en essais. Les essais sont réalisés en immersions-émersions alternées (10mn-50mn) ou en immersion continue en utilisant une eau de mer artificielle (solution A₂ du règlement AIR 0754). Nous opérons en flexion sous charge constante de façon à obtenir une contrainte de 80% de la limite élastique à 0,2% (R_{0,2}).

Dans le cas de tôles épaisses traitées industriellement et livrées à l'état normalisé T 651 (trempe, traction contrôlée 2%, revenu 194/190°C), une étude statistique portant sur 60 tôles provenant de coulées et dates de traitements thermiques différentes a fait apparaître un certain nombre de produits défectueux

(Fig.4). Les examens effectués ont montré que ces tôles étaient dans un état sous-revenu et n'avaient pas subi le traitement de revenu correct. En fonction de ces résultats une valeur de conductivité $\geq 20,5$ m. ohm-cm-2 a été retenue comme critère de contrôle rapide du traitement des tôles produites.

Des essais précédemment effectués en immersion continue avaient conduit à des ruptures plus ou moins rapides, même pour des tôles de conductivité supérieure à la valeur limite choisie, mais l'examen d'échantillons rompus, la comparaison avec des essais identiques effectués en corrosion simple, ont montré que la contrainte ne jouait aucun rôle dans le phénomène si ce n'est pour la rupture finale. (Fig.5).

Les essais en immersion continue sont donc moins sélectifs que ceux effectués en immersions-émersions alternées.

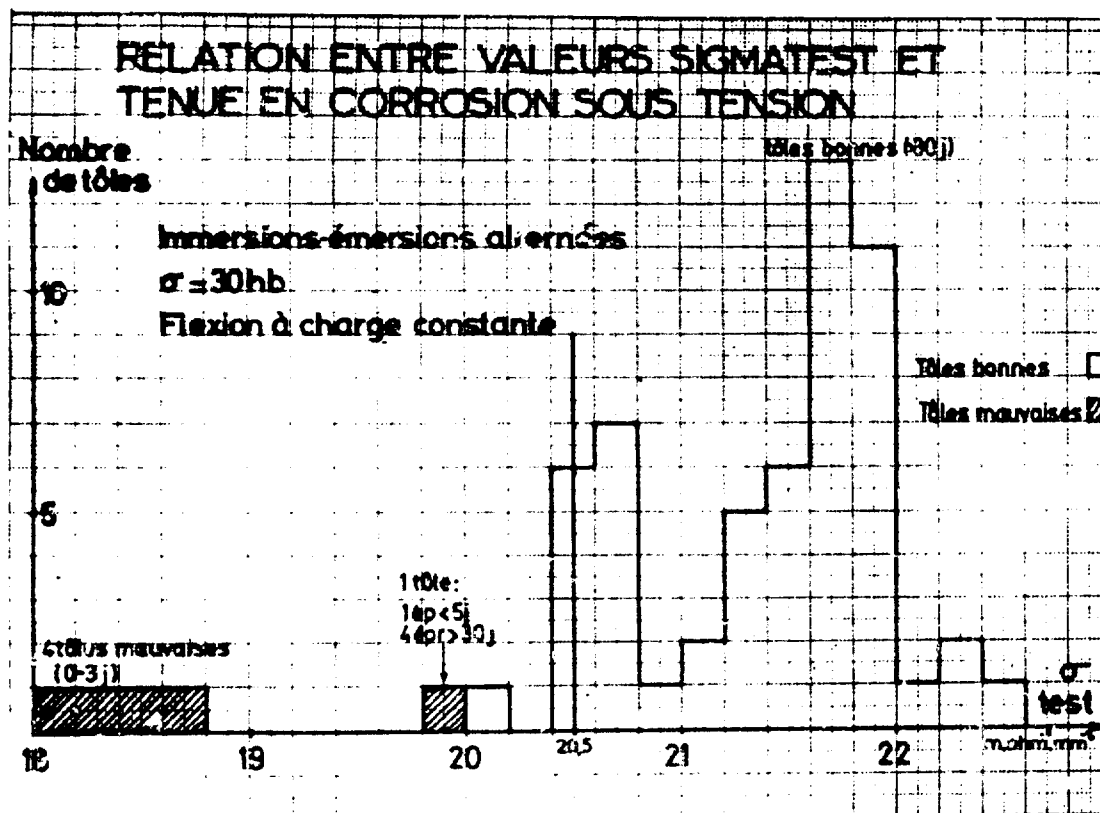


Fig.4 - C S T TOLES EPAISSES A-U2GN ETUDE STATISTIQUE EN I.E.A.

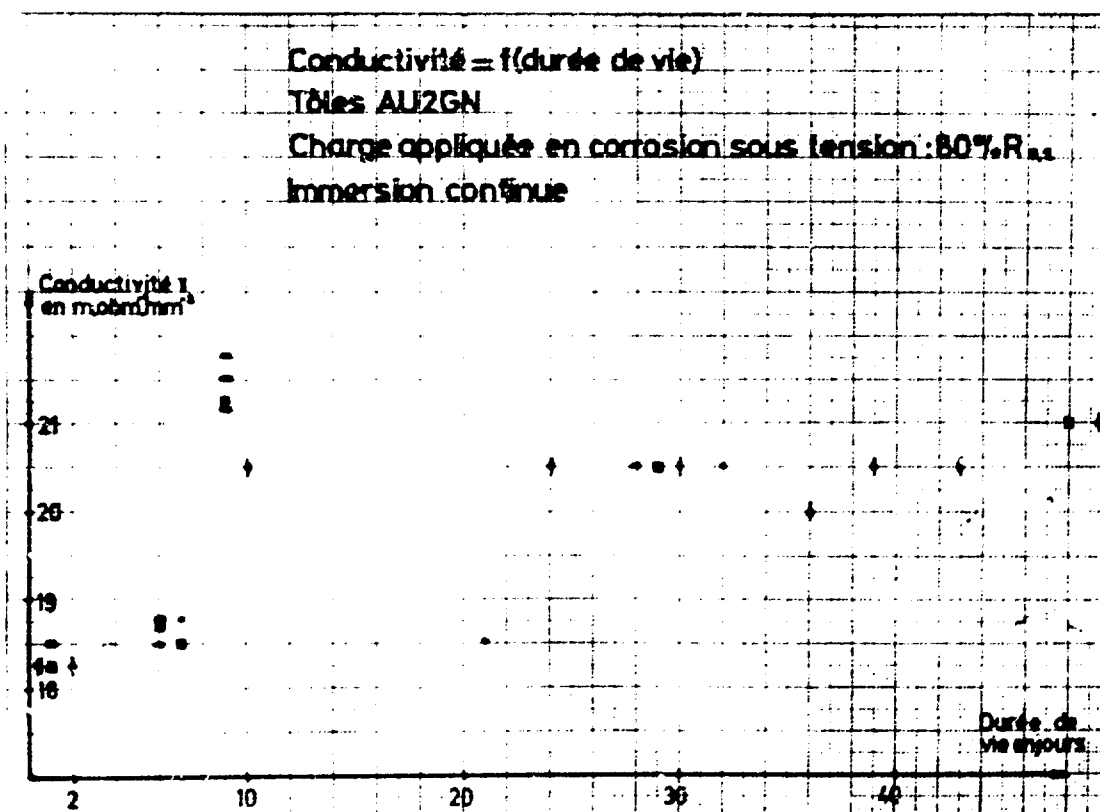


Fig.5 - C S T TOLES EPAISSES A-U2GN IMMERSION CONTINUE

Dans tous les cas on doit simultanément considérer les phénomènes avec et sans contrainte afin de déterminer la part de chaque paramètre dans le phénomène global. Pour cela on utilise une série de relations découlant de la formule de JOHNS :

$$I_r = \frac{\Delta R_T - \Delta R_N}{\Delta R_T} \times 100$$

$\Delta R_T = R_0 - R_T$ = diminution de la charge de rupture après C.S.T.

$\Delta R_N = R_0 - R_N$ = diminution de la charge de rupture après corrosion

qui permet de chiffrer la part de la contrainte dans l'essai de corrosion sous tension, ou indice de susceptibilité à la corrosion sous tension.

Un exemple de valeurs obtenues est fourni par la Fig. 6. La contrainte ne joue un rôle significatif que pour la tôle 8774 (état sous-revenu) ayant subi des ruptures rapides en C.S.T.

Enfin, pour les produits révélés sensibles à la corrosion sous tension, un critère important est la limite de non rupture, c'est à dire la contrainte en dessous de laquelle la corrosion sous tension ne se manifeste plus.

La Fig. 7 fournit les résultats obtenus avec une tôle à l'état sous-revenu, lors de sollicitations en flexion ou traction. On remarque que ce dernier essai semble beaucoup plus sévère que celui en flexion où le seuil de non rupture est de 20% de la limite élastique à 0,2% alors qu'il est inférieur à 10% pour l'essai en traction.

Fig. 6
DÉPOUILLEMENT D'ESSAIS DE CORROSION ET DE
CORROSION SOUS TENSION

Rep	R ₀ hb	R _T hb	R _N hb	R _T	R _N	I _T	I _N	V _{AT}
8774	41,8	25,4	37,5	39%	10%	74%	26%	1,85% h ⁻¹
1300	43,6	36,4	38,4	16,5%	11,9%	28%	72%	0,022% h ⁻¹
13001	44,6	34,7	34,6	22,4%	22,4%	0%	100%	0,035% h ⁻¹
13034	43,5	41	41,6	5,8%	4,4%	24%	76%	0,008% h ⁻¹
14231	43	29,7	33	31%	23%	25%	75%	0,043% h ⁻¹
17833	39,7	30,1	29,9	24,4%	24,8%	0%	100%	0,034% h ⁻¹
19200	42,2	34,7	34,3	17%	19,5%			0,023% h ⁻¹

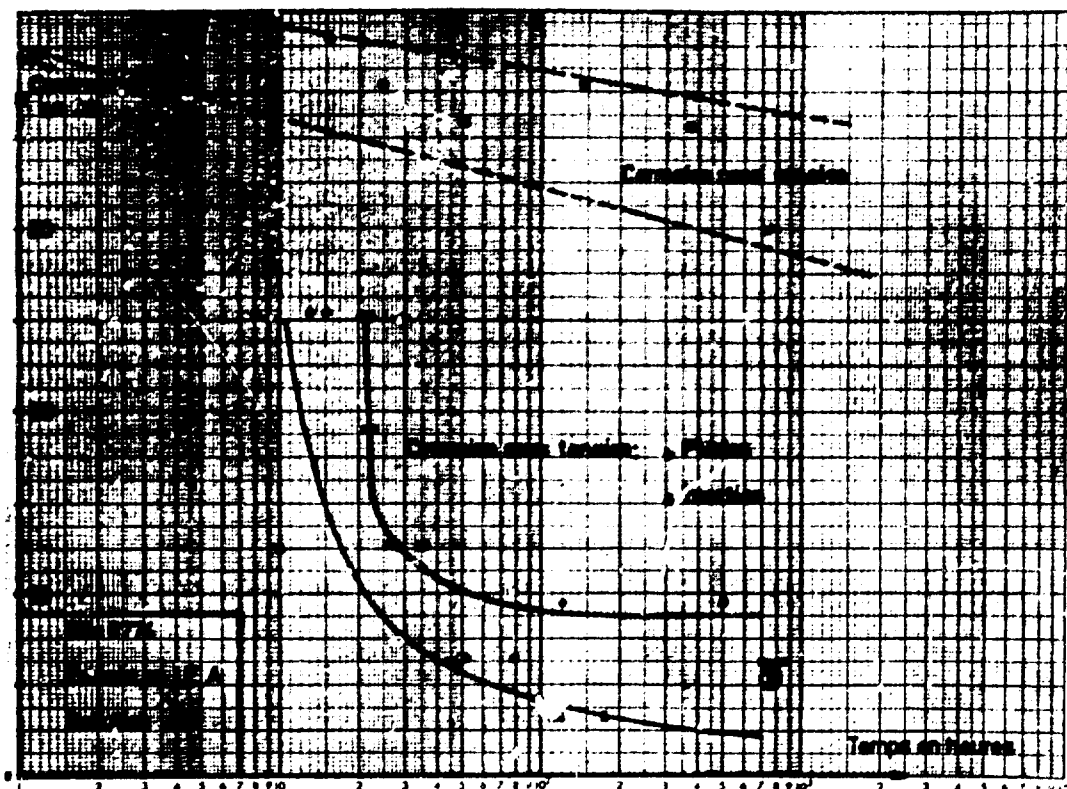


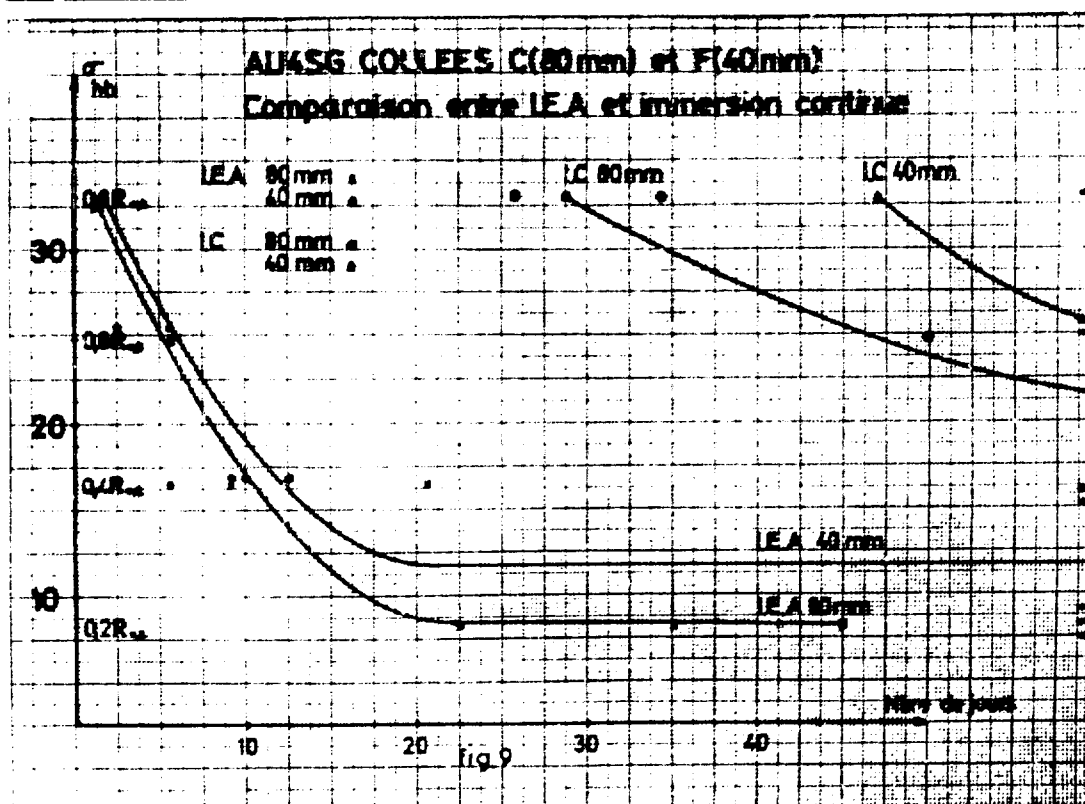
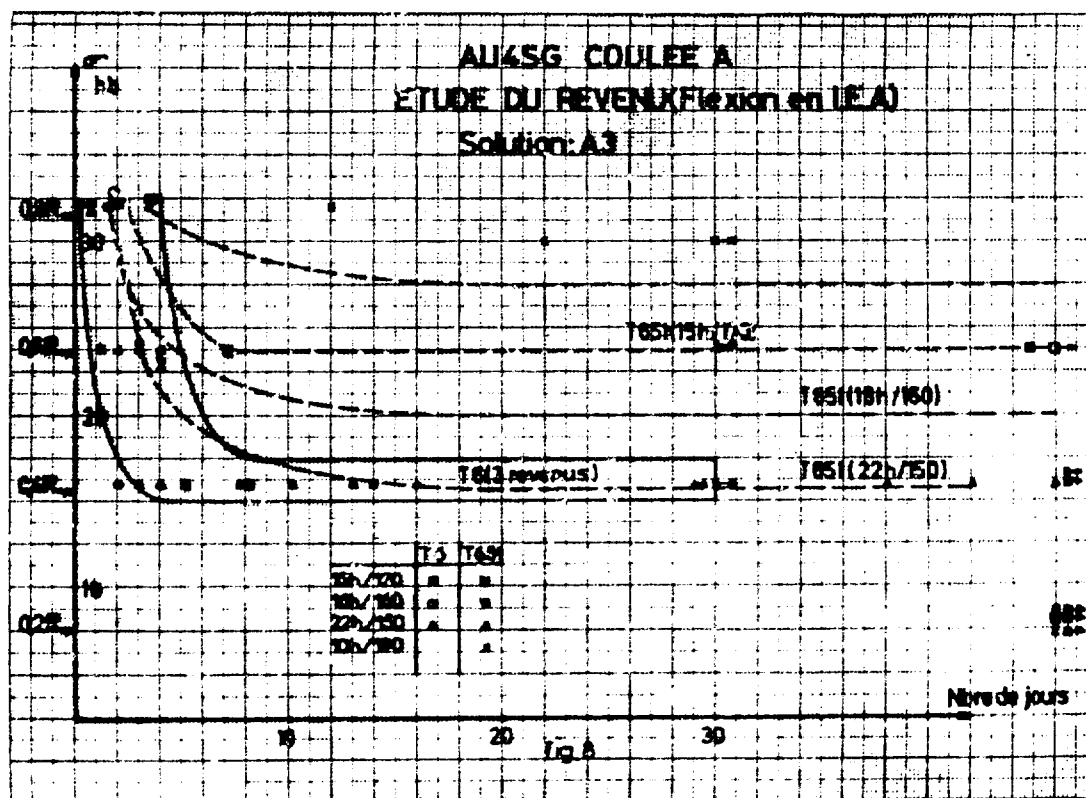
Fig. 7 - COURBES-CONTRAINTES-DURÉES DE VIE
COMPARAISON DES ESSAIS EN FLEXION ET TRACTION

3 - CORROSION SOUS TENSION DE L'A-U4SG : Cet alliage de composition :

Cu	Mg	Mn	Si	Fe	Zn	Ti	Ni
3,9-5,0	0,2 - 0,8	0,4 - 1,2	0,5-1,2	0,5	0,25	0,2	0,1

est largement utilisé dans l'industrie aéronautique française et britannique en raison de ses très bonnes caractéristiques statiques, mais le problème de l'élimination de sa susceptibilité à la C.S.T. en sens travers court n'a pas encore été résolu.

Nous avons essentiellement étudié le cas des tôles épaisses aux états T 6 et T 651 obtenus par des revenus de 22h/ 150°C, 16h/160°C ou 15h/ 170°C.



La figure 8 montre que l'A-U4SG reste sensible à la corrosion sous tension quel que soit le traitement effectué. Cependant, l'introduction d'une opération de traction contrôlée entre trempe et revenu semble apporter une certaine amélioration à la tenue en corrosion sous tension qui augmente avec la température de revenu; pour les états trempé-revenu T 6 on ne constate aucune différence entre les trois traitements étudiés. La fig.9 met en évidence une importante variation de comportement de l'alliage selon le type d'essai; de manière encore plus marquée que pour l'A-U2GN, l'essai en immersion continue se révèle peu sélectif pour l'étude de la corrosion sous tension de l'A-U4SG et laisse à penser que celle-ci est très influencée par l'aération de la solution.

Afin de confirmer cette observation nous avons procédé à des essais de corrosion sous tension en immersion continue, en solutions saturées en Azote ou Oxygène. Les essais ont été interrompus à la rupture de l'éprouvette en corrosion sous tension en présence d'oxygène et les éprouvettes restantes ont alors été tractionnées afin de déterminer les caractéristiques résiduelles et de calculer l'indice de susceptibilité dans chaque cas. La Fig. 10 fournit les résultats obtenus et met en évidence le rôle prépondérant de l'aération de la solution d'essai.

ESSAI	SOLUTION	RESULTATS	CONTRAINTE D'ESSAI	CHARGE DE RUPTURE APRES ESSAI	CHARGE DE RUPTURE INITIALE Ro
C.S.T.	NaCl 3% + O ₂	Rupture en 96 h.	35,2 hb	35,2 hb(R _t)	40,7 hb
C.S.T.	NaCl 3% + Argon	Non Rupture en 96 h.	35,2 hb	48,1 hb(R _t)	
Corrosion	NaCl 3% + O ₂	Exposition 96 h.	0	14,2 hb(R _n)	
Corrosion	NaCl 3% + Argon	Exposition 96 h.	0	48,3 hb(R _n)	

DETERMINATION DE L'INDICE DE SUSCEPTIBILITE
A LA CORROSION SOUS TENSION

$$I_T = \frac{P_n - R_t}{R_o - R_t} \times 100$$

SOLUTION	OXYGENEE	DESAREEE	I E A EN SOLUTION A3	I U EN SOLUTION A3
I _T	67%	14%	80 à 95%	≤ 40%

FIGURE 10

CORROSION ET CORROSION SOUS TENSION DE

L'A-U4SG

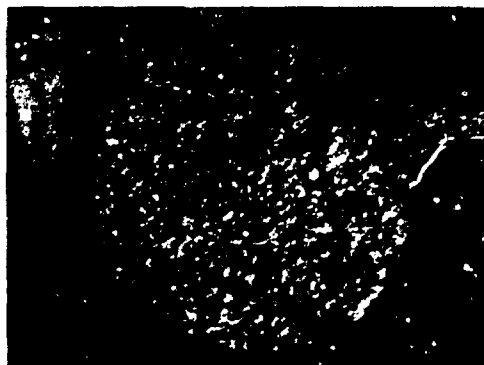
Influence de l'aération

4. TENTATIVE D'INTERPRETATION DES PHENOMENES

Les processus intervenant dans la corrosion et la corrosion sous tension en milieux aqueux faisant, le plus souvent, appel à des réactions électrochimiques, nous avons complété nos essais de corrosion par tracé des courbes de polarisation des matériaux, test de corrosion intercrystalline et examens micrographiques, afin d'établir une corrélation entre les phénomènes observés et les microstructures particulières.

4.1 - Cas de l'A-U2GN. - Les examens effectués après essais de corrosion et corrosion sous tension révèlent des différences significatives selon les états du matériau:

- aspect des ruptures (C1113.118-13.119) - seuls les échantillons sensibles à la CST présentent une rupture à lumbelle, cône fibres tendues. Pour les états non susceptibles, on observe une couronne sombre de corrosion, montrant que le phénomène ne dépend pas de la sollicitation mécanique.



Cliché n° 13.118 G.15
Tôle 8773 - Rupture en 24 h en essai
de corrosion sous tension



Cliché n° 13.119 G. 15
Tôle 7939 - Non rompue en C.S.T.
en 30 jours.

Reproduced from
best available copy.

- coupes micrographiques : Les éprouvettes rompues rapidement en essais de CST en IEA et IC ($\theta \leq 7^\circ$) présentent une rupture à départ intergranulaire ainsi que quelques criques secondaires intercrystallines sur le fût, fibres tendues uniquement (Fig. 14).

Pour les autres produits (non rupture en 30 j. en IEA), la corrosion présente un aspect nettement transcristallin et semble suivre les amas de précipités alignés par le laminage (Fig. 15). Ceux-ci, identifiés au Centre de Recherche du groupe PECHINEY à Voreppe, sont essentiellement du type $Al_9 Fe Ni$ ainsi que $Al_6 Cu_3 Ni$.

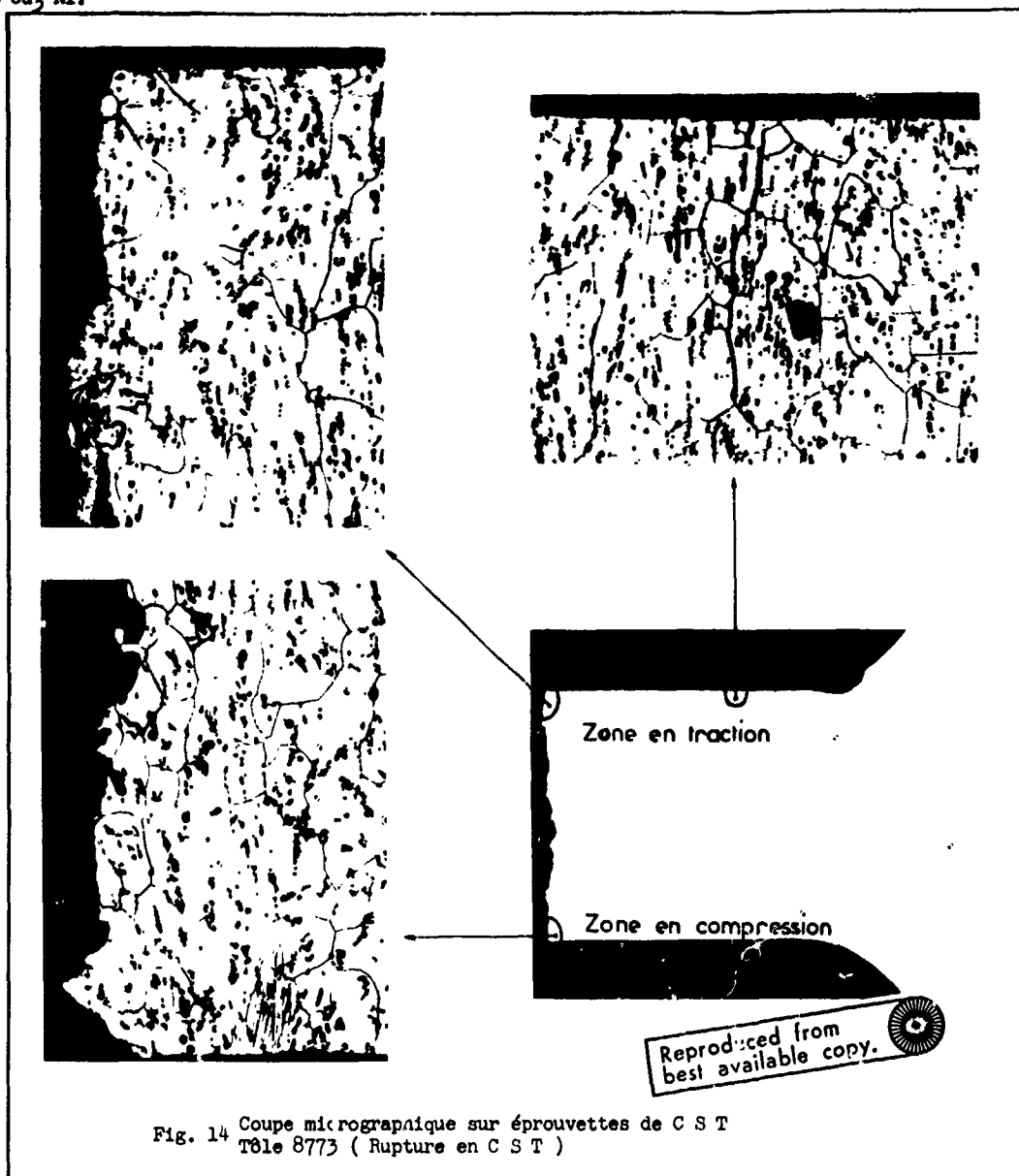


Fig. 14 Coupe micrographique sur éprouvettes de C S T
Tôle 8773 (Rupture en C S T)

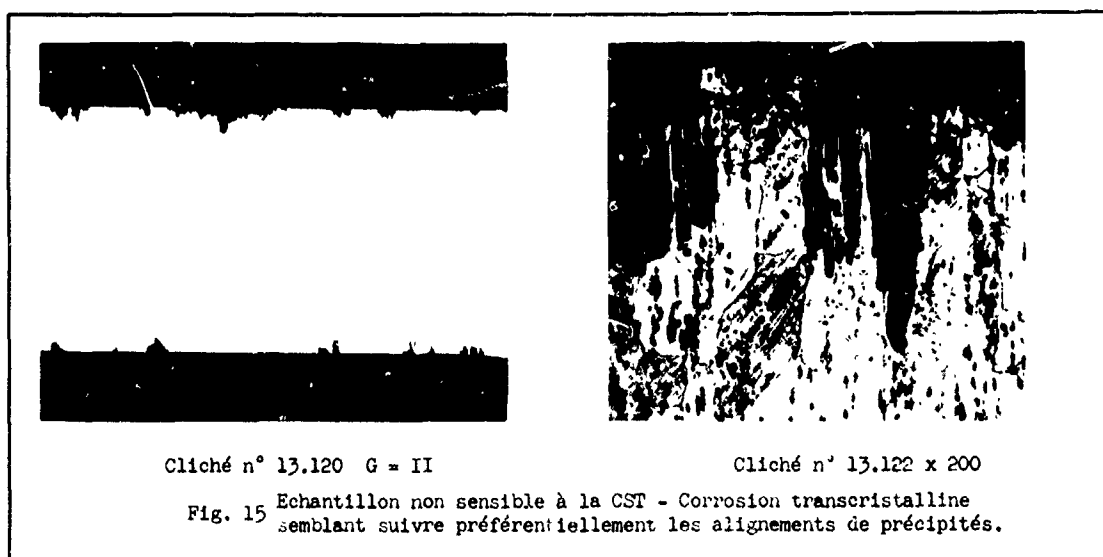
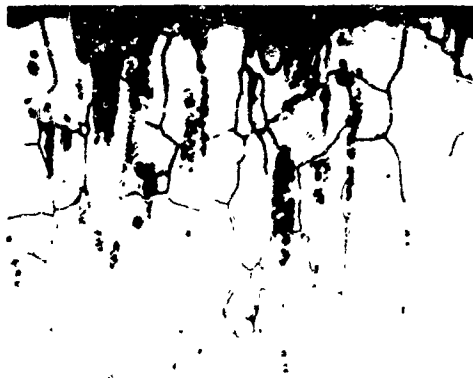
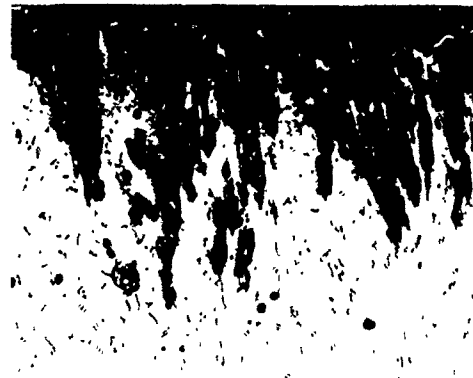


Fig. 15 Echantillon non sensible à la CST - Corrosion transcristalline
semblant suivre préférentiellement les alignements de précipités.



Cliché n° 11.695 G = 200
Tôle 8773 A - sous revenu



Cliché n° 11.708 G = 200
Tôle 6412 - revenu correct

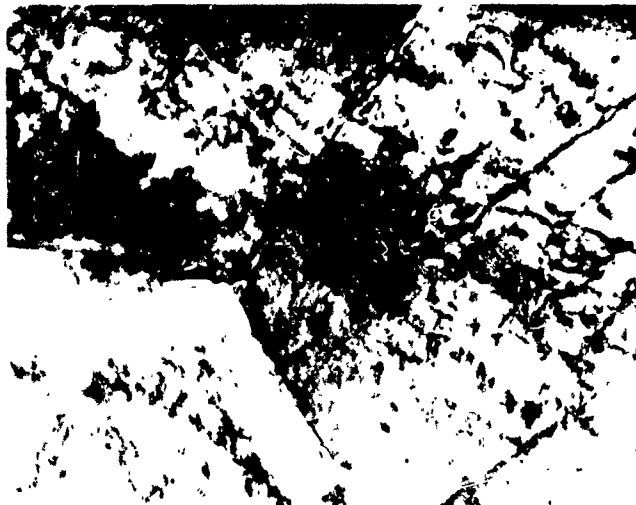
Fig. 16 - Test de corrosion intercrystalline

- enfin des tests de corrosion effectués à l'aide d'un réactif $\text{NaCl} + \text{H}_2\text{O}_2$ pendant 6h à 35°C montrent que seul l'alliage sous revenu est surtout sensible à la corrosion intercrystalline (Fig. 15).

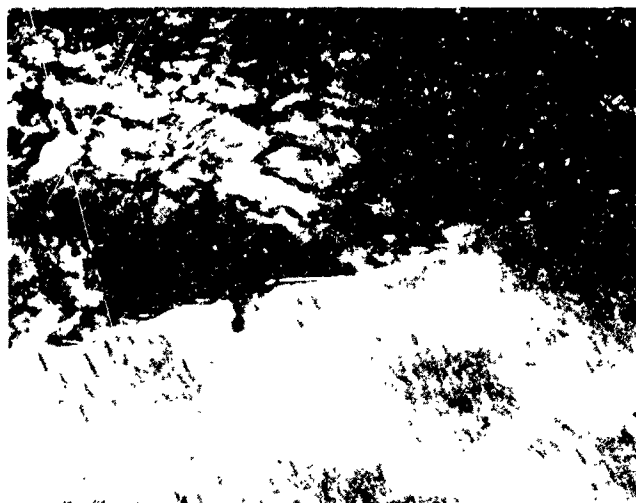
L'examen en microscopie électronique (cf. fig. 17) de lames minces prélevées dans les deux types de matériaux révèle des dislocations dans les deux cas ; toutefois :

- pour les états sensibles, la densité de dislocation est très importante et l'orientation marquée. Pour les états désensibilisés, la densité est moindre et l'orientation aléatoire. La précipitation aux joints de grains ne semble pas différente entre les deux états.

- la précipitation de phase durcissante d' Al_2Cu Mg n'est observable dans la matrice que pour les tôles non susceptibles à la corrosion sous tension.



Cliché n° 8773 A G = 20 000

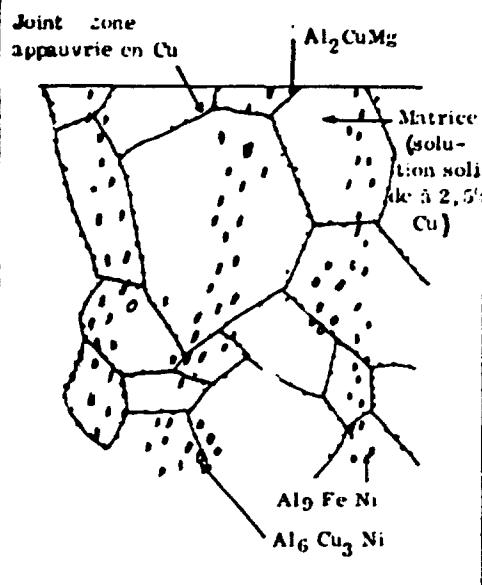
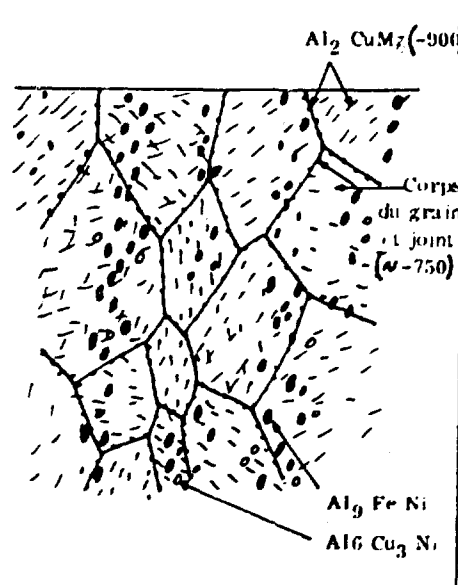


Cliché n° 289 G G = 15 000

Fig. 17 Micrographies électroniques Aspect des dislocations et de la précipitation

Reproduced from
best available copy.

Pour tenter d'expliquer les mécanismes de corrosion de l'A-U2GN aux états sous-revenu et T 651, nous avons indiqué sur le tableau ci-dessous les principales données pour chaque état : nature des principales phases ainsi que leur répartition et proportions approximatives en fonction de l'état structural, d'après les observations effectuées en microscopie optique et électronique.

REPARTITION DES PHASES DANS L'A-U2GN					
Etat sous revenu			Etat T - 651		
Principales phases	% dans l'alliage	Potentiel (-mV/ECS)	Principales phases	%	Potentiel
Sol. Sol. à 2,5% Cu	~90%	-650	Sol. Sol. appauvrie en Cu	~90%	-700mV
Zone appauvrie aux joints de grains, en raison de la précipitation préférentielle de Al ₂ Cu Mg	~2%	-725 à -700	Disparue ou "estompée"		
Précipités de Al ₂ Cu Mg aux joints de grains	~1%	-900	Précipitation généralisée de Al ₂ Cu Mg dans tout l'alliage	~4%	-900
Al ₉ Fe Ni	~5%	-550	Al ₉ Fe Ni	~5%	-550
Autres phases non considérées	~2%				
					

Les courbes de polarisation de ces états ont été établies en solution à 3% NaCl agitée et nous avons considéré que la courbe expérimentale de l'alliage est en réalité la résultante des courbes de réactions des principales phases dans le milieu choisi. Pour cette exploitation nous avons utilisé les valeurs expérimentales obtenues par S.J. Ketcham lors de l'étude d'alliages Al-Cu-Mg, sur des phases fabriquées en Laboratoire (PDD et courbes de polarisation de Al₂ Cu Mg, Al₂ Cu, sol-sol, Al pur), en tenant compte dans notre interprétation des proportions de ces phases (approximatives) dans les états que nous considérons.

Etat sous-revenu (Fig.n°20)	Etat 1 651 (Fig.21)
<p>* <u>Anode</u> : Sol.Sol (5) - <u>Cathode</u> : $Al_2 Fe Ni$ (2') courant de corrosion $\sim 2 \mu A/cm^2$ <u>conséquence</u> : attaque de la Sol-sol autour de ces précipités</p>	<p>* <u>Anode</u> : Sol.sol (5) <u>Cathode</u> : Al_2 ; $Fe Ni$ (2') <u>conséquence</u> : attaque de la Sol-sol autour de ces précipités avec courant de corrosion plus important</p>
<p>* <u>Anode</u> : $Al_2 Cu Mg$ (3) <u>Cathodes</u> : $Al_2 Fe Ni$ (2')-Sol-sol.(5') joint de grain (4') réaction prépondérante: attaque $Al_2 Cu Mg$ aux joints avec faible courant de corrosion</p>	<p>* <u>Anode</u> : $Al_2 Cu Mg$ (3) <u>Cathodes</u>: $Al_2 Fe Ni$ (2') et Sol-sol (5') attaque $Al_2 Cu Mg$ ($\sim 30 \mu A/cm^2$) piqûres fines</p>
<p>* <u>Anode</u> : Joint de grain (4) <u>Cathodes</u> : $Al_2 Fe Ni$ (2')-Sol-sol.(5') réaction prépondérante: attaque Al joint en présence Sol-sol. \Rightarrow corrosion intercrystalline ($\sim 5 \mu A/cm^2$)</p>	

Ainsi on constate que l'attaque du joint de grain n'intervient que pour un état trempé mûré ou sous-revenu, pour lequel la précipitation $Al_2 Cu Mg$ ne s'est effectuée que dans les zones les plus perturbées (joints de grains), créant ainsi un appauvrissement local en Cu .

Dans le cas de l'A-U2GN T 651, la phase durcissante d' $Al_2 Cu Mg$ a précipité finement dans tout le volume des grains; les potentiels du joint et de la matrice tendent alors vers une valeur commune et les effets de pile prépondérants sont entre matrice et précipités cathodiques, matrice et précipités $Al_2 Cu Mg$.

Enfin, pour essayer de mettre en évidence l'influence de la contrainte, nous avons mesuré simultanément l'évolution du PDD d'éprouvettes sous contrainte et sans contrainte (Fig. 22). Nous avons seulement observé que dans le cas de l'alliage sensible, le PDD se décale vers des potentiels plus anodiques (environ 20 mv) au cours d'une période de 2 à 10h après immersion, correspondant à l'apparition des premières criques. Ensuite, le potentiel se stabilise et ne varie pas de façon significative jusqu'à rupture, intervenant en 48h.

On peut penser que l'effet de la contrainte serait de déplacer les dislocations présentes dans les échantillons susceptibles et de créer des empilements sur les joints de grains augmentant ainsi les contraintes locales et la différence de potentiel entre joints de grains et matrice, d'où la vitesse de dissolution anodique (théorie de HOLL).

4.2 - Etude de l'A-U4SG : Les courbes de polarisation tracées en solution NaCl 3% avec agitation et barbotage d'oxygène ou d'Argon mettent en évidence l'influence de l'aération (Fig.27). Le potentiel de dissolution est déplacé vers des valeurs négatives et le courant de corrosion est fortement diminué par désaération.

En solution aérée, on a successivement les réactions :

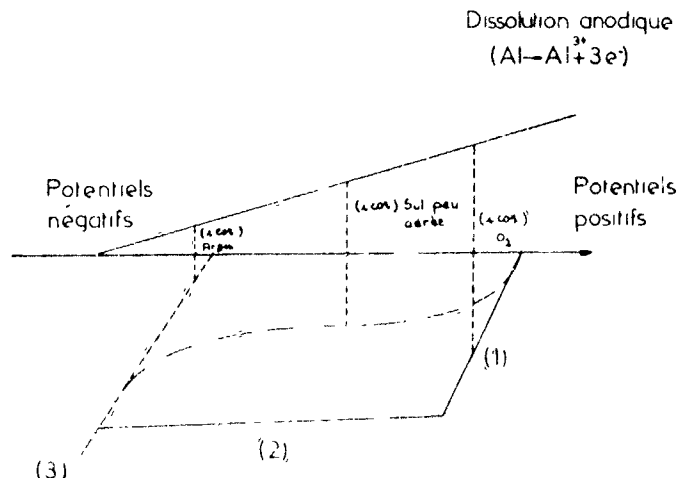
- $1/2 O_2 + H_2 O + 2 e^- \longrightarrow 2 OH^-$ (1) réduction de O_2
- Diffusion de O_2 (2)
- $H^+ + e^- \longrightarrow 1/2 H_2$ (3) dégagement de H_2

En solution, bien aérée, la réaction de réduction de l'oxygène conditionne sans doute le phénomène; pour une solution moins aérée, la réaction de diffusion devient prédominante, le courant de corrosion diminue et le potentiel devient plus négatif.

En solution privée d'oxygène, la réaction de l'hydrogène peut seule intervenir, le courant de corrosion diminue encore et le potentiel est déplacé vers des valeurs plus négatives.

Le schéma ci-contre illustre ces processus.

Ainsi, en solution désaérée, le courant de corrosion est très inférieur à celui obtenu en solution oxygénée; de plus, lors d'un processus de corrosion, les zones difficilement aérées (piqûres, criques) fonctionneront en anodes par rapport aux zones aérées (surface).



Influence de la contrainte : celle-ci ne se manifestant de façon sensible qu'en IEA ou solution avec O_2 , nous pensons que la contrainte a une influence sur la réaction de décharge de $l'O_2$ (1) en diminuant l'énergie nécessaire à cette réaction.

Si cette hypothèse s'avère exacte, la contrainte devrait n'influencer que la courbe de polarisation cathodique en milieu aéré.

D'autre part, la CST devrait être accélérée en milieu légèrement acidifié (déplacement de la réaction (1) vers les potentiels positifs).

Nous devons vérifier ces hypothèses par tracé de courbes de polarisation d'éprouvettes avec et sans contrainte.

5 - CONCLUSION

Les essais de corrosion sous tension tels que nous les avons couramment pratiqués en flexion à charge imposée constante sont sujets à critique:

- sollicitation à la contrainte maximale d'une seule fibre de l'échantillon.
- différence entre la contrainte calculée et celle réellement appliquée en raison de la flexion de l'échantillon entraînant une modification du bras de levier.
- la formule utilisée pour déterminer le facteur de susceptibilité à la corrosion sous tension fait intervenir une valeur R_p qui est, soit connue en traction lorsque les éprouvettes ne sont pas rompues en essai, soit en flexion (contrainte nominale appliquée) pour les éprouvettes rompues lors de l'essai de C.S.T. Les indices de susceptibilité à la corrosion sous tension que nous calculons ne doivent donc être considérés que comme des ordres de grandeur.

Ces restrictions étant faites on peut cependant admettre que ce type d'essai constitue une méthode d'exploration valable permettant des études systématiques des matériaux et de leurs traitements, à l'aide d'un appareillage relativement peu coûteux. Pour la détermination du seuil de contrainte admissible en corrosion sous tension, il est sans doute préférable de choisir un essai en traction à charge imposée constante.

Des essais effectués sur l'A-U2GN, il ressort que cet alliage n'est sensible à la corrosion inter-cristalline et à la corrosion sous tension que lorsque le revenu est insuffisant; dans ce cas la contrainte joue un rôle important dans le phénomène puisqu'elle intervient pour environ 75% dans la perte totale des caractéristiques mécaniques de l'alliage en corrosion sous tension. Ainsi, si l'on ne peut à proprement parler, qualifier ce phénomène de "fissuration en corrosion sous tension" - qui semble réservé au cas où les alliages ne montrent aucune susceptibilité à la corrosion inter-cristalline en l'absence d'une contrainte mécanique - on se trouve néanmoins en présence d'un phénomène nettement accéléré par la contrainte.

L'A-U2GN est rendu totalement insensible à la corrosion sous tension par un revenu qui lui confère simultanément des caractéristiques optimales; il peut donc être utilisé avec un maximum de sécurité pour des pièces de structure soumises à des contraintes permanentes, même en sens travers court.

Bien que sa sensibilité à la corrosion inter-cristalline soit faible après revenu, l'alliage A-U4SG reste très susceptible à la corrosion sous tension en sens TC en milieu aéré, quel que soit le traitement thermique essayé. Des précautions doivent donc être prises quant à son utilisation sur appareils; on doit en particulier éviter ou limiter les contraintes permanentes en travers court.

Enfin la considération des microstructures des alliages, l'exploitation des courbes de polarisation, nous ont permis de mettre en évidence certaines des réactions importantes intervenant dans les processus de corrosion et CST et de mieux comprendre l'influence des quelques paramètres liés à l'alliage ou au milieu d'essai.

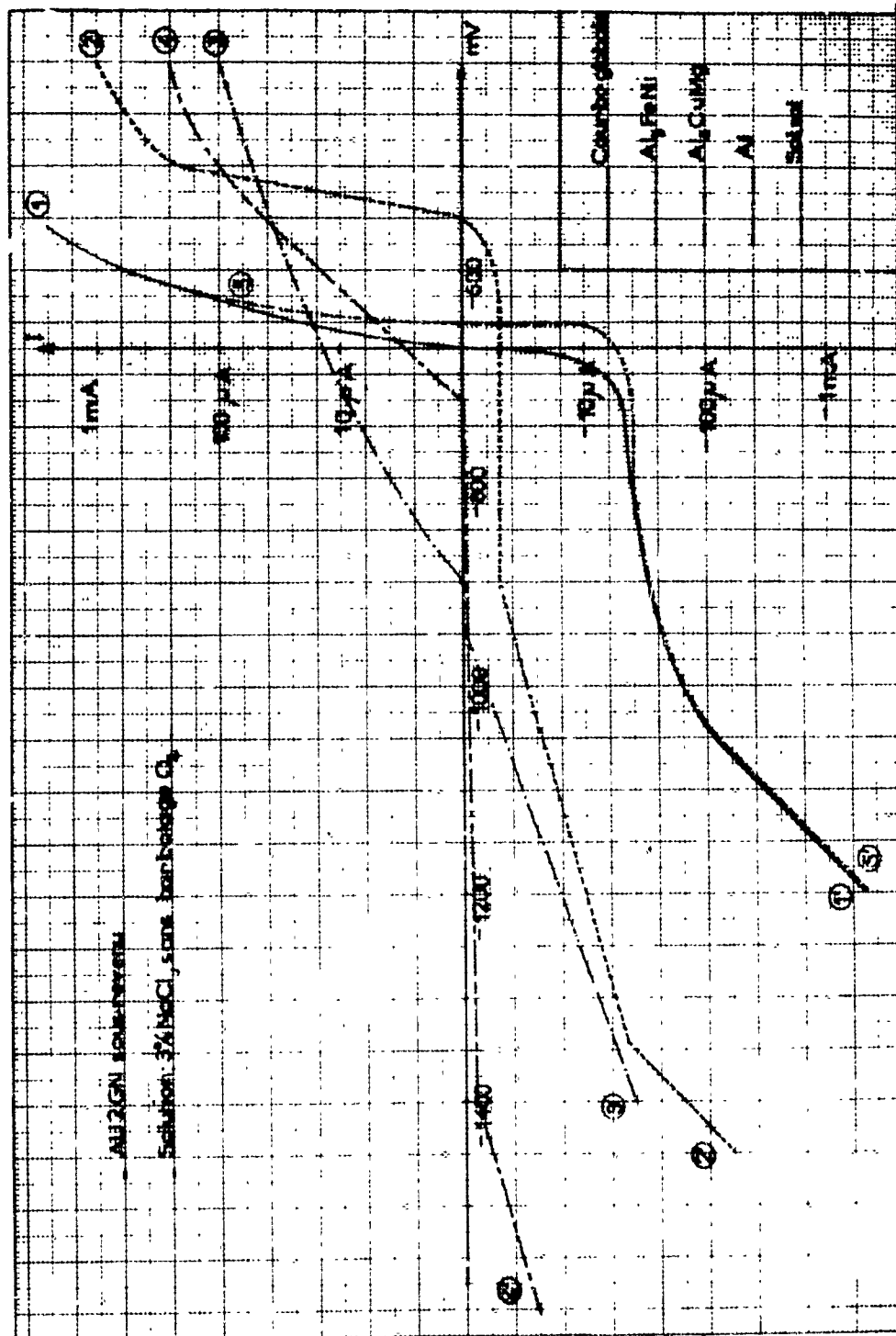
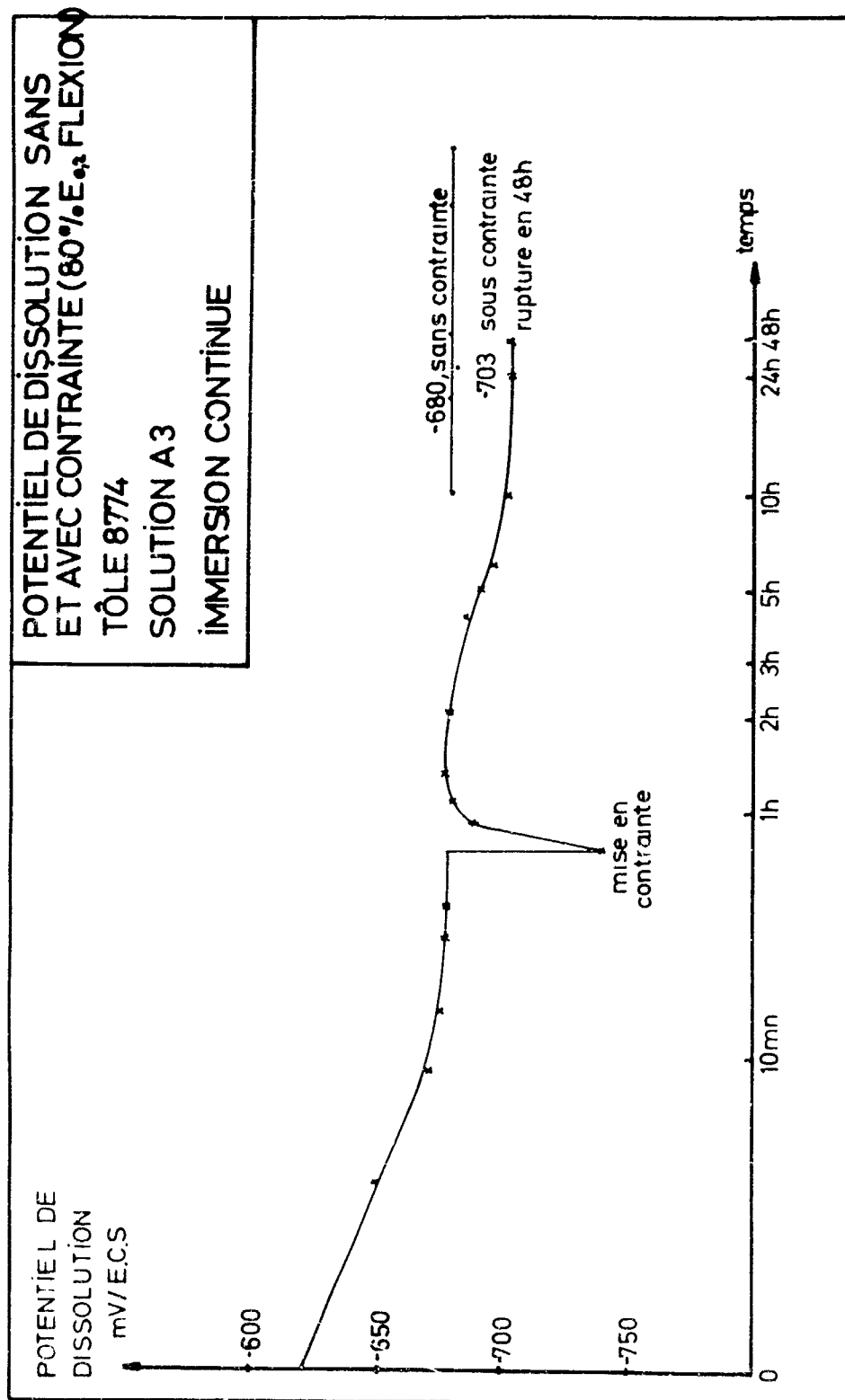


FIG. 20 - COURBES DE POLARISATION DE L'Al-Zn sous l'effet



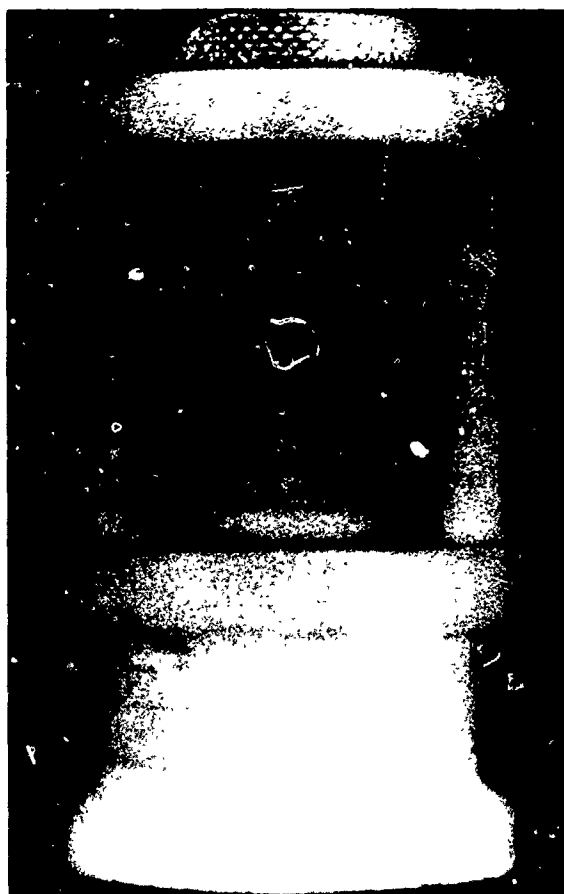


Fig. 3: Stressing fixture for the tension specimens

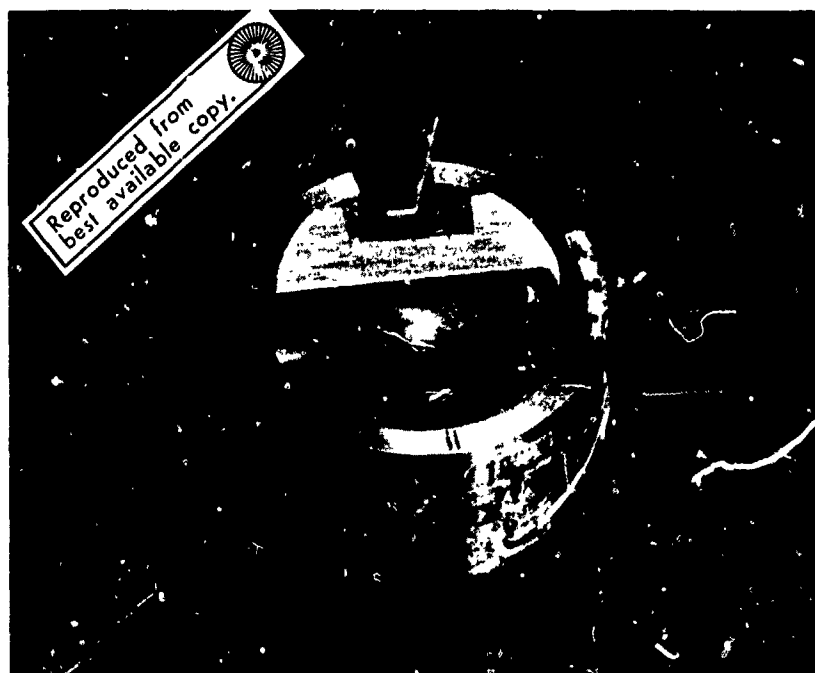


Fig. 4: Wedge loaded C-ring specimen with attached strain-gauge

RESULTS OF COMPARATIVE STRESS-CORROSION TESTS ON AlZnMgCu-ALLOYS
USING DIFFERENT TYPES OF SPECIMENS

Werner Lehmann

Industrieanlagen-Betriebsgesellschaft mbH
Hauptabteilung für Festigkeit, Konstruktion
und Werkstoffe
8012 Ottobrunn bei München, Einsteinstraße

SUMMARY

In order to evaluate and to compare the stress-corrosion behaviour of more complicated structural parts, for example die-forgings from the two different alloys 7079-T6 and AZ 74.61, various types of specimens were taken from critical locations on the forging. These critical locations are the area around the jack-point hole, the main parting plane and the area of the first two rows of bolt-holes. C-rings, precracked DCB-specimens or smooth tension specimens respectively were examined, using a standard 3.5 % NaCl alternate-immersion test. The test-specimens were periodically inspected in order to find out the time to failure (tension specimens), the time to the first crack or to complete fracture (C-rings) and the crack-length as a function of time as well as the threshold-value of K_{ISCC} (DCB-specimens).

After approximately five months of testing each type of specimen give specific results concerning the stress-corrosion behaviour. In this way it seems to be possible to get an almost complete information about susceptibility to stress-corrosion of a typical forging. In all three cases mentioned above the results show that forgings from the alloy AZ 74.61 are superior to those of 7079-T6.

RESULTS OF COMPARATIVE STRESS-CORROSION TESTS ON AlZnMgCu-ALLOYS USING DIFFERENT TYPES OF SPECIMENS

Werner Lehmann

1. Introduction

The majority of the published results in the area of stress-corrosion cracking have been concerned with a discussion of more or less well defined material properties. The tests were generally conducted with idealized specimens taken from plates, sheets and rods. Additionally only one test method was used in most cases. The latest research results, for example titanium alloys, have shown, that it is not completely possible to describe the stress-corrosion behaviour in this way. In order to evaluate the stress-corrosion behaviour of more complicated structural parts, for example forgings, the above methods are in our opinion insufficient. This is due to the fact, that the specific characteristics of structural parts, for example non-homogeneous grain-structure and more or less high internal stresses, can not be taken into consideration. On the other hand the testing of actual structural components, because of their complexity and the extend of the testing procedure, is normally not possible. It is therefore a reasonable method to test samples taken from critical locations on the structural part. Since it is expected that generally fatigue cracking is present in most structural elements, we are of the opinion that for a complete evaluation it is necessary to test precracked as well as smooth specimens. The crack-growth rate properties will be a valuable addition to the smooth specimen threshold-data in determining the maintenance inspection intervalls.

At IABG the tests being conducted have the specific goal of comparing the stress-corrosion behaviour of die-forgings from two different AlZnMgCu-alloys.

2. Test set-up and execution

2.1 Test material

Available for the test were fittings (die-forgings) from the two AlZnMgCu-alloys 7079-T6 and AZ 74.61.

The following fabrication plan was used by the manufacturer:

forging - heat treatment - mechanical finishing

This information is very important because the sequence of fabrication steps has an influence on the presence of more or less high internal stresses.

The following heat procedures were used:

AlZnMgCu-alloy 7079-T6

solution treatment: 20 - 60 min / 465 °C

water quenching: 40 - 60 °C

artificial ageing: 12 hr 120 °C + 8 hr 170 °C

AlZnMgCu-alloy AZ 74.61

solution treatment: 20 - 60 min / 465 °C

water quenching: 30 - 50 °C

artificial ageing: 24 hr 120 °C + 6 ÷ 10 hr 170 °C

The heat treatment of the alloys used was somewhat different from the normal treatment T6 and served to improve stress-corrosion behaviour especially in the case of 7079.

2.2 Sampling / type of specimens

Since inspection results have shown that there are three critical areas on the fitting, specimens were taken at the following locations:

- | | |
|--|-------------------|
| a) in the area around jack-point hole | C-ring specimens |
| b) in the main parting plane | DCB-specimens |
| c) in the area of the first two rows of bolt holes | tension specimens |

Figure 1 shows the type and the location of the various specimens. Figure 2 shows the dimensions of the various test specimens. A total of 40 tension specimens, 20 C-ring specimens and 10 precracked DCB-specimens were tested.

2.3 Specimen preparation / loading

After mechanical finishing the tension specimens and C-rings were etched in a solution of nitric acid, hydrofluoric acid and distilled water.

The time-to-failure tests of the tension specimens and C-rings were conducted at two different applied loads:

- at 85 percent of yield stress
- at 25 kp/mm²

The loading of the tension specimens was accomplished with spring-loaded stressing fixtures (see fig. 3).

The C-rings were loaded with a wedge, so that the desired stress was attained on the inside of the ring opposite the wedge (see fig. 4). The exact load was measured with strain gauges. In order to prevent damage of the inner surface of the ring, the strain gauges were attached to the outside surface. The point of highest loading was in the area of the parting plane, that is in the short-transverse direction. Internal stresses were neglected.

The DCB-specimens were bolt-loaded until a crack of 2 - 3 mm was introduced.

For the purpose of calculating the stress-intensity-factor K_I corresponding to each crack-length, the known expression for K_I , according to Hyatt

$$K_I = \frac{\sigma \cdot E \cdot h}{4} \left[\frac{3h(a + 0.6h)^2 + E^2}{(a + 0.6h)^3 + h^2 \cdot a} \right]^{1/2}$$

was used.

The stress-intensity at which the crack-growth ceases is denoted by K_{ISCC} .

To prevent galvanic corrosion the specimens were partially coated of wax.

2.4 Stress corrosion test conditions / test specimen inspection

A standard 3.5 % NaCl alternate-immersion test was performed (duration of immersion 10 min, duration of drying 30 min). The pH-factor of corrosion medium was between 7.8 and 8.6. Fig. 5 shows the complete corrosion test set-up. The use of a 3.5 % NaCl-solution for long test durations made it difficult to observe the cracks.

The test specimens were periodically inspected in order to obtain the following information:

- a) tension specimens under constant load: time to failure
- b) C-rings: time to the first crack, total number of cracks and time to complete fracture
- c) precracked DCB-specimens: crack length as a function of time and final crack length

In order to more exactly record the crack growth in the DCB-specimens, at the beginning of the test inspections were made every six hours.

3. Results of stress-corrosion testing

3.1 Tension specimens under constant load

After approximately 5 months of testing the following time-to-failure data can be reported (see also fig. 6):

- a) Test specimens of 7079-T6 alloy taken in the short-transverse direction had all failed between 7 and 13.5 hrs under the load of 85 % of yield stress and between 15 and 60 hrs under the load of 25 kp/mm^2 .
- b) Test specimens of 7079-T6 alloy taken in the long direction had all failed between 600 and 3000 hrs under a load of 85 % of yield stress and between 1150 and 3800 hrs under a load of 25 kp/mm^2 .
- c) Test specimens of AZ 74.61 alloy taken in short-transverse direction with two exceptions have not yet failed. Under a load of 85 % of yield stress the first failure occurred after 2000 hrs. No failure has occurred in the specimens taken in the long direction or under the load of 25 kp/mm^2 .

A comparison of the time to failure-data for smooth specimens of 7079-T6 and AZ 74.61 leads to a factor of one hundred and shows clearly the superiority of AZ 74.61.

Fig. 7 shows the fracture surface of a 7079-T6 and a AZ 74.61 specimen, both taken in the short-transverse direction. The 7079-T6 specimen shows the typical slate-like fracture surface, characteristic of a brittle stress-corrosion failure. The AZ 74.61 specimen shows in contrast a very rough and pitted fracture surface, which indicates a very slow attack of corrosion.

3.2 C-rings under constant deflection

The results of the test on the C-ring specimens are summarized in the table shown in fig. 8.

After 5 months of testing no cracking was observed in the C-ring-specimens from AZ 74.61 alloy. In contrast all of the rings machined from 7079-T6 alloy show cracks of varying length (first column of the table). The observed cracks are concentrated on the edge of the C-ring with the extreme short-transverse grain-structure (designated as side I in the table). The edge designated as side II represents the inner area of the forging with a equi-axial grain structure. The next two columns contain information on the time to first crack and to the complete fracture.

Fig. 9 shows a specimen from 7079-T6-alloy with many branched cracks on the inner and outer surface. The metal flow-lines are easy to see. Fig. 10 shows the intergranular cracks, typical of stress-corrosion cracking of high-strength aluminium alloys.

3.3 Precracked double cantilever beam (DCB) specimen

For each of the ten tested DCB-specimens following data was calculated:

- a) the crack-length on side I and side II of the specimen as a function of time
- b) the stress-intensity factor K_I as a function of crack-length
- c) the crack-growth-rate da/dt as a function of time
- d) the crack-growth-rate da/dt as a function of stress-intensity-factor K_I

In figures 11 through 14 the above data for one specimen of 7079-T6 and AZ 74.61 are compared. Additionally a comparison of data from side I and side II is shown. A comparison on the crack lengths in the fig. 11 shows clearly that the curves for the AZ 74.61-specimen (on the right of the figure) are considerably flatter than the curves for 7079-T6. Additionally the start of cracking occurs much sooner in the 7079-T6 specimen. The specimen from AZ 74.61 shows an incubation time. Differences in the data for side I and side II are also recognizable (grain-structure!).

The differences in stress-corrosion-behaviour of the two materials are also clearly shown in fig. 12. The flatter curves for the 7079-T6 specimen (on the left of the figure) indicate the higher crack-growth-rates. The curves end at the stress-intensity factors at which the unstable cracking ceases. This value corresponds to the so-called K_{ISCC} -value. The differences in the K_{ISCC} -values are easy to see.

Fig. 13 shows the crack-growth-rate data as a function of time. As in the other figures the differences in the data for the two alloys as well as for the two sides of each specimen are discernable. The peaks in each curve represent a non-uniform growth-rate.

Fig. 14 shows a log-log plot of the crack-growth-rate da/dt as a function of the stress-intensity factors K_I . As in the previous plots the curves represent the data for only one test-specimen of each alloy. Once again a comparison of the data for the two alloys shows the superiority of AZ 74.61. This superiority in stress-corrosion-behaviour of the alloy AZ 74.61 is depicted not only by the higher threshold value of K_{ISCC} but also by the lower maximum value of crack-growth rate. In the case where a short transverse grain-structure is predominant (side I of the specimen), a relative rapid increase of crack-growth rate can be observed when the values for K_I increase. This also demonstrates the influence of the varying grain-structure within the fitting.

Since the depiction of $da/dt = f(K_I)$ allows for the clearest comparison of the behaviour of the alloys 7079-T6 and AZ 74.61, all of the data for the five specimens of each alloy have been plotted in the diagrams shown in fig. 15. In the upper diagram the combined data for sides I and II of the DCB-specimen form two distinct bands. From this diagram can be obtained the following values for the stress-intensity factor K_{ISCC} :

$$\begin{aligned} \text{for the alloy 7079-T6: } K_{ISCC} &\sim 7 \text{ ksi } \sqrt{\text{inch}} \\ \text{for the alloy AZ 74.61: } K_{ISCC} &\sim 18 \text{ ksi } \sqrt{\text{inch}} \end{aligned}$$

The single data point for AZ 74.61 obtained from Hyatt lies on the right-hand limit of our band. The reason for this may be that Hyatt's specimens was taken from a plate, whereas our specimens were taken from a die-forging in the area of the parting plane.

The two-step heat-treatment of the fittings resulted in particular for the 7079-T6 specimens in an improvement of the stress-corrosion behaviour. In contrast Hyatt used a normal T6-heat treatment process. For this reason our test-results for 7079-T6 and AZ 74.61 are grouped relatively closer to each other. When the data are separated into side I and side II as in the two lower diagrams the influence of the varying grain-structure of the two sides is recognizable. This is especially noticeable with the 7079-T6 alloy.

4. Conclusions

It has been shown that it is possible to compare the stress-corrosion behaviour of die-forged structural elements manufactured from different alloys by testing various types of specimens taken from critical locations on the forging. Using this method it is possible to obtain values for each alloy for the time to failure under constant load, which is the total time for incubation and crack-growth; for the time to first crack under constant deflection and for the crack-growth rate and stress intensity factor K_{ISCC} .

The results obtained in all three cases indicate the superiority of the stress-corrosion behaviour of the alloy AZ 74.61.

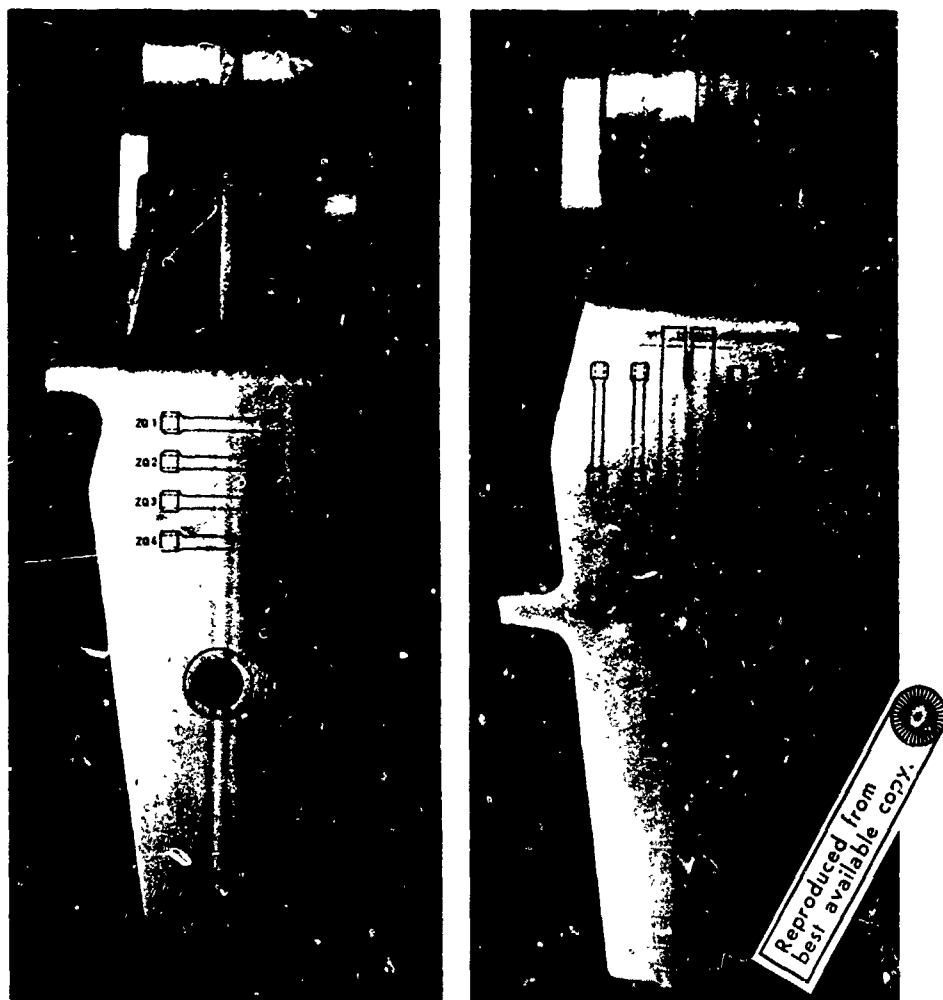


Fig. 1: Location of the specimens on the fitting

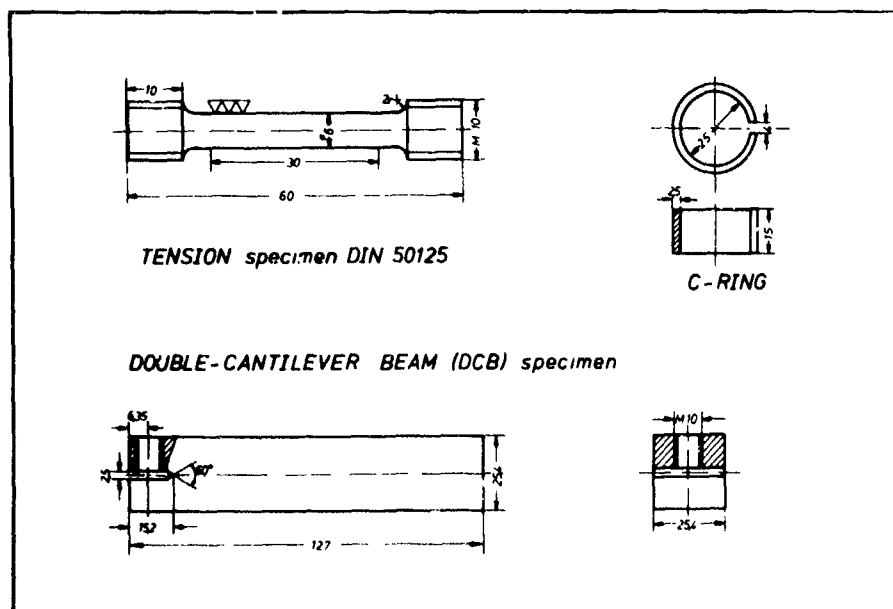


Fig. 2: Type and dimensions of the specimens



Fig. 3: Stressing fixture for the tension specimens

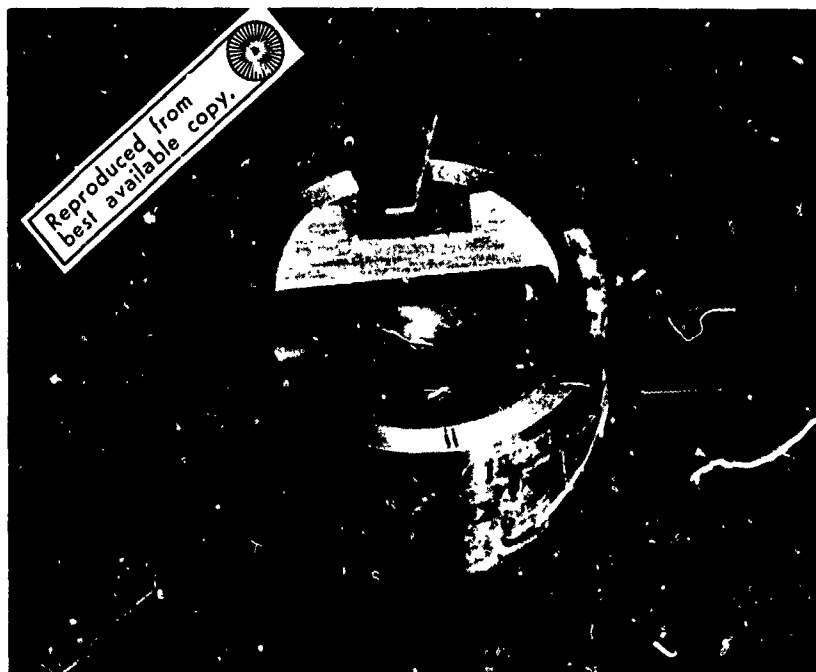


Fig. 4: Wedge loaded C-ring specimen with attached strain-gauge



Fig. 5: Alternate immersion test set-up

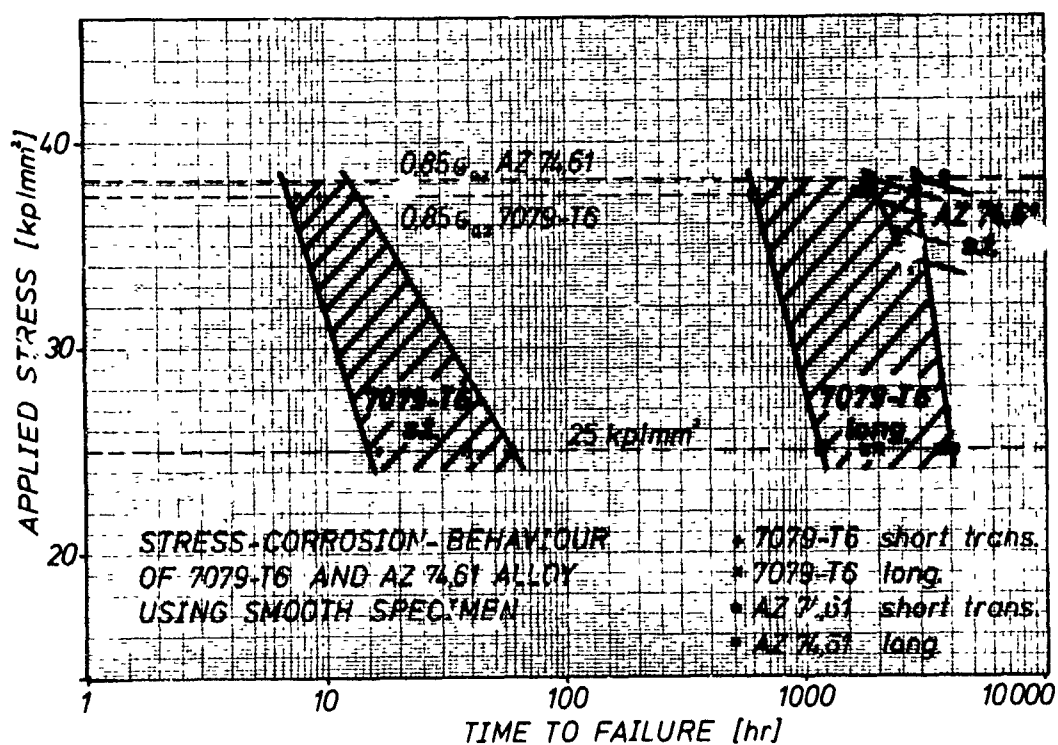
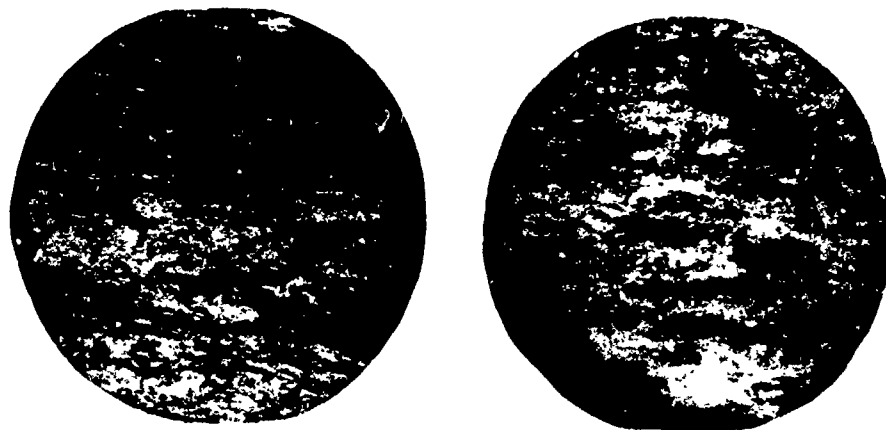


Fig. 6: Stress-corrosion-behaviour of 7079-T6 and AZ 74.61 alloy using smooth specimen



7079-T6

AZ 74.61

— 1mm

Fig. 7: Typical fracture surfaces for specimens of 7079-T6 and AZ 74.61

Specimen No.	Alloy	Stress level	RESULTS OF STRESS CORRUPTION - TEST USING C-RINGS						
			Total number of cracks	Number of cracks		Time to first failure in hr		Time to fracture in hr	
				Side I *	Side II *	Side I *	Side II *	direction a **	direction b **
1 CO	7079 - T6	0,85 $\sigma_{0,2}$	2	1	1	258	307	307	356
2 CO			3	2	1	451	691	670	766
3 CO			2	2	-	148	-	597	837
4 CO			3	2	1	54	331	331	356
5 CO	7079 - T6	0,85 $\sigma_{0,2}$	3	1	2	42	198	119	220
8 CO			3	2	1	148	620	476	691
6 CO	AZ 74	0,85 $\sigma_{0,2}$	-	-	-	-	-	-	-
7 CO	AZ 74	0,85 $\sigma_{0,2}$	-	-	-	-	-	-	-
9 CO			-	-	-	-	-	-	-
10 CO			-	-	-	-	-	-	-
1 CU	7079 - T6	25 kp/mm ²	3	2	1	282	2000	1668	2168
2 CU			1	1	-	2339	-	no fracture	-
3 CU			2	1	1	476	499	no fracture	no fracture
4 CU			2	1	1	102	307	258	356
5 CU	7079 - T6	25 kp/mm ²	6	3	3	102	356	331	389
8 CU			2	2	-	102	-	412	2000
6 CU	AZ 74	25 kp/mm ²	-	-	-	-	-	-	-
7 CU	AZ 74	25 kp/mm ²	-	-	-	-	-	-	-
9 CU			-	-	-	-	-	-	-
10 CU			-	-	-	-	-	-	-

* Side I - surface of forging
Side II - inner area of forging

** direction a - direction of failure axial
direction b - direction of failure radial

Fig. 8: Table of C-ring test results

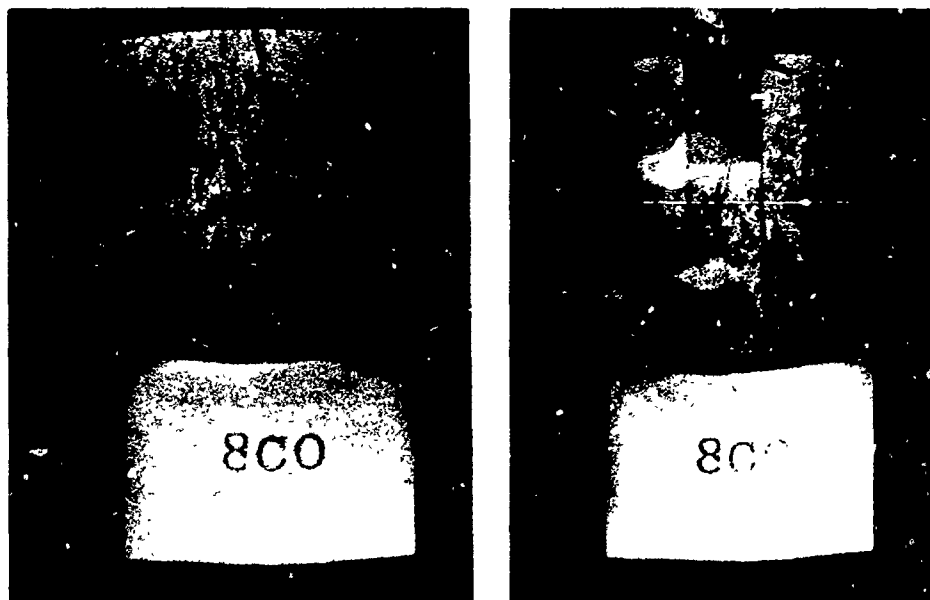


Fig. 9: Stress-corrosion cracking on a C-ring specimen of 7079-T6

Reproduced from
best available copy.



— 10 μ

Fig. 10: Typical intergranular cracking on a 7079-T6 specimen

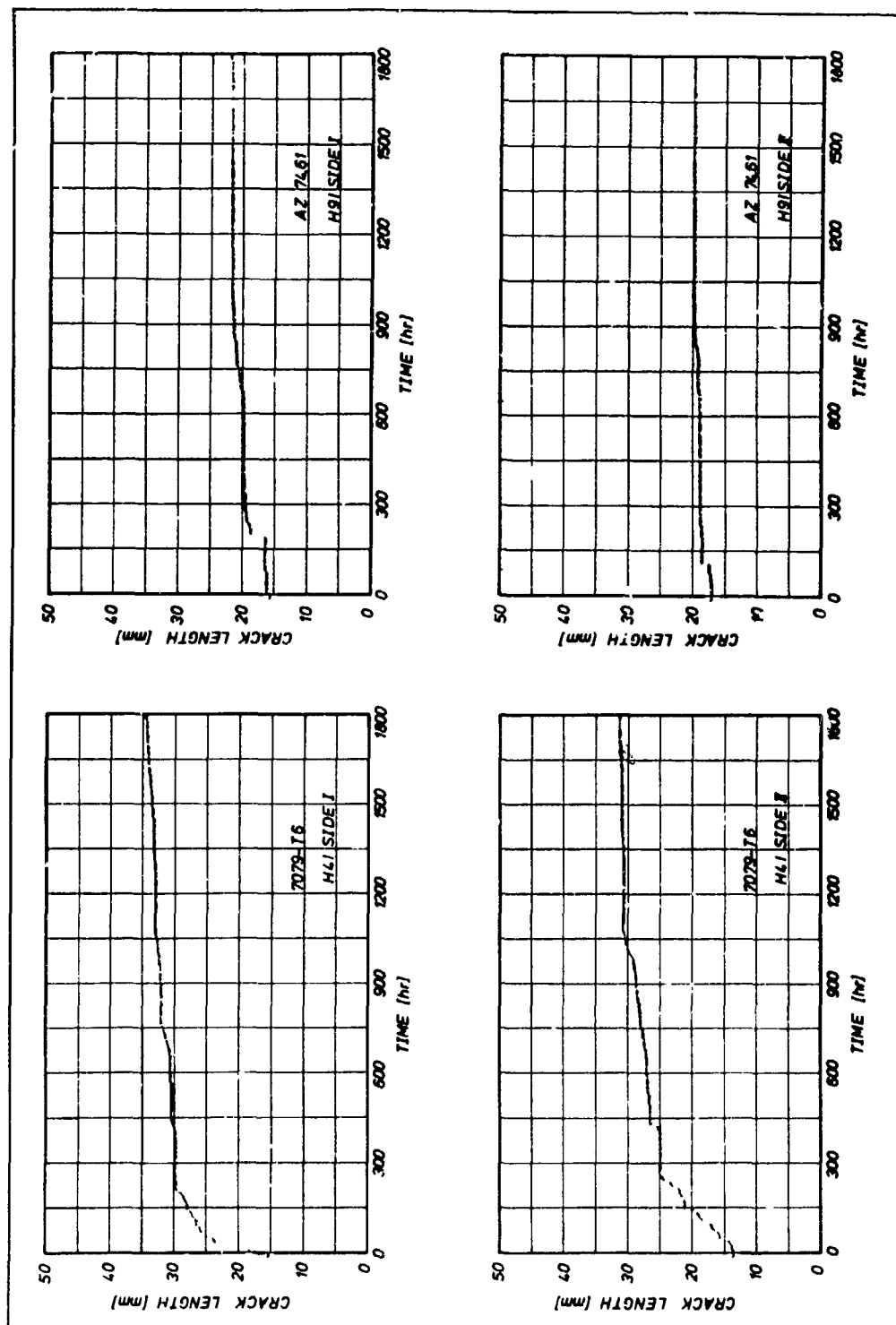


Fig. 11: Crack length as a function of time

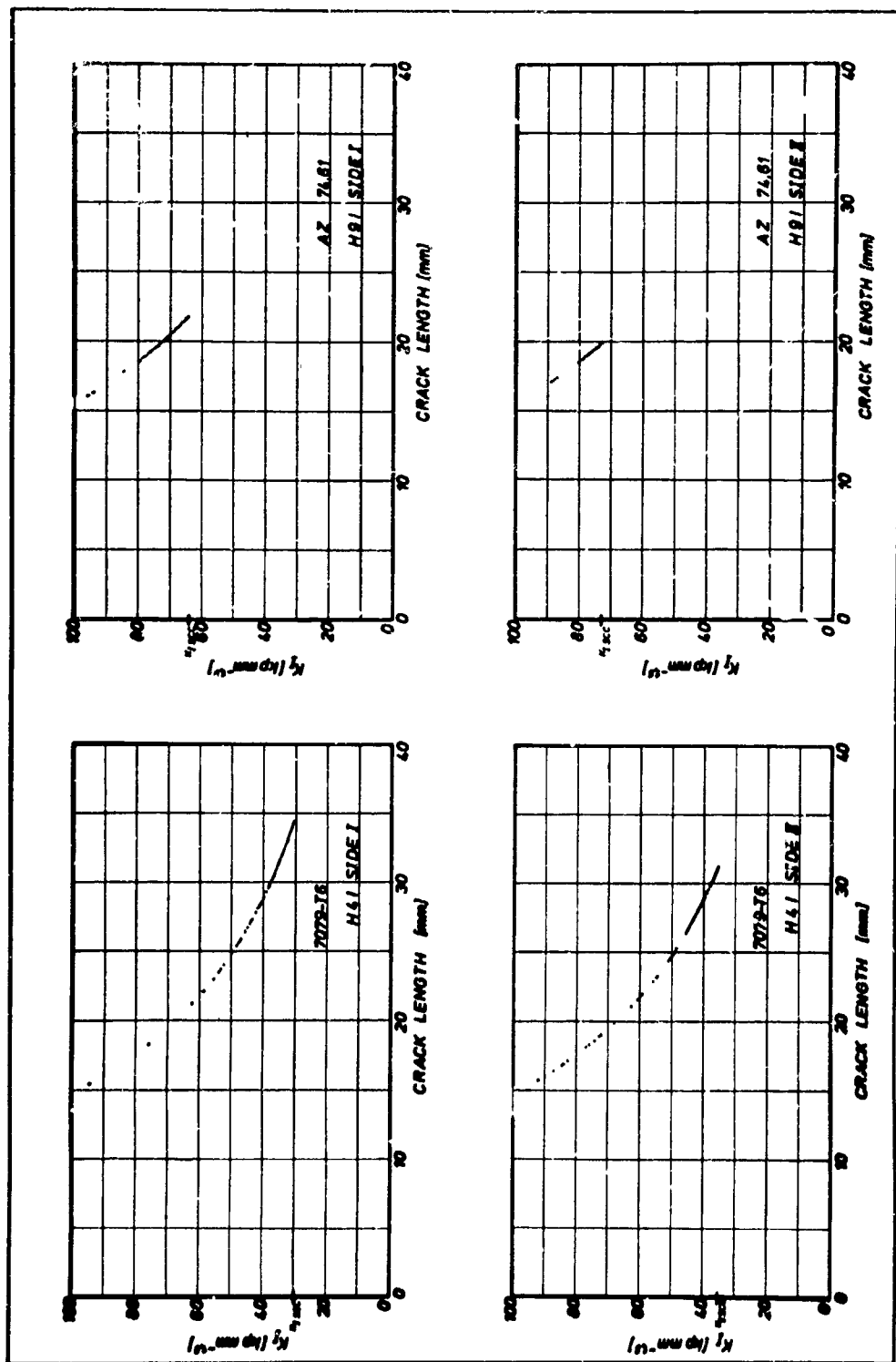


Fig. 12: Stress-intensity factor K_I as a function of crack-length

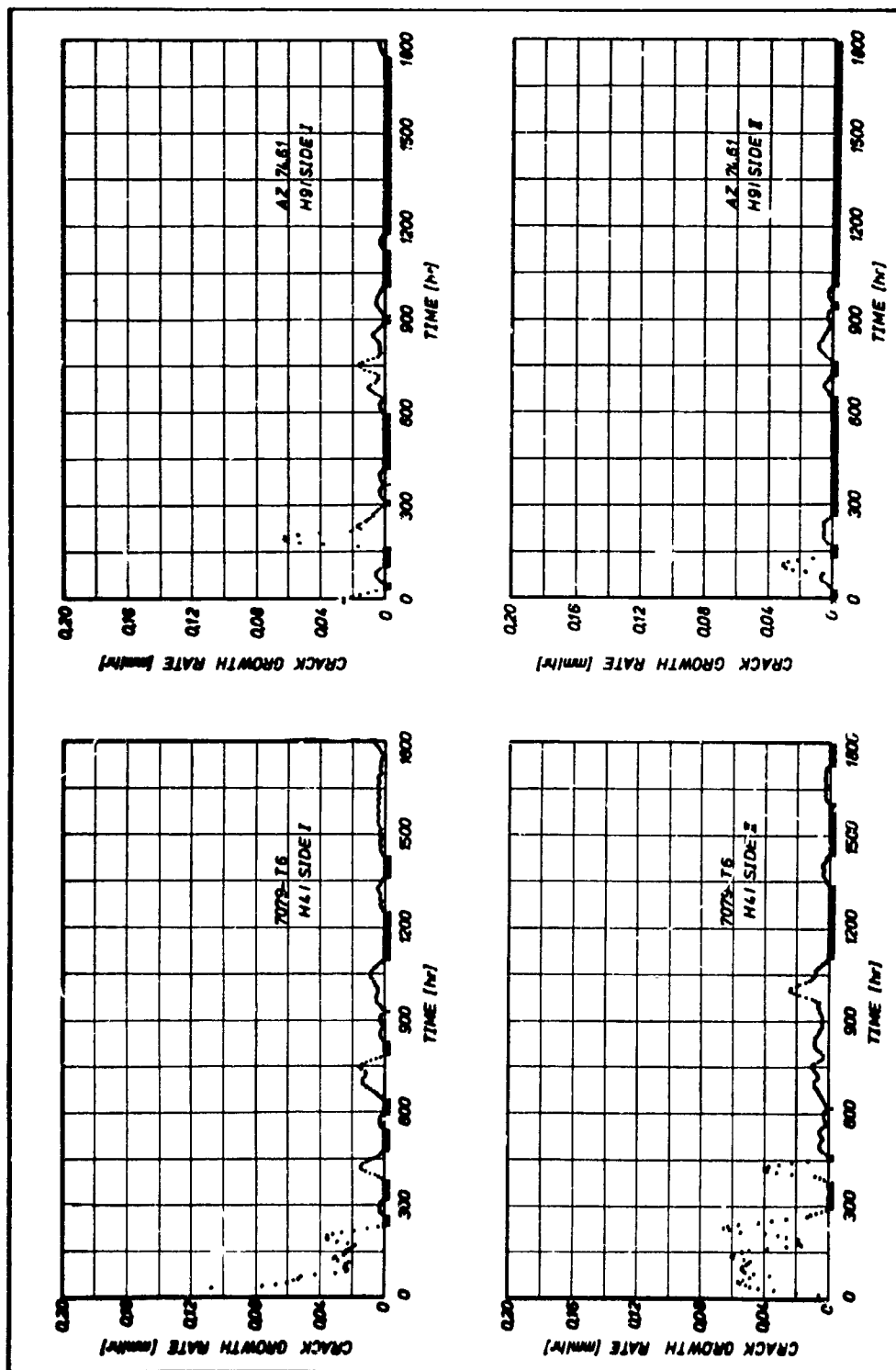


Fig 13: Crack growth rate as a function of time

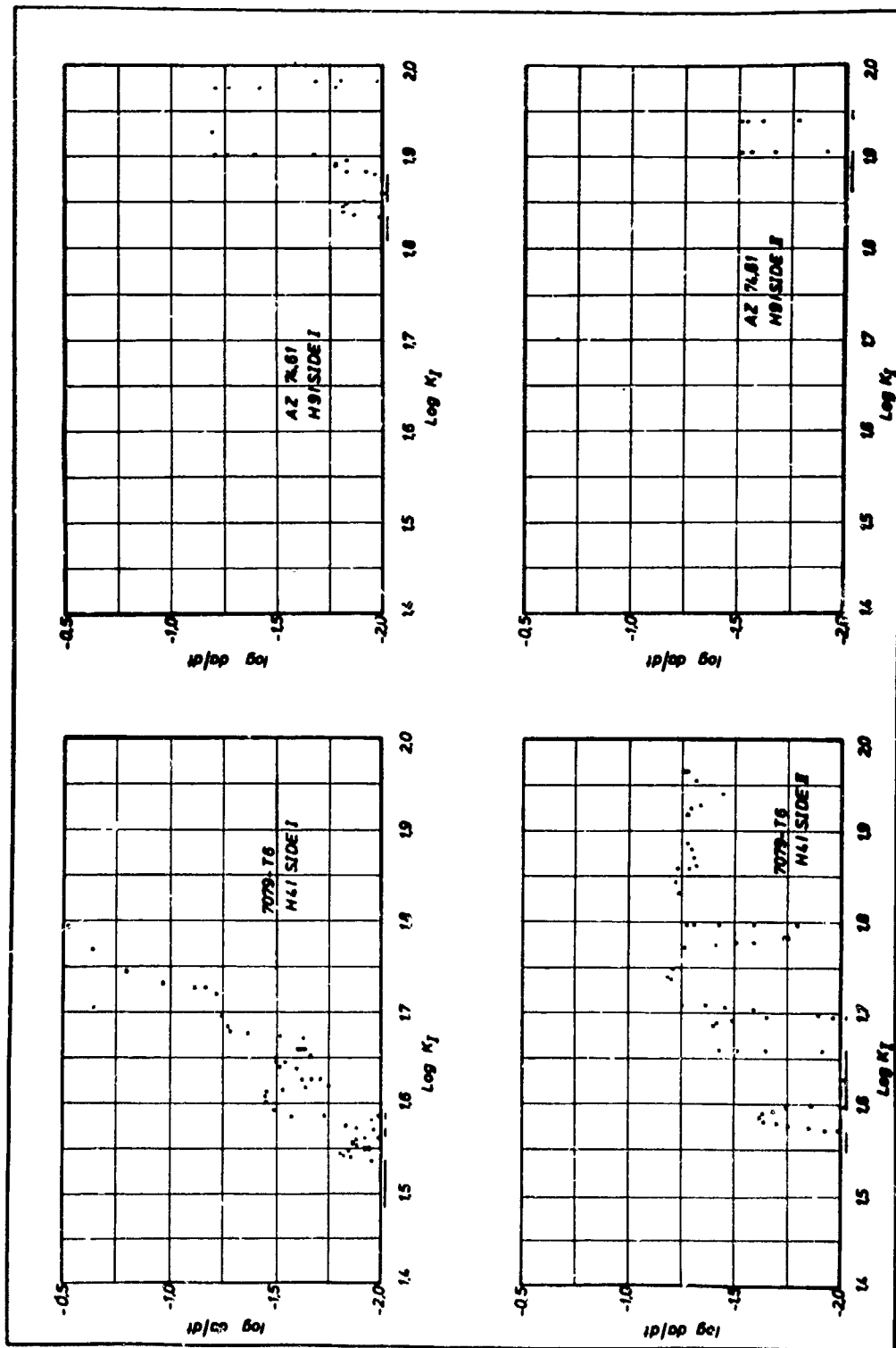


Fig. 14: Example of crack growth rate as a function of stress intensity factor K_I

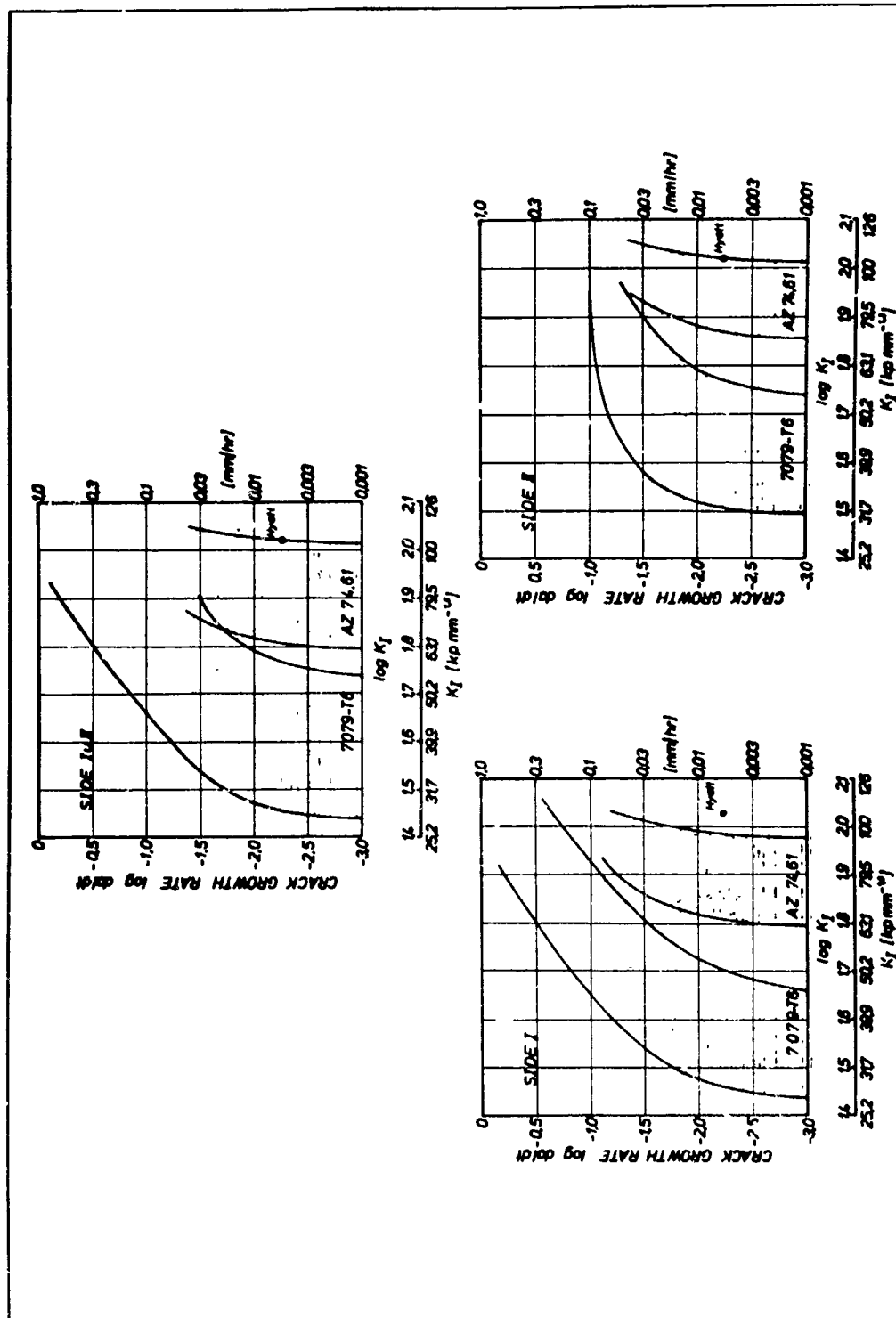


Fig 1: Crack growth rate for all DCB-specimens as a function of stress intensity factor K_I

STRESS CORROSION CRACKING OF MARTENSITIC PRECIPITATION
HARDENING STAINLESS STEELS

Michael Henthorne
Supervisor, Corrosion Research
Carpenter Technology Corporation
Reading, Pennsylvania 19603 USA

SUMMARY

Stress corrosion cracking tests on two precipitation hardening stainless steels, Custom 455 and Custom 450, have been used to study the effects of heat treatment, product size, type of test specimen and test environment. Smooth specimens (tensile, bent beam and U-bend) and precracked cantilever beams have been tested in sodium chloride solution, salt spray and a natural marine atmosphere.

The cracking resistance of Custom 455 improves significantly as the aging temperature is increased i.e. as the yield strength decreases and the toughness increases. Specimens cut from large product sizes (e.g. billet) have lower fracture toughness than smaller sizes (e.g. bar) and this is reflected in K_{ISCC} values. No normal failures were obtained for Custom 450 with either the smooth or precracked specimens.

The validity of K_{ISCC} as a design criteria is questioned. Possible methods of predicting K_{ISCC} from K_{IC} and electrochemical measurements related to pitting and/or crevice corrosion are suggested. The differences between stress corrosion and cracking in galvanic corrosion situations are discussed.

STRESS CORROSION CRACKING OF MARTENSITIC PRECIPITATION HARDENING STAINLESS STEELS

Michael Henthorne

Martensitic, precipitation hardening stainless steels offer an attractive combination of:

1. Corrosion resistance
2. High strength
3. Toughness
4. Ease of fabrication and heat treatment

Their corrosion resistance eliminates the need for painting or plating and their high strength and toughness permit weight and cost savings. The unique properties of this family of materials has led to the development of several new alloys in recent years. These are finding increased use in aerospace and a wide variety of other industries.

Like all martensitic steels, the precipitation hardening grades can be susceptible to stress corrosion cracking at ambient temperatures. Their successful application is, to a major extent, dependent upon an awareness of this.

This paper deals primarily with two alloys—Custom 455 and Custom 450. Data are presented for smooth and precracked specimens with particular attention being given to the role of heat treatment and product size. The interpretation of test data and suggestions for improved test methods are also discussed.

COMPOSITION AND MECHANICAL PROPERTIES

Typical compositions and tensile properties are shown in Tables 1 and 2. Both alloys are fully martensitic.

Table 1 TYPICAL ALLOY COMPOSITIONS

Alloy	C	Mn	Si	P	S	Cr	Ni	Mo	Cu	Cb	Ti
Custom 455	.02	.1	.1	.015	.005	11.5	8.5	—	2.3	.2	1.2
Custom 450	.03	.3	.3	.015	.005	15	6.5	.3	1.5	.7	—

Custom 455 is designed for uses requiring yield stresses in excess of 200 ksi and for a wide variety of corrosents can be considered to have corrosion resistance intermediate between AISI Types 410 and 304 stainless.

Custom 450 was developed for applications requiring the corrosion resistance of Type 304. It can be used in either the annealed or aged conditions.

Table 2 TYPICAL ROOM TEMPERATURE TENSILE PROPERTIES
(1" ROUND BAR)

Alloy	Condition	0.2% YS		UTS	% El. in 4D	% R.A.
		ksi	kg/mm ²			
Custom 455	Aged 900°F	245	172	250	10	45
"	" 950°F	225	158	235	12	50
"	" 1000°F	200	141	210	14	55
Custom 450	Annealed	118	83	141	13	50
"	Aged 900°F	186	131	195	14	57
"	" 1000°F	169	119	173	17	62
"	" 1150°F	93	65	143	23	69

STRESS CORROSION CRACKING DATA

Smooth Specimens

Results obtained with a variety of smooth specimens and test media are shown in Table 3. Note that for Custom 455:

1. Resistance to cracking improves with increasing aging temperature. This is attributed to an increase in toughness since corrosion and pitting resistance do not significantly change.
2. Bent beam specimens stressed to 90% of the 0.2% flow stress are just as susceptible to cracking in salt spray as are U-bends. Although there is a specimen thickness difference to consider, the similar behavior is attributed to the probability that in the 900°F age condition cracking is largely controlled by pit formation. Once a pit forms, an applied stress of 90% of the 0.2% flow stress is quite adequate to cause rapid crack propagation.
3. Tensile specimens in 3.5% NaCl at 75°F did not crack whereas bent beams at the same stress level in salt spray at 95°F did fail. This is attributed largely to the

greater incidence of pitting in a spray as compared to a solution.

4. The Kure Beach marine test site was slightly more severe than salt spray. This is attributed to the presence of sand particles at the former. These can deposit on the specimen surface and induce pitting.
5. There is considerable scatter in results.

Table 3 STRESS CORROSION TESTS WITH SMOOTH SPECIMENS

Alloy	Tensile Specimens (a) in 3.5% NaCl (pH 5, 75°F)	Days to Failure		
		Bent Beams (b) in 20% Salt Spray Spray (pH 7, 95°F)	U-Bends (c) in 20% Salt Spray (pH 7, 95°F)	U-Bends at Kure Beach, N.C. 80' Lot 800' Lot
Custom 455 Aged 900°F	NF, NF, NF, NF	115, 337, 229 427, NF	4, 141, 463 NF, NF	1, 2, 3 2, 23, 24
Custom 455 Aged 1000°F			NF, NF, NF, NF	NF, NF NF
Custom 450 Aged 900°F	NF, NF, NF, NF		NF, NF, NF, NF, NF, NF, NF, NF, NF, NF, NF	NF, NF, NF, NF, NF

(a) Tensile specimens with gauge length 9/16", diameter 1/10", stressed to 90% of 0.2% flow stress. NF signifies no failure in 90 day test for Custom 455 and 45 day test for Custom 450.

(b) Bent beams (4.8" x .5" x .05") 2 point loading to 90% of 0.2% flow stress in 20% salt spray. NF signifies no failure in 505 day test.

(c) U-bends (3.88" x .38" x .105"). NF signifies no failure in 300 days for salt spray and 1200 and 400 days at Kure Beach for Custom 455 and 450 respectively. Salt spray for Custom 450 test was 5%.

The data shown in Table 3 for smooth specimens of Custom 450 show it to be immune to cracking. Some U-bend samples were cut transverse to the rolling direction and still resisted cracking.

Precracked Specimens

Data for precracked cantilever beam specimens of Custom 455 are summarized in Figure 1. As predicted from the smooth specimens there is a marked increase in K_{Isc} as the aging temperature is increased. Note that failures occurred in material aged at 1000°F whereas smooth specimens were immune. The change in K_{Isc} with aging temperature is largely a reflection of K_{Ic} changes. K_{Isc} is about 85% of K_{Ic} for all conditions.

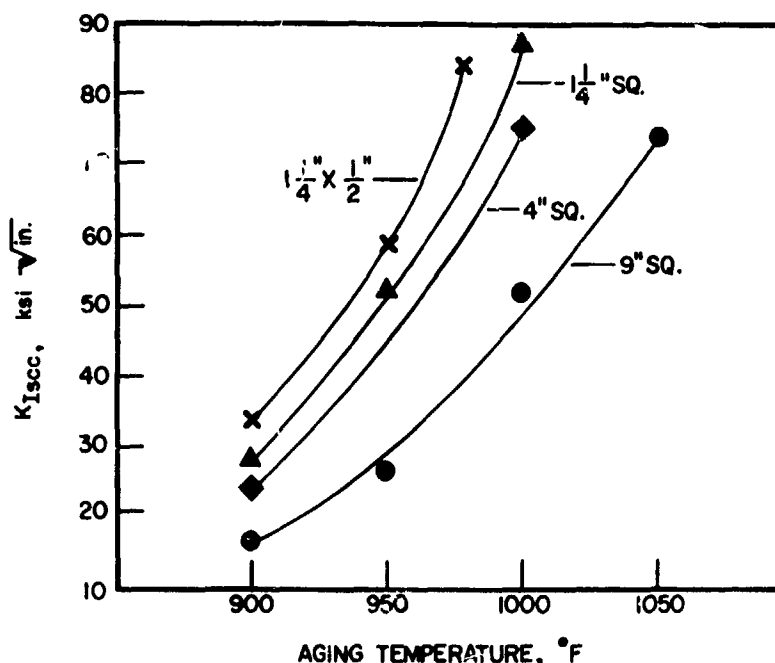


Figure 1. Effect of Original Size and Aging Temperature on K_{Isc} for Custom 455 in 3.5% NaCl, pH 5, 75°F.

Carter et al(1) also obtained no failures in material stressed up to 85% of K_{Ic} .

Figure 1 shows a marked influence of product size and emphasizes the need to define this when discussing K_{Isc} . Again, changes due to product size are largely a function of K_{Ic} changes. Grain size decreased from ASTM 2 for the 9" square to ASTM 7 for the 1-1/4" square. All of the data shown in Figure 1 is for beams cut longitudinal to the working direction. Transverse cut specimens were evaluated for the 9" square material and yielded K_{Ic} and K_{Isc} values about 10% lower.

Custom 450 was also tested in 3.5% NaCl solution (pH 3.6) at 75°F. The notch and precrack were perpendicular to the 3/4" thick plate used for this study. K_{Ic} was 75 KSI $\sqrt{\text{in.}}$ for full hardened material (aged 900°F). No failures were obtained in stress corrosion tests at stress intensities as high as 90% of K_{Ic} (1800 hour tests). This confirms the smooth specimen results showing the alloy to be highly resistant to cracking in chloride media.

SIGNIFICANCE OF K_{Isc}

There is almost a linear relationship between K_{Isc} and yield strength for Custom 455 as expected from previous experience with AISI 4340 and 18 Ni maraging steel - see Figure 2. K_{Isc} -yield strength relationships for three defect sizes are plotted in Figure 2 using the following relationship and assuming the existence of yield point stresses(2).

$$a_{crit} = 0.2 (K_{Isc} / \sigma_{YS})^2$$

Where a_{crit} is the critical defect length (assuming long, thin defects).

Theoretically, a material whose product form and heat treatment put it above the calculated line for defects of size "X" will resist cracking in this media provided there are no defects larger than size "X".

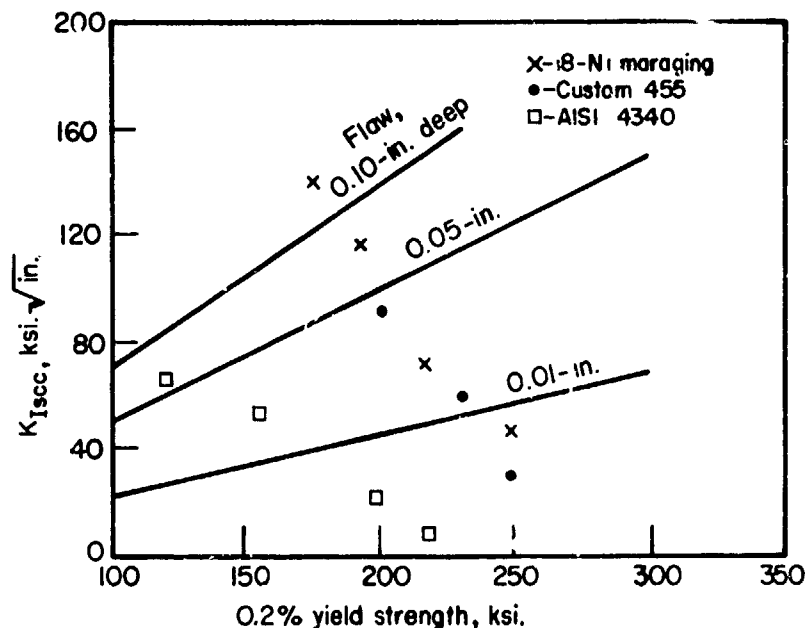


Figure 2. K_{Isc} —Yield Strength Relationships, 3.5% NaCl, pH5

The validity of using K_{Isc} as a design criteria is questionable, however. During our work on Custom 450 we noticed an interesting phenomena which Brown has also reported(3) for a precipitation hardening 13Cr-8Ni-2Mo stainless steel. We observed failure of cantilever beam specimens away from the notch and precrack as shown in Figure 3. Cracking started at a pit formed in the crevice between the corrosion cell and the specimen. Some aging scale left on the specimen probably accelerated the attack.

Brown logically uses the type of failure shown in Figure 3 as evidence that a prime function of a precrack is to serve as a crevice for local chemistry changes - more specifically a lowering of the pH to produce a potential -pH condition conducive to the formation of hydrogen. In a case such as shown in Figure 3 the crevice at the cell wall was more capable of producing corrosion and hydrogen than the one at the bottom of the notch. The fact that a crevice existed along the sides of the specimen at the cell wall would also give a potentially greater source of hydrogen.

In addition to helping explain the role of crevices the behavior in Figure 3 is very significant in that it definitely points to a weakness in the use of K_{Isc} data in design work. The initial stress intensity in the stress corrosion crack area of the specimen shown in Figure 3 must have been very low indeed, whereas the test data predict $K_{Isc} = K_{Ic} = 75 \text{ KSI } \sqrt{\text{in.}}$.

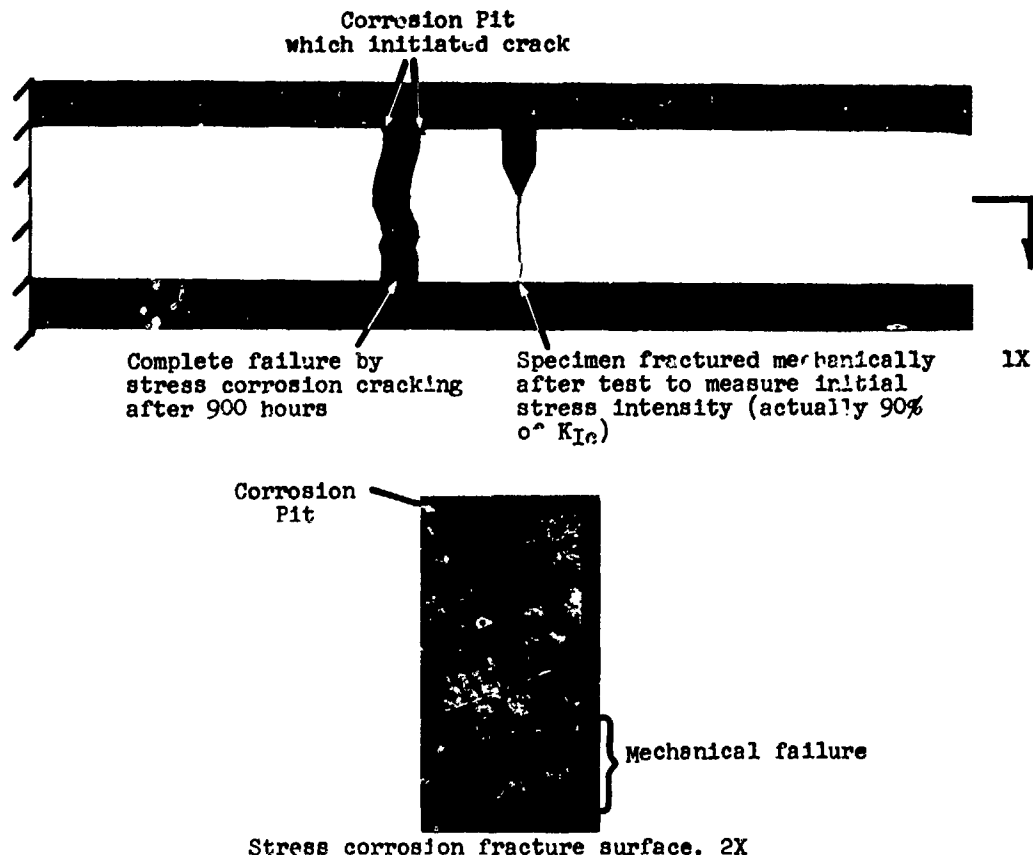


Figure 3. Stress Corrosion Cracking Initiated at Crevice Between Corrosion Cell and Test Specimen. 3.5% NaCl, pH 3.6, 75°F.

Another question relating to the use of K_{Isc} can be described with the following example. Steel A has a K_{Ic} of 70 and a K_{Isc} of 60. Steel B has a K_{Ic} of 50 but does not fail by stress corrosion cracking in tests of the type described here i.e. $K_{Isc} = K_{Ic} = 50$. Which material is most suitable for service in media similar to that used in the testing? Strictly from a mechanics point of view one might select steel A as having the highest K_{Isc} . However, since steel B apparently has better corrosion resistance it might be expected to be less susceptible to chemistry changes that could occur in more serious crevice (and longer exposure times) in service.

Data developed in recent years⁽³⁻⁵⁾ indicate more and more that stress corrosion cracking in high strength steels is caused by hydrogen. To resist cracking a steel must therefore have good general, pitting and crevice corrosion resistance to minimize the amount of hydrogen produced, and good toughness to be able to tolerate small amounts of hydrogen that do enter the metal. These two items (toughness and corrosion resistance) are believed to be the governing factors in determining whether cracking will occur. Obviously there are other important factors e.g. role of surface chemistry in determining how much of the hydrogen produced enters the metal and the behavior of this hydrogen in the strained lattice.

An example of the need for both toughness and corrosion resistance to resist cracking is shown in Table 4. Custom 455 has relatively good corrosion resistance and its K_{Isc} is a high percentage of K_{Ic} . Custom 450 has even better resistance and it does not fail at all in the test. Note that the good corrosion resistance of both of these alloys is dependent upon the fact that the hardening precipitate does not deplete the matrix of large amounts of corrosion resistant elements (e.g. chromium). The experimental alloy on the other hand is quite susceptible to cracking even though it has the highest toughness. Its poor performance is attributed to the presence of corrosion resistant elements in the hardening precipitate. The depletion of the matrix in these elements lowers the alloy's corrosion resistance. This results in a ready source of hydrogen (from the corrosion reaction). U-bends of the experimental alloy also failed very readily, even in high humidity without any chlorides.

Table 4 INFLUENCE OF HARDENING PRECIPITATE ON K_{Isc} (3.5% NaCl, pH 5, 75°F)

Alloy	Aging Temp.	K_{Ic} (KSI, $\sqrt{\text{in.}}$)	$K_{Isc}/K_{Ic} \%$	Hardening Precipitate
Custom 455	950 F	67	87	Laves (Fe, Ti)
Custom 450	900°F	75	100	Laves (Fe, Nb, Mo)
Experimental	975°F	105	<50	R Phase (Cr, Mo, Co, Fe)

The probability that stress corrosion cracking in this type of material is largely dependent upon two factors (1) toughness (2) corrosion and chemistry changes in crevices, pits etc. suggests alternative means of evaluation.

One could feasibly increase the severity of the precracked test by introducing crevices on the sides of the specimen adjacent to the crack but this might prove difficult to quantify. Alternatively one might be able to dispense with the stress corrosion test altogether in some systems. For Custom 455 for example, K_{ISCC} is very much dependent upon K_{IC} because the factors which change K_{IC} have little effect on corrosion resistance. Possibly this behavior could be predicted from pitting potentials and/or protection potentials⁽⁶⁾ derived from anodic polarization data. This approach might also predict the type of phenomena shown in Figure 3.

K_{IC} and pitting/protection potentials can be determined in a few hours and the use of some function of these to predict stress corrosion cracking behavior could perhaps eliminate the need for many stress corrosion tests. The writer wishes to emphasize that he is suggesting this as a possible approach and realizes (as noted above) that many other factors can be important in a stress corrosion situation.

CONTACT WITH ACTIVE METALS

Precipitation hardening stainless steels may come into contact with more active metals during service. This occurs frequently in systems using active metals for galvanic protection or (particularly in aerospace applications) where low density metals such as aluminum are in widespread use.

This contact with active metals such as aluminum can result in cracking of the stainless steel. This is not stress corrosion cracking but hydrogen cracking due to hydrogen produced on the stainless steel which is serving as a cathode.

In predicting the performance of high strength stainless steels in this situation it is sometimes erroneously assumed that a material with better stress corrosion cracking resistance (e.g. low K_{IC}/K_{ISCC} ratio) will be more resistant. This is not necessarily so and depends upon why a material has the low ratio. If it is resistant to stress corrosion cracking because of high toughness then this property will be useful in resisting hydrogen cracking when in contact with active metals. On the other hand if it owes its stress corrosion cracking resistance primarily to good corrosion and crevice corrosion resistance then these properties are of no use in avoiding the galvanic corrosion problem and could in fact aggravate it by increasing one of the driving forces (potential difference). For example, the experimental alloy in Table 4 would very probably be superior to the other alloys in a galvanic corrosion/hydrogen cracking situation even though its stress corrosion cracking resistance is inferior.

Toughness, potential differences, area ratios, design parameters and polarization characteristics (particularly for the active metal) are more useful for predicting performance in these situations than are stress corrosion cracking data.

CONCLUSIONS

1. Smooth and precracked specimens of Custom 455 show improved stress corrosion cracking resistance as the aging temperature is increased. Aging temperatures of 950°F and preferably higher are normally used for applications where stress corrosion cracking is a suspected possibility.
2. K_{ISCC} for Custom 455 decreases with increasing product size in the same way as K_{IC} .
3. No regular failures were obtained in either smooth or precracked specimens of full hardened Custom 450. The alloy is therefore superior to other precipitation hardening stainless steels. However, it is not immune to failure in chloride solutions as evidenced by cracking under large crevice areas.
4. Precracked specimens show much better reproducibility than smooth specimens for a grade such as Custom 455 and represent a more severe test.
5. The use of K_{ISCC} as a design criteria is questionable in view of the probability that design factors (e.g. crevices) in service could cause the corrosion aspect of cracking to dominate and produce cracking at lower stress intensities.
6. Stress corrosion cracking in these materials is believed to be caused by hydrogen and to be very much dependent upon the interplay of (1) toughness and (2) corrosion resistance. It is suggested therefore that it might be possible to predict stress corrosion cracking resistance based on a consideration of K_{IC} and anodic polarization parameters such as pitting and/or protection potentials.
7. Failure of martensitic stainless steels in contact with more active metals (e.g. aluminum) is not stress corrosion cracking and stress corrosion test data is of limited value for predicting performance in these situations.

REFERENCES

1. C.S. Carter, D.G. Farwich, A.M. Ross and J.M. Uchida, Corrosion, Vol. 27, May, 1971, pp. 190-195.
2. B.F. Brown, "Stress-Corrosion Cracking—A Perspective Review of the Problem," Report 7130, Naval Research Laboratories, Washington D.C., June 16, 1970.
3. B.F. Brown, "ARPA Coupling Program on Stress-Corrosion Cracking—Final Technical Report," Report 7168, Naval Research Laboratories, Washington D.C., September 21, 1970.
4. B.F. Brown, "On the Electrochemistry of Stress Corrosion Cracking of High Strength Steels," 4th International Congress on Metallic Corrosion, September, 1969, Amsterdam, The Netherlands. Proceedings to be published by NACE, Houston, Texas.
5. B.E. Wilde, Corrosion, Vol. 27, August, 1971, pp. 326-333.
6. B.E. Wilde and E. Williams, J. Electrochem. Soc., Vol. 117, June, 1970, pp. 775-779.

**INVESTIGATION OF AN ACCELERATED STRESS CORROSION
CRACKING METHOD**

by

M.Hugo, J.Bellot and E.Herzog
Société Nouvelle des Aciéries de Pompey (54)
France

INVESTIGATION OF AN ACCELERATED STRESS CORROSION CRACKING METHOD

M. HUGO, J. BELLOT and E. HERZOG

Abstract

The authors suggest an accelerated slow strain rate tensile method of testing which could be very useful for inspection purposes. Slow straining in nitrate, NaOH and acid environments are described.

I. INTRODUCTION

The choice of correct and rapid testing methods is quite intricate when the material is exposed to both corrodent and stress. Accelerated methods of testing are necessary either for selecting a material appropriate to withstand a certain stress level, either for the same material under different service conditions or for selection of the most appropriate type of assembly i.e. weldment, heat treatment before and after welding, the life of bolts and rivets. Life and safety concerns should also deal with the unforeseen factor i.e. with higher stress levels, yielding and straining in notched areas or with a plastic accommodation of the structure. The simplest stress distribution is found in uniaxial tensile testing; a great number of tests are however required since different stress levels are to be tried both in the elastic and plastic ranges.

With a stable material, these tests run over a long time as a result of which numerous points on a stress vs. time curve are to be plotted. An attempt was made to develop a more rapid method of testing likely to put forward initiation and propagation of particular paths of corrosion such as pits, grain boundaries along slip planes. These various types of attack frequently appear at the vicinity of the yield point, and after yielding in the plastic area. The authors decided therefore to proceed at slow strain rate, starting for example at a 0,7 to 0,5 fraction of yield point up to rupture i.e. at a 0,8 - 1,6 % elongation rate per hour. Strain rate is dependent on the purpose of investigation, in our case, the ageing of mild steel and our aim being a result after 24 to 50 hours. In unalloyed steels, C and N atoms diffuse rapidly at 100/130°C, the temperature boiling range of nitrates, caustic soda and acid solutions. This diffusion promotes intergranular corrosion in some cases in presence of passivating and specifically adsorbable anions.

Our investigation has been carried out at a rate of 10⁻⁵ cm . sec⁻¹ i.e. the diffusion rate of C + N atoms in α ferrite. Indeed, with high rates (10 %/h), the strain rate exceeds the propagation rate of intergranular corrosion and rupture is of a mixed type i.e. a superficial intergranular attack and ductile cup and cone rupture over the major part of the section. This method of testing has already been described in earlier publications dealing with research on C and low alloy steels by the laboratories of Prof. PARKINS, BOHNENKAMP and Société Nouvelle des Acières de POMPEY. These studies were carried out on smooth cylindrical specimens.

As regards titanium, stainless, copper and aluminium alloys, more work was reported on sharp notched pre-cracked test bars (see bibliography). There exist of course other publications in this connection, we only quoted a few examples. The aim of the present paper is to emphasize the practical interest of such testing methods likely to be used for inspection purposes. It does not require costly facilities and test interpretation is easy. We had no further considerations in mind and did not use other techniques such as electro-chemical measurements.

II. EXPERIMENTAL TECHNIQUES

In our corrosion tests, we always use the same type of specimen in the same material conditions, whatever be the method retained i.e. a tensile test bar, ϕ 4 mm, with smooth surface, polished mechanically, useful length 30 mm and 5 mm radius to threaded ends. This sample can be strained in a tensile-corrosion dead load and lever type testing device, under the following conditions :

1. without stress
2. under constant stress
3. with slow tensile strain rate
4. under stress relaxation (was not used).

The present paper describes the results obtained with conditions 1, 2 and 3 on different steels and with different corrodents. A closed container the upper part of which was cooled, carried the boiling solution. Thus concentration remained constant.

III. RESULTSCorrosion in boiling nitrates

The behaviour of normalized rimmed steels, Al or Si killed steels (carbon range : 0,02 to 0,7 %) was observed in a solution containing 57 % of calcium nitrate and 3 % of ammonium nitrate ; density 1,3 and pH 6,5 at 108°C.

Our aim was to show the s.c.c. determining influence of the carbon content in the different methods of investigation.

. Without stress

In certain cases, intergranular corrosion initiation mechanisms can be observed by a corrosion test without stress. Specimens were immersed in the boiling solution. Exposure time : 100, 200 and 300 hours. The effect of the corrodent has been observed through microscopic examination of a longitudinal section. Owing to potential differences between the grain face (passivated) and the boundary (active) difficult to measure at this scale, all C-steels were, to some extent, susceptible to intergranular corrosion. Depth of intergranular corrosion increases within a decreasing C content. At a carbon range of 0,02 to 0,06, intergranular penetration rate increases with time (figure 1). Intergranular crack initiation and propagation have been noted (without applied stress) (micrography - fig. 2). From a certain carbon content i.e. $C \geq 0,12$, depth of intergranular corrosion is constant after an exposure time of 200 hours. Cracks are stopped by pearlitic areas (fig. 3). Figure 4 shows depths of intergranular attack versus carbon contents of the steels investigated after a 300 hours exposure time. On the other hand, very pure, C-free iron is not subject to grain boundary attack as steel with C + N stabilized by Ti.

. Under constant stress

Steels with different carbon contents were loaded under constant conditions for stresses under, equal to and above yield point (E 0,2). The specimens were cut along their axis and the depth of intergranular attacks was measured. Results are shown in figure 5. Properly speaking, steels with a carbon range of 0,01 to 0,06 do not have a non rupture level. This situation is confirmed by the fact that they already exhibit propagation of intergranular cracks without stress. Under 0,4 E 0,2 and rupture after ~ 300 hours, intergranular cracks reaching 1 mm of depth were observed on each side of the rupture. Non rupture level increases with carbon content ; for $C \geq 0,12$ %, it is nearly equal to E 0,2. Beyond this content, uniform general intergranular corrosion (depth 40 to 60 μ) is observed on the specimens which have not ruptured after 500 h exposure, (stress $> E 0,2$). Depth of attack varies with grain size and with the distribution of pearlitic alignments which act as crack arresters.

. With slow strain rates

Specimens were strained slowly in oil and nitrates at an initial rate of 10^{-5} cm s $^{-1}$ at 110°C (0,8 %/h). The stress-strain curves were recorded by a dynamometric ring provided with strain gages. The tensile specimen was gripped within a tight vessel containing the boiling solution. A comparison was made of the stress-strain curves obtained in the nitrates and in oil (at 110°C).

- yield point E 0,2
- maximum stress reached during testing R
- specimen life time t
- elongation and reduction of area (%)
- strain hardening
- time to rupture ratio $\frac{t_{oil}}{t_{corrodent}}$
- maximum depth of cracks on the broken specimen :
 - a). near the threaded ends : slightly strained area
 - b). near the rupture, a heavily strained area

As an example, we show the curves registered for the steels containing 0,02, 0,17 and 0,7 % of C. The rupture energy for slow strained specimens under corrosion could be compared to that of uncorroded ones.

. Steel containing 0,02 % of C

In oil, rupture is induced after 15 hours with an elongation of 22 % and maximum R of 54 kg/mm 2 . In nitrates, brittle fracture occurs after 2 hours with a maximum load of 28 kg/mm 2 (figure 6).

Propagation of scc during straining is represented by fig. 7 ; these tests were interrupted at different steps of the curve.

First step : Examination after the first curve jog showed one 0,25 mm crack starting at each end of the tensile specimen, and numerous other minute cracks of 0,02 mm.

Second step : After the 2nd discontinuity, the cracks near the end had reached 0,45 mm, while the minute cracks distributed over the length of the specimens measured 0,02 - 0,03 mm

Third step : At the third discontinuity, numerous mouths of cracks (depth 0,5 mm) had appeared, which, after slight elongation induced rupture of the specimen. Intergranular crack propagation thus initiates near yield point elongation.

. Steel with 0,17 % C

The first cracks (figure 8) are only detected at the first discontinuities of the stress-strain curve in the plastic range. When C content increases, these discontinuities appear farther in the plastic range. Crack propagation is located in the plastic area of the curve. Above a C content of 0,5/0,6, the slope of the stress-strain curve becomes smooth after yield point.

. Steel with 0,7 % C

Figure 9 shows the yield point followed by a smooth curve. Under the present slow strain rate conditions, a crack in steel containing 0,7 % carbon, propagates at the point of mechanical instability due to stress concentration as a result of the reduction of area. The test was run for 2 h 20 for a maximum R of 55 kg/mm 2 (microscopic examination shows an intergranular crack in pearlitic structure - fig. 10). The table (fig. 11) summarizes the main characteristics obtained with the three test methods. Slow strain rate tensile testing arrived much more rapidly at the same order of merit for the tested C-steels. Consequently, this method deserves closer investigation.

Corrosion in NaOH environment

The action of NaOH on stress cracking corrosion is much slower than that of the ammonium nitrates. In a first stage, slow straining was used in order to determine the most dangerous concentration for intergranular corrosion in mild steels containing 0,02 % C (fig. 12) (strain rate was reduced to 0,8 %/h against 1,6 %/h in nitrates). The criteria retained for corrosion in 35 % NaOH boiling solution were :

- the specimen life time
- the loss of reduction of area
- the depth of intergranular attacks
 - a). in the body of the specimen
 - b). in the necking area

. Corrosion under constant stress

Intergranular corrosion without stress and imposed potential may occur under certain extreme conditions in steels used in industry in caustic soda solutions. Grain boundaries are attacked, grains are disintegrated and dissolved. This process also occurs under static load and under $E 0,2$ stresses or above. Time to rupture is usually very long. The effect of a 35 % caustic soda solution on specimens under a stress near $E 0,2$ was observed after different exposure times (the steels were identical to those tested in nitrate environments) (fig. 13). Increase of C content influences favourably the intergranular corrosion resistance both in NaOH and nitrate environment.

. Stress corrosion cracking with slow tensile straining

Correlation found between the E loss (ΔE), the crack depth under slow straining conditions and the behaviour of steel under constant load is satisfactory (table V - fig. 14).

Acid corrosion

Slow rate straining was used for the determination of the intergranular corrosion resistance of austenitic steels in an acid environment. The test solution had the following chemical composition :

140 g/l P_2O_5 250 g/l CaO
600 g/l NO_3H

Tests were carried out at the boiling temperature of 132°C. A duplicate test has been made on a standard steel Z 6 CN 18-10 at various heat treatments (C 0,05 Cr 17 Ni 10) :

- a). hyperquenching 1100°C 30'
- b). and subsequent annealing at + 700°C 30' (carbide precipitation)

. Mechanical characteristics

Table VI (fig. 15)

Treatment	Temperature	E kg/mm ²	R_m kg/mm ²	A %	E %
1100°C T.E.	20	23	56	65	80
	130	19	45	43	80
1100°C T.E. + 700°C 30'	20	23	57	65	79
	130	19	46	42	80

. Direct attack (without stress)

On hyperquenched and sensitized austenite at 700°C. After a test duration of 15 days, generalized intergranular corrosion depth of 300 μ had occurred.

. Corrosion under constant stress

Table VII (fig. 16)

Treatment	Stress kg/mm ²	Specimen Life time	Intergranular corrosion
1100°C T.E.	17	SR 240 h	none
1100°C T.E. + 700°C	17	118 h	intergranular corrosion over whole specimen. Brittle fracture without deformation $\Delta E = 100$ %

- . Slow rate straining corrosion
($v = 0,8 \text{ \%}/h$)

Table VIII (fig. 17)

Treatment	Specimen Life Time	R maxi kg/mm ²	A %	ΔE %	Stress cracking corrosion
1100°C T.E.	97 h	47	52	0	entirely intergranular
1100°C T.E. + 700°C	9 h	17	0	100	

The susceptibility to intergranular corrosion of this steel, at sensitized condition, is strongly enhanced by slow tensile straining. (fig. 18)

IV. CONCLUSIONS

The interest of slow rate tensile strain testing (0,8 to 1,6 \%/h of elongation) has been shown for the following cases :

- C-steels in concentrated solutions of boiling nitrates and caustic soda
- sensitized stainless steel 18/10 in an acid environment.

Compared with tests under constant stress and stresses equal to yield point, the economy of time is considerable and the number of tests reduced. In a caustic soda environment, intergranular rupture is achieved between 30 and 40 hours, whereas a test at E 0,2 needs 100 times more. This method of testing allows determination of the parameters which accelerate or induce rupture e.g. concentration of a corrodent, degree of cold work etc. A rapid assessment of rupture risks, danger of initiation and propagation of particular corrosion types is possible.

In our opinion, the latter point is the most important one i.e. providing the possibility of assessing these dangers in ductile and carbon steels in a given environment and under given conditions. Last but not least, the comparison and inspection of materials by a standard test, quite easy, become possible thanks to time limitation.

B i b l i o g r a p h y

- (1) HENTHORNE (M.), PARKINS (R.N.) Corr. Sci. 1966, p. 357-369
- (2) PARKINS (R.N.), HUMPHRIES Corr. Sci. 1967, p. 747-761
- (3) BOHNENKAMP Arch. Eisenh. 1968, p. 363
- (4) HERZOG (E.), BACKER (L.), HUGO (M.), VALERO (M.) Mém. Sci. Rev. Mét. 1967 p. 413/421
- (5) BELLOT (J.), HUGO (M.), ROLIN (M.), HERZOG (E.) Mém. Sci. Rev. Mét. 1968 p. 607/625
- (6) ORMAN (S.) Corr. Sci. 1969, p. 849
1965, p. 745

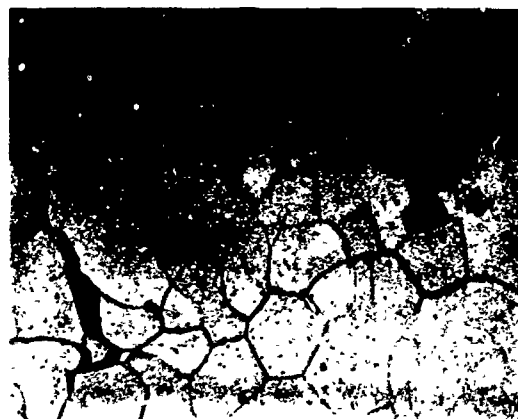
Table I

C content (%)	Depth of intergranular attack		
	Exposure time		
	100 hours	200 hours	300 hours
0,02/0,04	40 μ	70 μ	210 μ
0,17	10 μ	25 μ	25 μ
0,70	5 μ	10 μ	10 μ

Figure 1



C = 0,02 Gr x 500



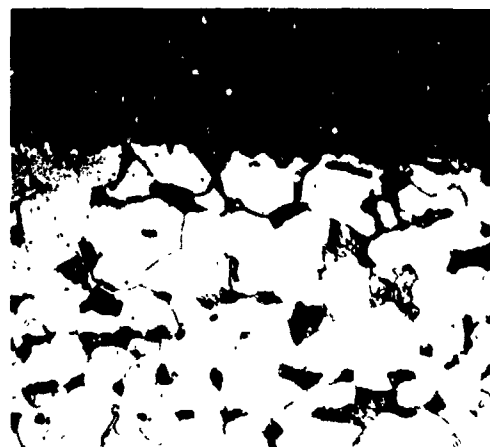
Corrosion tests in boiling nitrate solution
(without stress 300 hours)
Propagation of intergranular attack

Figure 2

Reproduced from
best available copy.

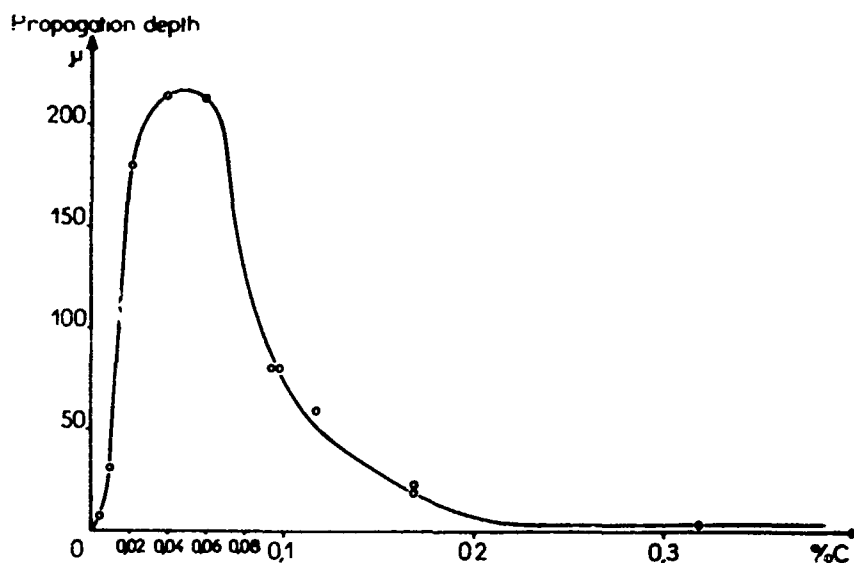


NITRATES

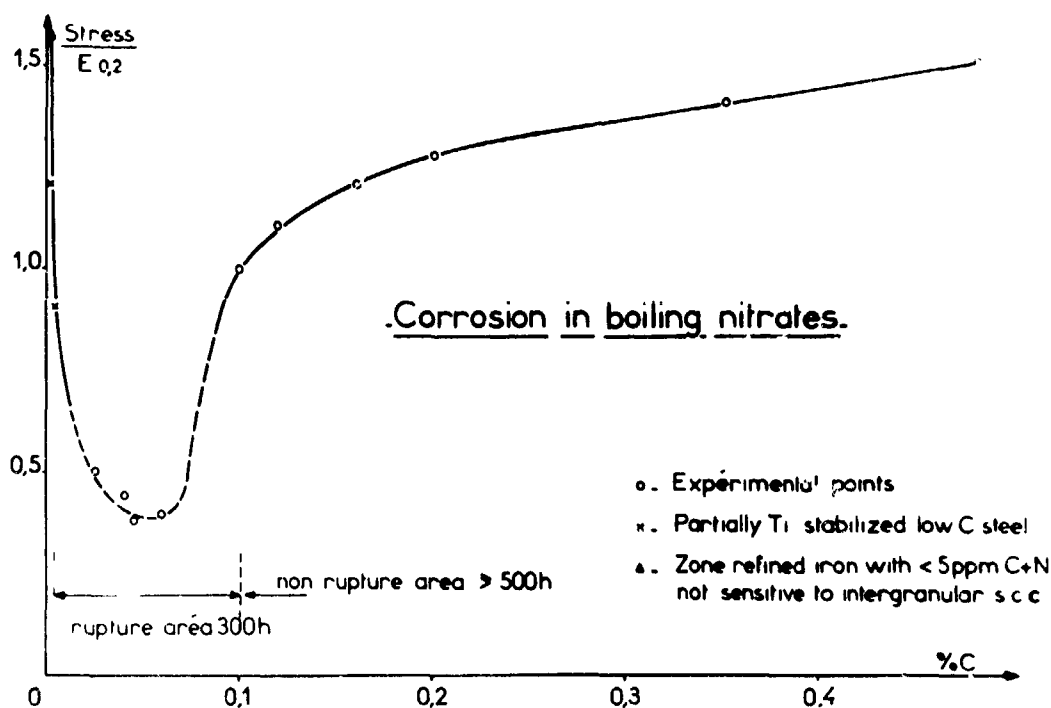


NaOH
cracks arrested on pearlite
C = 0,17 steel

Figure 3



Relation between C. content and intergranular corrosion depth (tests without stress) 300 hours immersion in boiling nitrates at 110°C. $\text{Ca}(\text{NO}_3)_2$ 57%
 NH_4NO_3 3%
 H_2O 40% **Fig. 4**



Constant load testing in nitrates relation between C content and non rupture stress level (500 hours) **Fig. 5**

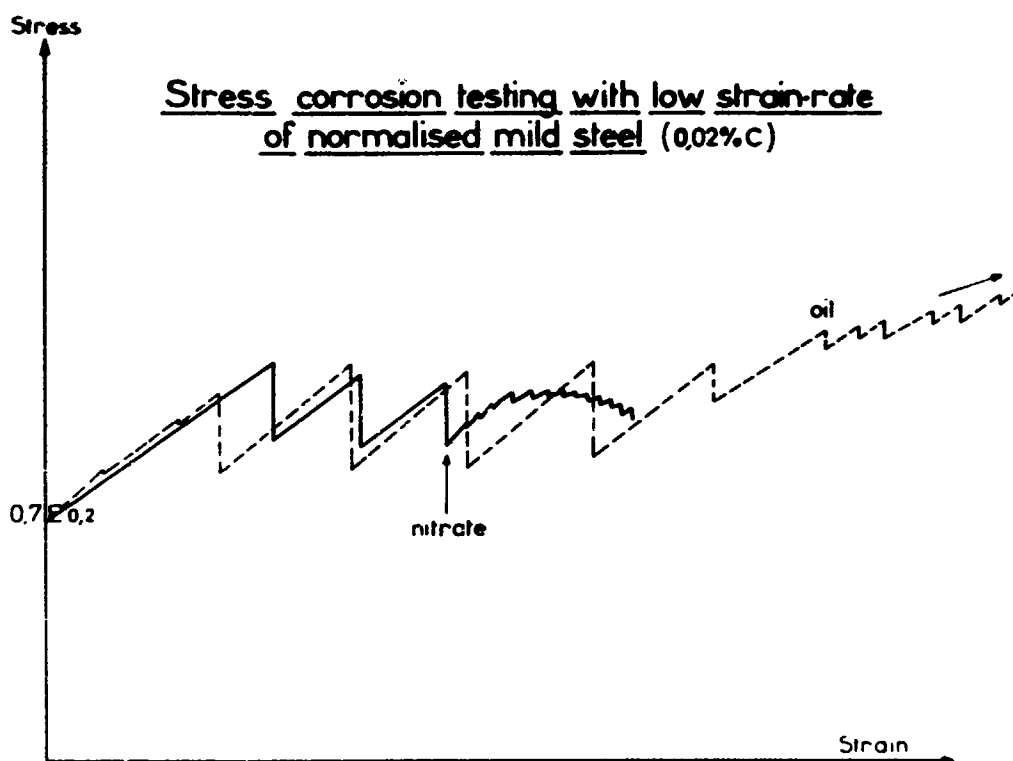


fig 6

Stress corrosion testing with low strain-rate
of normalised mild steel (0.02%C)

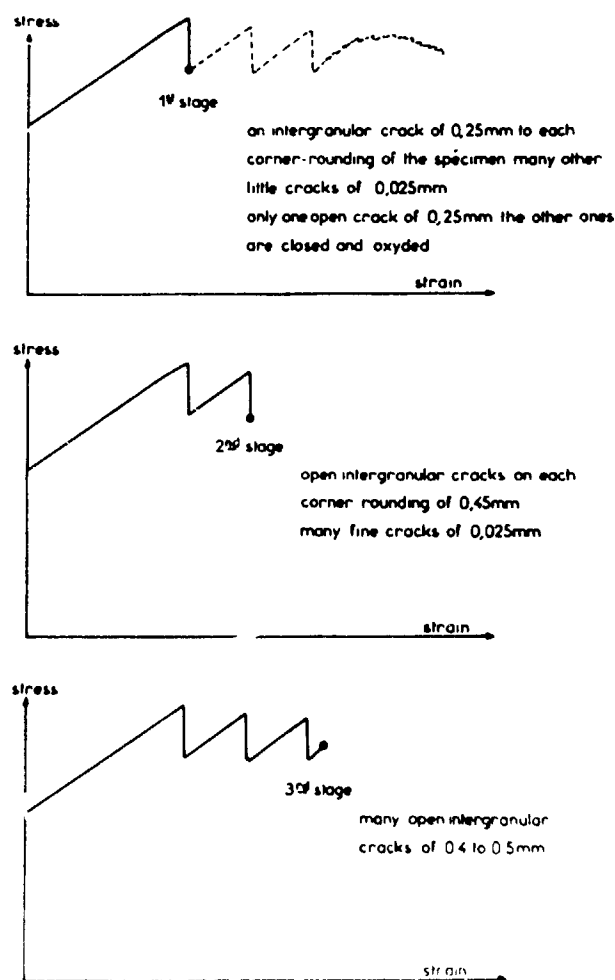


fig 7

Stress corrosion in 110°C nitrates
mild steel (0,17%C) - normalised

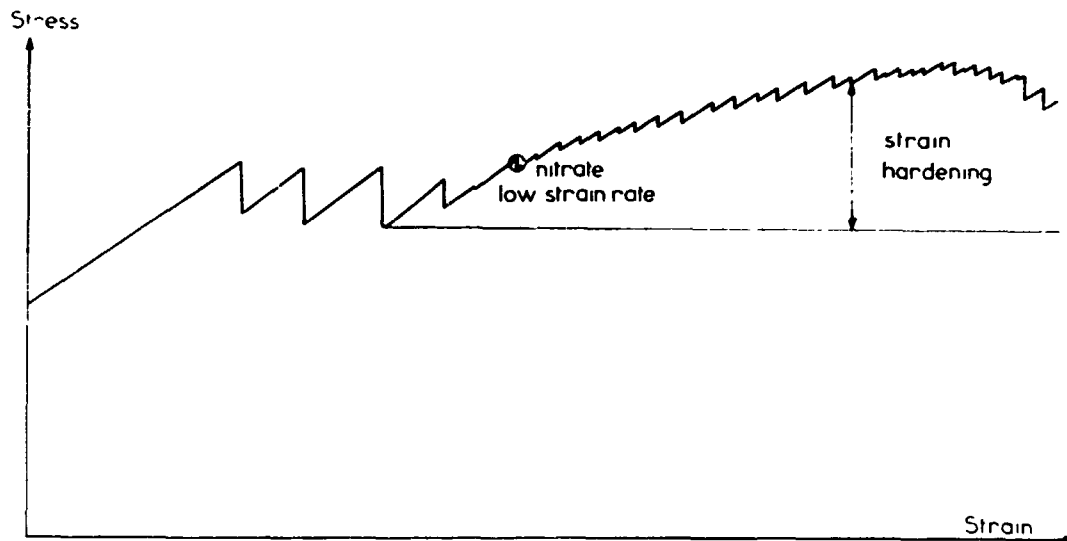


fig 8

Stress corrosion testing with low strain-rate
of normalised high carbon steel (0,7%C)

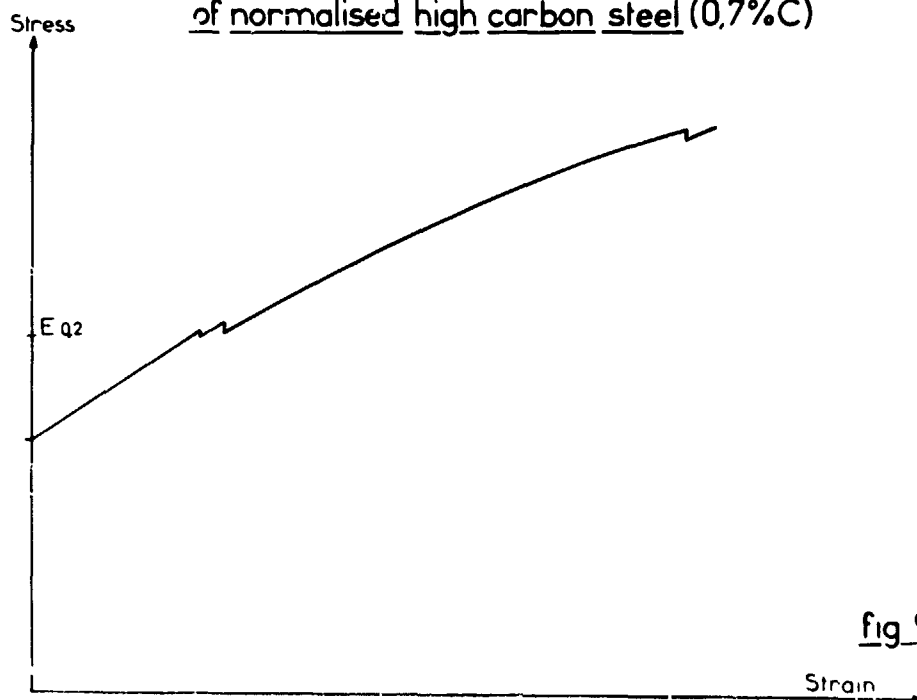


fig 9



Intergranular crack in pearlitic structure

Figure 10

Table II

	C 0,02	C 0,17	C 0,70
1). <u>without stress</u> Depth of penetration at 300h Propagation rate	210 increasing	25 nought	10 nought
2). <u>with stress</u> Stress without rupture (t_{NR}) Depth of penetration after 500h (t_{NR})	ncught > 1 mm (0,4 E/300 h)	1,2 E 40/50 μ	1,7 E 30/40 μ
3). <u>Slow rate tensile straining</u> R maxi kg:mm ² E kg:mm ² Strain hardening R-E Time ratio $\frac{oil}{corrodent}$	25 20/28 nought 8	38 23/28 10 5	55 35 20 4
Range of stress propagation	Elastic (without stress)	Plastic (after yield point elongation)	Point of mechanical instability (necking area)
Maximum depth of cracks after slow straining	≥ 1 mm	100 μ	50 μ
Σ to rupture %	0	2/3 %	4/5 %

Figure 11

Table III

Concentration of boiling NaOH %	Life time h	R maximum kg/mm ²	Loss of reduction of area %	Corrosion types
15	44	43	2,8	Localized intergranular penetration of 15 μ
25	41	40	5,5	+ numerous intergranular penetration of 25 μ
35	26	40	50	Generalized intergranular corrosion 200 μ and 400 μ in Σ
45	35	43	7	Transgranular and important dissolution

Figure 12

Table IV

Steels	E 0,2 130°C kg/mm ²	Stress kg/mm ²	Life time hours	Observations regarding corrosion types
C 0,02	22	20	SR 720 h	Grain disintegration-intergranular cracks of 150 μ
		25	R 1 828 h	Brittle rupture, grain disintegration, intergranular cracks ≥ 1 mm
C 0,17	23	25	SR 720 h	Grain disintegration, intergranular cracks 25 μ
		25	SR 1 440 h	Grain disintegration, intergranular cracks 45 μ
		25	SR 2 880 h	Grain disintegration, intergranular cracks 45 μ
C 0,35	35	40	SR 720 h	Grain disintegration. Intergranular corrosion 10 μ
		40	SR 1 440 h	Grain disintegration, intergranular corrosion 15 μ
		40	SR 2 880 h	Grain disintegration, intergranular corrosion 15 μ

R = rupture SR = without rupture

Figure 13

Table V

Steels	Specimen life time (h)	R maximum kg/mm ²	$\Delta \Sigma$ %	Corrosion
C 0,02	26	40	52	Generalized intergranular corrosion from 200 μ to 400 μ in Σ
C 0,17 (rimmed)	37	50	35	Generalized intergranular corrosion 40 to 150 μ in Σ
C 0,17 (Si killed)	43	35	30	ditto
C 0,35	30	50	30	Generalized intergranular corrosion 40 and 90 μ in Σ

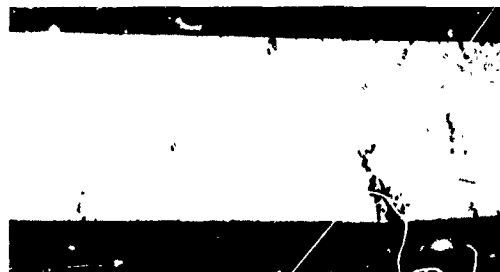
Σ necked area near rupture

Figure 14

ACID CORROSION Stainless steel 18/10



Gr x 2



Gr x 11



Gr x 270

Intergranular corrosion feature in acid environment

Figure 18

MICROSCOPIC IDENTIFICATION OF STRESS-CORROSION
CRACKING IN STEELS WITH HIGH YIELD STRENGTH

E. H. Phelps
Applied Research Laboratory
U. S. Steel Corporation
Monroeville, Pennsylvania

Abstract

The microscopic features of stress-corrosion cracking in steels with high yield strength are reviewed with the objective of establishing specific characteristics by which stress corrosion can be identified. Photomicrographs of stress-corrosion cracking obtained under known exposure conditions on specimens of alloy steels, of precipitation hardenable stainless steels, and of maraging steels are presented and discussed. The most consistent feature of stress-corrosion cracking in these steels is that it usually initiates at multiple sites on the steel surface. Cracking may be intergranular or transgranular depending on the alloy system and the environment. Branching occurs in some instances but is not a consistent characteristic of stress-corrosion cracking in steels with high yield strength.

MICROSCOPIC IDENTIFICATION OF STRESS-CORROSION CRACKING IN STEELS WITH HIGH YIELD STRENGTH

E. H. Phelps

Introduction

When service failures are encountered, it is essential that a correct diagnosis of the cause of failure be made so that appropriate corrective steps can be taken to prevent further occurrences. When stress-corrosion cracking is the suspected cause of failure, a careful microscopic examination is probably the most important diagnostic tool available. In this paper, the general guidelines that have been used in the past for diagnosing stress-corrosion cracking will be reviewed and compared with the microscopic appearance of stress-corrosion cracks produced in steels with high yield strength under known exposure conditions. The intent is to provide a guide that will assist future investigators concerned with the performance of the higher strength steels.

Metallographic techniques are used to examine cracks by cutting and polishing cross sections or surface sections, the former being the most common method. The sections should preferably be cut to include secondary cracks, if they are present. The most informative procedure is to first examine the polished specimen before etching and again examine after etching. The unetched condition is most suitable for revealing the details of the crack path. Light etching permits the observer to determine the relationship between the crack path and the microstructure. The scanning electron microscope (SEM) is an extremely powerful tool for examining the fracture face itself. Replica techniques can also be used for this purpose but they are very time consuming and do not provide the large depth of field that can be obtained with the SEM.

The following criteria for diagnosing cracks as stress-corrosion cracks have been discussed previously^{1)*} and are presented here to serve as a basis for the discussion to follow.

1. One criterion is to determine whether the path of cracking is the same as the characteristic path for stress-corrosion cracking in the alloy system involved. For example, in annealed stainless steel, stress-corrosion cracking characteristically follows a transgranular path, whereas in carbon steel it characteristically follows an intergranular path. It should be recognized, however, that this criterion may sometimes be misleading when metallurgical or environmental factors have an influence on the path of cracking. As an example, some alloys are known to exhibit both intergranular and transgranular cracking. As another example, it is known that the path of cracking in some alloys can be controlled between transgranular and intergranular paths simply by changing the environment.
2. Perhaps the most useful criterion in metallographic examinations is that stress-corrosion cracks usually follow branched paths through the metal. This is a fairly general characteristic and applies whether the cracks are transgranular or intergranular. Even this criterion is not universally applicable, however, because sometimes stress-corrosion cracks are not branched.
3. Another characteristic of stress-corrosion cracks is that they usually initiate at many points on the surface, whereas mechanically induced cracks generally have one point of initiation. However, this is also a general rather than a universal characteristic.

Microscopic Appearance of Stress-Corrosion Cracking in Steels With High Yield Strengths

The microscopic appearance of stress-corrosion cracking in a number of different heat-treated martensitic steels with high yield strengths is presented in Figures 1 to 14. Figures 1 to 11 are metallographic cross sections and in all cases the path of cracking is from the top of the photomicrograph. Figures 12 to 14 are photomicrographs taken with

* See References.

the scanning electron microscope. All the cracks shown developed under known conditions on several different types of stress-corrosion specimens. Some specimens were exposed to laboratory solutions, whereas others were exposed to marine atmosphere, flowing sea water, or tidal exposure. The latter exposures were conducted at the International Nickel Company's test facilities at Harbor Island and Kure Beach, North Carolina. Each figure includes pertinent information concerning the steel tested, exposure conditions, and exposure time. The chemical compositions of the steels are presented in Table I.

The photomicrographs shown were selected as being generally representative of the stress-corrosion cracks produced by the stated exposure conditions. They were chosen from the results of a number of different research programs conducted by the Applied Research Laboratory over the past several years. With the exception of Figures 13 and 14 which show the appearance of cracks produced by applied cathodic current, all the cracks in the photomicrographs are considered to be stress-corrosion cracks in accordance with the definition²⁾ of this phenomenon, "Cracking resulting from the combined effect of corrosion and stress." However, for some of the cracks shown, the actual crack propagation mechanism may involve embrittlement by hydrogen generated at the cathodes of local corrosion cells on the steel surface. Cracks of this type are nevertheless still regarded as examples of stress-corrosion cracking, the definition of which does not imply a mechanism.

The salient features of each of the photomicrographs are as follows:

Figure 1: Cr-Mo-Si-V alloy steel in marine atmosphere

Crack path appears to be intergranular with respect to prior austenite grain boundaries. Relatively little branching is evident.

Figure 2: Ni-Cr-Mo alloy steel in H₂S solution

Crack path is transgranular as evidenced by straight portions of cracks. Crack shows extensive branching, and multiple initiation of cracking is evident at corrosion pits.

Figure 3: 12Cr-Mo-V stainless steel in marine atmosphere

Crack exhibits extensive branching and is intergranular with respect to prior austenite grain boundaries.

Figure 4: Precipitation hardenable stainless steel in marine atmosphere

Crack is unbranched and transgranular as evidenced by straight path.

Figure 5: 18Ni-Co-Mo maraging steel in marine atmosphere

Photomicrograph shows multiple sites of crack initiation at corrosion pits. Crack path is not apparent.

Figure 6: 18Ni-Co-Mo maraging steel in marine atmosphere

Photomicrograph shows multiple crack initiation at corrosion pits. Cracks exhibit relatively extensive branching, but path with respect to grains is not evident.

Figure 7: 18Ni-Co-Mo maraging steel in marine atmosphere

Crack shows moderate branching and is predominantly intergranular.

Figure 8: 18Ni-Co-Mo maraging steel in marine atmosphere

Crack is relatively unbranched and appears to follow planes in the structure. Intergranular and transgranular cracking are both evident.

Figure 9: 18Ni-Co-Mo maraging steel in sulfide solution

Crack is highly branched and transgranular.

Figure 10: 12Ni-5Cr-3Mo maraging steel with weld bead in tidal zone

Crack is unbranched in weld metal and heat-affected zone but starts to branch as it approaches base metal. Path is predominantly intergranular in base metal.

Figure 11: 18Ni-Cr-Mo maraging steel in flowing sea water

This photomicrograph shows the tip of a propagating crack in a precracked wedge-open-loading specimen. Note that the tip area contains a large number of branched, transgranular cracks. Application of fracture mechanics to correctly determine the stress intensity is not possible with this type of crack-tip behavior.

Figure 12: 12Cr-Mo-V stainless steel in 3 percent NaCl with applied anodic current

With these exposure conditions, earlier work³⁾ indicated that the cause of crack propagation is active-path corrosion. Recently, however, it has been proposed⁴⁾ that hydrogen absorption is responsible for crack growth even with applied anodic current. In this mechanism, hydrogen absorption takes place in the crack-tip region as a result of cathodic discharge of protons resulting from hydrolysis of anodic-dissolution products. Anodic dissolution is thus considered to be necessary for crack-tip acidification but is not the primary crack-growth mechanism. The scanning electron micrograph clearly shows that the initial portion of the crack is intergranular and that corrosion on some of the grain surfaces has occurred. The original machined surface and a region of ductile tearing are also evident.

Figure 13: 12Cr-Mo-V stainless steel in 3 percent NaCl with applied cathodic current

With applied cathodic current, the mechanism of crack propagation is hydrogen embrittlement.³⁾ The scanning electron micrograph shows that the crack in the area shown is intergranular. Crack branching is evident at the grain intersections.

Figure 14: 12Cr-Mo-V stainless steel in 3 percent NaCl with applied cathodic current

This photomicrograph shows the appearance of a different area of the same specimen described in Figure 13. In contrast to Figure 13, the mode of crack propagation in the area shown is quasi-cleavage.

Summary

On the basis of the photomicrographs presented herein along with previous experience, certain generalizations appear to be justified with respect to microscopic identification of stress-corrosion cracking in heat-treated martensitic steels with high yield strength.

1. Perhaps the most consistent observation is that multiple points of surface initiation are usually observed regardless of the particular alloy or environment.
2. Branching may or may not be observed. If branching is observed in an investigation of a service failure, it is certainly suggestive of a stress-corrosion mechanism as the cause of failure. However, absence of branching does not necessarily mean that stress-corrosion is not a factor.
3. With respect to the path of cracks across grains or along grain boundaries, the following patterns are generally followed:

<u>Steel</u>	<u>Environment</u>	<u>Pattern</u>
Alloy steel	Marine	Intergranular
Alloy steel	Sulfide	Transgranular
Precipitation-hardenable stainless steel	Marine	Transgranular
Maraging steel	Marine	Intergranular or Transgranular
Maraging steel	Sulfide	Transgranular

Acknowledgment

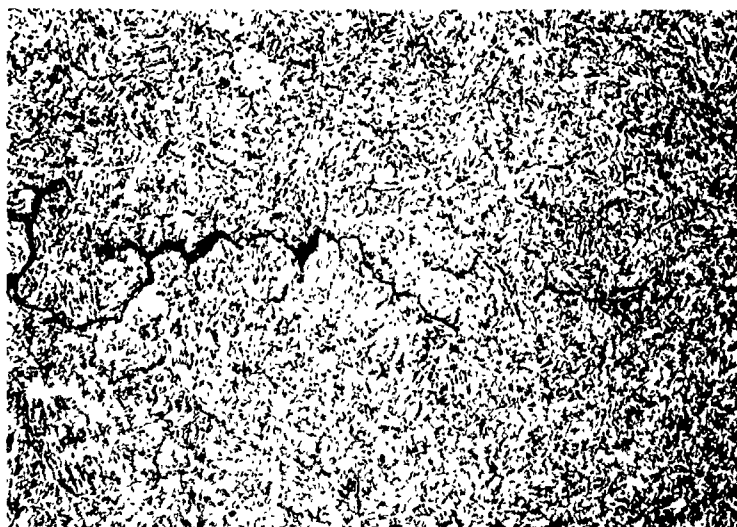
The author wishes to express his appreciation to A. W. Loginow and C. D. Kim, who conducted the research from which the photomicrographs presented herein were taken. The excellent metallographic work was done by W. L. Mann.

References

1. E. H. Phelps and M. E. Komp, "Techniques for Diagnosis of Corrosion Failures," Metals Engineering Quarterly, August 1970, p. 24.
2. Corrosion Handbook, H. H. Uhlig, Editor, John Wiley and Sons, New York, 1948.
3. E. H. Phelps, "A Review of the Stress Corrosion Behavior of Steels with High Yield Strength," Proceedings of Conference on Fundamental Aspects of Stress Corrosion Cracking, National Association of Corrosion Engineers, 1967.
4. B. E. Wilde, "The Mechanism of Cracking of High Strength Martensitic Stainless Steels in Sodium Chloride Solutions," to be published in Corrosion.

Table I
Chemical Composition of Steels Investigated
Percent, by weight

Figure Reference	Steel Type	C	Mn	P	S	Si	Ni	Cr	Mo	V	Ti	Al	Co
1	Cr-Mo-Si-V	0.39	0.93	0.009	0.014	1.5	-	2.00	0.48	0.07	-	0.04	-
2	Ni-Cr-Mo	0.13	0.29	0.009	0.011	0.25	2.97	1.60	0.51	-	-	-	-
3	12Cr-Mo-V	0.25	0.50	0.019	0.015	0.45	0.63	12.16	0.98	0.33	-	-	-
4	Precipitation Hardenable Stainless	0.07	0.68	-	-	0.32	6.9	14.8	2.5	-	-	1.1	-
5	18Ni-Co-Mo	0.014	0.028	0.007	0.012	0.007	18.0	-	4.72	-	0.44	-	7.85
6,7	18Ni-Co-Mo	0.02	0.037	0.002	0.009	0.034	18.0	-	4.85	-	0.44	-	7.84
8,9	18Ni-Co-Mo	0.016	0.084	0.006	0.008	0.13	18.1	-	4.74	-	0.97	-	8.47
10	12Ni-5Cr-3Mo	0.032	0.073	0.007	0.013	0.062	12.0	5.0	3.4	-	0.24	0.41	-
11	18Ni-Co-Mo	0.003	0.02	0.001	0.003	0.003	17.1	-	4.68	-	0.51	-	7.75
12,13,14	12Cr-Mo-V	0.25	0.57	0.03	0.023	0.31	0.65	12.5	1.13	-	0.32	-	-



Reproduced from
best available copy.

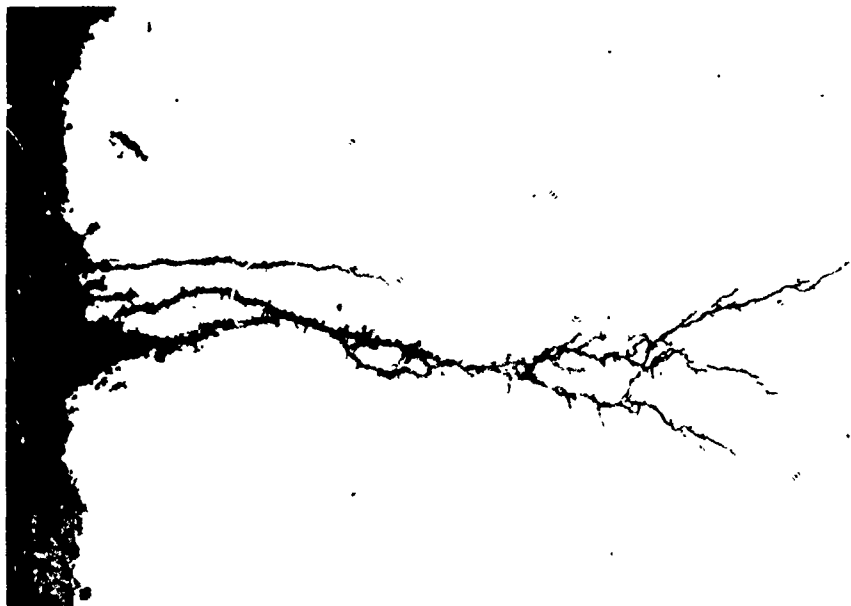
Superpicrel

X500

Steel Type: Cr-Mo-Si-V-alloy steel
Heat Treatment: Quenched and tempered at 700 F (644K)
Yield Strength: 237,000 psi (1634 N/mm²)
Type Specimen: Bent Beam
Stress Level: 75% Yield strength
Environment: Marine atmosphere
Exposure Time: 11 Days

LM-1-R

Figure 1



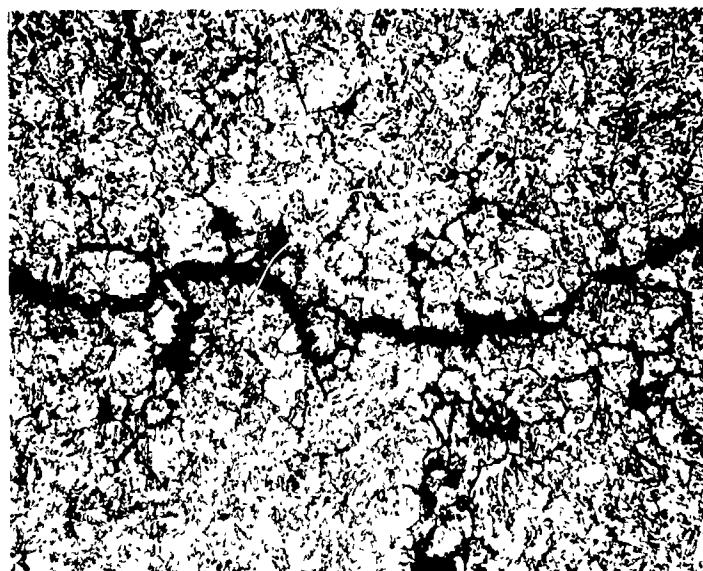
Unetched

X250

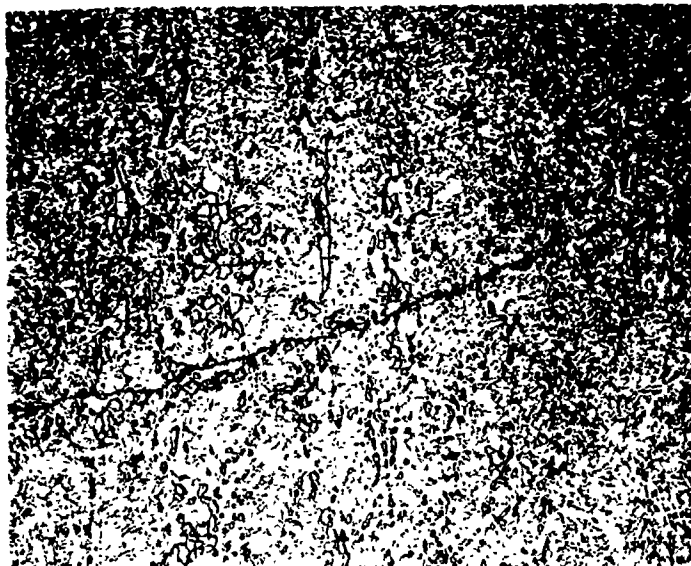
Steel Type: Ni-Cr-Mo alloy steel
Heat Treatment: Quenched and tempered at 1035 F (830K)
Yield Strength: 150,000 psi (1034 N/mm²)
Type Specimen: Tension
Stress Level: 30,000 psi (207 N/mm²)
Environment: 3% NaCl, 0.5% HAC, saturated with H₂S
Exposure Time: 6 hours

LM-649-A-1

Figure 2



Reproduced from
best available copy.



Vilella's Reagent

X500

Steel Type: 12Cr-Mo-V stainless steel
Heat Treatment: Quenched and tempered at 900 F (755K)
Yield Strength: 205,000 psi (1413 N/mm²)
Type Specimen: Bent beam
Stress Level: 75% Yield strength
Environment: Marine atmosphere
Exposure Time: 1 Day

1M-1-D

Figure 3

Vilella's Reagent

X500

Steel Type: Precipitation hardenable stainless
Heat Treatment: Conditioned and tempered at 1050 F (839K)
Yield Strength: 186,000 psi (1282 N/mm²)
Type Specimen: Bent beam
Stress Level: 75% Yield strength
Environment: Marine atmosphere
Exposure Time: 16 Days

1M-1-E

Figure 4



Reproduced from
best available copy.



Unetched

X250

Steel Type: 18Ni-Co-Mo maraging steel
Heat Treatment: Hot-rolled and aged at 900 F (755K) for 3 hours
Yield Strength: 236,000 psi (1627 N/mm²)
Type Specimen: Tension
Stress Level: 75% Yield strength
Environment: Marine atmosphere
Exposure Time: 370 Days

LM-296-E-1

Figure 5

Unetched

X100

Steel Type: 18Ni-Co-Mo maraging steel
Heat Treatment: Annealed and aged at 900 F (755K) for 3 hours
Yield Strength: 240,000 psi (1655 N/mm²)
Type Specimens: Bent beam
Stress Level: 75% Yield strength
Environment: Marine atmosphere
Exposure Time: 316 Days

LM-1064-A-2

Figure 6



Reproduced from
best available copy.

Fry's Reagent X250

Steel Type: 18Ni-Co-Mo maraging steel
Heat Treatment: Annealed and aged at 900 F (755K)
for 3 hours
Yield Strength: 248,000 psi (1710 N/mm²)
Type Specimen: Tension
Stress Level: 75% Yield strength
Environment: Marine atmosphere
Exposure Time: 330 Days

1M-296-B-1

Figure 7



Fry's Reagent

X250

Steel Type: 18Ni-Co-Mo maraging steel
Heat Treatment: Annealed and aged at 900 F (755K)
for 3 hours
Yield Strength: 279,000 psi (1924 N/mm²)
Type Specimen: Bent beam
Stress Level: 75% Yield strength
Environment: Marine atmosphere
Exposure Time: 107 Days

1M-349-D-1

Figure 8



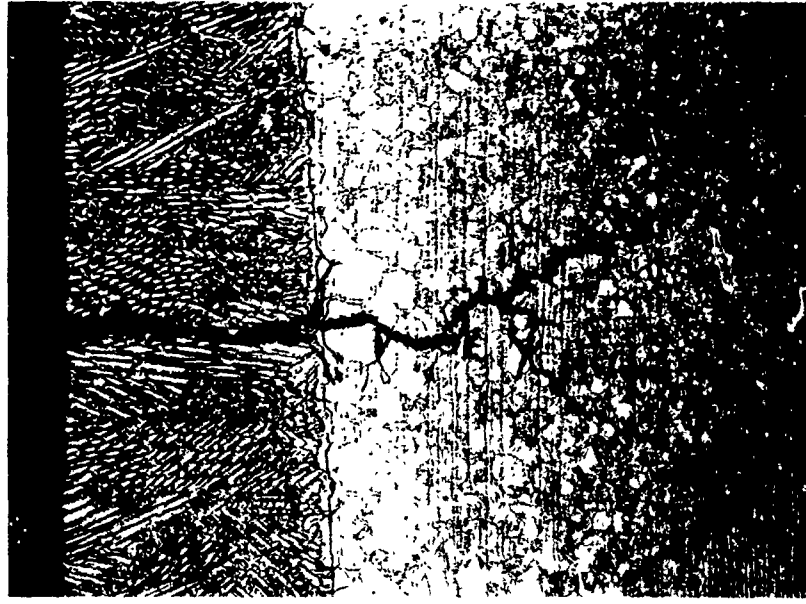
Fry's Reagent

X250

Steel Type: 18Ni-Co-Mo maraging steel
Heat Treatment: Annealed and aged at 900 F (755K) for 3 hours
Yield Strength: 279,000 psi (1924 N/mm²)
Type Specimen: Bent beam
Stress Level: 75% Yield strength
Environment: 3% NaCl saturated with H₂S
Exposure Time: 2 Hours

LM-349-E-1

Figure 9



Weld bead

Heat-affected zone

Reproduced from best available copy.

Base metal

Nital-41cral

X100

Steel Type: 12Ni-5Cr-3Mo maraging steel with weld bead
Heat Treatment: Annealed and aged at 900 F (755K) for 3 hours after welding (base metal)
Yield Strength: 183,000 psi (1262 N/mm²)
Type Specimen: U-bend
Stress Level: Yield stress
Environment: Tidal zone
Exposure Time: 9 Days

LM-393-A-1

Figure 10

Machined
Surface

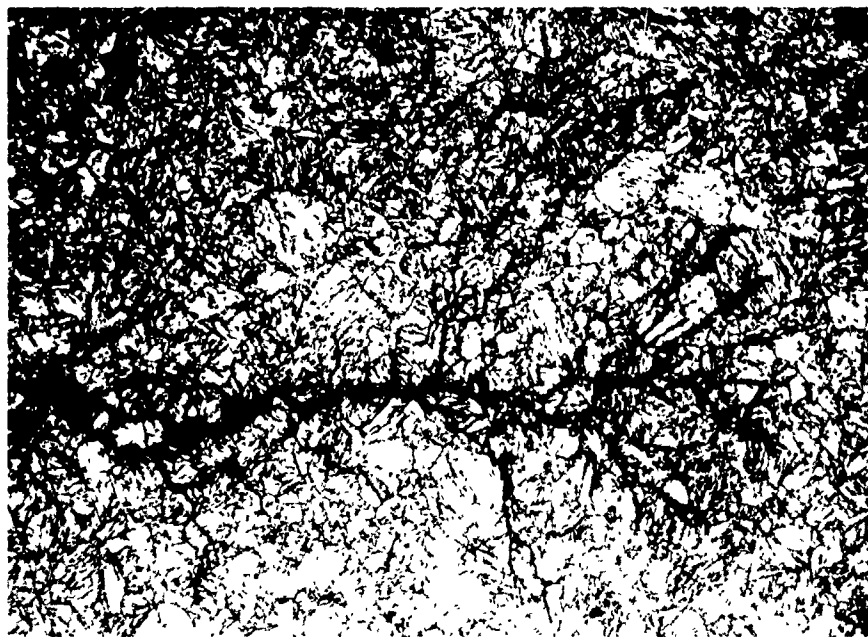


Reproduced from
best available copy.

Intergranular
Attack

Ductile
Tear

Figure 12



Fry's Reagent

X500

Steel Type: 18Ni-Co-Mo maraging steel
Heat Treatment: Double Austenitized and aged at 900 F (755K)
Yield Strength: 256,000 psi (1765 N/mm²)
Type Specimen: Wedge-open-loading K_{IC} type
Stress Level: Initial K, 97.5 ksi /in. (107.1 MNm^{-3/2})
Environment: Flowing sea water
Exposure Time: 6 Months

LM-977-A-1

Figure 11

SEM

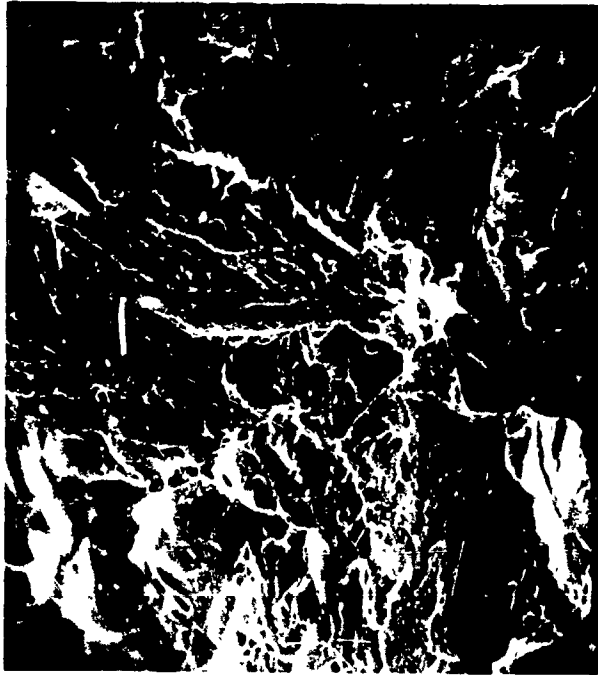
X1500

Steel Type: 12Cr-Mo-V stainless
Heat Treatment: Quenched and tempered at 900 F (755K)
Yield Strength: 188,000 psi (1296 N/mm²)
Type Specimen: Tension
Stress Level: 75% Yield strength
Environment: 3% NaCl with 3 ma/in² (4.66A/m²) anodic current
Exposure Time: 1.6 Hours

CDK-1



Reproduced from
best available copy.



SEM

X3500

Steel Type: 12Cr-Mo-V stainless steel
Heat Treatment: Quenched and tempered at 900 F
(755K)
Yield Strength: 188,000 psi (1296 N/mm²)
Type Specimen: Tension
Stress Level: 75% Yield strength
Environment: 3% NaCl with 3 ma/in² (4.66A/m²)
cathodic current
Exposure Time: 3.4 Hours

CDK-2

Figure 13

SEM

X3500

Steel Type: 12Cr-Mo-V stainless
Heat Treatment: Quenched and tempered at 900 F
(755K)
Yield Strength: 188,000 psi (1296 N/mm²)
Type Specimen: Tension
Stress Level: 75% Yield strength
Environment: 3% NaCl with 3 ma/in² (4.66A/m²)
applied cathodic current
Exposure Time: 3.4 Hours

CDK-3

Figure 14

HOT SALT STRESS CORROSION CRACKING OF TITANIUM ALLOYS —
OVERVIEW AND IMPACT ON SPACE SHUTTLE APPLICATION

By

W. Barry Lisagor^{*} and James E. Gardner^{**}

NASA Langley Research Center
Hampton, Virginia, U.S.A.

^{*} Materials Engineer, Structural Materials.

^{**} Aerospace Technologist, Structural Materials.

SUMMARY

The proposed application of titanium alloys as thin gage radiative metallic heat shields in the thermal protection system of space shuttle vehicles has generated renewed interest in hot salt stress corrosion cracking, and how it may impact space shuttle design considerations. The test program described herein was conducted to determine if onset of hot salt stress corrosion cracking would occur in the cumulative exposure of time, temperature, and stress currently considered for titanium heat shields in the shuttle mission. In addition, efforts were made to assess the effects of cyclic exposure on cracking, to compare the resistance to cracking of the two proposed prime candidate alloys (Ti-6Al-4V and Ti-6Al-2Sn-4Zr-2Mo) and to determine the effect of Mach 3 airflow on cracking behavior. The results indicate that cracking will occur on salt coated specimens continuously exposed in laboratory ovens for 100 hours at temperatures and stresses proposed for shuttle TPS application. However, both cyclic exposure and exposure in a Mach 3 airstream tend to decrease the damage observed. The Ti-6Al-4V alloy exhibited a higher threshold stress than the Ti-6Al-2Sn-4Zr-2Mo alloy but suffered more apparent damage once onset of cracking occurred.

HOT SALT STRESS CORROSION CRACKING OF TITANIUM ALLOYS - OVERVIEW AND IMPACT ON SPACE SHUTTLE APPLICATION

by

W. Barry Lisagor and James E. Gardner
NASA Langley Research Center
Hampton, Virginia, U.S.A.

INTRODUCTION

The proposed application of titanium alloys to space shuttle vehicles has generated renewed interest in the phenomenon of hot salt stress corrosion cracking, and its relevance to particular shuttle requirements. If titanium alloys are to be utilized as thin gage radiative metallic heat shields in the shuttle thermal protection system, the effects of hot salt stress corrosion cracking on design considerations must be determined. Much of the data and understanding of the hot salt problem were developed in support of supersonic aircraft application and will be directly applicable to space shuttle technology. However, space shuttle requirements will involve higher use temperatures but shorter cumulative high-temperature exposure times than have been considered before for the aircraft application. Additional testing to the shuttle exposure conditions is therefore necessary to insure optimum design.

Although the general hot salt stress corrosion cracking mechanism has been substantiated by experimental programs, the effects of specific environmental variables on the cracking process are not completely understood. Thus, engineering data on hot salt stress corrosion cracking in environments which simulate the proposed application must be obtained in order to make meaningful predictions on the criticality of the problem for that application.

Data on the hot salt stress corrosion cracking of candidate alloys are particularly needed at proposed use temperatures exceeding 6000° F. For example, titanium alloy sheet has been proposed for use in the space shuttle thermal protection system for maximum operating temperatures as high as 1000° F. This paper presents a review of the most recent work on hot salt stress corrosion cracking both for mechanisms of damage and engineering data found in the literature. Identification and description of some research tools found to be particularly suitable for the study of this phenomenon are included. Finally, the results of a preliminary study of the effects of hot salt exposure on titanium alloys subjected to exposures indicative of proposed space shuttle application are presented.

BACKGROUND

Historically, hot salt stress corrosion cracking has been an unusual problem compared to other, more classical, forms of stress corrosion cracking. Its occurrence has been widely demonstrated in controlled laboratory tests, but no service failures have been directly related to hot salt stress corrosion cracking even though laboratory tests indicate that failures from this phenomenon should result from some use conditions. Also, the basic mechanism, hydrogen embrittlement of the material in the vicinity of salt deposits, has been well supported experimentally. Lingwall and Ripling (ref. 1) proposed a hydrogen embrittlement mechanism and supported it by tests on the thermal and mechanical behavior of materials and on anodic protection experiments. Ondrejcin and others (ref. 2) have presented a comprehensive mechanistic study, again identifying a hydrogen embrittlement mechanism, supported by several metallurgical and chemical experiments. Hydrogen concentration determinations have been made by vacuum fusion analysis reported by Gray (ref. 3) and Lisagor and others (ref. 4) showing increases in hydrogen content near the fracture surfaces of stress rupture specimens exposed in a hot salt environment. Gray has also recently reported (ref. 5) a new analytical technique for measuring hydrogen content by ion-microprobe mass-spectrometric analysis. The technique involves the removal of very small thicknesses of material by a focused beam of argon ions and analyzing the material removed by mass-spectrometry. Hydrogen contents approaching 10,000 ppm were measured in areas adjacent to the fracture surface of stress rupture specimens.

In addition to the recent information found in the literature on hot salt stress corrosion cracking mechanisms, data reflecting the engineering performance of specific alloys with respect to this phenomenon are available (refs. 6 and 7). Although this information resulted from studies which were more concerned with aircraft application, the general materials behavior observed could be meaningful for certain space shuttle operating conditions.

TEST SPECIMENS AND PROCEDURES

Materials and Specimens

The titanium alloys included in the study are the prime candidate alloys proposed for space shuttle application: Ti-6Al-4V in the annealed condition, and Ti-6Al-2Sn-4Zr-2Mo in the duplex annealed condition. The materials were procured as commercially produced to manufacturer's internal specifications. The alloys were in sheet form with a nominal gage thickness of 0.040 inch.

The specimen used for the test program was of the self-stressed type developed at the Langley Research Center of the National Aeronautics and Space Administration (ref. 8). The configuration and details of the specimen are shown in figure 1. Strips of each alloy 0.040 by 0.25 by 4.0 inches are preformed at each end as in figure 1(a) and spotwelded together as in figure 1(b). In this configuration, the specimen has a uniform outer fiber stress in the curved section. The stress level is determined by the radius of curvature and can be calculated by its chord height (ref. 8). Specimens of both alloys were stressed such that the nominal outer fiber stresses at exposure temperature were 24 and 45 ksi. Unexposed specimens in this configuration are bend tested at room temperature to determine degree of bend ductility (fig. 1(c)). Specimens damaged by environmental exposure resulting in stress corrosion cracking or embrittlement show varying losses of bend ductility (fig. 1(d)) compared to unexposed specimens. This specimen configuration was selected for this test program because it has been shown to be extremely sensitive for revealing damage caused by hot salt exposure and is easily exposed to a wide variety of test conditions. However, the specimen is of the constant deflection type and care should be taken to determine that stress relaxation has not affected observed results when exposures involve high temperatures and stresses.

High-Temperature Exposure Procedures

Laboratory Oven Exposures.— Specimens of both alloys were salt coated in the curved test section to a uniform salt film density of 10 mg/in² by repetitively spraying them with a 3.5-percent NaCl solution and warm air drying. This salt density is slightly higher than that reported by Ashbrook for a severe service exposure (ref. 9). Specimens stressed to both stress levels were then exposed to the desired time-temperature exposure conditions in laboratory ovens in which slowly moving air at ambient pressure was circulated. Specimens of both alloys were salt coated and exposed together for each exposure condition. Specimens were exposed at 700°, 800°, 900°, and 1000° F for a total accumulated exposure time of 100 hours. Some specimens were exposed continuously at temperature for 100 hours while others were exposed for either four cycles of 25 hours or for 100 cycles of 1 hour with cooling to ambient temperature between cycles. This was done in order to assess the effect of frequency of cycling at the higher temperatures. Cycle length has been shown to be highly significant in similar tests at 600° F (ref. 4).

Wind-Tunnel Exposures.— Specimens of both alloys stressed to 24 ksi were also exposed in a small, continuously operating, Mach 3 wind tunnel known as the Supersonic Materials Environmental Test System (SMETS) located at the Langley Research Center. Specimens were salt coated using the same procedure as was described for the laboratory oven exposures and were exposed at 700° F for 100 hours cumulative exposure time. Static pressure on the specimen surfaces was approximately 0.06 atmosphere for the wind-tunnel tests. Both continuous and cyclic exposure were used as in the laboratory oven tests. The tunnel test section, with specimens in place for exposure, is shown in figure 2. The test section is 3 by 5 inches and holds 28 self-stressed specimens for a given exposure. Dummy specimens are positioned at the front and rear of the test section to insure smooth airflow over the actual test specimens. At various positions along the test section, other dummy specimens are positioned to monitor and control exposure temperature. Salt coated and control specimens of each alloy were exposed together for each exposure condition.

Room-Temperature Bend Test and Analysis Procedures

After completion of each laboratory oven or wind-tunnel exposure condition, specimens were bend tested at room temperature to determine relative bend ductility compared to unexposed specimens. The test was conducted by loading the specimens in axial compression (fig. 1(c)) until fracture occurred. The maximum load and the specimen deflection to fracture were recorded.

After bend testing, specimens were examined using low magnification stereo microscopy and scanning electron microscopy to observe the severity of cracking, and to conduct a detailed characterization of individual surface cracks and their resulting fracture surfaces.

RESULTS AND DISCUSSION

Environmental Tests

Continuous Exposure.— Exposure conditions were selected to determine if hot salt cracking would be initiated in the regime of time, temperature, and stress which might be considered for the space shuttle thermal protection system application. In addition, the performance of the two alloys, the effects of cyclic versus continuous exposure, and the effects of airstream velocity on hot salt cracking were compared.

Results of tests on both the Ti-6Al-4V and Ti-6Al-2Sn-4Zr-2Mo alloys after exposure at 700°, 800°, and 900° F in a laboratory oven are shown in figure 3. The nominal outer fiber stress of the specimens at temperature was 24 ksi. Plotted on the ordinate is the relative bend ductility of specimens after exposure, shown as a percentage of the bend ductility determined for unexposed specimens. The relative bend ductility, which is a very sensitive indicator of damage caused during the exposure, is shown as a function of exposure temperature for a continuous 100-hour exposure. The data shown by the open symbols are for an average of four (4) salt coated test specimens; upper and lower limits are shown as

well as the average value. Each closed symbol represents a test specimen which was exposed for the same time, temperature, and stress indicated without salt. The results indicate that the Ti-6Al-4V alloy is more resistant to hot salt cracking than the Ti-6Al-2Sn-4Zr-2Mo alloy at an exposure stress of 24 ksi.

Post-test examination of all specimens revealed no secondary corrosion cracks (fig. 4) in the Ti-6Al-4V alloy at this stress level, indicating that the decrease in relative bend ductility observed was a result of low-temperature aging. The Ti-6Al-2Sn-4Zr-2Mo alloy, however, did contain secondary corrosion cracks (fig. 4) indicating that the threshold stress for this alloy is lower than 24 ksi for a continuous, 100-hour exposure at these temperatures.

Data are shown on figure 5 for both alloys with a nominal outer fiber stress of 45 ksi and exposed continuously for 100 hours at 700°, 800°, and 900° F. The threshold stress for onset of cracking was exceeded for the Ti-6Al-4V alloy at this stress level. The relative bend ductility for the Ti-6Al-4V alloy was reduced to approximately 20 percent, compared to the 80-percent level for specimens exposed at 24 ksi. However, Ti-6Al-2Sn-4Zr-2Mo alloy specimens at 700° F exhibited a somewhat higher relative bend ductility than was observed at the lower stress. This was unexpected and may possibly be due to the inherently less ductile behavior of this alloy and to the type of bend test utilized. It should be noted, however, that the test is primarily designed to indicate threshold levels for crack initiation, and not to measure degree of damage once onset of cracking has occurred. The slight increase in relative bend ductility observed for both alloys at 900° F may be attributed to stress relaxation at this temperature. Specimens were also exposed at 1000° F, but were not included on the figures after post-exposure X-ray stress analysis revealed that extensive stress relaxation had occurred.

The surface appearance after exposure and testing of both alloys stressed to 45 ksi is shown in figure 6. The Ti-6Al-4V alloy exhibited more severe cracking at these exposure conditions than did the Ti-6Al-2Sn-4Zr-2Mo alloy, but both exhibited secondary cracking which can be seen adjacent to the primary fracture in each case.

Analysis by Scanning Electron Microscopy.— The photomicrographs of figures 4 and 6 provide reasonable observation of the secondary cracking caused by the hot salt exposure, but limitations on conventional optical microscopy prevent a detailed analysis at high magnification of these cracks. Specimens examined using scanning electron microscopy can be characterized in much more detail.

Scanning electron micrographs of a Ti-6Al-4V specimen, after exposure and bend testing, are shown in figure 7. Small surface cracks are apparent in the area adjacent to the primary fracture (fig. 7(a)). Cracks tend to be numerous and low magnification scans enable one to survey areas of interest and concentrate when desirable to more detailed analysis at higher magnifications. Detailed examination of a single surface crack (figs. 7(b)-(e)) at higher magnification shows that embrittlement associated with the hot salt stress corrosion cracking process is highly localized. From the surface of the specimen to a depth of approximately 20μ, the fracture surface exhibits a brittle appearance that is primarily intergranular (fig. 7(e)). However, the fracture morphology changes to a ductile, dimple type rupture beyond the locally embrittled depth (fig. 7(d)).

With the aid of the scanning electron microscope, analysis can be made from the lowest magnification, where several surface cracks are visible, to a detailed characterization of the fracture morphology of a single preselected surface crack.

Cyclic Exposure.— The results of the continuous exposure tests indicate that hot salt stress corrosion cracking does occur in time, temperature, and stress conditions encompassing values which may be encountered in shuttle operating conditions. However, the results were obtained in continuous 100-hour tests and effects of cycling and air velocity were not included. The results of tests on both alloys in which the cycle duration and number were varied to accumulate a total exposure time of 100 hours are shown in figure 8. Exposure temperature for these tests was 700° F, and results of tests on both 24 and 45 ksi stressed specimens are shown. The results suggest that cycle duration and frequency have a significant effect on the extent of hot salt stress corrosion cracking of both alloys with shorter cycle duration and higher frequency resulting in much less damage. This effect of cycle duration and frequency suggests the need for clearly defining the thermal and load histories which are expected in areas where titanium alloys will be utilized so that accurate assessments of the significance of the hot salt problem may be made. Again, the lower stressed specimens of the Ti-6Al-2Sn-4Zr-2Mo alloy showed greater loss in bend ductility contrary to what might be expected.

Effect of Air Velocity.— A comparison of the cracking behavior of specimens exposed in laboratory air ovens and of those exposed in the small wind tunnel are shown in figure 9. Tests on the Ti-6Al-2Sn-4Zr-2Mo alloy exposed at 700° F and 24 ksi nominal outer fiber stress are shown. Relative bend ductility is shown as a function of cycle duration and frequency to a cumulative 100-hour exposure. The results indicate that very little damage was observed on specimens exposed in the wind tunnel for either continuous or cyclic exposures. This may be attributed to either the removal of salt from the specimen surfaces which was observed to occur, or to variations in the chemical processes which must occur for cracking to take place. The principal chemical reactions, the pyrohydrolysis of the salt to hydrogen halide and reaction of the hydrogen halide with the surface oxide (ref. 2), may be pressure

dependent. Laboratory oven exposures were made at atmospheric pressure while wind-tunnel exposures resulted in a static pressure of 0.06 atmosphere on the specimens. The combined effects of short-cycle duration and high-velocity airflow result in little or no direct damage caused by hot salt.

CONCLUDING REMARKS

The following concluding remarks are made based on the results of the study described herein:

1. Hot salt stress corrosion crack initiation does occur in the time-temperature-stress regime of conditions considered desirable for optimum space shuttle operation, based on continuous 100-hour tests of salt coated titanium alloy specimens. However, cyclic exposures, particularly of short duration, and exposures in Mach 3 airflow both tend to decrease the amount of damage observed to the point where little or no direct damage was observed on specimens exposed for 100 hours in 1-hour cycles. The need for clearly defined operating conditions of surface temperature and load, accurately determined as functions of time is obvious, and additional multiparameter tests appear in order to determine if hot salt stress corrosion cracking must be considered in the design of hardware.
2. The Ti-6Al-4V alloy exhibited a higher threshold stress than the Ti-6Al-2Sn-4Zr-2Mo alloy at the temperatures investigated. At higher stress levels, the Ti-6Al-4V alloy appeared to show more sensitivity to cracking and somewhat more degradation. The Ti-6Al-2Sn-4Zr-2Mo alloy did not exhibit secondary cracking as severe as the Ti-6Al-4V alloy at stress levels exceeding the threshold value for both alloys.
3. The mechanism for hot salt stress corrosion cracking appears to be more clearly defined than other stress corrosion phenomena. This mechanism has been supported with the aid of recently developed research tools such as the ion microprobe mass analyzer and scanning electron microscope.

REFERENCES

1. Lingwall, R. G.; Ripling, E. J.: Mechanism of Hot Salt Stress Corrosion Cracking of Titanium Base Alloys. Final Report on Elevated Temperature Stress Corrosion of High Strength Sheet Materials in the Presence of Stress Concentrators. NASr-50, NASA CR-88979, August 1967.
2. Ondrejcin, R. S.; Rideout, S. P.; and Louthan, M. R., Jr.: The Hot Salt Cracking of Titanium Alloys. Presented at the International Symposium on Stress Corrosion Mechanisms in Titanium Alloys. Georgia Institute of Technology - National Association of Corrosion Engineers. January 27-29, 1971.
3. Gray, H. R.: Hot Salt Stress Corrosion of Titanium Alloys: Generation of Hydrogen and Its Embrittling Effect. NASA TN D-5000, January 1969.
4. Lisagor, W. B.; Gardner, J. E.; and Royster, D. M.: The Effects of Dynamic and Static Environments and Surface Flaws on the Hot-Salt Stress Corrosion Cracking of Titanium Alloys. Presented at the International Symposium on Stress Corrosion Mechanisms in Titanium Alloys. Georgia Institute of Technology - National Association of Corrosion Engineers. January 27-29, 1971.
5. Gray, H. R.: Role of Hydrogen in Hot-Salt Stress-Corrosion of a Titanium Alloy. Presented at the International Symposium on Stress Corrosion Mechanisms in Titanium Alloys. Georgia Institute of Technology - National Association of Corrosion Engineers. January 27-29, 1971.
6. Royster, D. M.: Hot-Salt-Stress-Corrosion Cracking and Its Effect on Tensile Properties of Ti-8Al-1Mo-1V Titanium-Alloy Sheet. NASA TN D-4674, August 1968.
7. Royster, D. M.: Hot-Salt-Stress-Corrosion Cracking and Its Effect on Tensile and Stress-Rupture Properties of Ti-6Al-4V Titanium-Alloy Sheet. NASA TN D-5417, September 1969.
8. Heimerl, G. J.; and Braski, D. N.: A Stress Corrosion Test for Structural Sheet Materials. Materials Research and Standards, Vol. 5, No. 1, January 1965.
9. Ashbrook, R. L.: A Survey of Salt Deposits in Compressors of Flight Gas Turbine Engines. NASA TN D-4999, January 1969.

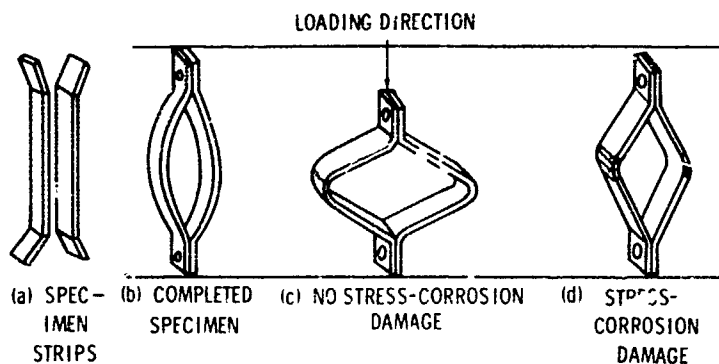


Figure 1.- Details of self-stressed specimen and difference of bend ductility with and without stress corrosion damage.

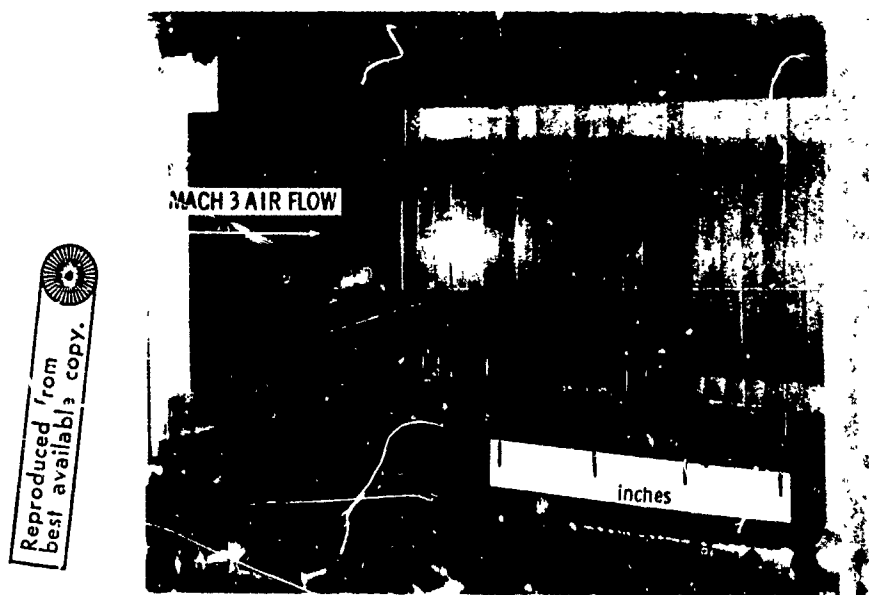


Figure 2.- Tunnel test section showing specimens in place for exposure

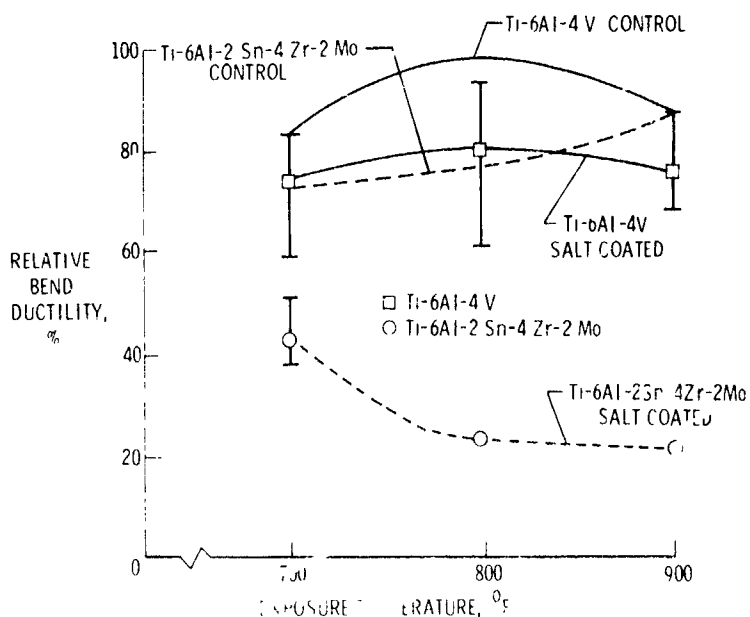


Figure 3 - Effect of temperature and hot salt on bend ductility of titanium alloys exposed continuously for 100 hours at a stress of 24 ksi (Closed symbols are control specimens)

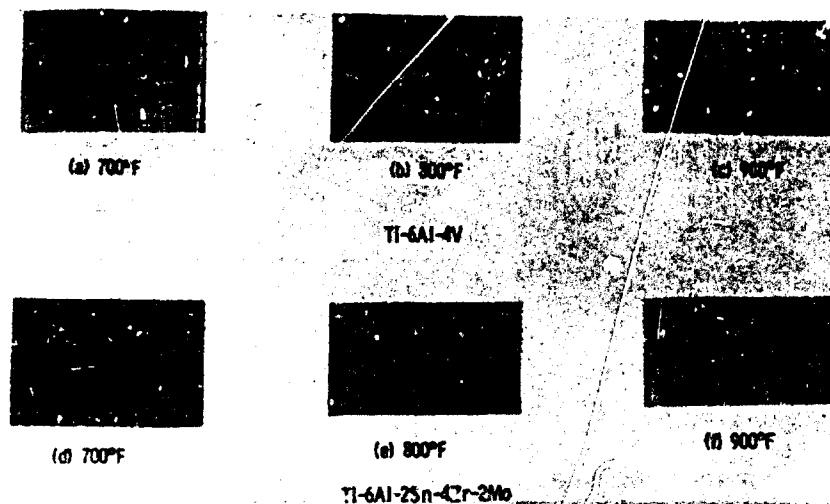


Figure 4.- Surface appearance near vicinity of primary fracture of salt coated titanium alloys exposed continuously for 100 hours at a stress of 24 ksi. (5X magnification.)

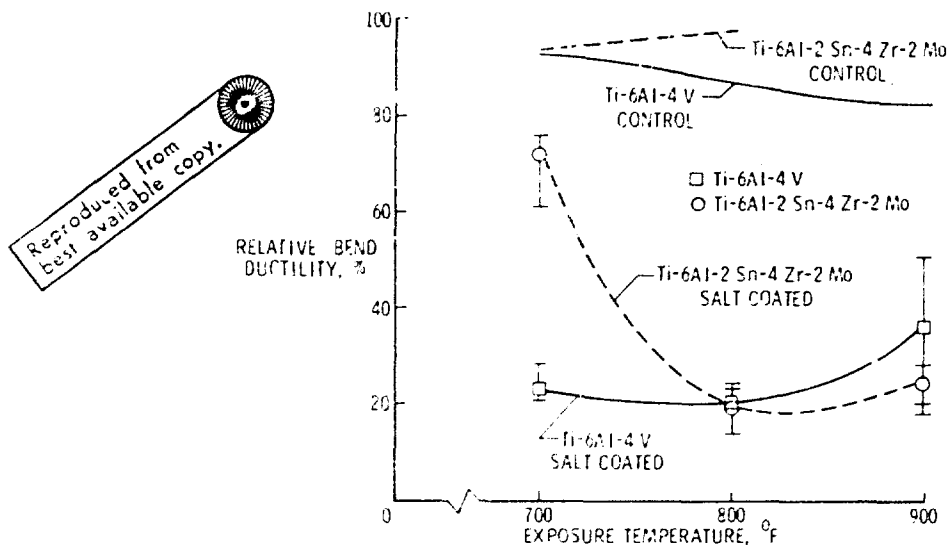


Figure 5.- Effect of temperature and hot salt on bend ductility of titanium alloys exposed continuously for 100 hours at a stress of 45 ksi. (Closed symbols are control specimens.)

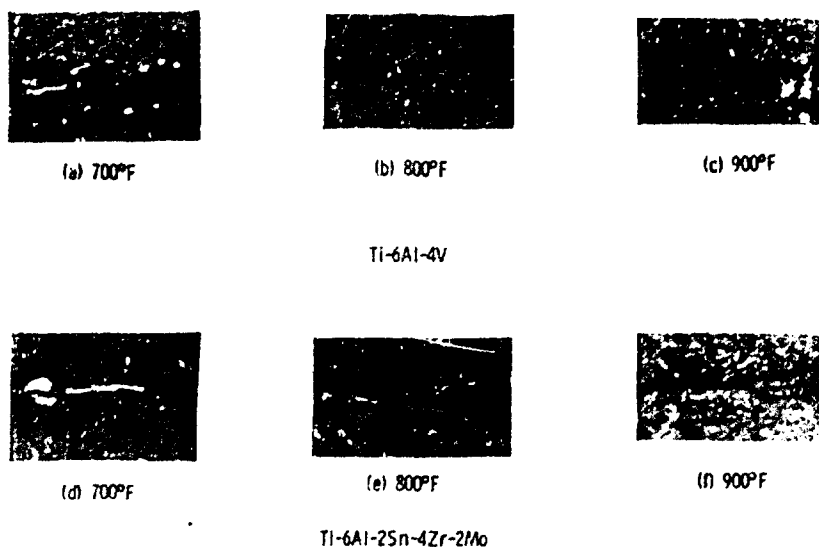


Figure 6.- Surface appearance near vicinity of primary fracture of salt coated titanium alloys exposed continuously for 100 hours at a stress of 45 ksi. (5X magnification.)



1.0 mm

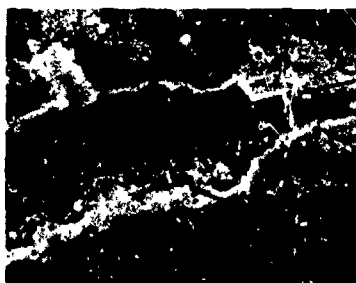
(a) low magnification
surface appearance
showing cracks near
primary fracture



0.5 mm

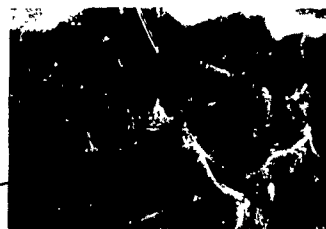
(b) enlarged view of
single surface crack
near primary fracture

Figure 7.- Scanning electron microscope images of a Ti-6Al-4V salt coated self-stressed specimen after exposure and bend testing.



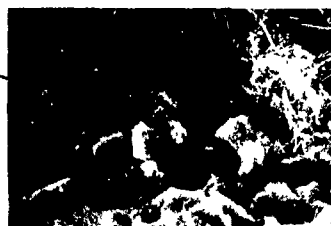
50 μ m

(c) fracture appearance
within surface crack



10 μ m

(d) ductile fracture area
beyond brittle region



10 μ m

(e) brittle fracture area
near surface of specimen

Figure 7.- Concluded.

Reproduced from
best available copy.



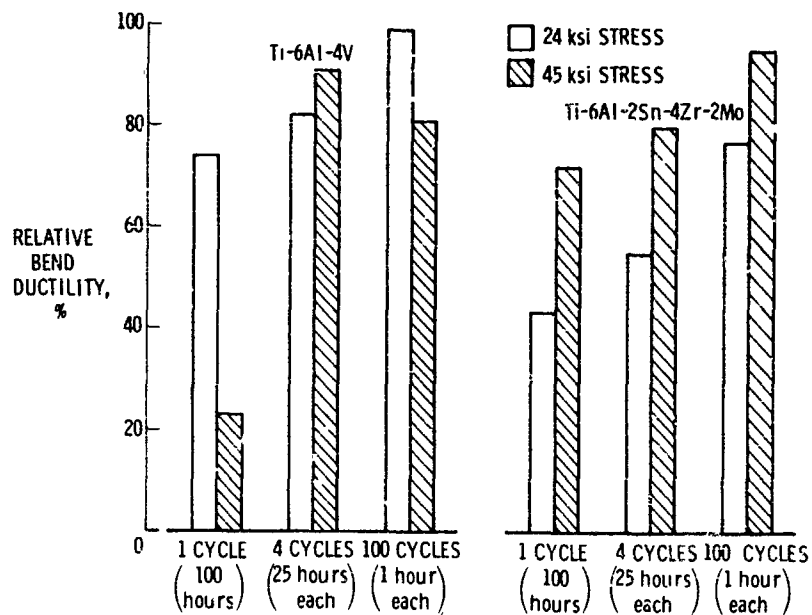


Figure 8.- Effect of stress level and cyclic exposure on relative bend ductility of titanium alloys. (Specimens exposed at 700° F for a total time of 100 hours.)

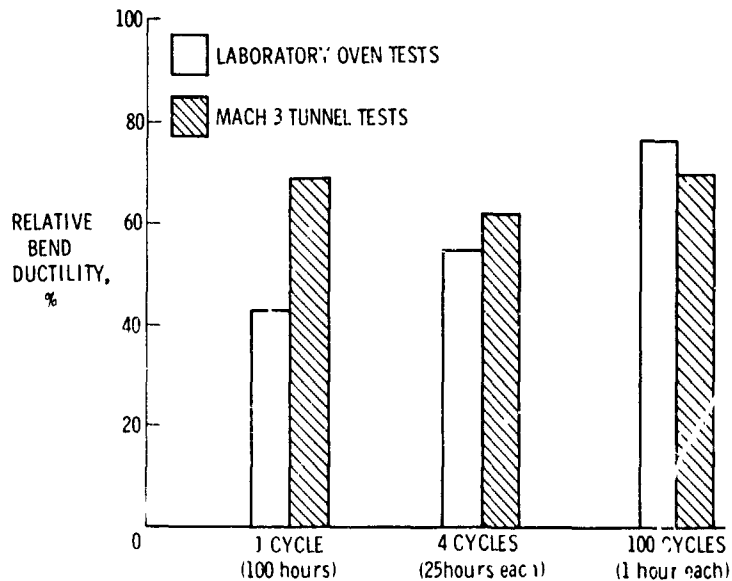


Figure 9.- Effect of air velocity and cyclic exposure on relative bend ductility of Ti-6Al-2Sn-4Zr-2Mo stressed to 24 ksi. (Specimens exposed at 700° F for a total time of 100 hours.)

**THE USE OF SLOW STRAIN-RATE EXPERIMENTS IN
EVALUATING RESISTANCE TO ENVIRONMENTAL CRACKING**

by

James E. Reinoehl
Senior Electrochemist
Corrosion Research Division
Battelle
Columbus Laboratories
505 King Avenue
Columbus, Ohio 43201, USA

and

Walter K. Boyd
Chief
Corrosion Research Division
Battelle
Columbus Laboratories
505 King Avenue
Columbus, Ohio 43201, USA

THE USE OF SLOW STRAIN-RATE EXPERIMENTS IN EVALUATING RESISTANCE TO ENVIRONMENTAL CRACKING

by

James E. Reinoehl

Walter K. Boyd

SUMMARY

This paper describes an experimental procedure to evaluate resistance to stress-corrosion cracking. Relative degrees of susceptibility to environmental cracking and embrittlement can be determined as a function of mechanical ductility parameters (e.g., reduction in area, elongation, etc) or as a function of electrochemical polarization parameters (e.g., electrode potential, pH, solution composition, etc) by pulling cylindrical tensile specimens at a suitable slow strain rate while they are subjected to controlled electrochemical and environmental conditions (e.g., electrode potential, solution composition, temperature, etc).

INTRODUCTION

Most corrosion experiments are time consuming since they involve exposing specimens to a corrosive environment until some deterioration occurs. Similarly, most environmental cracking tests involve exposing stressed specimens of simple or complex configurations to an aggressive environment which, by prior experience, has been shown to promote cracking of the alloy. When a specimen cracks in less time than the duration of the experiment, the relative susceptibility of that alloy to environmental cracking can be expressed quantitatively by the time to failure. Unfortunately, however, some specimens will not be subject to environmental cracking for very long periods of time; if these resist cracking for the duration of the experiment, the alloy is commonly considered to be "immune" to cracking. To be sure of true immunity, however, one would have to expose the specimen for infinite time. Obviously, this is impractical in engineering applications, so that a number of subjective judgments must be made in evaluating time-exposure data.

One method which is commonly used to speed up the generation of time-exposure data is to increase the severity of the test by such means as (1) increasing the relative aggressiveness of the environment by altering its composition, temperature, pressure, etc., or (2) increasing the relative susceptibility of the alloy by means of a suitable heat treatment, or the introduction of a notch or precrack. Many of these experimental conditions are difficult to reproduce in repetitive exposures or even to retain during a lengthy exposure. Thus the data that result from exposure tests are subject to considerable scatter.

Many of the objections can be circumvented by selecting the environmental and stressing variables such that all specimens will fail within a definite period of time. For example, if tensile specimens are pulled at a slow strain rate of about $1\%/hr$ while subjected to cracking or noncracking environments, fracture will occur within a day whether it be by a ductile mechanical mode or by a brittle environmental cracking mode. By carefully controlling the strain rate and electrochemical conditions, then a wide range of different mechanical and corrosion behaviors can be induced. Thus, ductility parameters such as percent reduction in area or percent elongation may provide quantitative information about the relative degrees of susceptibility of different materials to environmental cracking in a specific environment or the relative degree of aggressiveness of different environments in promoting cracking of a specific material. Complementary microscopic examinations of the fractured specimens provide additional information regarding the mechanisms which were involved in the fracture process. However, regardless of possible controversies over describing the mechanism involved, the numerical data obtained provide objective engineering information as to the mechanical properties of materials under carefully controlled environmental conditions. This paper describes the apparatus used for slow strain-rate tests of environmental cracking and discusses the influence of a number of electrochemical and mechanical parameters in promoting environmental cracking and embrittlement.

THE SLOW STRAIN-RATE TECHNIQUE

Apparatus

The apparatus used in the environmental cracking test at slow strain rates are similar to those described by Parkins and coworkers.⁽¹⁾ The principal components are pictured in Figure 1. The actual test cell is seen in the middle of the photograph. A length of glass (or TFE) tubing between two rubber stoppers confines approximately 50 ml of solution around a cylindrical tensile specimen machined from the alloy to be examined. The remainder of the apparatus serves to control the mechanical and electrochemical conditions of the test.

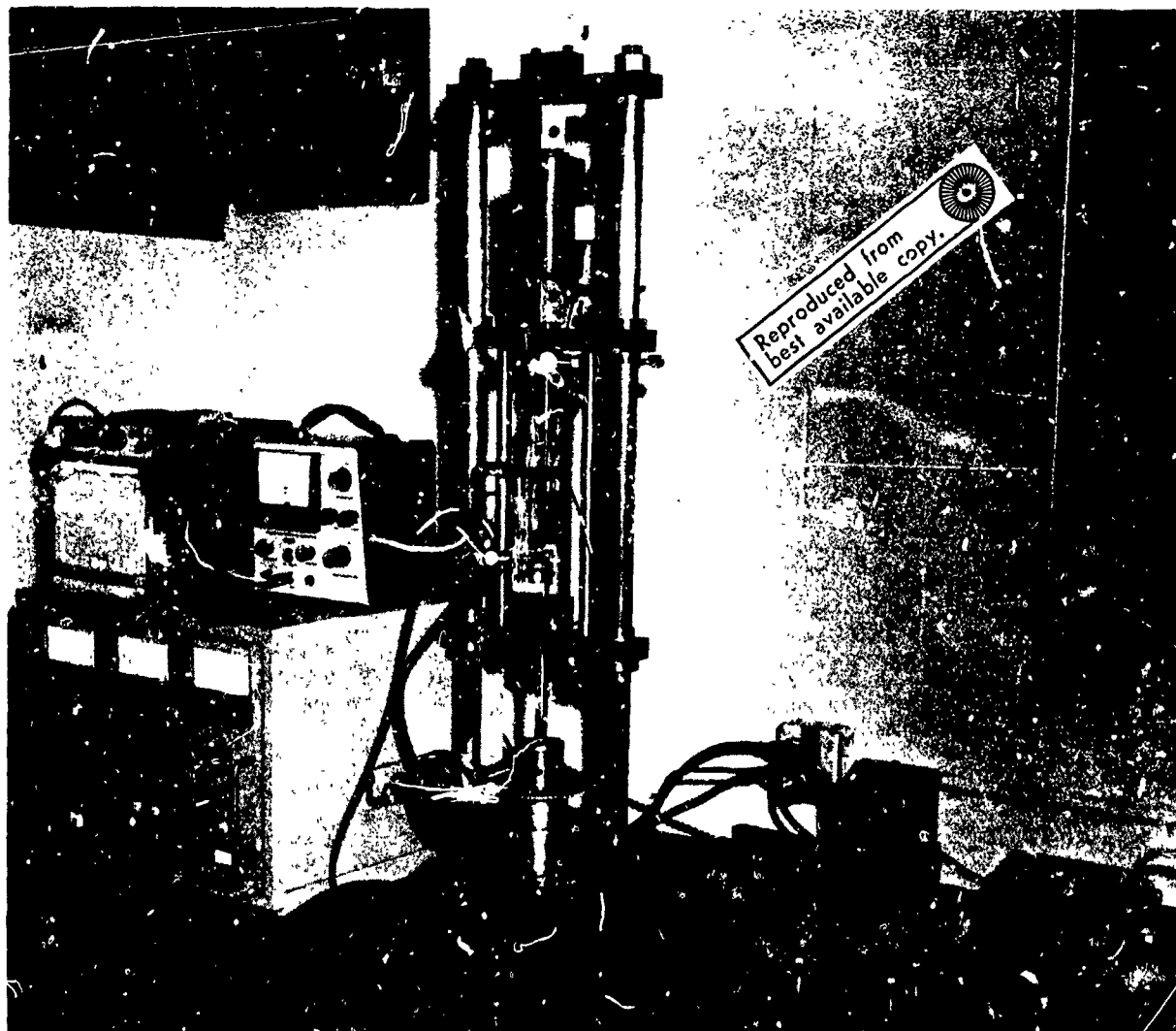


FIGURE 1. APPARATUS FOR CONDUCTING ENVIRONMENTAL CRACKING TESTS AT SLOW STRAIN RATES AND APPLIED POTENTIALS

A 1/4-hp motor is connected to a series of gears so as to move the crosshead at a fixed rate. Since one end of the cylindrical tensile test specimen is affixed to the moving crosshead and the other end is affixed to a stationary load cell, the specimen is slowly extended at a rate which is determined by the combination of gears selected. The apparatus pictured is constructed to achieve strain rates in the range between about 5.4 and 0.4%/hr during plastic deformation of the gage length of the tensile specimen. These strain rates conveniently induce varying degrees of SCC in mild steels in test times ranging from several hours (for the fastest strain rate) to several days (for the slowest). While the slowest strain rate promotes the greatest degree of SCC, an intermediate strain rate of about 1%/hr has been found to be the most convenient to use for screening tests on mild steels in caustic and carbonate-bicarbonate environments since it gives one result per machine per day. These strain rates are slower than the slowest strain rate of common commercial tensile testing machines. The faster strain rates which are attained on commercial testing machines are believed to be suitable only for evaluating alloy-environment combinations which are very susceptible to environmental cracking phenomena. For example, some iron-nickel alloys will develop stress-corrosion cracks in 12% $MgCl_2$ solutions when tested at strain rates as fast as 1%/minute.⁽²⁾

While a slow strain rate may induce environmental cracking and embrittlement under conditions which would be unexpected on the basis of experience with tests conducted under static loads, ductile fracture still will occur in most environments unless the electrochemistry of the system is diligently controlled. The potentiostat shown in Figure 1 is used to control the potential of the specimen at a value, with respect to a saturated calomel reference electrode, which is selected on the basis of relevant features of potential/current curves. For example, selective corrosion attack and environmental cracking are expected to be most severe at imposed potentials corresponding to regions of negative slope in the potential/current curve. Also, a breakdown potential similar to that used to describe the onset of pitting may characterize environmental cracking conditions.⁽³⁾ Accordingly, a few specific ranges of potentials can be selected which will optimize the chances of occurrence of environmental cracking phenomena and relative amounts of loss of ductility can be determined as a function of potential in each range. It is noted that a plot of relative loss of ductility as a function of potential will frequently give a bell-shaped curve that is not unlike a probability distribution. Degrees of severity of cracking can thus be shown for specific combinations of mechanical and electrochemical conditions.

A cracking tendency may also be enhanced by conducting the slow strain-rate test at an elevated temperature. A pronounced cracking tendency may be observed at near boiling when identical mechanical and electrochemical conditions give little if any loss of ductility at room temperature. The effect of temperature on the propensity of mild steel to develop stress-corrosion cracks in an ammonium-nitrate solution is shown in Figure 2. The degree of severity of cracking increases steadily with temperature

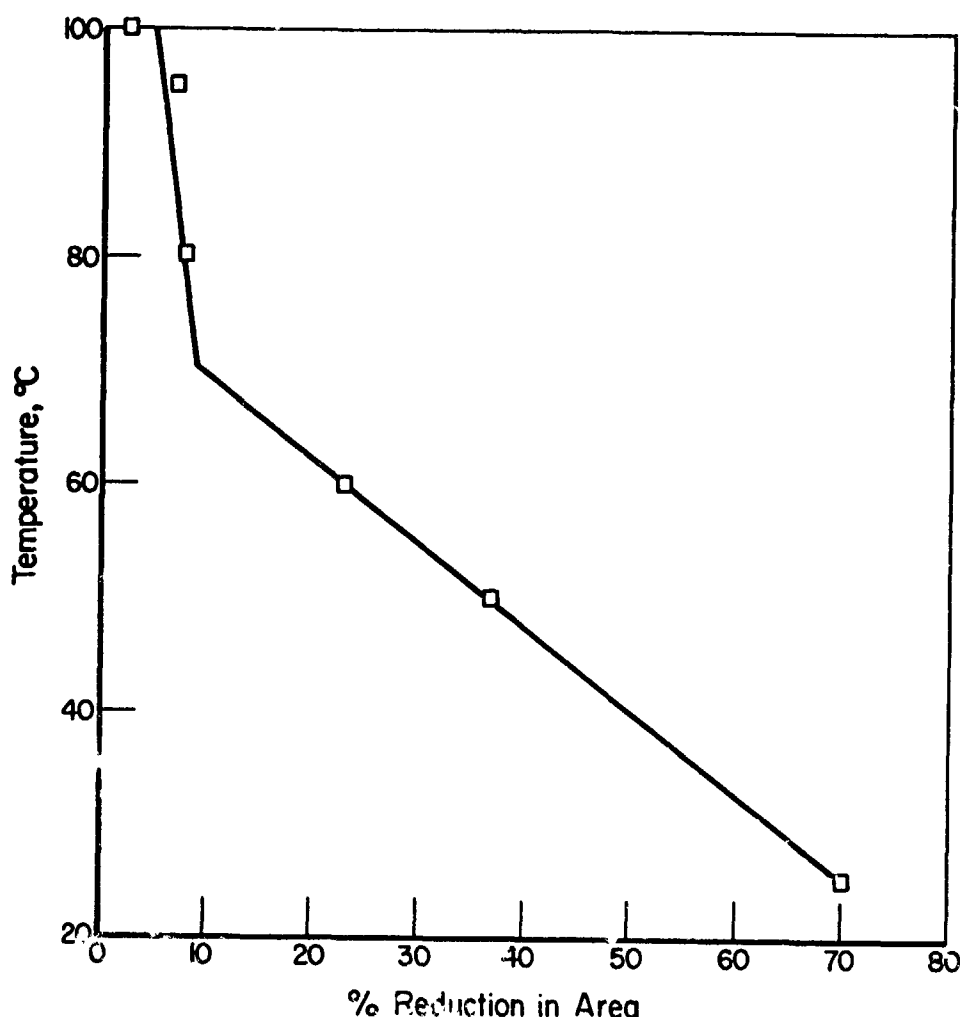


FIGURE 2. EFFECT OF TEMPERATURE ON THE LOSS OF DUCTILITY OF A CARBON-MANGANESE STEEL IN 20% NH_4NO_3 SOLUTION AT A STRAIN RATE OF 0.36%/HR

until ductile mechanical behavior is virtually lost at temperatures above 70°C. While these data indicate that cracking will not occur at ambient temperature for these experimental conditions, they also give no indication of a unique threshold temperature below which stress-corrosion cracking will not occur. Accordingly, a slower strain rate combined with a carefully selected controlled potential might be expected to induce a cracking tendency even at temperature below ambient. Also, careful selection of the mechanical, electrochemical, and thermal conditions of a slow strain-rate test might induce losses of ductility in some seemingly innocuous environments.

INTERPRETATION OF RESULTS

Relative susceptibilities to environmental cracking may be classified by comparing times to fracture or ductility parameters (e.g., reduction in area or elongation, as determined from the fractured specimen) with similar parameters determined for a purely ductile fracture. Relative cracking tendencies thus may be expressed as a percent loss of ductility.⁽⁴⁾ Cracking is confirmed by visual and metallographic examination. The latter has the added benefit of showing a wide variety of "pit" configurations associated with nucleation sites for stress-corrosion cracks.

Additional information can be gained by recording the load, measured by the load cell (Figure 1), on a strip-chart recorder. Mechanical properties such as yield stresses, ultimate tensile stresses, and fracture stresses may thus be compared for varying degrees of susceptibility to environmental cracking. Different types of environmental cracking and embrittlement give markedly different load-time curves much the same as ductile and brittle materials have characteristically different behaviors. The plastic deformation and fracture behavior of a material under the influence of a controlled liquid environment may thus be studied. It is also informative to note natural corrosion potentials of the alloy in the environment before and after the test. These may reflect the presence or absence of a passive film on the alloy. When potentiostatic control is maintained on the specimen, current transients may be recorded as an indication of the electrochemical kinetic processes which occur as the specimen is being plastically strained.

Thus, both mechanical and electrochemical parameters may be recorded simultaneously in the slow strain-rate test for environmental cracking. These may be interpreted in terms of fracture mechanics concepts or in terms of preferential corrosion behavior. Since both mechanical and electrochemical phenomena interact in environmental cracking, proper interpretation of these data may reveal the mechanical and the electrochemical contributions to the process of environmental cracking.

CONCLUSIONS

Relative degrees of susceptibility to environmental cracking and embrittlement can be determined as a function of mechanical ductility parameters (e.g., reduction in area, elongation, etc) or as a function of electrochemical polarization parameters (e.g., electrode potential, pH, solution composition, etc) by pulling cylindrical tensile specimens at a suitable slow strain rate while they are subjected to controlled electrochemical and environmental conditions (e.g., electrode potential, solution composition, temperature, etc). A definite result is obtained within hours or days by this method whether the combination of alloy and environment is highly susceptible or highly resistant to environmental cracking. By careful selection and control of electrochemical, metallurgical, and mechanical variables so as to promote optimum conditions for environmental cracking, an objective evaluation of the relative susceptibilities of different alloy compositions and structures may be made. Also, an improved understanding of environmental cracking phenomena results from the determination of the optimum electrochemical, metallurgical, and mechanical conditions for their promotion.

REFERENCES

- (1) Humphries, M. J., and Parkins, R. N., "Stress-Corrosion Cracking of Mild Steels in Sodium Hydroxide Solutions Containing Various Additional Substances", Corrosion Science, 7, (11), 747-761 (1967).
- (2) Scully, J. C., and Hoar, T. P., "Mechanochemical Anodic Dissolution of Iron-Nickel Alloys in Hot Chloride Solution at Controlled Electrode Potential", Proc. 2nd International Congress on Metallic Corrosion, New York, March 11-15, 1963, pp 184-187.
- (3) Prazhak, M., Toushek, Ya., and Spanilyi, V., "Role of Anion Adsorption in Pitting Corrosion and Stress-Corrosion Cracking of Metals", Protection of Metals, 5, (4), 329-333 (1969).
- (4) Herzog, E., Hugo, M., and Bellot, J., "Nouvelles methodes d'investigation de la corrosion des aciers dans les solutions de soude caustique", Corrosion-Traitements, Protection, Finition, 18, (5), 287-294 (1970).

EXPERIMENTAL TECHNIQUES USED TO STUDY STRESS
CORROSION MECHANISMS IN AIRCRAFT STRUCTURAL ALLOYS

G. M. Koch, W. E. Krupp and K. E. Weber
Materials Research Laboratory
Advanced Design and Research Laboratories
Lockheed-California Company
P. O. Box 551
Burbank, California 91503

EXPERIMENTAL TECHNIQUES USED TO STUDY STRESS CORROSION MECHANISMS IN AIRCRAFT STRUCTURAL ALLOYS

G. M. Hoch, W. E. Krupp and K. E. Weber
Materials Research Laboratory
Advanced Design and Research Laboratories
Lockheed-California Company
P. O. Box 511
Burbank, California 91503

INTRODUCTION

Stress corrosion testing is generally performed for one or more of the following reasons: (1) to compare the susceptibility of various materials and fabrication methods, (2) to evaluate methods for protection or alleviation, and (3) to identify proper design practices. These tests fall into two major categories, conventional and fracture mechanics. Conventional tests use uncracked specimens to determine time-to-failure versus applied stress, threshold stress values, and crack growth rates. Specimens used in conventional testing include smooth tensile, bent beam, U-bend and C-ring. These are exposed to test environments by continuous immersion, alternate immersion, salt spray, sea coast or industrial atmosphere exposure. On the other hand, fracture mechanics tests make use of precracked specimens to determine time-to-failure versus stress intensity (K_{I1}), threshold stress intensity (K_{Isc}), and cracking rate (da/dt). In addition to the notched and precracked types mentioned above, other specimens used for these tests include compact tension, wedge-opening-loading, double-cantilever-beam and tapered-cantilever-beam. Exposure techniques are essentially the same, with the exception that environmental contact may be limited to only the crack region utilizing masking techniques. In these tests, standardized methods are used where appropriate for efficient production of reliable low cost data.

In addition to the aforementioned, a separate type of research activity is performed to examine the fundamental mechanisms that produce stress corrosion susceptibility in a particular material/environment combination. The objective of these tests is the development of sufficient information to indicate methods of alleviation, such as (1) modifying the structure of the material, (2) altering the service media, and (3) changing the nature of the boundaries separating environment and material. This paper will discuss some of the specialized experimental techniques used at Lockheed-California Company to examine various aspects of the stress corrosion phenomenon in aircraft structural alloys.

CRACK MORPHOLOGY STUDIES

Microscopic cracking patterns can be traced through the thickness of a specimen by removing successive layers of material to reveal interior planes and discern the three-dimensional morphology of a crack. This can be used to determine cracking paths, crack branching, stress state and zones of plastic deformation.

In one set of experiments⁽¹⁾ specimens of 7075-T6 aluminum alloy were loaded to fracture in the presence of 3.5 percent NaCl solution, using the three-point bending configuration shown in Figure 1. Microscopic examination of specimen surfaces revealed intergranular cracking parallel to the principal tensile stress and hinges of plastic deformation indicative of plane stress conditions, as shown in Figure 2. Controlled amounts of material were removed from the specimens by lepping. The interior planes thus revealed were polished and photographed at 23X. A representative photomicrograph of an interior plane is shown in Figure 3. This photograph shows the cracking parallel to the principal tensile stress as previously noted in Figure 2. In addition, a transgranular crack perpendicular to the principal stresses and emanating from the precrack at the notch may be seen. The technique of removing successive layers of material was repeated until the center of the specimen was reached⁽²⁾. The cracking pattern at various depths was traced on clear plastic sheets which were assembled to form the three-dimensional model shown in Figure 4.

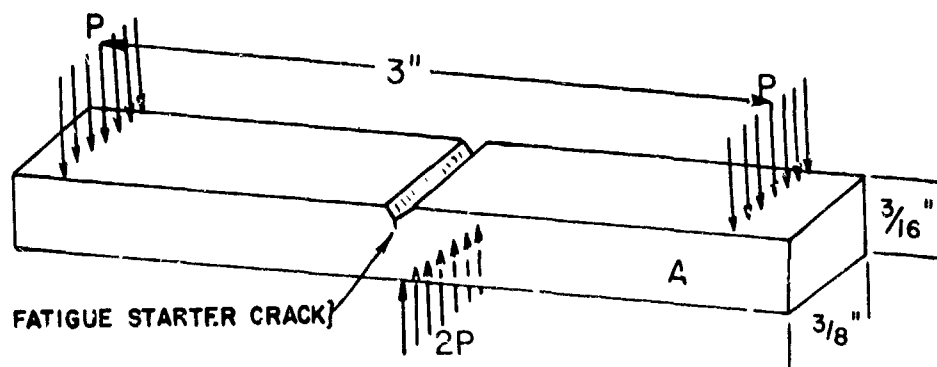


Figure 1. Specimen geometry and loading arrangement for three-point bend stress corrosion test.



Figure 2. Surface of 7075-T6 specimen. Cracking parallel to principal tensile stress and plastic deformation hinges indicative of plane stress.



Figure 3. Cracking pattern on a plane 0.055 inch from the surface of a 7075-T6 specimen. Intergranular cracking, separated from transgranular cracking by 0.013 inch.

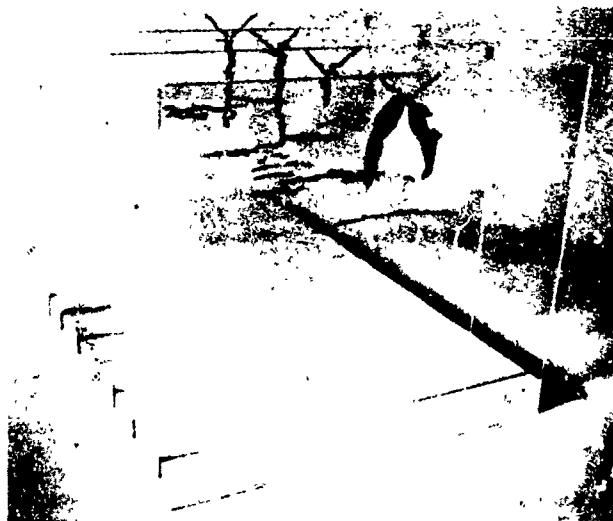


Figure 4. Three-dimensional model of stress corrosion cracking in 7075-T6 bend specimen.

Time lapse photographic techniques have been employed to follow the progression of stress corrosion cracking. One face of a precracked specimen was lightly polished, the specimen was immersed in a corrosive solution, and the desired stress applied. Special 16mm motion picture equipment was used to record one frame every 90 seconds, or 40 frames each hour. Figure 5 shows representative frames from two of the motion pictures, showing crack growth in 1% NaCl and CCl_4 to occur at nearly identical rates⁽³⁾.

Transmission and scanning electron microscopy have also been used to examine fracture surfaces and reveal microstructural features associated with susceptible alloys. One example of the use of SEM is presented in Figures 6 and 7, which show the fracture surfaces of wedge-opening-loading specimens of 7075-T6 alloy exposed to 3.5 percent NaCl solution. Special note should be made of the elliptical regions of localized stress corrosion separated from the main crack front and surrounded by regions of ductile tear. One mechanism advanced to explain this structure requires the diffusion of a contaminating species through the plastic zone ahead of the main crack, producing localized regions of stress corrosion cracking surrounded by uncracked material⁽¹⁾.

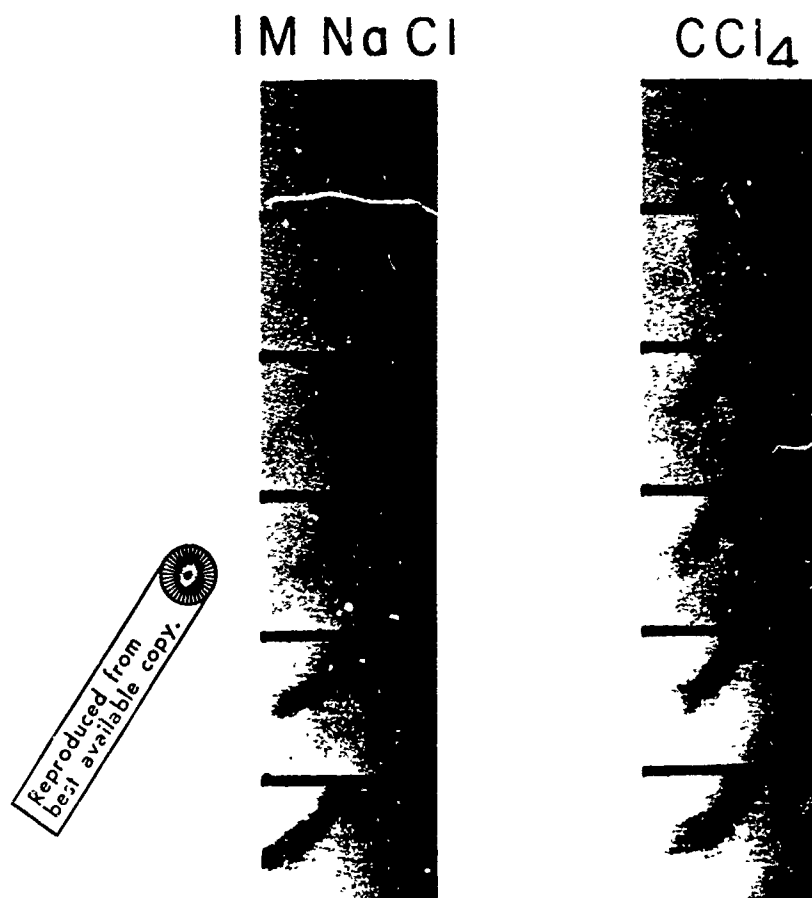


Figure 5. Stress corrosion cracking of Ti-8Al-1Mo-1V in 1M NaCl solution and anhydrous CCl₄.

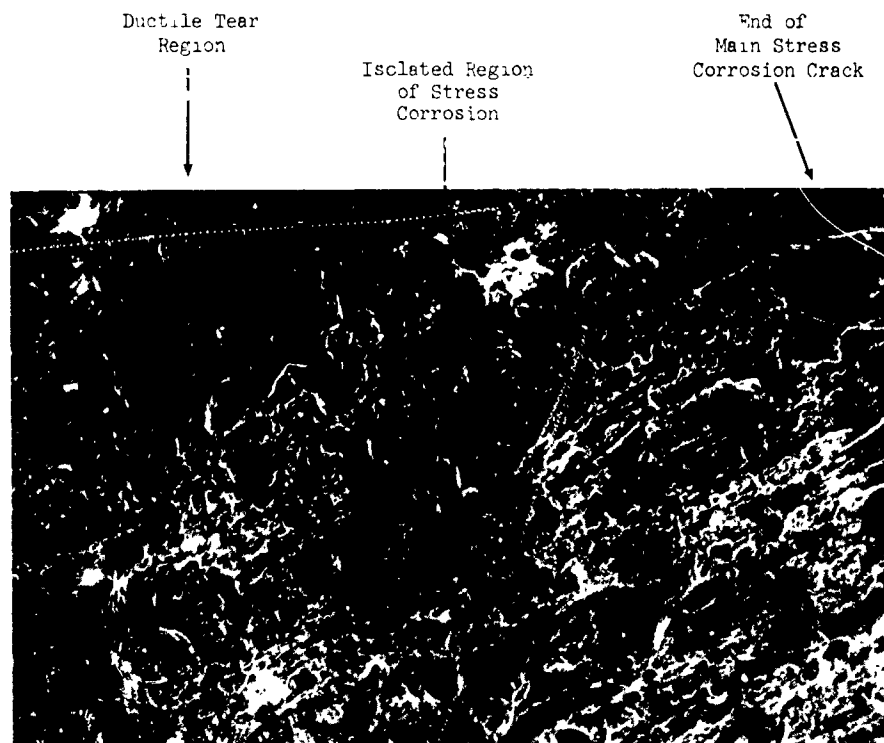


Figure 6. Transition between stress corrosion and ductile tear in Ti-8Al-1Mo-1V specimen exposed to 3.5% NaCl at $K_{I1} = 1.7 \text{ ksi}\sqrt{\text{in.}}$. Magnification = 100X

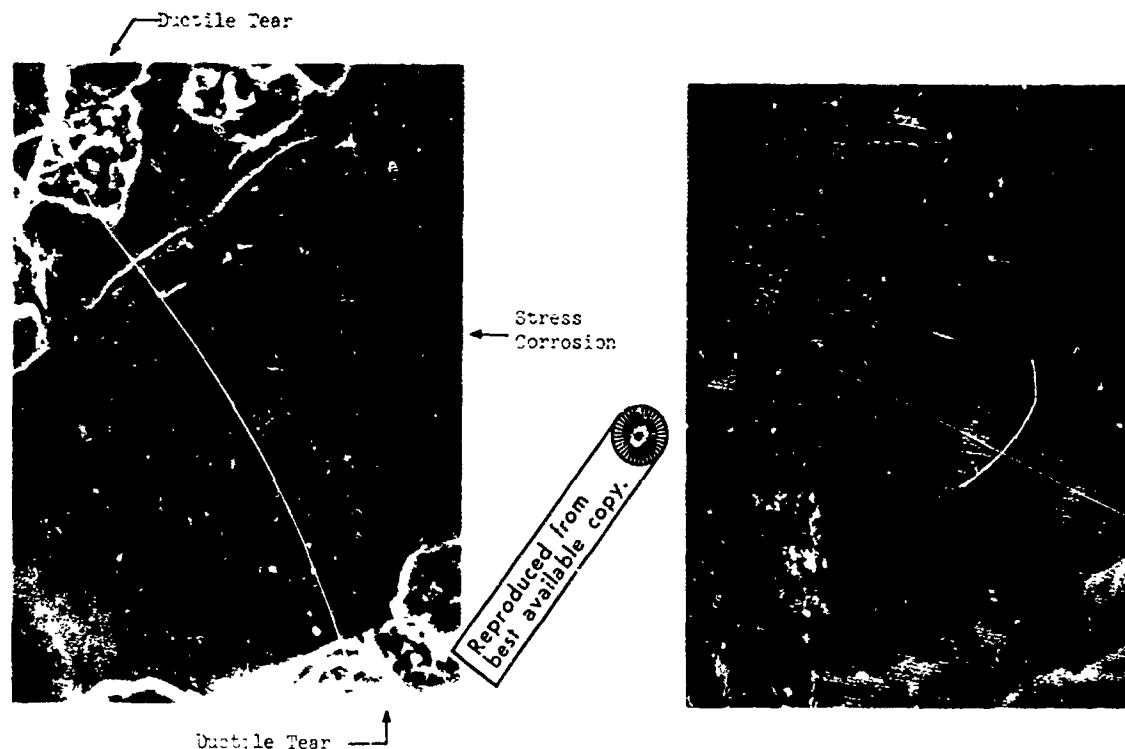


Figure 7a. Isolated region in 7075-T6 specimen exposed to 3.5% NaCl at $K_{II} = 19.7$ ksi/in., showing stress corrosion surrounded by ductile tear. Magnification = 1000X

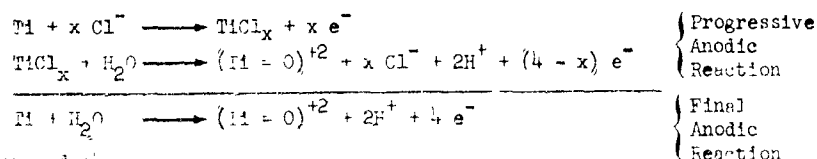
Figure 7b. Isolated region in 7075-T6 specimen exposed to 3.5% NaCl at $K_{II} = 9.0$ ksi/in., showing stress corrosion surrounded by ductile tear. Magnification = 3000X

CONTAMINANT IDENTIFICATION

The mechanical properties of metals are greatly influenced by the distribution of alloying elements, impurities and contaminants in their microstructure. Autoradiography can be used to determine the microsegregation of any element that has a radioactive isotope^(4,5). Such data are useful in stress corrosion work to identify contaminating elements, determine diffusion rates and isolate accumulation sites.

Radioactive elements are introduced into the corrosive media being studied, e.g. tritium oxide in water or chlorine-36 in NaCl solution. Exposure of stressed specimens to the corrosive media permits transfer of the tagged contaminant. Subsequent to the test the surface of the specimen which retains the radioactive element is placed in intimate contact with an emulsion layer suitable for detecting beta or gamma radiation. After exposure, the solidified film is peeled from the metal surface, developed by photographic techniques, and examined. Observations of darkened areas in the emulsion are correlated with the microstructure of the test specimen to determine the location of the radioactive material. An example presented in Figure 8 shows retention of chlorine-36 in the stress corroded region of a Ti-8Al-1Mo-1V fracture surface⁽⁶⁾. The developed film can be analyzed using existing techniques⁽⁷⁾ to determine the concentration of the radioactive contaminant in the metal surface. Use of the dilution factor for the isotope in the carrier media allows calculation of the actual contaminant concentration. Mechanical sectioning of the test specimen to reveal interior planes allows observation of the distribution of the contaminant in the third dimension and determination of diffusion rates through the material. An example of the distribution of chlorine-36 on an interior plane of a 7075-T6 aluminum alloy specimen is shown in Figure 9.

Identification of corrosion products can be accomplished by analysis of the corroident fluid. For example, consider a series of tests performed with Ti-8Al-1Mo-1V specimens exposed to 1M NaCl or CCl_4 and loaded in three-point bending to 80 percent of the air failure value. Portions of the corroidents were extracted from the vicinity of the crack during testing and analyzed spectrophotometrically. Figure 10 shows the resultant ultra violet absorption spectra. It has been suggested that the absorption peaks in both liquid media were due to the tetravalent type structure ($Ti = O$). These results were used in conjunction with other data⁽⁶⁾ to develop a series of chemical reactions to describe Ti-8Al-1Mo-1V stress corrosion. These reactions are as follows:



where x does not exceed 4.

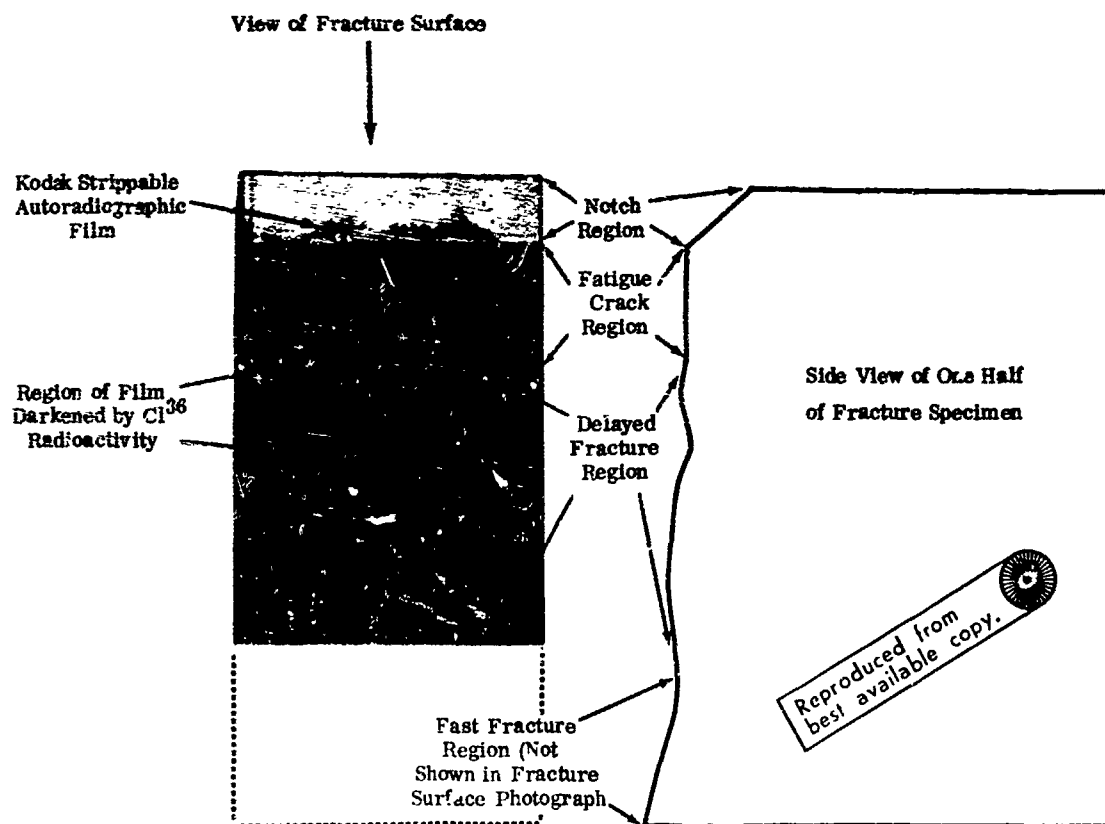


Figure 8. Autoradiographic study of radioactive Cl^{36} retention on the Ti-8Al-1Mo-1V alloy fracture surface.



Figure 9. Replicas of interior plane 0.015 inch from the surface of a 7075-T6 specimen. Darkened areas caused by decomposition of emulsion locate radioactive chlorine-36 accumulation.

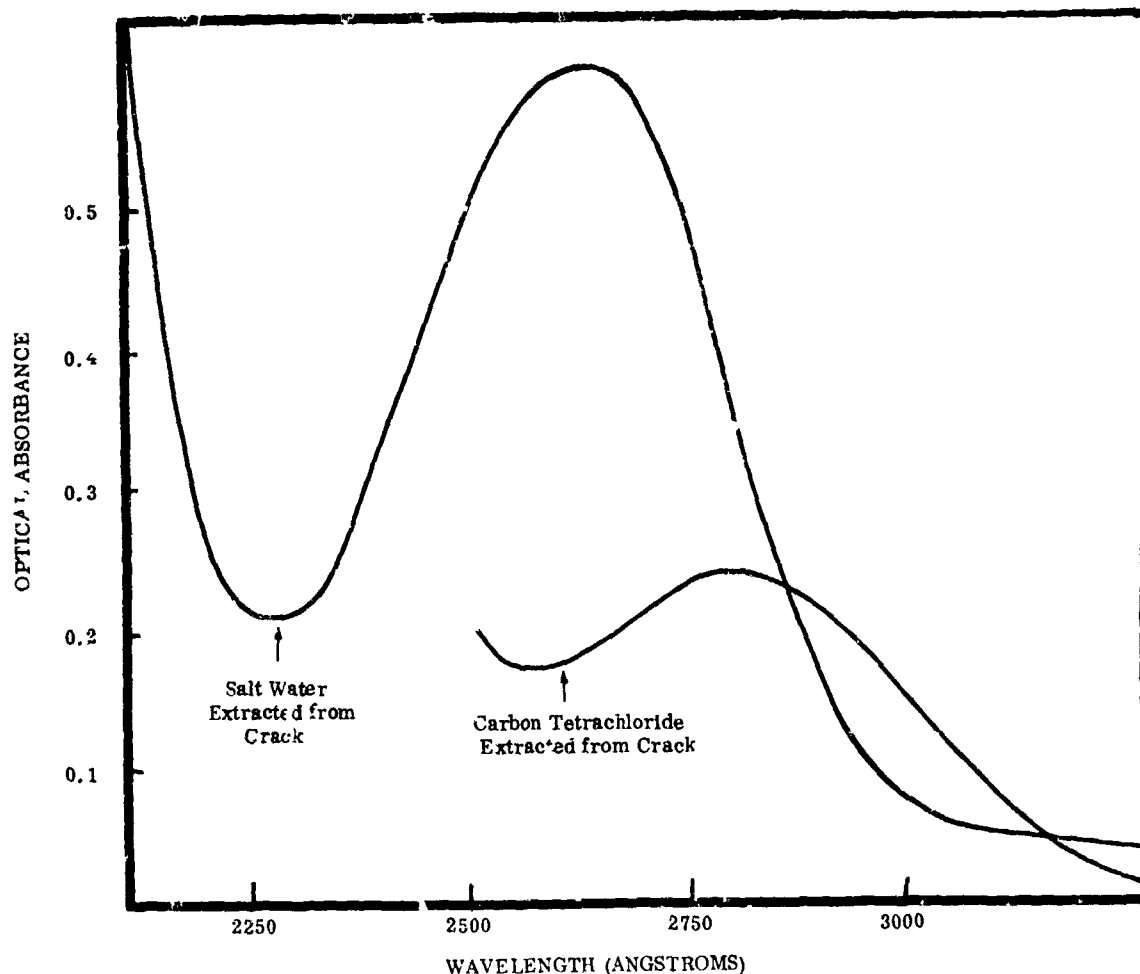


Figure 10. Optical absorbance spectra of Ti-8Al-1Mo-1V corrosion product.

ELECTROCHEMISTRY

Crack-tip corrosion cell activity can be delineated by use of pH and oxidation/reduction indicators⁽⁶⁾. The pH indicators function by using color changes to detect pH shifts associated with electrochemical processes active in the vicinity of the crack. For the Ti-8Al-1Mo-1V alloy under discussion, passive regions external to the crack tend to become cathodic, with an attendant increase in alkalinity due to the formation of hydroxyl ions. On the other hand, anodic regions within the crack tend to become acidic due to the production of hydrogen ions. The pH sensitive dyes can be used very effectively to identify these anodic and cathodic regions. Similarly, certain oxidation reduction indicators will respond in regions where these electrochemical processes are occurring.

Solutions of 1M NaCl solution containing either phenolphthalein pH indicator or a starch-potassium iodide oxidation indicator were added to the notch region of precracked specimens of Ti-8Al-1Mo-1V. These specimens were loaded to 80 percent of the air failure value in three-point bending. Sketches of the appearance of the notch region during exposure are shown in Figure 11. As the crack progressed in solutions containing phenolphthalein, red coloration was produced along the sloping sides of the notch, indicating hydroxyl ion formation, while the solution at the apex of the notch immediately adjacent to the notch remained colorless. On the other hand, solutions containing the starch-iodide indicator yielded a characteristic blue color in the anodic crack region.

This experiment and others described earlier indicate that the corrosion cell voltage tends to move positive ions, such as titanium out of the crack and drive negative ions, such as chloride, into the crack. Thus, chloride ion is indicated as the damaging species for Ti-8Al-1Mo-1V^(1,3,6). The observation of corrosion cell activity at the crack tip led to the conclusion that protection might well be attained by interfering with the electrochemical reactions involved.

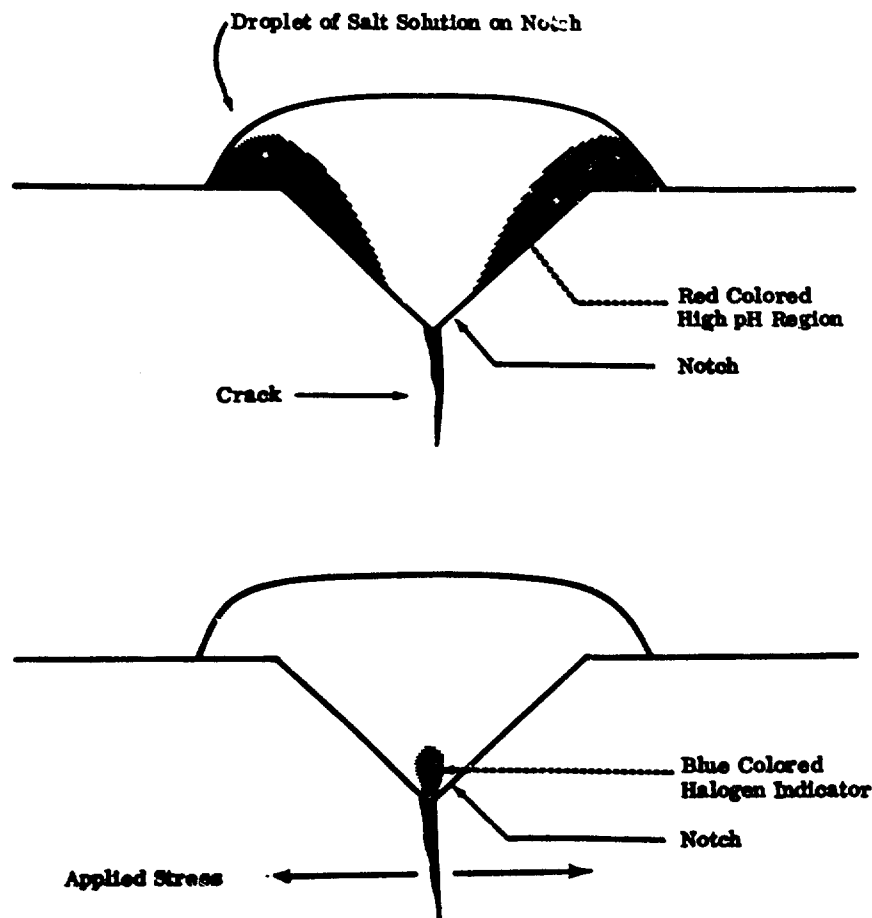


Figure 11. Diagram of appearance of notch in Ti-8Al-1Mo-1V after exposure to 1M NaCl corrosive containing indicators.

Electrode potential measurements have provided one of the most effective methods for evaluating the electrochemical aspects of stress corrosion susceptible alloys. Potential measurements long ago provided evidence that both ferric (Fe^{+3}) and cupric (Cu^{+2}) ions actively absorb on titanium surfaces from aqueous solutions⁽⁸⁾. Hence, electrode potential measurements were used to determine the passivating ability of a number of inhibitors. The basic equipment used in these investigations consisted of an electrometer connected in a circuit between a saturated calomel reference electrode and the test sample, both of which were in contact with the aqueous media. An experimental apparatus used for potential measurements on wire samples is shown in Figure 12. The flask which contained the aqueous solution was modified so that the wire could be passed through the flask wall and stressed by dead weight loading. It was soon discovered that there was no particular advantage in working with stressed samples, and the bulk of the experimentation was accomplished using alloys in the unstressed condition. Results of these screening studies revealed that iridium (Ir^{+4}), gold (Au^{+3}), ferric (Fe^{+3}), and cupric (Cu^{+2}) were among the ionic species that produced the greatest degree of passivation for the Ti-8Al-1Mo-1V alloy in 1M NaCl solutions. Electrode potential shifts as great as 1.2 volts in the noble direction were produced by certain of these materials when present at concentrations of approximately 0.001 moles per liter.

These same ionic passivators were subjected to further evaluation in mechanical tests to determine their effectiveness in preventing stress corrosion cracking. Duplex annealed Ti-8Al-1Mo-1V notched and precracked three-point bend specimens were loaded to 80 percent of the air failure value and immersed in a 1M NaCl solution to which a trace of the passivator had been added. All of the ionic passivators mentioned previously substantially increased the time to failure in this alloy. It was discovered that inhibitor concentrations as low as 0.005 percent by weight were effective. Comparison of the electrochemical and mechanical test results demonstrated that a direct correlation existed between the ability of an ionic passivator to inhibit stress corrosion cracking and the electrode potential change which resulted when that passivator was brought in contact with the alloy. Passivators which displayed more than approximately 0.5 volt change during the screening tests were found to effectively inhibit cracking; those which produced less than 0.5 volt change were ineffective.

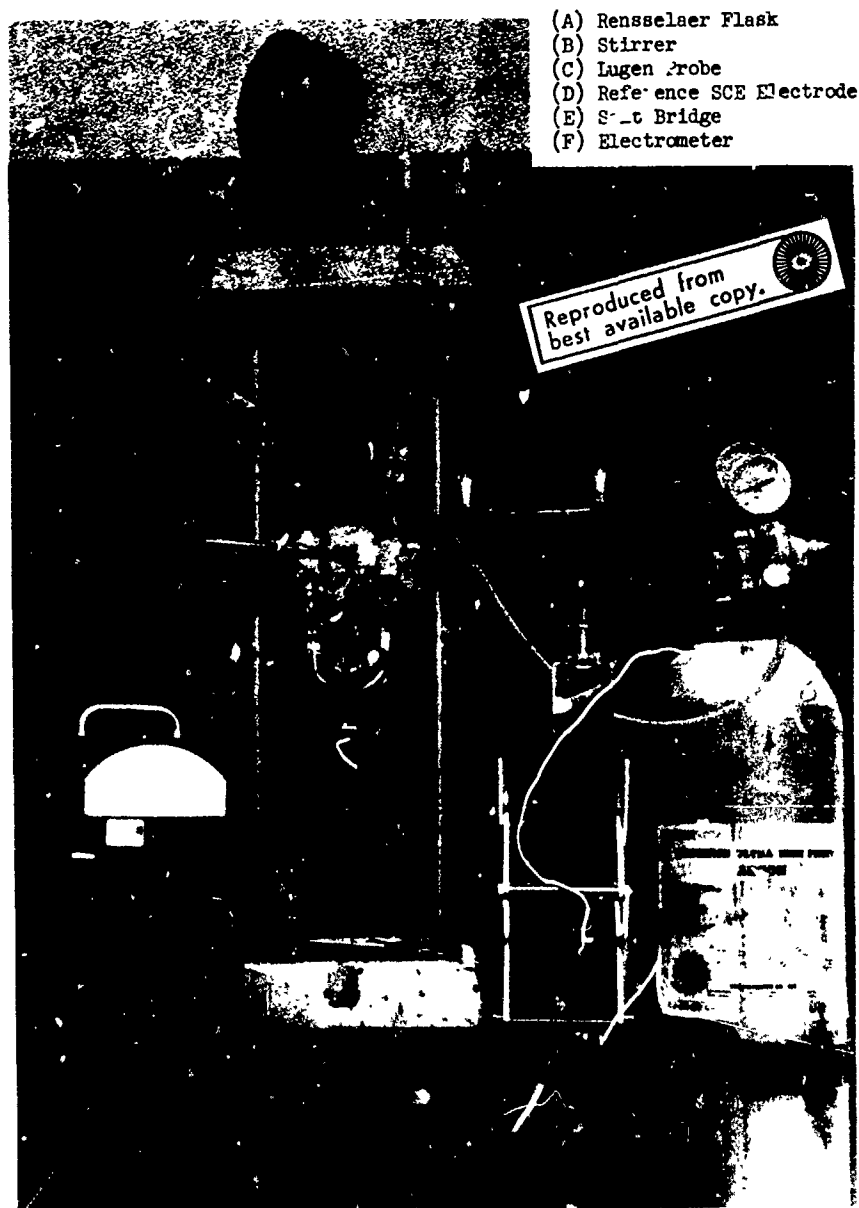


Figure 12. Equipment for electrode potential measurements.

It was postulated that retardation of crack growth in titanium by these inhibitors resulted from the fact that both the anode and cathode regions of the electrochemical cell within the crack became passivated to similar noble potentials by absorbed ionic material. This served to substantially drop the total voltage difference of the cell which in turn reduced the tendency of the corrosive negative ions (e.g. Cl^-) to be attracted to the anodic crack tip region where metal dissolution normally occurs. Thus, these inhibitors apparently functioned by destroying the normal electrochemical ion transport mechanisms that are required for sustaining stress corrosion crack growth in this alloy. It is possible that inhibitors of this type could be employed in sealants to help prevent or arrest crack growth.

CONCLUSION

The diverse assembly of investigative techniques described in this paper point up the need for interdisciplinary efforts in stress corrosion research. Techniques and procedures from many fields, including mechanics, metallurgy, chemistry and physics must be utilized if the desired level of understanding is to be attained.

REFERENCES

1. M.P. Kaplan, D.S. Cowgill, J.S. Fritzen, W.E. Krupp, S. Krystkowiak and K.E. Weber, "A Study of the Mechanics of Fracture in Stress Corrosion Cracking," Corrosion, V. 26 (1970) p. 7
2. S. Krystkowiak and D.S. Cowgill, "Titanium Stress Corrosion Cracking Morphology," Proceedings of First Annual Meeting of the International Metallographic Society, Denver, Colorado, November 1968
3. K.E. Weber, S. Krystkowiak and J.S. Fritzen, "Similarities of Titanium Stress Corrosion Cracking in Salt Solutions and Carbon Tetrachloride," DMIC Memo 228, Battelle Memorial Institute, Columbus, Ohio, March 1967
4. C. Leymonie, Radioactive Tracers in Physical Metallurgy, John Wiley and Sons, New York, N.Y., 1963
5. A.W. Rogers, Techniques of Autoradiography, Elsevier House, London, England, 1969
6. D.S. Cowgill, J.S. Fritzen, S. Krystkowiak, W.E. Krupp and K.E. Weber, "Crack Morphology Studies in the Ti-8Al-1Mo-1V Alloy," presented at ASTM/ARPA Symposium on Stress Corrosion, Atlanta, Georgia, October 1968
7. N.A. Tiner, "Use of Electron Microautoradiography for Evaluating Microsegregation of hydrogen in Titanium Alloys," ASM Transactions, V. 61 (1968) p. 195
8. H.H. Uhlig and A. Geary, J. Electrochem. Soc., V. 101 (1954) p. 215

FRACTURE INITIATION AND STRESS CORROSION CRACKING
OF WELDED JOINTS OF α TYPE TITANIUM ALLOYS

by

C.Chassain and P.R.Krahe
Centre des Matériaux de l'Ecole des Mines de Paris
91 - Corbeil - France

ABSTRACT

The almost instantaneous failure of some welded joints of certain Ti, Al, Sn α type alloys when in contact with carbon tetrachloride vapour, was studied and related to the slight surface contamination developed during argon-arc welding. Analysis of the contaminated layers with the Castaing-Slodzian ion probe showed that a substantial amount of oxygen penetration had occurred during the welding operation. Testing showed that the susceptibility to stress corrosion was related to the extent of this penetration and micro-cracks were observed to form on the welded surfaces after loading but before contact with the corrosion medium. As oxygen in solid solution in titanium reduces its ductility these mechanical cracks will propagate under the action of a constant load deeper into the more contaminated samples. If the K_I at the crack tip exceeds the $K_{I_{SCC}}$ at the moment of contact with the corrosion medium the cracking will proceed by stress corrosion and will lead, under higher stresses, to the almost instant failures observed.

RESUME

La rupture quasi-instantanée de joints soudés d'alliages de titane de type α lorsque mis en contact avec les vapeurs de trichloréthylène, a été étudiée et reliée à la contamination superficielle lors des opérations de soudage à l'arc sous atmosphère d'argon.

Les analyses des couches contaminées au moyen d'un analyseur ionique de Castaing-Slodzian, ont montré qu'une pénétration relativement importante d'oxygène avait lieu lors de ce soudage. Nos essais ont montré que la susceptibilité à la C.S.T. était en relation avec la profondeur de cette contamination. La formation de microfissures a pu être observée sur les surfaces soudées lorsqu'elles sont mises sous contraintes avant le contact avec le milieu de C.S.T. L'oxygène en solution solide dans le titane réduisant fortement sa ductilité, ces criques mécaniques peuvent se propager profondément dans les échantillons les plus contaminés. Lors de la mise en contact avec le milieu, si le K_I existant alors en tête de ces fissures dépasse le $K_{I_{SCC}}$, la fissuration intervient par C.S.T. et sous fortes charges des ruptures presque instantanées peuvent survenir.

FRACTURE INITIATION AND STRESS CORROSION CRACKING OF WELDED JOINTS OF α TYPE TITANIUM ALLOYS.

by

C. Chassain and P.R. Krahe

1. INTRODUCTION

The stress corrosion cracking (SCC) of welded joints of some α titanium alloys when in contact with chlorinated hydrocarbons has been known for a long time (1). In particular, very rapid failure was reported by Brown (2) and Vialatte (3), who studied the SCC of the alloy TA5E in carbon tetrachloride. To explain this behaviour, Brown suggested that stress corrosion was initiated at pre-existing micro-cracks formed by the mechanical failure of the oxides present at the weldment's surface. Two experimental observations made by Vialatte gave further weight to this hypothesis: the first concerned the micro-cracks found on the weld's surface before contact with the SC medium and after loading and the second the suppression of the phenomenon once matter was removed from the weldment's surface.

However, since no control was exerted on the amount of matter removed from the weld's surface, the question as to whether the removal of just the oxide film would inhibit SCC remained unanswered, and so these observations did not prove Brown's hypothesis. Indeed our results show that the removal of only the oxide film will not eliminate SCC.

2. RESULTS

The susceptibility of alloys TA5E and TAE Zr 5 to SCC in carbon tetrachloride vapour was evaluated by the three point constant load flexion testing of 5 mm wide specimens, cut out of a 2,5 mm thick and 110 mm wide plate having a welding seam in the middle. The results are given in fig.1 as curves of failure time against loading stress. For stresses near the elastic limit (80 - 90 hbars) the failure times are very short, varying from 1 to 10 minutes.

Experiments showed that the samples would become insensitive to SCC if at least 5 μ were removed from the welded surface by any of the following ways: mechanical and electro-polishing, grinding or chemical cleaning. However if after this treatment the samples were re-contaminated by a brief heating under a torch flame ($\sim 700^\circ\text{C}$), they again became sensitive and would fail at the times and stresses given by fig.1.

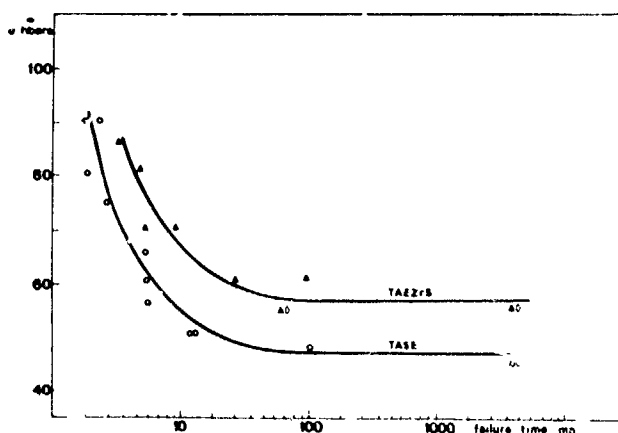


Fig.1 - Stress versus failure time for three point flexion of welded specimens.

The ion probe results are summarized in figs. 2 and 3 for the following four different surface treatments and stress corrosion susceptibilities.

- | | | |
|----------------------------------|---|-----------------|
| 1) Not welded | : | Not susceptible |
| 2) Welded | : | Susceptible |
| 3) Welded and chemically cleaned | : | Not susceptible |
| 4) As 3 plus flame contamination | : | Susceptible |

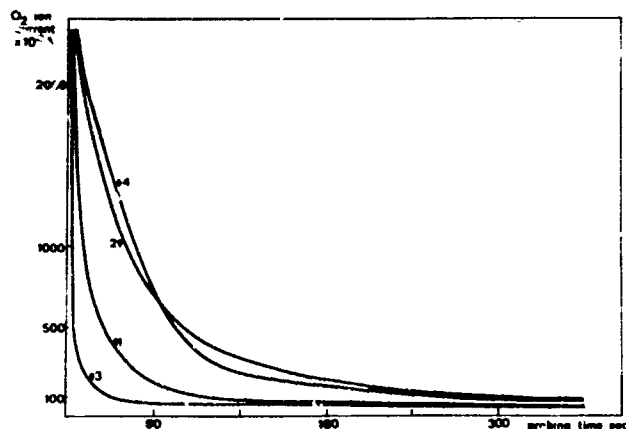


Fig. 2 - Oxygen penetration curves for the following surface conditions : 1) not welded, 2) welded 3) welded and chemically cleaned, 4) welded chemically cleaned and flame recontaminated.

These curves are plots of the analysed secondary O_2^- ion current against the probing time. Since the bombardment erodes the metal at a rate nearly equal to 100 Å/sec, they represent the oxygen distribution from the surface down into the metal. The high initial concentration observed in the immediate vicinity of the surfaces is due to absorbed O_2 and to thin surface oxides. When the contamination becomes more severe - treatment 4 - the surface oxide becomes thicker as can be seen by the plateau observed on the corresponding curve, fig. 3. It is interesting to note that even for this heavily contaminated state, the oxide thickness did not exceed 0.2μ while it was necessary to remove around 5μ of material from the weld's surface in order to eliminate stress corrosion susceptibility, this latter figure being near the depth where the oxygen concentration falls down to the matrix level, fig. 2.

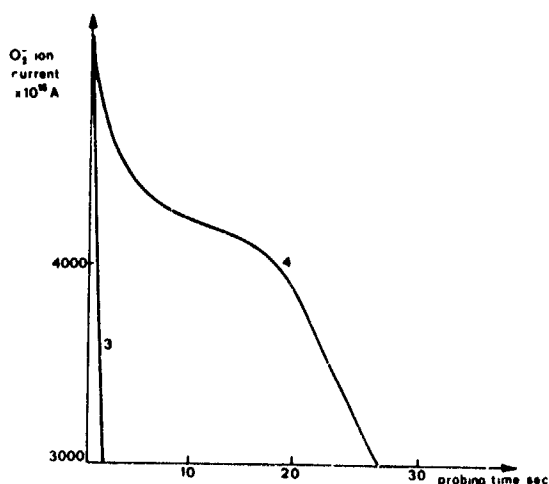


Fig. 3 - Oxygen rich portion of fig. 2 curves 3 and 4

The oxygen penetration in the metal is clearly different according to the surface treatment given to the sample, being more extensive in the heavily contaminated samples which are also the more susceptible to stress corrosion. It is therefore apparent that the extent of the concentration gradient below the weld's surface is the determining factor on the initiation of SCC of these alloys in carbon tetrachloride vapour.

That the presence of a thin surface oxide plays a small role on this process is shown in fig. 4, which corresponds to the oxygen penetration in a sample chemically cleaned and re-oxidised anodically. Although the presence of the oxide is clearly seen by the plateau this sample is not susceptible to SCC, as one would expect from the shallow penetration curve observed.

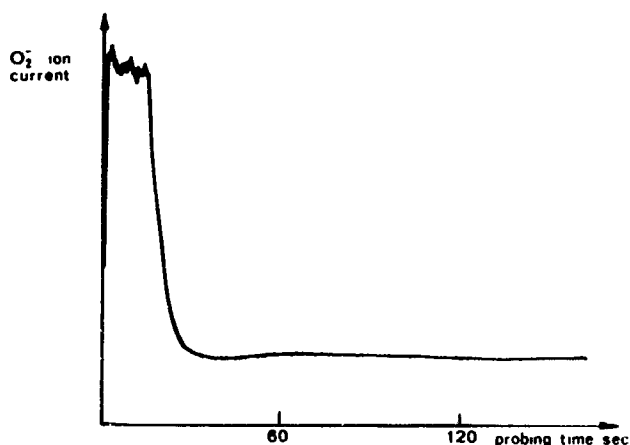


Fig. 4 - Oxygen penetration curve for the following condition : welded, chemically cleaned and oxidised anodically in a H_2SO_4 solution.

3. A MODEL FOR THE OBSERVED STRESS CORROSION INITIATION

It is well established that certain elements like oxygen when in solid solution in titanium greatly diminish its plasticity by impairing its usual modes of deformation, i.e. slip and twinning (4) (5). We can therefore associate a ductility gradient with each oxygen concentration gradient observed.

Before immersion in the stress corrosion medium but after loading the sample, micro-cracks can be initiated on the sample's surface and can propagate into the diffusion zones : some of these micro-cracks are seen on fig. 5. At constant load their propagation and therefore their final length will depend essentially on the ductility at the crack tip. The longer mechanical micro-cracks are to be found in the more extensively contaminated samples.



Fig. 5 - Mechanical failure of the welded surfaces before immersion in carbon tetrachloride, X 5000.

For the particular test employed in the present study, the stress intensity factor, K_I , at the crack tip will be highest for the longer cracks. If K_I exceeds the lowest stress intensity factor needed for the development of stress corrosion in the environment under consideration ($K_{I_{SCC}}$), the crack will begin to grow as soon as the sample comes in contact with the stress corrosion medium. If K_I is lower than $K_{I_{SCC}}$, the crack will not propagate. In this way we can account for the almost instant cracking of the weldments and for the relation between stress corrosion susceptibility and extent of contamination

4. ACKNOWLEDGMENTS

The authors wish to thank the Société Nationale d'Etudes et de Construction des Moteurs d'Avions (SNECMA) for the financial support given to this study, and the CAMECA, for the use of their ion probe.

5. REFERENCES

- (1) R. Meredith and W.L. Arter.
Welding Research Supplement. Sept. 1957, p.415-s
- (2) H. Brown.
Battelle Memorial Institute, Columbus, Ohio, DMIC,
Memorandum 60, August 1960.
- (3) M. Vialatte et C. Apert.
Corrosion - Traitements - Protection - Finition.
Vol.16, N°5, Aout-Septembre 1968, p.246.
- (4) E.K. Molchanova.
Phase Diagrams of Titanium Alloys.
Israel Program for Scientific Translations, Jerusalem 1965.
p.119 - 126.
- (5) A. Dubertret.
Métaux, Corrosion, Industrie.
Mars 1971, N° 547, p.88.

PRELIMINARY REPORT ON THE RESEARCH ON THE INFLUENCE
OF THERMOMECHANICAL TREATMENTS ON STRESS CORROSION
CRACKING BEHAVIOUR OF AISI 4340 STEEL

by

R. De Santis - L. Matteoli - T. Songa

Istituto di Ricerche Breda - Milano and Bari

PRELIMINARY REPORT ON THE RESEARCH ON THE INFLUENCE
OF THERMOMECHANICAL TREATMENTS ON STRESS CORROSION
CRACKING BEHAVIOUR OF AISI 4340 STEEL

R. De Santis - L. Matteoli - T. Songa

This contribution refers some data on a research, sponsored by the Italian Air Force, on the influence of thermomechanical treatments on the stress corrosion cracking of AISI 4340 steel.

The interest in this research has been aroused by the anomalous behaviour of carbon and alloy heat-treatable steels upon cold deformation after low temperature tempering. The phenomenon was firstly observed in 1953 by Matteoli and Andreini (4).

It has been proved that these steels, heat treated to a tensile strength superior to 150 kg/mm², undergo a reduction in hardness, when submitted to a subsequent cold deformation.

It has also been proved that the hardness characteristics can be partially or completely recovered with a second tempering treatment, after the deformation, performed at the same temperature of the first tempering.

The research in progress is intended to establish whether the above-mentioned thermomechanical treatments could influence the stress corrosion cracking behaviour of the 4340 AISI steel.

For the research two grades of 4340 AISI steel have been selected: air melted and electroslag remelted.

Fig. 1 and 2 show the experimental results obtained by testing the hardness of two specimens of both steel grades subjected to the thermomechanical treatments, illustrated in the same figures.

The hardness recovery of the steels tempered at 200°C, is very small, if not absent, and sometimes it takes place after very long tempering time. This phenomenon is very marked, on the contrary, for the 300°C tempered steels. In this case long tempering time causes a second decrease of the hardness in a way, which is typical for ageing phenomena.

No clear relation seems to exist between the metallurgical grade of the material and the behaviour upon deformation and second tempering. Moreover there are significant differences in the results obtained on different specimens of the same material.

These interesting aspects of the problem are still under examination.

No complete explanation exists about the decrease in hardness upon deformation. Among the possible hypotheses the most plausible one seems to be the intervention of an effect of the extra strain energy (supplied by the deformation) in restoring the lattice of the metal.

Stress corrosion cracking tests are now in progress on specimens from both steels in the quenched and tempered conditions, both at 200°C and at 300°C, in the cold deformed conditions after tempering and in the maximum hardness recovered conditions.

To evaluate the stress corrosion cracking behaviour of the steels, cantilever beam specimens,

side grooved and fatigue precracked, are used. The typical specimen geometry is shown in fig. 3.

The use of cantilever beam specimens is due to the two following basic considerations:

- 1) at any given stress intensity above K_{ISCC} the cantilever specimen rupture occurs in the shortest time compared with other specimens with different geometry giving the same apparent threshold limit
- 2) the tests with an increasing K are more representative of the real situation rather than a decreasing K or the very difficult constant K tests

Side grooving of the specimens has been selected because of the complete suppression of any shear lip and of the consequent setting up of pure plane-strain conditions in the whole section.

The obvious reason for fatigue precracking is due to the opportunity not to rely upon the "natural" development of a stress raiser (such as a corrosion pit) in conducting stress corrosion tests on high strength and notch sensitive materials.

After notch and side groove machining, fatigue cracks are induced at the base of the notch by fatigue in air. During fatiguing the crack propagation rate is continuously checked with an electrical resistance meter device as to assure that the ratio of the total flaw depth to the total specimen thickness is in the range 0.25 ± 0.35 for all the specimens.

Side grooving has proved itself very satisfactory in maintaining the fatigue crack in axis with the notch and in allowing the fatigue crack to grow nearly straight (see fig. 4). This is very important because, during cracking in these conditions crack velocity and also the crack driving force are uniform.

For the stress corrosion test the specimens are loaded in bending with devices similar to those proposed by Brown in 1966 (1).

The corrosive medium is 3% sodium chloride solution in distilled water. The contact of the electrolyte with the specimen occurs by continuous dripping of the solution on the notch. References 2, 3 and 5 give more detailed information on the working procedure.

Stress corrosion cracking tests are still in progress and the results on K_{ISCC} values are not yet available. The influence of the thermomechanical treatments on the Fracture Mechanics parameters are however expected to be significant.

REFERENCES

- 1) Brown B. F. "A new Stress-Corrosion Cracking Test for high strength alloys"
Materials Research and Standards 6 (1966) 129
- 2) De Santis R., Songa T. "Aspetti metodologici nello studio della corrosione sotto tensione di acciai ad elevata resistenza"
Ingegneria Meccanica 19 n. 8 (1970) 37
- 3) De Santis R. "Metodologie di prova nello studio della corrosione sotto tensione di acciai ad alto limite di snervamento"
La Metallurgia Italiana 77 n. 12 (1970) 461
- 4) Matteoli L., Andreini B. "Prove di fatica su acciai deformati a freddo ed aventi subito una diminuzione di durezza"
La Metallurgia Italiana 60 n. 9 (1953) 3
- 5) Songa T., De Santis R. "Teorie sulla corrosione sotto tensione degli acciai ad elevata resistenza"
Ingegneria Meccanica 19 n. 6 (1970) 45

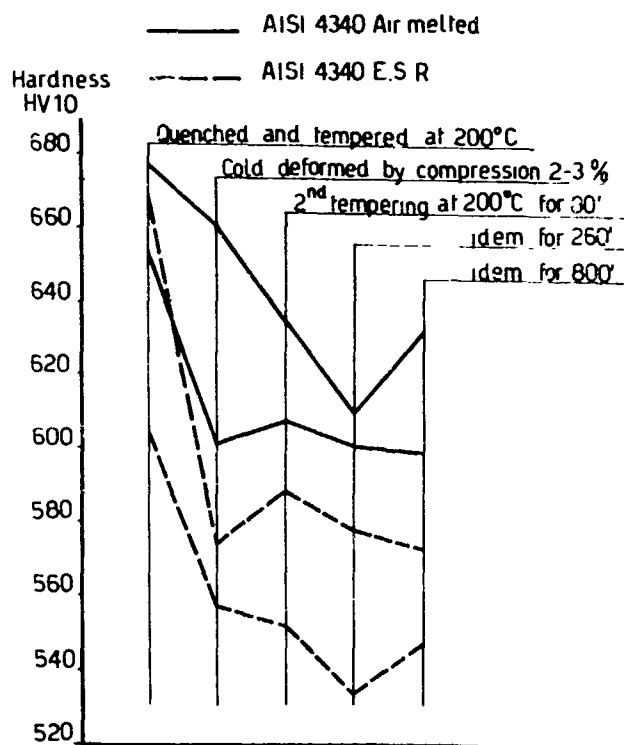


fig. 1

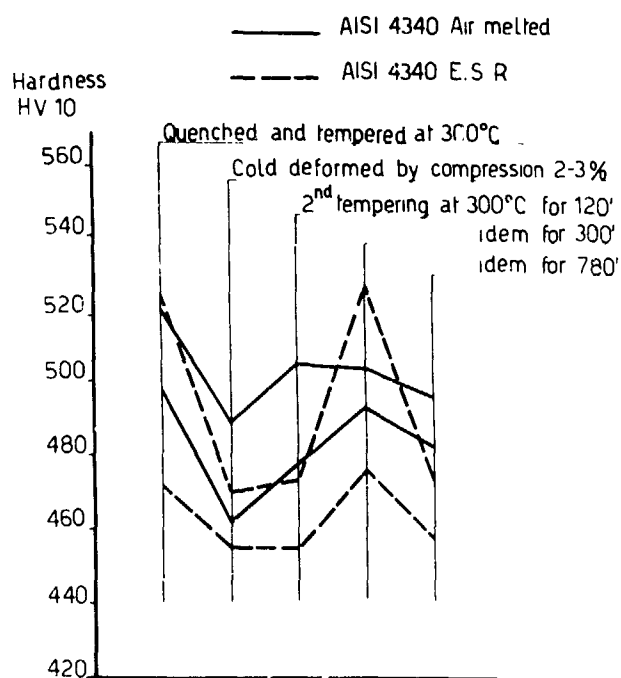


fig. 2

fig 1 - 2 - Hardness variations consequent to the thermomechanical cycles illustrated in the figures

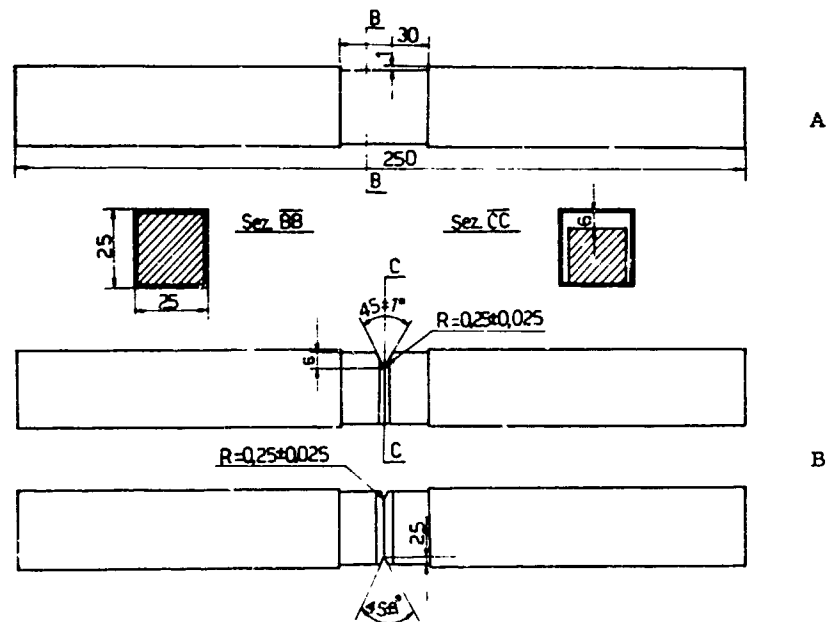


fig. 3 - Stress Corrosion Cracking Specimens Geometry

A = Specimen ready for deformation

B = Specimen ready for S.C.C test

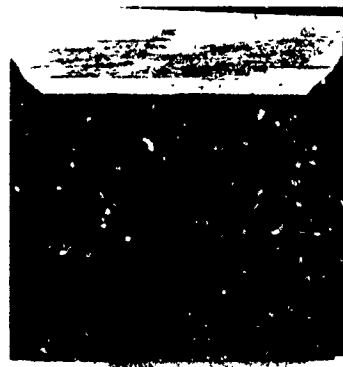


fig 4 - Appearance of the fatigue crack penetration in the specimen

PRELIMINARY RESULTS OF MECHANICAL AND STRESS-CORROSION TESTS ON
PLATES OF 7075 ALLOY PRODUCED BY A NEW PROCESSING TECHNIQUE

by

E. DI RUSSO, M. CONSERVA, M. BURATTI
Research Metallurgists of the Metallography Department
of the Experimental Institute of Light Metals
C.P.129 - 28100 Novara (Italy)

SUMMARY

The primary and secondary properties of hot rolled plates of 7075 alloy, obtained with a new processing technique, are briefly described. These new materials show a significant reduction of the transverse effect in respect to the conventionally produced plates. Improved characteristics of ductility, fracture-toughness and stress-corrosion resistance are attained in the short transverse direction, along with strength levels equal to or higher than those of similar materials produced in the traditional way.

On décrit brièvement les propriétés primaires et secondaires des ébauches à chaud d'alliage 7075, obtenus avec un nouveau procédé technologique. Ces nouveaux matériaux présentent une significative réduction de l'effet de travers en comparaison avec les ébauches produits conventionnellement.

Une amélioration de la ductilité, de la tenacité à la rupture et de la résistance à la corrosion sous tension, est réalisée avec niveaux de résistance mécanique égaux ou plus élevés que ceux des similaires matériaux produits avec le procédé traditionnel.

PRELIMINARY RESULTS OF MECHANICAL AND STRESS-CORROSION TESTS ON PLATES OF 7075 ALLOY
PRODUCED BY A NEW PROCESSING TECHNIQUE

by
E. DI RUSSO, M. CONSERVA, M. BURATTI

The scope of this technical note is to present some preliminary results of mechanical and stress-corrosion tests performed on plates of 7075 alloy, produced by a new processing technique. Although the stress-corrosion behaviour, which is the main topic of this meeting, is not considered in detail, anyhow it may be interesting to describe briefly the properties of these new products characterized by a significant reduction of the transverse effect.

As is known, the transverse effect is especially prevalent in plates of 7075 alloy of normal industrial production.

The material obtained with the new processing technique, represents an important development towards the production of plates with better combination of strength-ductility-fracture-toughness-stress-corrosion resistance in the (short) transverse direction; on the other hand it can allow a more valuable study to be made of the relationship existing between the above mentioned properties, taking as comparison term a conventionally produced material.

The most important ways till now followed for attaining a more attractive combination of the main properties which characterize the service behaviour of a plate of 7075 alloy, are the following:

- increase of the degree of purity (very low content of Fe and Si);
- ingot homogenization at very high temperature and for long soaking times;
- high solidification rate in order to reduce the D.A.S. (dendrite arm spacing) down to $20\pm 30 \mu\text{m}$;
- two-step ageing cycle.

Another way is to employ ancillary elements different from chromium; obviously if the alloy is completely free from chromium, we have a new alloy; a typical example is given by Zergal alloys, where zirconium is substituting for chromium.

By chance it is to be noted the increasing development of Zr bearing Zergal like alloys, to replace 7075 type materials.

All the factors above mentioned have improved the properties of the wrought products of 7075 alloy, but today they represent only a starting point to go on.

For further substantial improvements it is necessary to follow new routes, taking into consideration the basic structural factors involved in the transverse effect.

The fracture path in specimens subjected to mechanical and stress-corrosion testing, follows preferentially the original cast grain boundaries, which survive in the plate and are orientated in the working direction. Actually what we call "grains" are constituted by aggregates of sub-grains of some μm in diameter. This type of fracture occurs above all when the products is stressed in the short-transverse direction. It is worthwhile remembering that secondary undissolved or insoluble phases and oxide inclusions are preferentially localized along the original grain boundaries and this fact enhances the transverse effect.

The new processing, developed under contracts with the Italian Ministry of Defence and the U.S. Department of the Army and forming the object of a recent patent application, makes possible the complete destruction of the cast structure and the formation of new grain boundaries not having any relationship with the original primary ones. At the same time, the new grains are much smaller than those present in a conventionally produced material. Also in this case, these new grains represent definite aggregates of sub-grains.

The table I lists some data of mechanical and stress-corrosion tests performed on two 25 mm-thick plates of high purity 7075 alloy, produced respectively by conventional practice and by the new processing, and heat treated T6 and according to a two-step ageing cycle. The conditions adopted in the second step of ageing ($160^\circ\text{C} \times 13 \text{ hrs}$) were intentionally chosen for comparison purpose; they determine in fact a stress-corrosion resistance higher than the typical one of the T6 treatment but insufficient to make a conventionally produced plate free from stress-corrosion phenomena in the short-transverse direction.

As can be seen, after a T6 treatment the new processing causes a strong improvement in elongation and reduction in area and such improvement is reached without any changement of the UTS and YS levels. The results referring to the plate produced by common practice represent the best which may be obtained on the 7075 alloy conventionally processed. After two-step ageing cycle, the differences in reduction in area between the two

materials remain unchanged, while the level of strength is almost the same for the two plates.

Although these data have been obtained on the long-transverse direction, it is reasonable to assume that analogous improvements in ductility may be attained in the short-transverse direction.

Preliminary fracture-toughness tests on the short transverse have indicated also a significant improvement of K_{IC} values caused by the new working process; the fig.1 shows the outstanding difference in the aspect of the fracture surface of two specimens after testing.

Stress-corrosion tests performed in the short-transverse direction using "tuning" fork specimens stressed in tension on the external surface at 60% of Y.S. and subjected to alternate immersion in 3.5% NaCl solution, have indicated (tab.I) the great improvement of resistance to cracking which may be reached by the new technological cycle and suitable ageing treatment (generally performed at $160^{\circ}\text{C} \times 16 \pm 24$ hrs).

On the basis of our knowledge about the relationship between ageing conditions, micro-structure and stress-corrosion behaviour, we have directed our attention on an outstanding structural feature linked with the new cycle; that is a precipitation of chromium bearing compounds which is quite different in the distribution and size of the particles from that commonly observed in conventional products of 7000 alloys.

It has been demonstrated that this precipitation acts on the ageing structures at high temperature and exerts a positive influence on the general plasticity of the aluminium matrix.

Such chromium distribution seems to favour the structural modifications induced in Al-Zn-Mg-Cu alloys by a controlled overageing treatment which is responsible for the increase of the stress-corrosion resistance.

It is obvious that the possibility to have at disposal products of 7075 alloy of definite composition and subjected to the same ageing treatment and showing same levels of strength, but different levels of ductility and toughness, may be a useful tool for a better evaluation of the parameters linked with the stress-corrosion phenomena as well as of the significance of the stress-corrosion test data obtained with pre-cracked specimens.

For this purpose, extensive investigations on Al-Zn-Mg-Cu system alloys are now in progress. In the stress-corrosion tests, together with pre-cracked specimens of DCB type, smooth specimens are used of the previously mentioned (constant deflection) type. This specimen has the stressed surface plained and metallographically polished (fig.2), hence it allows an easy inspection to be made of the crack appearance both visual and at the optical microscope. Besides, using an especial, designed electrolytic cell, it is possible to follow continuously at the optical microscope the nucleation of the crack and its enlargement during the stress-corrosion test.

Tab.I - Results of tensile, fracture-toughness and stress-corrosion tests performed on the plates of high purity 7075 alloy produced respectively by conventional and not conventional processing

Cycle	Heat treatment	long-transverse				short-transverse	
		UTS kg/mm ²	YS0.2% kg/mm ²	E %	R A. %	K _{IC} $\frac{\text{kg}}{\text{mm}^2} \sqrt{\text{mm}}$ (TW)	failure (*) times hours
conventional	T6(TA)	62.0	55.2	8.4	17	95	170 - 310
	TA ₁ + A ₂	60.9	54.9	8.6	26	109	247 - 310
not conventional	T6(TA)	61.6	56.2	10.6	34	120	248 - 310
	TA ₁ + A ₂	60.7	54.2	11.0	44	125	>1560

T = s.h.t. at 470 °C x 2 hrs: quenching in water at r.t.

A₁ = ageing at 120 °C x 24 hrs; A₂ = ageing at 160 °C x 13 hrs

(*) Alternate immersion test in salt solution on "U" shaped specimens

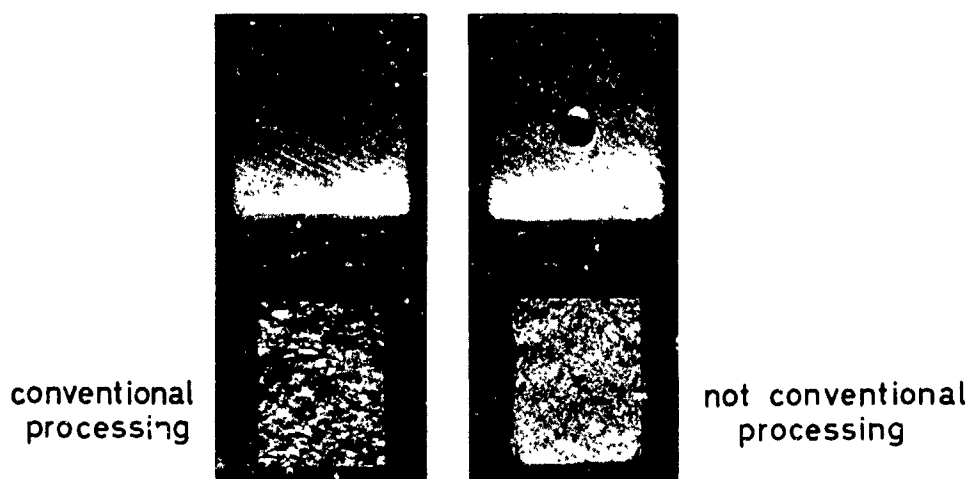
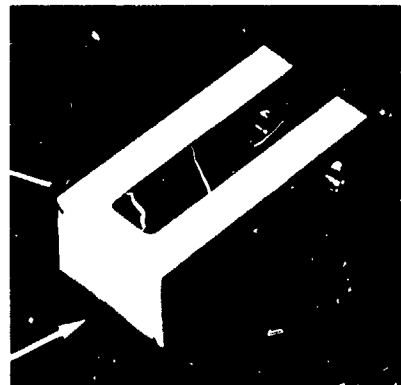
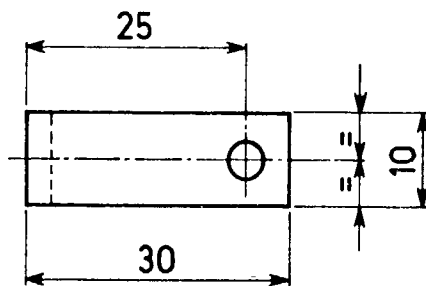
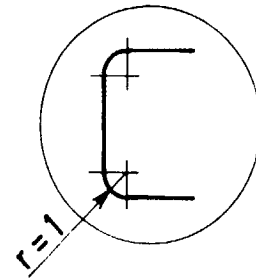
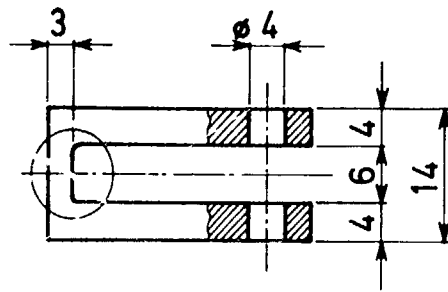


Fig.1 - Fracture surfaces of fracture-toughness specimens (short-transverse direction) of the h.p. 7075 alloy plates produced respectively by conventional and not conventional processing (Magn.X2)

Dimensions in mm.



Surface polished by
metallographic technique

Fig.2- Smooth specimen used in the stress-corrosion test. (Constant deflection type).

WRITTEN DISCUSSIONS OF PAPERS PRESENTED AT THE MEETING

Paper 1 - Engineering Utility and Significance of Stress Corrosion Cracking Data, presented by W. E. Anderson

R. P. Wei - In your presentation you indicated that the following criteria will be used for assessing the usefulness of laboratory stress-corrosion testing results for practical application:

$$\frac{1}{\pi} \left(\frac{K}{\sigma_{ys}} \right)^2 < ? < a < ? < L, W$$

Would you please expand on this point? Do you include conditions other than that for linear elastic fracture mechanics?

W. E. Anderson - If the cracking problem is clearly linear elastic, the general stress level will be well below yield and the relative dimensions indicated by the formulation will hold. In these cases, I have no hesitation in using the G or K representations of test specimens and structure, recognizing that there may or may not be continuous correlation between stress field parameter and the particular environmental cracking behavior. As the criteria tend more to be violated I become more cautious, finally "trusting" only to ad hoc test conditions.

W. Schütz - You mentioned that silver may induce stress-corrosion cracks in titanium parts. Do you know that some aircraft companies in the United States and Germany use silver plating on titanium parts to reduce fretting corrosion damage?

W. E. Anderson - Dr. Schütz points out (with regard to the jet-engine compressor-disc failure) that silver plating is currently used on a number of titanium aircraft parts. Yes, I have no doubt, I hope they are in locations that don't get too hot.

F. Bollenrath - Which are the correlations between the 3-atom-bonds per unit cell and the stress concentration factor for crack propagation?

W. E. Anderson - Regarding Professor Bollenrath's question, I was only trying to develop some appreciation for the activity level of each atom bond before the cracking process ruptured it, by whatever mechanism. Any "correlation" is determined by the material response to the imposed conditions. I assumed each aluminum atom vibrated about 10^{12} times per second and that about three atom bonds would be broken if the crack advanced one unit cell of 4\AA . (Would two bonds per cell be a better choice?) Also, "rapid" cracking was taken to be about 10^3 m/sec.

Paper 5 - Some Important Considerations in the Development of Stress Corrosion Cracking Test Methods, presented by R. P. Wei.

R. N. Parkins - Many service stress corrosion failures, especially in the chemical industry, involve very ductile materials in thin sections. Linear elastic analysis methods are usually not strictly applicable under these conditions. To what extent will future developments in fracture mechanics technology permit its application to these practical situations?

R. P. Wei - Dr. Parkins referred to service stress corrosion failures, especially those in the chemical industry, that involved very ductile materials in thin sections. If these failures occurred at nominal stress levels well below the yield strengths of the materials, it is not quite clear that linear elastic fracture mechanics analysis could not have been applied. The applicability of the analysis depends on the size of the crack-tip plastic zone in relation to the size of the crack and other planar dimensions of the body. More specific information will be needed for this determination. Many attempts are being made to incorporate the effect of crack-tip plasticity into the fracture mechanics analyses. We are hopeful that some useful results will emerge soon.

W. G. Clark, Jr. - With regard to the effect of exposure time on measured K_{Isc} values, what parameter was used to determine that the stress-corrosion process was not in operation during the shorter periods of time? Perhaps a fractographic examination of a broken specimen exposed for only a short time would indicate that stress-corrosion cracking is a problem at the nominal stress intensity involved. Were the test specimens involved in your study precracked in air or in the environment?

R. P. Wei - The data shown in Tables I and II of our paper do not imply that stress corrosion was not taking place at the shorter times. In fact, they are used to illustrate the dangers involved in making such an assumption. These results reflect principally the effect of incubation (defined as the period in which the rate of crack growth is much less than 10^{-6} inch per minute). Both displacement-gage measurements, made during testing, and post fracture examination of the fracture surfaces were used for establishing this incubation period.

The particular specimens used in these studies were pre-cracked in air, although specimens for other alloys that were pre-cracked in the aggressive environment still showed incubation, as well as the other stages of crack growth.

G. J. Danek, Jr. - In what materials did you fatigue precrack in the presence of the environment?

R. P. Wei - The materials that have been fatigue pre-cracked in the presence of environments used in subsequent stress corrosion cracking studies include AISI 4340, H-11 and 18Ni maraging steels, and high-strength titanium alloys.

Paper 6 - Current Progress in the Collaborative Testing Programme of the Stress Corrosion Cracking (Fracture Mechanics) Working Group, presented by A. H. Priest.

R. N. Parkins - While not wishing to disagree with your interpretation of the results from the experiments involving different temperatures, it would be unfortunate if it was thought that temperature invariably had no effect upon stress-corrosion cracking. Indeed, I wonder in relation to the results in this work (coupled with the doubts that begin to emerge about the reproducibility and significance of K_{ISCC}) whether had measurements of crack growth rate been made in these experiments instead of K_{ISCC} , a temperature dependence might not have been observed.

A. H. Priest - I agree that had the crack growth rates been measured in these tests a systematic variation with temperature would have been observed. Indeed investigations by individual laboratories have shown that the rate of crack growth displays an Arrhenius type of relationship with temperature.

It does not follow, however, that K_{ISCC} values will show a similar relationship since there is evidence that these depend upon the formation of a stretch zone at the crack tip which is likely to be governed by the plastic flow properties of the metal. Such properties will be relatively independent of test temperature and over the range investigated the variation of K_{ISCC} is probably insignificant.

A more thorough investigation of this type of factor has been initiated as part of the next stage of the collaborative programme. I disagree strongly with Dr. Parkins (who is a member of the Working Group) that the K_{ISCC} values of this group are either lacking in reproducibility or of doubtful significance. If evidence could be produced of the greater reproducibility of any other stress corrosion test conducted by as many laboratories I should believe he was on firmer ground.

When one bears in mind that the results from the collaborative programme were conducted on so many different types and sizes of specimen and that for several of the laboratories this was their first experience of this type of test, the results of the collaborative programme are remarkably consistent; the reproducibility would be encouraging if only one laboratory had participated, let alone thirteen.

If, on the other hand, Dr. Parkins is referring to the variation of K_{ISCC} values within a particular alloy system then this simply illustrates the sensitivity of fracture toughness parameters to real metallurgical effects. The influence of inclusion spacing and tensile properties on K_{ISCC} values described at this meeting indicates the importance of this type of factor which is equal to that of the influence of surface chemistry.

I do not wish to debate the significance of K_{ISCC} as a design parameter in this reply; only time and experience will provide the answer. It is interesting to note, however, that at the 1967 Stress Corrosion Specialists meeting only one out of seven papers was specifically concerned with fracture mechanics, at the 1971 meeting only seven out of twenty-one were not. One may extrapolate from there.

Paper 7 - The Science Committee Conference on the Theory of Stress Corrosion Cracking of Alloys, presented by J. C. Scully

G. Bollani - It would be interesting to know whether the branching of the crack reported in your last slide is attributable to microstructural characteristics of the material (grain boundaries, etc.), or has to be explained on fracture mechanics grounds

J. C. Scully - From all the evidence presented by Dr. Speidel in his paper on aluminum alloys and from other speakers at the conference it does seem reasonable to conclude that crack branching is controlled by considerations of fracture mechanics. This is also the conclusion drawn in my own work on austenitic stainless steels. By branching I mean a bifurcation followed by the propagation of both new fronts. It is also possible to obtain a semblance of branching in situations where some metallurgical feature is highly reactive but in such cases the main crack has many short digressions. That is quite a different case.

Paper 8 - Measuring the Degree of Conjoint Action Between Stress and Corrosion in Stress Corrosion, presented by F. H. Cocks.

H. L. Marcus - Did your comments about titanium 6Al-4V alloy imply an intergranular failure mechanism for this alloy?

- F. H. Cocks - No. The results of the precorrosion test procedure shows that there is a very long initiation stage which is not accelerated by the application of stress. This method does not, however, give information on the mechanism responsible for this initiation stage. Such information has to be obtained by other means, e.g., metallography.
- H. L. Marcus - In your description of the effect of surface preparation on the initiation-non-stressed condition you indicate that grain deformation is the primary cause of time effects. Dr. F. Mansfield of our laboratory has shown a large effect on the pitting potential for various surface preparations of aluminum alloy 7049 in various heat-treatment conditions. I suggest that many changes take place at the surface to change this "initiation" stage.
- F. H. Cocks - Undoubtedly there will be found to be many different explanations of precorrosion effects which may be observed in different alloys and environments. In the case of alloys which crack intergranularly, however, it seems reasonable to expect machining or shot-peening treatments to have a large effect on the initiation period. This is so because such treatments disrupt the grain boundary structure at the surface, and this layer of disruption must be penetrated by normal corrosion processes before stress corrosion can begin. There may, as you point out, be other processes occurring during the stress corrosion initiation period as well. Regardless of the cause of the initiation period, however, the precorrosion testing method I described provides a quantitative means for measuring how important this stage is in the overall failure process.
- Paper 10 - Stress Corrosion Testing of Welded Joints, presented by T. G. Gooch.
- W. G. Clark, Jr. - In your testing of welded joints, how do you account for the effect of residual stresses? How can you report stress-corrosion threshold values if you do not know the applied stress?
- T. G. Gooch - The question of residual welding stresses must be considered in relation to both laboratory testing and service. Once 3-point bend specimens are machined from a weld for SCC testing, tensile residual stresses will be largely relieved. Thus experimental derivation of K_{ISCC} ignores their contribution to the applied stress. However, unless there has been an effective stress relief treatment, residual stresses will constitute a significant addition to service loading. It may be difficult to establish precisely what residual stress exists, and a conservative approximation must be made. This should allow for local stress concentrations and joint geometry. For example, transverse to a weld, the stresses will normally be of the order of parent material yield stress. Along a weld they may be determined by the weld metal yield stress. In the linear elastic regime, it may be possible to determine the total acting K level by superimposing the contributions from residual and service stresses. This is comparable to the general yielding situation of adopting an additive strain approach to obtain a resultant total strain. In both cases, it should be possible to assess service performance in the light of NDT sensitivity. However, considerably more work is required before the effects of residual stresses can be fully defined.
- Paper 11 - Screening Tests of Susceptibility to Stress Corrosion Cracking, presented by G. J. Bieffer.
- W. K. Boyd - In our laboratory we have recently studied cathodic protection of 18Ni(200) maraging and HY140 steels in actual sea water. No hydrogen embrittlement was noted at three times the current densities required for protection. This has been attributed to the formation of a calcareous deposit on the surface which minimizes hydrogen pick-up. However, if hydrogen sulphide is present cracking will occur very readily.
- G. J. Bieffer - Your statement suggests that the deliberate formation of a calcareous deposit would be a means of preventing hydrogen embrittlement cracking. However, in most service conditions, the formation and maintenance of a protective calcareous deposit on an immersed steel structure would not be practical.
- Paper 12 - Stress Corrosion Testing of Titanium Alloys, presented by S. J. Ketcham.
- F. Bollenrath - Low-stressed welds commonly show some creep at room temperature. Did you observe a correlation between the lifetime of test pieces taken from weld joints and the holding time from fabrication and loading of the C-ring to the introduction of the corrosive environment?
- S. J. Ketcham - The precracked and double edge notched tensile specimens fabricated from the weldments were tested under dead load so stress relaxation due to room temperature creep should not be a factor. This may have occurred, however, with the 4-point loaded bend specimens. Room temperature creep may also account for the fact that the notched C-rings either failed within 30 minutes or not at all. The C-rings, incidentally, were loaded in the corrosive environment.
- Paper 13 - Factors Influencing Threshold Stress Intensity Values and Crack Propagation Rates During Stress Corrosion Cracking Tests at High-Strength Steels, presented by P. McIntyre.

4
R. DeSantis -

In your report you indicate K_{Isc} values obtained on steels heat treated at 600°C. Such materials are characterized by very high toughness values so that very thick specimens are required to meet plane strain conditions. How did you conduct your tests? What were the dimensions of your specimens? How did you overcome the difficulties associated with testing very thick specimens?

P. McIntyre -

Dr. DeSantis questions the validity of our K_{Isc} values for steels tempered at 600°C on the grounds that the specimens would not meet the specimen size criterion that the thicknesses, B , must exceed:

$$2.5 \left(\frac{K}{\text{yield stress}} \right)^2$$

I believe he has come to this false impression for the following reasons:

- (1) He has inserted K_{Ic} values in the expression to calculate B values where he should have used K_{Isc} values.
- (2) He has assumed that the steels we are investigating have carbon levels in the region of 0.2% when in fact they are 0.4% carbon low alloy steels and therefore possess high yield strengths.

A typical K_{Isc} value of such steels after tempering at 600°C is 40 ksi $\sqrt{\text{in.}}$ and a typical 0.2% proof stress is 200 ksi.

Inserting these values in the expression,

$$B = 2.5 \left(\frac{40}{200} \right)^2 = 0.1 \text{ in.}$$

The specimens we used were 0.394 in. square which is well in excess of the above minimum size requirement.

Paper 19 -

Influence of Test Method on Stress Corrosion Behavior of Aluminum Alloys in Sea Water, presented by G. J. Danek.

E. DiRusso -

In the work presented, alloys of 6000-type are included in those wrought products which were subjected to stress-corrosion testing. Also for these alloys K_{Isc} values are given. I have never found "true" stress-corrosion failures in alloys of the Al-Mg-Si system but only stress-accelerated corrosion phenomena. Is it correct to assume that K_{Isc} values are actually representative of stress-corrosion resistance for such alloys?

G. J. Danek -

In using K_{Isc} to describe the threshold stress intensity value for 6061-T652 tested in seawater, it is not intended to imply that the alloy is susceptible to stress corrosion cracking in the traditional sense. The term stress corrosion cracking has been traditionally defined as intergranular cracking in an environment. But with a fatigue crack it is possible for the specimen to fail without such development of intergranular cracking. Slight lowering of the K value for 6061-T652 may be due to other effects such as creep or lowering of surface energy by adsorption of impurities to facilitate crack propagation.

Paper 22 -

Stress Corrosion Cracking of Martensitic Precipitation Hardening Stainless Steels, presented by M. Henthorne.

P. Merklen -

In the case of intergranular corrosion what is the value to be assigned to K_{Isc} when it is determined by introducing a fatigue precrack which is transgranular? How will this transgranular crack propagate in the corrosive medium where we normally have intergranular corrosion cracking?

M. Henthorne -

The question raised by Mr. Merklen is an interesting one and is of course applicable to precracked specimens in general and not just my presentation. I suspect that in most cases, a transgranular fatigue crack is not much of a hindrance to intergranular stress corrosion cracking for at least two reasons. First, I believe a prime function of the precrack is to serve as a crevice and it does this independent of crack path. Secondly, in a commercial alloy and a typical precracked specimen, the fatigue crack front will cross about 1000 grain boundaries. It therefore seems very probable that at many points along the crack front the stress conditions will be quite favorable for a change in crack path if there is any electrochemical impetus to do so. In stress intensity situations close to K_{Isc} then differences between the fatigue crack path and stress corrosion mode may be more significant - a possibility supported by the papers (this volume) by Priest and McIntyre.

J. A. Davis -

Dr. Henthorne proposed a hydrogen embrittlement mechanism for stress-corrosion cracking of pH steels with hydrogen produced by the corrosion reaction. I feel that measurements of pH at the crack tip and at some distance from the crack tip indicate anodic dissolution continuously occurs at the crack tip with the cathodic reaction occurring at a finite distance from the crack tip. Protons

- F. H. Cocks - No. The results of the precorrosion test procedure shows that there is a very long initiation stage which is not accelerated by the application of stress. This method does not, however, give information on the mechanism responsible for this initiation stage. Such information has to be obtained by other means, e.g., metallography.
- H. L. Marcus - In your description of the effect of surface preparation on the initiation-non-stressed condition you indicate that grain deformation is the primary cause of time effects. Dr. F. Mansfield of our laboratory has shown a large effect on the pitting potential for various surface preparations of aluminum alloy 7049 in various heat-treatment conditions. I suggest that many changes take place at the surface to change this "initiation" stage.
- F. H. Cocks - Undoubtedly there will be found to be many different explanations of precorrosion effects which may be observed in different alloys and environments. In the case of alloys which crack intergranularly, however, it seems reasonable to expect machining or shot-peening treatments to have a large effect on the initiation period. This is so because such treatments disrupt the grain boundary structure at the surface, and this layer of disruption must be penetrated by normal corrosion processes before stress corrosion can begin. There may, as you point out, be other processes occurring during the stress corrosion initiation period as well. Regardless of the cause of the initiation period, however, the precorrosion testing method I described provides a quantitative means for measuring how important this stage is in the overall failure process.
- Paper 10 - Stress Corrosion Testing of Welded Joints, presented by T. G. Gooch.
- W. G. Clark, Jr - In your testing of welded joints, how do you account for the effect of residual stresses? How can you report stress-corrosion threshold values if you do not know the applied stress?
- T. G. Gooch - The question of residual welding stresses must be considered in relation to both laboratory testing and service. Once 3-point bend specimens are machined from a weld for SCC testing, tensile residual stresses will be largely relieved. Thus experimental derivation of K_{ISCC} ignores their contribution to the applied stress. However, unless there has been an effective stress relief treatment, residual stresses will constitute a significant addition to service loading. It may be difficult to establish precisely what residual stress exists, and a conservative approximation must be made. This should allow for local stress concentrations and joint geometry. For example, transverse to a weld, the stresses will normally be of the order of parent material yield stress. Along a weld they may be determined by the weld metal yield stress. In the linear elastic regime, it may be possible to determine the total acting K level by superimposing the contributions from residual and service stresses. This is comparable to the general yielding situation of adopting an additive strain approach to obtain a resultant total strain. In both cases, it should be possible to assess service performance in the light of NDT sensitivity. However, considerably more work is required before the effects of residual stresses can be fully defined.
- Paper 11 - Screening Tests of Susceptibility to Stress Corrosion Cracking, presented by G. J. Bieffer.
- W. K. Boyd - In our laboratory we have recently studied cathodic protection of 13Ni(200) n.a.raging and HY140 steels in actual sea water. No hydrogen embrittlement was noted at three times the current densities required for protection. This has been attributed to the formation of a calcareous deposit on the surface which minimizes hydrogen pick-up. However, if hydrogen sulphide is present cracking will occur very readily.
- G. J. Bieffer - Your statement suggests that the deliberate formation of a calcareous deposit would be a means of preventing hydrogen embrittlement cracking. However, in most service conditions, the formation and maintenance of a protective calcareous deposit on an immersed steel structure would not be practical.
- Paper 12 - Stress Corrosion Testing of Titanium Alloys, presented by S. J. Ketcham.
- F. Bollenrath - Low-stressed welds commonly show some creep of room temperature. Did you observe a correlation between the lifetime of test pieces taken from weld joints and the holding time from fabrication and loading of the C-ring to the introduction of the corrosive environment?
- S. J. Ketcham - The precracked and double edge notched tensile specimens fabricated from the weldments were tested under dead load so stress relaxation due to room temperature creep should not be a factor. This may have occurred, however, with the 4-point loaded bend specimens. Room temperature creep may also account for the fact that the notched C-rings either failed within 30 minutes or not at all. The C-rings, incidentally, were loaded in the corrosive environment.
- Paper 13 - Factors Influencing Threshold Stress Intensity Values and Crack Propagation Rates During Stress Corrosion Cracking Tests at High-Strength Steels, presented by P. McIntyre

produced during hydrolysis of the anodic reaction products must diffuse away from the crack tip before they are reduced to hydrogen atoms. The hydrogen atoms can then be absorbed and diffuse to the crack tip region. However, the fact that anodic dissolution continuously occurs at the crack tip indicates crack propagation is at least partially by an anodic dissolution mechanism.

- M. Henthorne — Anodic dissolution is essential for crack propagation since, as Dr. Davis notes, it indirectly produces the hydrogen. I agree that anodic dissolution probably does move the crack forward finite amounts but suspect this is minor propagation compared to that resulting from hydrogen beyond the crack tip. Much of the anodic reaction will occur on the walls close to the crack front as noted by Dr. Davis. In the absence of hydrogen to propagate the crack I believe either stifling of the corrosion reaction or lateral growth (i.e., pitting) will occur. Of course in other systems, e.g., mild steel in nitrates, I believe anodic dissolution plays a major role in moving the crack forward.
- Paper 24 — Microscopic Identification of Stress Corrosion Cracking in Steels With High-Yield Strength, presented by E. H. Phelps.
- T. G. Gooch — Work at The Welding Institute on transformable steels has shown failure mode to depend on both material microstructure and susceptibility, and on applied stress intensity. With increasing susceptibility or decreasing stress intensity, there is a transition from ductile to cleavage to intergranular failure. Mixed mode failure is common. A twinned martensitic structure has been found to be most susceptible to hydrogen induced stress corrosion, and this microstructure is particularly associated with intergranular failure. Results obtained appear consistent with Dr. Phelps' data.
- Paper 29 — Preliminary Report on the Research on the Influence of Thermomechanical Treatments on Stress Corrosion Cracking Behavior of AISI 4340 Steel, presented by R. DeSantis.
- W. Barrois — Don't you suppose that the variation in hardness is analogous to that observed with numerous alloys stretched in the course of a tensile test. I think that this is a type of Bauschinger effect related to the stability of dislocation pile-ups corresponding to deformations and residual quenching stresses which are on the scale of grains and precipitates.
- R. DeSantis — The possibility of the intervention of a phenomenon similar to the Bauschinger effect to explain the variation in hardness of the steels has been considered. We must however point out that the phenomenon occurs not only in straining the metal in compression (as is typical for the Bauschinger effect) but also in straining in tension. It occurs also only on heat treatable steels tempered at low temperature without any prior mechanical hardening process. We agree however that the decrease in hardness is related to the distribution of the dislocations in the material.